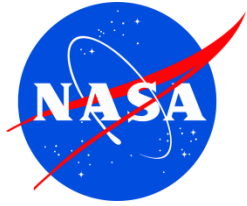


NASA/TP-2013-217376



Badhwar-O'Neill 2011 Galactic Cosmic Ray Flux Model Description

*Engineering Directorate
Avionic Systems Division*

*National Aeronautics and Space Administration
Lyndon B. Johnson Space Center
Houston, TX 77058*

June 2013

THE NASA STI PROGRAM OFFICE . . . IN PROFILE

Since its founding, NASA has been dedicated to the advancement of aeronautics and space science. The NASA Scientific and Technical Information (STI) Program Office plays a key part in helping NASA maintain this important role.

The NASA STI Program Office is operated by Langley Research Center, the lead center for NASA's scientific and technical information. The NASA STI Program Office provides access to the NASA STI Database, the largest collection of aeronautical and space science STI in the world. The Program Office is also NASA's institutional mechanism for disseminating the results of its research and development activities. These results are published by NASA in the NASA STI Report Series, which includes the following report types:

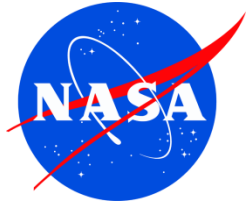
- **TECHNICAL PUBLICATION.** Reports of completed research or a major significant phase of research that present the results of NASA programs and include extensive data or theoretical analysis. Includes compilations of significant scientific and technical data and information deemed to be of continuing reference value. NASA's counterpart of peer-reviewed formal professional papers but has less stringent limitations on manuscript length and extent of graphic presentations.
- **TECHNICAL MEMORANDUM.** Scientific and technical findings that are preliminary or of specialized interest, e.g., quick release reports, working papers, and bibliographies that contain minimal annotation. Does not contain extensive analysis.
- **CONTRACTOR REPORT.** Scientific and technical findings by NASA-sponsored contractors and grantees.
- **CONFERENCE PUBLICATION.** Collected papers from scientific and technical conferences, symposia, seminars, or other meetings sponsored or cosponsored by NASA.
- **SPECIAL PUBLICATION.** Scientific, technical, or historical information from NASA programs, projects, and mission, often concerned with subjects having substantial public interest.
- **TECHNICAL TRANSLATION.** English-language translations of foreign scientific and technical material pertinent to NASA's mission.

Specialized services that complement the STI Program Office's diverse offerings include creating custom thesauri, building customized databases, organizing and publishing research results . . . even providing videos.

For more information about the NASA STI Program Office, see the following:

- Access the NASA STI Program Home Page at <http://www.sti.nasa.gov>
- E-mail your question via the Internet to help@sti.nasa.gov
- Fax your question to the NASA Access Help Desk at (301) 621-0134
- Telephone the NASA Access Help Desk at (301) 621-0390
- Write to:
NASA Access Help Desk
NASA Center for AeroSpace Information
7121 Standard
Hanover, MD 21076-1320

NASA/TP-2013-217376



Badhwar-O'Neill 2011 Galactic Cosmic Ray Flux Model Description

*Engineering Directorate
Avionic Systems Division*

*National Aeronautics and Space Administration
Lyndon B. Johnson Space Center
Houston, TX 77058*

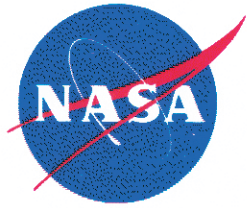
June 2013

Available from:

NASA Center for AeroSpace Information
7121 Standard Drive
Hanover, MD 21076-1320

National Technical Information Service
5285 Port Royal Road
Springfield, VA 22161

This report is also available in electronic form at <http://ston.jsc.nasa.gov/collections/TRS>



Prepared by: Patrick M. O'Neill June 5, 2013
Patrick M. O'Neill date
Radiation Physicist
Electronic Design and Manufacturing Branch / EV5
patrick.m.oneill@nasa.gov
281-483-5180

And: Charles C. Foster June 10, 2013
Charles C. Foster date
Foster Consultant Services, LLC
fosterchc@nventure.com
253-565-2574

Reviewed by: Kim, Myung-Hee Y June 6, 2013
Kim, Myung-Hee Y date
JSC-SK [UNIVERSITIES SPACE RESEARCH ASSOC-DIV OF SPACE LIFE SCIENCES]
myung-hee.y.kim@nasa.gov
281.244.2993

Approved by: Darilyn Peddie 6/11/13
Darilyn Peddie date
EV5 Branch Chief
Electronic Design and Manufacturing Branch / EV5
darilyn.gaston.peddie@nasa.gov
281-483-8279

Acronyms

ACE	Advanced Composition Explorer
AU	astronomical unit
BO'11	Badhwar-O'Neill 2011
CRIS	Cosmic Ray Isotope Spectrometer
EFS	Engelmann, Ferrnando, Soutoul
GCR	Galactic Cosmic Ray
HEAO	High Energy Astronomy Observatory
IMP-8	Interplanetary Monitoring Platform 8
ISS#	International Sunspot Number
LEO	low Earth orbit
LIS	Local Interstellar Spectrum
MeV	megaelectron volts
NOAA	National Oceanic and Atmospheric Administration
NSCR	NASA Space Cancer Risk
SEE	Single Event Effect

Contents

1.0	Introduction.....	1
2.0	Galactic Cosmic Ray Spectrum – Model and Measurements.....	2
2.1	Radiation Environment Assumptions.....	2
2.2	Local Interstellar Spectrum	2
	<i>Solar Modulation Parameter (Φ)</i>	3
	<i>Solar Modulation Parameter (Φ) from International Sunspot Number Time Lag</i>	5
	<i>Oxygen Flux (80 MeV/n) Model vs IMP-8 and ACE</i>	6
3.0	Galactic Cosmic Ray Flux Measurements vs Badhwar-O’Neill 2011 Model.....	7
	<i>High Energy Heavy Ions ($z=1$ to 28)</i>	7
	<i>Low Energy Heavy Ions ($z=1$ to 28) – NOT ACE (Arbitrary Data Measurements)</i>	7
	<i>Low Energy Heavy Ions ($z=5$ to 28) – ACE Only</i>	8
	<i>Adjusted PHI vs Time</i>	8
	<i>Deepest Solar Minimum</i>	8
4.0	Conclusion	9
	References.....	10
	Appendix A: Data References	11
	Appendix B: Data References Rejected.....	13
	Appendix C: High Energy Spectra	16
	Appendix D: Low Energy Spectra.....	94
	Appendix E: Low Energy ACE Spectra for Solar Minimum and Maximum Periods.....	178
	Appendix F: PHI from ISS# ADJUSTED to get Best Model – Data Fit.....	202

(This page intentionally left blank)

1.0 Introduction

Ionizing Galactic Cosmic Ray (GCR) radiation exposure is a major risk factor for astronauts and electronics for deep space exploration.

The purpose of this work is to provide an accurate GCR energy spectrum that can be used by radiation health physicists for astronaut exposures^{1,2} and for Single Event Effect (SEE) rate prediction codes CRÈME-MC [<https://creme.isde.vanderbilt.edu/>] and CREME96.³ GCRs are the major cause of "quiet time" SEEs in spacecraft in the solar system and beyond.

Accurate knowledge of the GCR spectrum is needed, especially during solar minimum when the GCR flux is at its maximum.

All GCR energy spectra (measurements and model) reported in this paper apply in free space – beyond the Earth's magnetosphere. An appropriate magnetic cutoff code such as that used by CRÈME-MC or CREME96 should be used to get the GCR flux within the Earth's magnetic field.

New results presented in this paper model the "quiet time" GCR flux over the period from 1955 to 2012 and provide the most comprehensive comparison that has been compiled, to date, between model and GCR in-flight measurements made above the magnetic cutoff, from balloons (high latitude) and satellites (high altitude).

This data set spans Solar Cycle 19 to 24 and confirms the maximum flux attained during the past six solar minima. This includes the most recent solar minimum, which is by far the deepest minimum since the measurements began. The Badhwar-O'Neill model parameters are uniquely influenced by measurements from the NASA Advanced Composition Explorer (ACE) Cosmic Ray Isotope Spectrometer (CRIS) that is currently measuring the low energy (~50 - 300 MeV/n) spectrum for all ions from lithium ($z=3$) to nickel ($z=28$). See the ACE Web site: <http://www.srl.caltech.edu/ACE/>.

This is a significant improvement to the overall accuracy of modeling the true GCR spectrum – now based on 55 years of cosmic ray measurements – because spacecraft designers need the actual history of GCR fluxes since it is the best knowledge of actual worst-case conditions. Badhwar-O'Neill 2011 (BO'11) is the only GCR model that utilizes all of the GCR measurements made from 1955 to 2012.

BO'11 has an improved method of determining the solar modulation parameter. The BO'11 model now uses the International Sunspot Number (ISS#) to determine level of solar modulation and an improved time delay function.

We also added the ability of the BO'11 model to calculate GCR flux for the elements from copper ($z=29$) to plutonium ($z=94$). In this range, GCR flux measurements are essentially nonexistent; therefore, we used the relative abundance data^{4,5} multiplied by our silicon spectrum ($z=14$).

To get the BO'11 model, send a request to patrick.m.oneill@nasa.gov.

2.0 Galactic Cosmic Ray Spectrum – Model and Measurements

2.1 Radiation Environment Assumptions

The steady GCR flux is the dominant cause of SEEs for hard components (those not susceptible to protons) in low Earth orbit (LEO) and for all components in orbits above LEO (such as Molniya, Geosynchronous, Lunar, and Mars). Of all the elements, carbon, oxygen, silicon, and iron cause most of these SEEs because they represent the most abundant of the more ionizing elements. It is especially critical that these elements be modeled precisely.

The BO'11^{6,7,8,9} uses the spherically symmetric Fokker-Planck equation that accounts for cosmic ray propagation in the heliosphere due to diffusion, convection, and adiabatic deceleration. The boundary condition is the constant energy spectrum (called the Local Interstellar Spectrum (LIS)) for each GCR element at the outer edge of the heliosphere (~100 AU). The Fokker-Planck equation modulates the LIS to a given radius from the sun, assuming steady-state heliosphere conditions.

2.2 Local Interstellar Spectrum

The BO'11 model uses a physically significant, simple, analytical form for the LIS of each element. The model uses the same power law that GCR physicists have used since Fermi¹⁰ first demonstrated shock acceleration for GCRs in the Milky Way.

The LIS for each element is

$$j_{lis}(E) = j_0 \beta^\delta (E + E_0)^{-\gamma} \quad (1)$$

Where E is the elemental particle's kinetic energy/nucleon and E₀ is the particle's rest energy/nucleon (938 MeV/n for every particle), β is particle speed relative to the speed of light.

The model has three free parameters: γ, δ, and j₀ for each element.

Methods that determine Φ from the current measurement of solar activity at the sun – such as sunspot number – tend to precede the GCR modulation. The heliosphere's response has a lag of 8 to 14 months to account for changes in solar activity. On the other hand, direct measurement of the GCR flux by a spacecraft instrument samples the current state of the heliosphere. The sunspot method has the advantage of predicting future GCR fluxes; however, the spacecraft method more precisely emulates the actual GCR flux.

Analysis shows that the correlation of the spectra of all the significant GCR elements (z=1 to 28) is better using direct sampling of the heliosphere by spacecraft to determine Φ. This is important to the SEE analyst who needs to know the actual history of GCR fluxes. The SEE analyst needs knowledge of actual worst-case conditions for spacecraft designs.

The BO'11 model now uses the ISS# rather than actual GCR flux to determine the value of Φ from a flight instrument. However, actual spacecraft data were used to calibrate the sunspot number for periods

where they overlap – Interplanetary Monitoring Platform (IMP)-8 from 1974 to 1997 and ACE from 1997 to present.

Table 1. LIS for BO'11

1.	1	2.774776	-1.770769	1.0295355E-03
2.	2	2.779642	-2.250157	5.3713091E-05
3.	3	3.205505	-0.6939054	6.3668558E-08
4.	4	3.368330	3.078184	7.7654974E-08
5.	5	3.385599	1.853244	1.7529467E-07
6.	6	2.981311	-0.2386665	1.4104538E-06
7.	7	3.162869	0.7369495	2.5751683E-07
8.	8	2.917556	-0.5048721	1.5013566E-06
9.	9	3.259731	2.065278	1.5567499E-08
10.	10	2.962981	0.1020193	2.1901934E-07
11.	11	3.152998	1.074219	2.9699576E-08
12.	12	2.948759	-0.1119917	2.8983834E-07
13.	13	2.994864	0.5002707	4.4308159E-08
14.	14	2.879053	-0.1195741	2.6550569E-07
15.	15	3.096346	2.159097	7.0265607E-09
16.	16	2.933176	0.7371805	4.6928129E-08
17.	17	3.176697	2.664137	6.0050547E-09
18.	18	3.032804	1.131401	1.3141148E-08
19.	19	3.140759	1.496659	8.1740321E-09
20.	20	2.962995	-1.8125730E-02	2.7298233E-08
21.	21	3.094214	0.6650744	3.9951229E-09
22.	22	3.109239	3.4904722E-02	1.2611869E-08
23.	23	3.071073	0.1630669	6.6375319E-09
24.	24	2.995401	-0.1453178	1.6220483E-08
25.	25	2.915389	7.7002598E-03	1.3574155E-08
26.	26	2.773206	-0.5354044	2.0045466E-07
27.	27	2.822085	7.3928069E-03	8.0848961E-10
28.	28	2.818860	0.3198831	1.0219478E-08

Solar Modulation Parameter (Φ)

The Fokker-Planck equation uses a single parameter – the solar modulation parameter (Φ) – to account for attenuation of the LIS due to the state of the heliosphere. Larger values of Φ cause lower GCR flux. In units of rigidity (volts), Φ is proportional to the momentum/charge required for a particle to penetrate the heliosphere.

The solar modulation parameter (Φ) is directly associated with solar activity and can be determined (in principle) by a number of methods. The various solar indices – eg, sunspot number, radio and X-ray flux, neutron monitor rates, spacecraft GCR measurements, and even tree rings – indicate the temporal variation of the sun's intensity.

One value of Φ describes the state of the heliosphere and applies at a specific time for all of the elements from hydrogen ($z=1$) through plutonium ($z=94$).

The solar modulation parameter (Φ) is directly associated with solar activity and determines the modulated GCR flux for any given time. Prior versions of the Badhwar-O'Neill model used neutron monitor (Climax) count to determine $\Phi(t)$ for periods when actual spacecraft instrument data were not available, such as periods prior to 1974. However, we now use the ISS# for all times.

However, we do not use the ISS# directly. First, we properly account for the time lag using the formulas described below. Then, we calibrated the "time delayed" ISS# by multiplying it by a constant. This calibration produces the excellent agreement with the Φ values derived from IMP-8 and ACE, shown in Figure 1.

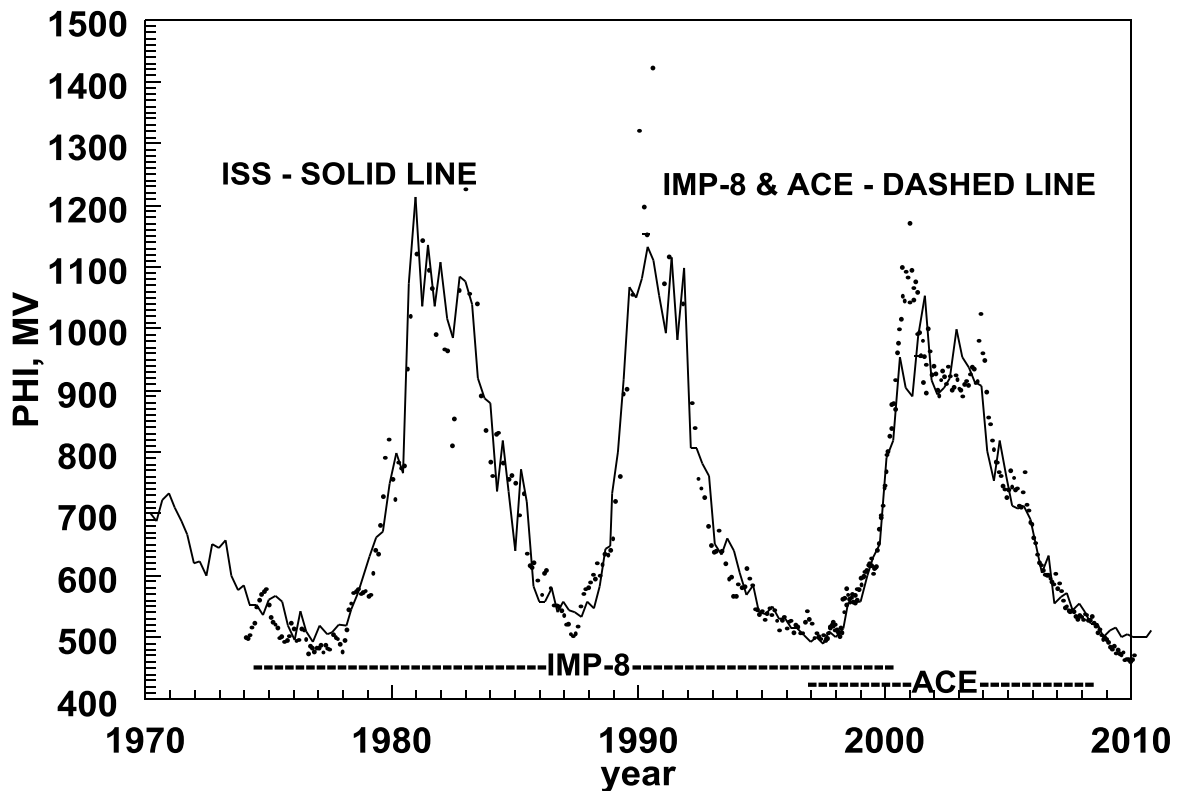


Figure 1. Solar Modulation Parameter (Φ) as derived from ISS# and from actual spacecraft instruments – IMP-8 and ACE.

One of the significant differences in BO'11 versus prior models is that the sunspot number coefficient for deriving the modulation parameter (Φ) for heavier ions ($z>1$) is roughly half that used for protons ($z=1$) during the "plateau" (eg, centered around 1996.5) solar minimum cycles. During "peaked" (eg, centered around 1987.5) solar minimum cycles, the same coefficient is used for all $z=1$ to 28.

The ISS# was downloaded from the National Geographic Data Center – National Oceanic and Atmospheric Administration (NOAA) (<http://www.ngdc.noaa.gov/ngdc.html>).

Solar Modulation Parameter (Φ) from International Sunspot Number Time Lag

The secret to deriving $\Phi(t)$ from the ISS# is the formula for accounting for the time delay between the time of the solar activity (the sunspots) and the time this effect (the magnetic field disturbance) reaches into the heliosphere enough to significantly modulate the GCR flux.¹¹

The time delay formula used for BO'11 is shown in Figure 2.

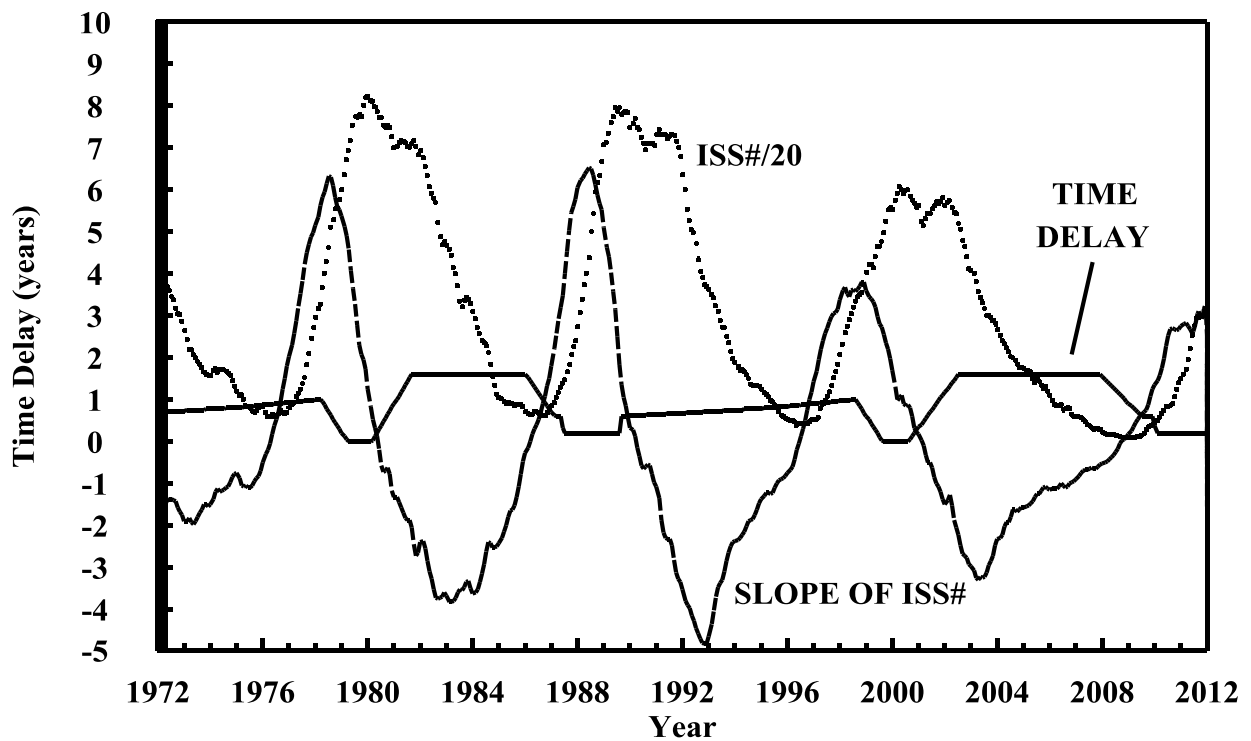


Figure 2. Time delay (in months) between solar events (sunspots) and their impact on the heliosphere regarding modulation of GCR ions.

Oxygen Flux (80 MeV/n) Model vs IMP-8 and ACE

Figure 3 demonstrates the BO'11 model quality of fit for oxygen.

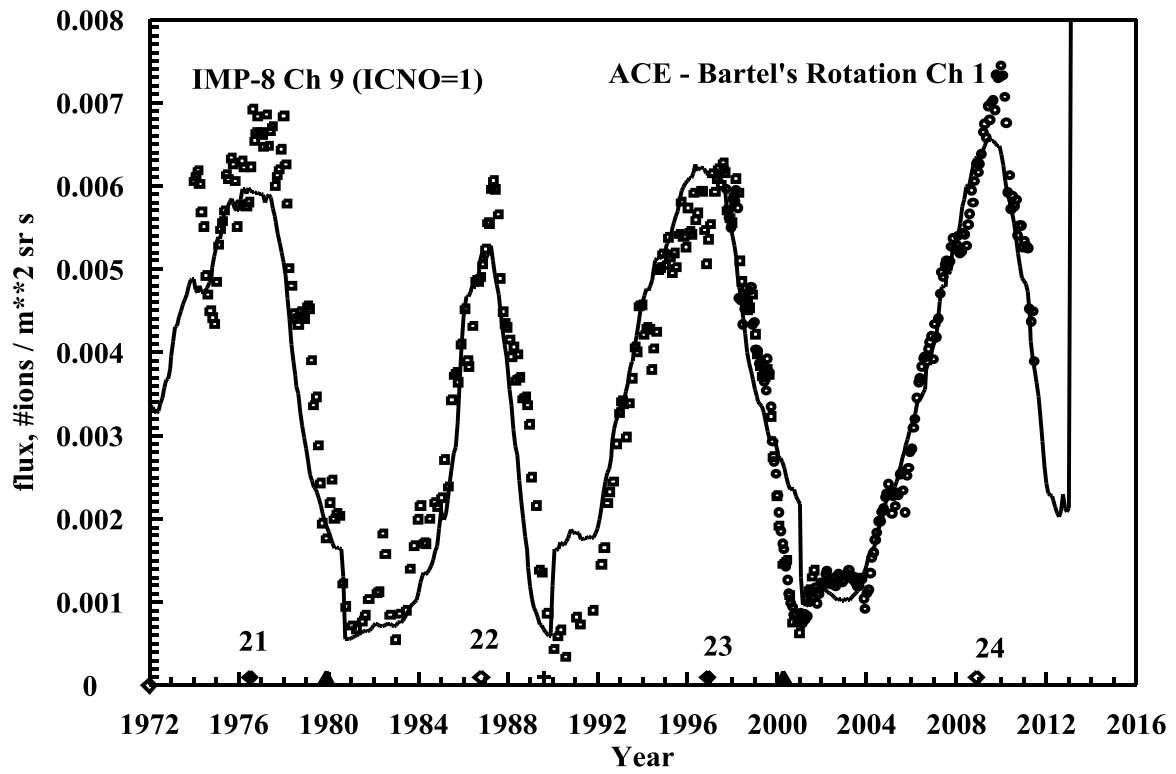


Figure 3. Oxygen Flux (80 MeV/n) Model (line) versus IMP-8 (squares) and ACE (circles) measurements.

3.0 Galactic Cosmic Ray Flux Measurements vs Badhwar-O'Neill 2011 Model

High Energy Heavy Ions (z=1 to 28)

The high-energy (>3000 MeV/n) measurements provide the foundation for the BO'11 parameter fit. The high energy data are used to determine two of the three fit parameters – the slope (γ) and the absolute magnitude (j_0) of the LIS.

At these and higher energies, the flux becomes less subject to solar modulation; therefore, the measurements can be used to determine the LIS. This allows precise data fitting even though the flux is low in this energy region.

Large instruments are used, and instruments can collect data for long periods (high energy ions are not subject to solar modulation). Engelmann, Ferrnando, Soutoul (EFS) (High Energy Astronomy Observatory (HEAO)) continuously collected data for 8 months. The balloon flights (JUL, ORTH) were only 1 day, and their collection factors were about the same as the EFS ($\sim 700 \text{ cm}^2 \text{ sr}$).

Appendix C shows all of the high-energy flux measurements for $z=1$ to 28 ions. The average error (per data point) is shown on each plot for each data set. The solar modulation parameter (PHI) is shown on each plot even though, at these energies, it makes little difference. The average error (per data point) for all the ions in the high energy region is typically around 15%.

Low Energy Heavy Ions (z=1 to 28) – NOT ACE (Arbitrary Data Measurements)

The low energy (50 - 1000 MeV/n) measurements determine the BO'11 model free parameter (δ) of the LIS.

For the abundant elements (B, C, N, O, Si, Fe), low energy (50 - 1000 MeV/n) measurements are available from several sources and ACE are typical.

For some of the less-abundant elements (Be, Li, Ne, Mg, Ca and Ni), only one source (at most) of data is available in addition to ACE data.

However, for the vast majority of the elements – the least abundant species (F, Na, Al, P, S, Cl, Ar, K, Sc, Ti, V, Cr, Mn, and Co) – ACE is the only source of low energy measurements.

The GCR flux measurements for abundant elements – such as hydrogen, helium, carbon, oxygen, silicon, and iron – appear in the literature from 1955 to 1997. Spectra measurements are especially numerous for the 1960s, '70s, and '80s. Some measurements of the other elements are also available in the older data, although sparsely. Flight instruments have measured hydrogen and helium spectra extensively for years. A short balloon flight (~ 16 hours), such as one using the IMAX (Isotope Matter – Antimatter Experiment) with a large superconducting magnet spectrometer, can accurately determine the "quiet time" GCR spectrum for these highly abundant species.

The solar modulation parameter (PHI) is shown on each plot. At these low energies, the PHI is very important. PHI is derived from the ISS#, as described above.

Appendix D shows all of the low-energy flux measurements for $z=1$ to 28 ions. The average error (per data point) is shown on each plot for each data set. Since the flux is greater for solar minimum, accurate fit during the minimum periods ($\text{PHI} < 650 \text{ MV}$) is more important. These periods were mainly used to determine the LIS parameter (δ). The average error (per data point) for all the ions near solar minimum for the "Arbitrary Data" is typically around 15%.

Low Energy Heavy Ions (z=5 to 28) – ACE Only

Appendix E shows the low-energy flux measurements for $z=5$ to 28 ions for both solar minimum and maximum. The average error (per data point) for the "best" fit and the "1 sigma" fit is shown on each plot for each data set. Each plot also shows the error distribution with the mean and standard deviation. Note that all of fits essentially (84%) lie below the "1 sigma" error fit.

Since the flux is greater for solar minimum, accurate fit during the minimum periods ($\text{PHI} < 650 \text{ MV}$) is more important. These periods were mainly used to determine the LIS parameter (δ). The mean fit error for the ACE solar minimum data is typically $<10\%$ for all the ions.

Adjusted PHI vs Time

Review of the plots in the preceding appendices shows that the major source of error between the GCR data measurements and the BO'11 model is the value of PHI derived from the ISS#. Therefore, it is instructive to see how much improvement occurs when the value of PHI is adjusted such that the BO'11 model fits the data measurements most accurately.

Appendix F shows the adjusted PHI to get best model – data fit for all low-energy ACE & Arbitrary Data flux measurements for $z=1$ to 28 ions for both solar minimum and maximum.

Deepest Solar Minimum

The current solar minimum (Cycle 23) is the quietest time, according to average monthly sunspot numbers since 1912. This is a good opportunity to observe a worst-case GCR spectrum since that should be a maximum of about 10 to 15 months after the sunspot minimum.

The monthly average sunspot number from NOAA reached a minimum for Cycle 23 around October 2009. The minimum value of Φ , as derived from ACE oxygen data, occurred around January 2010 and was approximately 430 MV. This compares to a value of about 500 MV for the Cycle 22 minimum, as observed by ACE in 1997. Of interest is the fact that the ACE oxygen flux is approximately 20% higher for the Cycle 23 minimum than that for the Cycle 22 minimum.

4.0 Conclusion

The BO'11 model now agrees reasonably well for the "early" and the "recent" measurements.

The new interactive Web-based model "NASA Space Cancer Risk (NSCR)-2012," developed by the NASA JSC Space Radiation Program Element, incorporated the BO'11 model for its GCR space environment.

The radiation health community uses the BO'11 GCR model for astronaut protection. The BO'11 model is integral to the NASA transport code HZETTRAN, and it is used by the electronic parts community as well.

References

- ¹Cucinotta, F.A. et al., "Managing Lunar and Mars Mission Radiation Risks Part I: Cancer Risks, Uncertainties, and Shielding Effectiveness," NASA/TP-2005-213164 (July 2005).
- ²W. Schimmerling, W. and Cucinotta, F.A. "Dose and dose rate effectiveness of space radiation," *Radiat Prot Dosimetry*, **122** (1-4): 349-353 (December 2006).
- ³Tylka, A.J. et al., *IEEE Trans. on Nucl. Sci.*, **44**, 2150 (1997).
- ⁴Mewaldt, R.A. et al., "Elemental Composition and Energy Spectra of Galactic Cosmic Rays," Proc. From Conference on Interplanetary Particle Environment, JPL Publication 88-28, pp 121-132, JPL, Pasadena, CA, April 15, 1988.
- ⁵Mewaldt, R.A. et al., "The Cosmic Ray Radiation Dose in Interplanetary Space – Present Day and Worst-Case Evaluations," 29th International Cosmic Ray Conference Pune (2005) 00, 101-104.
- ⁶Badhwar, G. D. and O'Neill, P.M. "Galactic Cosmic Radiation Model and Its Applications," *Advances in Space Research*, **17** No. 2, (1996).
- ⁷O'Neill, P.M. "Badhwar – O'Neill Galactic Cosmic Ray Model Update Based on Advanced Composition Explorer (ACE) Energy Spectra from 1997 to Present," *Advances in Space Research*, **37**, 1727 (2006).
- ⁸Adams, J.H. Jr., Heiblim, S., and Malott, C. "Evaluation of Galactic Cosmic Ray Models," *IEEE Nuclear and Space Radiation Effects Conference*, Quebec City, Quebec (July 2009).
- ⁹Badhwar, G.D. and O'Neill, P.M. "Time Lag of Twenty Two Year Solar Modulation," Proceedings of the International Cosmic Ray Conference, SH 6.21, Calgary, July 19-30, 1993.
- ¹⁰Fermi, E., "On the Origin of the Cosmic Radiation," *Phys. Rev.*, **75**, 1169-1174 (1949)
- ¹¹Nymmik, R.A. "Time Lag of galactic Cosmic Ray Modulation: Conformity to General Regularities and Influence on Particle Energy Spectra," *Adv Space Res*, **26**, No. 11, 1875-2000 (2000).

Appendix A: Data References

(Used for Badhwar-O'Neill 2011 Model)

Pro07PAM and He07PAM

Adriani, O. et.al. "PAMELA Measurements of Cosmic-Ray Proton and Helium Spectra." *Science* 1-42. Web. 3 March 2011.

HE66B

Badhwar, G.D. et. al., "Measurements of the Low-Energy Cosmic Radiation during the Summer of 1966." *Phys. Rev.* **163**, 1327-1342 November 1967.

Pro63BHM, PRO65BHM, HE63BHM and He65BHM

Balasubrahmayan, V.K., et. al., "Low Energy Galactic Cosmic Rays." *Recent Advances in Cosmic Ray Research*. North Hollywood, CA: Western Periodicals Co., 1966. 101-127. Print.

Pro94CAP and He07CAP

Boezio, M. et.al. "The Cosmic-Ray Proton and Helium Spectra between 0.4 and 200 GV." *The Astrophysical Journal* **518**. 457-472. (1999). Print.

C77CW, MG77CW, NE77CW, and Ox77CW

Chappell, J.H. and W.R. Webber, "High Energy Cosmic ray Charge and Energy Spectra Measurements." *International Cosmic Ray Conference*, Paris, France, **2**, 59-61 (1981).

Li9899, Li9900, Be9899 and Be9900

de Nolfo, G.A., et.al. "New Measurements of the Li, Be and B Isotopes as a Test of Cosmic Ray Transport Models." *28th International Cosmic Ray Conference* (2003).

B76DPAT, C76DPAT, MG76DPAT, NE76DPAT, Ox76DPAT

Derrickson, J.H. et. al. "The Absolute Energy Spectra of Galactic Cosmic Rays Measured in the Fall of 1976." *Dept. of Chemistry*, University of Alabama in Huntsville, Huntsville, Alabama, (1976)

BE80EFS, B80EFS, C80EFS, CL80EFS, Co80EFS, CR80EFS, F80EFS, K80EFS, MG80EFS, MN80EFS, NA80EFS, NE80EFS, Ni80EFS, OX80EFS, P80EFS, S80EFS, TI80EFS and V80EFS
Engelmann, J.J. et al, "Charge Composition and Energy Spectra of Cosmic-Ray Nuclei for Elements from Be to Ni. Results from HEAO-3-C2. " *Astron. Astrophys.*, **233**, 96-111 (1990).

PRO61FG, PRO62FG, PRO63FG, HE61FG, and HE62FG

Fichtel, C.E., et. al. "Modulation of Low Energy Galactic Cosmic Rays." *International Cosmic Ray Conference*, Jaipur, **2**, 240-245 July 1961.

C72Jul, Li72Jul and Ox72Jul

Juliusson, Einar "Charge Composition and Energy Spectra of Cosmic-ray Nuclei at Energies above 20 GeV per Nucleon." *Astrophys. J.*, **191**, 331-348 July 1974.

B74LW4, C74LW4 and Ox74LW4

Lezniak, J.A. and W.R. Webber, "The Charge Composition and Energy Spectra of Cosmic-ray Nuclei from 3000 MeV per Nucleon to 50 GeV per Nucleon." *Astrophys. J.*, **223**, 676-696 July 1978.

PRO92IMX, HE92IMX

Menn, W., et.al., "The Absolute Flux of Protons and Helium at the Top of the Atmosphere Using IMAX." *Astrophys. J.*, **533**, 281-297 April 2000.

PRO61MV, PRO62MV and PRO63MV

Meyer, Peter and Rochus Vogt, "Changes in the Primary Cosmic Ray Proton Spectrum in 1962 and 1963." *International Cosmic Ray Conference, Jaipur*, **3**, 49-55 December 1963.

Ni75M

Minagawa, Gary, "The Abundances and Energy Spectra of Cosmic Ray Iron and Nickel at Energies from 1 to 10 GeV per amu," *Astrophys. J.*, **248**, 847-855 September 1981.

PRO63OW, PRO65OW, PRO66OW, HE63OW and HE65OW

Ormes, J.F. and W.R. Webber, "Proton and Helium Nuclei Cosmic-Ray Spectra and Modulations between 100 and 2000 Mev/Nucleon." *Journal of Geophysical Research, Space Physics*, **73**, 4231-4245, 1 July 1968.

PRO70RY and HE70RY

Ryan, M.J. et.al. Cosmic Ray Proton and Helium Spectra above 50 GeV, *Physical Review Letters* **10** 985-988, April 1972.

PRO65RE, PRO66RE, PRO67RE, PRO68RE, PRO69RE, HE65RE, HE66RE, HE67RE, HE68RE and HE69RE

Rygg, Thomas A. and James A. Earl. "Balloon Measurements of Cosmic Ray Protons and Helium over Half a Solar Cycle 1965-1969." *Journal of Geophysical Research* 7445-7469, 10 November 1971. Print.

Pro97BES, PRO98BES, PRO99BES, PRO00BES, PRO02BES, HE97BES, HE98BES, HE99BES, HE00BES, HE02BES and HE93WSA

Shikaze, Y. et.al. "Measurements of 0.2 to 20 GeV/n cosmic-ray proton and helium spectra from 1997 through 2002 with the BESS spectrometer." *Elsevier* (2007): 1-29. Web. 21 April 2007.

HE66vRW

Von Rosenvinge, T.T. and W.R. Webber, "A Comparison of the Energy Spectra of Cosmic Ray Helium and Heavy Nuclei," *Astrophys. J.*, **5**, 342-359 (1969).

Appendix B: Data References Rejected **(Not Used in Badhwar-O'Neill 2011 Model)**

B77CW

Chappell, J.H. and W.R. Webber, "High Energy Cosmic ray Charge and Energy Spectra Measurements." *International Cosmic Ray Conference*, Paris, France, **2**, 59-61 (1981).

Ox90CGW

Chenette, D.L. et. al., "The LET Spectrum and it's Uncertainty During the CRRES", *Adv. Space Res.*, **14**, 809-813 (1994).

Pro78EK, Pro79EK, Pro80EK, Pro81EK, He78EK, and He81EK

Evenson, Paul, et. al., "Measurements of Galactic Hydrogen and Helium Isotopes from 1978 through 1983", 19th ICRC, La Jollo, 60-63, (1985).

He54FNW and He57FNW

Freier, P.S., et. al., "Flux and Energy Spectrum of Cosmic-Ray α Particles during Solar Maximum", *Physical Review*, **114**, 365-370, 1 April 1959.

Ox85GMA, Ox86GMA, Ox87GMA, Ox88GMA, Ox748GMA, He78GMA, He86GMA and He87GMA

Garcia-Munoz, M. "Data of Garcia Munoz on Oxygen and Helium." Message to Gautum Badhwar. 26 June 1991. Fax.

Pro83GMS, Pro84GMS, He83GMS and He84GMS

Garcia-Munoz, M. et. al., "The 1973-1984 Solar Modulation of Cosmic Ray Nuclei", 19th ICRC, La Jollo, 409-412 (1985).

Pro71GMM, Pro73GMM, Pro74GMM, He71GMM, He73GMM, He74GMM, B73GMM, Ox73GMM and C73GMM

Garcia-Munoz, M., et al., "The Anomalous 4He Component in the Cosmic-ray Spectrum at <50 MeV per Nucleon During 1972-1974," *Astrophys. J.*, **202**, 265-275 November 1975.

Pro82GMP, ProGMP84, He82GMP and He84GMP

Garcia-Munoz, M. et. al., "The Dependence of Solar Modulation on the Sign of the Cosmic Ray Particle Charge", *J. of Geophysical Research*, **91**, A3, 2858-2866, 1 March 1986.

B748GMS, Ox74GMSL, Ox74GMSH, C74GMSL and C74GMSH

Garcia-Munoz, M. et. al. "The Energy Dependences of the Ratios of Secondary to Primary Elements in the Cosmic Radiation." 16th ICRC, Kyoto, Japan, **1**, 6 August 1979.

Pro72GMM and He72GMM

Garcia-Munoz, M. et. al., "A New Test for Solar Modulation Theory: The 1972 May-July Low-Energy Galactic Cosmic-Ray Proton and Helium Spectra", *Astrophys. J.*, **182**, L81-L84 (1973).

Pro66G, Pro67G, Pro69G, Pro70G, He66G, He67G, He69G, and He70G

Garrard, Thomas Lee 1973, "A Quantitative Investigation of the Solar Modulation of Cosmic-Ray Protons and Helium Nuclei", Phd Thesis, California Institute of Technology, Pasadena, California.

S72Jul, P72Jul, NA72Jul, K72Jul, F72Jul, Cr72Jul, CL72Jul, Ni72Jul, Be72Jul, NE72Jul, MG72Jul, B72Jul, V72Jul, and Ti72Jul

Juliusson, Einar, "Charge Composition and Energy Spectra of Cosmic-Ray Nuclei at Energies above 20 GeV per Nucleon", *Astrophysical J.*, **191**, 331-348, 15 July 1974.

S74LW3, NA74LW3, F74LW3, Ni74LW3, Be74LW3, Ox74LW3, NE74LW3, MG74LW3, C74LW3, B74LW3

Lezniak, J.A. and W.R. Webber, "The Charge Composition and Energy Spectra of Cosmic-ray Nuclei from 3000 MeV per Nucleon to 50 GeV per Nucleon," *Astrophys. J.*, **223**, 676-696 (July 1978)

Pro68LW and He68LW

Lezniak, J.A. and W.R. Webber, "Solar Modulation of Cosmic Ray Protons, Helium Nuclei, and Electrons", *J. of Geophysical Research*, **76**, 1605-1625.

Li69M, Be69M, Ox69M, C69M, and B69M

Mason, G.M., "Interstellar Propagation of Galactic Cosmic-Ray Nuclei $2 \leq Z \leq 8$ in the Energy Range 10-1000 MeV Per Nucleon", *Astrophys. J.*, **171**, 139-161, 1 January 1972.

He58feb, He58jul, He59apr, He59may, and He59jun

McDonald, Frank B., "Primary Cosmic-Ray Intensity near Solar Maximum", *Physical Review*, **116**, 462-463 15 October 1959.

He55Mw, He55MwA and He55MwB

McDonald, Frank B. and William R. Webber, "Proton Component of the Primary Cosmic Radiation", *Physical Review*, **115**, 194-202 1 July 1959.

NA72Orth, F72Orth, Li72Orth, Be72Orth, Ox72Orth, Ne72Orth, MG72Orth, C72Orth, B72Orth
Orth, Charles D., et al, "Abundances and Spectra for Cosmic-ray Nuclei from Lithium to Iron for 2 to 150 GeV Per Nucleon," *Astrophys. J.*, **226**, 1147-1161 (December 1978)

PRO65R, PRO68R, PRO69R, PRO71R, PRO72R, PRO74R, He65R, He68R, He69R, He71R, He72R, and He74R

Rockstroh, J.M. 1977, "Details of the Solar Modulation Problem", Thesis, U of N.H., New Hampshire.

Pro98SMM and He98SMM

Sanuki, T. et al., "Precise Measurement of Cosmic-Ray Proton and Helium Spectra with the BESS Spectrometer," *Astrophys. J.*, **545**, 1135-1142 December 2000.

Pro87S

Seo, E.S., et. al., "Measurement of the Cosmic Ray Proton and Helium Fluxes from 200 MeV to 100 GeV During the 1987 Solar Minimum." *Nucl. Tracks Radiat. Meas.*, **20**, 431-444 July 1992.

Ox76SSS, C76SSS and B76SSS

Simon, M., H., Spiegelhauer and W.K.H. Schmidt, et al., "Energy Spectra of Cosmic-ray Nuclei to Above 100 GeV per Nucleon," *Astrophys. J.*, **239**, 712-724 July 1980.

C71SBS

Smith, L.H. et. al., "A Measurement of Cosmic-Ray Rigidity Spectra Above 5 GV/c of Elements from Hydrogen to Iron", *Astrophys. J.*, **180**, 987-1010, 15 March 1973.

Pro77Vm, Pro79Vm, He77Vm and He79Vm

Von Roseninge, T.T. et. al., "The Modulation of the Galactic Cosmic Ray Between 1 and 17 AU", 16th ICRC, Kyoto, **12**, 170 (1979).

Pro77Wy and He77Wy

Webber, W.R. and S.m. Yushak, "Measurements of Cosmic Ray ²H and ³He Nuclei Above 100 MeV/nuc Using Balloon Borne Telescope". 16th ICRC, Kyoto, 383-388 (1979).

Pro87W , Pro89W, He87W and He89W

Webber, W.R. et. al., "A Measurement of the Cosmic-Ray ²H and ³He Spectra and ²H/⁴He and ³H/⁴He Ratios in 1989", *Astrophysical J.* **380**, 230-234, 10 October 1991.

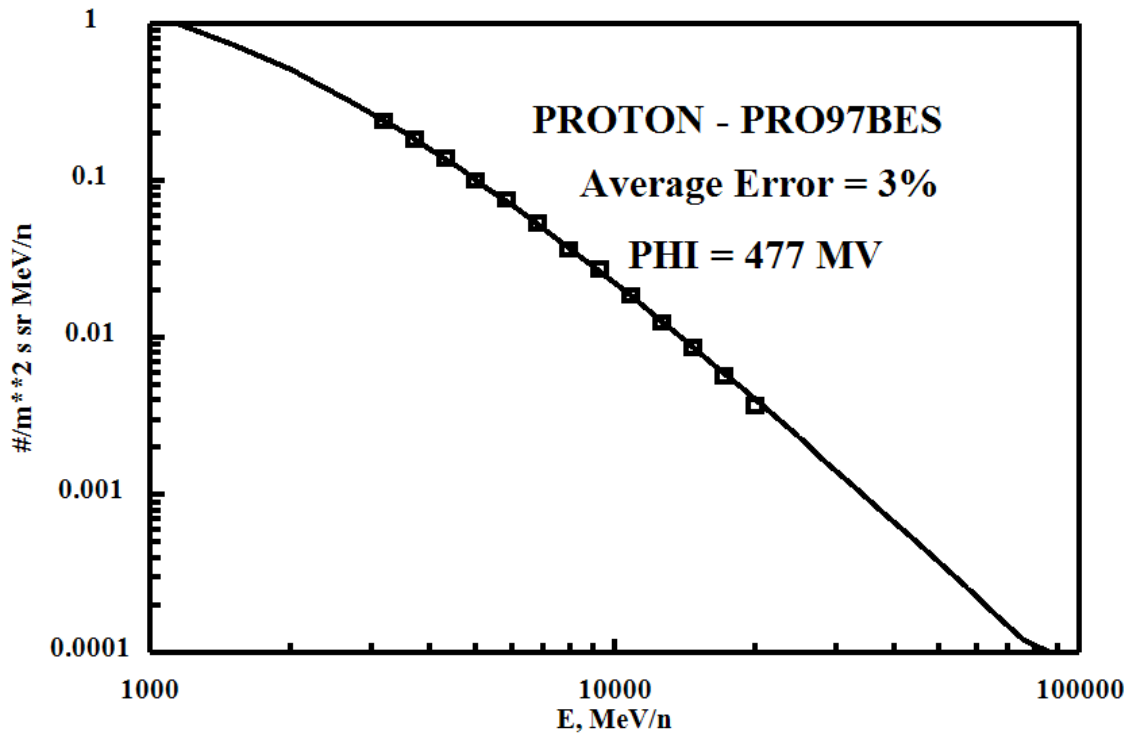
Appendix C: High Energy Spectra

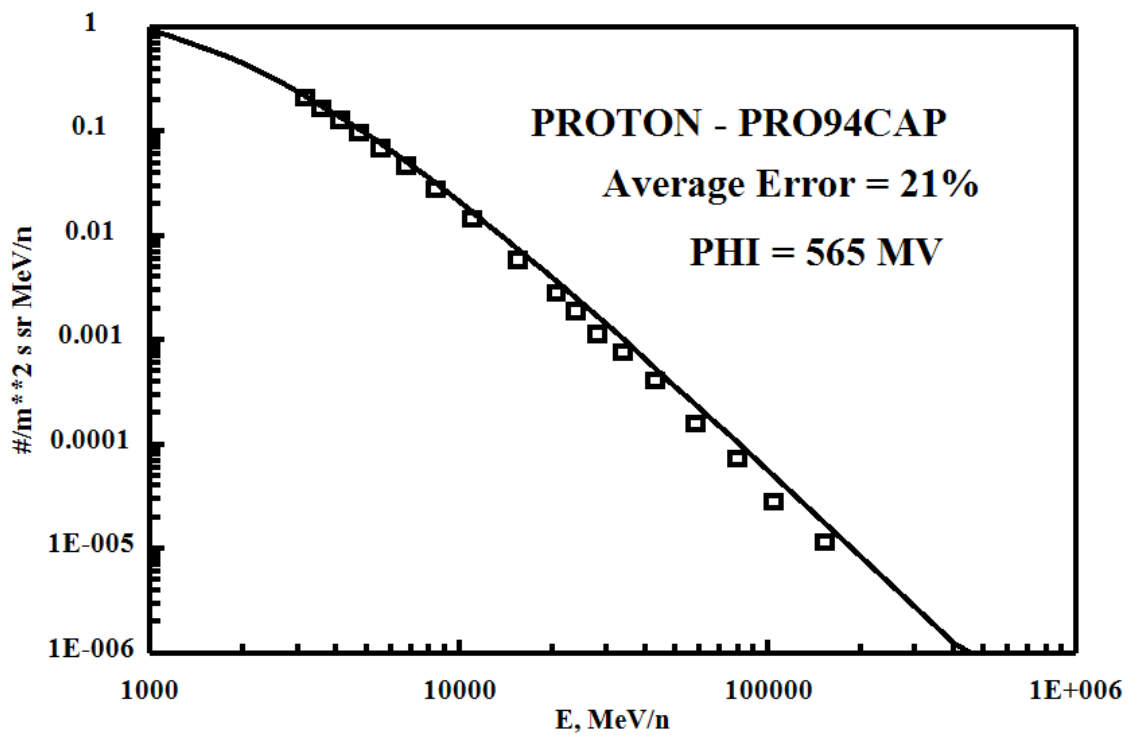
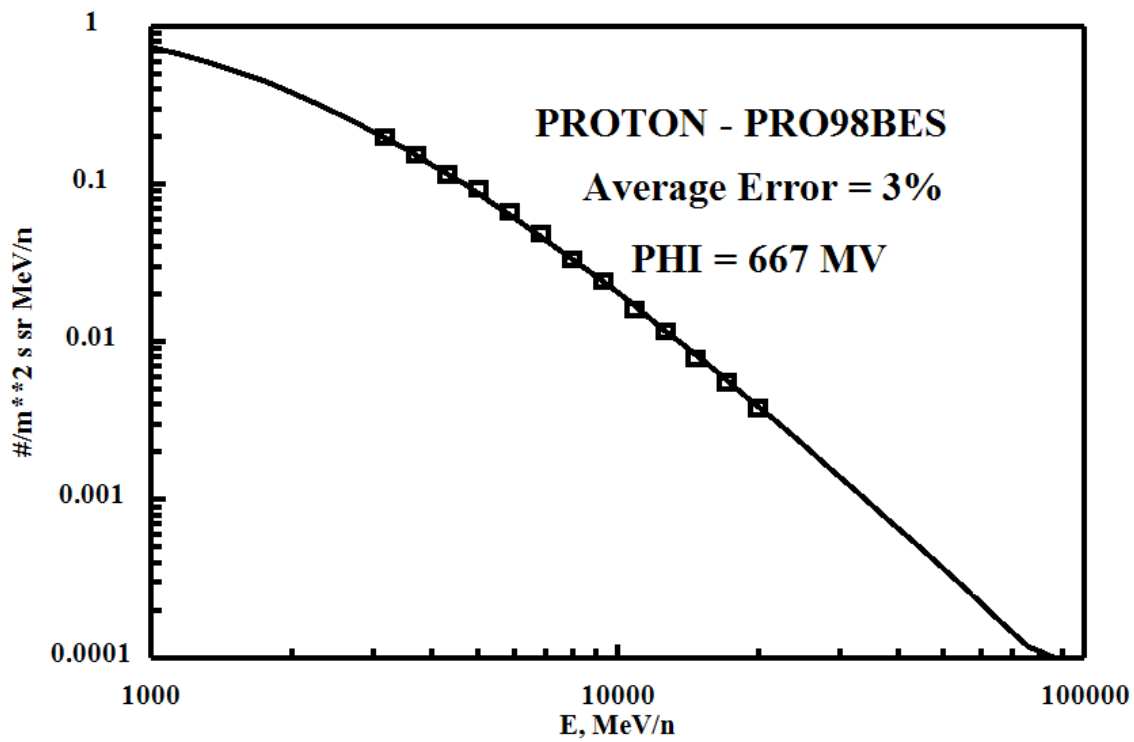
Line = BO'11 Model

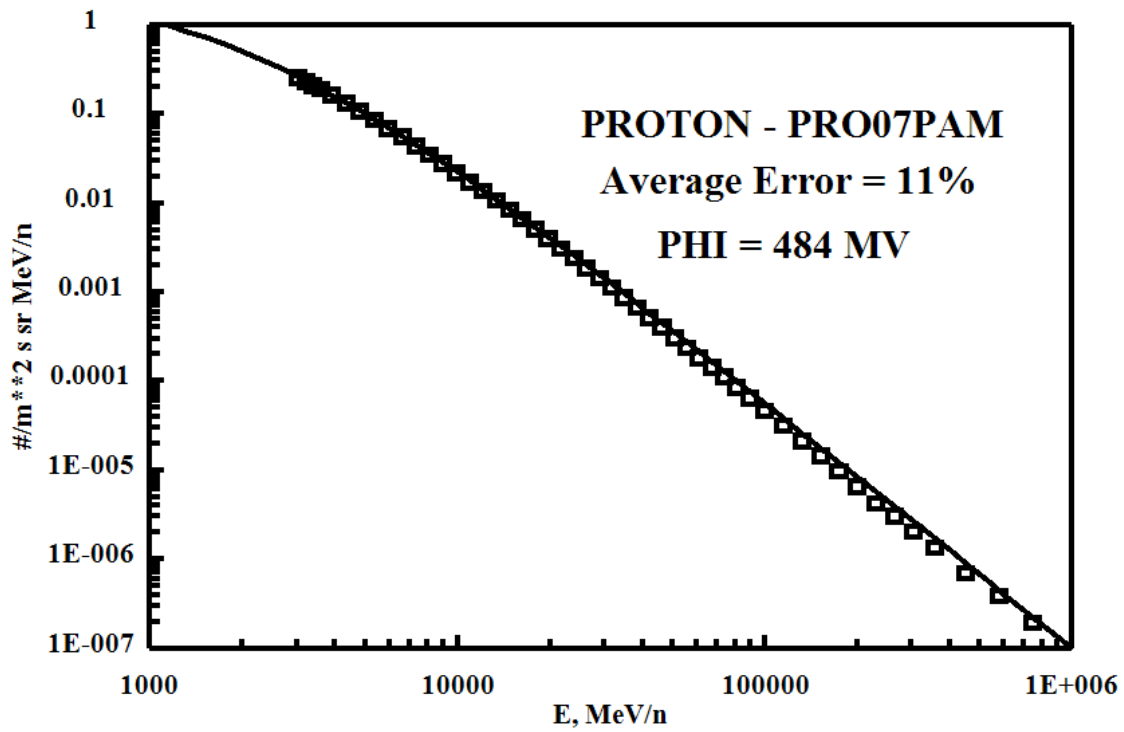
Arbitrary Data Measurements (squares) are correlated with the references (eg, PRO97BES)

Note: The average error indicated on each plot applies only to data points >3000 MeV/n and each plot only shows the measured data points >3000 MeV/n even though that data set may contain data points with energies < 3000 MeV/n.

<u>PROTON - High Energy, Solar Minimum</u>			
<u>Files Used (Arbitrary 1's)</u>			
FILE	DATE	PHI (MV)	ERROR=ABS (FLUX-DATA)
Pro97BES.dat	1997.570	477.0878	2.607838
Pro98BES.dat	1998.575	666.7952	2.724817
Pro94Cap.dat	1994.605	565.4738	20.53057
Pro07Pam.dat	2007.000	484.1927	11.05974
BO AVERAGE ERROR =		9.230742	



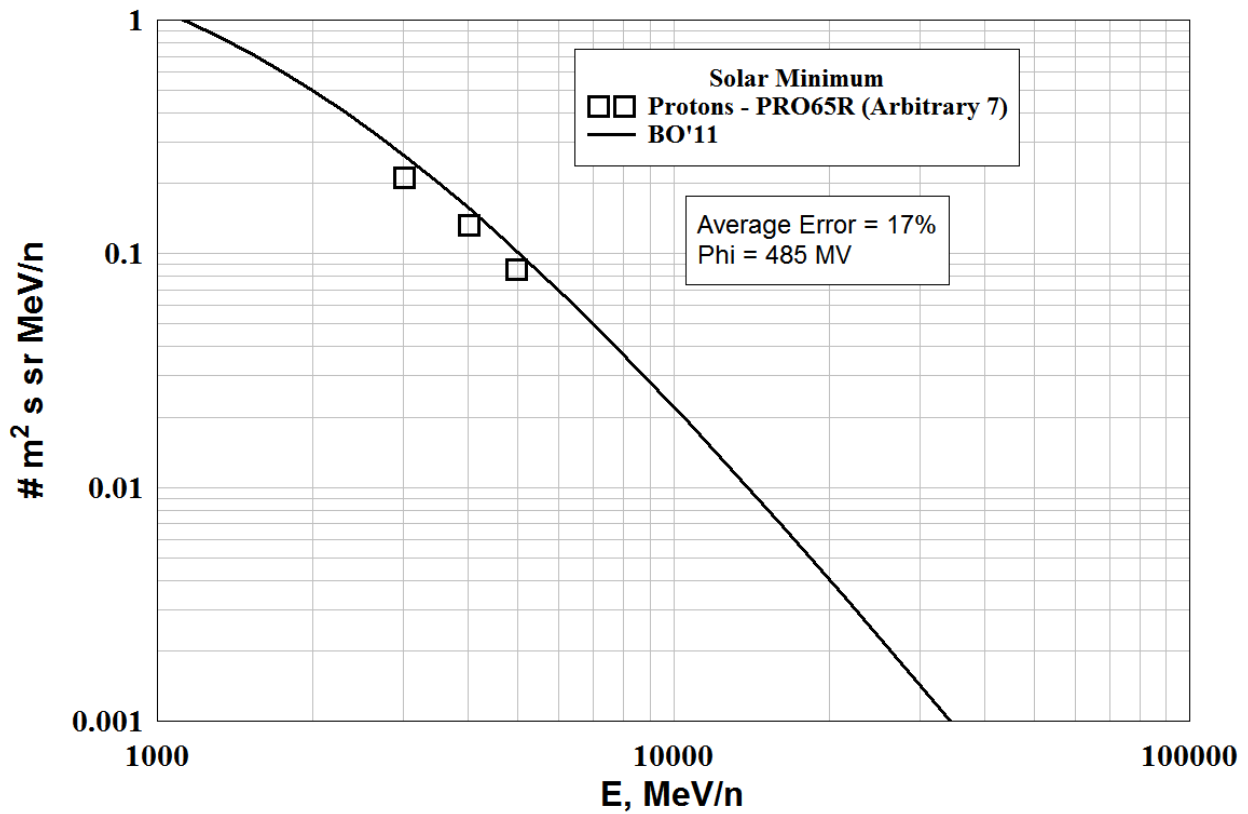
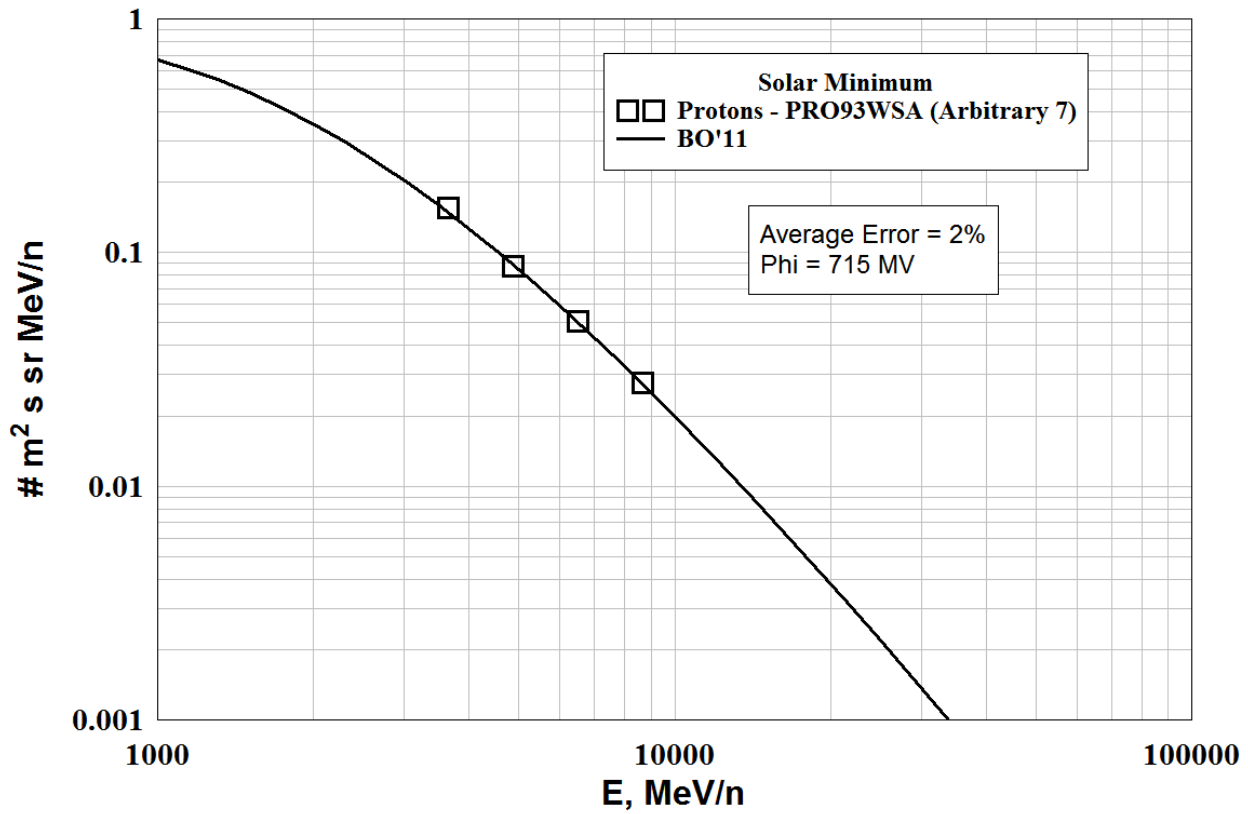


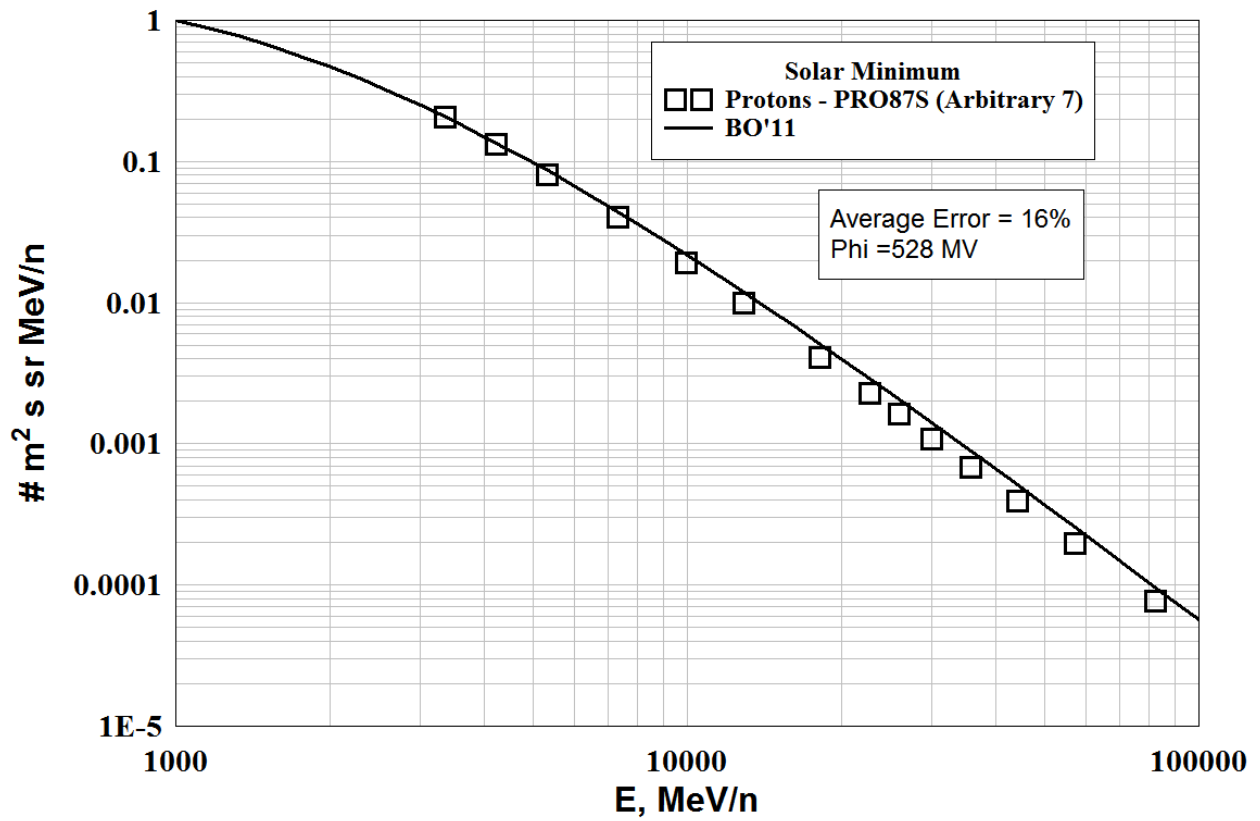
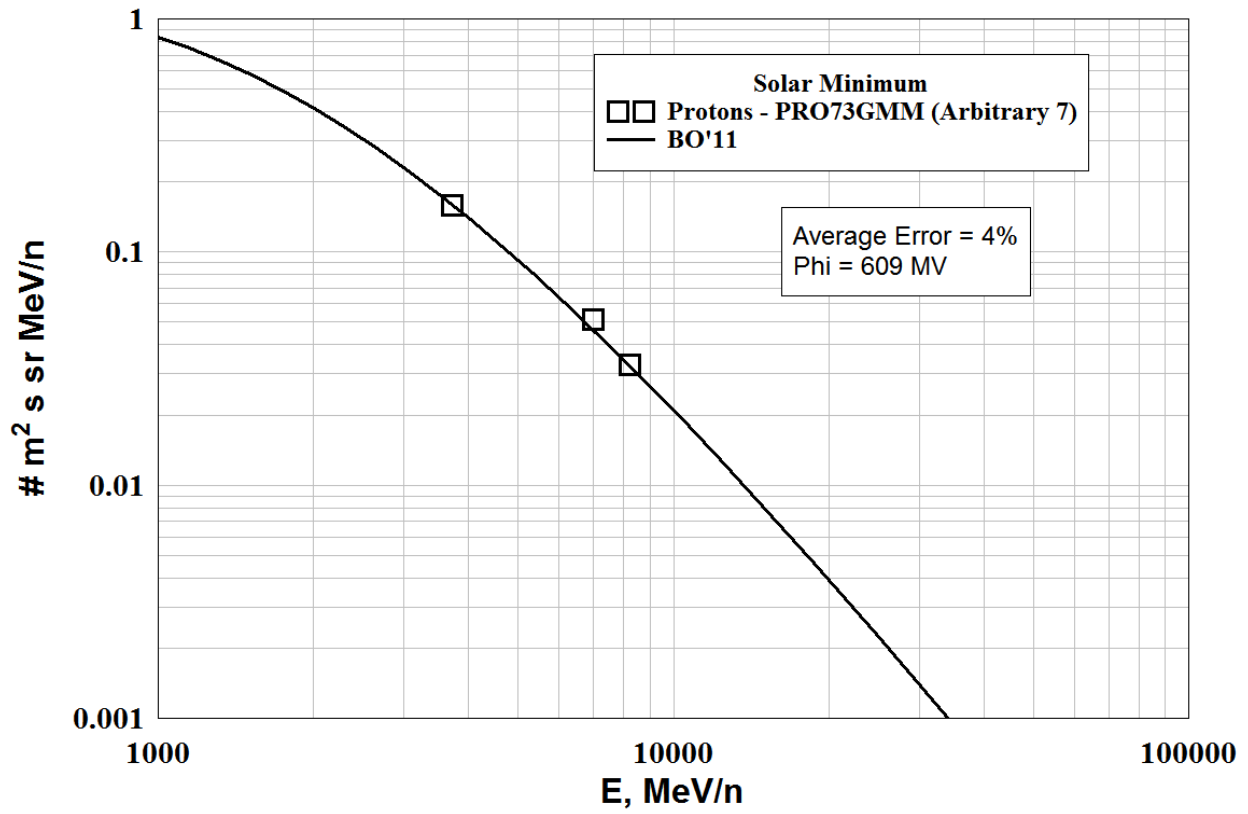


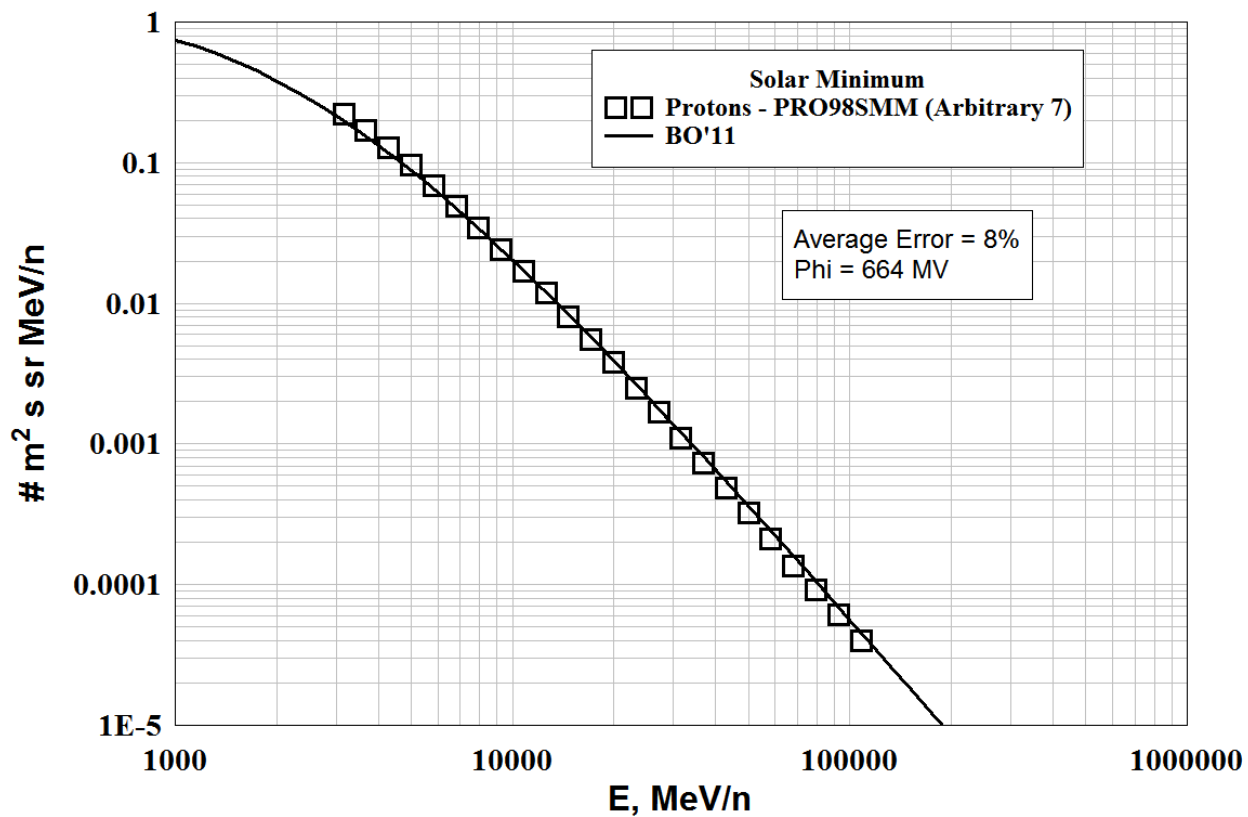
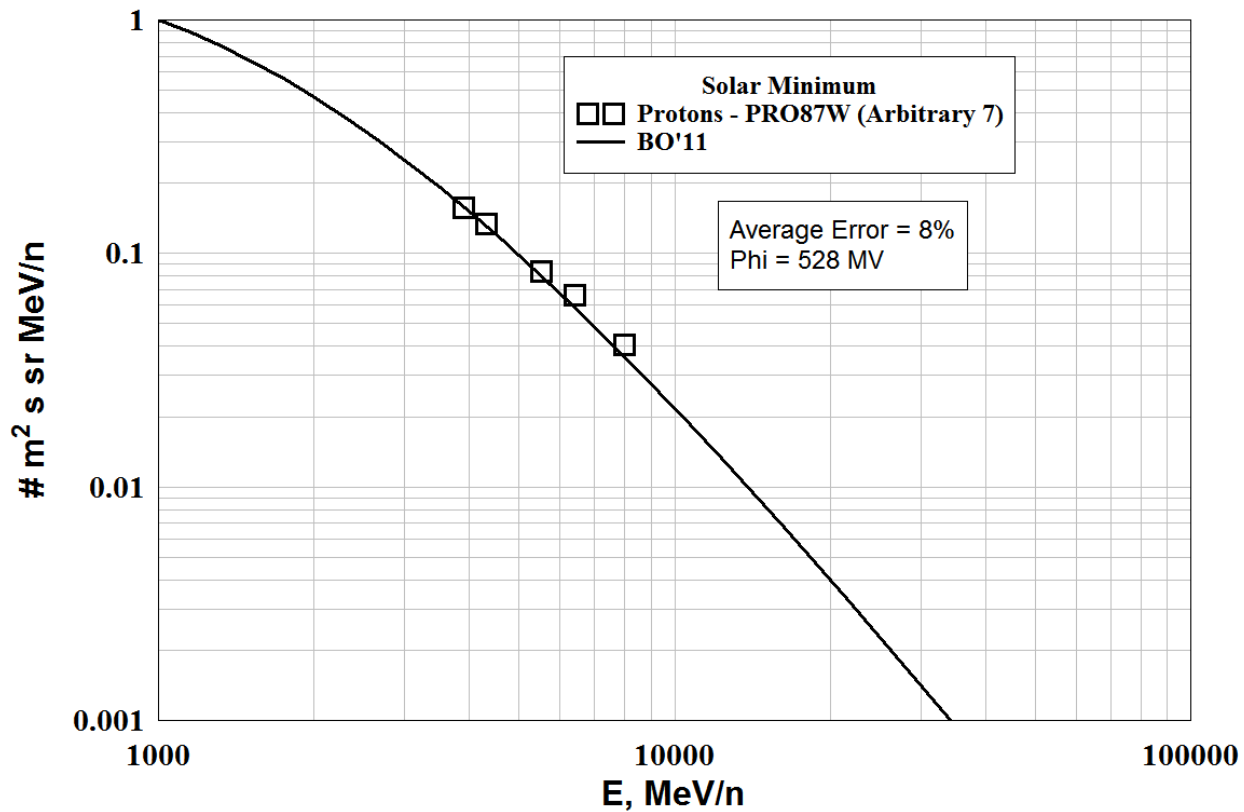
PROTON - High Energy, Solar Minimum

Additional Files

FILE	DATE	PHI (MV)	ERROR=ABS (FLUX-DATA)
Pro93WSA.dat	1993.567	715.0115	2.078370
Pro65R.dat	1965.573	484.6338	17.28930
Pro73GMM.dat	1973.408	609.1092	4.228811
Pro87S.dat	1987.638	527.9987	15.98243
Pro87W.dat	1987.641	528.4525	6.262641
Pro98SMM.dat	1998.567	664.4254	7.867101
BO AVERAGE ERROR =		8.951442	





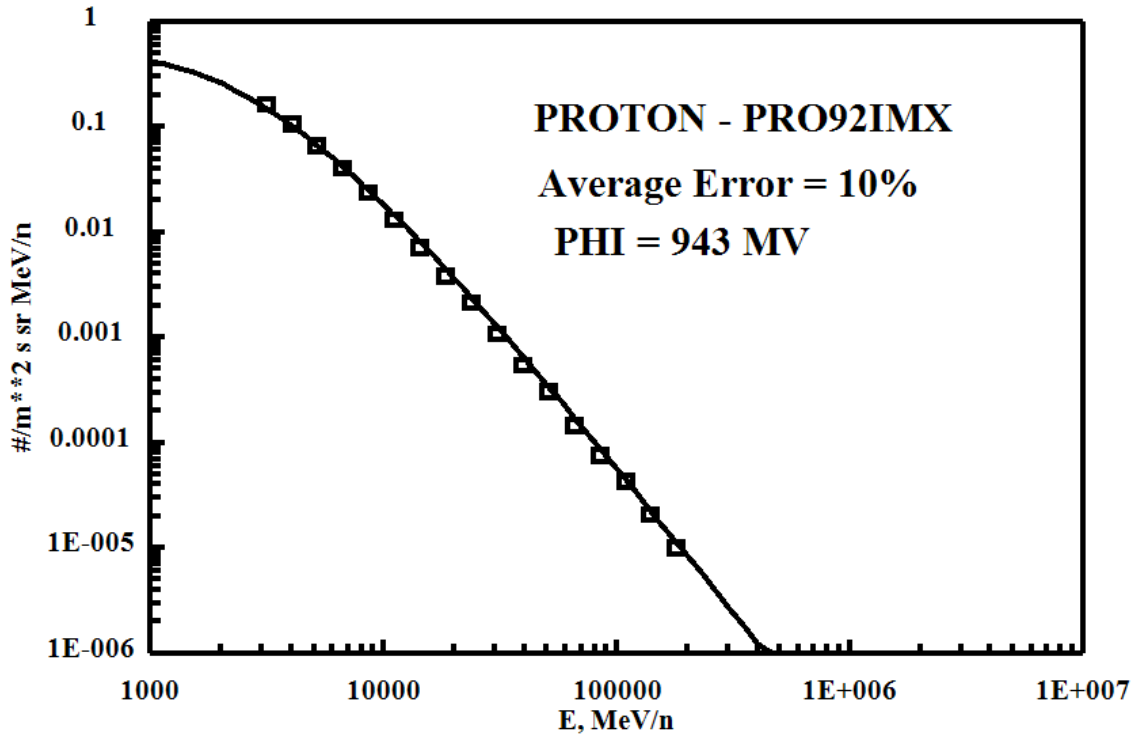


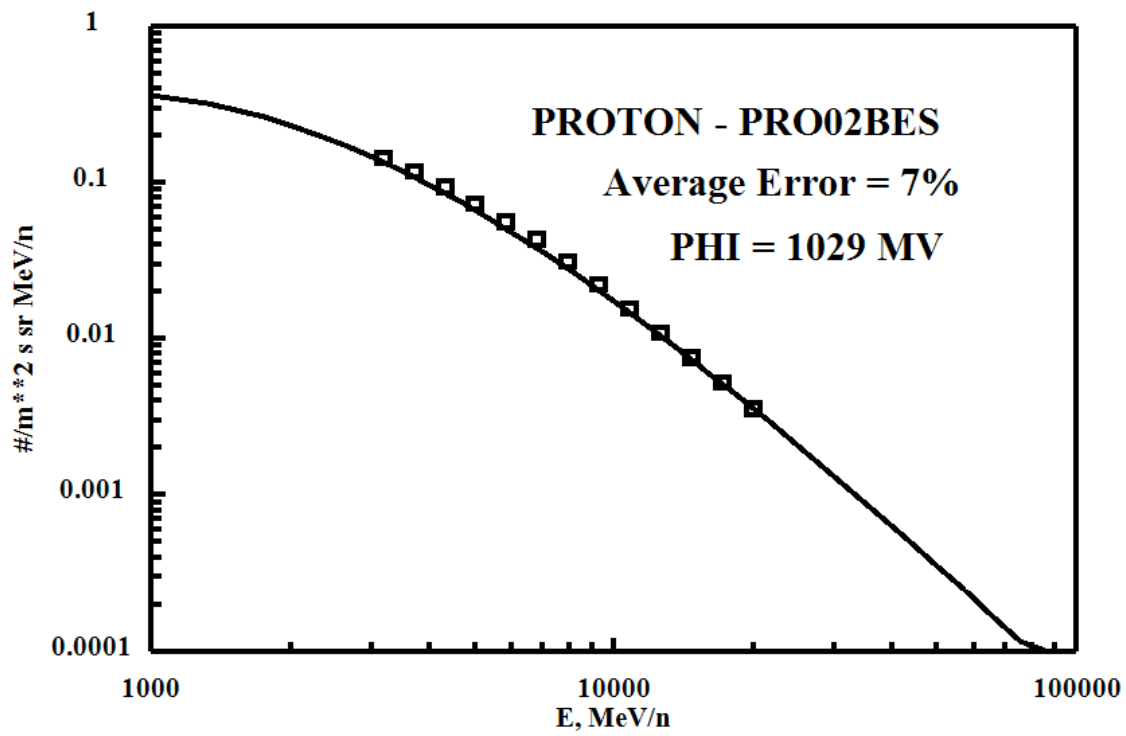
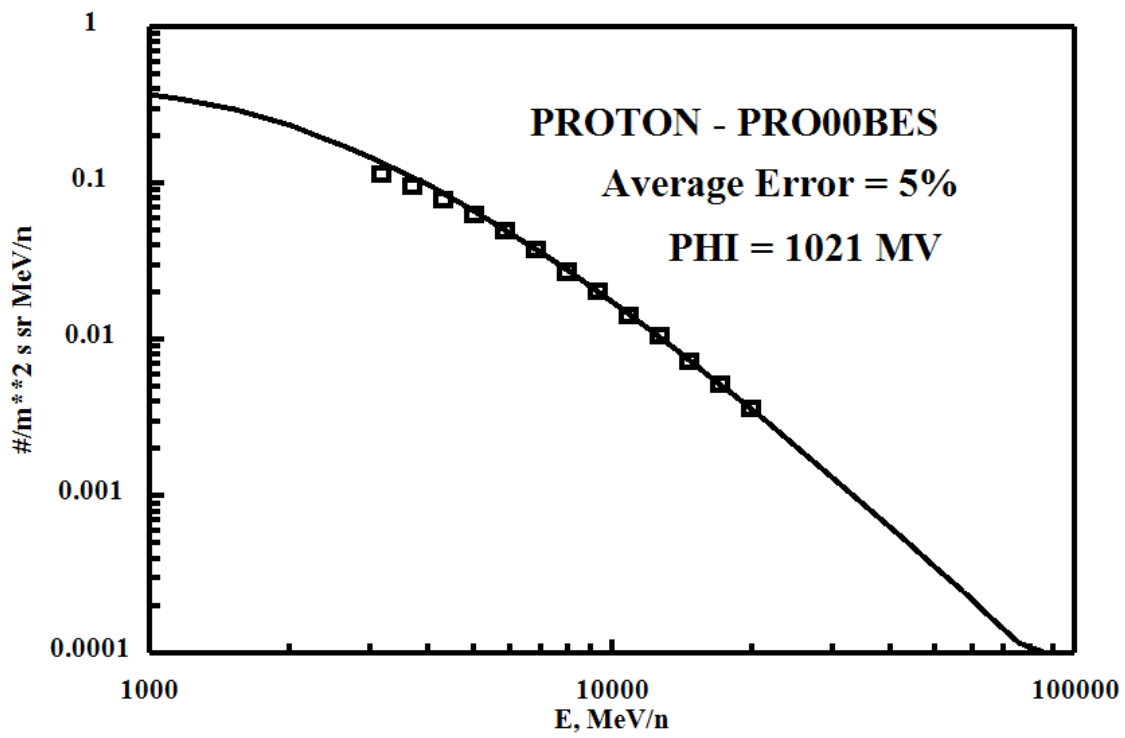
PROTON - High Energy, Solar Maximum

Files Used (Arbitrary 1's)

FILE	DATE	PHI (MV)	ERROR=ABS (FLUX-DATA)
Pro92IMX.dat	1992.540	942.8263	10.04087
Pro70Ry.dat	1970.874	946.1595	22.56775
Pro99BES.dat	1999.611	865.3713	11.89829
Pro00BES.dat	2000.608	1020.844	4.726431
Pro02BES.dat	2002.600	1029.817	7.111317

BO AVERAGE ERROR = 11.26893

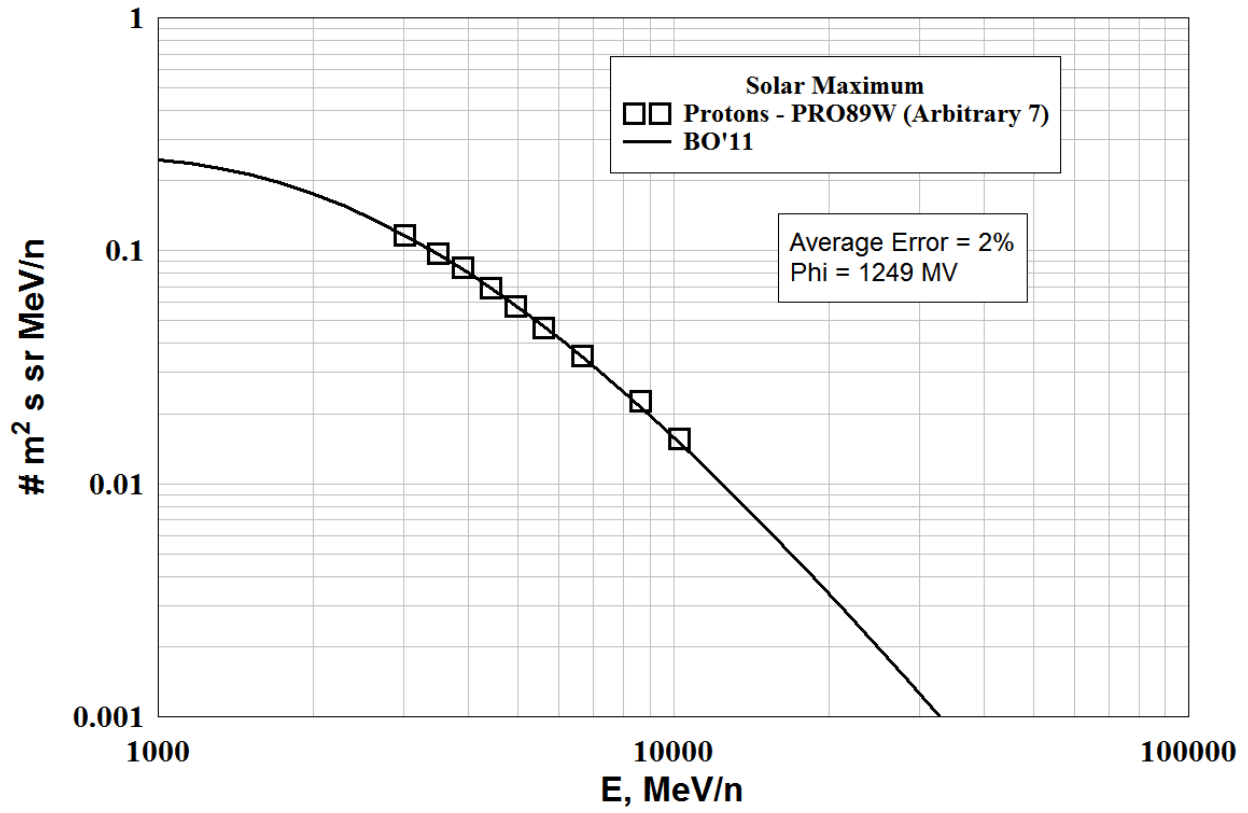




PROTON - High Energy, Solar Maximum

Additional Files

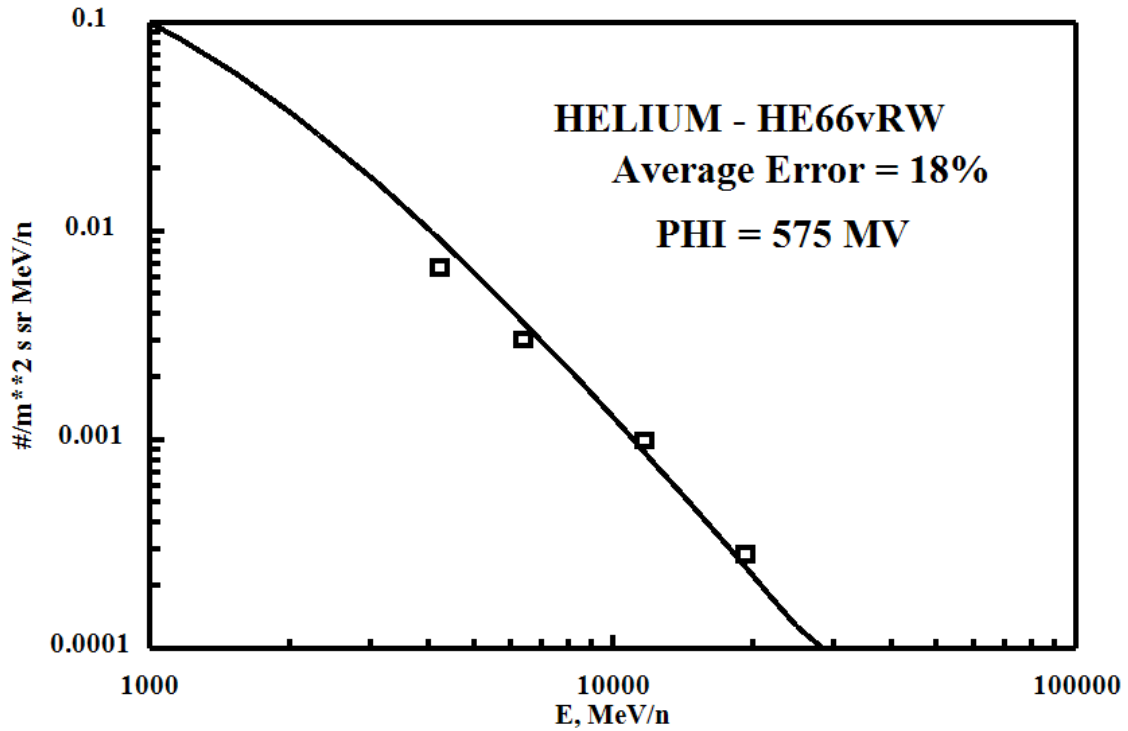
FILE	DATE	PHI (MV)	ERROR=ABS (FLUX-DATA)
Pro89W.dat	1989.682	1248.804	1.847661
BO AVERAGE ERROR =			1.847661

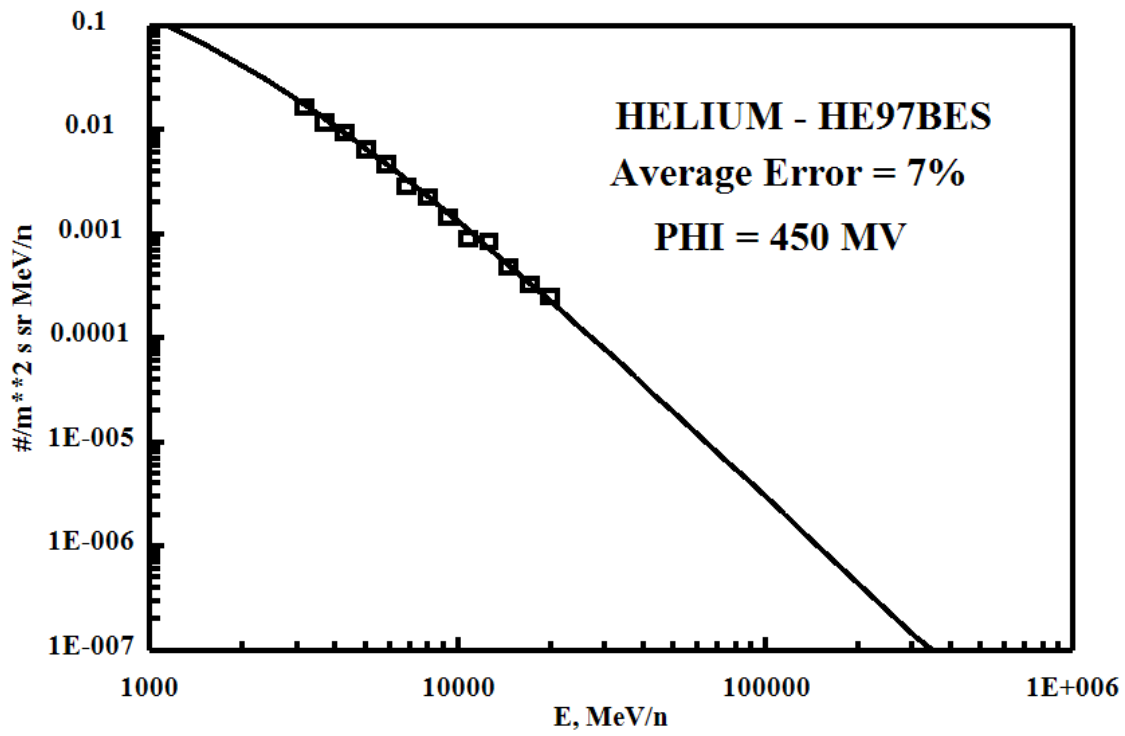
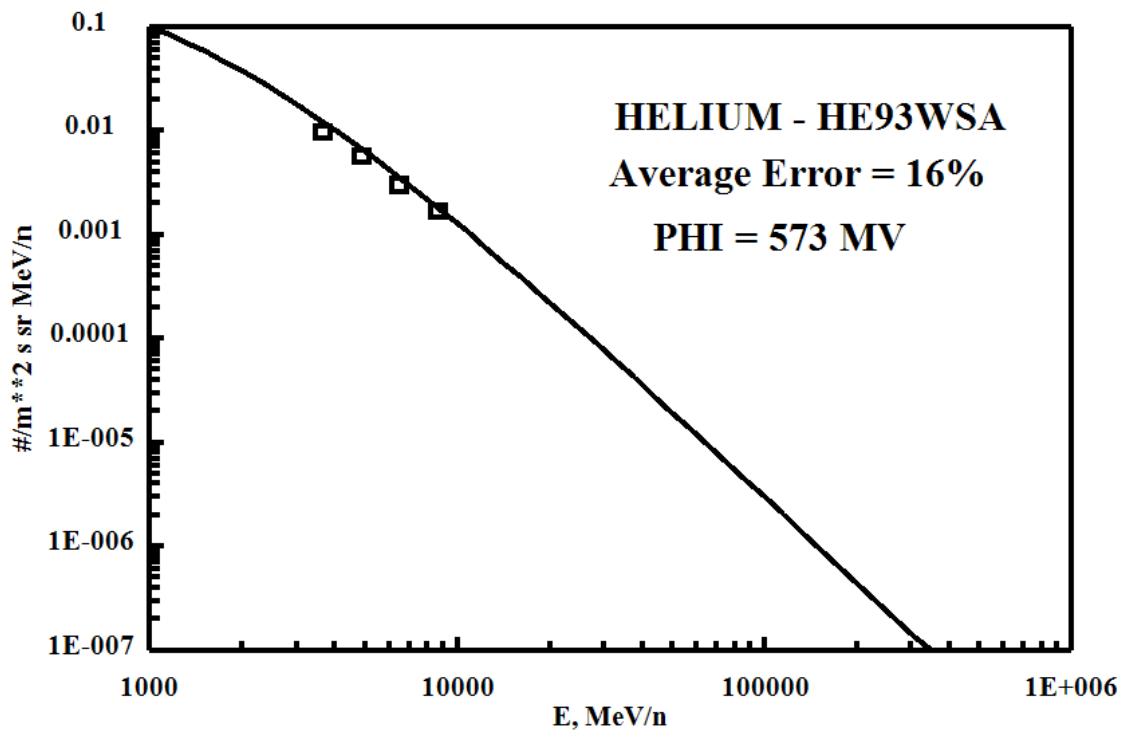


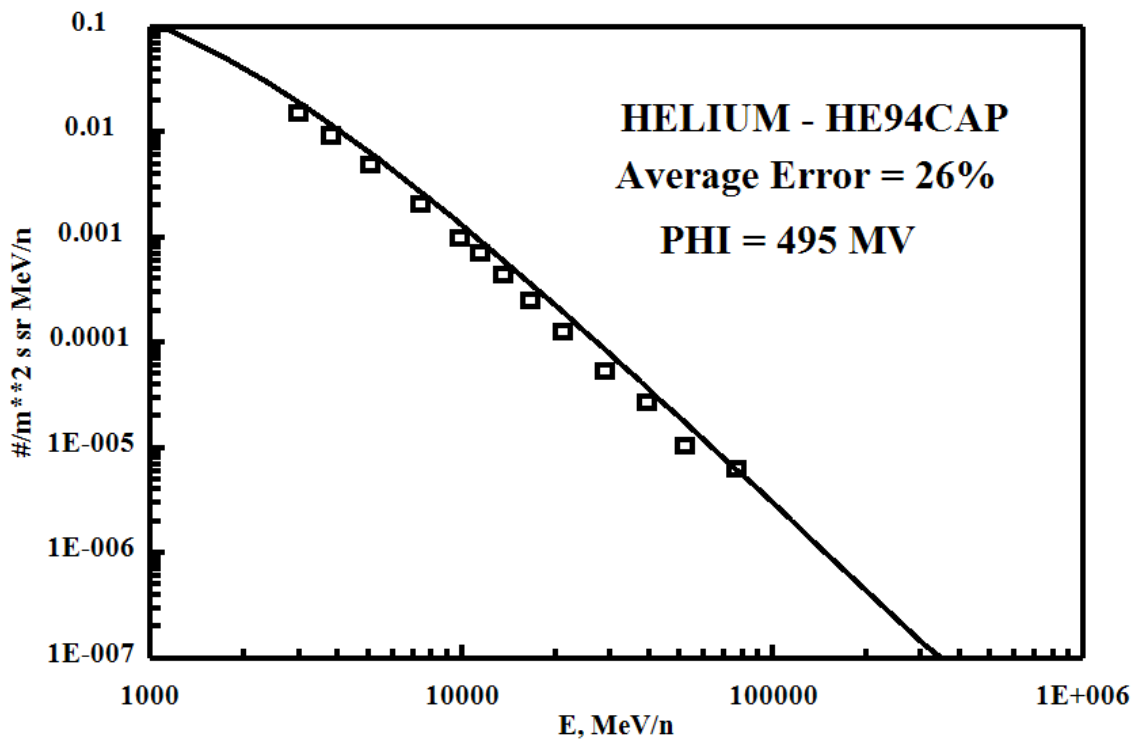
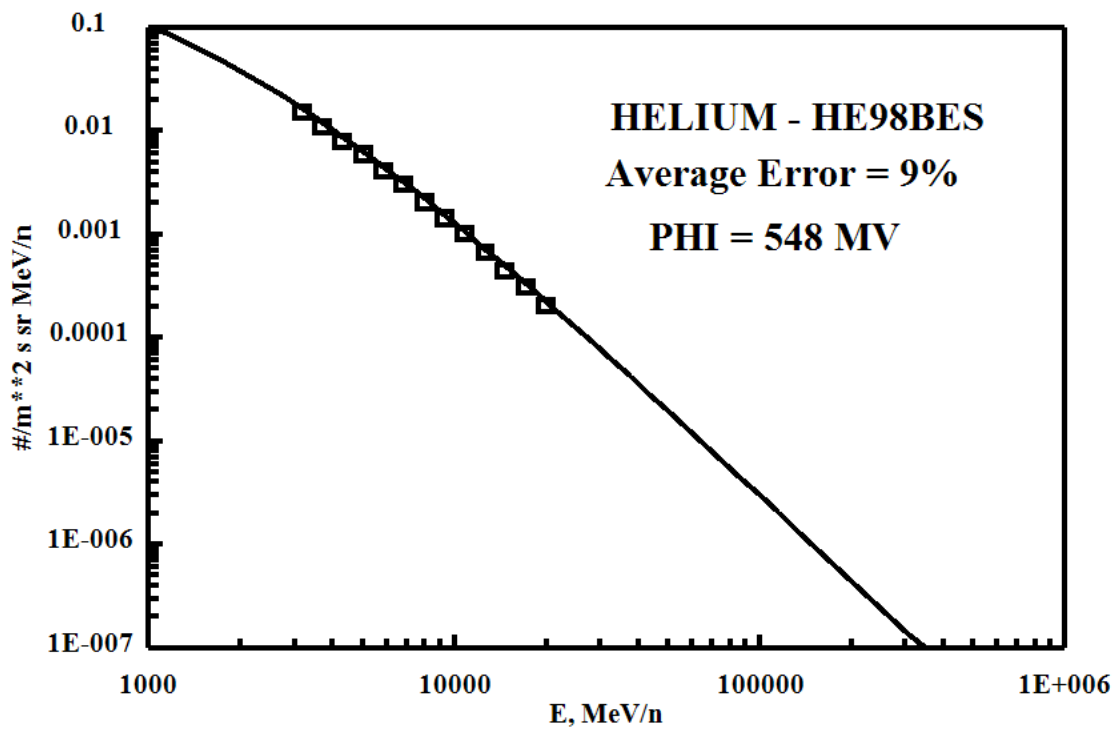
HELIUM - High Energy, Solar Minimum

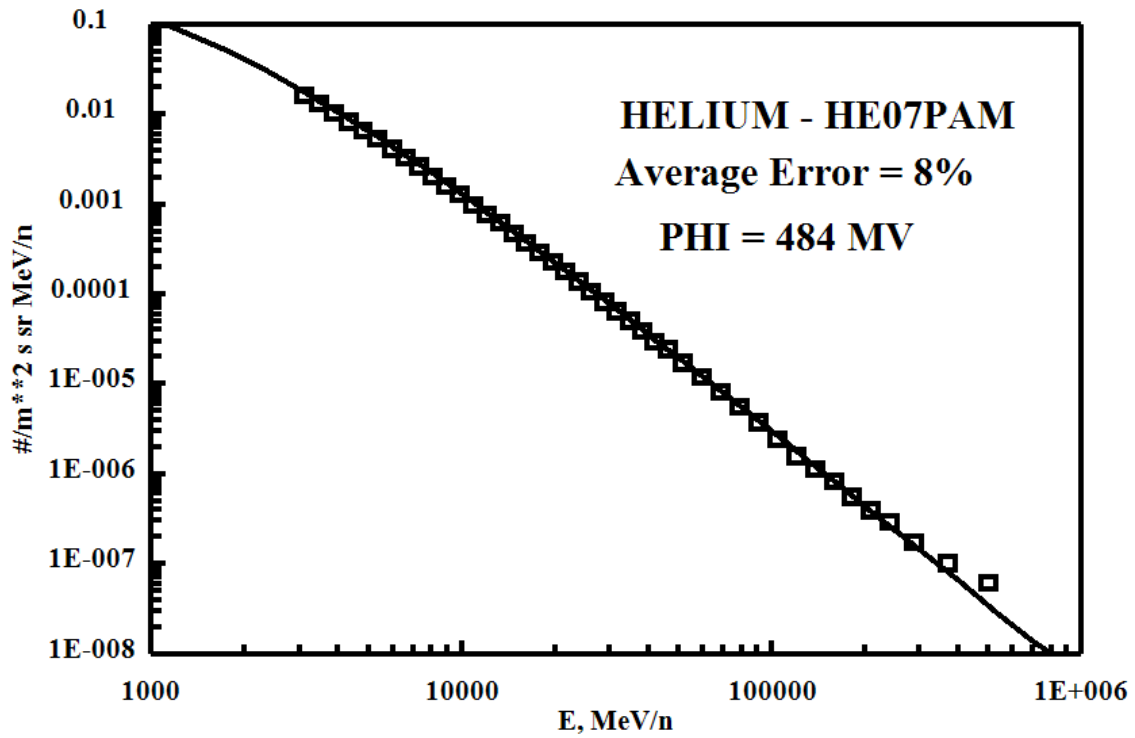
Files Used (Arbitrary 1's)

FILE	DATE	PHI (MV)	ERROR=ABS (FLUX-DATA)
He66vRW.dat	1966.564	575.2775	17.96216
He93WSA.dat	1993.567	572.9689	15.66373
He97BES.dat	1997.570	449.6011	7.057961
He98BES.dat	1998.575	547.9679	8.550315
He94Cap.dat	1994.605	495.4308	26.45465
He07Pam.dat	2007.000	484.1927	7.836141
BO AVERAGE ERROR =			13.92083





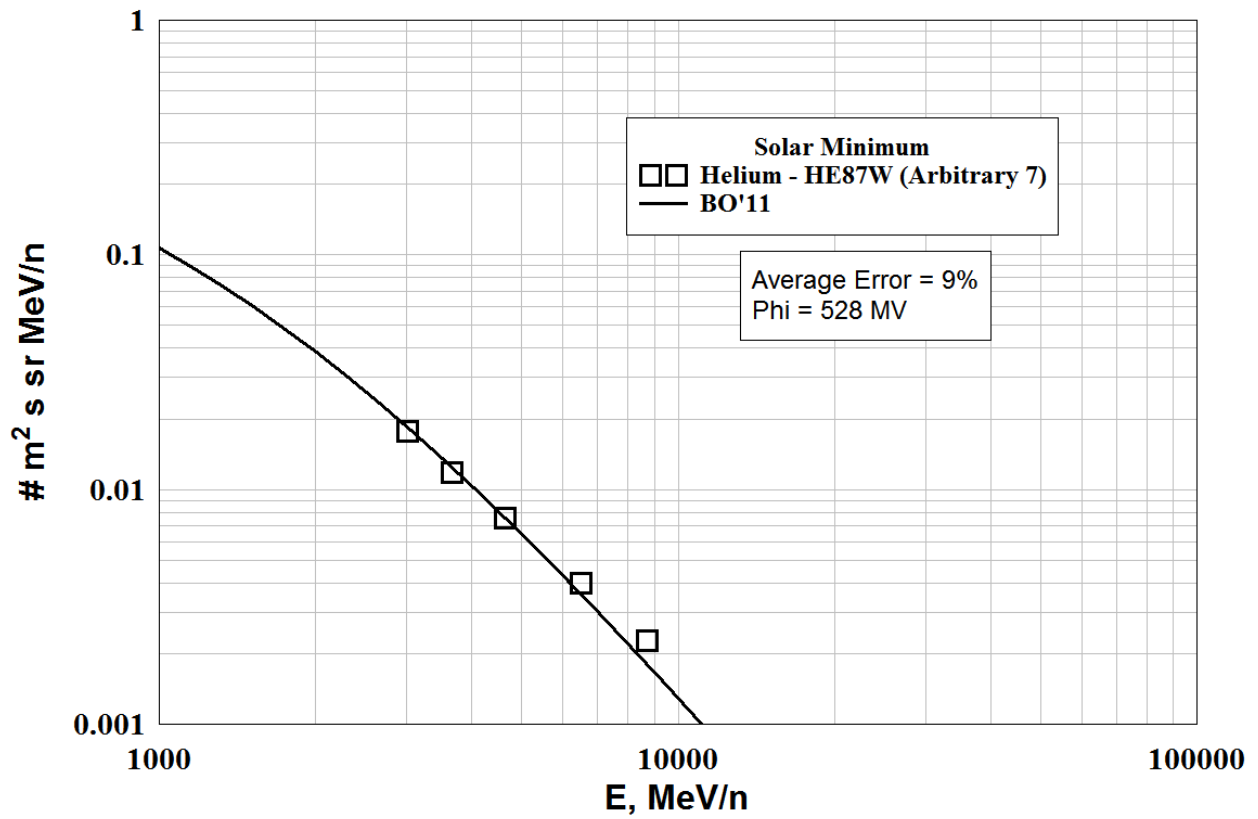
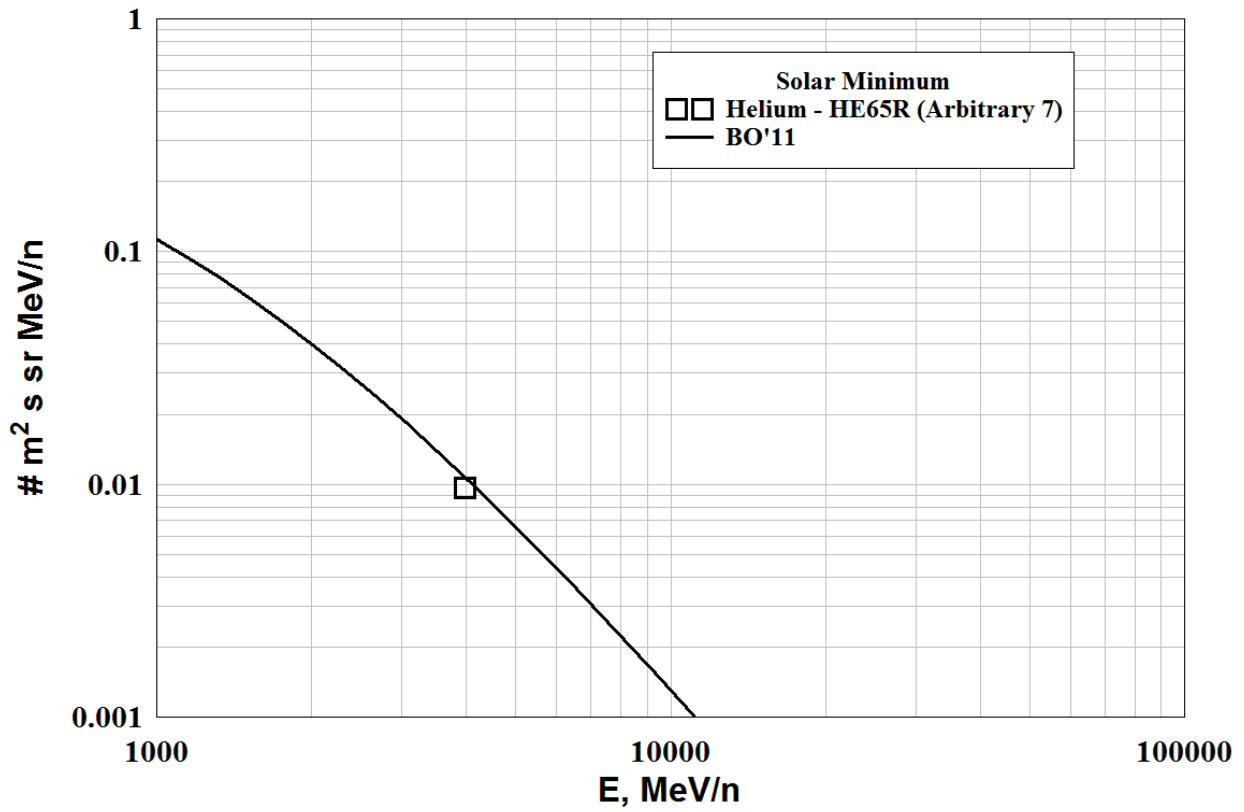


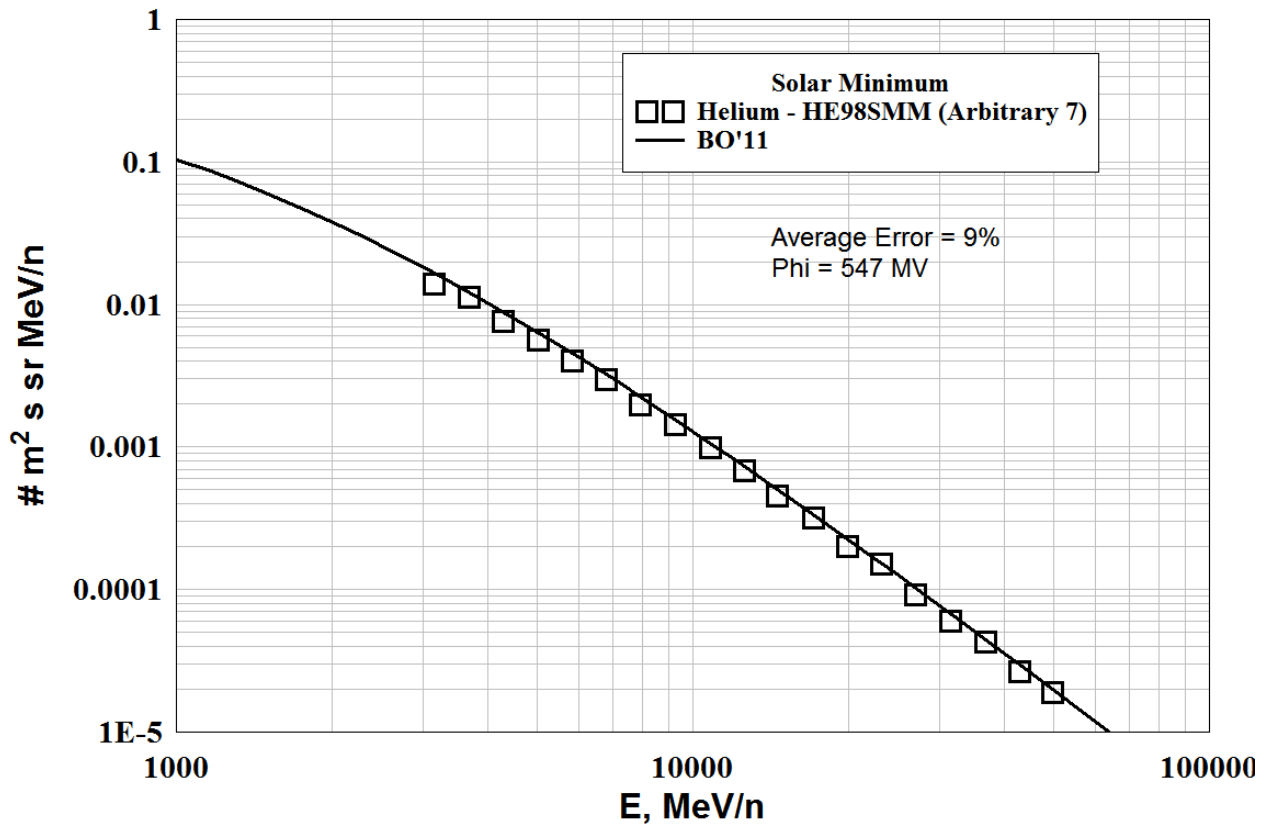
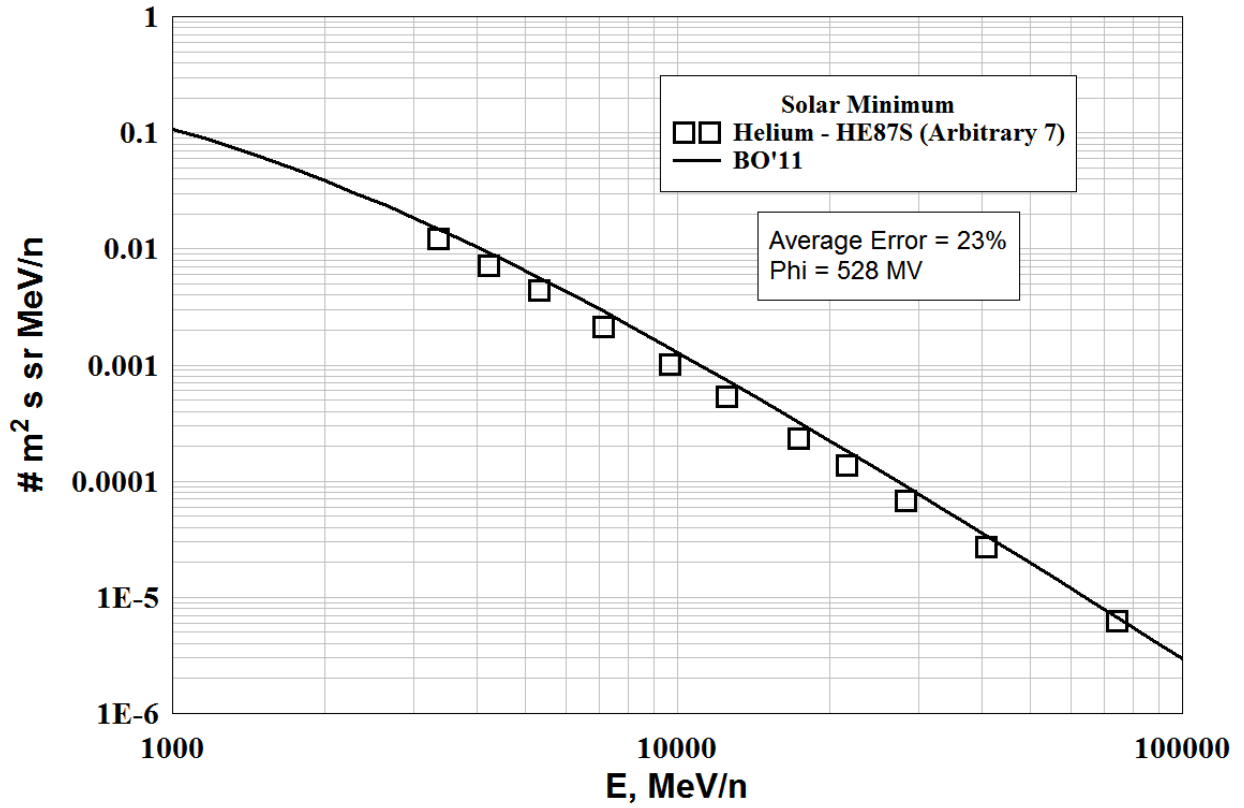


HELIUM - High Energy, Solar Minimum

Additional Files

FILE	DATE	PHI (MV)	ERROR=ABS (FLUX-DATA)
He65R.dat	1965.573	484.6338	10.29496
He87W.dat	1987.641	528.4525	9.036066
He87S.dat	1987.638	527.9987	22.94393
He98SMM.dat	1998.567	546.7391	9.349790
BO AVERAGE ERROR =			12.90619



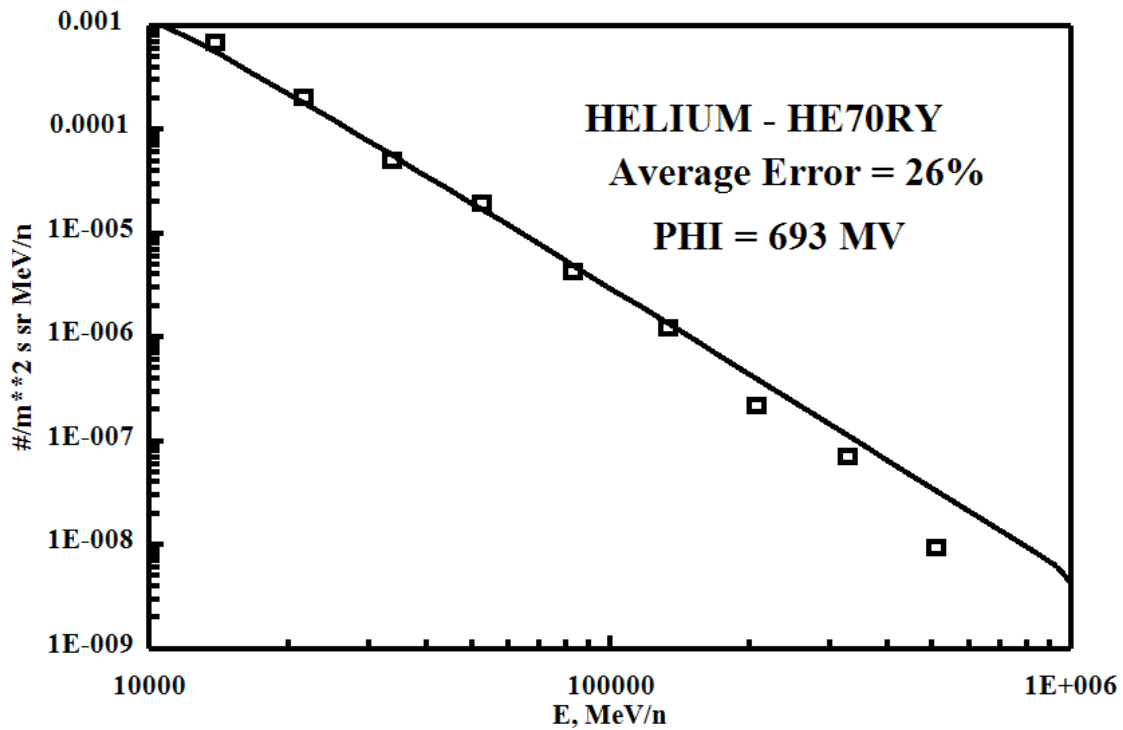


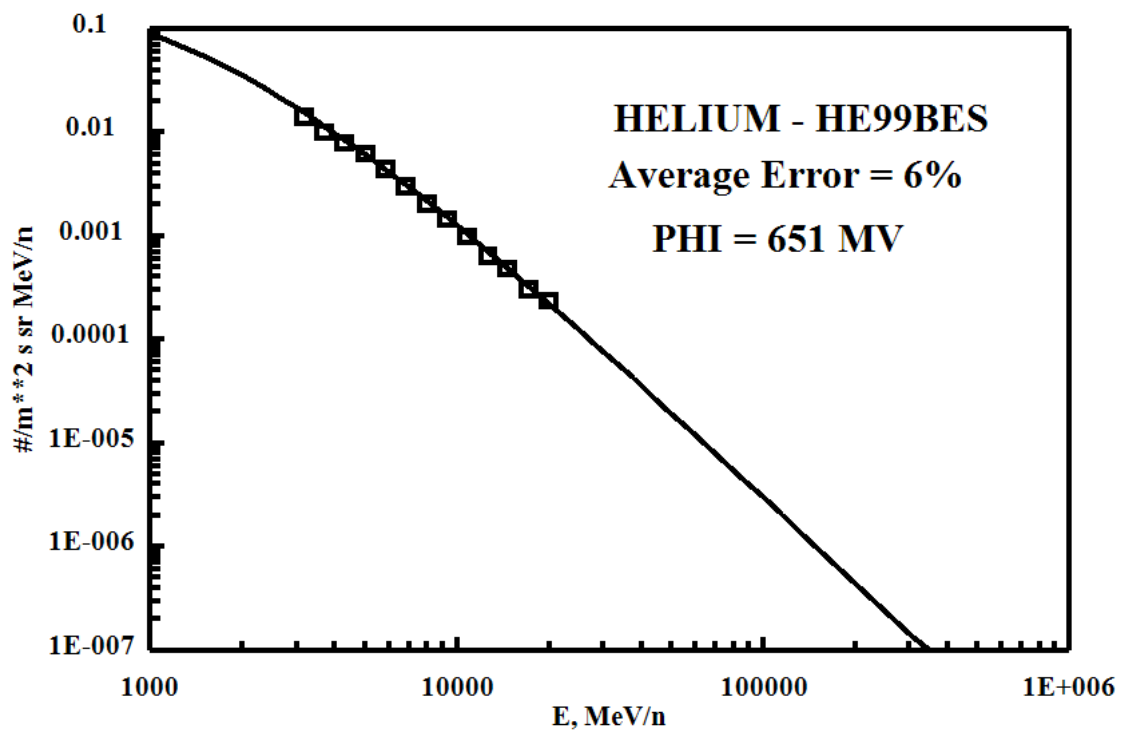
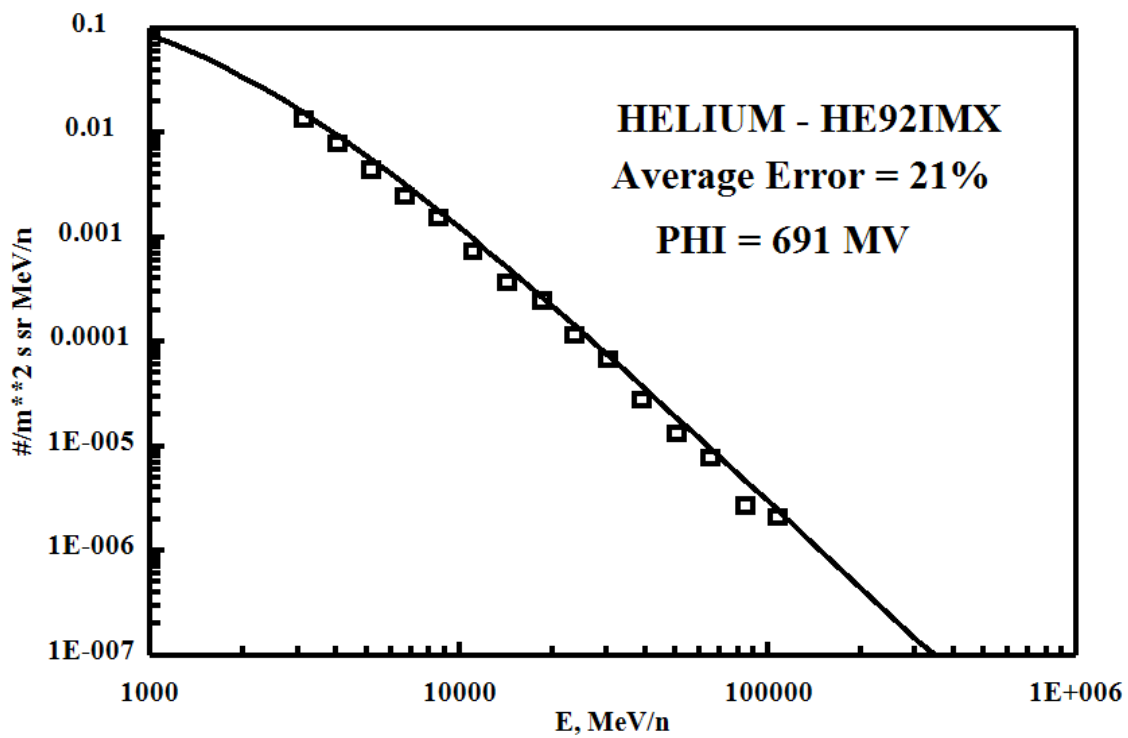
HELIUM - High Energy, Solar Maximum

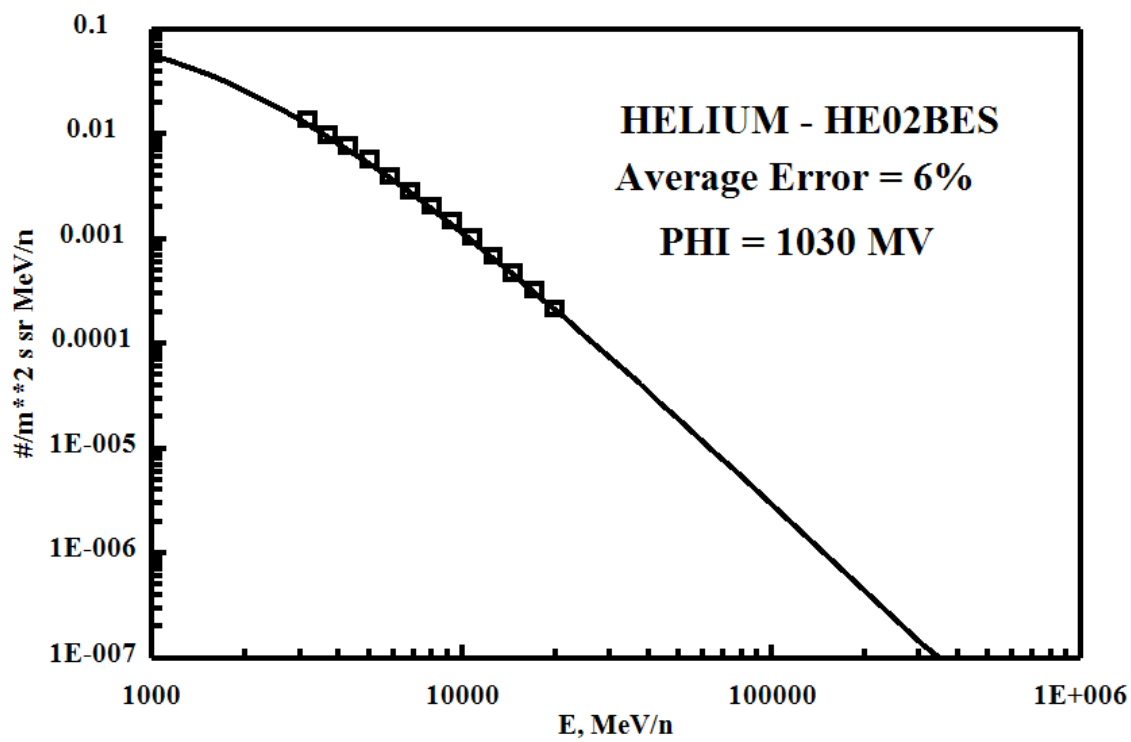
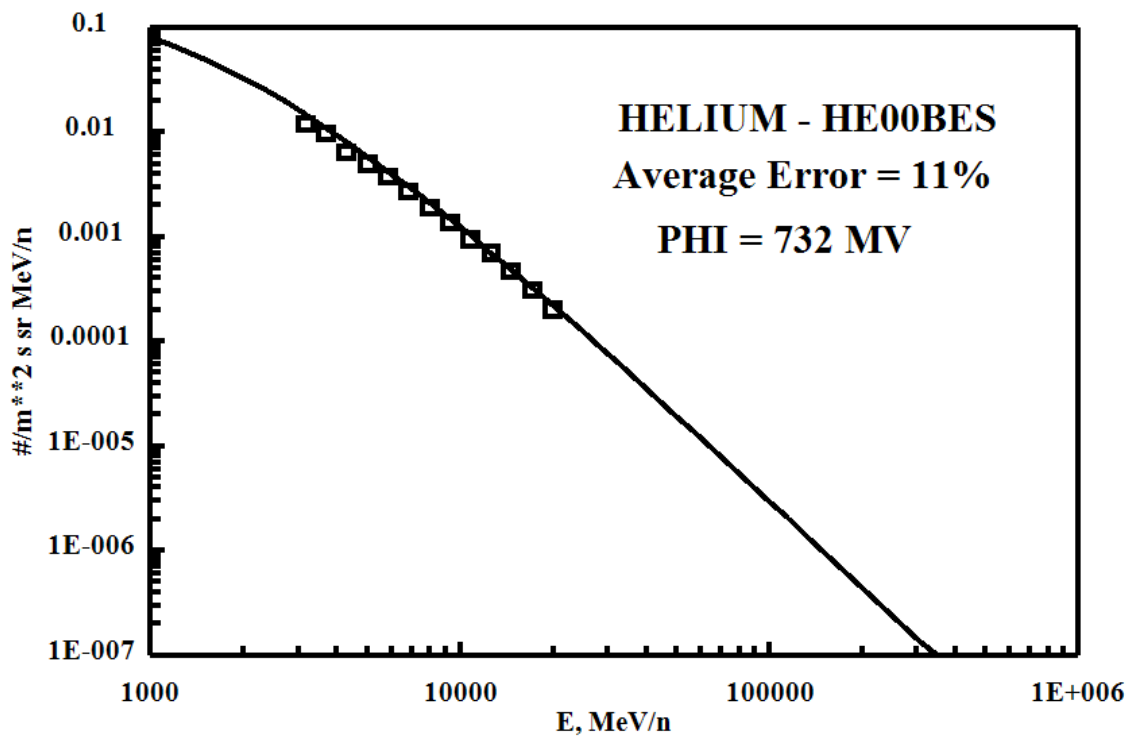
Files Used (Arbitrary 1's)

FILE	DATE	PHI (MV)	ERROR=ABS (FLUX-DATA)
He70Ry.dat	1970.874	692.8234	26.41482
He92IMX.dat	1992.540	691.0951	20.73852
He99BES.dat	1999.611	650.9333	5.717887
He00BES.dat	2000.608	731.5487	10.60942
He02BES.dat	2002.600	1029.817	6.292054

BO AVERAGE ERROR = 13.95454



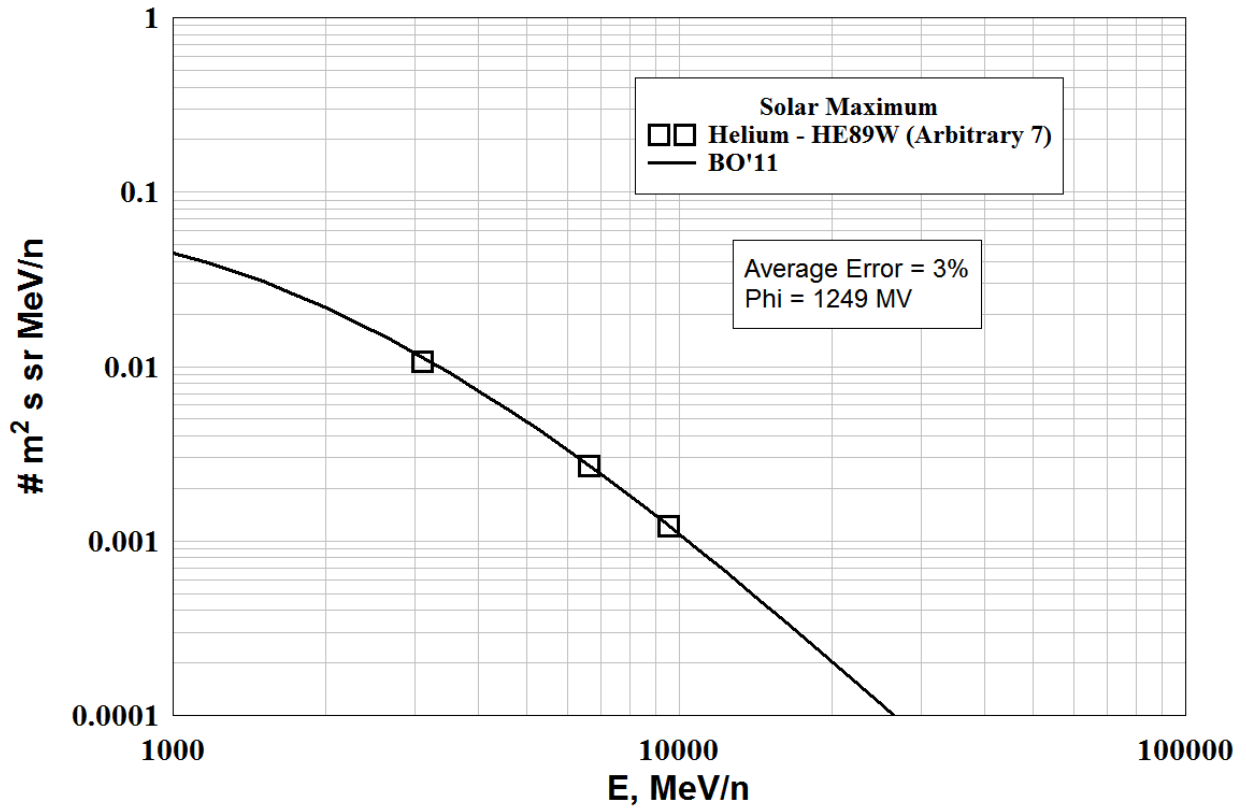




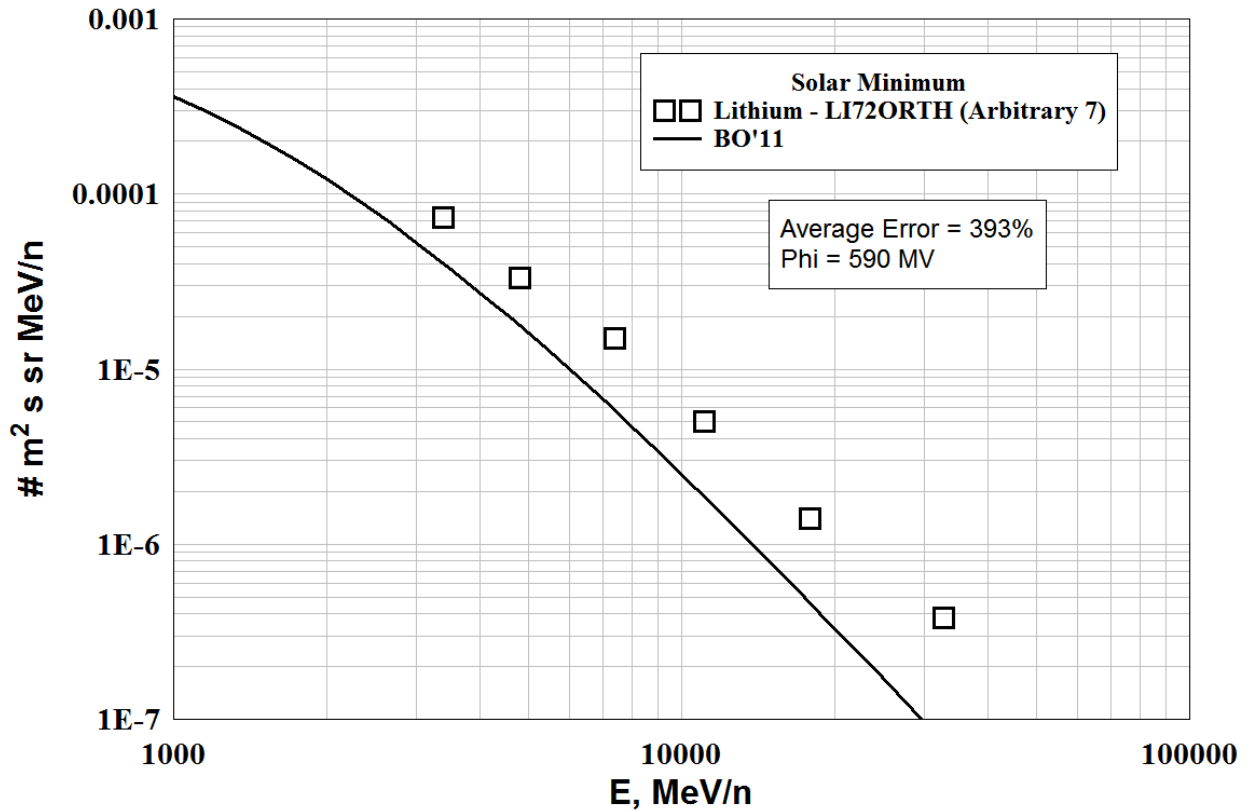
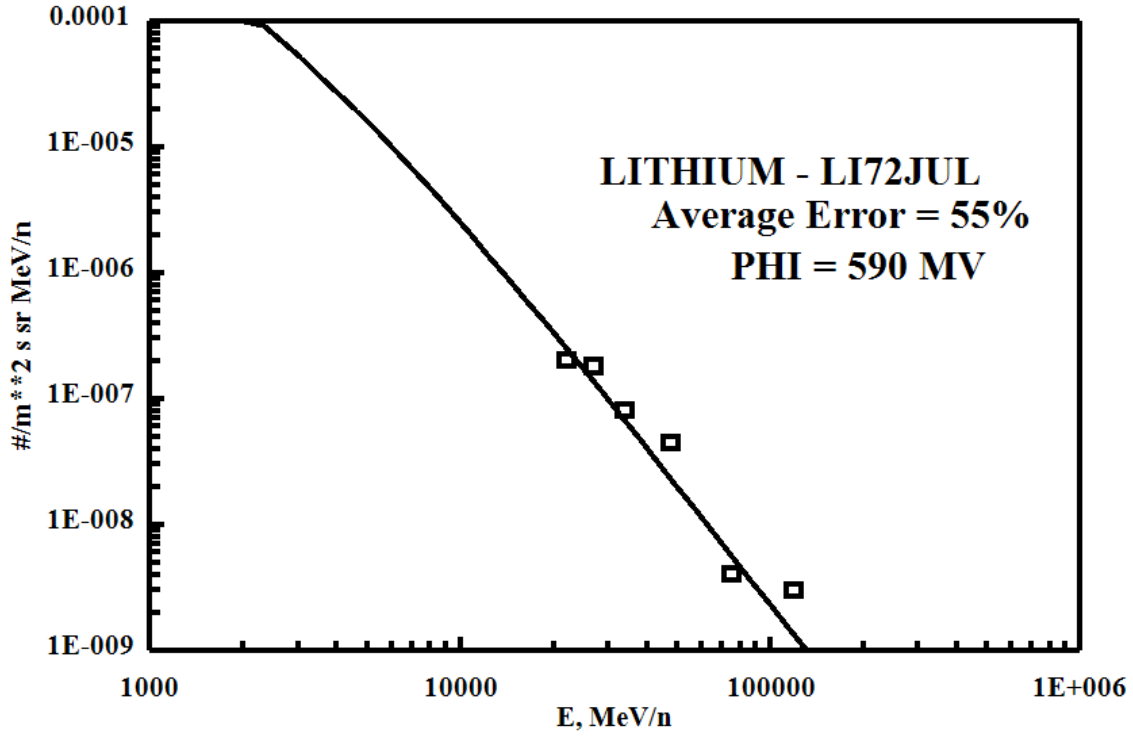
HELIUM - High Energy, Solar Maximum

Files Rejected - (Arbitrary 7's)

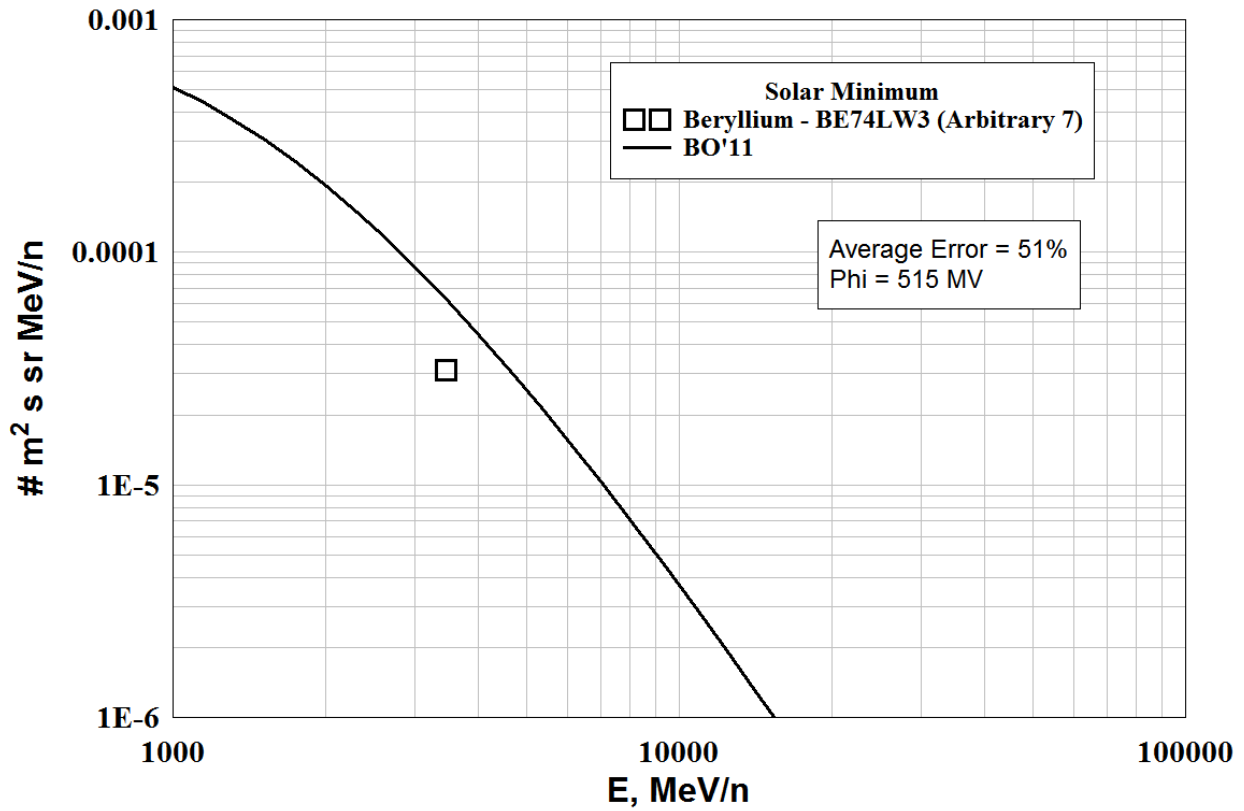
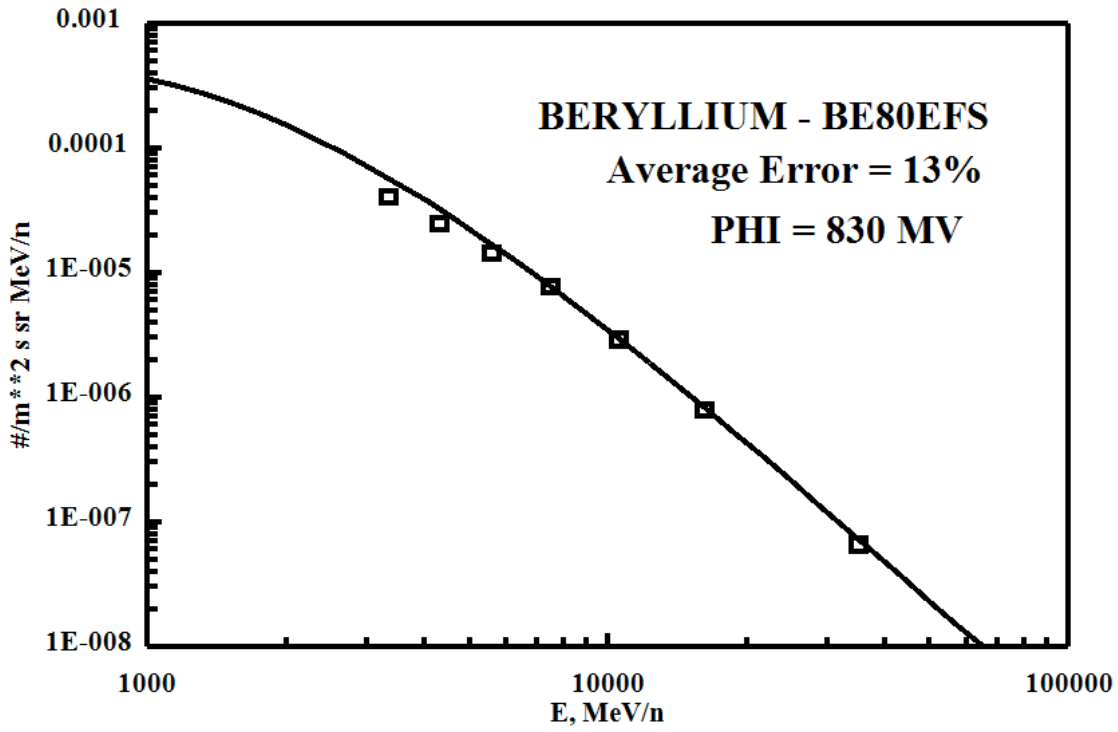
FILE	DATE	PHI (MV)	ERROR=ABS (FLUX-DATA)
He89W.dat	1989.682	1248.804	2.722097
BO AVERAGE ERROR =			2.722097

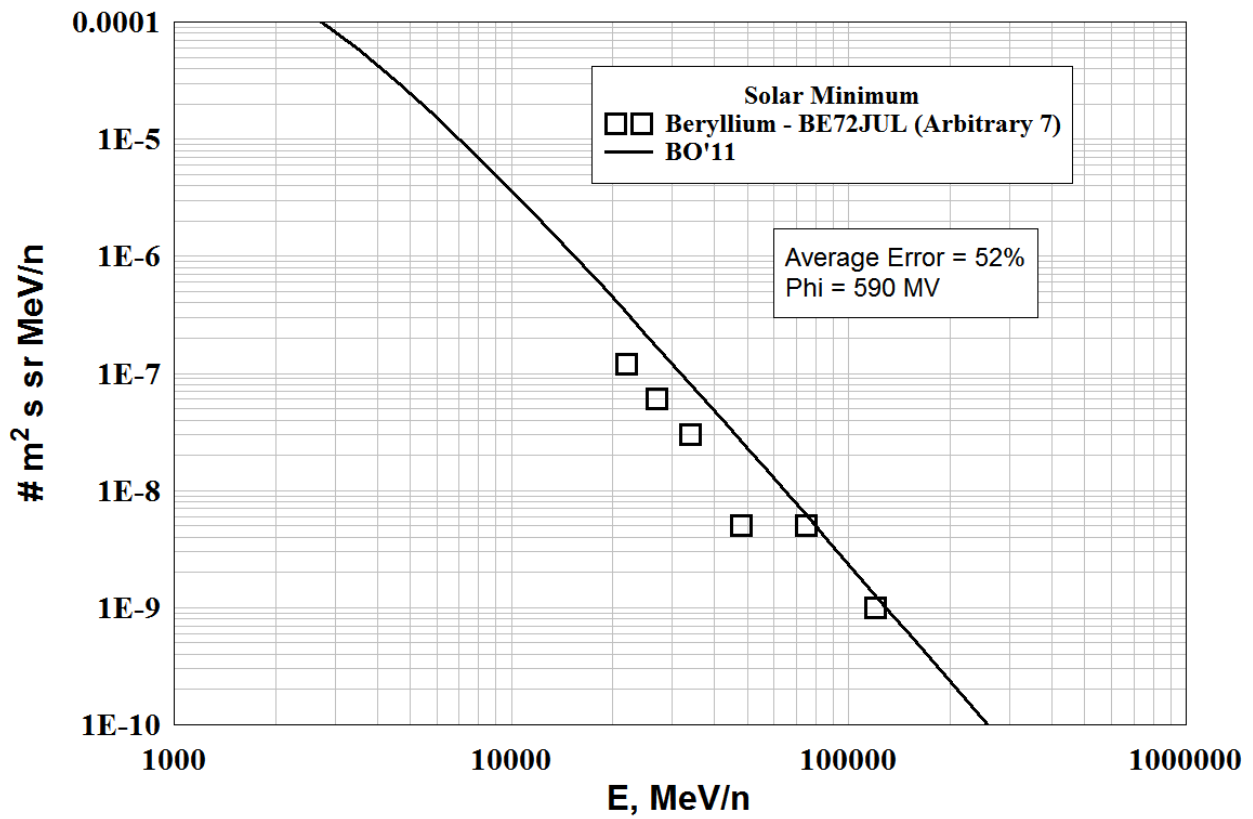
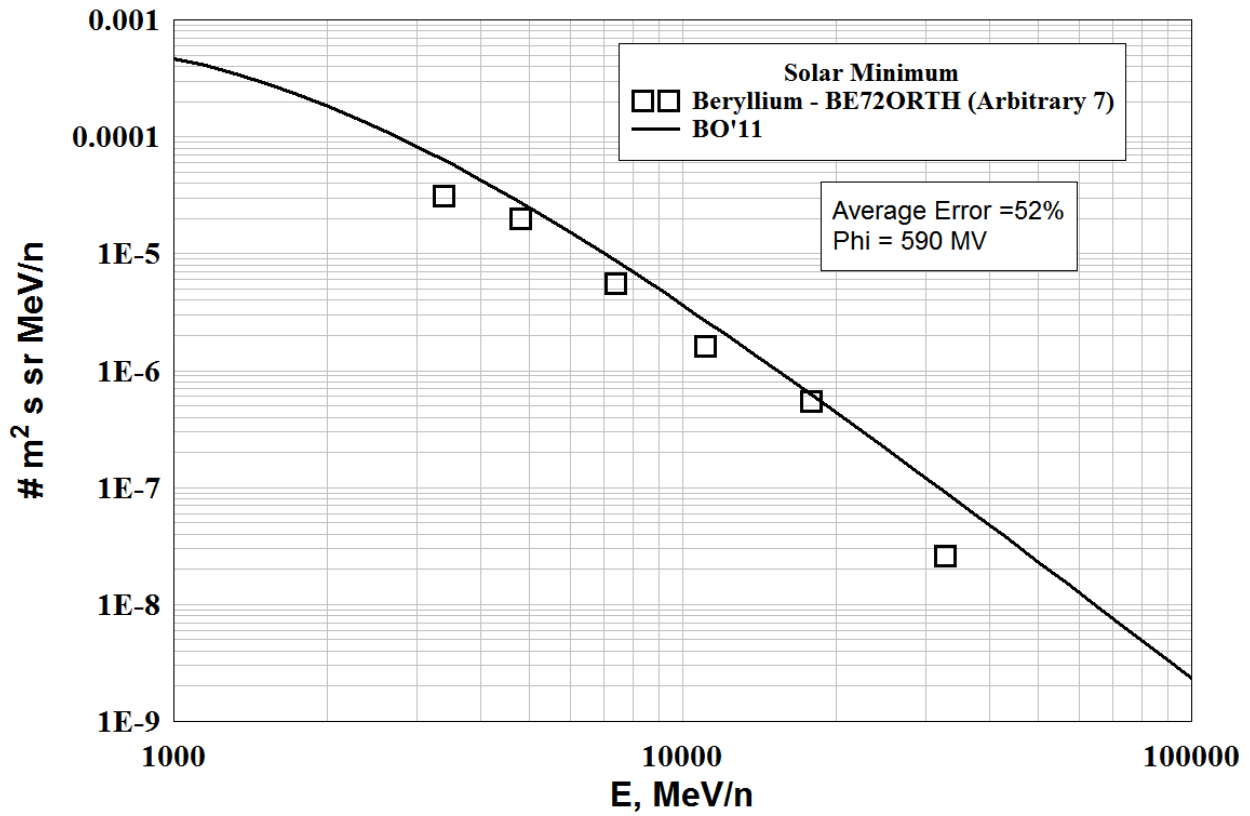


LITHIUM - High Energy

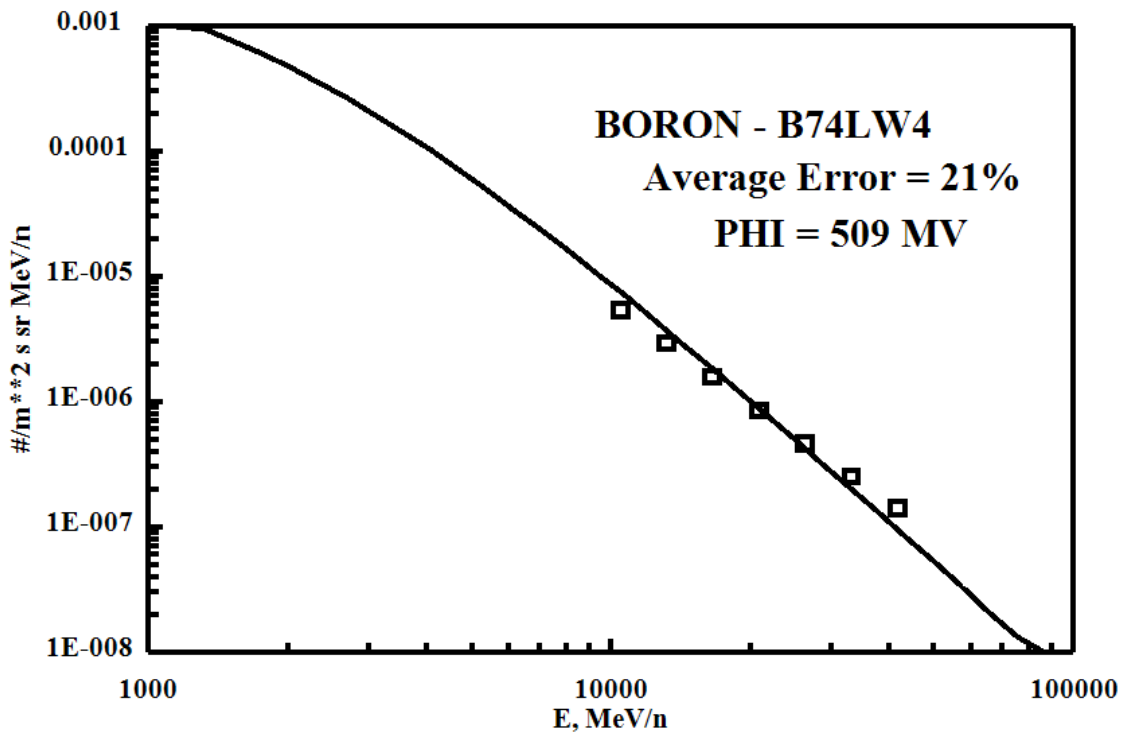
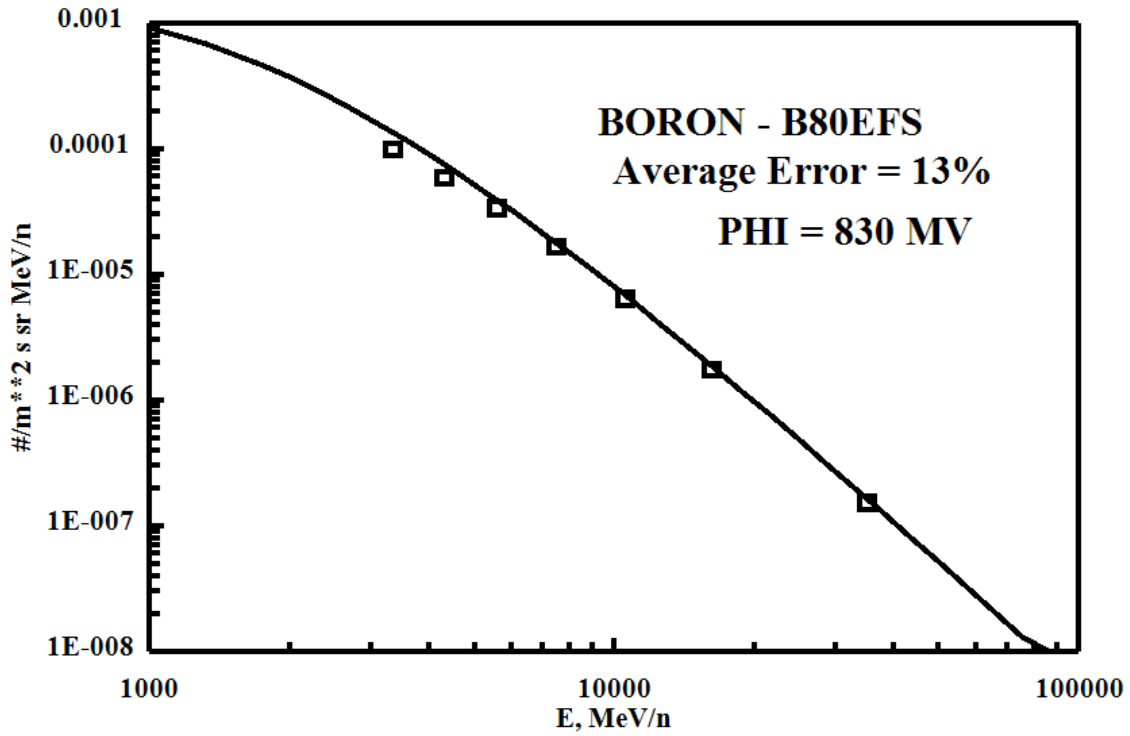


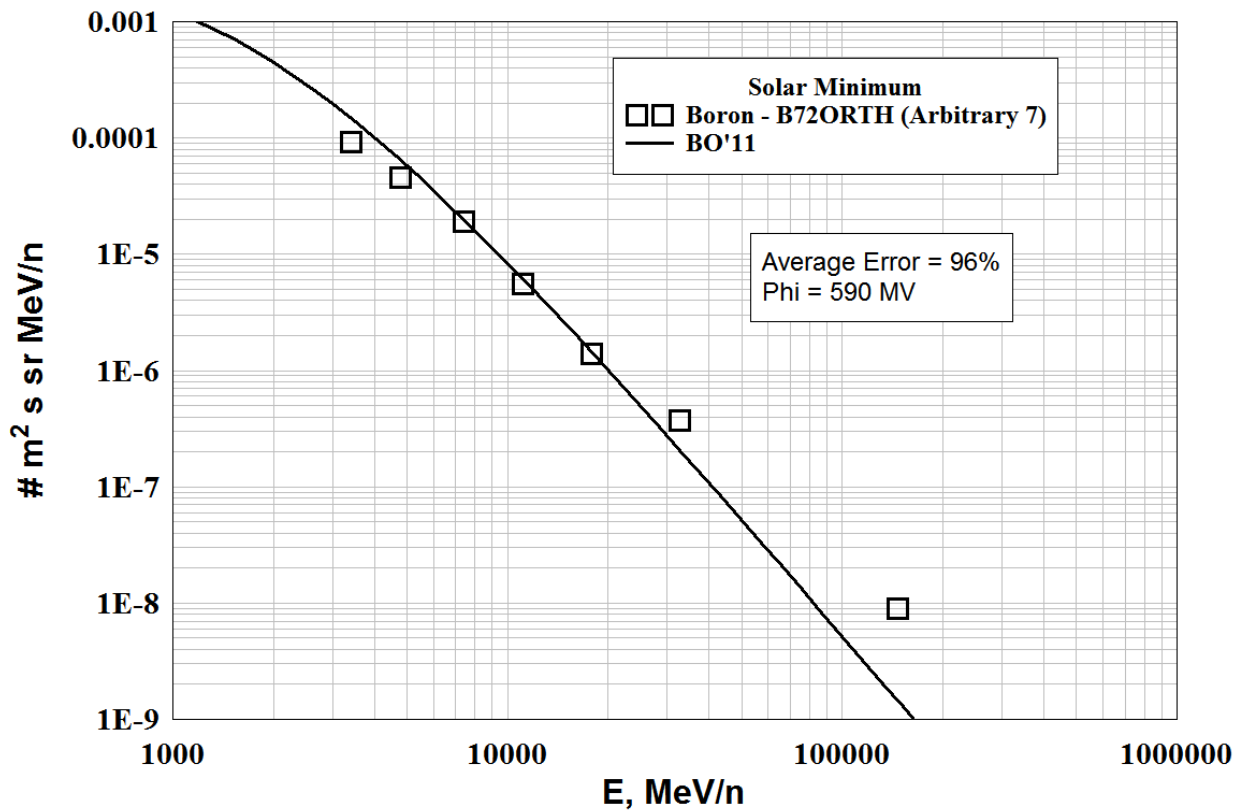
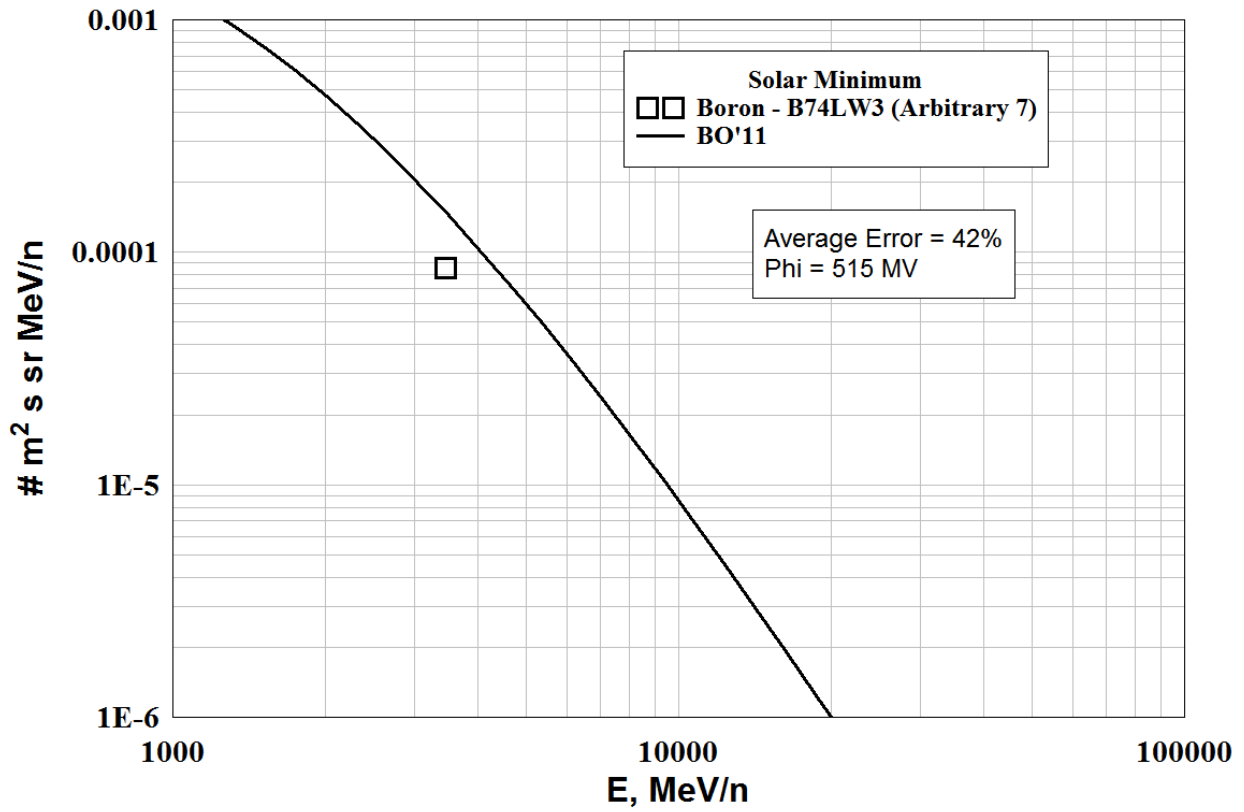
BERYLLIUM - High Energy

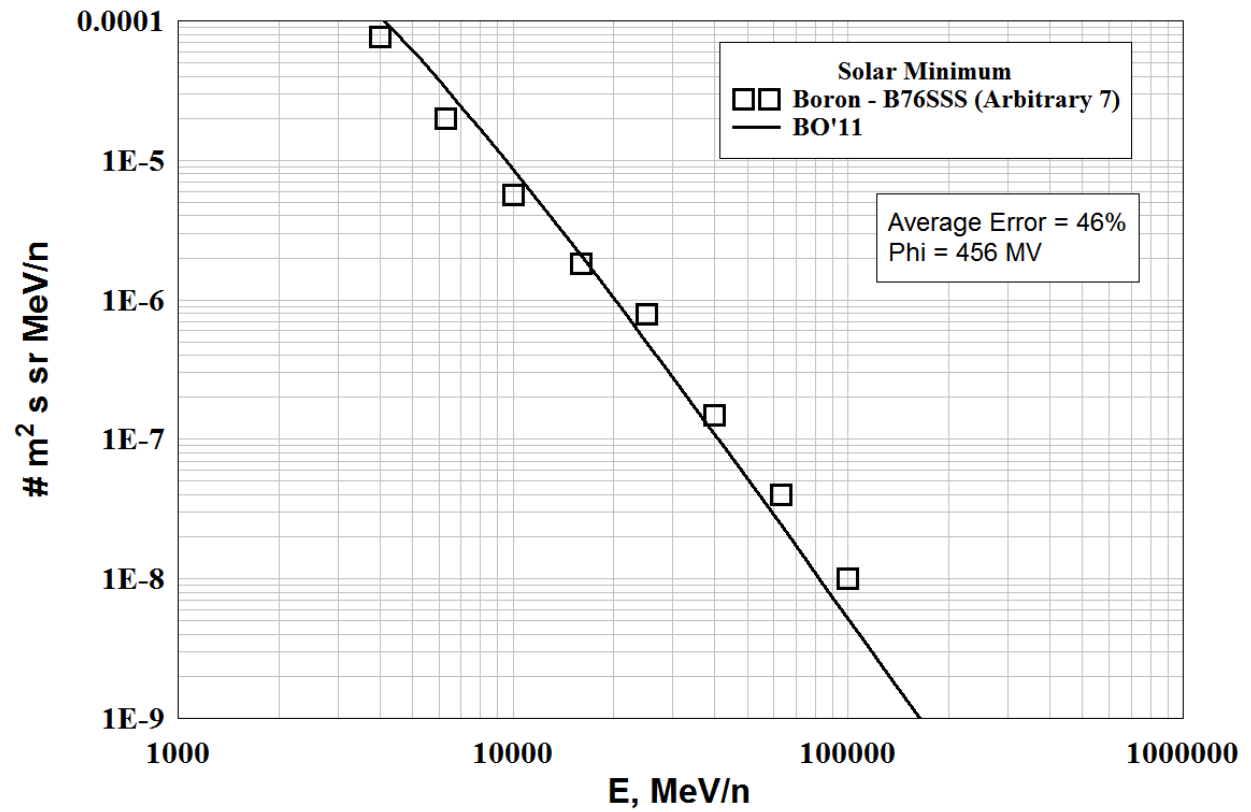
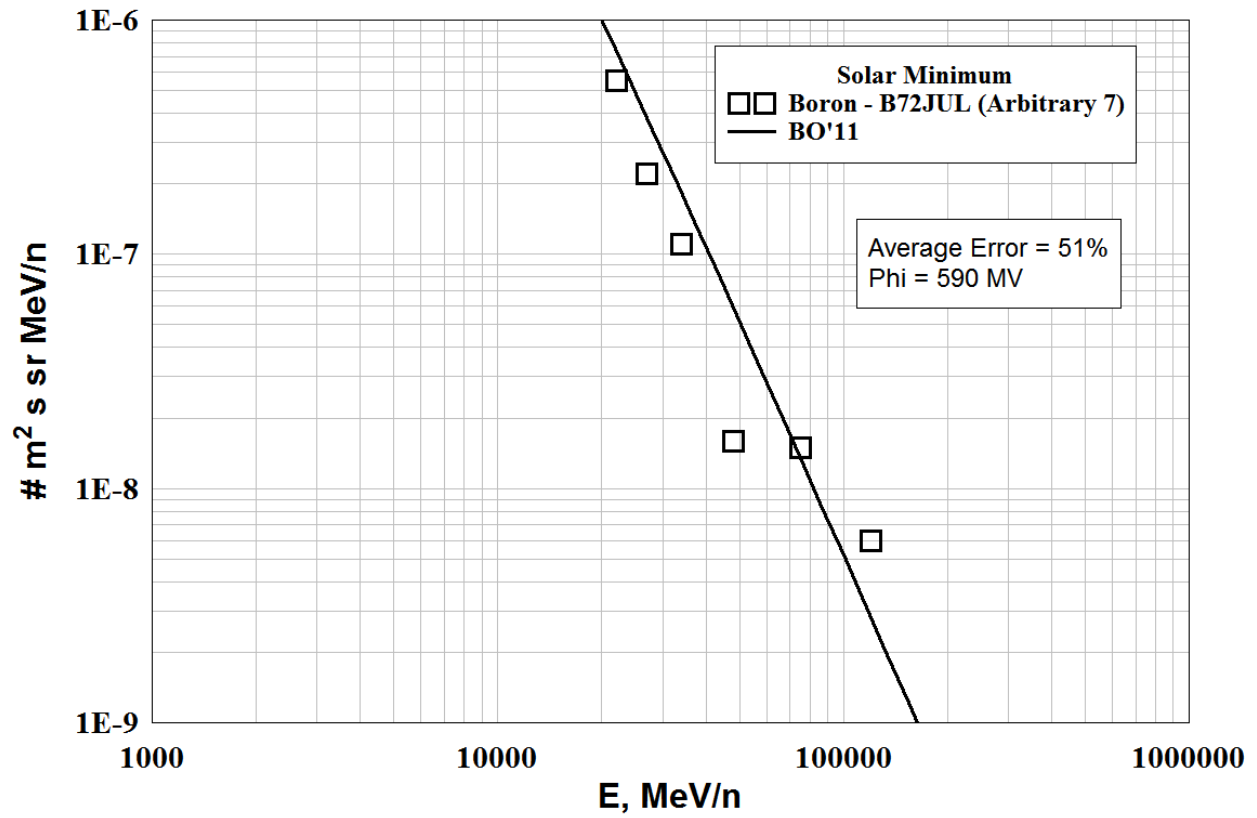


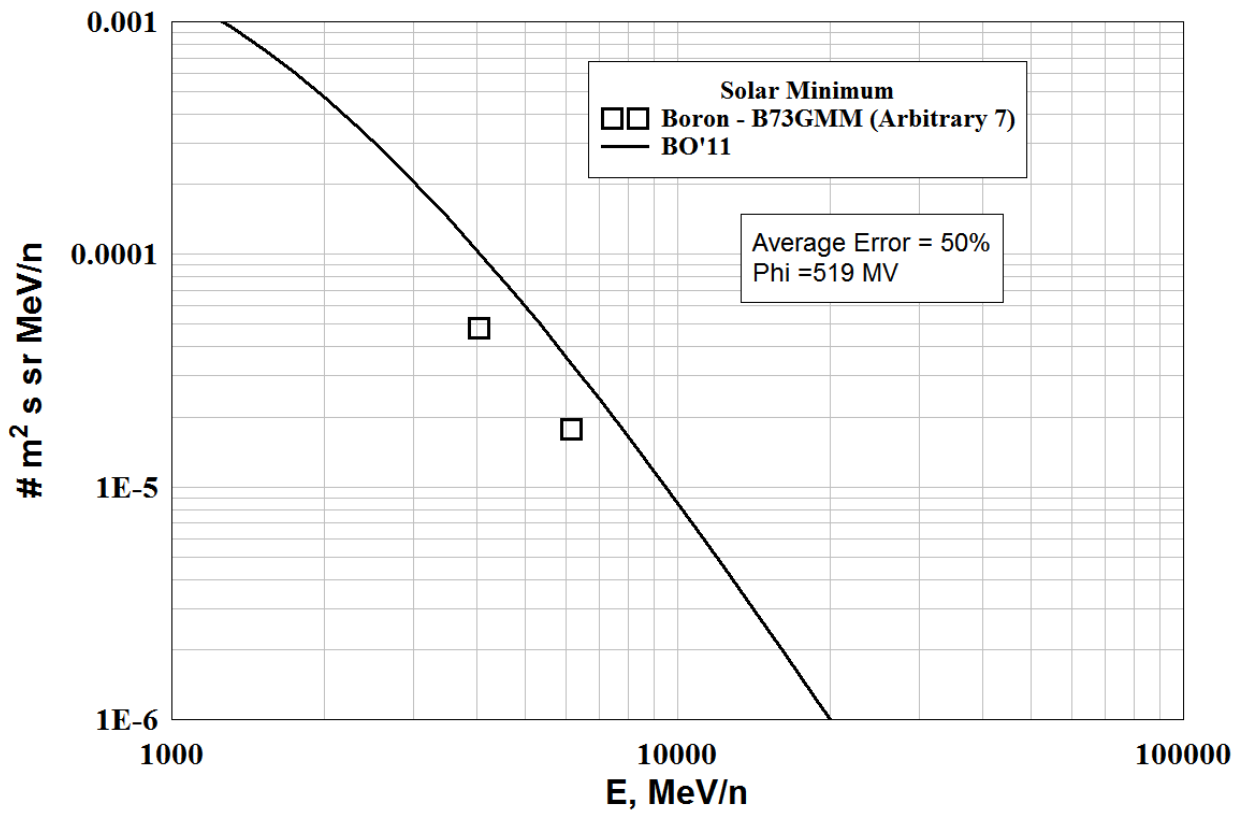
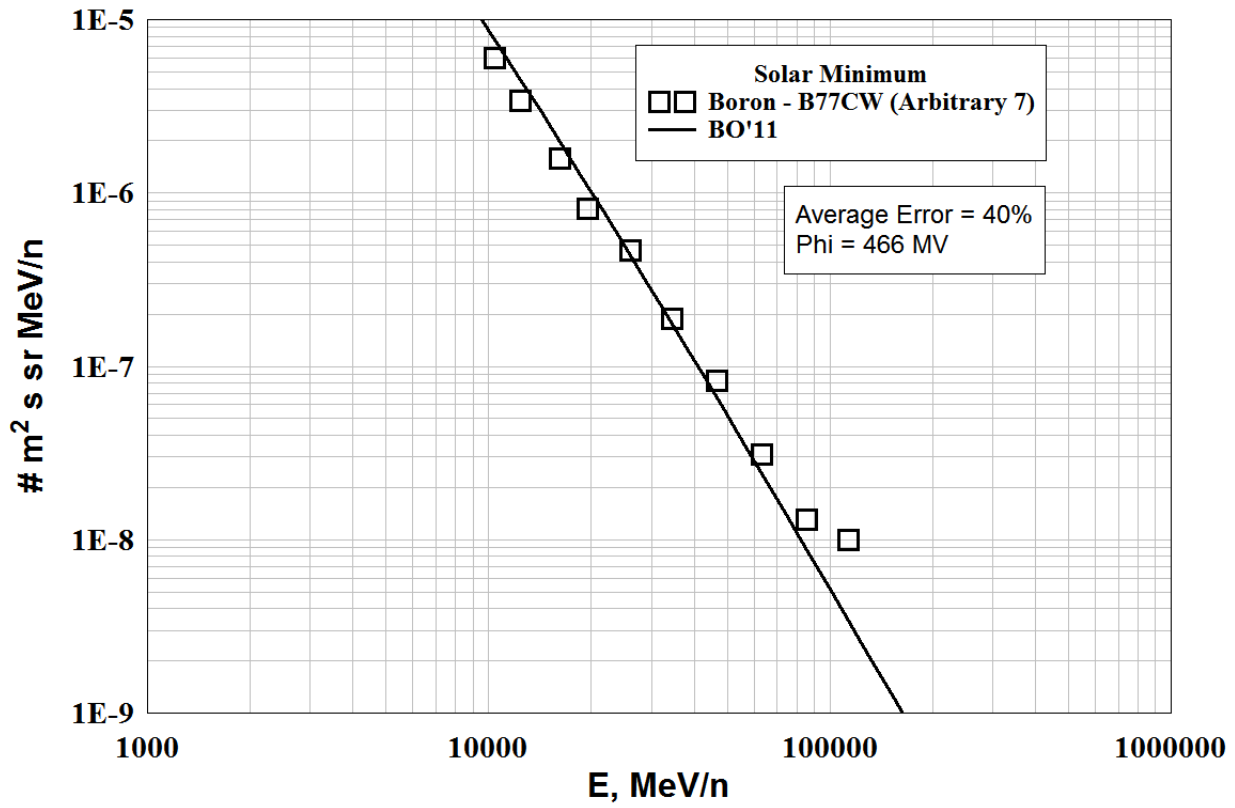


BORON - High Energy









CARBON - High Energy, Solar Minimum

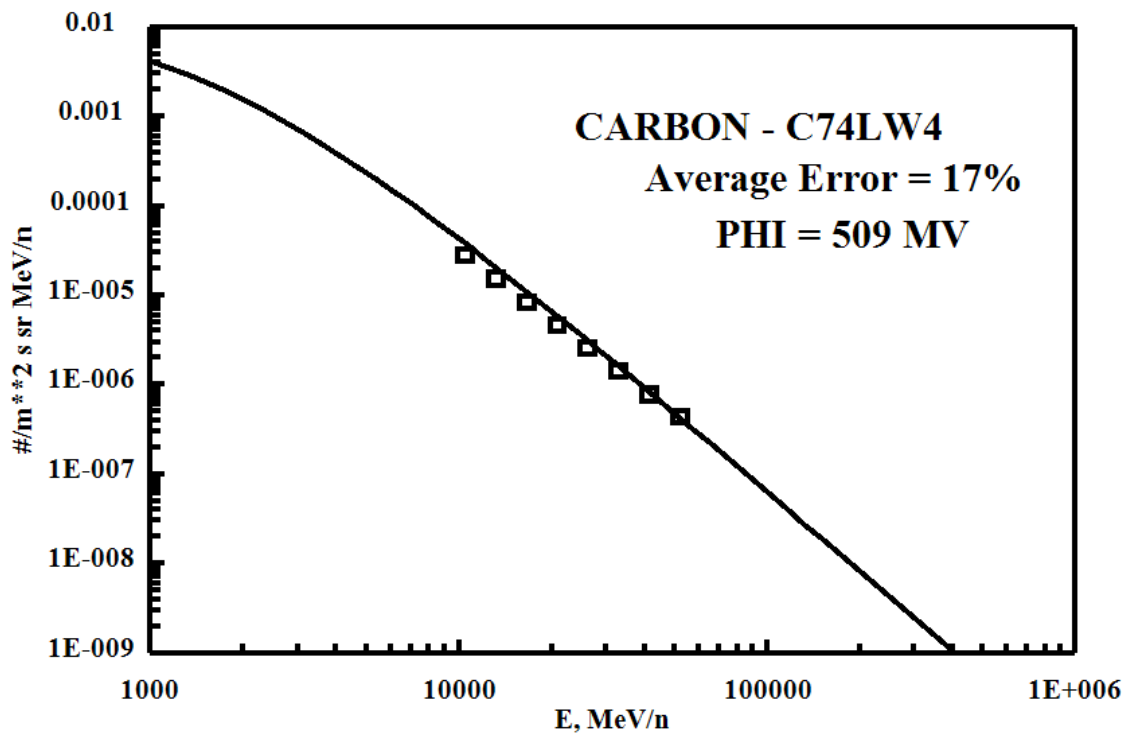
Files Used (Arbitrary 1's)

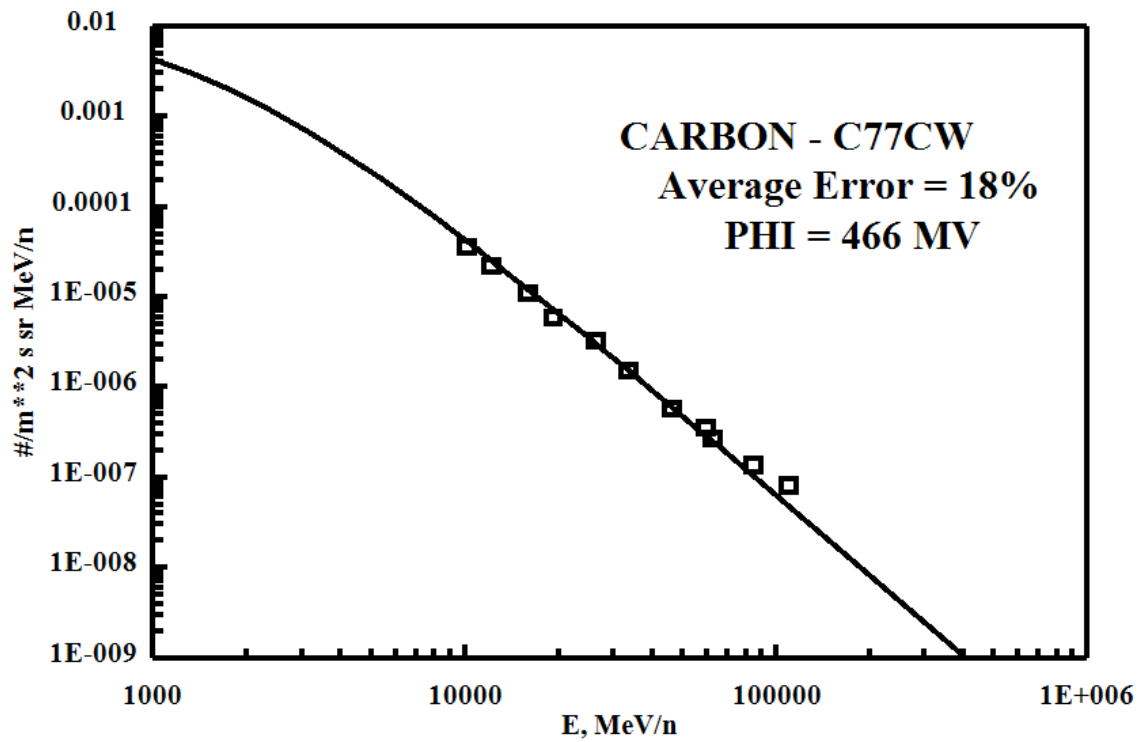
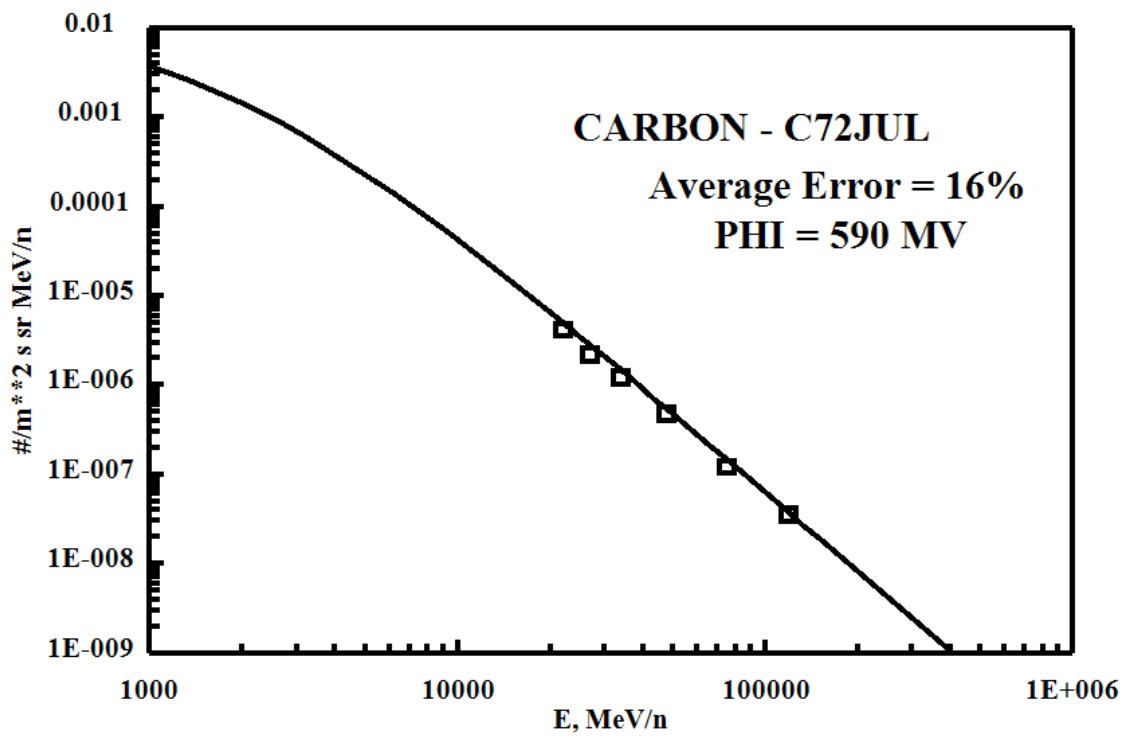
FILE	DATE	PHI (MV)	ERROR=ABS (FLUX-DATA)
C74LW4.dat	1974.726	509.2871	16.84722
C72Jul.dat	1972.751	590.1960	15.72787
C77CW.dat	1976.000	465.6418	18.20770
BO AVERAGE ERROR =			16.92760

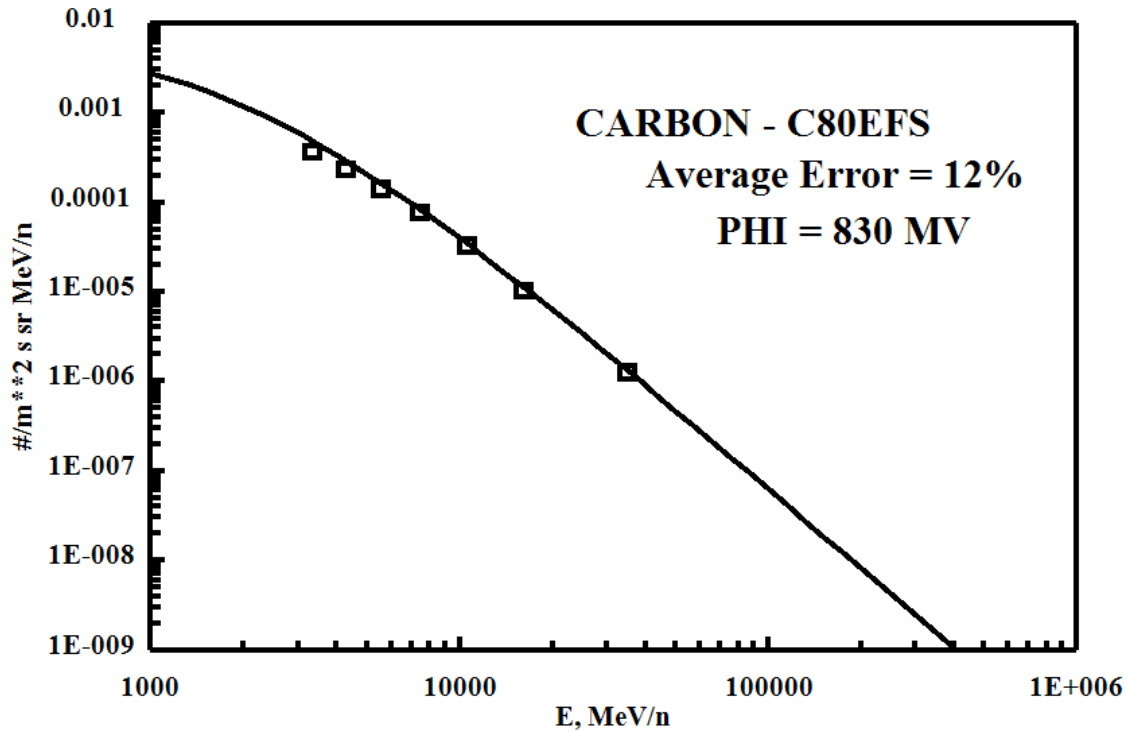
CARBON - High Energy, Solar Maximum

Files Used (Arbitrary 1's)

FILE	DATE	PHI (MV)	ERROR=ABS (FLUX-DATA)
C80EFS.dat	1979.795	830.2713	12.06566
BO AVERAGE ERROR =			12.06566







CARBON - High Energy, Solar Minimum

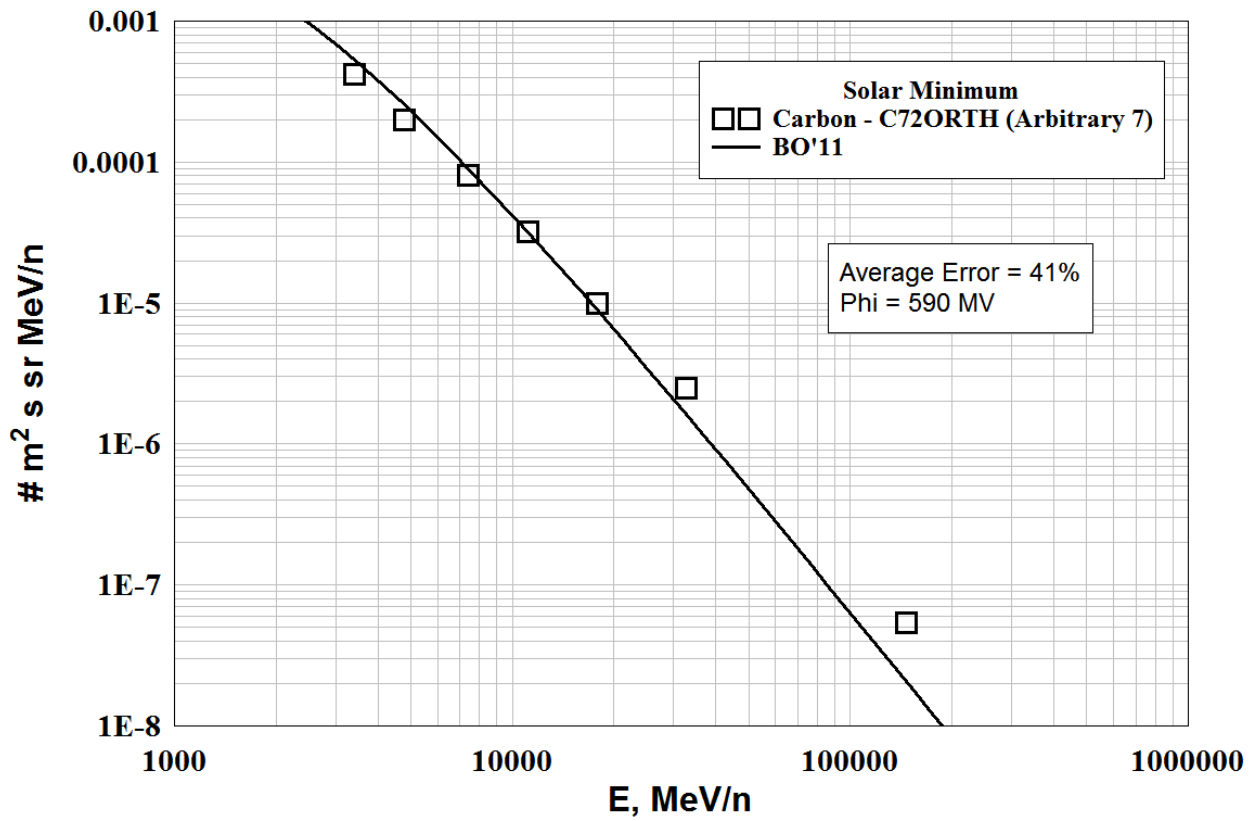
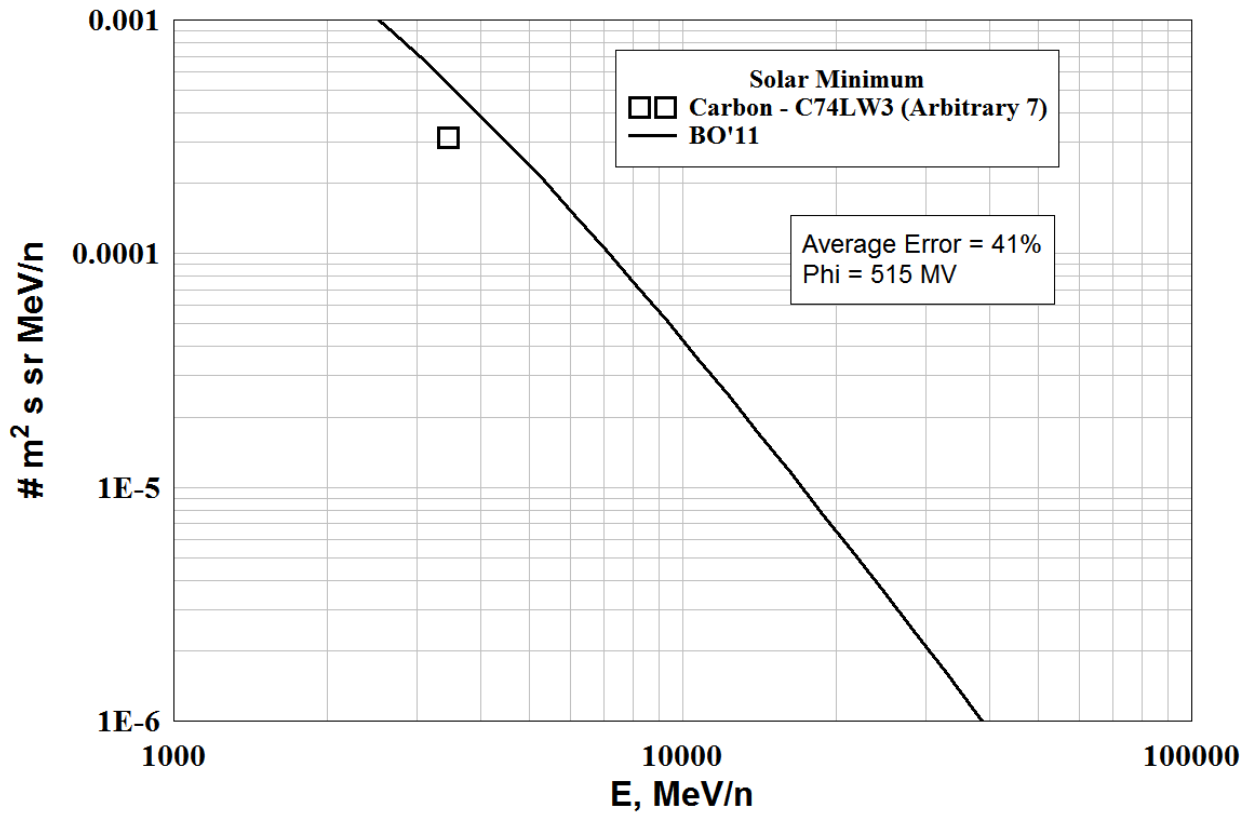
Files Rejected - (Arbitrary 7's)

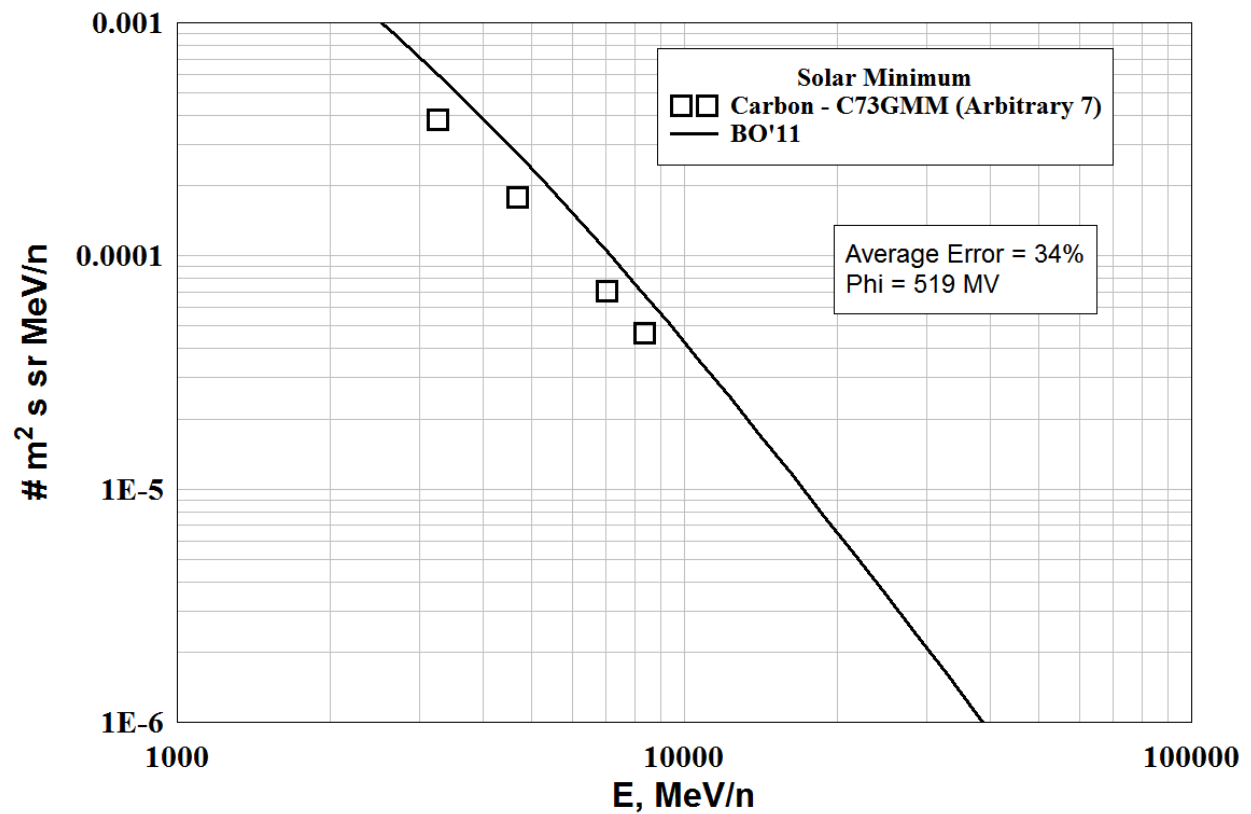
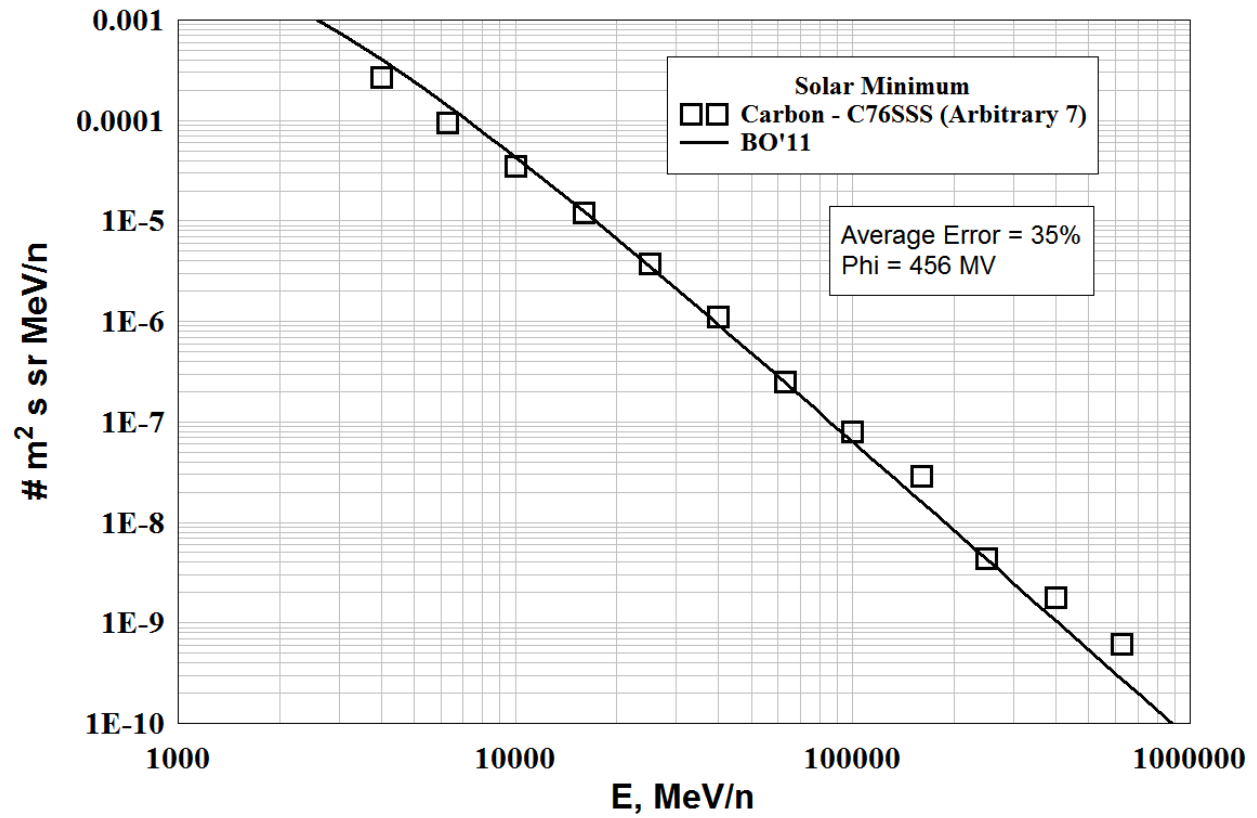
FILE	DATE	PHI (MV)	ERROR=ABS (FLUX-DATA)
C74LW3.dat	1974.553	515.0297	41.14713
C72Orth.dat	1972.748	590.3618	40.04637
C76SSS.dat	1976.789	456.1017	34.74538
C73GMM.dat	1973.353	519.4824	33.88317
BO AVERAGE ERROR =			37.45551

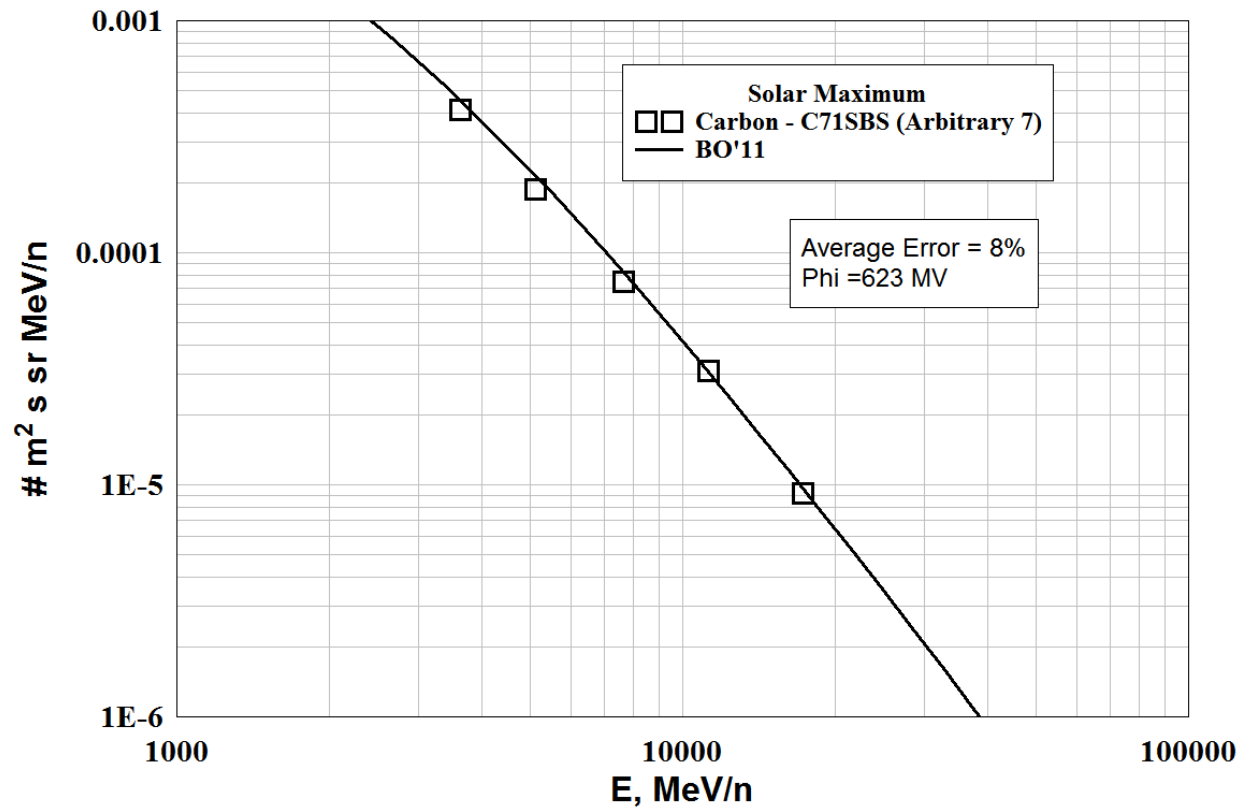
CARBON - High Energy, Solar Maximum

Files Rejected - (Arbitrary 7's)

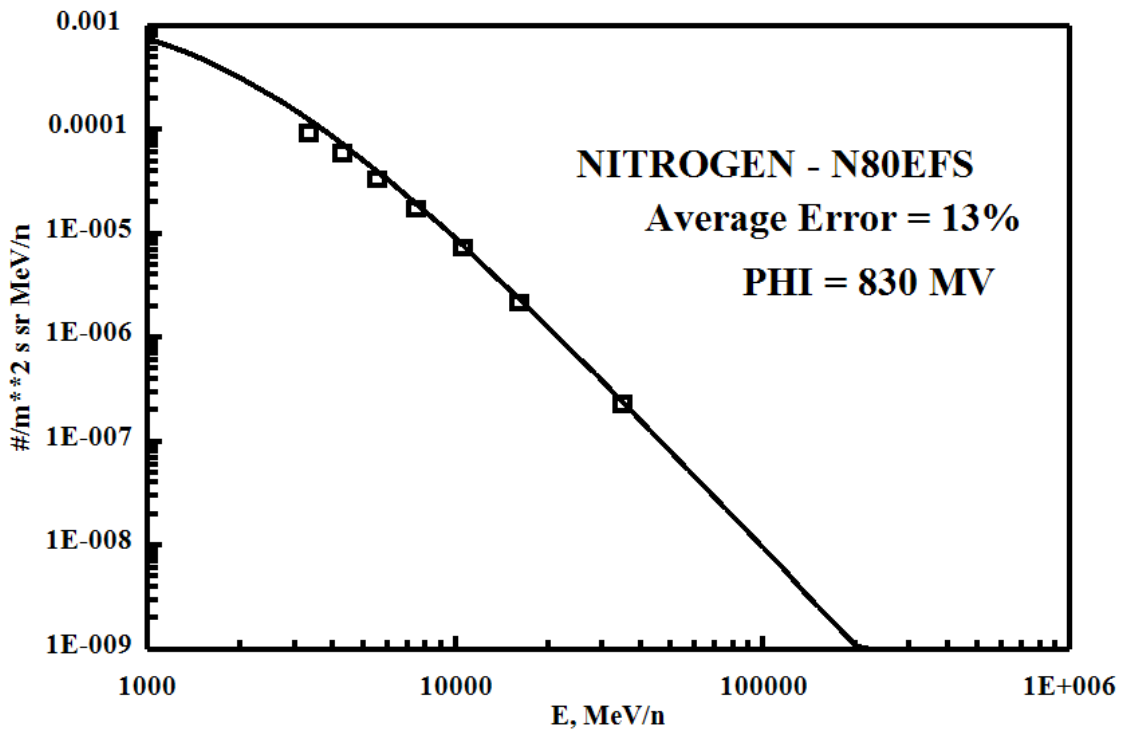
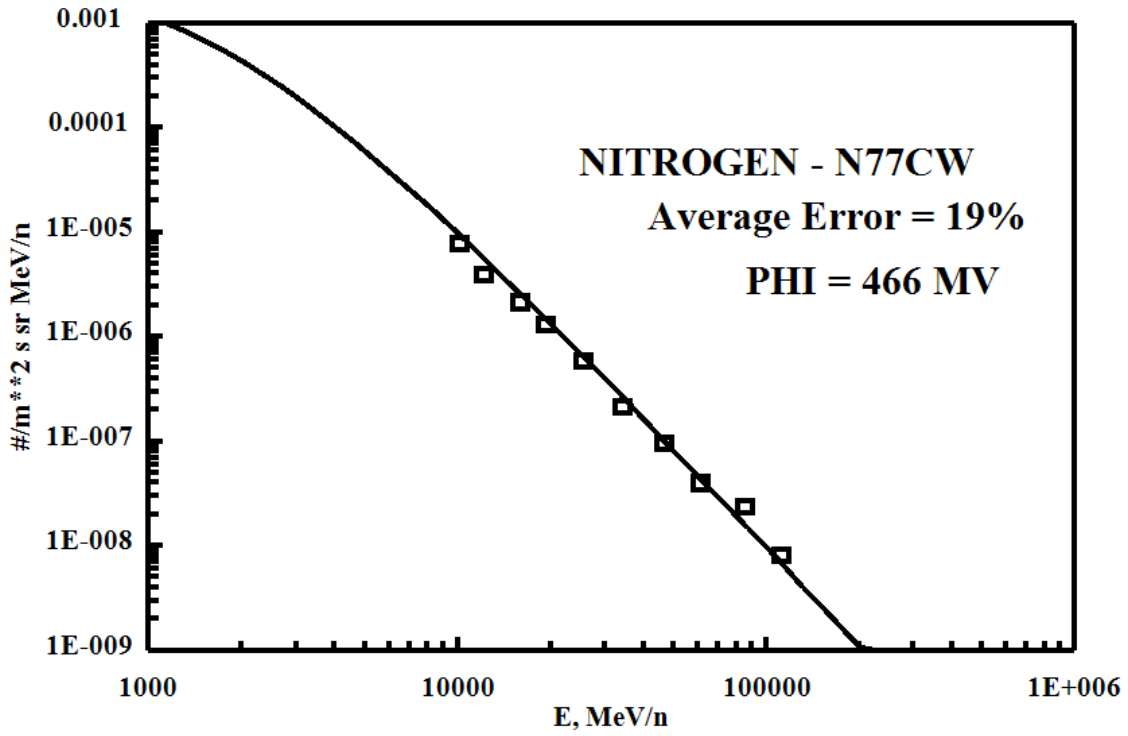
FILE	DATE	PHI (MV)	ERROR=ABS (FLUX-DATA)
C71SBS.dat	1971.370	623.2165	7.713494
BO AVERAGE ERROR =			7.713494

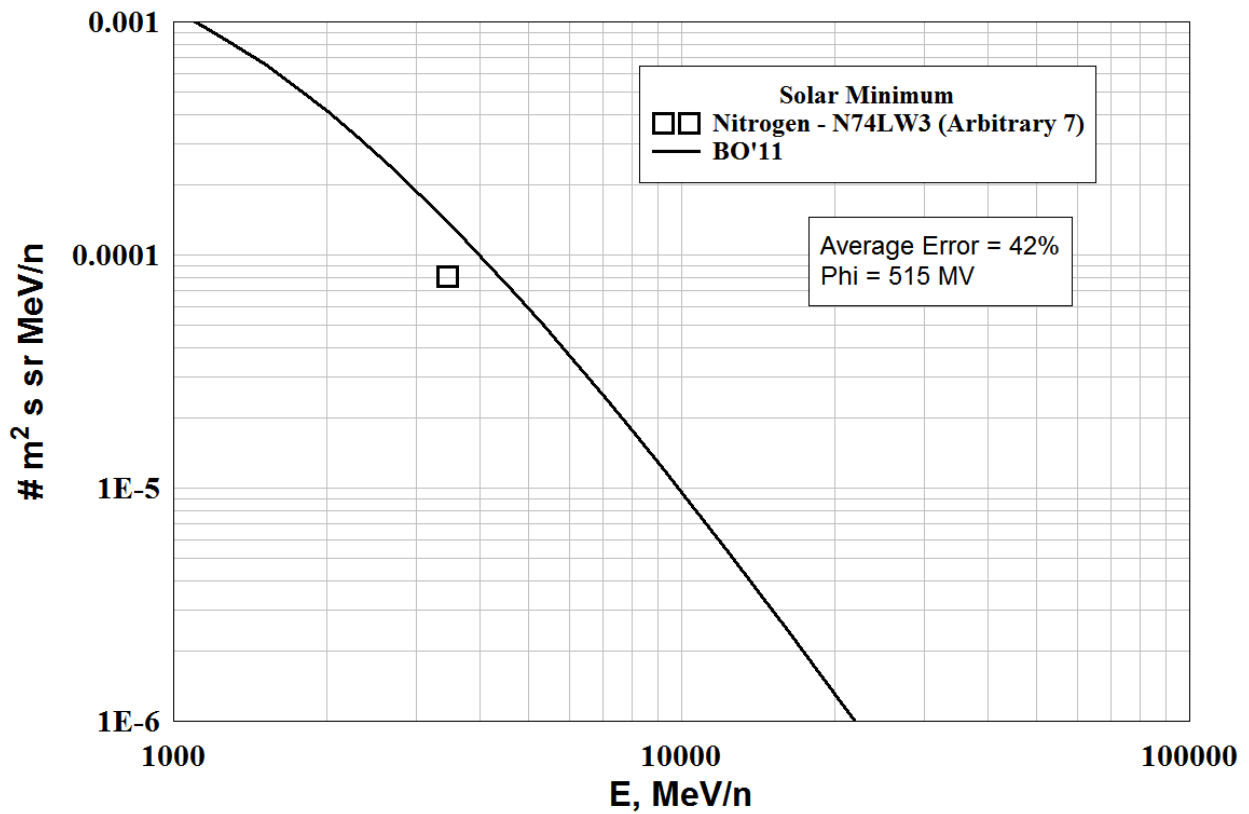
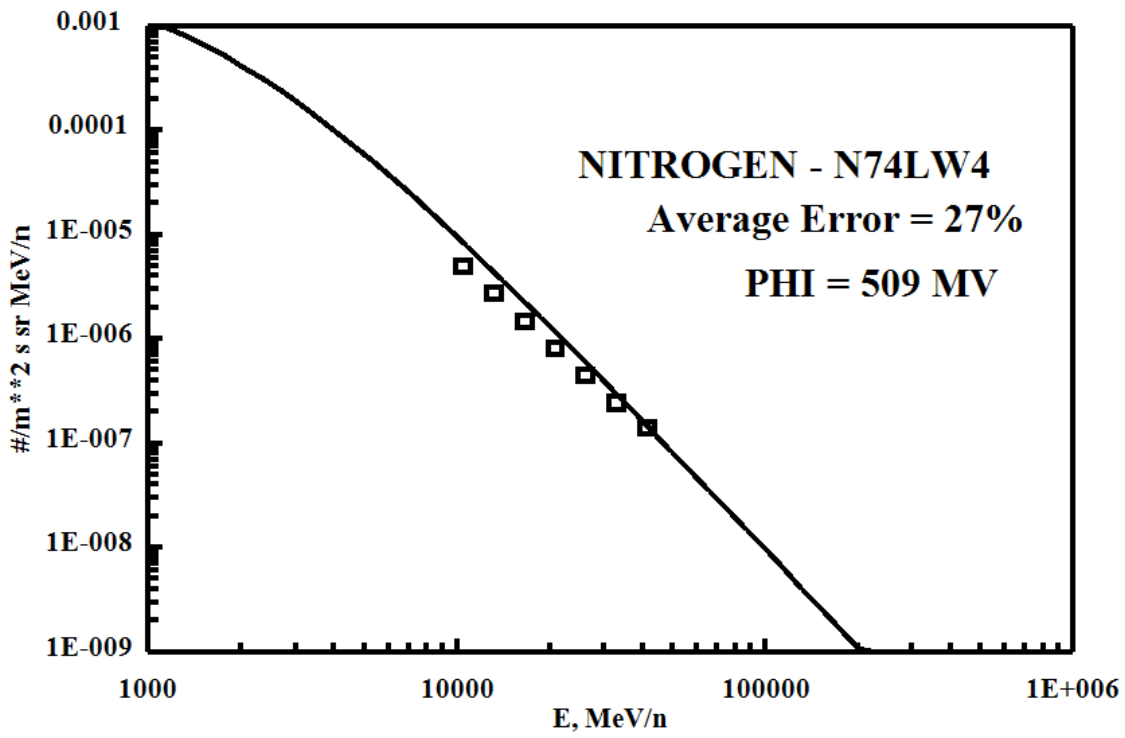


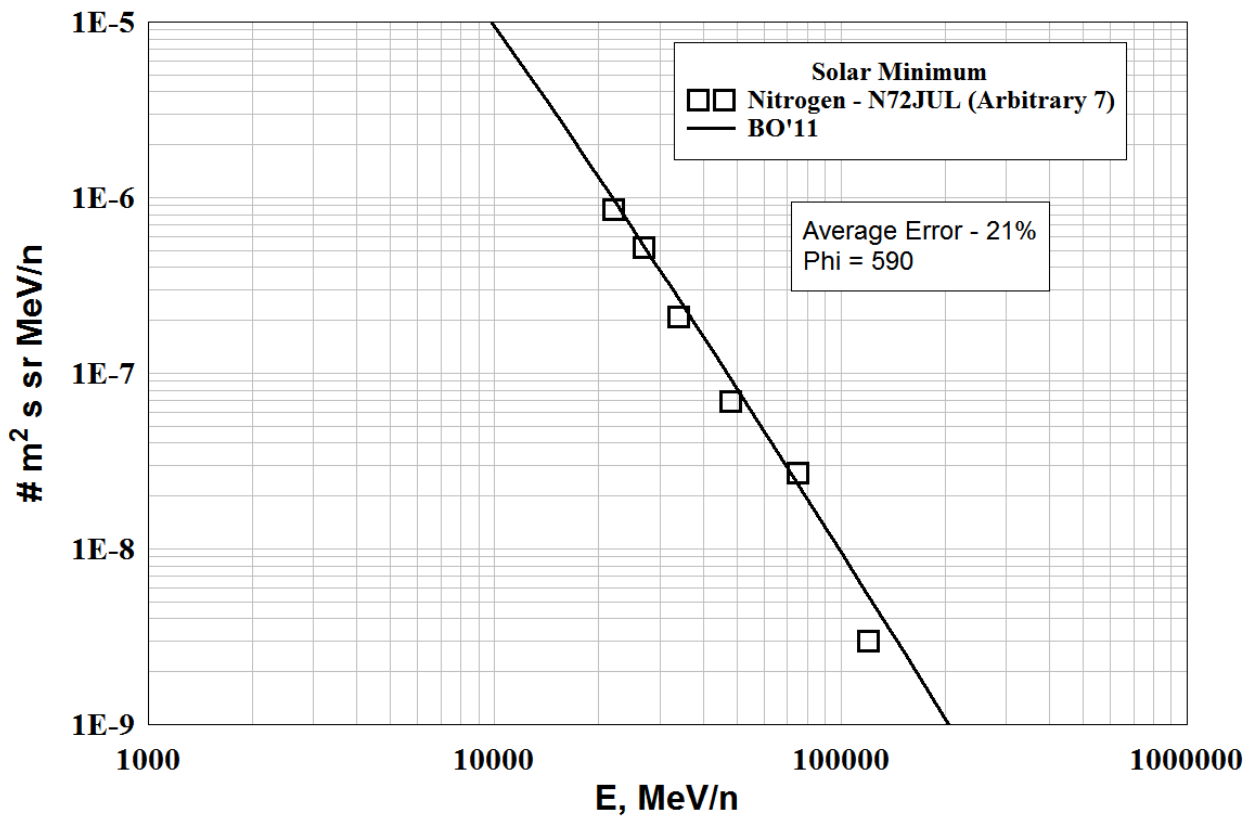
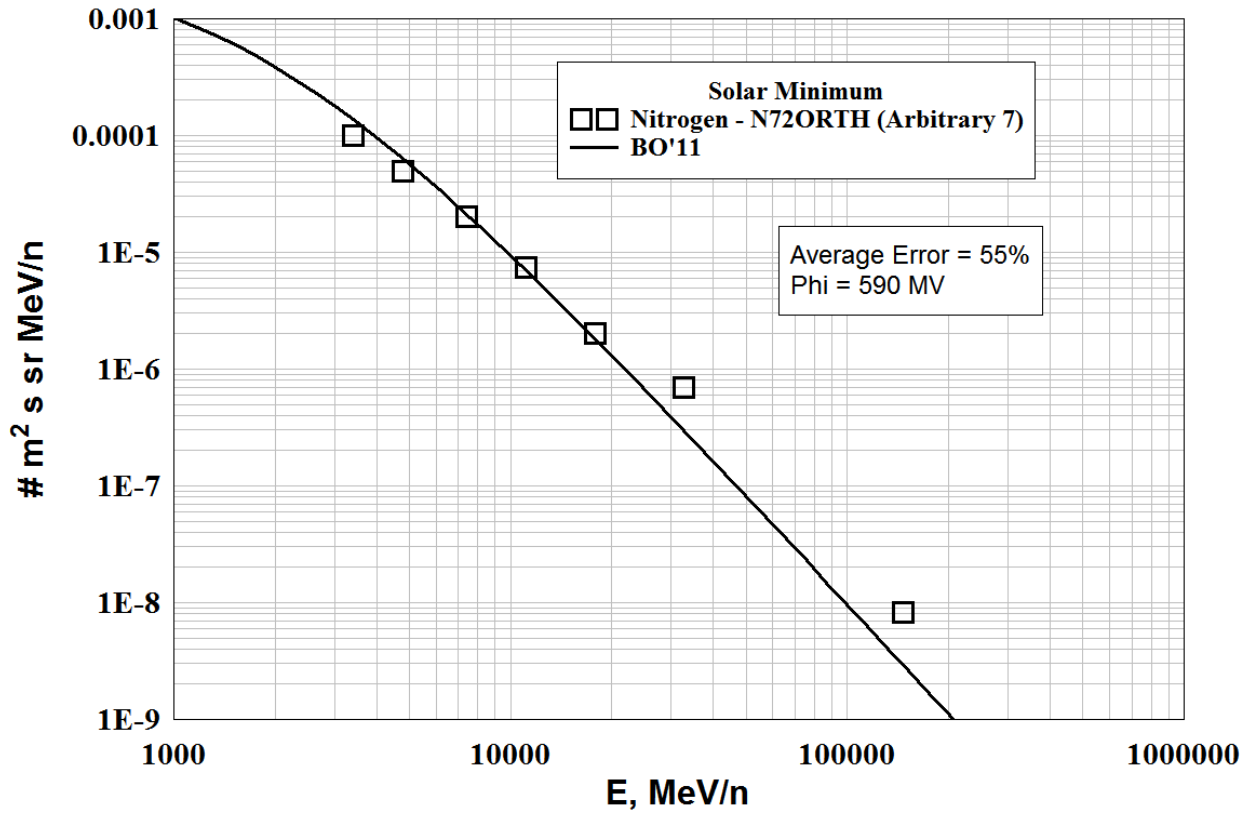


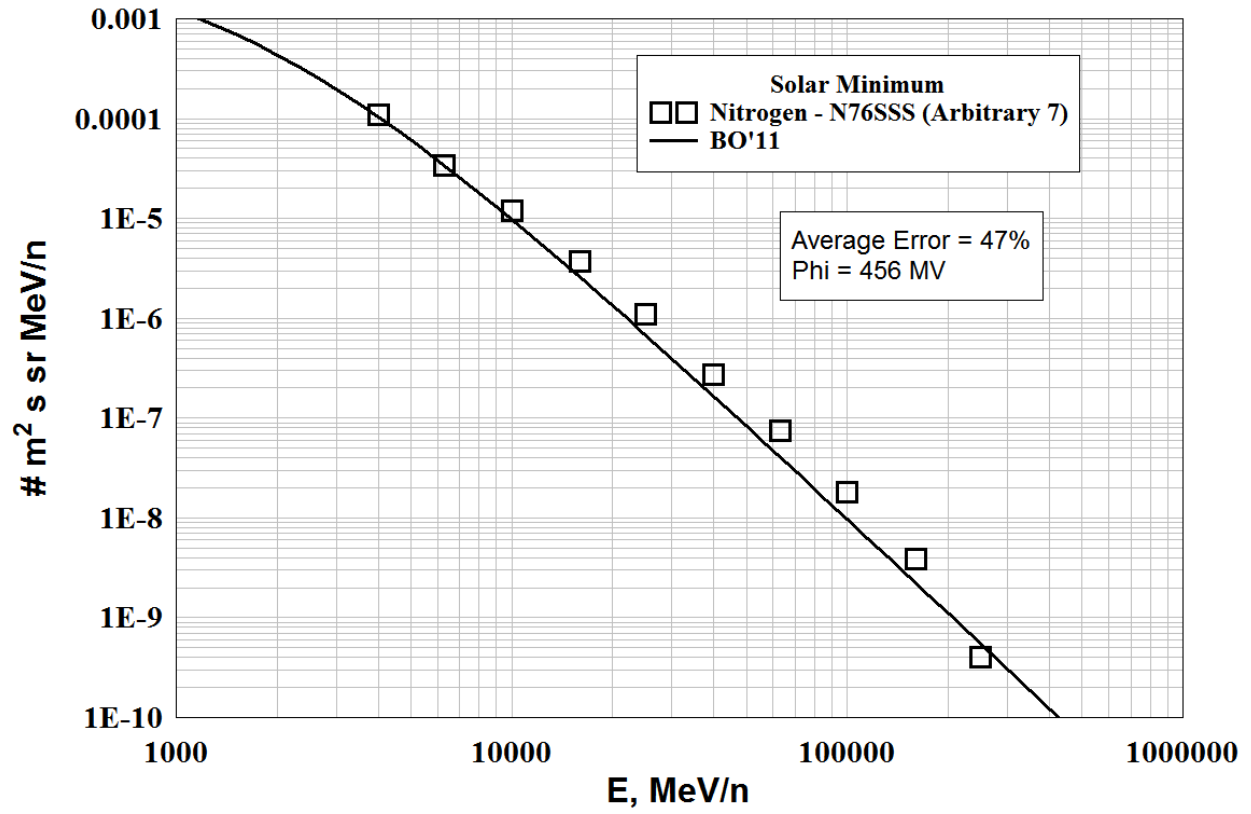


NITROGEN - High Energy







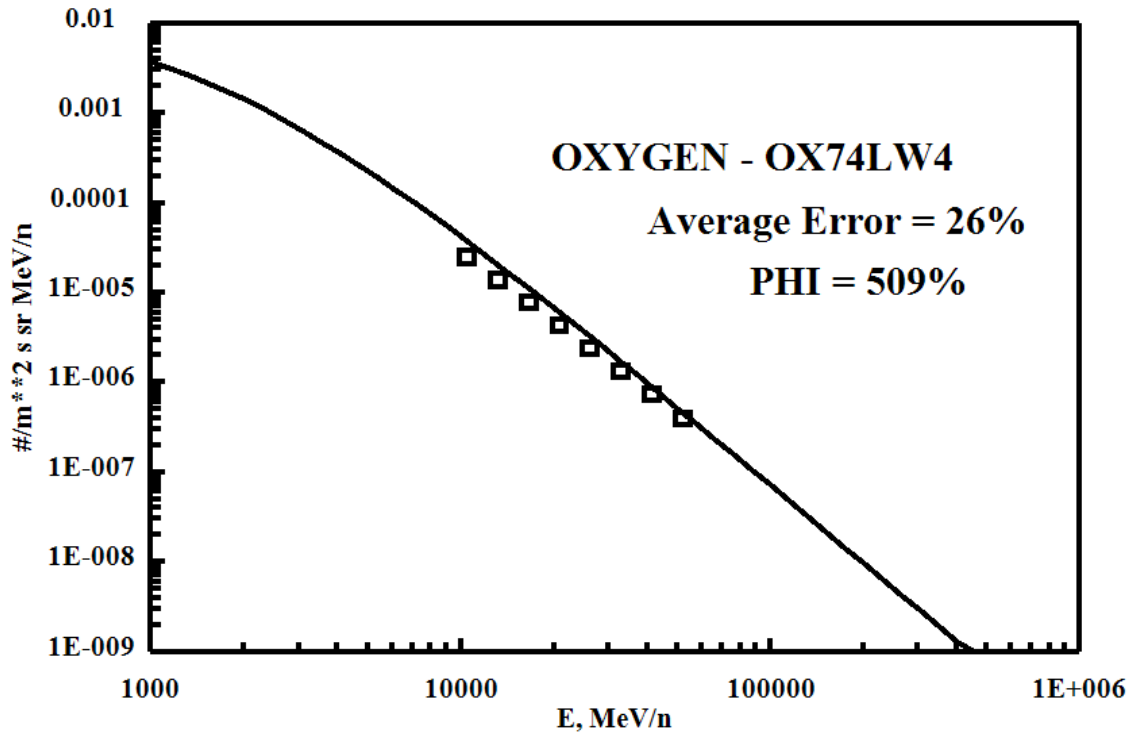


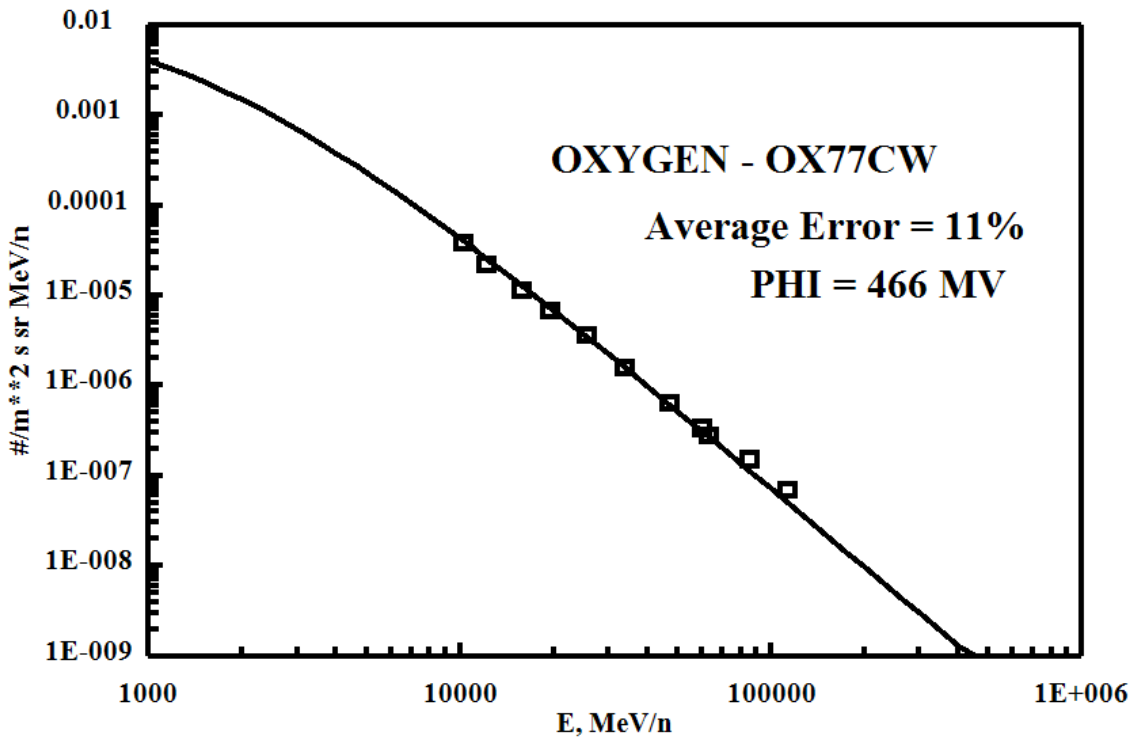
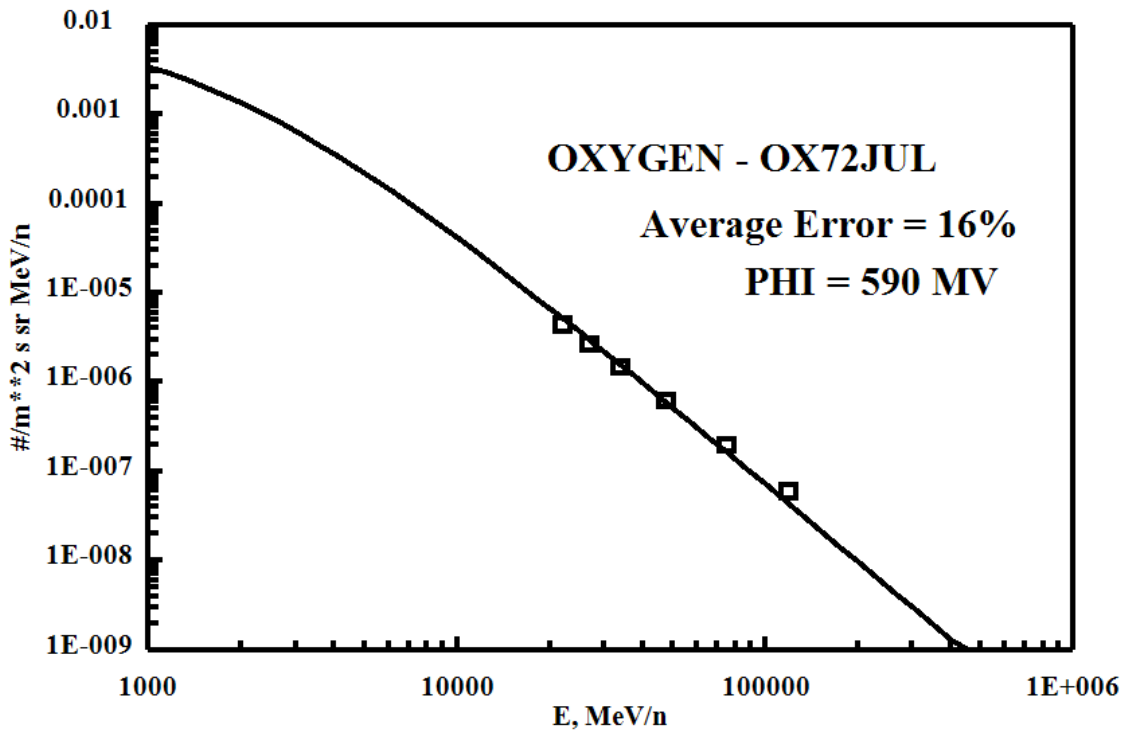
OXYGEN - High Energy, Solar Minimum

Files Used (Arbitrary 1's)

FILE	DATE	PHI (MV)	ERROR=ABS (FLUX-DATA)
Ox74LW4.dat	1974.726	509.2871	26.42744
Ox72Jul.dat	1972.751	590.1960	15.76700
Ox77CW.dat	1976.000	465.6418	11.35872

BO AVERAGE ERROR = 17.85105

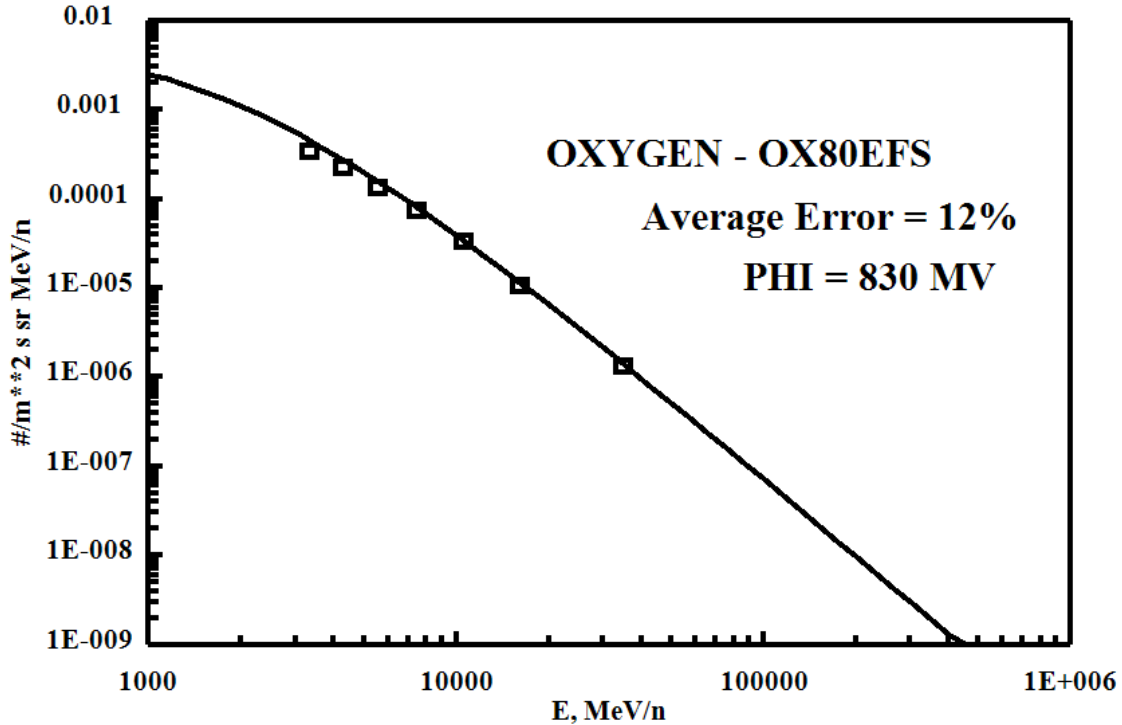




OXYGEN - High Energy, Solar Maximum

Files Used (Arbitrary 1's)

FILE	DATE	PHI (MV)	ERROR=ABS (FLUX-DATA)
Ox80EFS.dat	1979.795	830.2713	12.03748
BO AVERAGE ERROR = 12.03748			



OXYGEN - High Energy, Solar Minimum

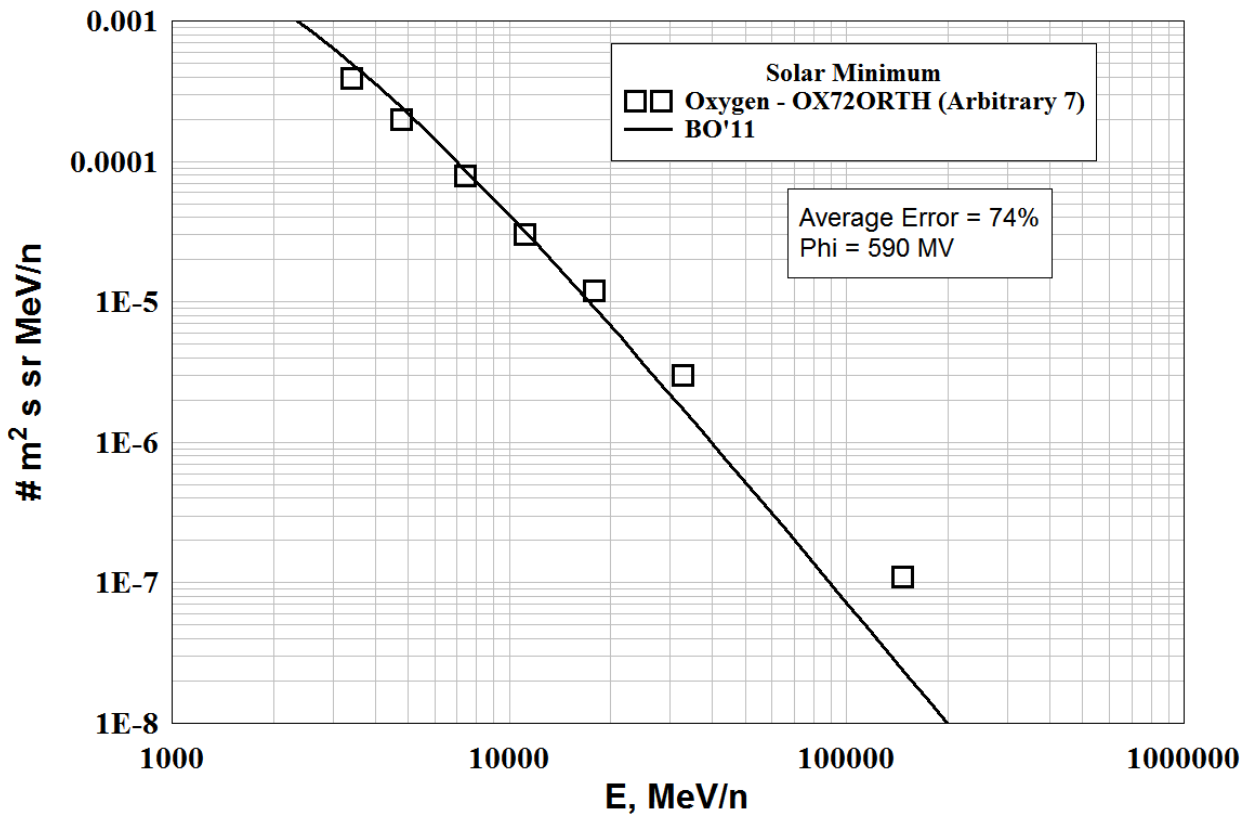
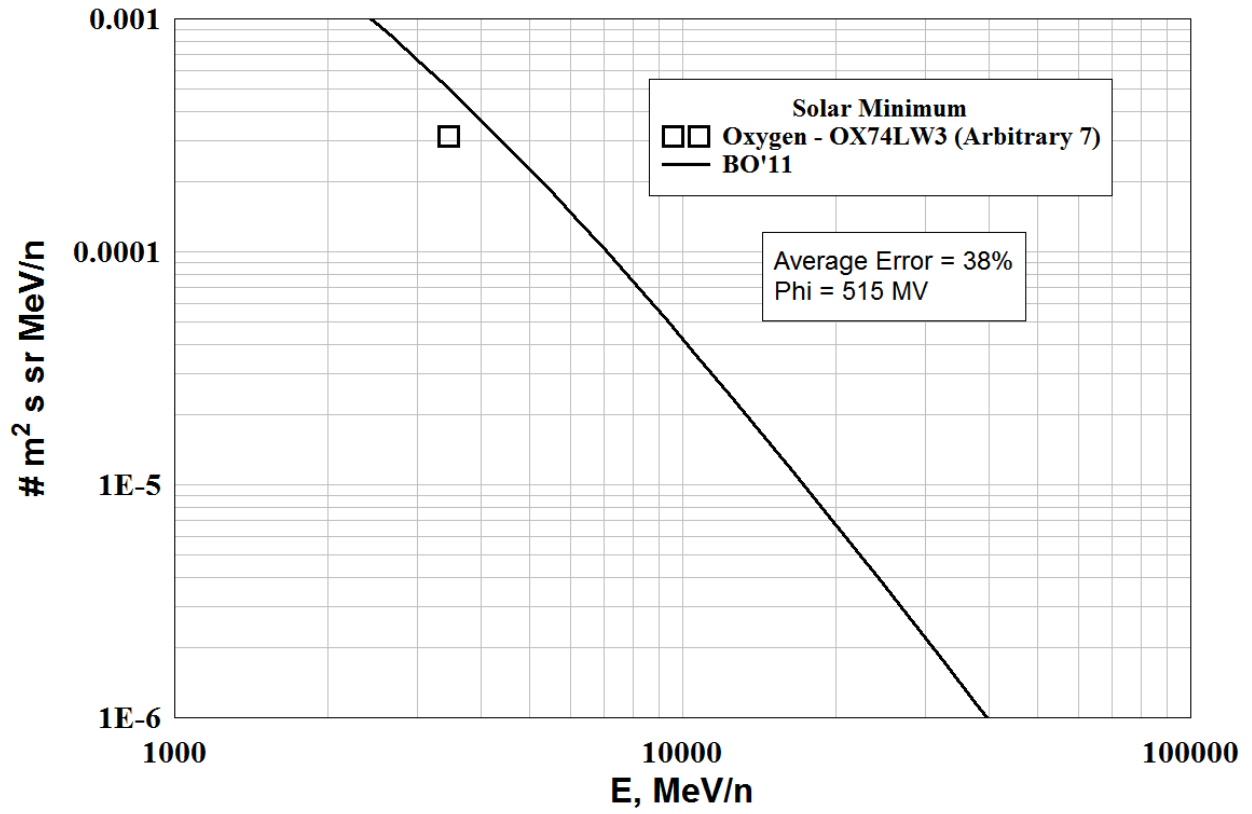
Files Rejected - (Arbitrary 7's)

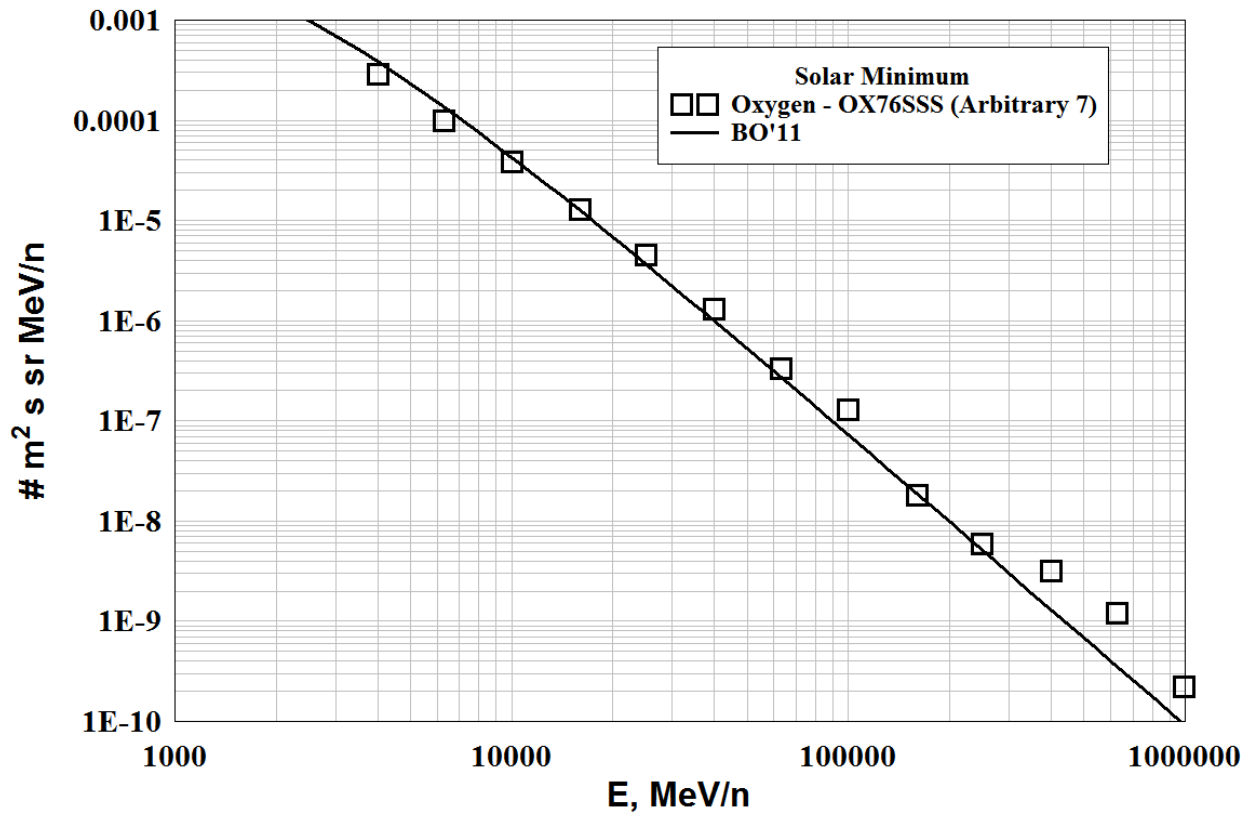
FILE	DATE	PHI (MV)	ERROR=ABS (FLUX-DATA)
Ox74LW3.dat	1974.553	515.0297	37.76938
Ox72Orth.dat	1972.748	590.3618	73.77858
Ox76SSS.dat	1976.789	456.1017	58.54860
BO AVERAGE ERROR = 56.69885			

OXYGEN - High Energy, Solar Maximum

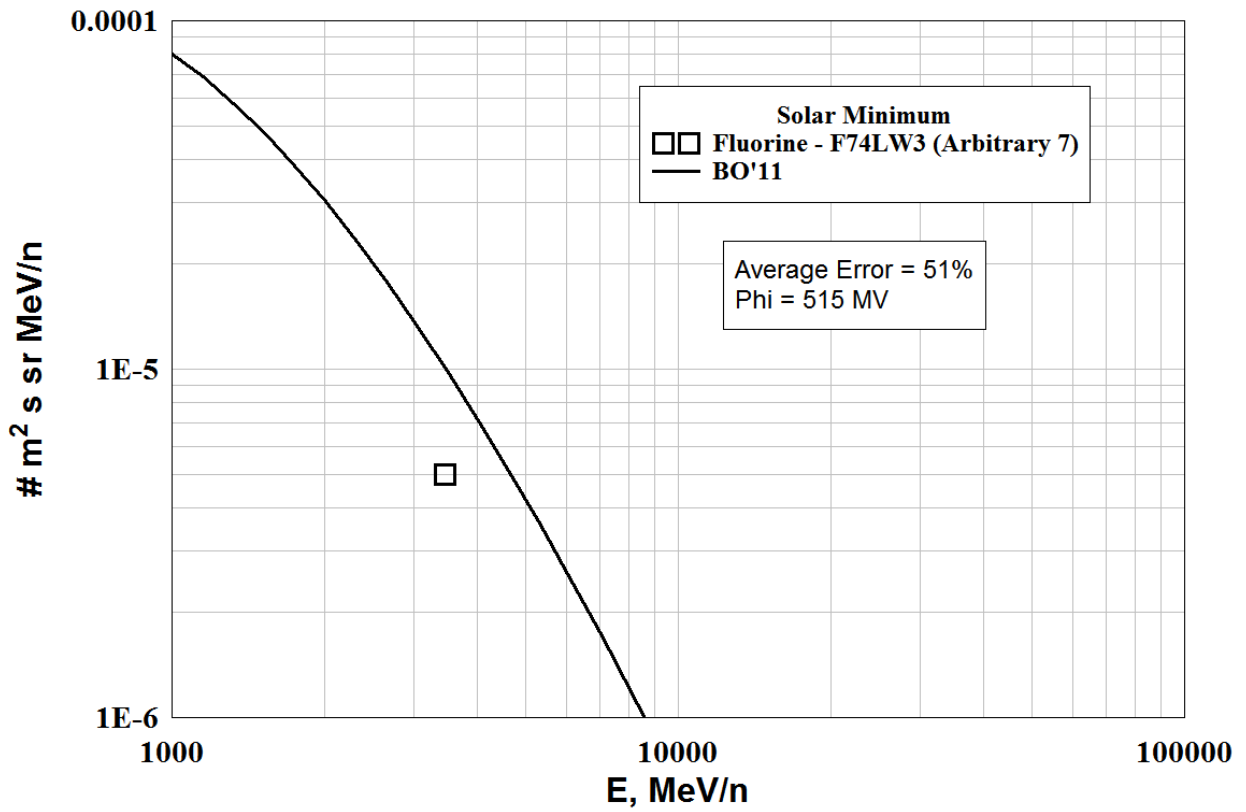
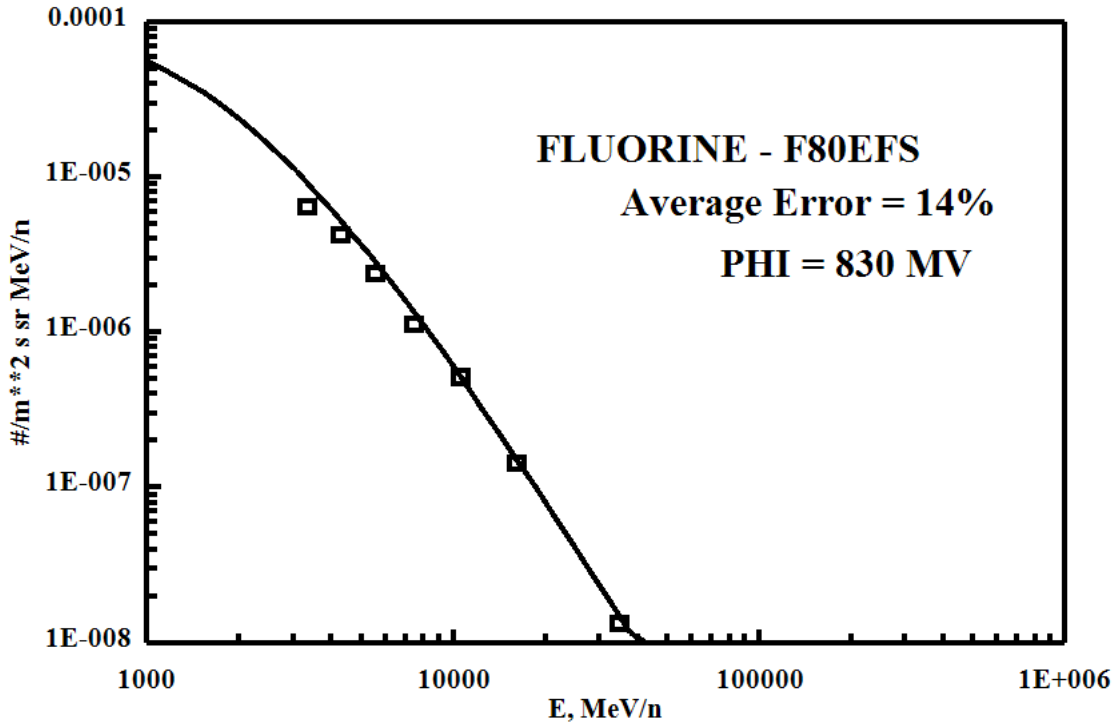
Files Rejected - (Arbitrary 7's)

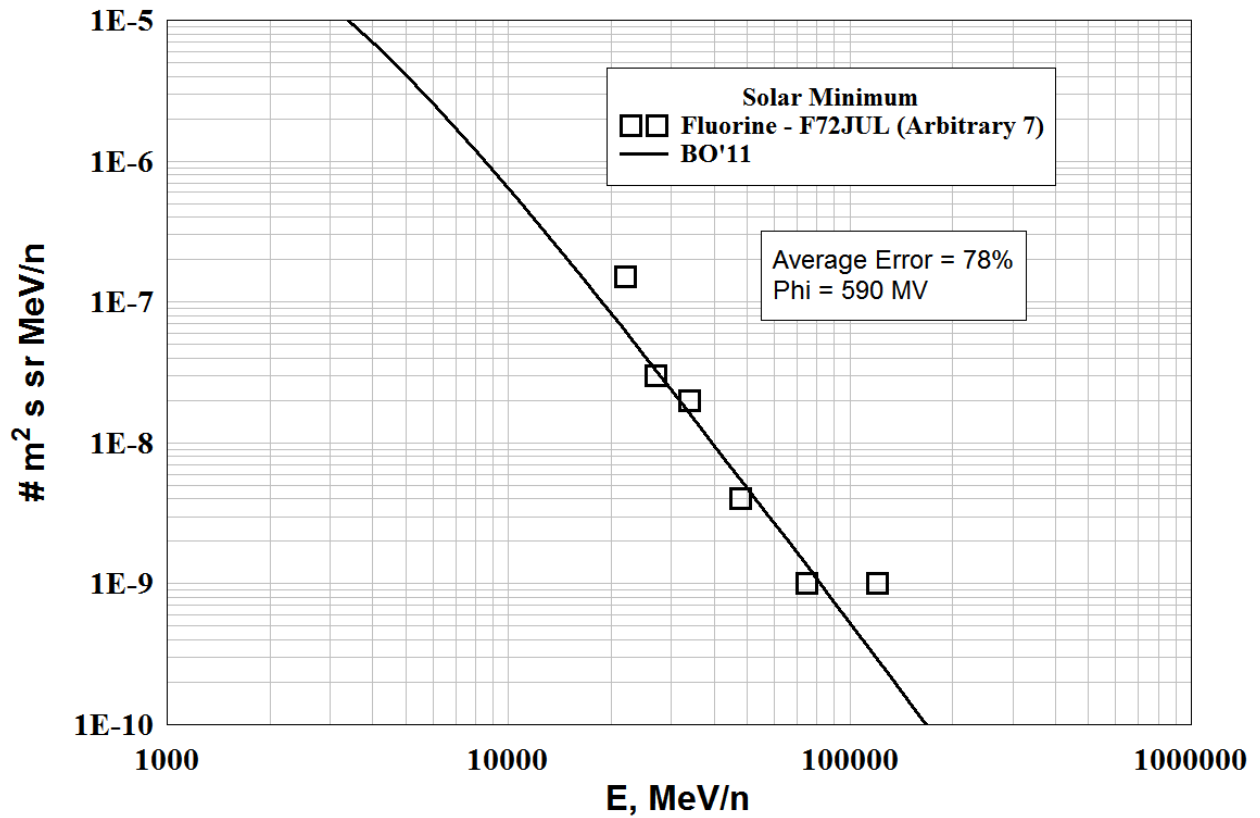
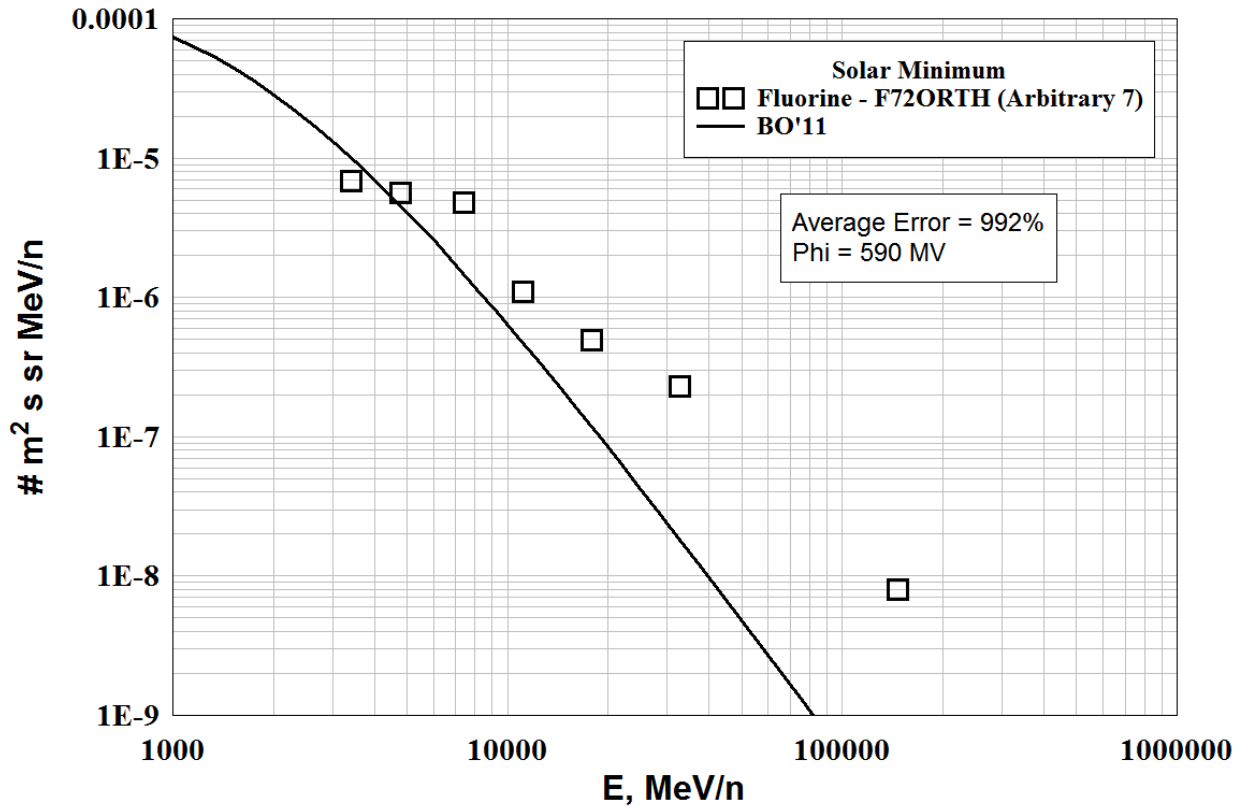
-----NO FILES-----



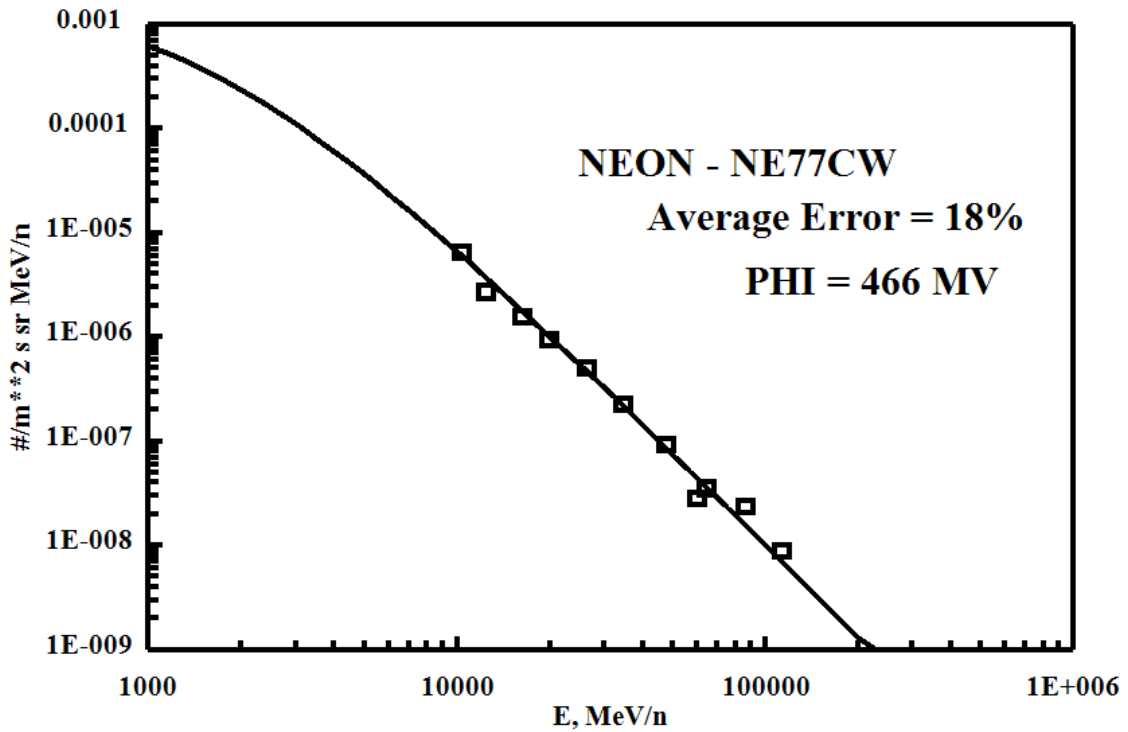
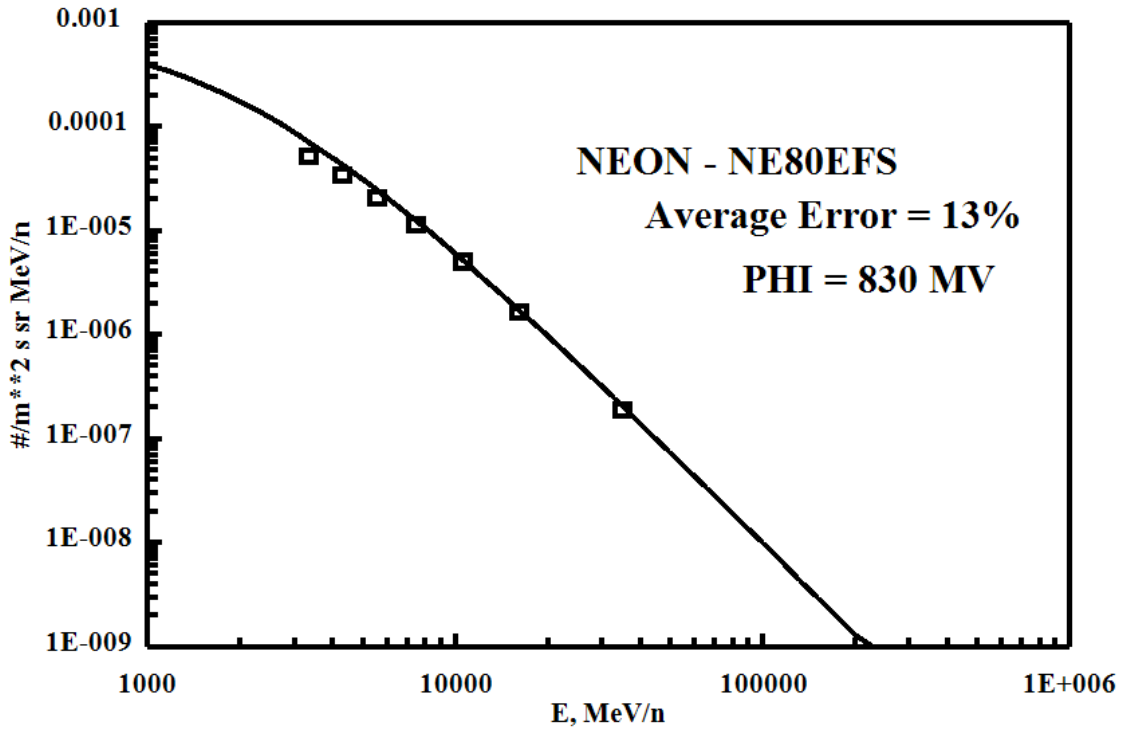


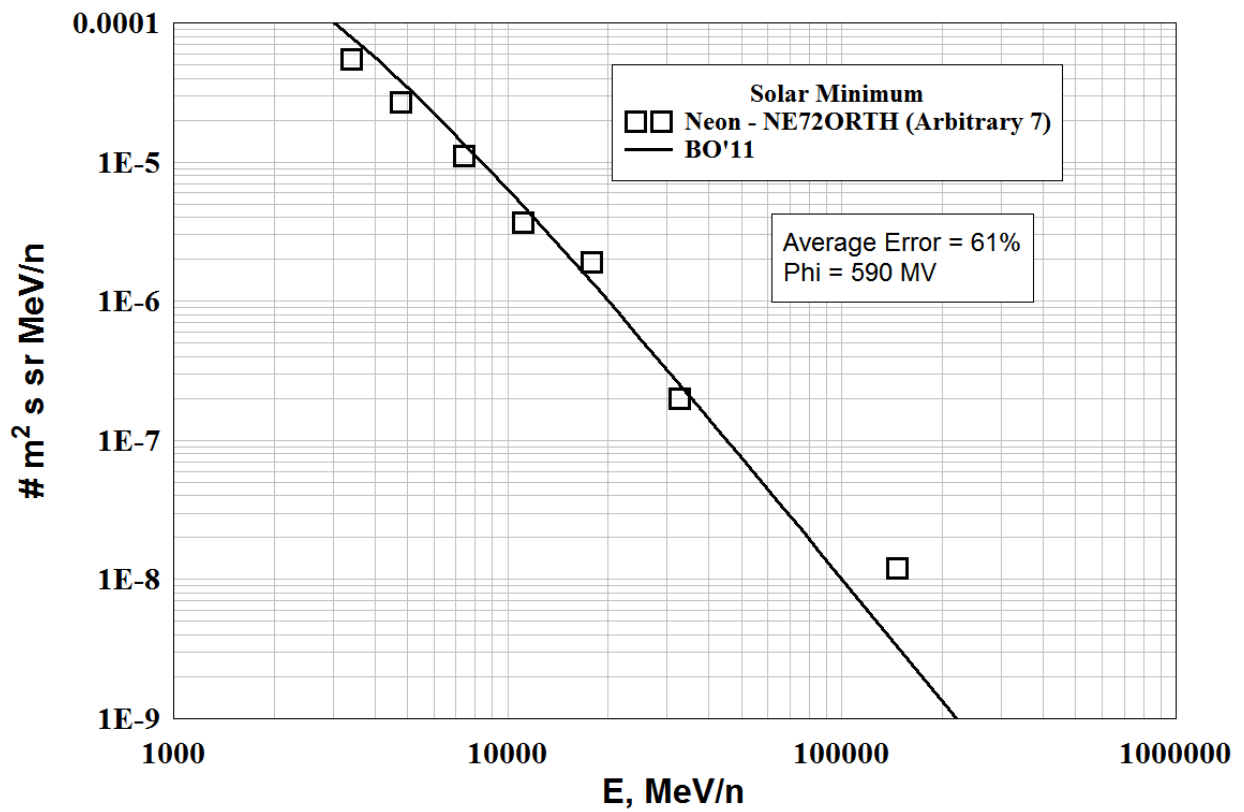
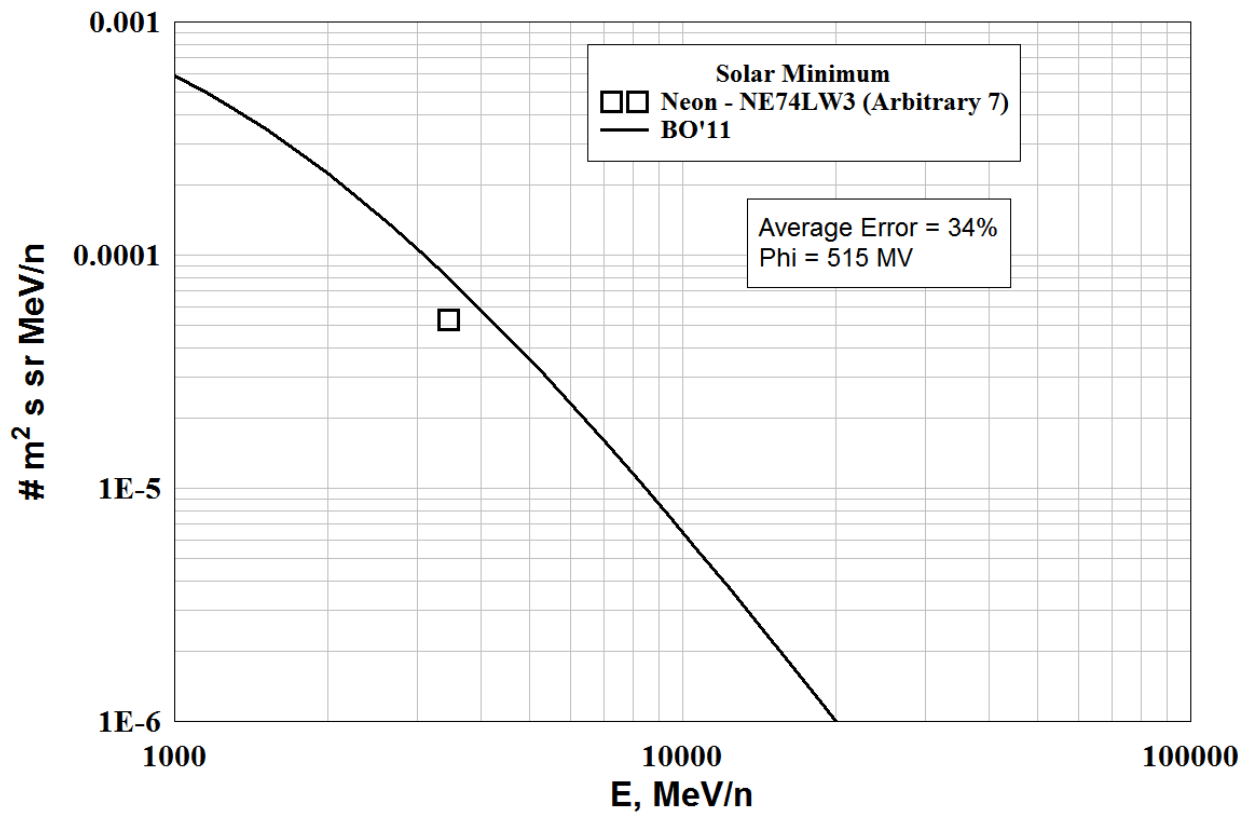
FLUORINE - High Energy

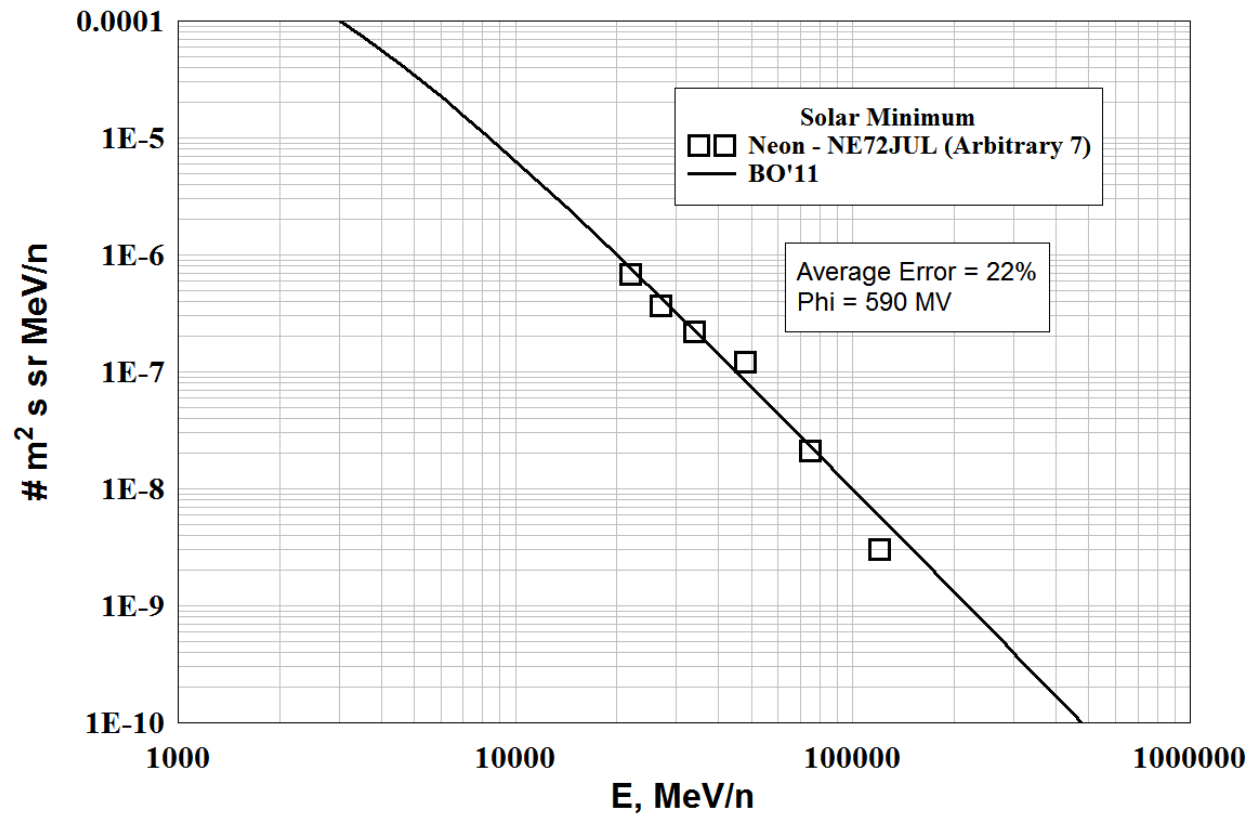




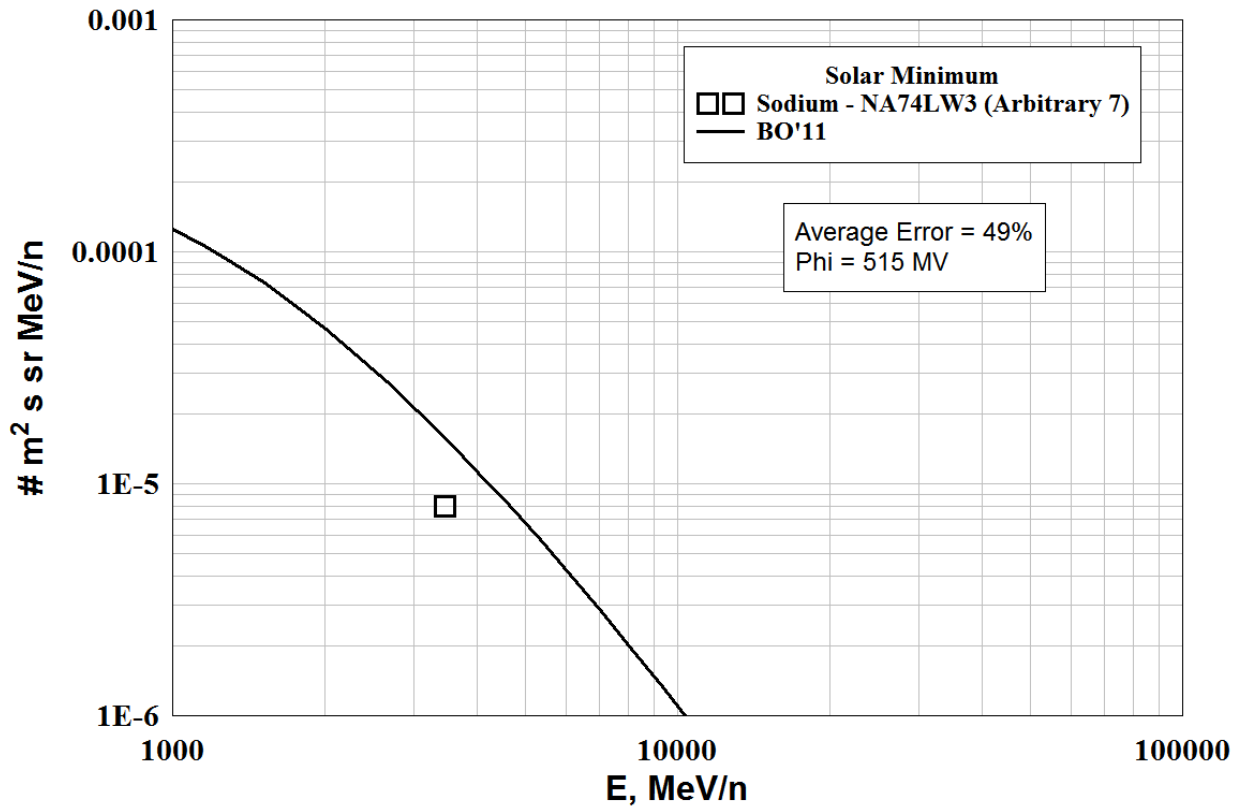
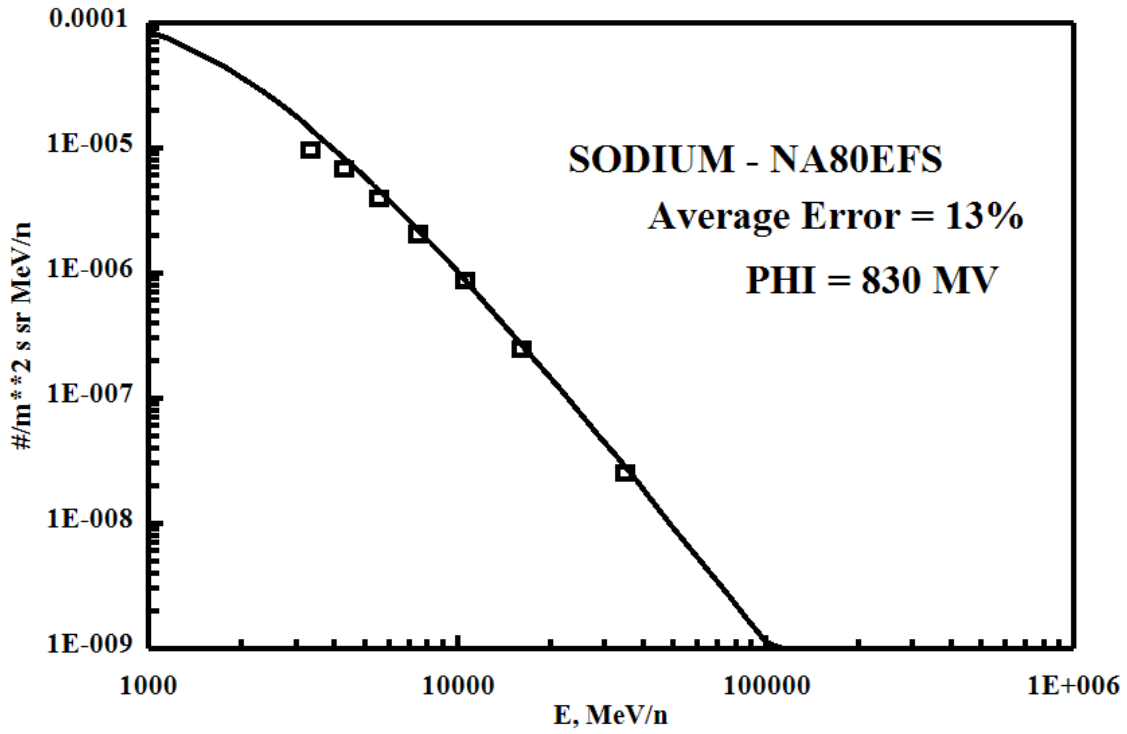
NEON - High Energy

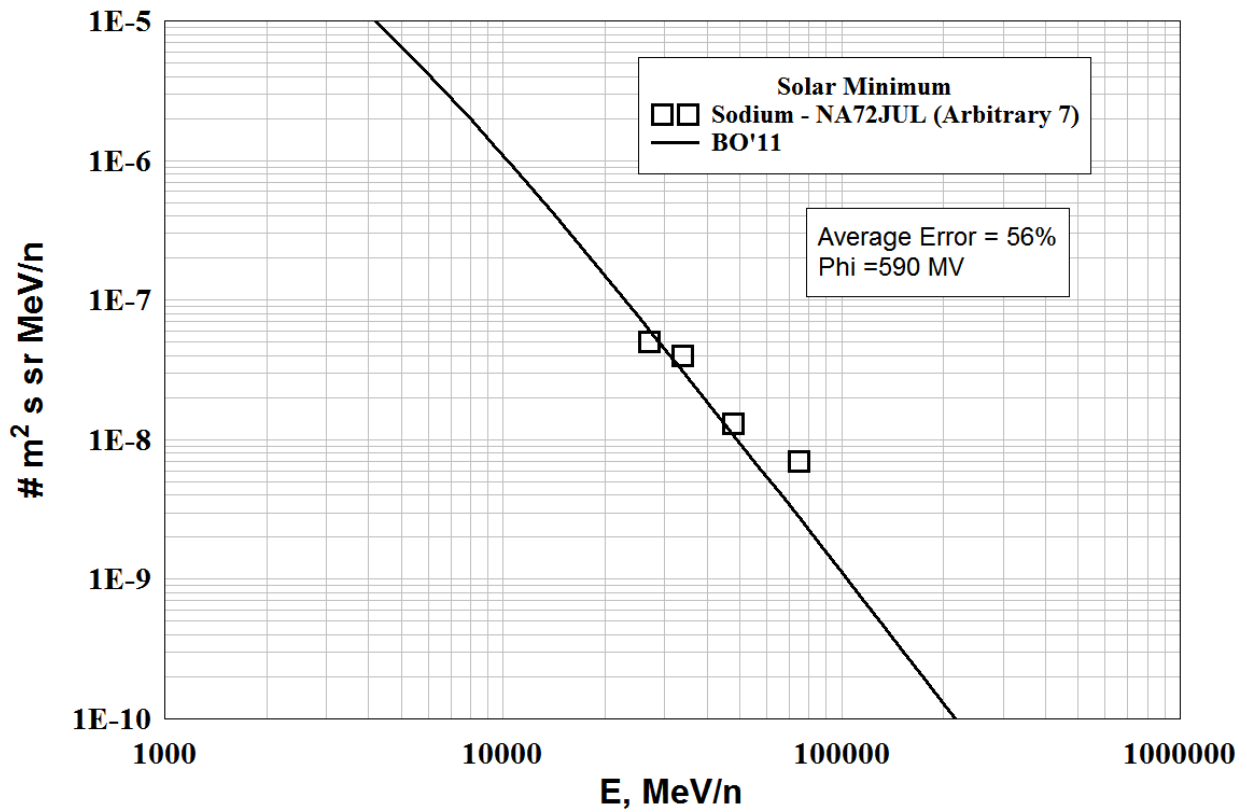
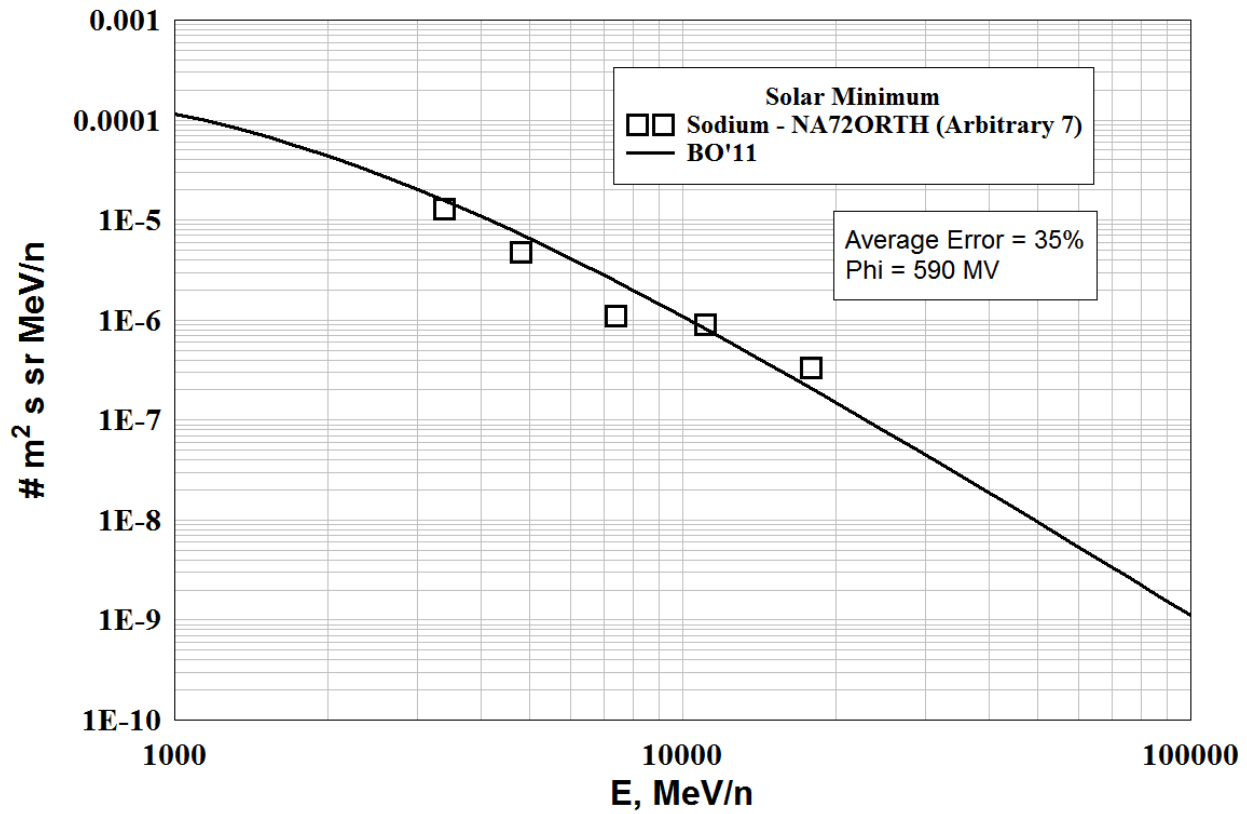




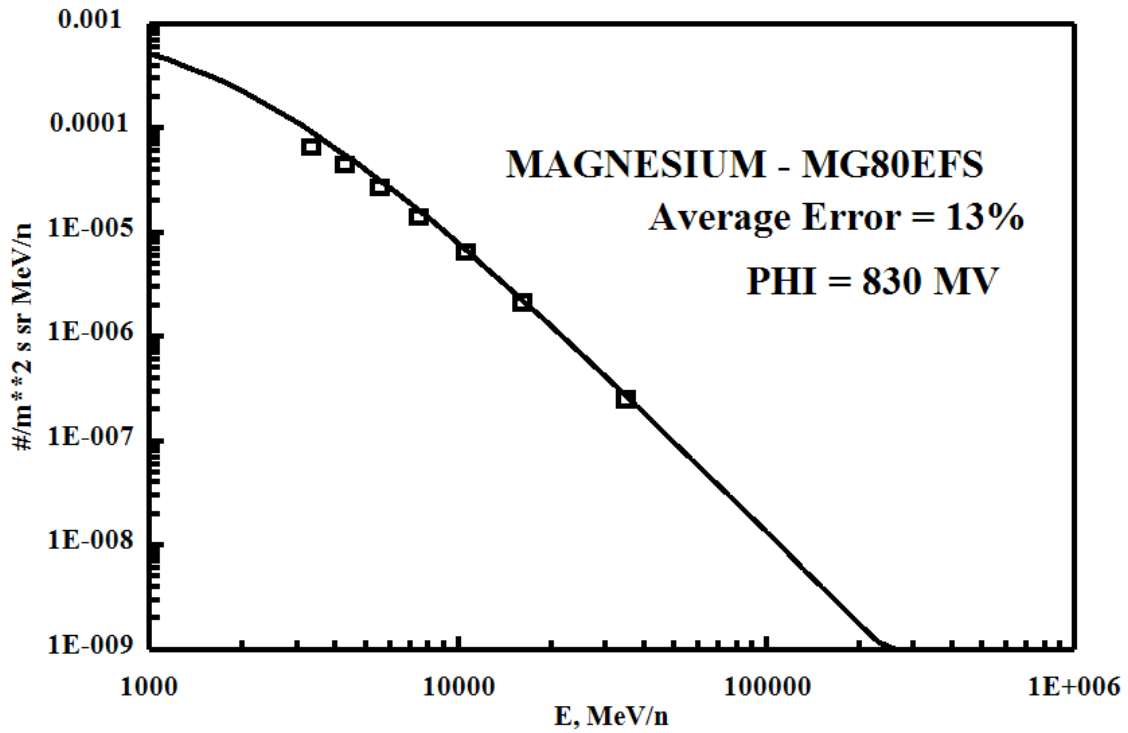
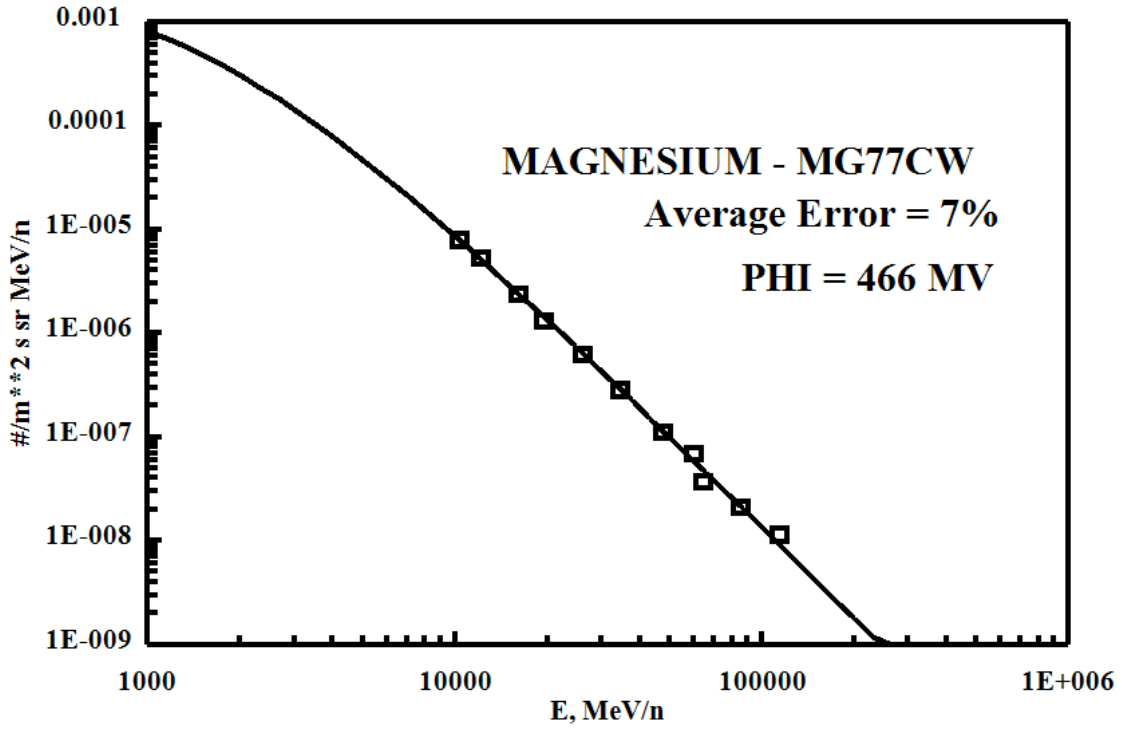


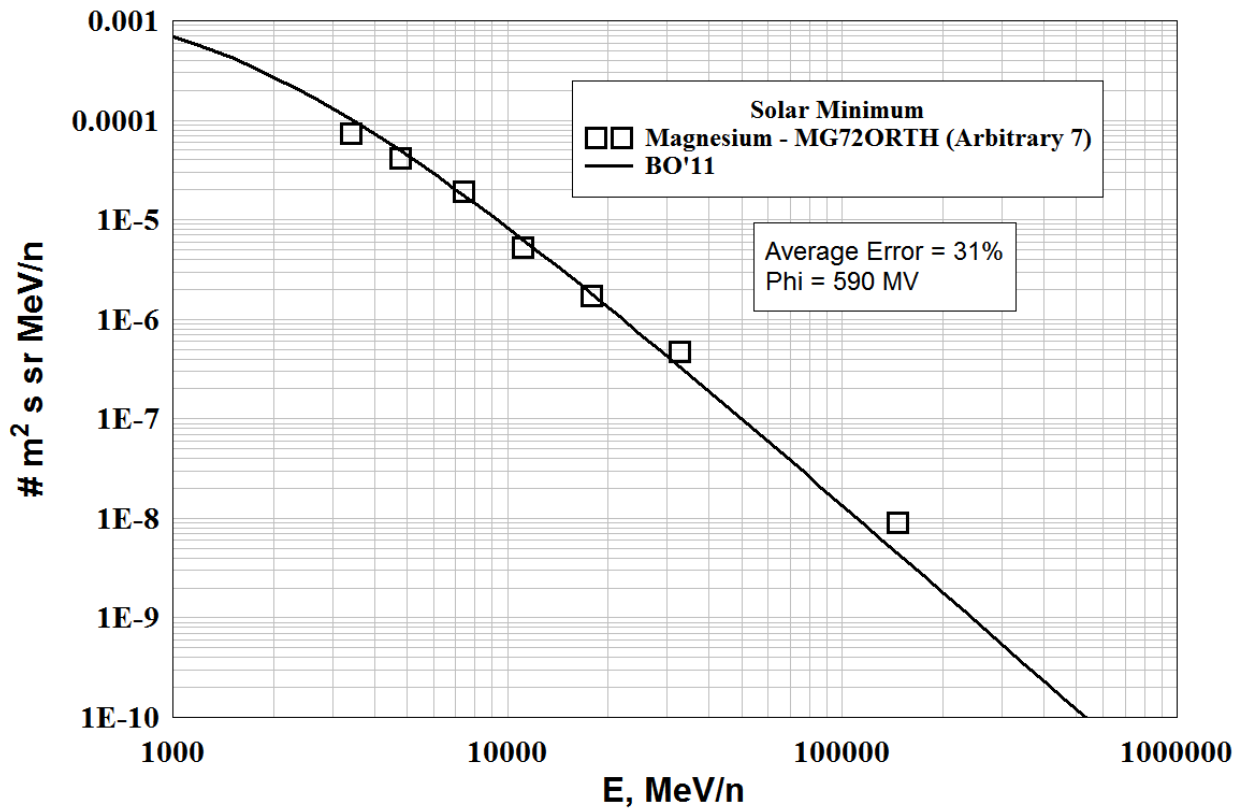
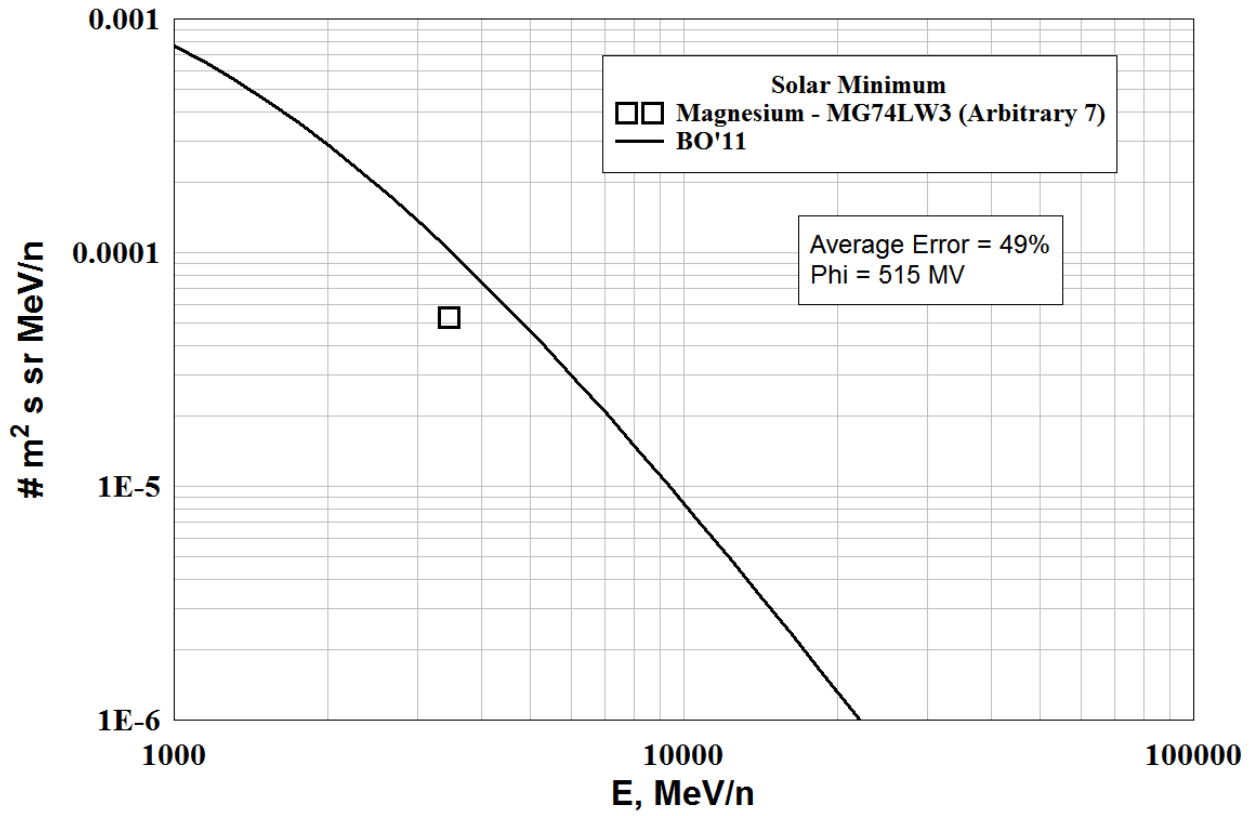
SODIUM - High Energy

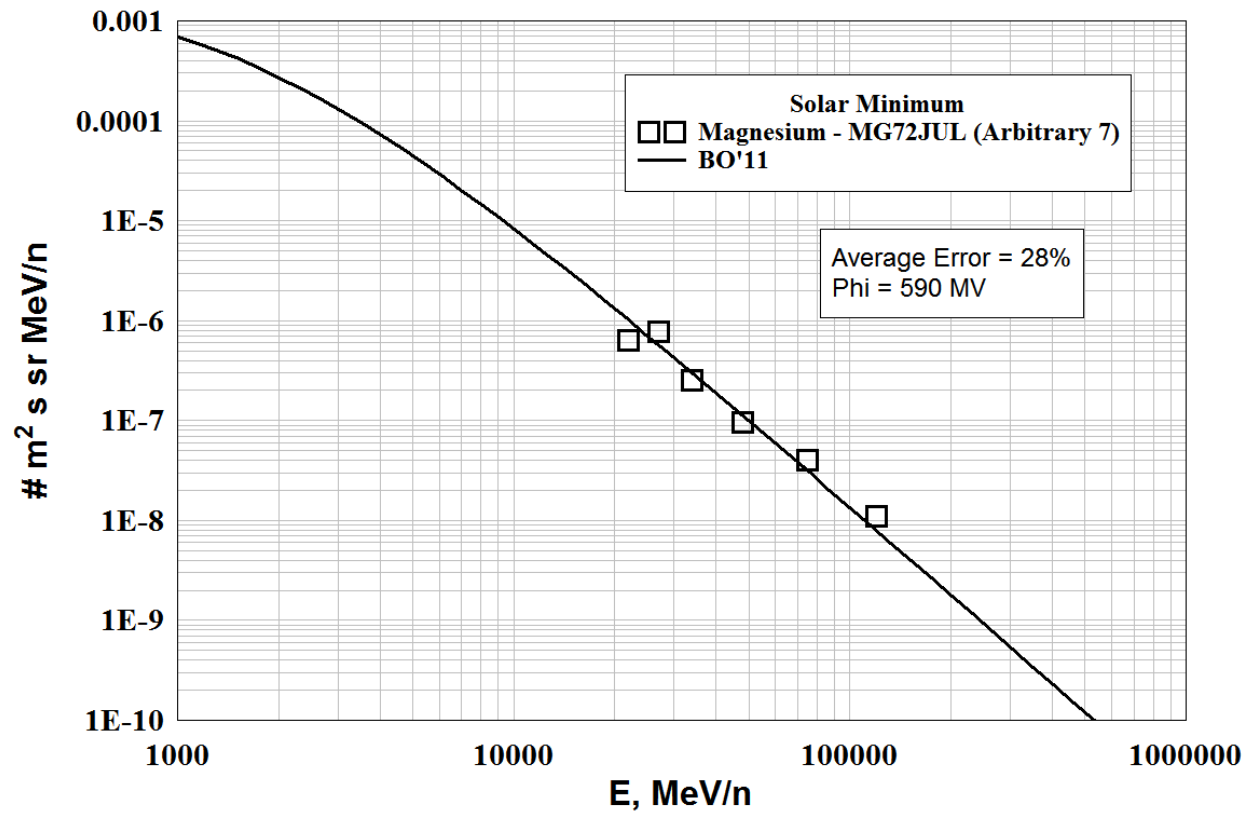




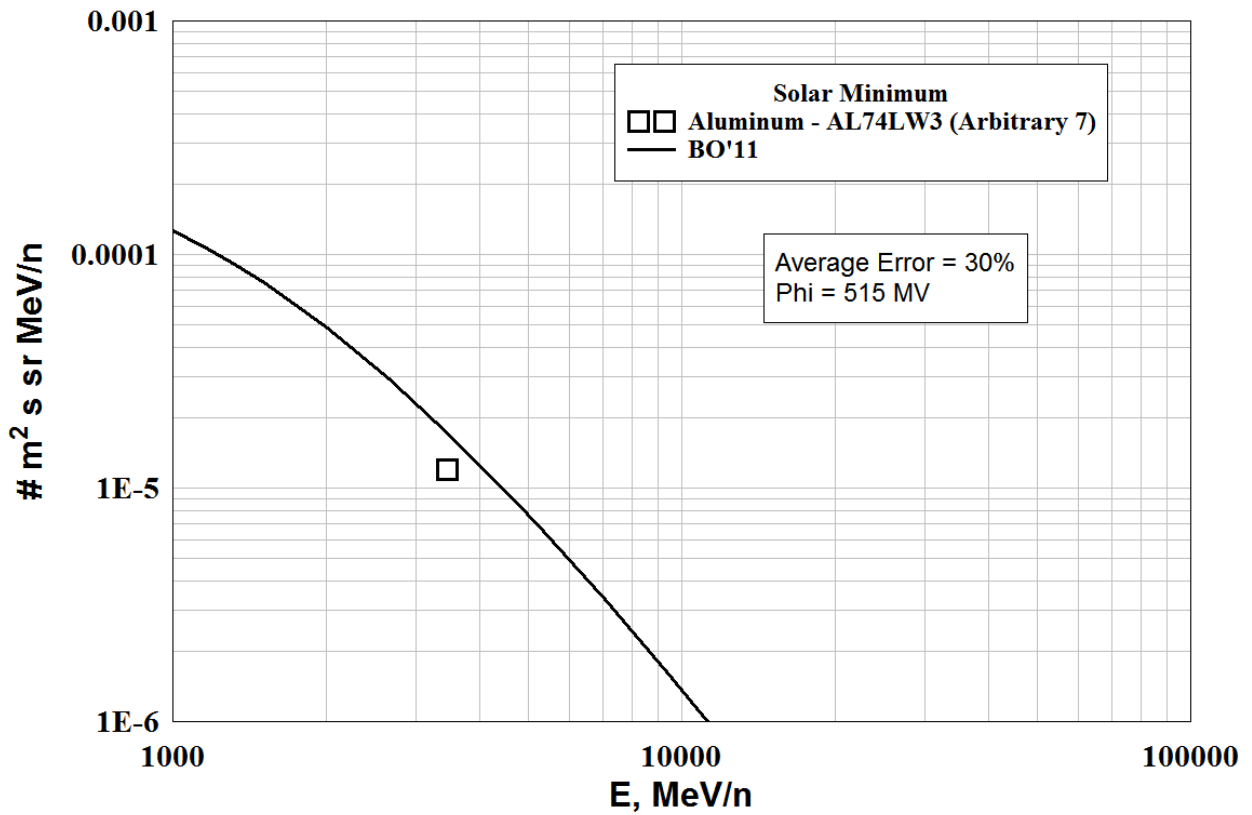
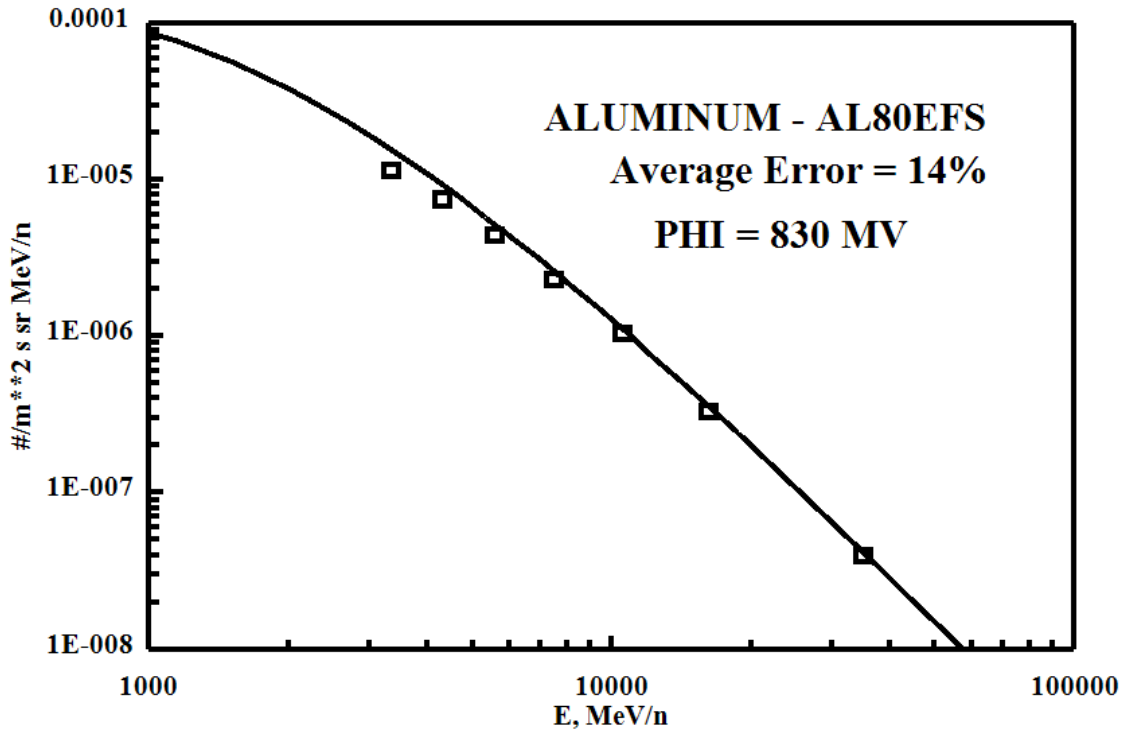
MAGNESIUM - High Energy

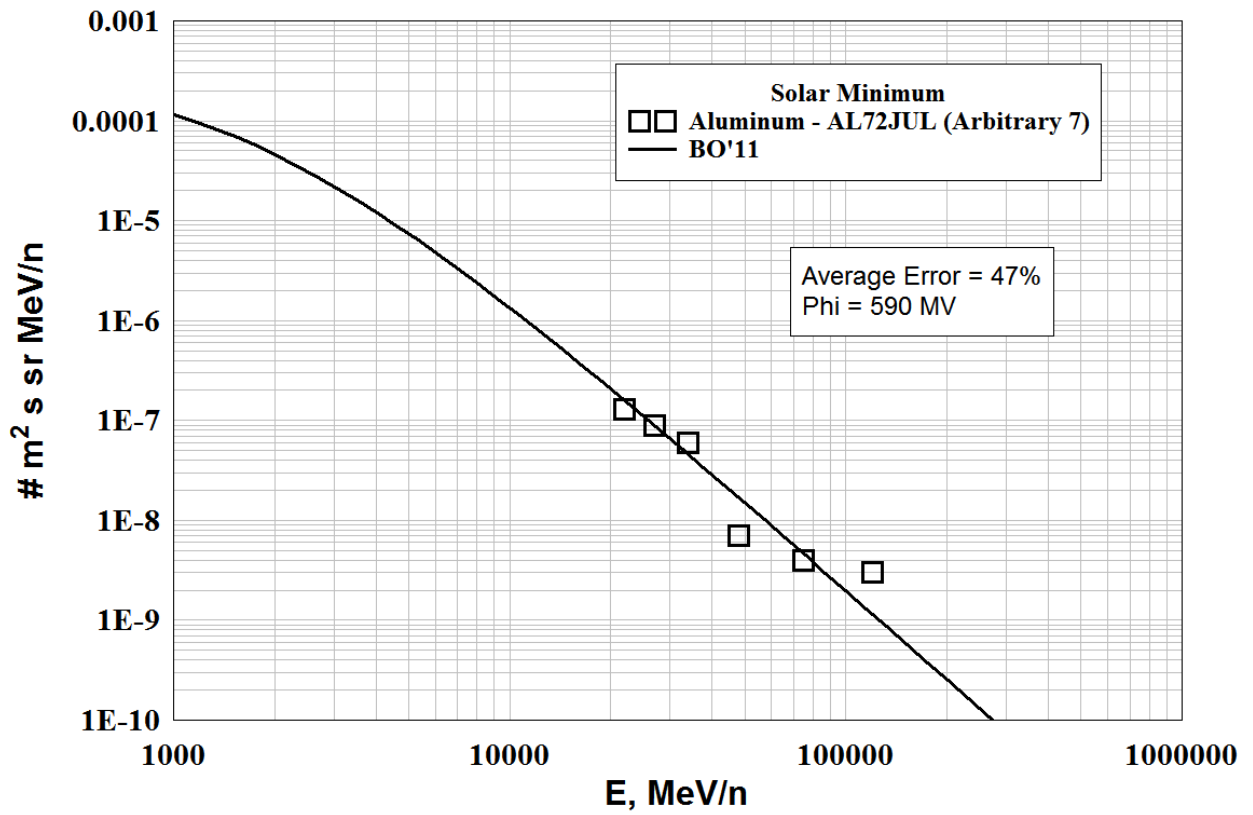
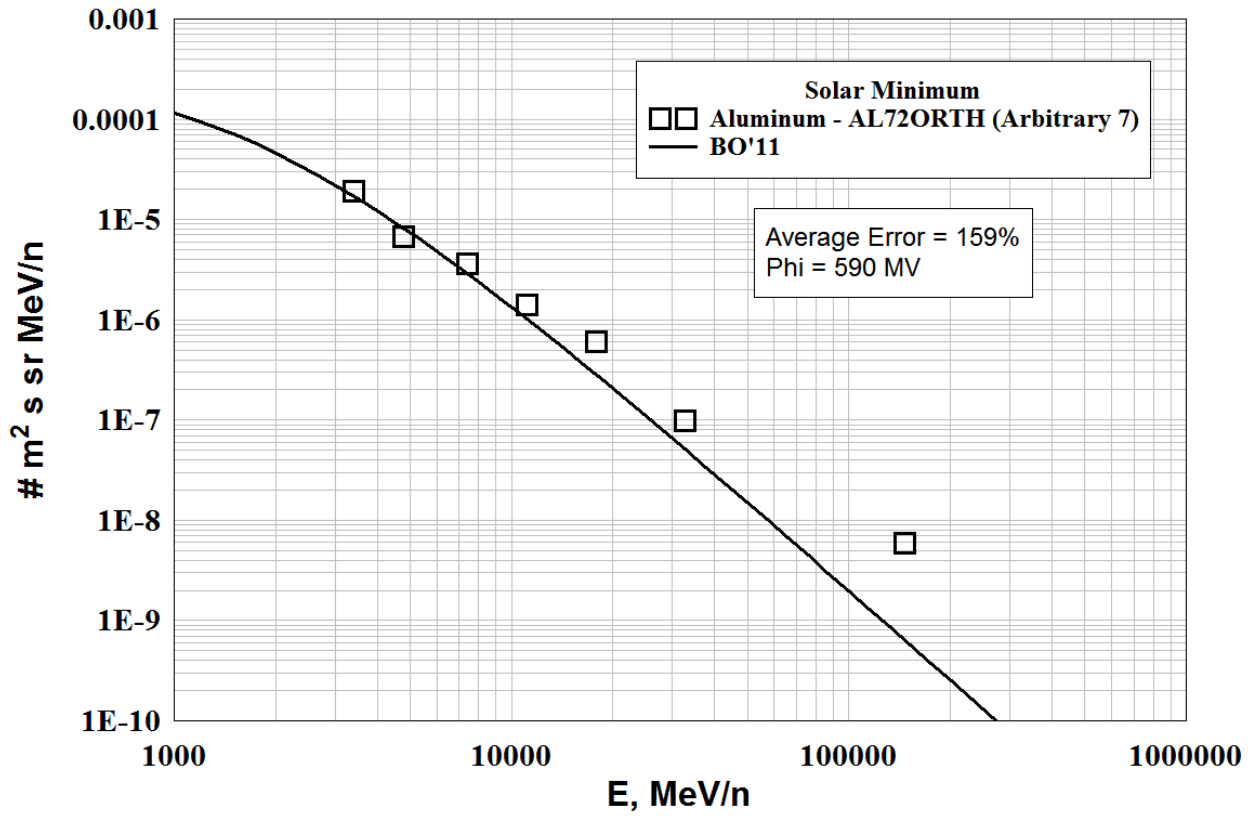






ALUMINUM - High Energy





SILICON - High Energy, Solar Minimum

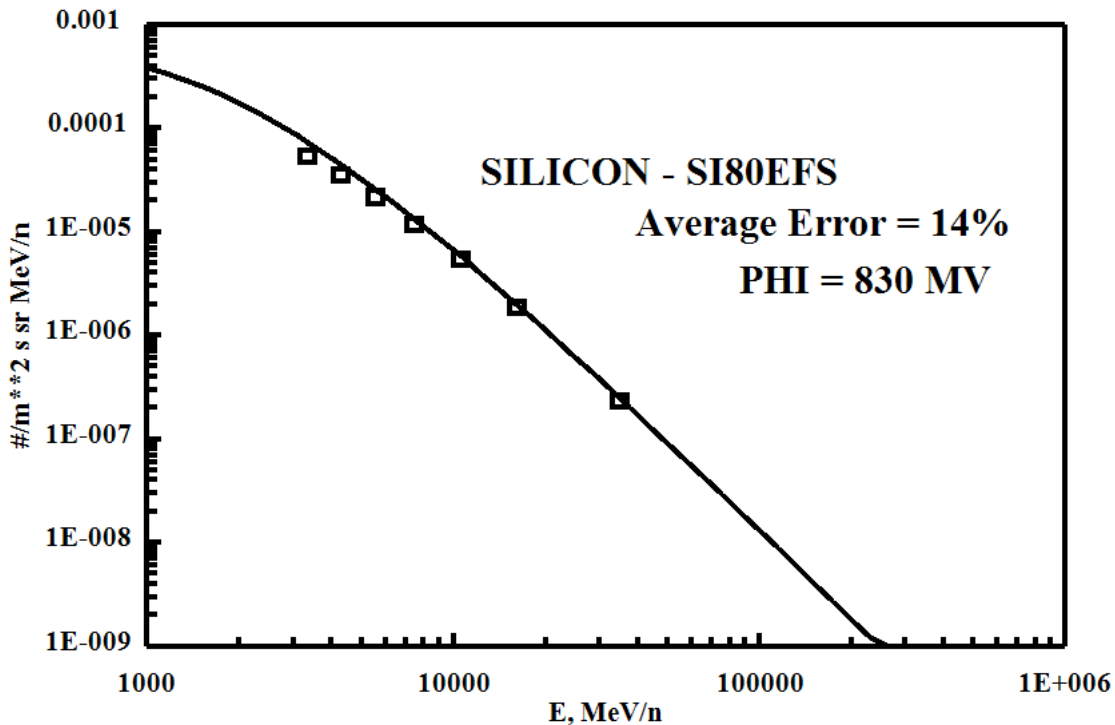
Files Used (Arbitrary 1's)

-----NO FILES-----

SILICON - High Energy, Solar Maximum

Files Used (Arbitrary 1's)

FILE	DATE	PHI (MV)	ERROR=ABS (FLUX-DATA)
SI80EFS.dat	1979.795	830.2713	13.52751
BO AVERAGE ERROR =			13.52751



SILICON - High Energy, Solar Minimum

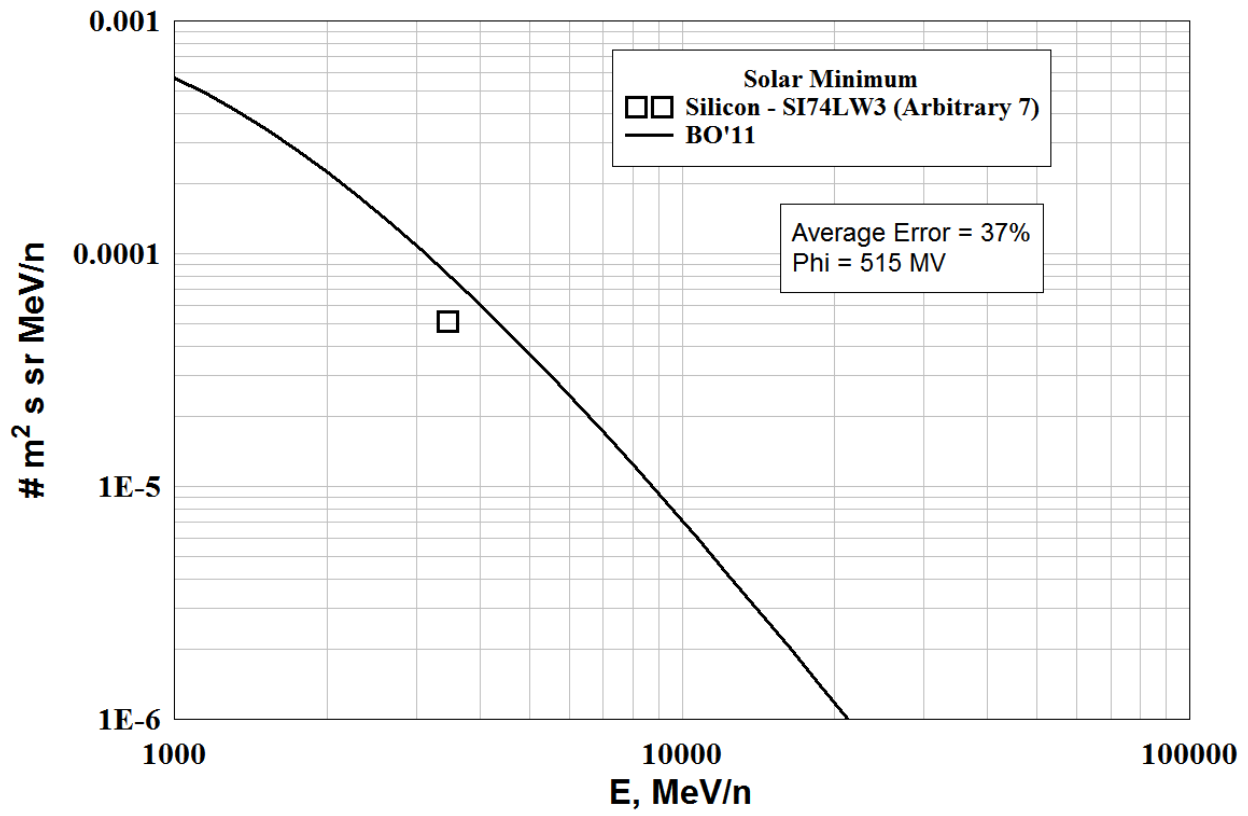
Files Rejected - (Arbitrary 7's)

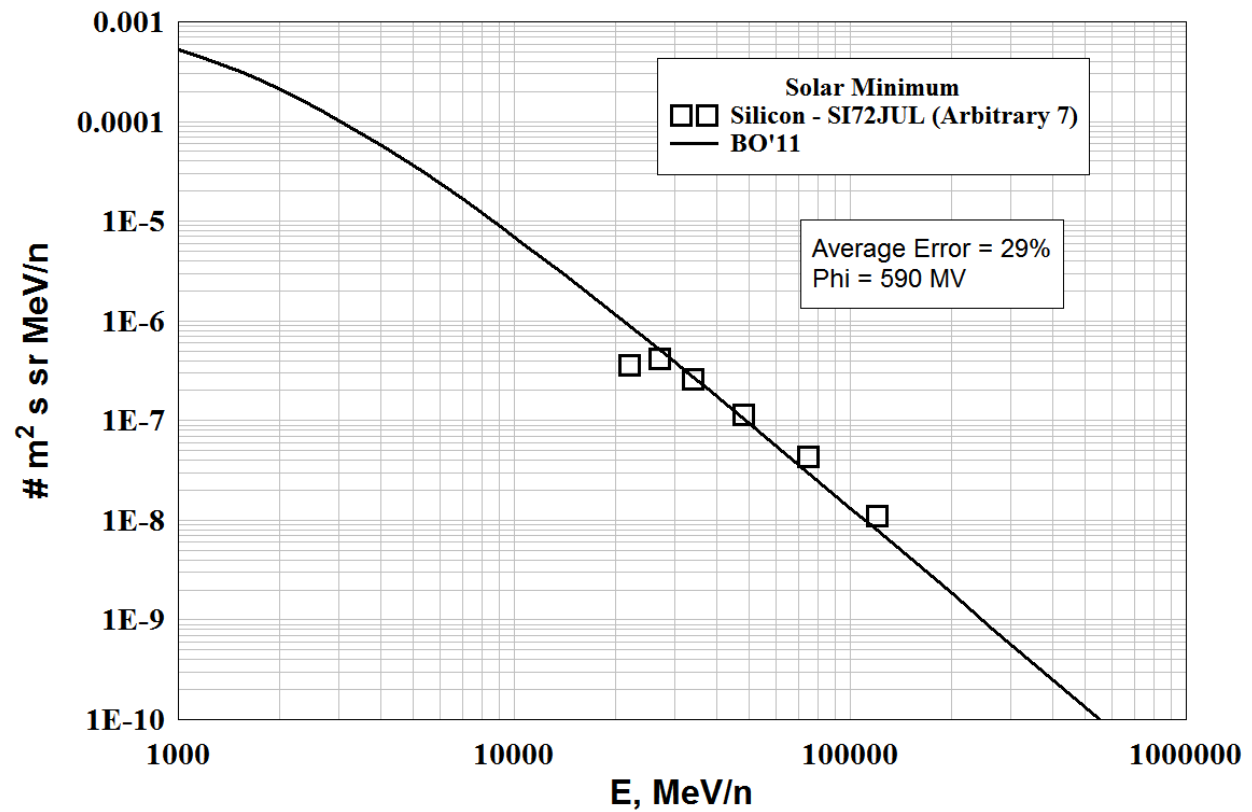
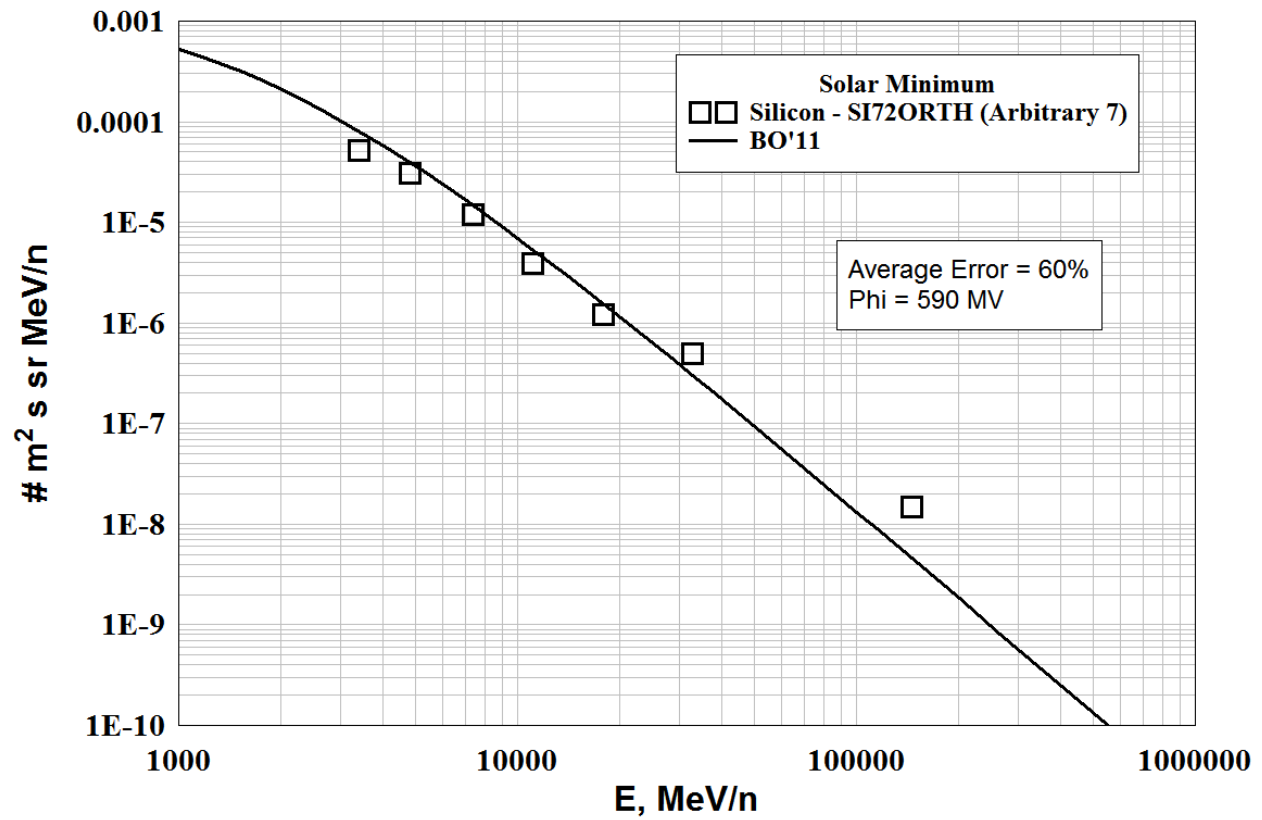
FILE	DATE	PHI (MV)	ERROR=ABS (FLUX-DATA)
SI74LW3.dat	1974.553	515.0297	37.47513
SI72Orth.dat	1972.748	590.3618	60.49501
SI72Jul.dat	1972.751	590.1960	29.15157
BO AVERAGE ERROR =			42.37391

SILICON - High Energy, Solar Maximum

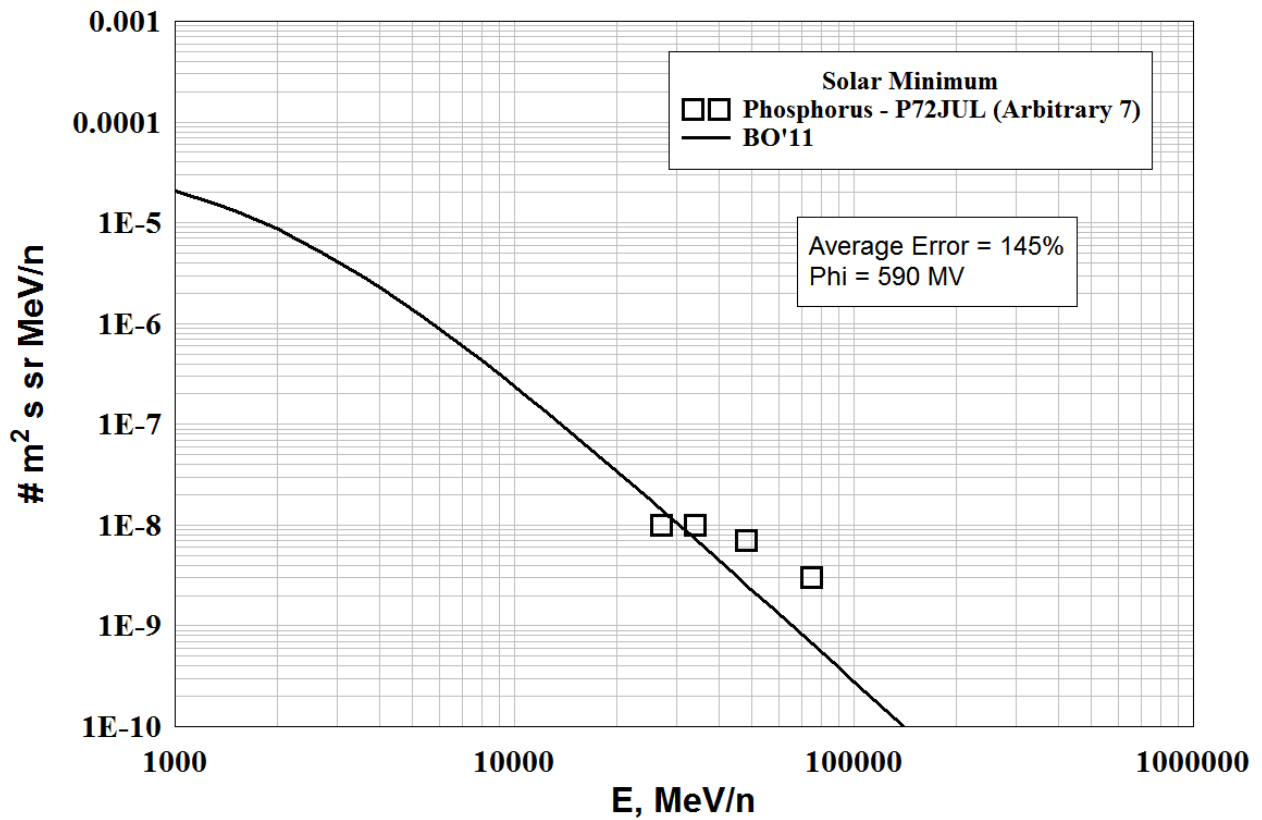
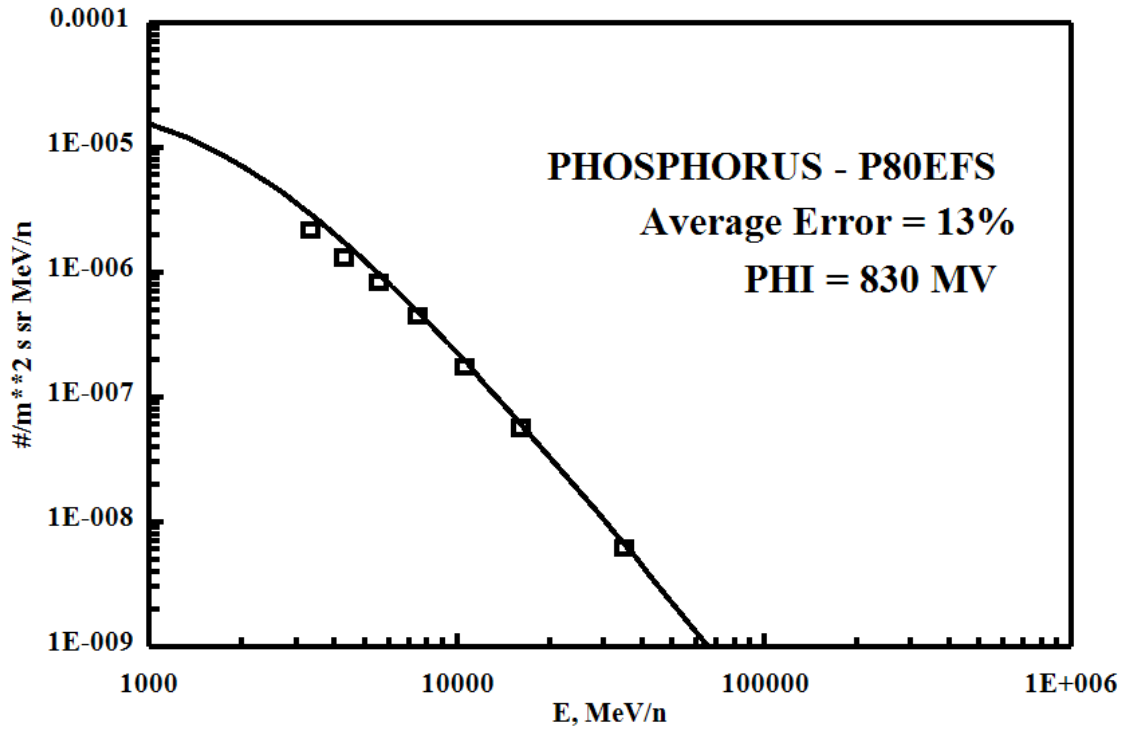
Files Rejected - (Arbitrary 7's)

-----NO FILES-----

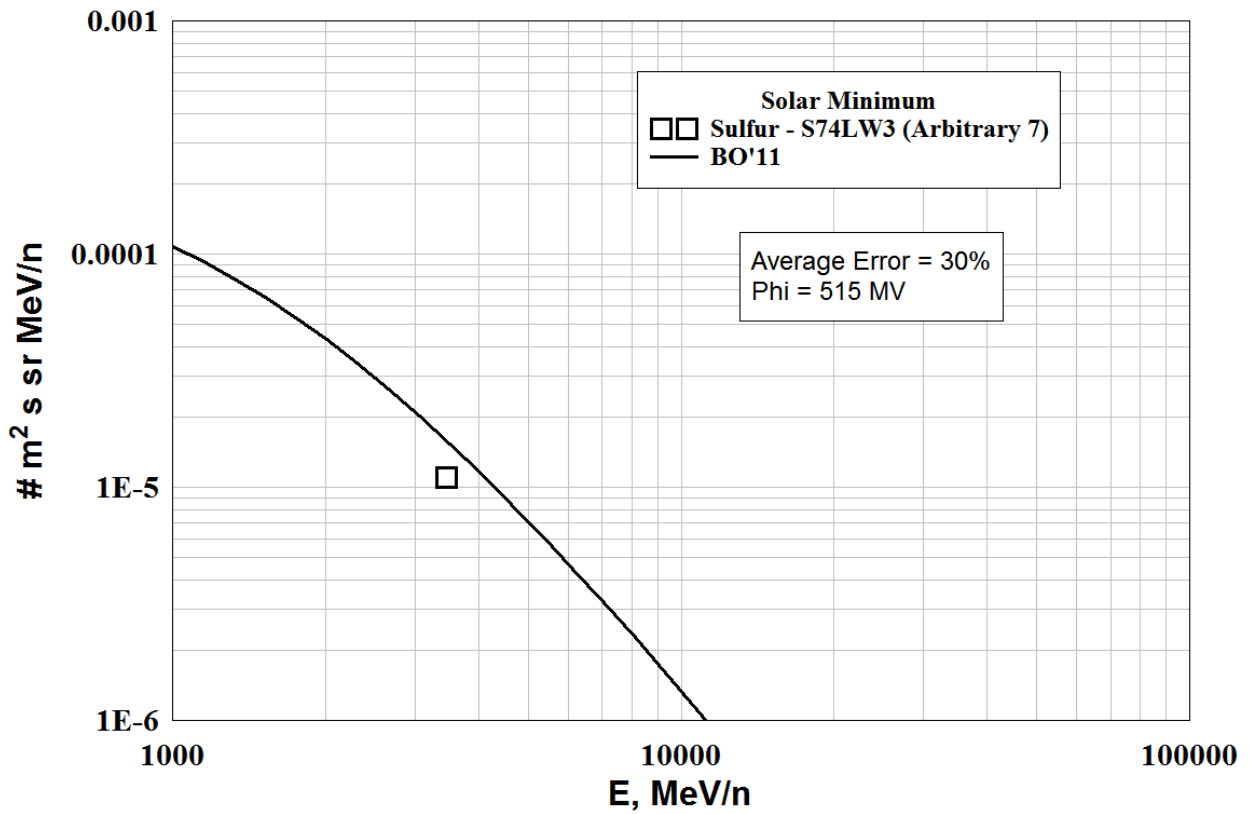
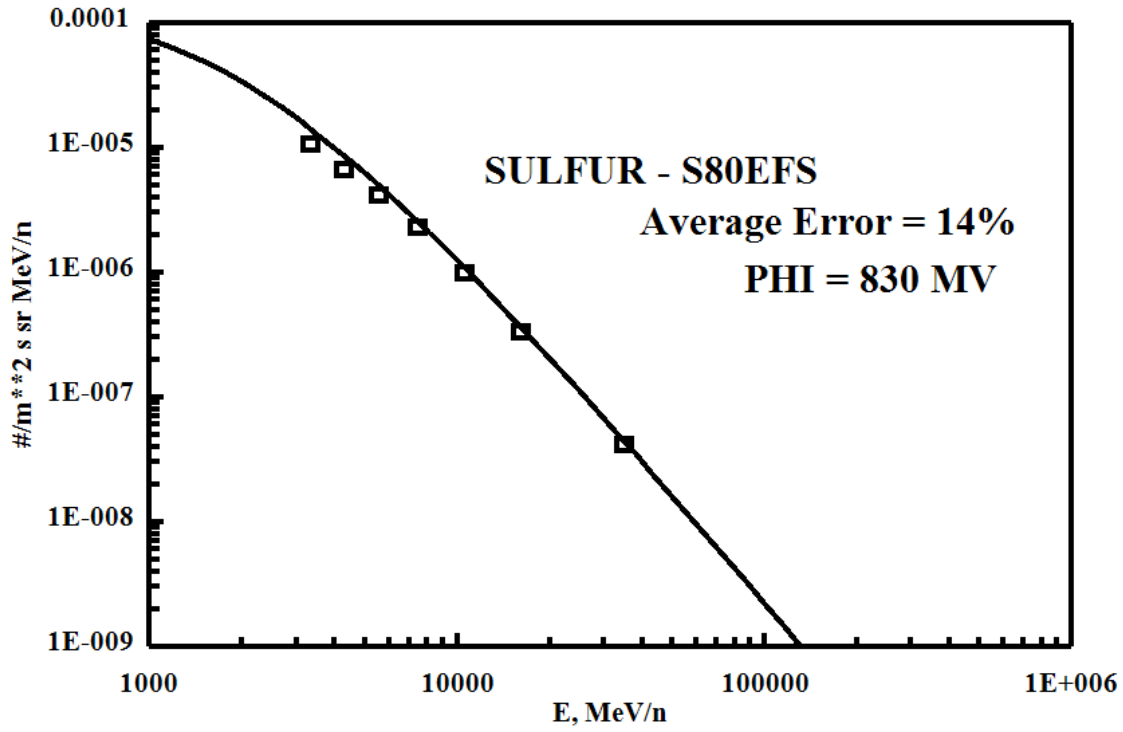


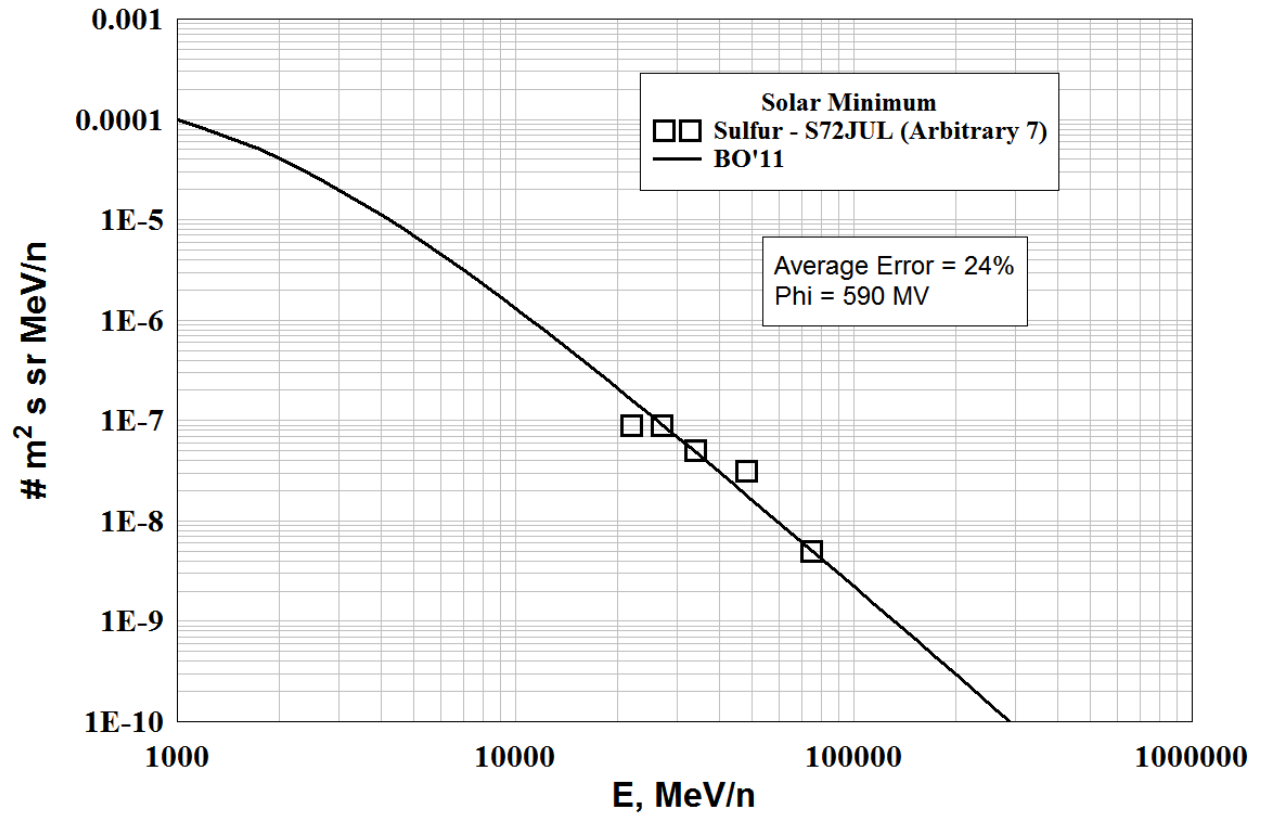


PHOSPHORUS - High Energy

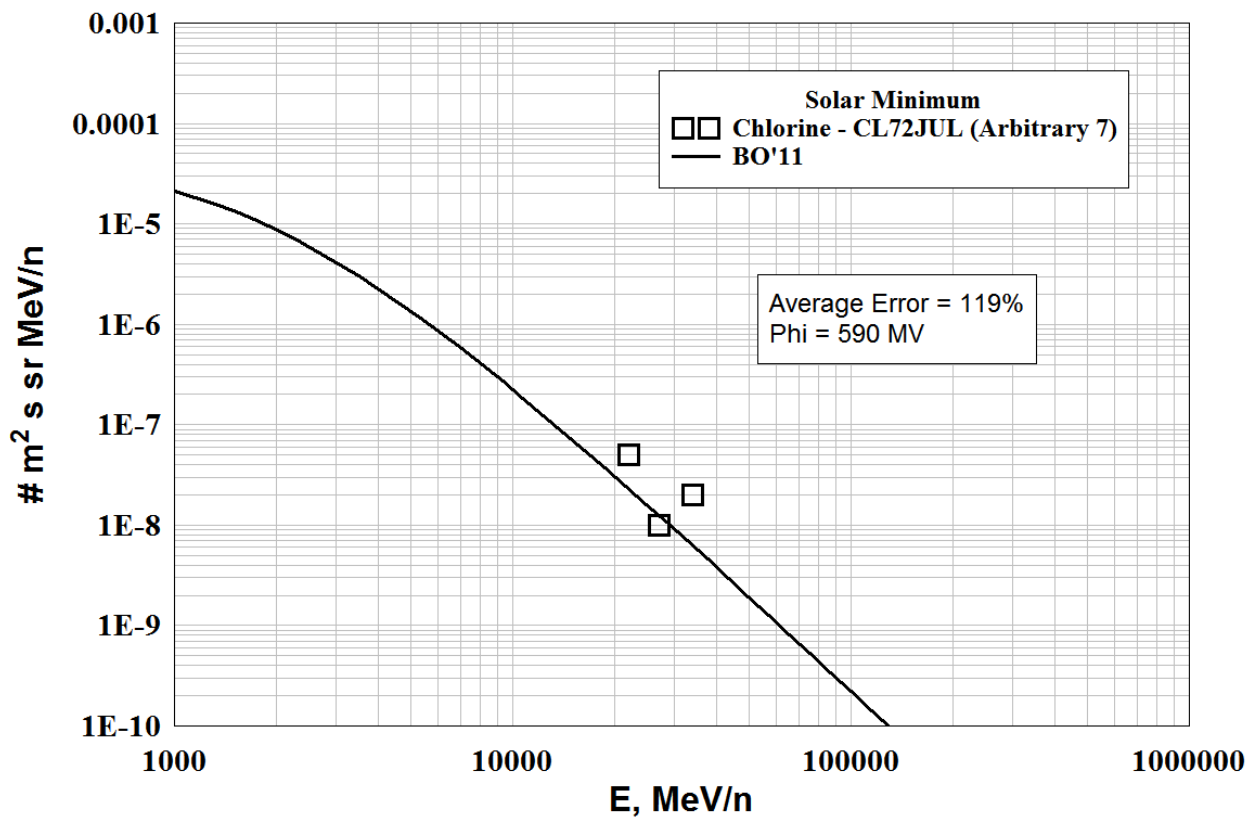
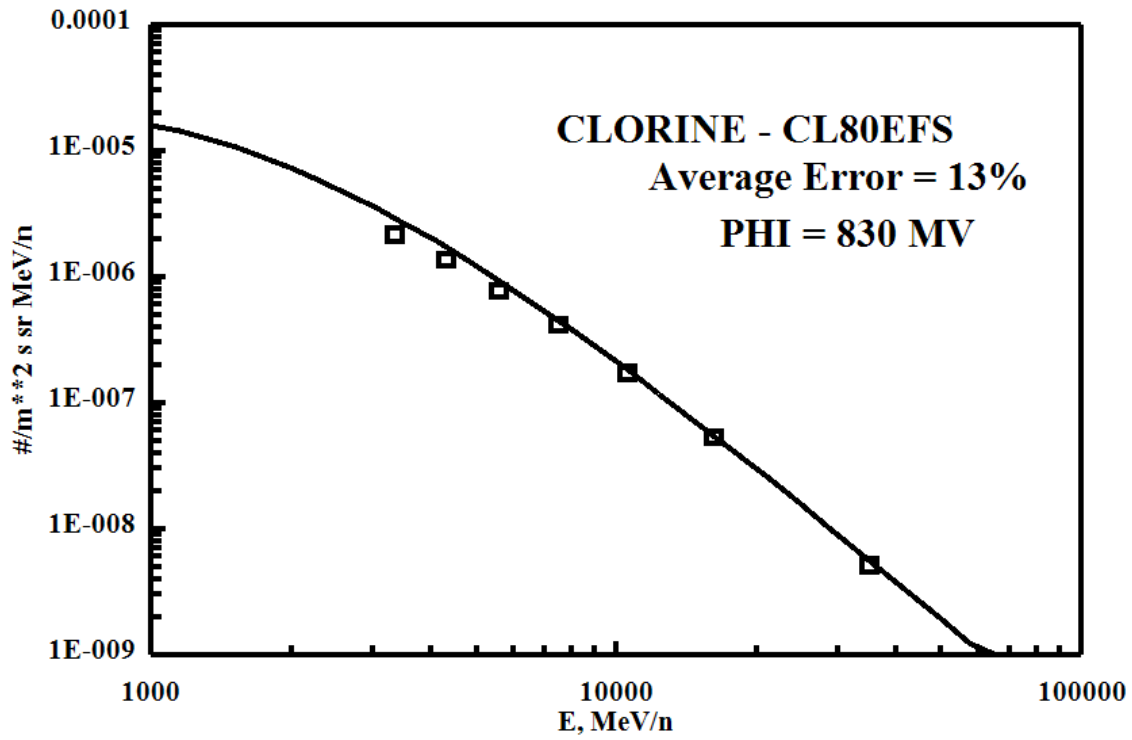


SULFUR - High Energy

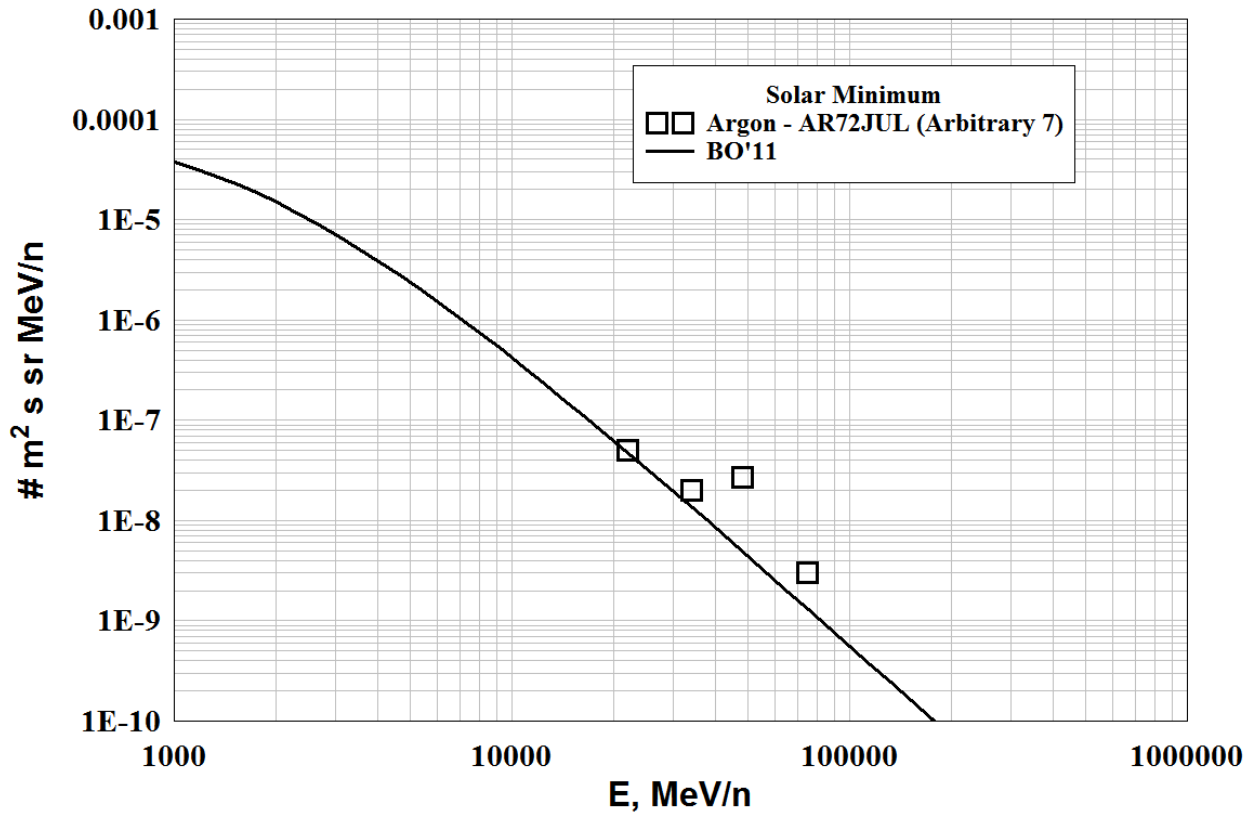
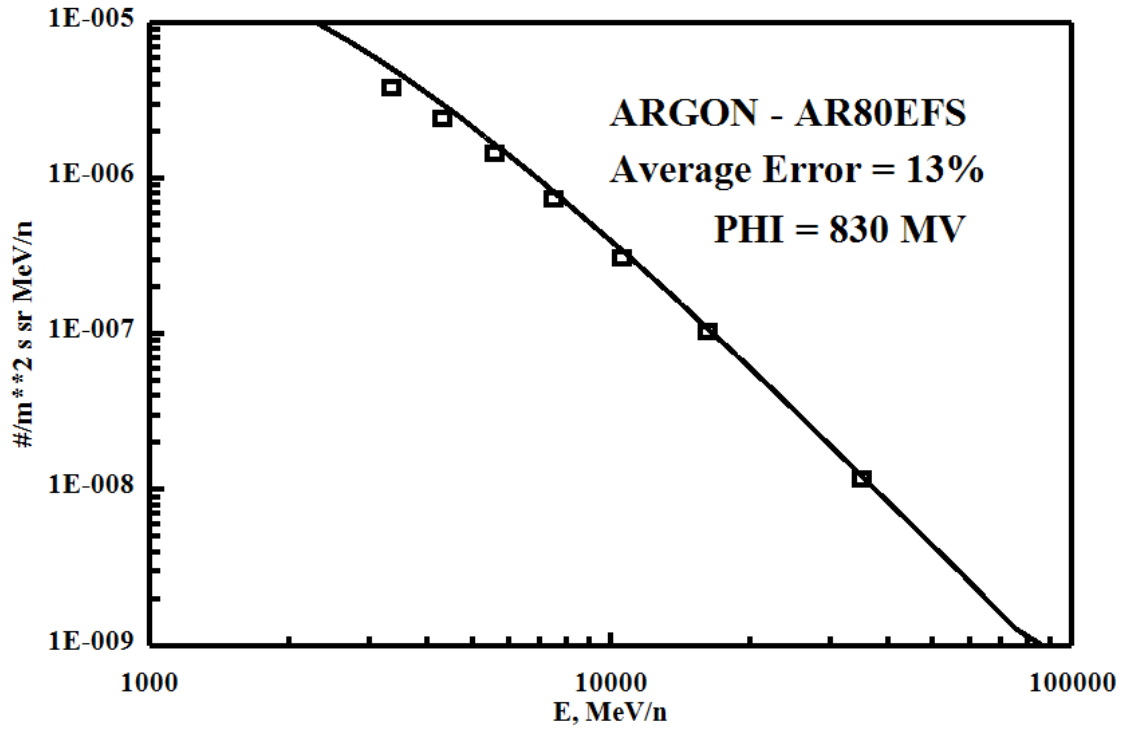




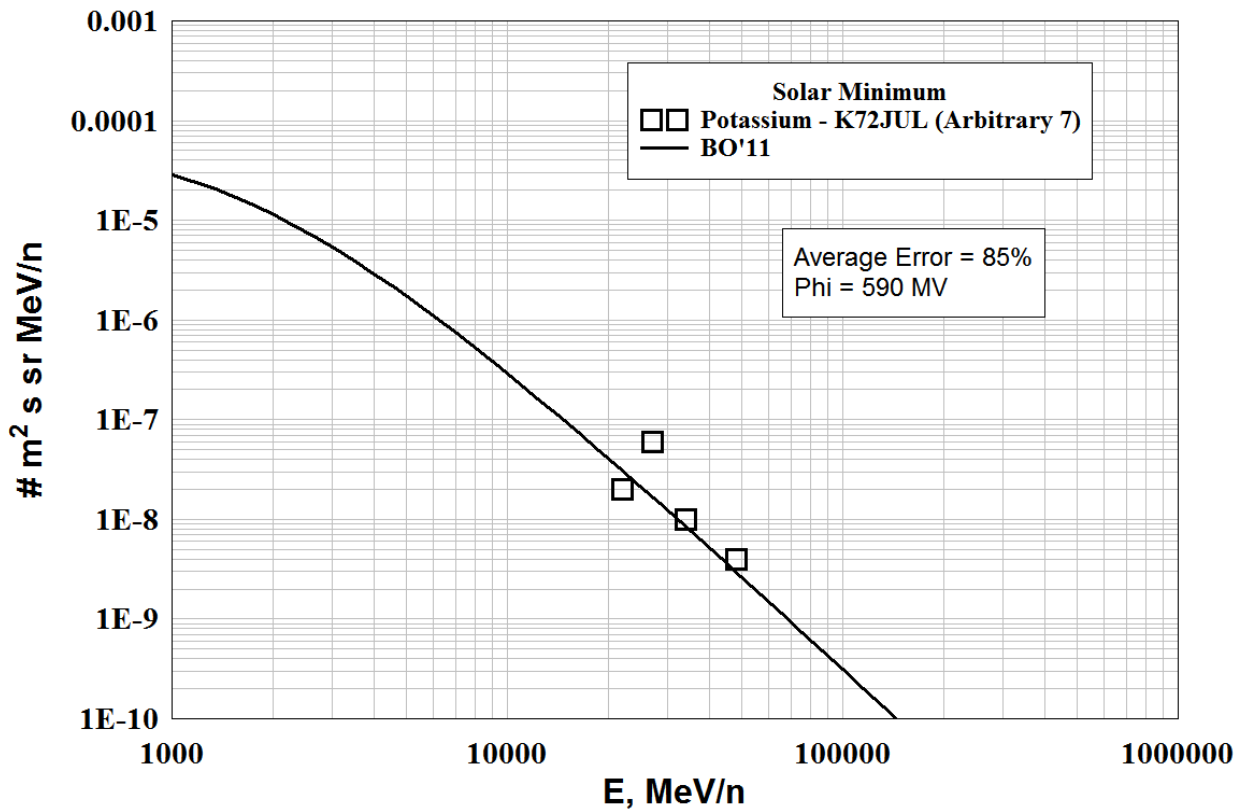
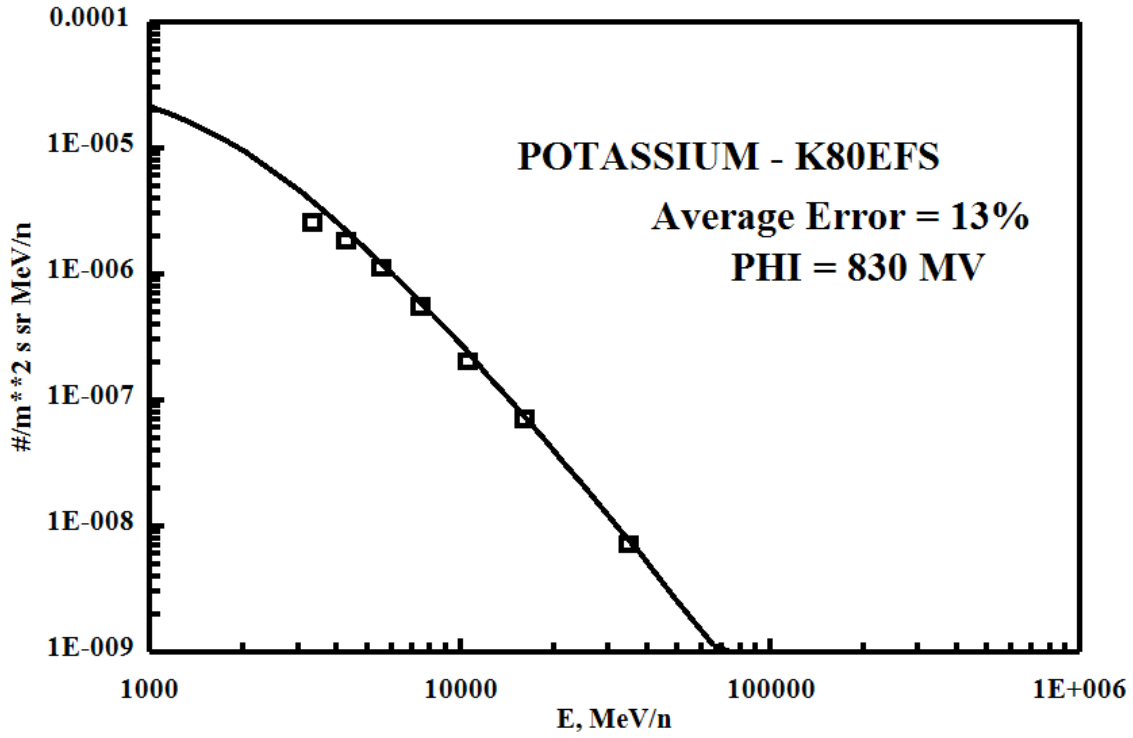
CLORINE - High Energy



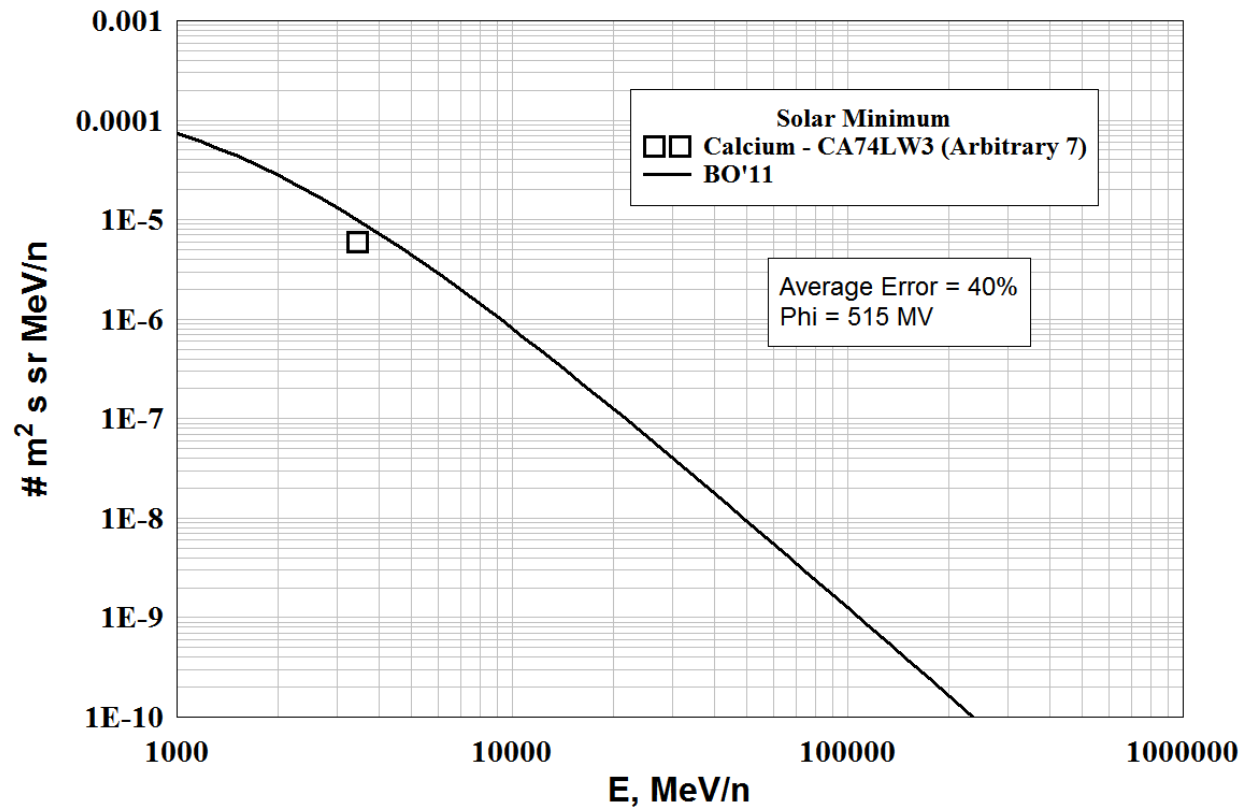
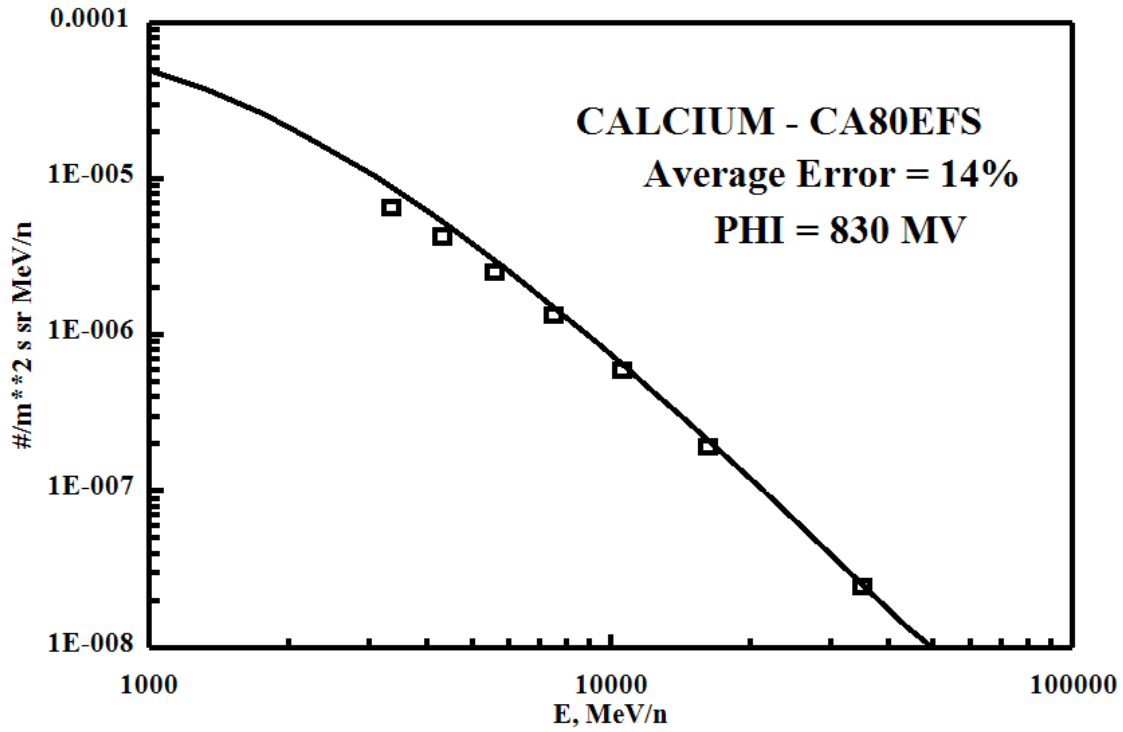
ARGON - High Energy

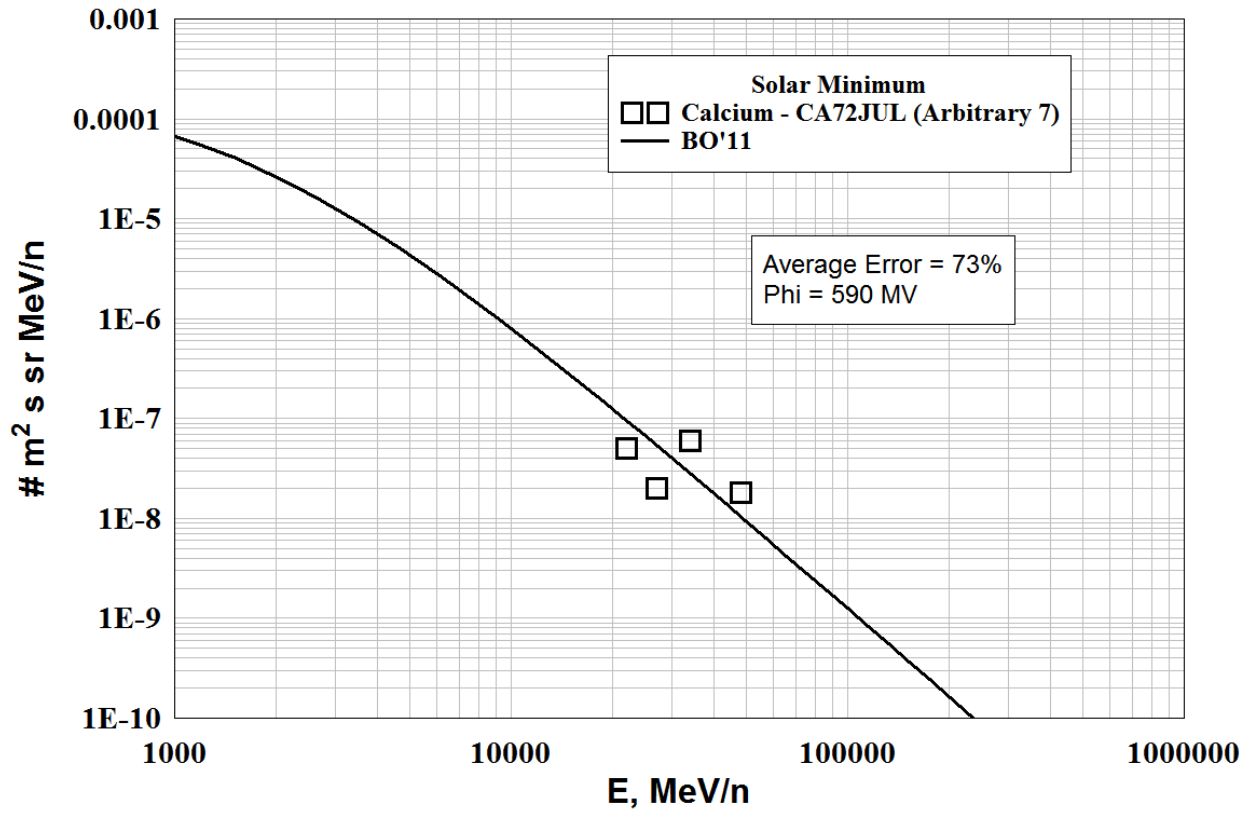


POTASSIUM - High Energy

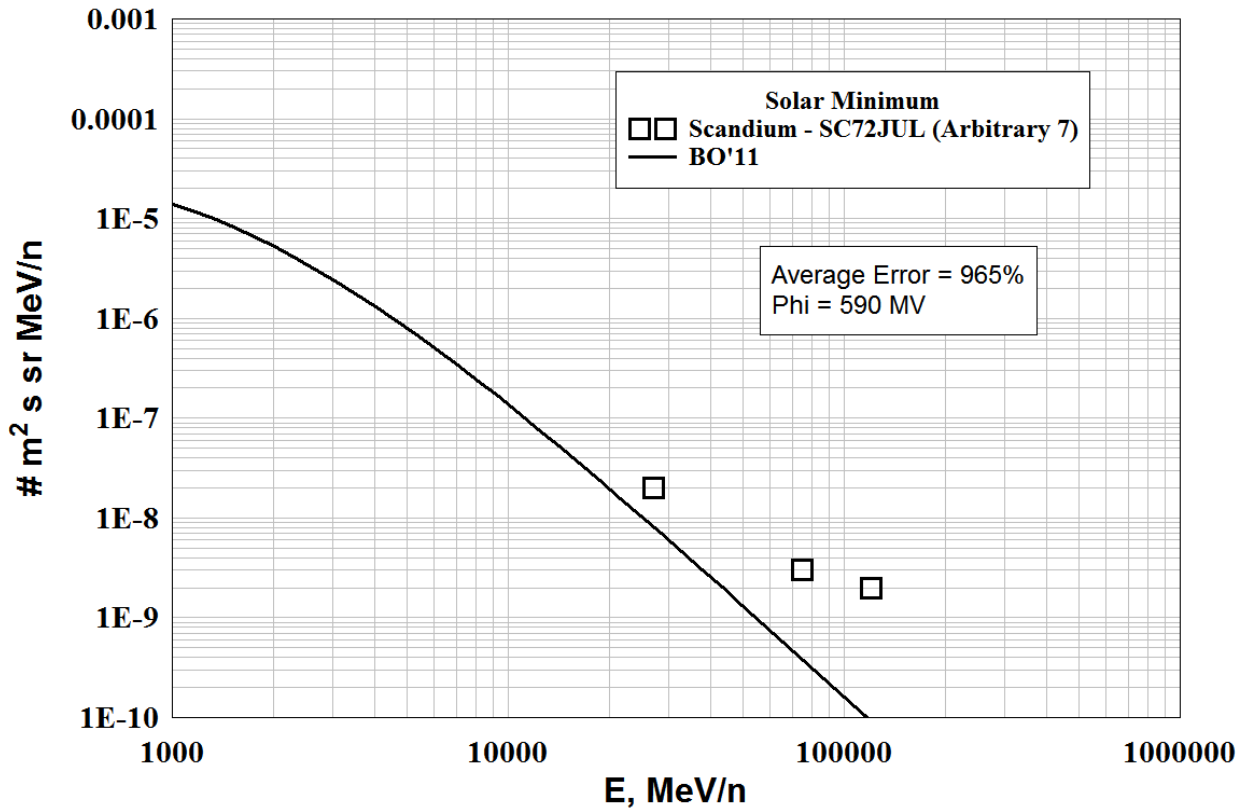
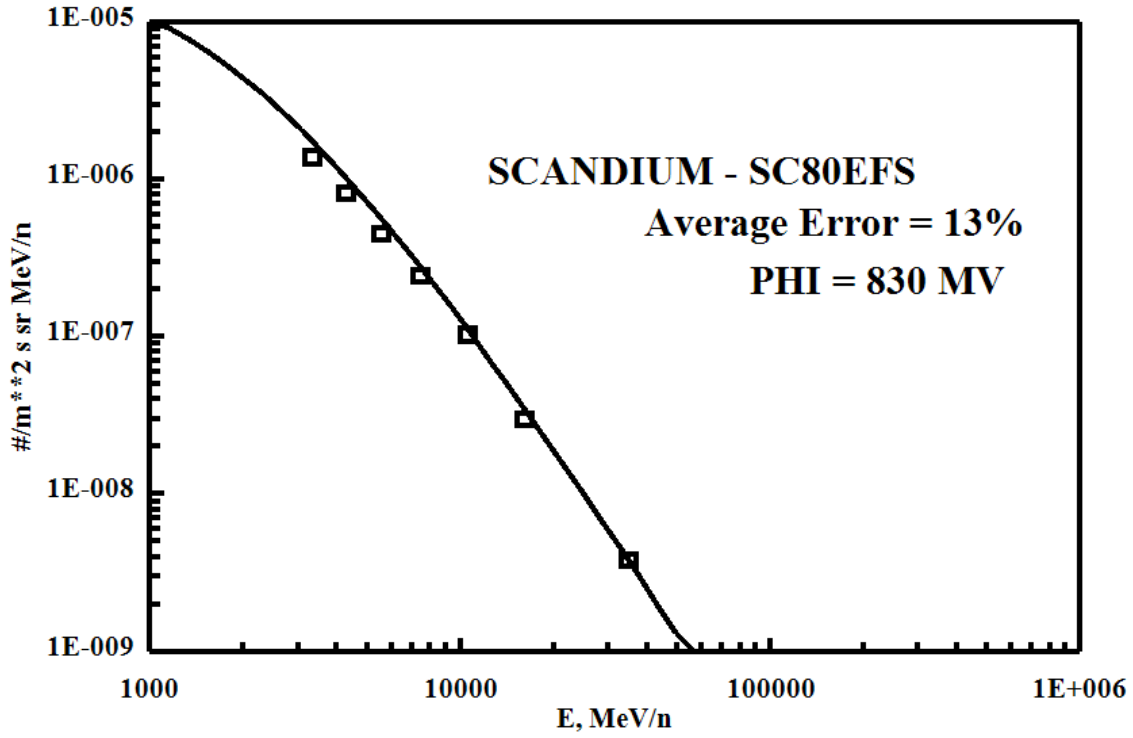


CALCIUM - High Energy

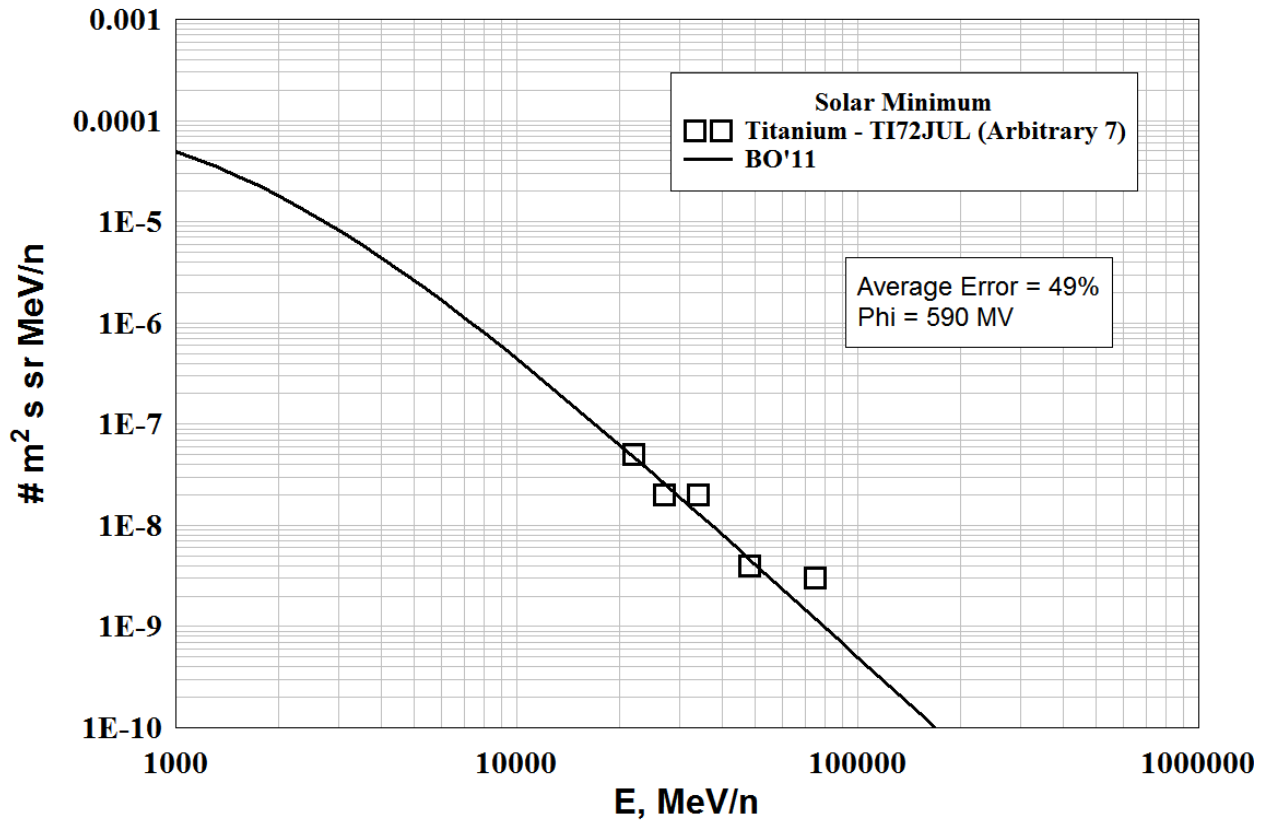
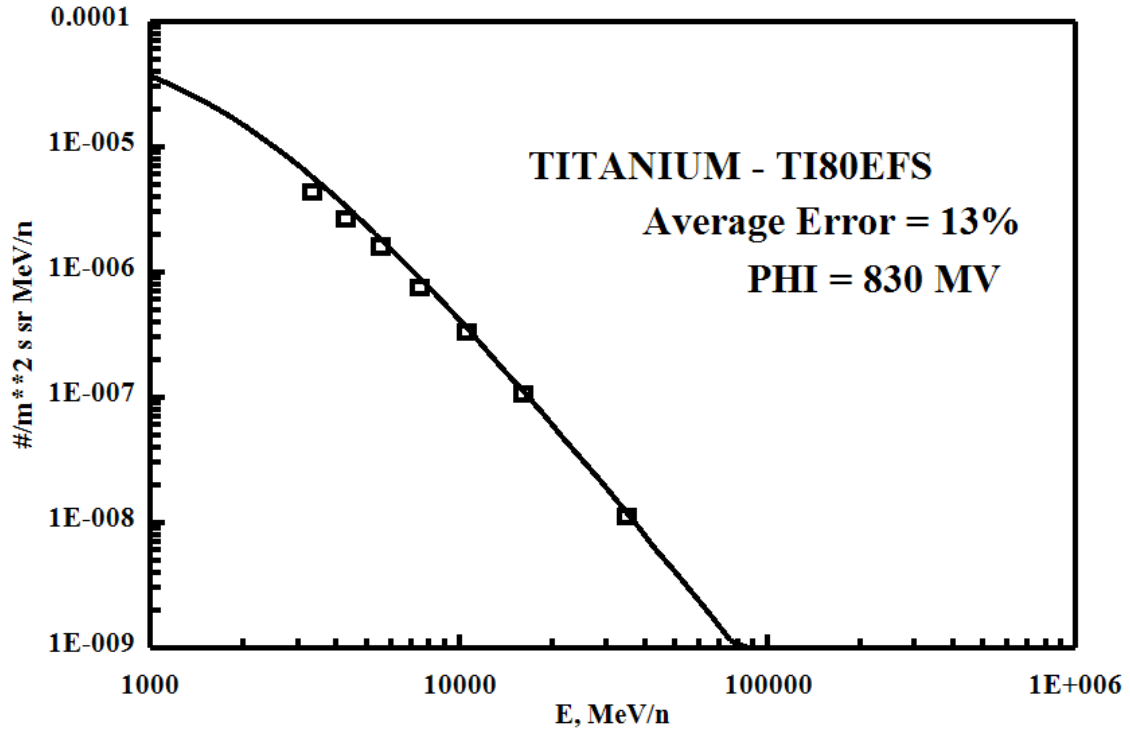




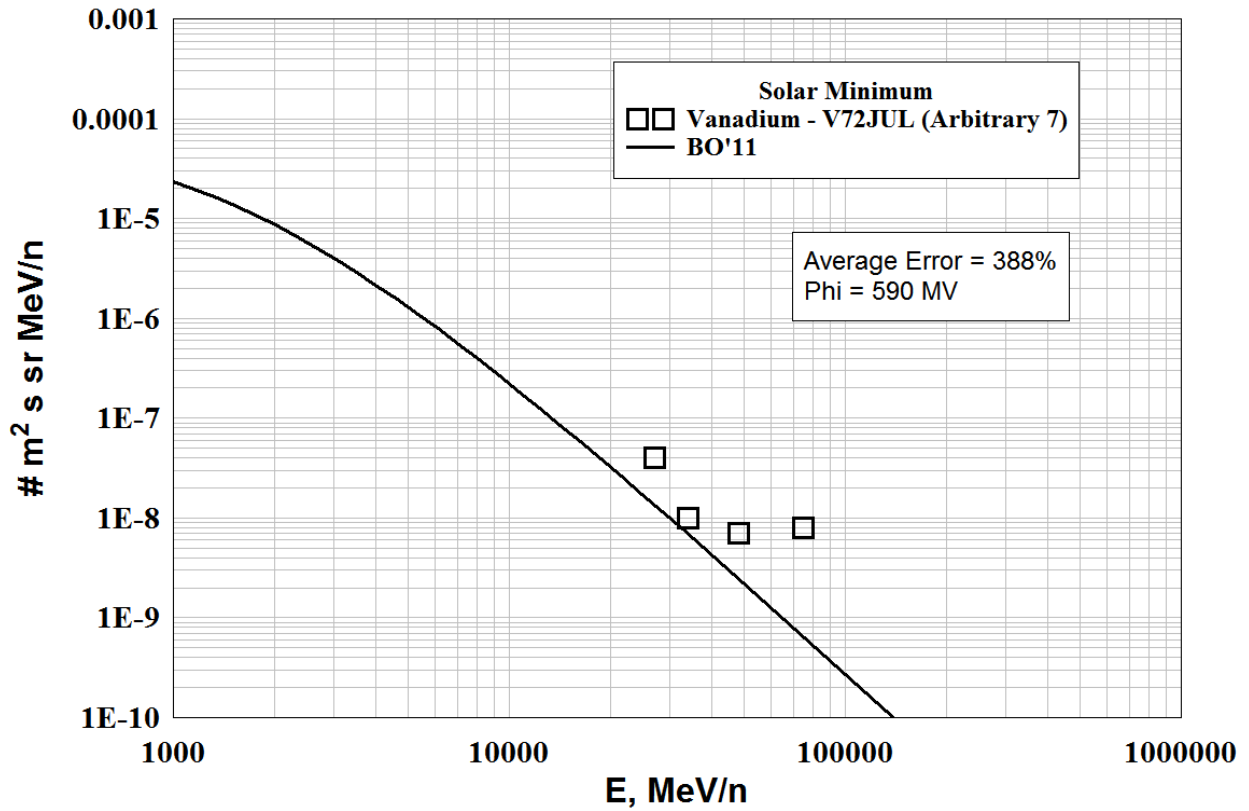
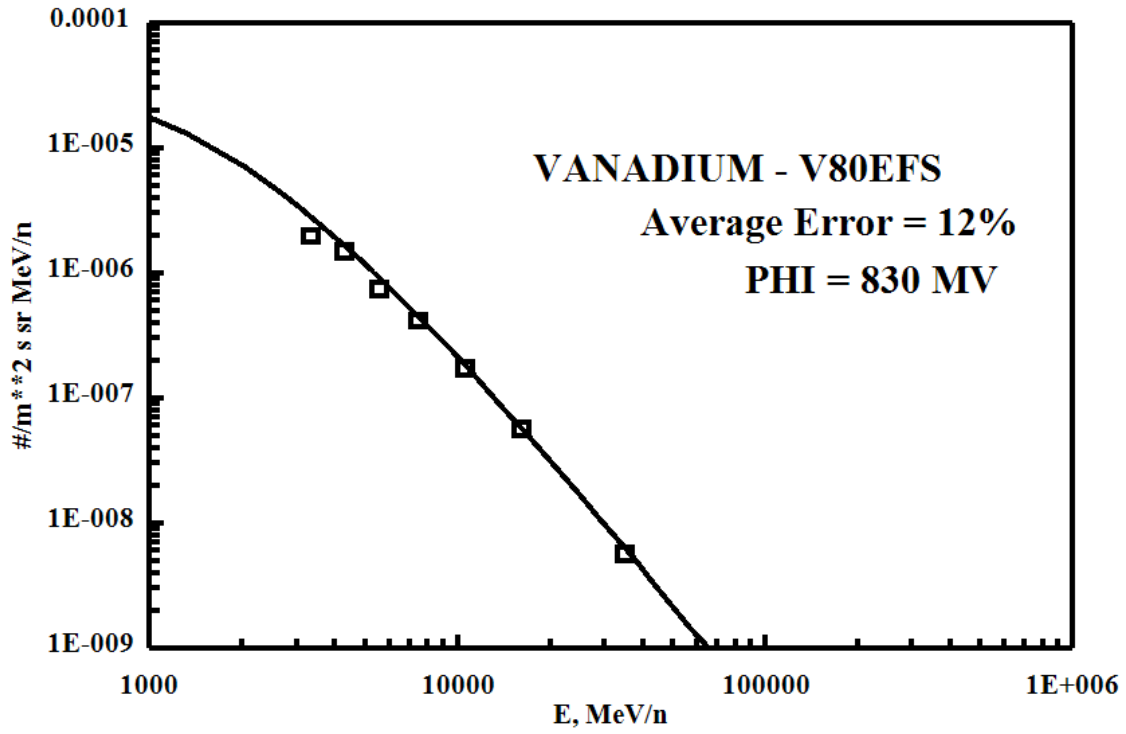
SCANDIUM - High Energy



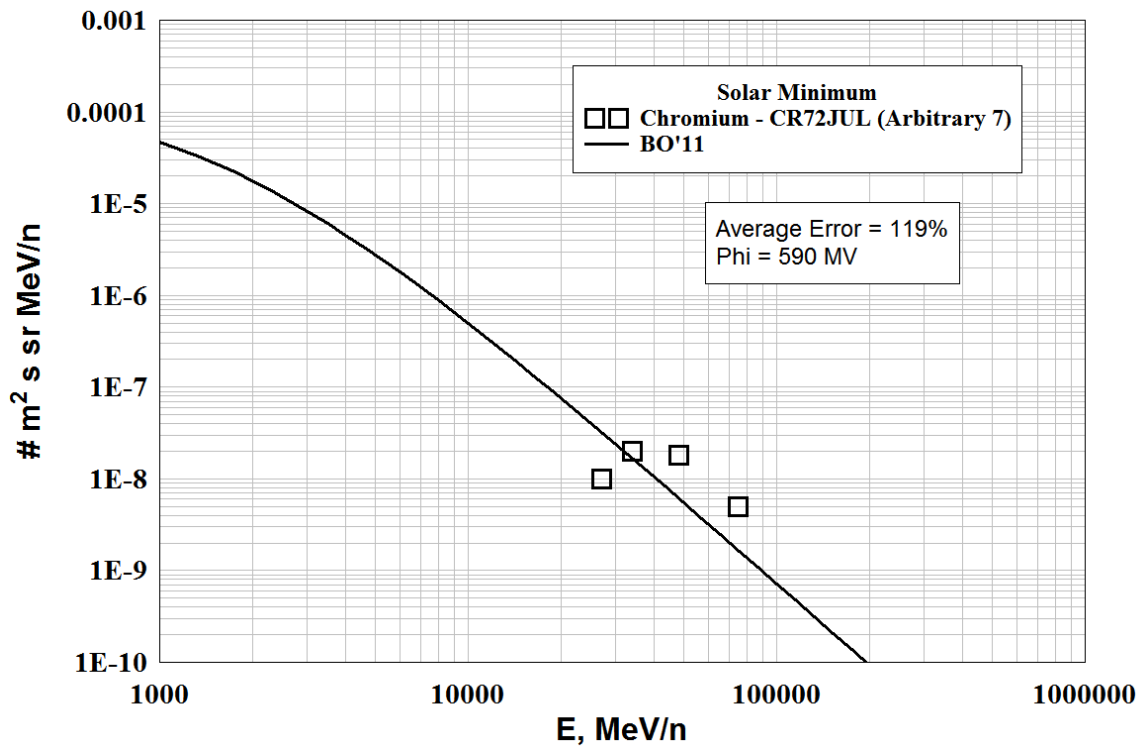
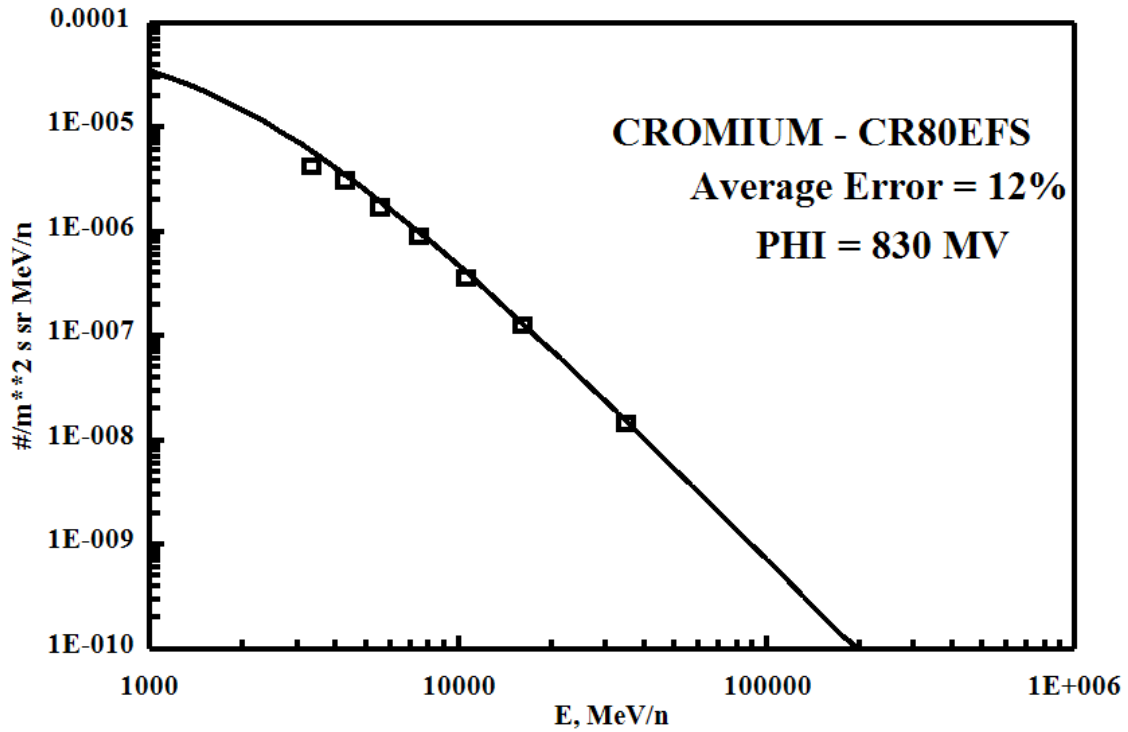
TITANIUM - High Energy



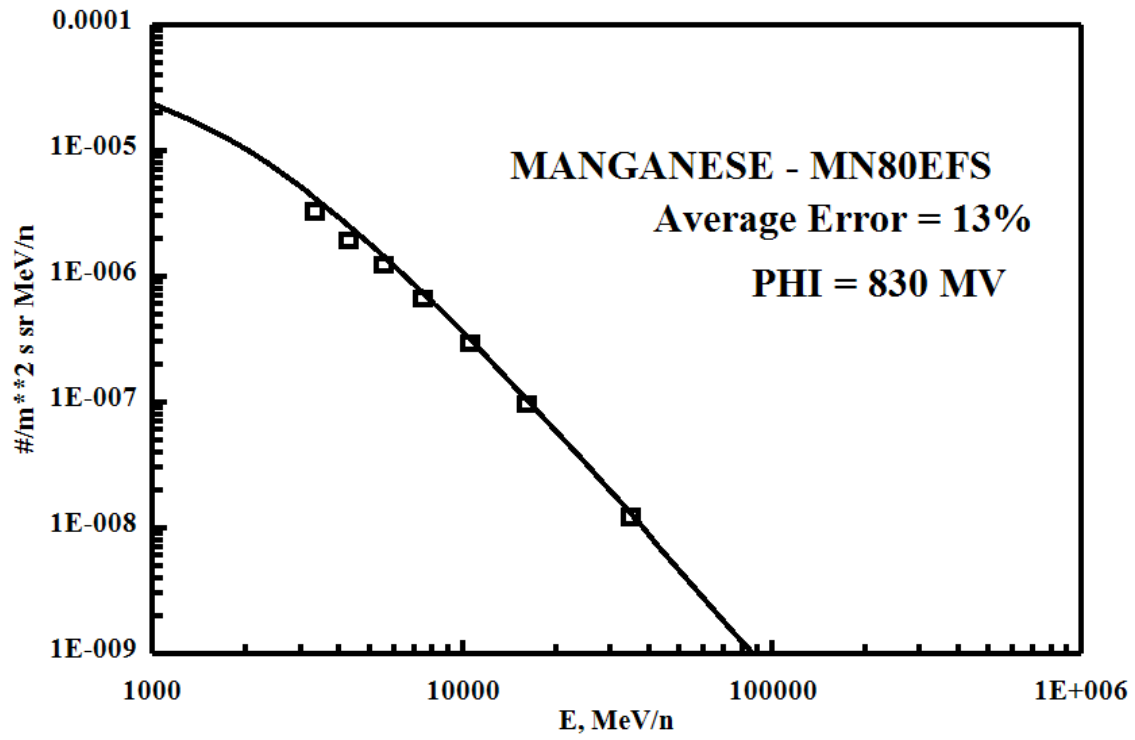
VANADIUM - High Energy



CHROMIUM - High Energy



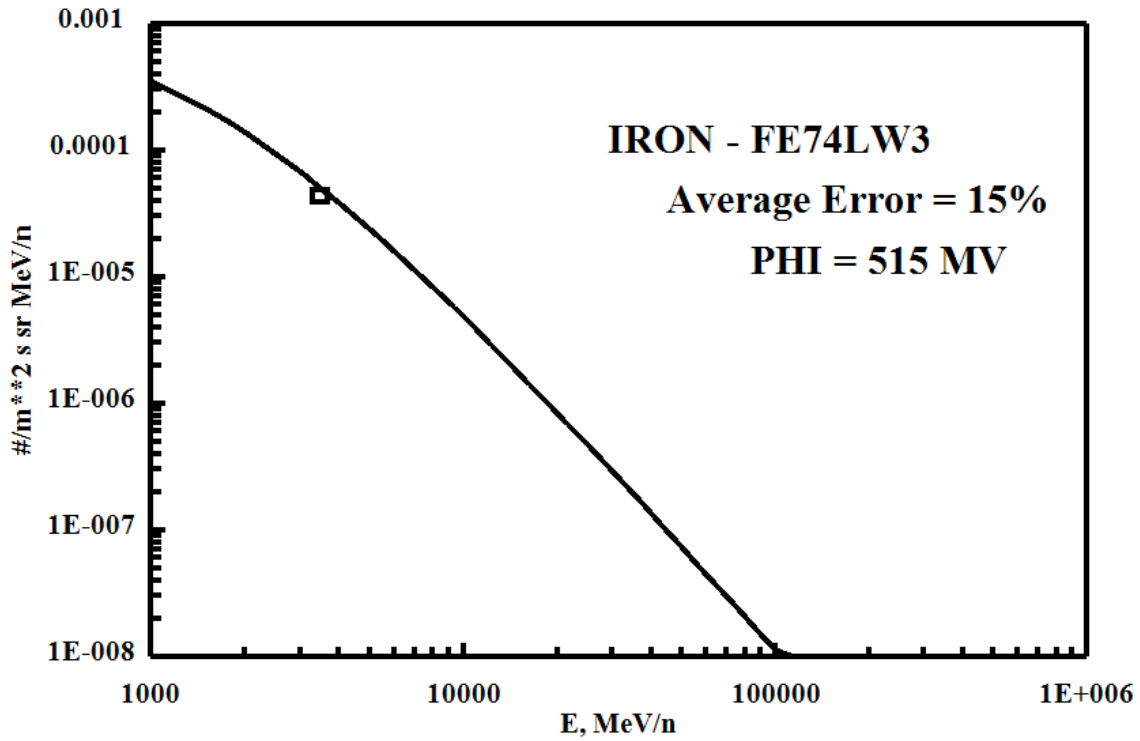
MANGANESE - High Energy

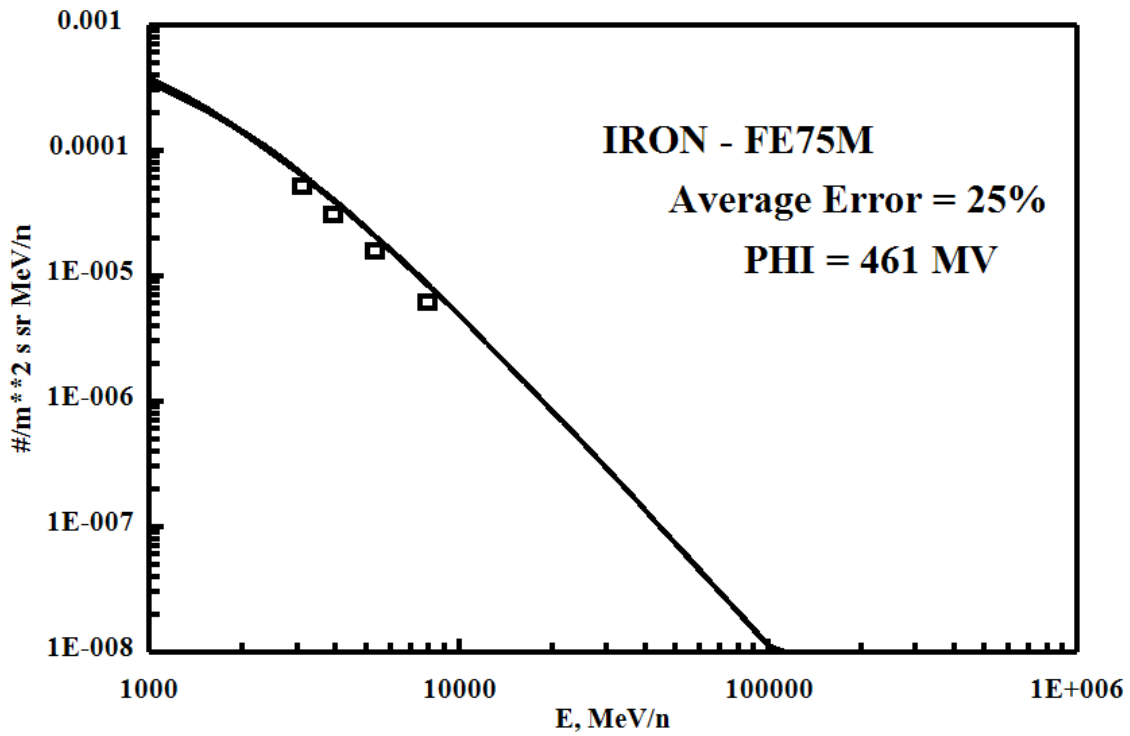
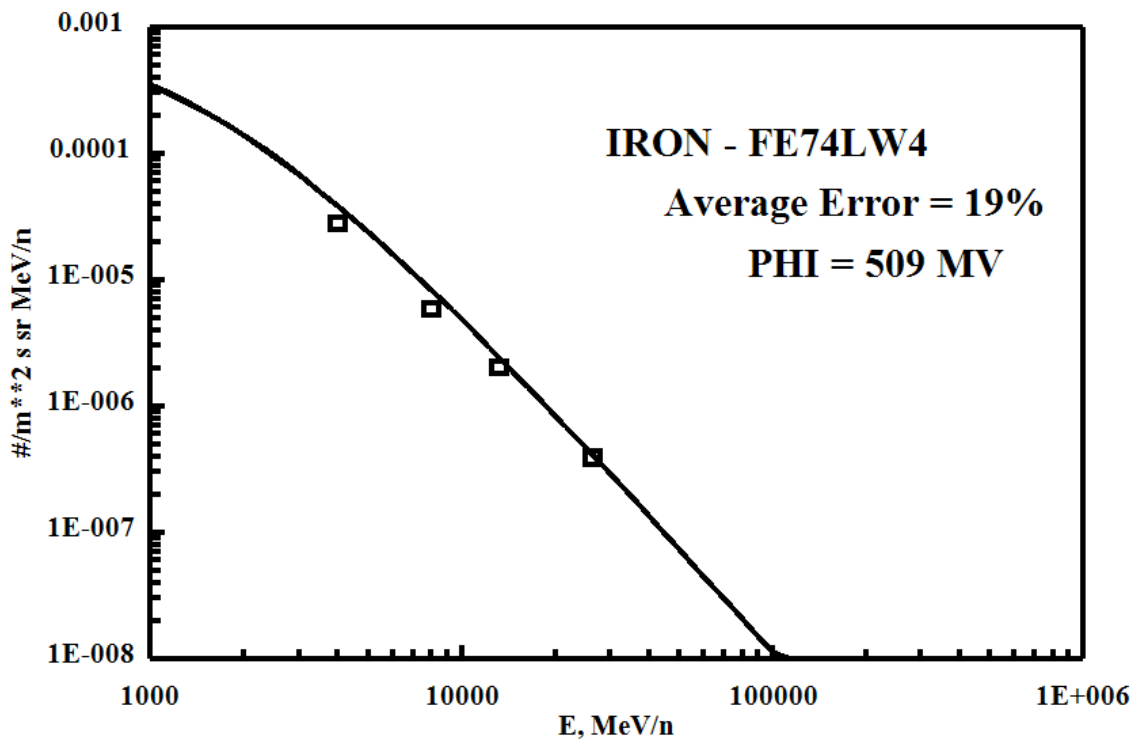


IRON - High Energy, Solar Minimum

Files Used (Arbitrary 1's)

FILE	DATE	PHI (MV)	ERROR=ABS (FLUX-DATA)
Fe74LW3.dat	1974.553	515.0297	15.00534
Fe74LW4.dat	1974.726	509.2871	19.22553
Fe75M.dat	1975.740	461.3481	24.97471
BO AVERAGE ERROR =			19.73519

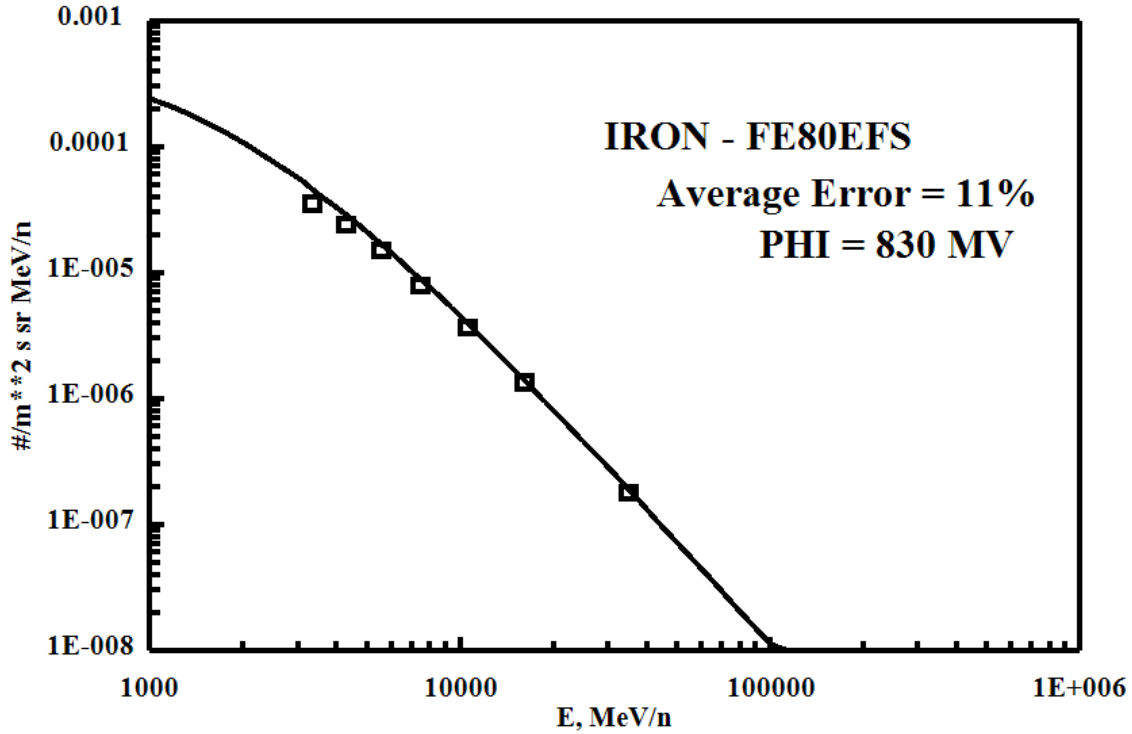




IRON - High Energy, Solar Minimum

Files Used (Arbitrary 1's)

FILE	DATE	PHI (MV)	ERROR=ABS (FLUX-DATA)
Fe80EFS.dat	1979.795	830.2713	11.20485
BO AVERAGE ERROR =			11.20485



IRON - High Energy, Solar Minimum

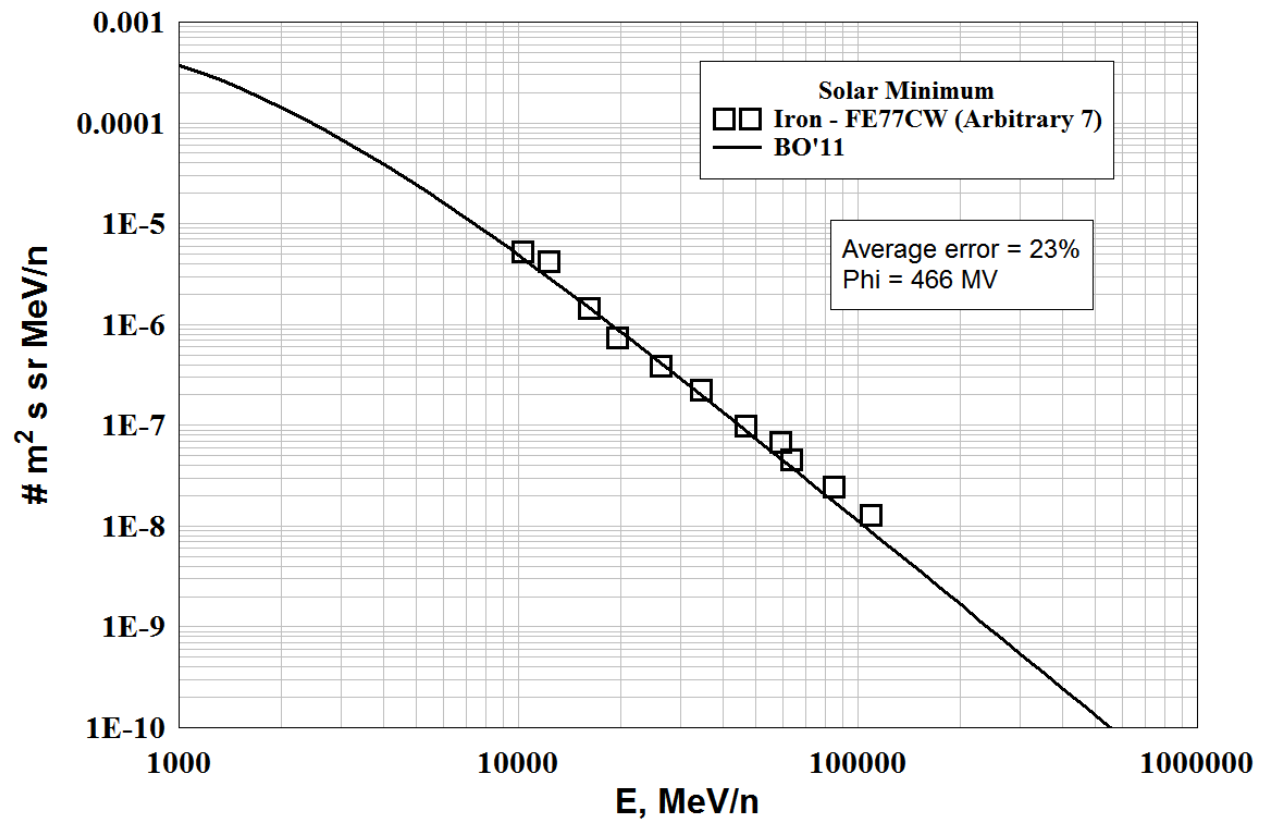
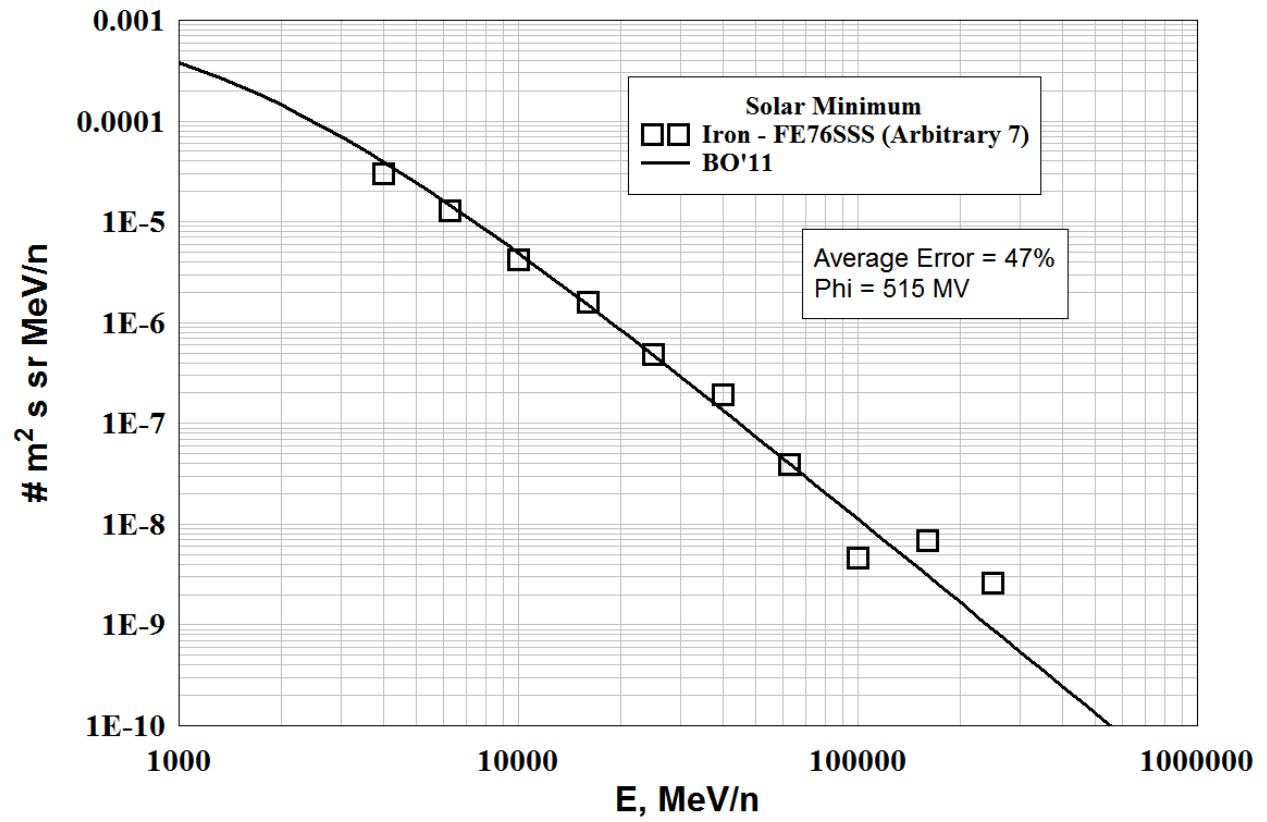
Files Rejected - (Arbitrary 7's)

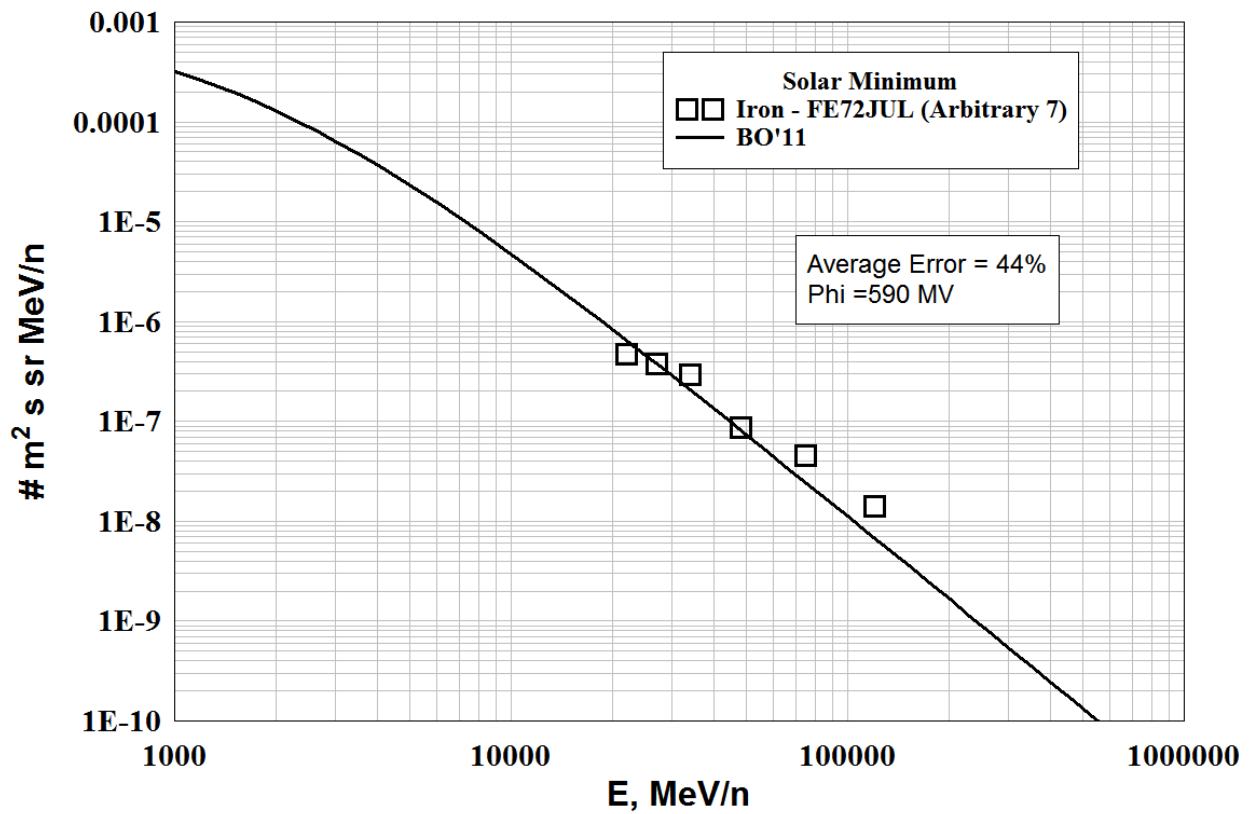
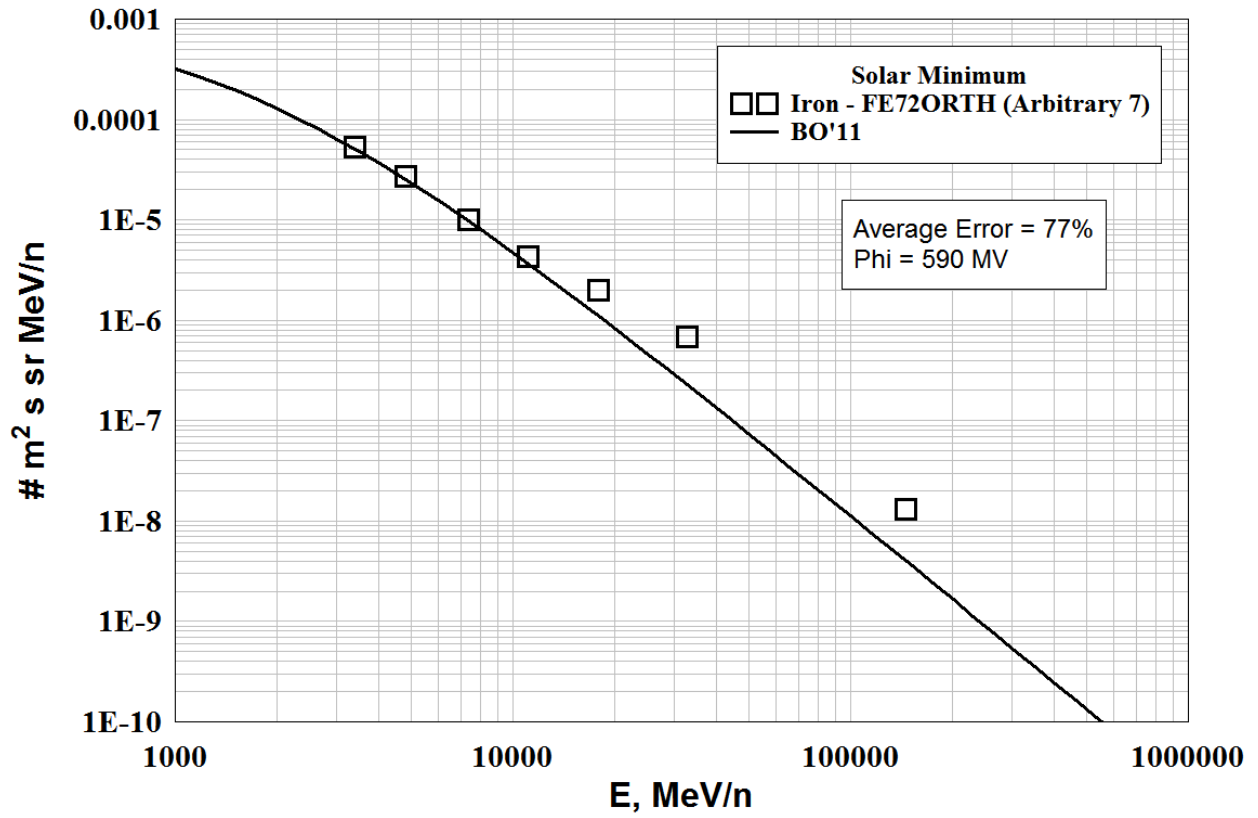
FILE	DATE	PHI (MV)	ERROR=ABS (FLUX-DATA)
Fe76SSS.dat	1976.789	456.1017	46.58792
Fe77CW.dat	1976.000	465.6418	23.15557
Fe72Orth.dat	1972.748	590.3618	77.43135
Fe72Jul.dat	1972.751	590.1960	43.69837
BO AVERAGE ERROR =			47.71830

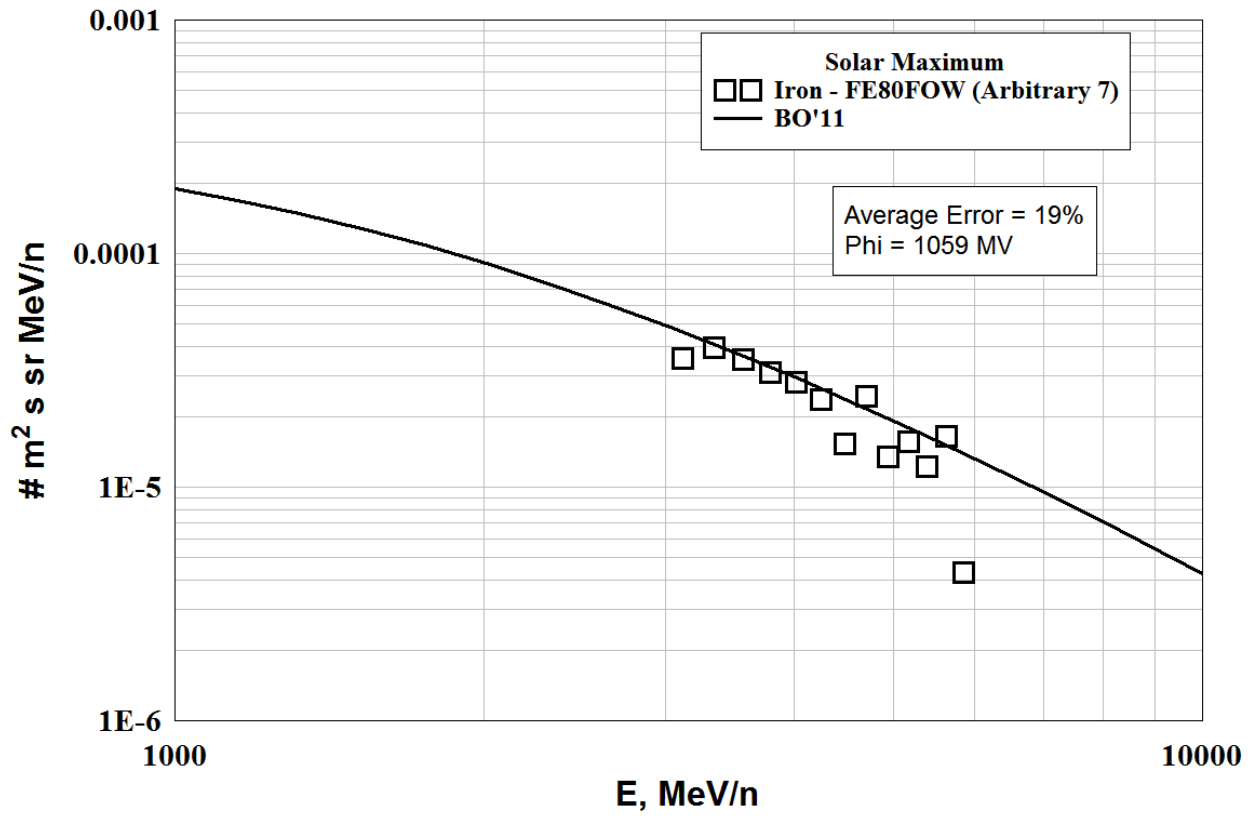
IRON - High Energy, Solar Maximum

Files Rejected - (Arbitrary 7's)

FILE	DATE	PHI (MV)	ERROR=ABS (FLUX-DATA)
Fe80FOW.dat	1979.416	1059.079	19.21520
BO AVERAGE ERROR =			19.21520

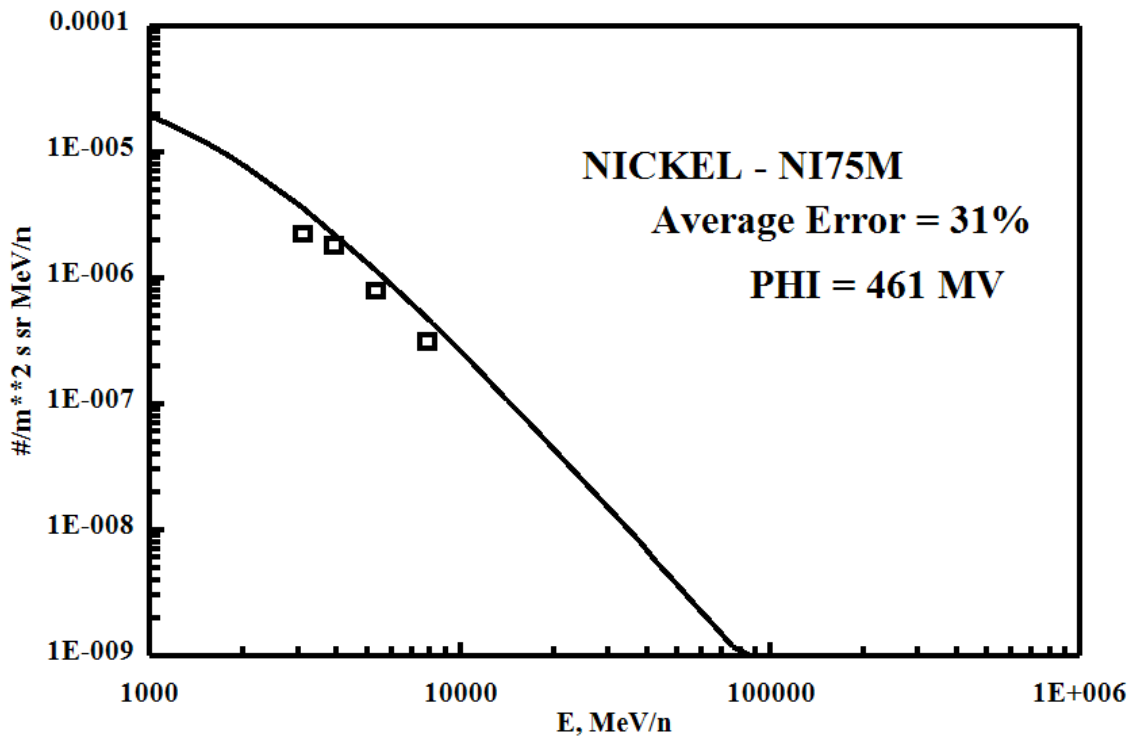
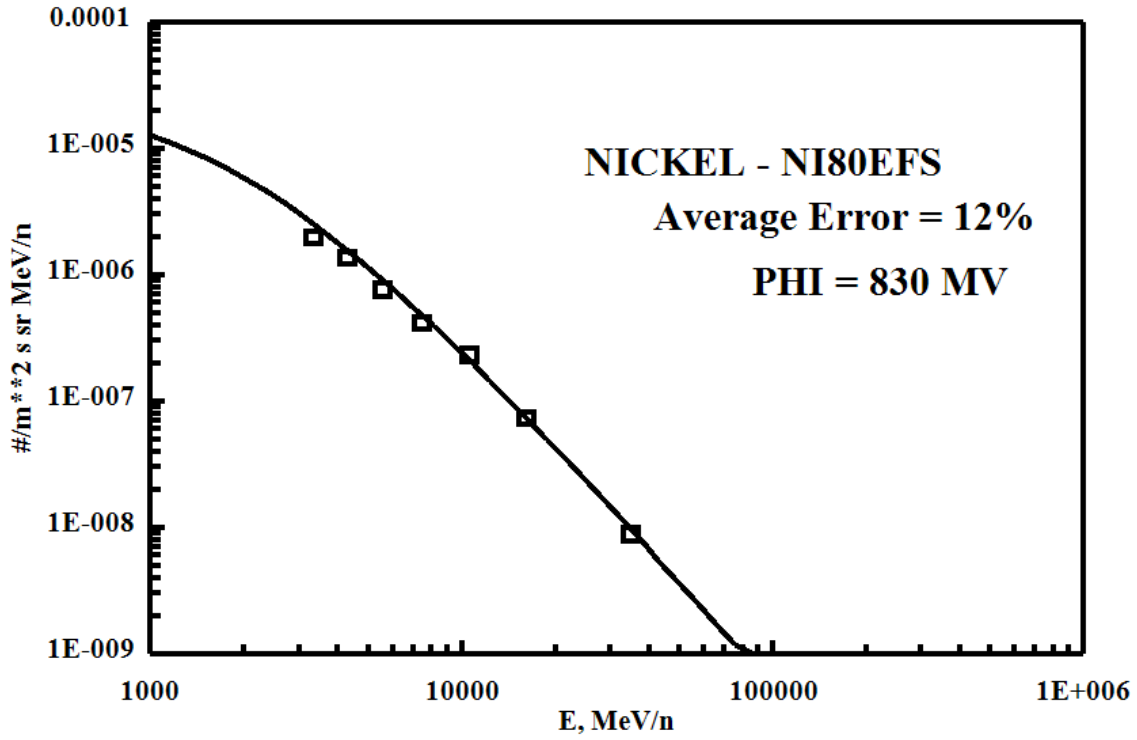


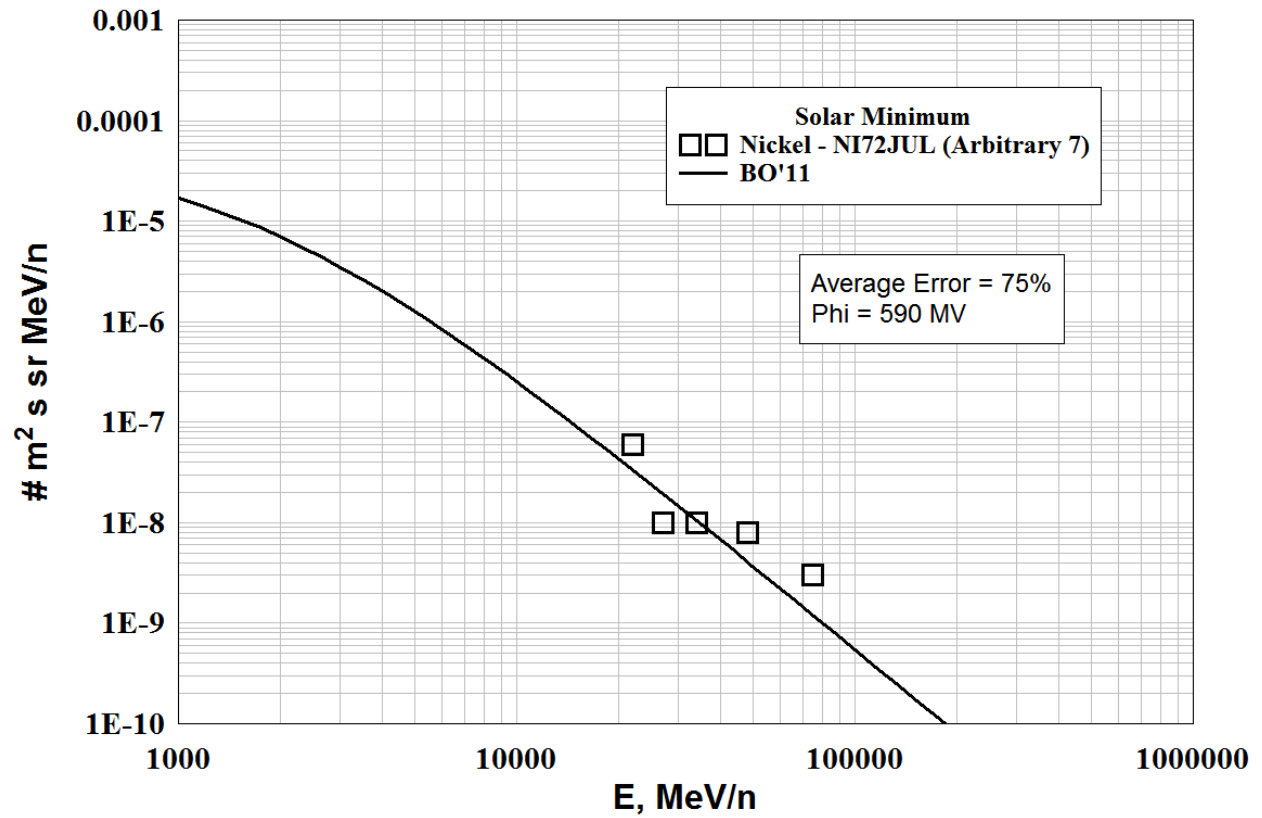
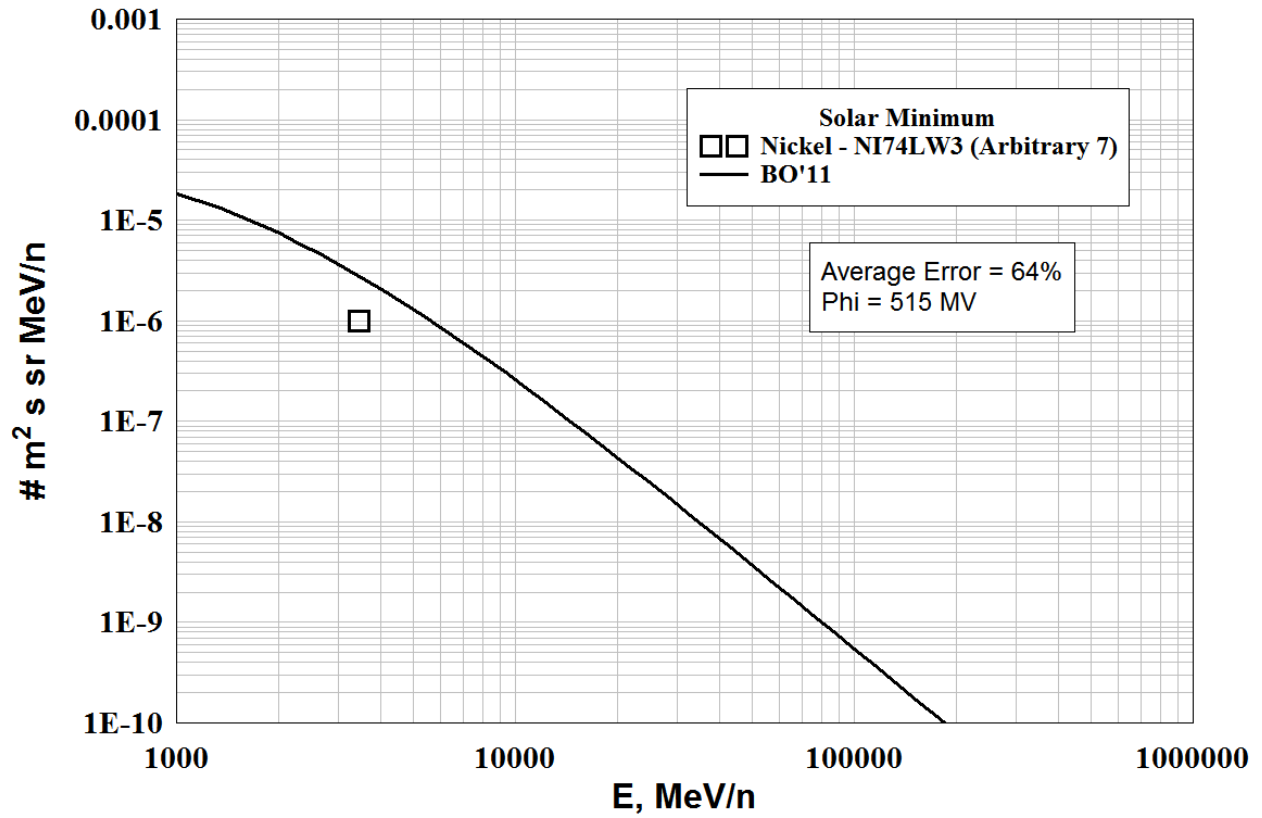




COBALT - High energy - NONE

NICKEL - High energy





Appendix D: Low Energy Spectra

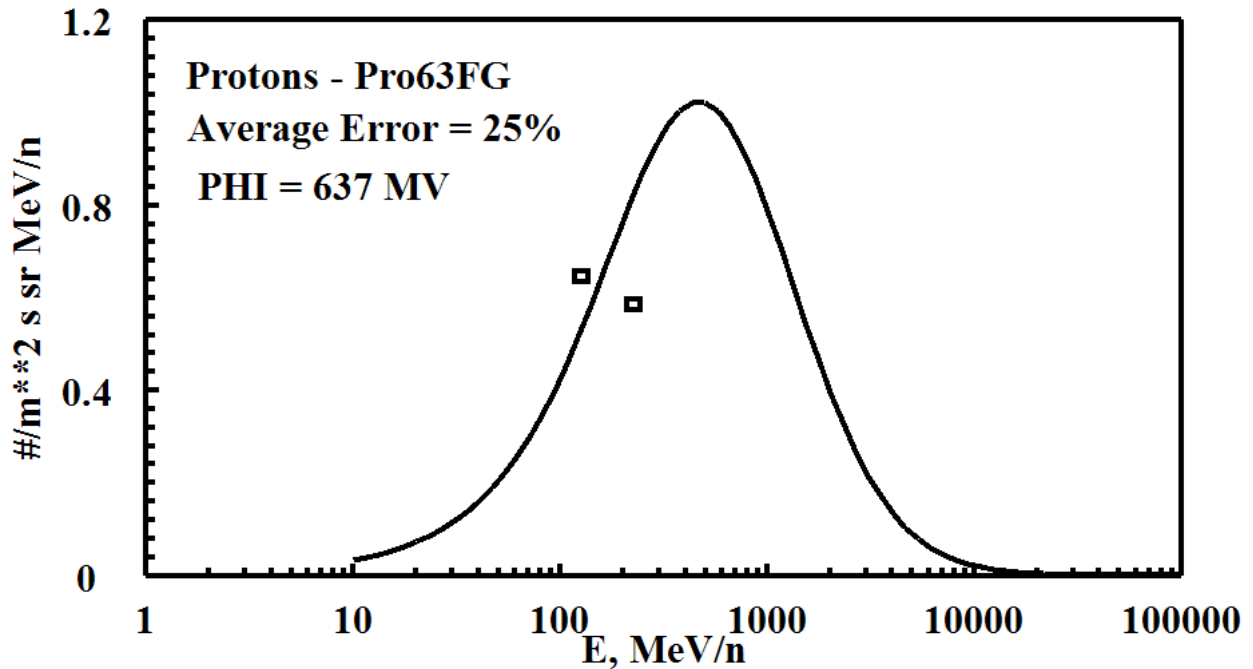
Line = BO'11 Model

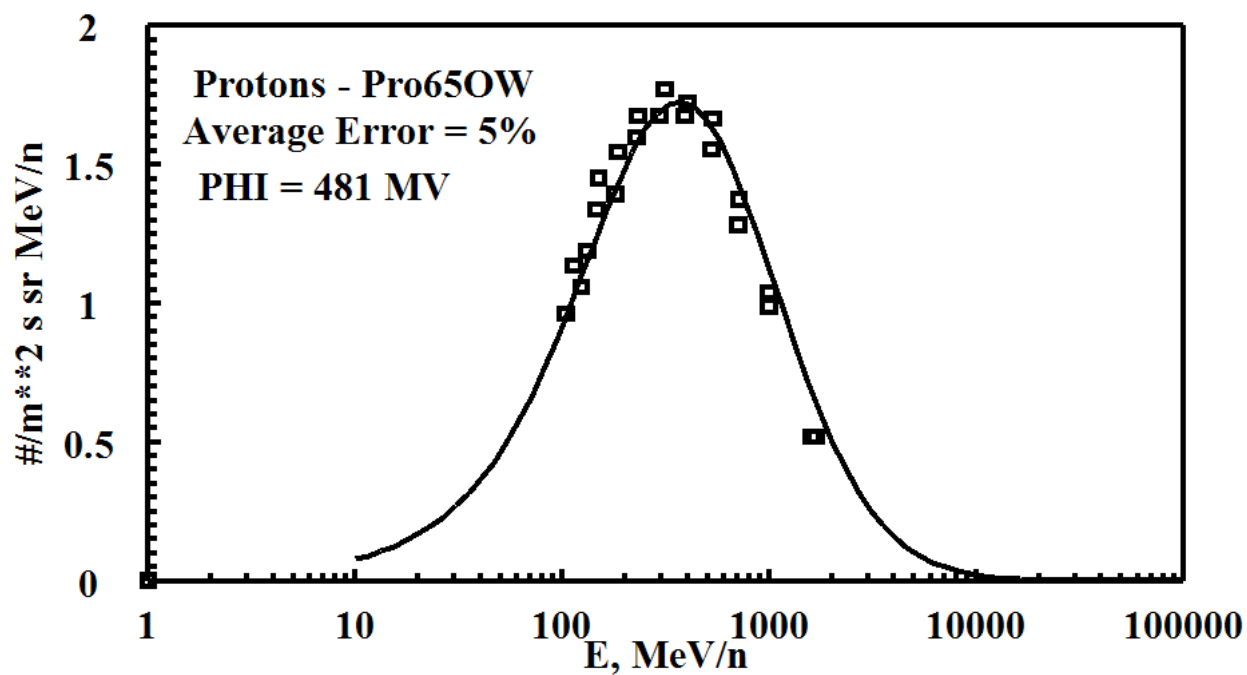
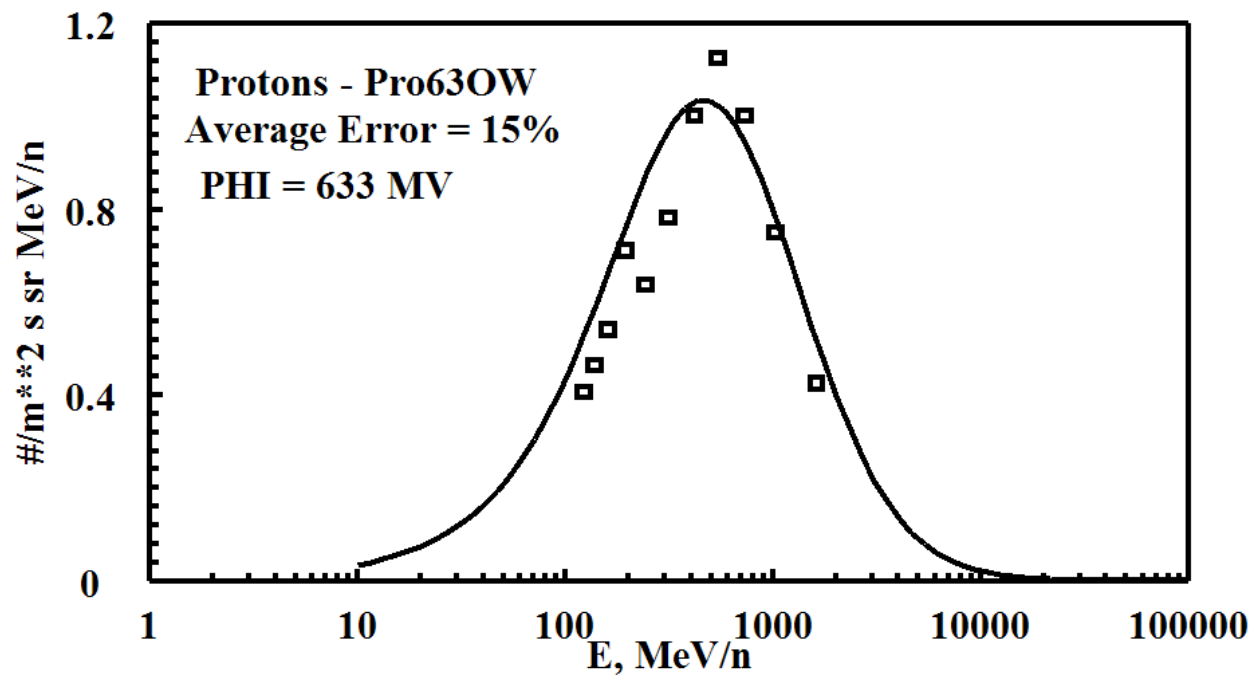
Measurement (squares) are correlated with the references (eg, PRO66B)

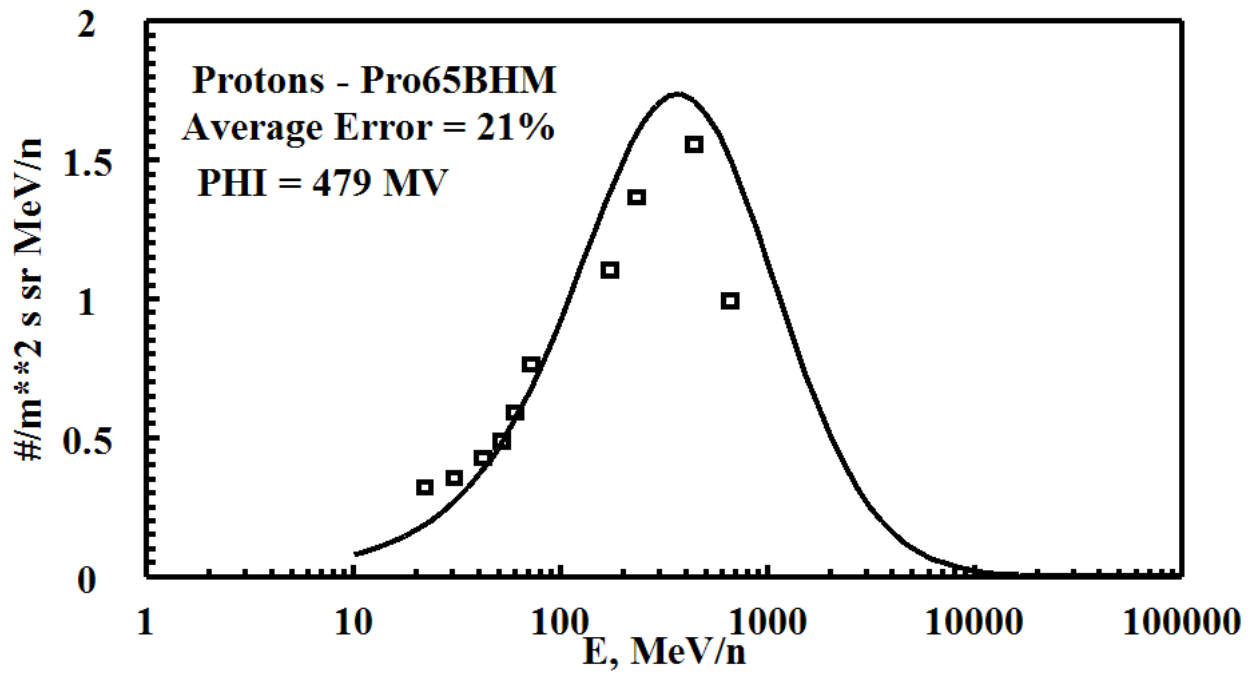
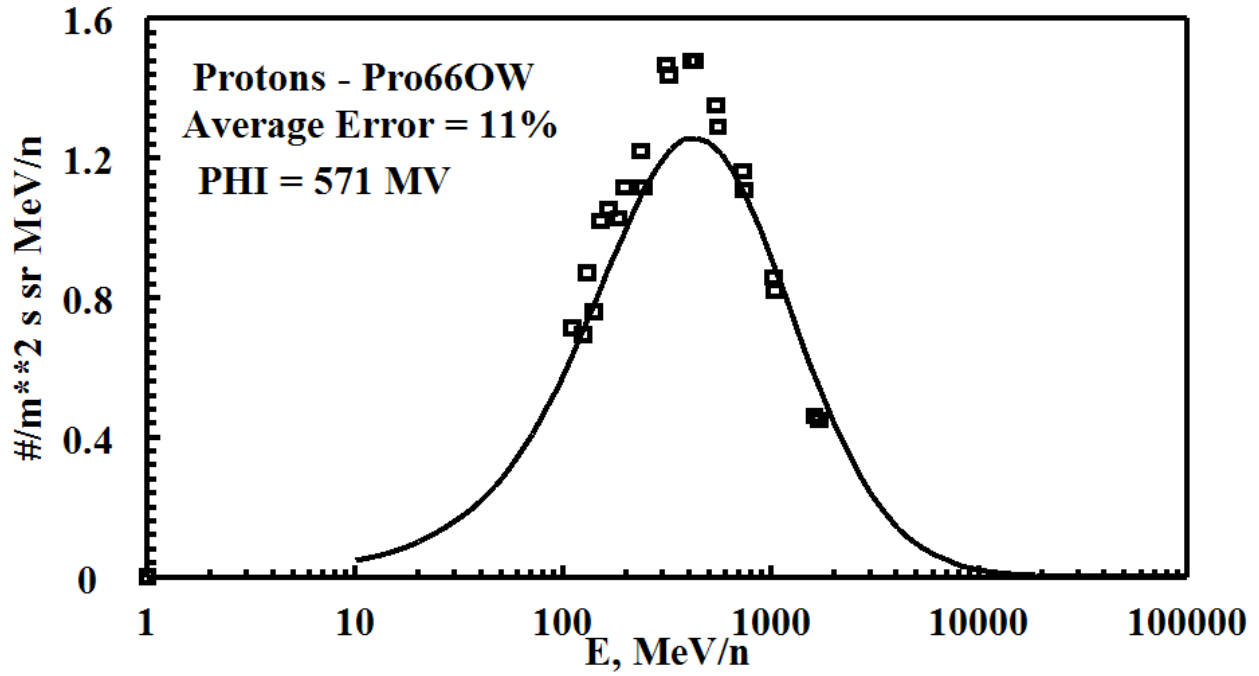
Note: The average error indicated on each plot applies only to data points <3000MeV/n, but each plot shows all of the measured data points that exist in each data set.

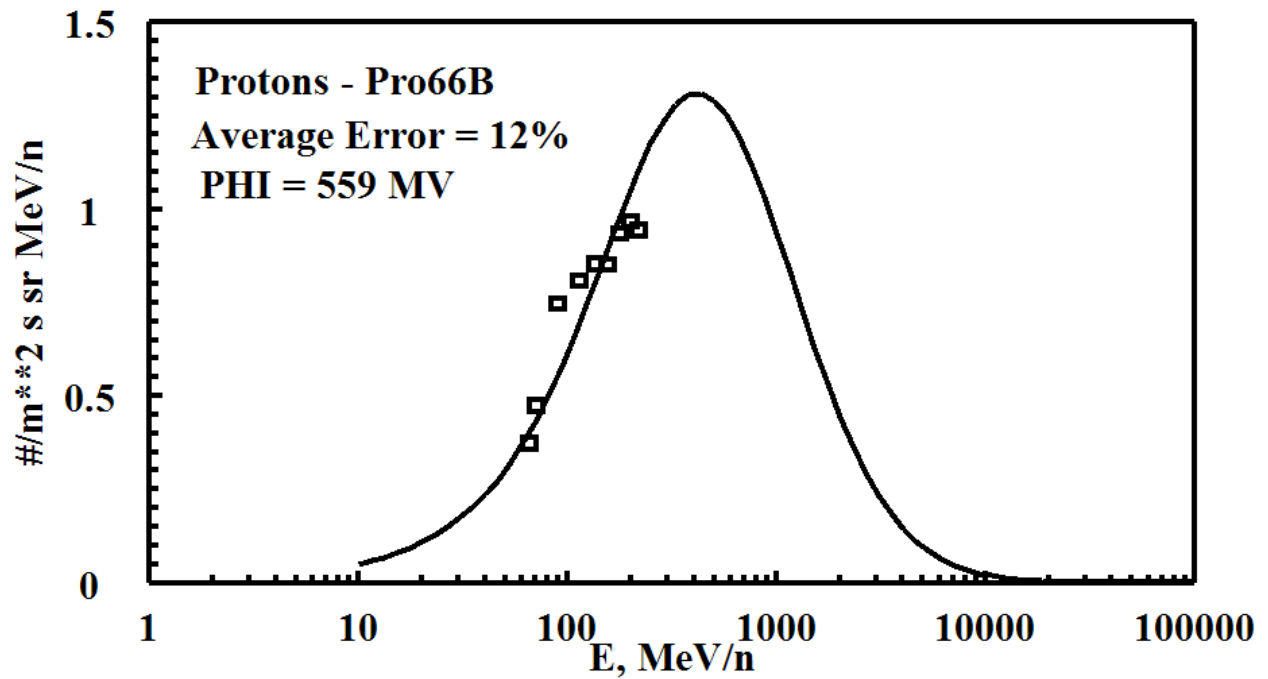
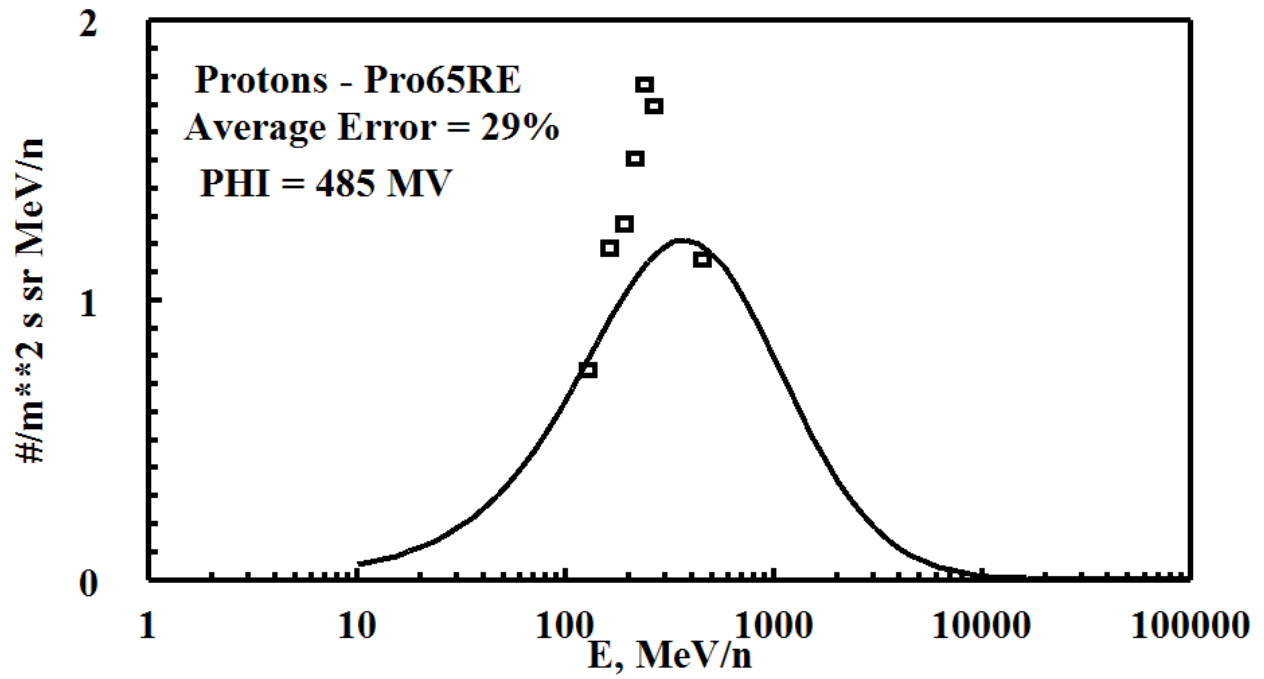
PROTONS - Low Energy, Solar Minimum Files Used (Arbitrary 1's)

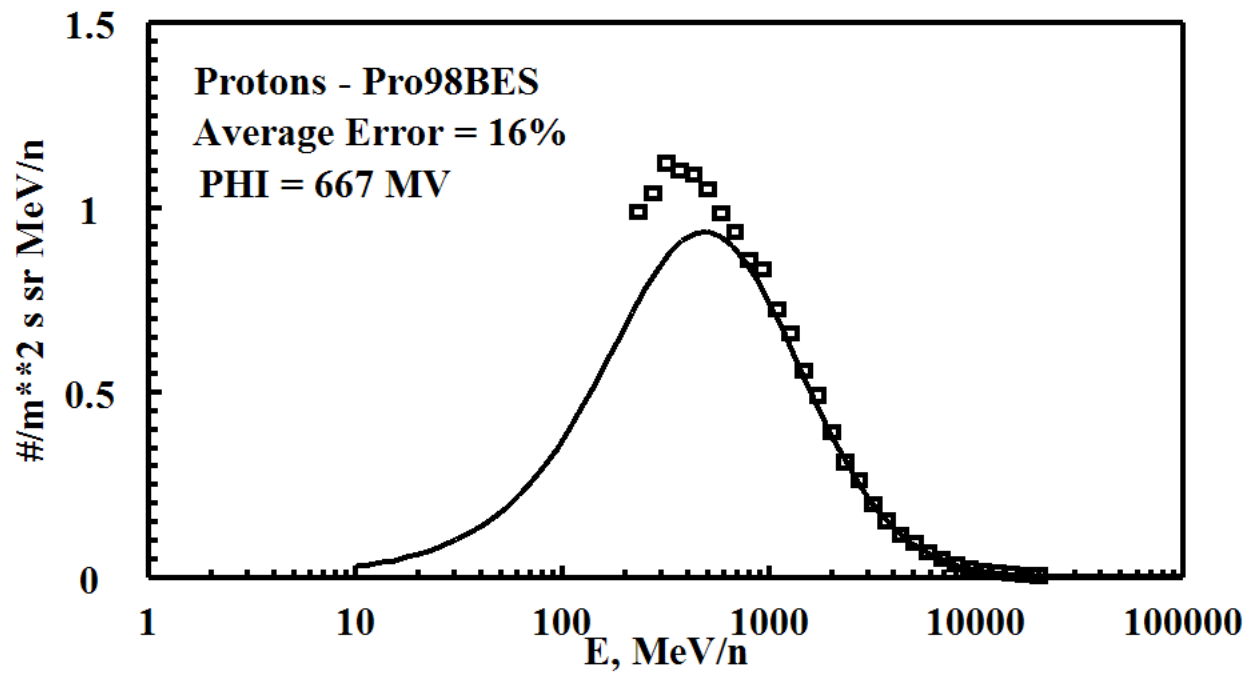
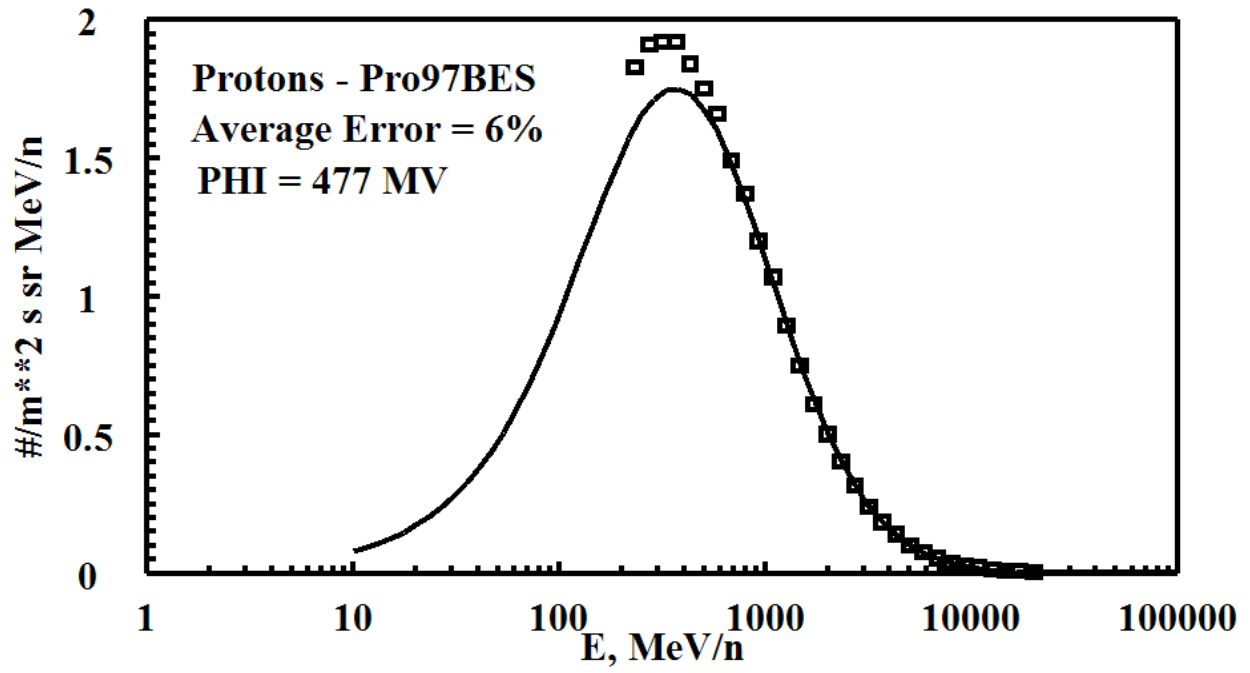
FILE	DATE	PHI (MV)	ERROR=ABS (FLUX-DATA)
Pro63FG.dat	1963.455	637.1404	24.62225
Pro63OW.dat	1963.575	632.7310	15.02571
Pro65OW.dat	1965.501	481.2304	4.917985
Pro66OW.dat	1966.548	571.2632	11.36108
Pro65BHM.dat	1965.447	479.2167	20.51697
Pro65RE.dat	1965.627	485.0185	28.88208
Pro66B.dat	1966.499	559.3981	11.73762
Pro97BES.dat	1997.570	477.0878	6.410701
Pro98BES.dat	1998.575	666.7952	16.14731
Pro94Cap.dat	1994.605	565.4738	11.24284
BO AVERAGE ERROR =			15.08645

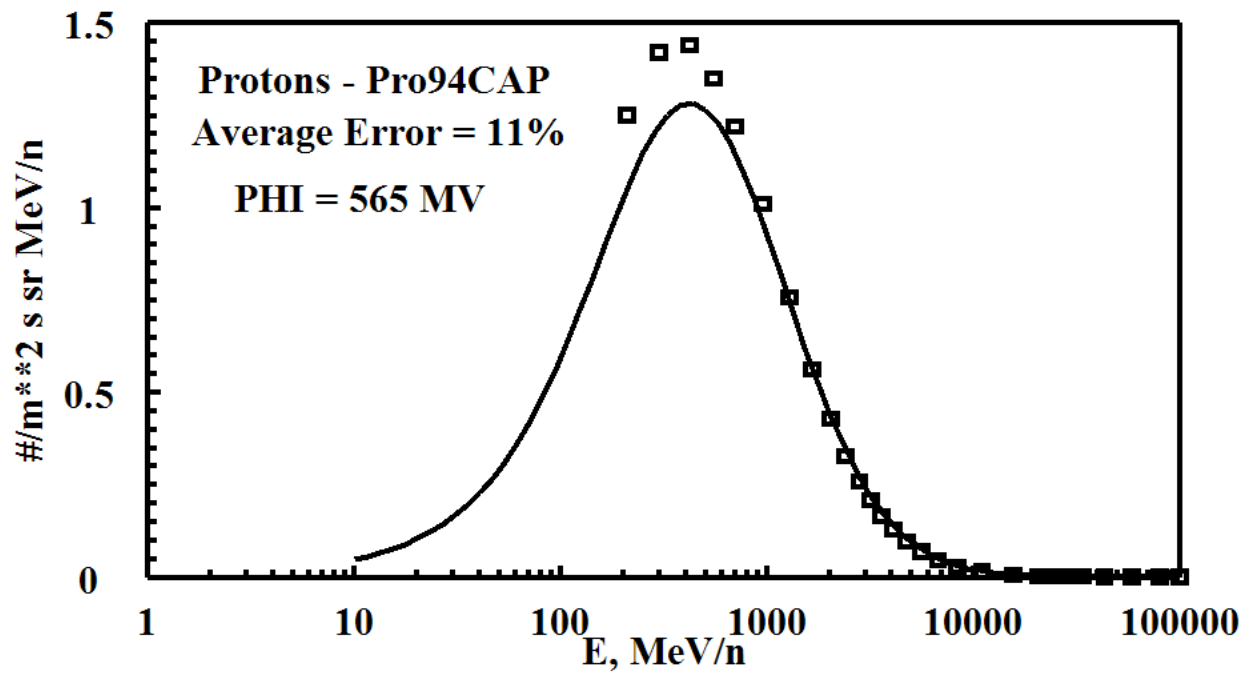






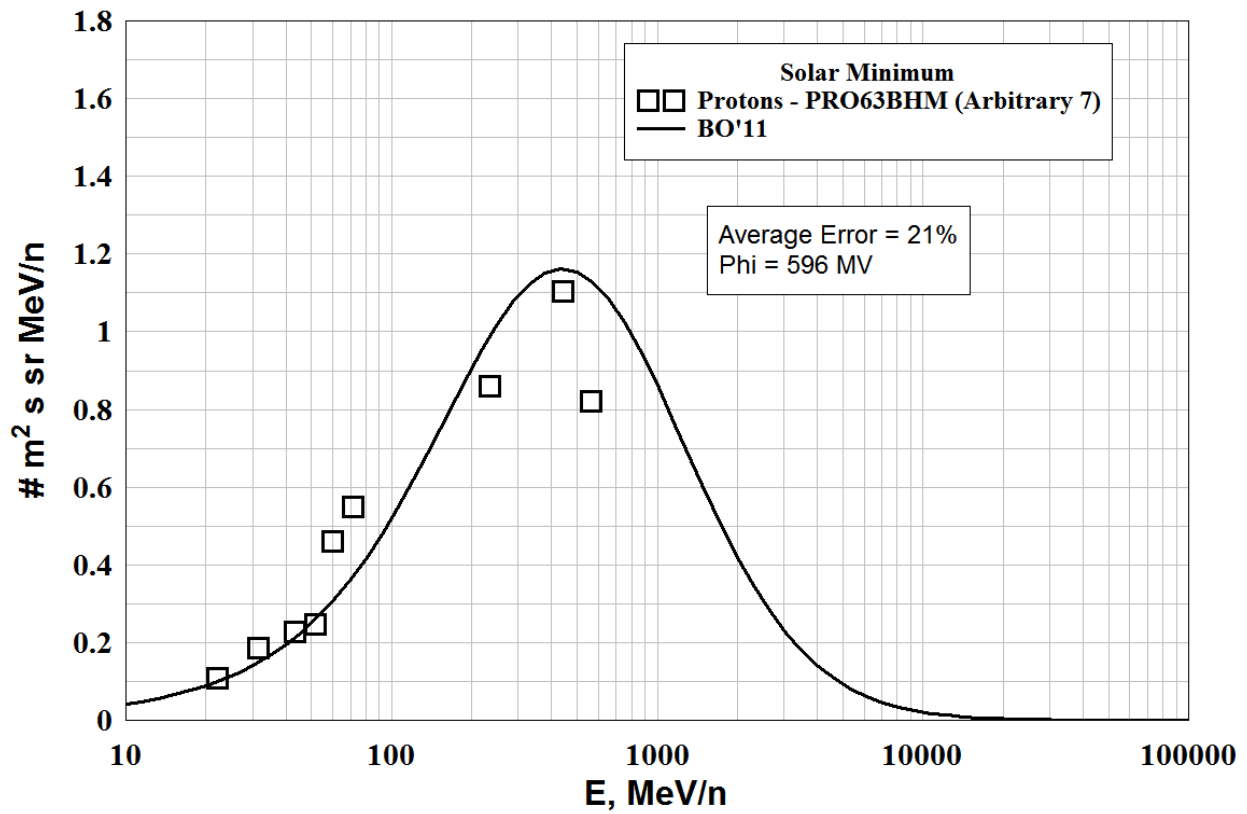
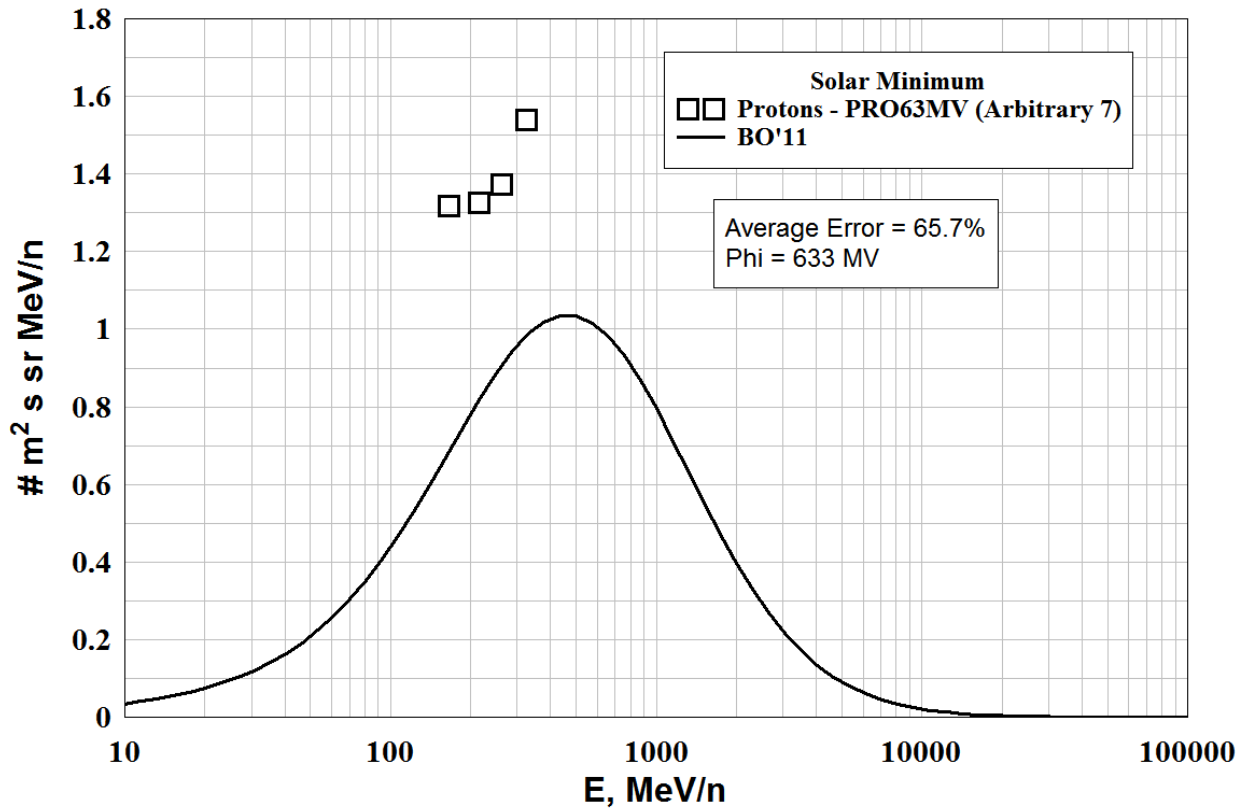


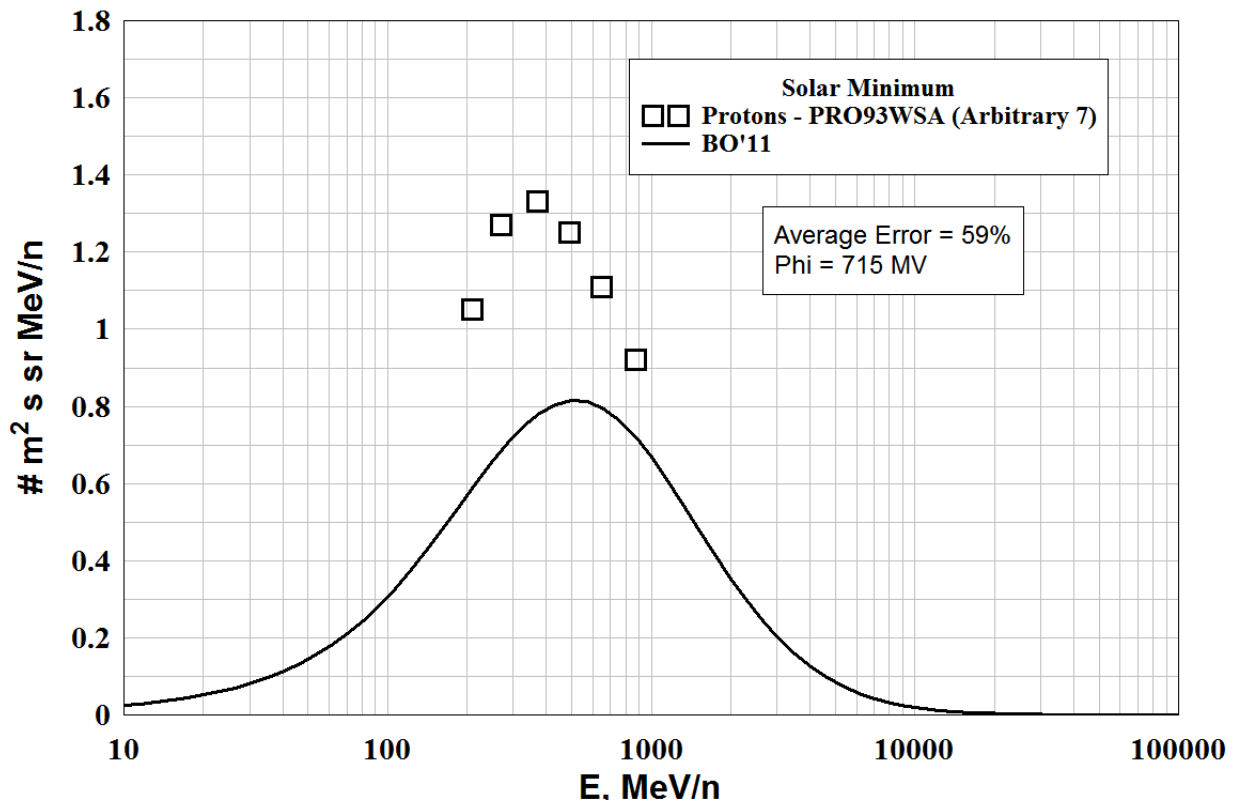
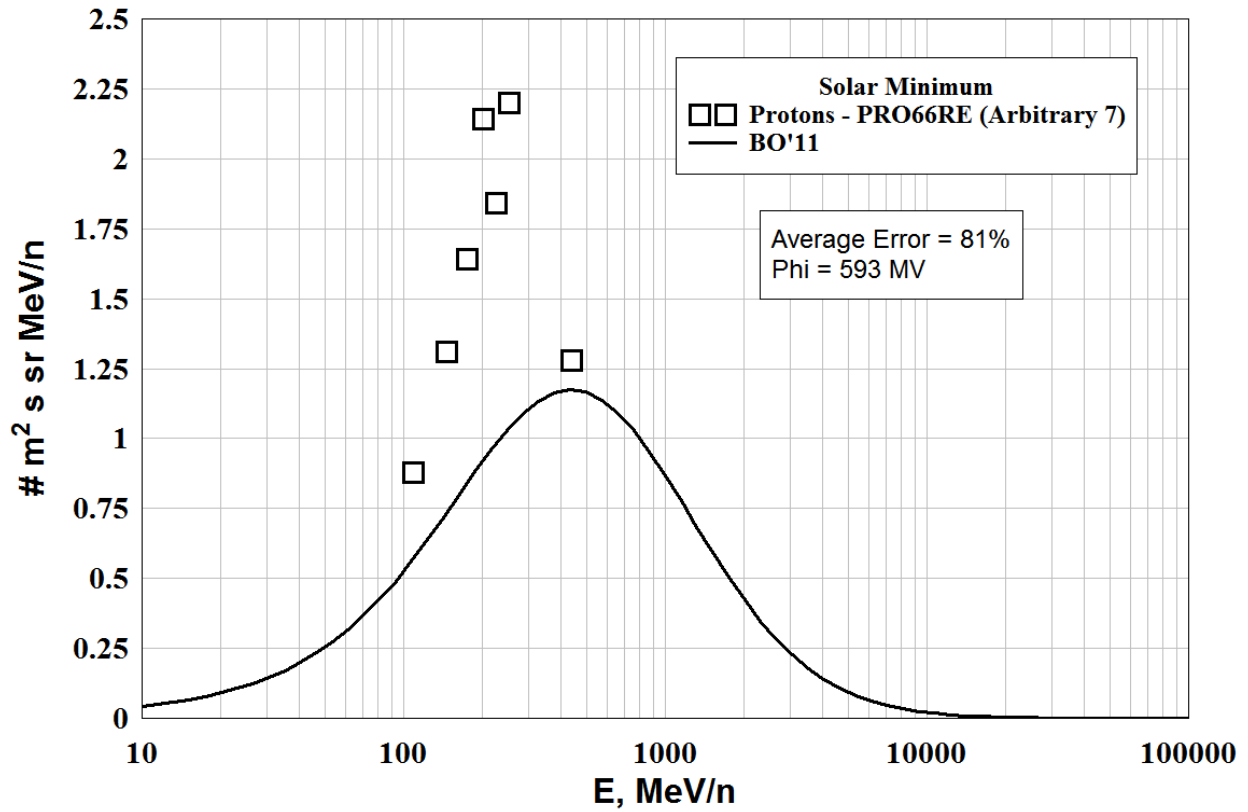


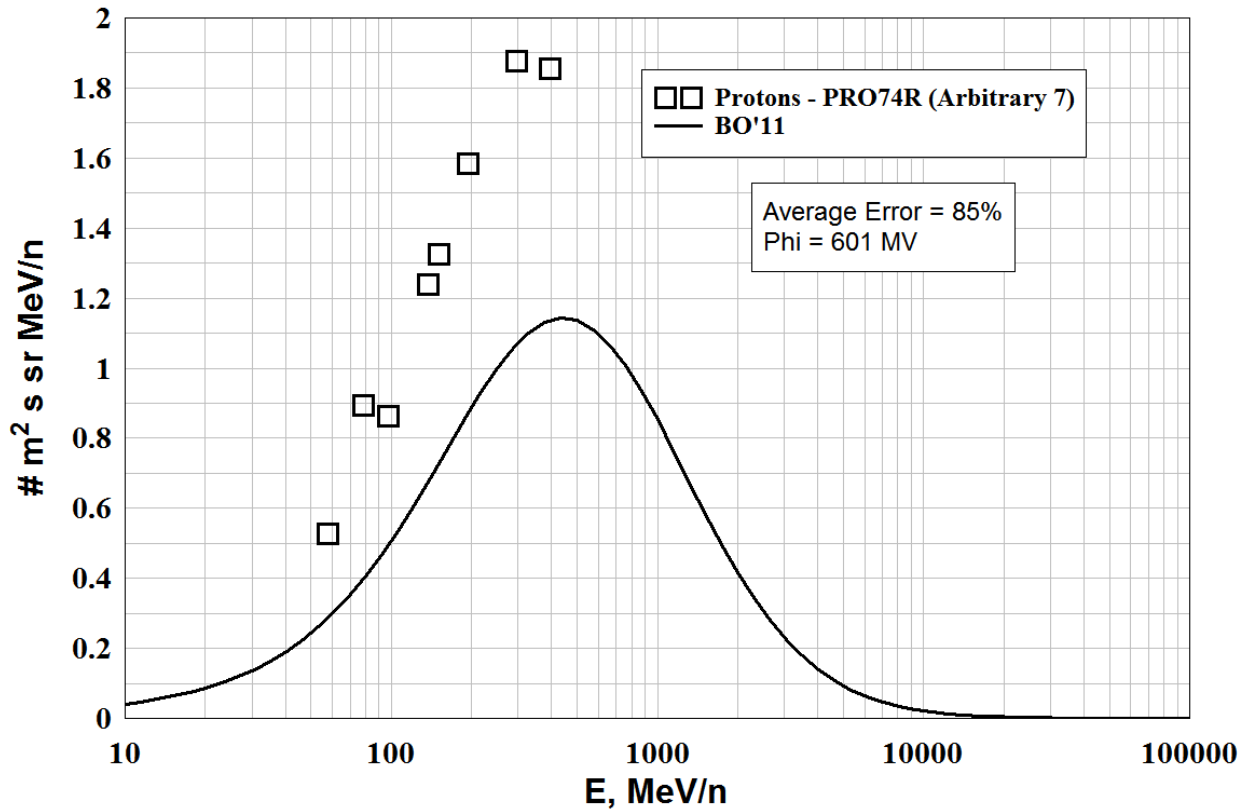
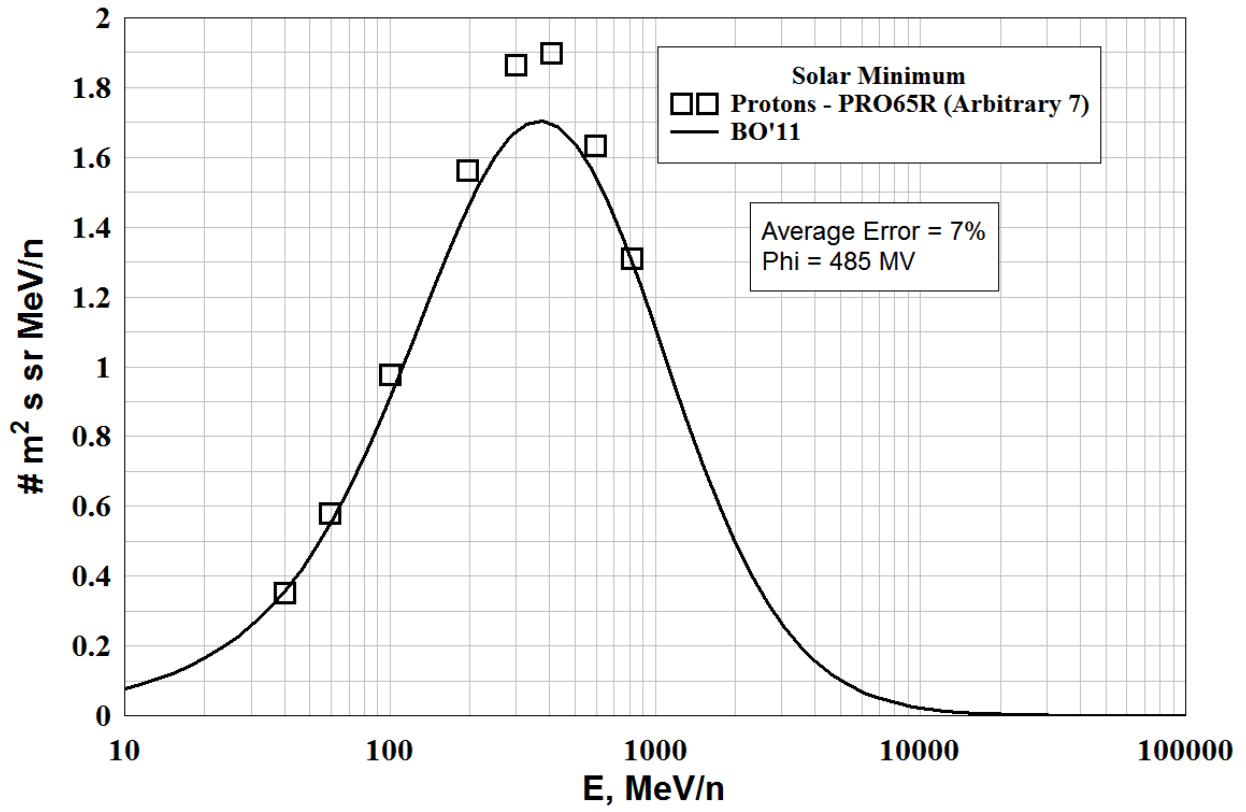


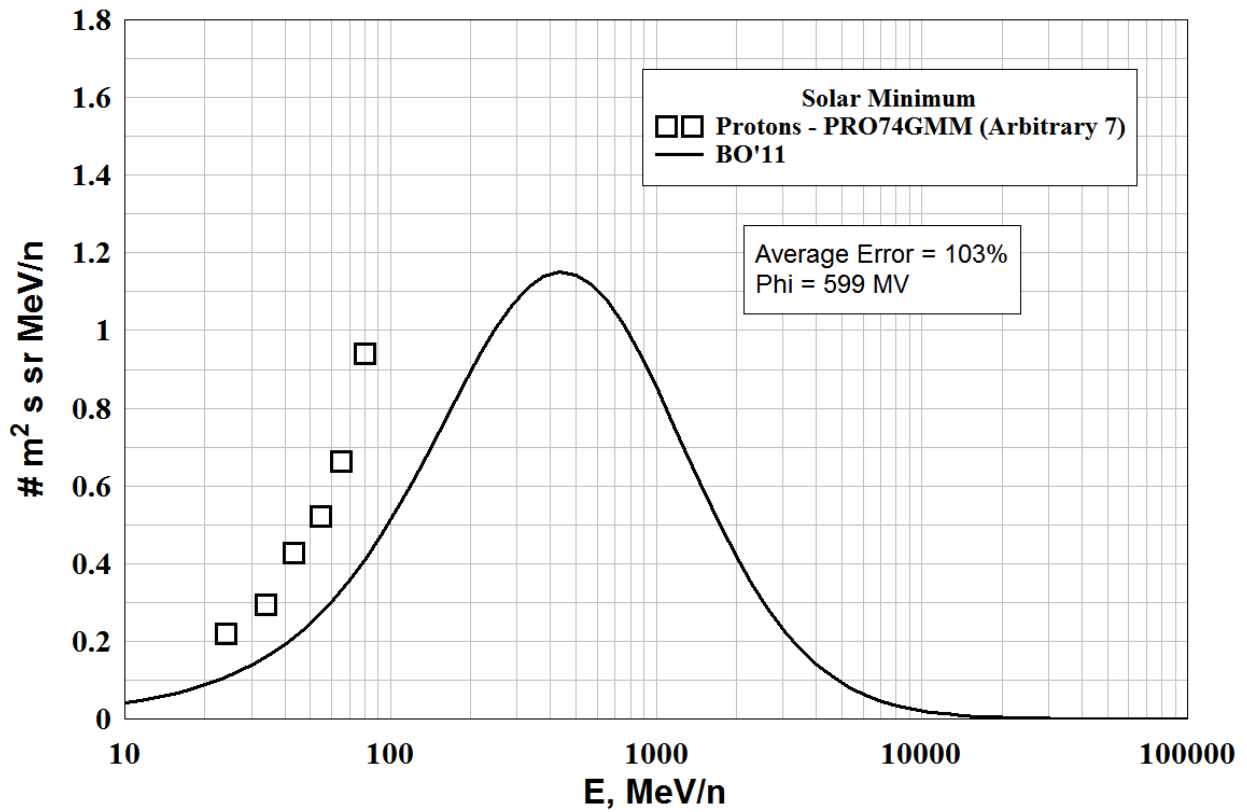
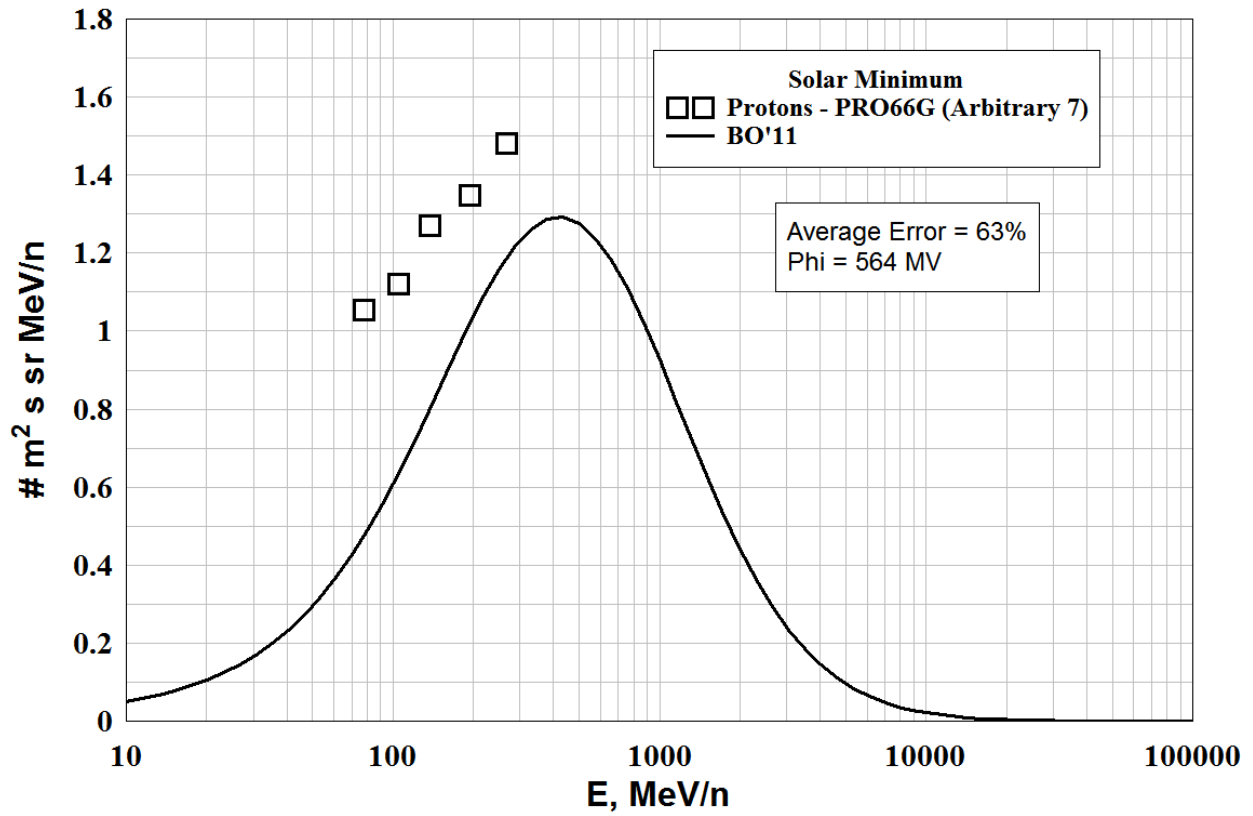
Files Rejected - (Arbitrary 7's)

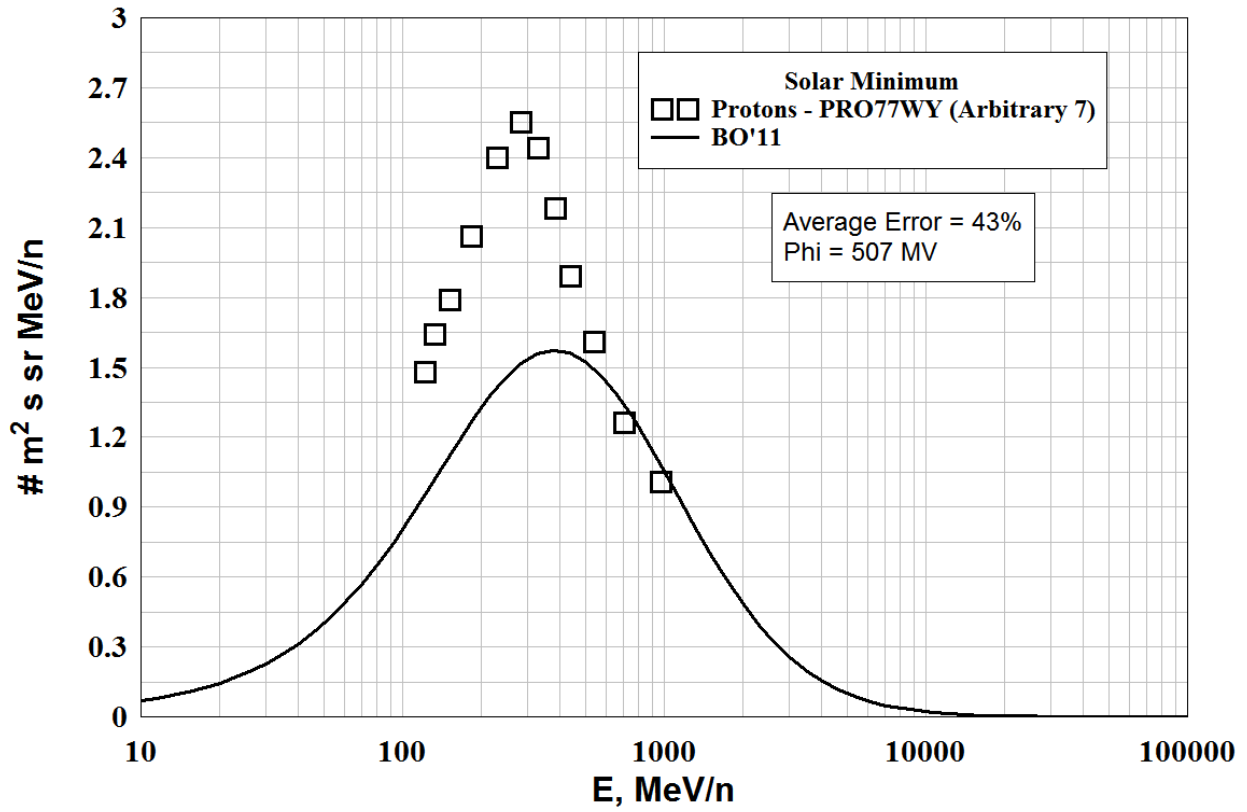
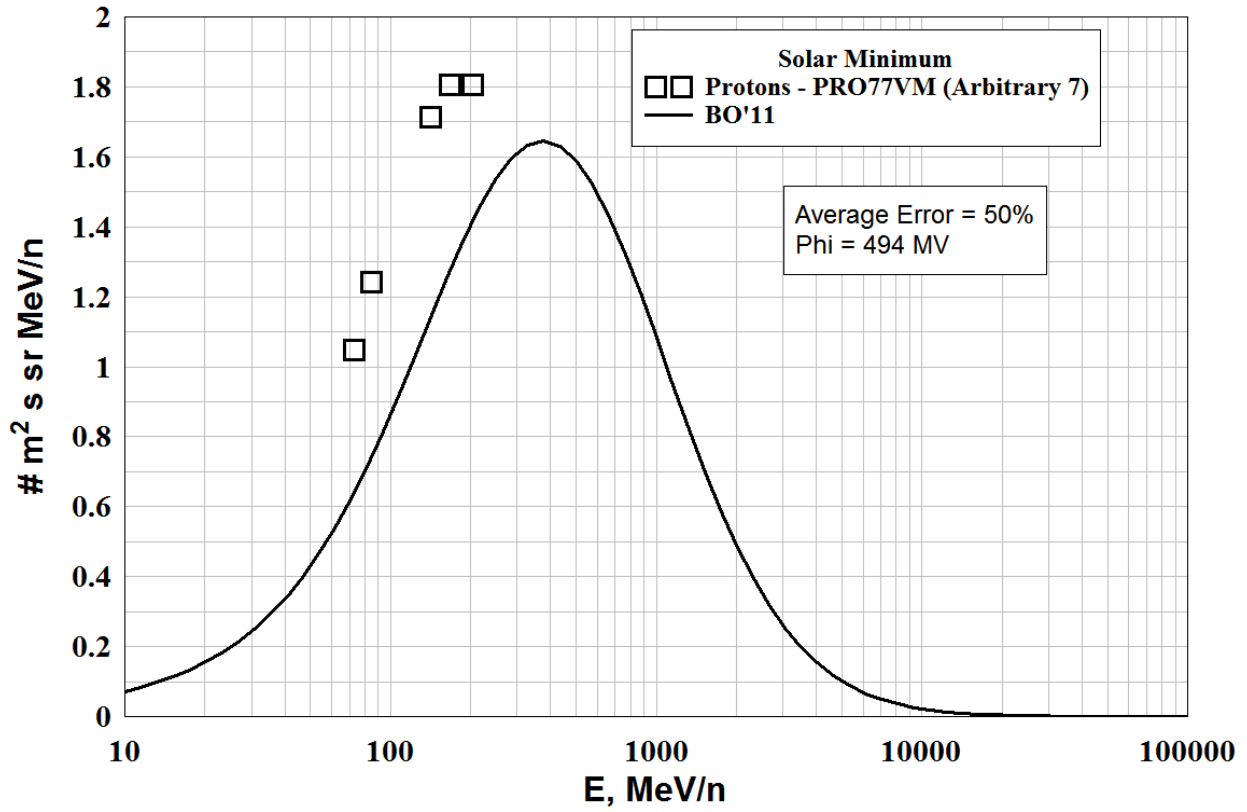
FILE	DATE	PHI (MV)	ERROR=ABS (FLUX-DATA)
Pro63MV.dat	1963.545	632.8328	65.65573
Pro63BHM.dat	1963.836	596.1647	21.15664
Pro66RE.dat	1966.641	593.0267	81.42393
Pro93WSA.dat	1993.567	715.0115	59.40961
Pro65R.dat	1965.573	484.6338	6.760087
Pro74R.dat	1974.499	601.2664	84.52446
Pro66G.dat	1966.517	563.7659	63.43481
Pro74GMM.dat	1974.542	599.4113	102.8642
Pro77Vm.dat	1977.252	494.4139	50.16814
Pro77Wy.dat	1977.510	507.0742	42.78721
pro78ek.dat	1978.584	818.9930	278.7522
Pro87S.dat	1987.638	527.9987	44.09135
Pro87W.dat	1987.641	528.4525	26.30991
BO AVERAGE ERROR =			71.33372

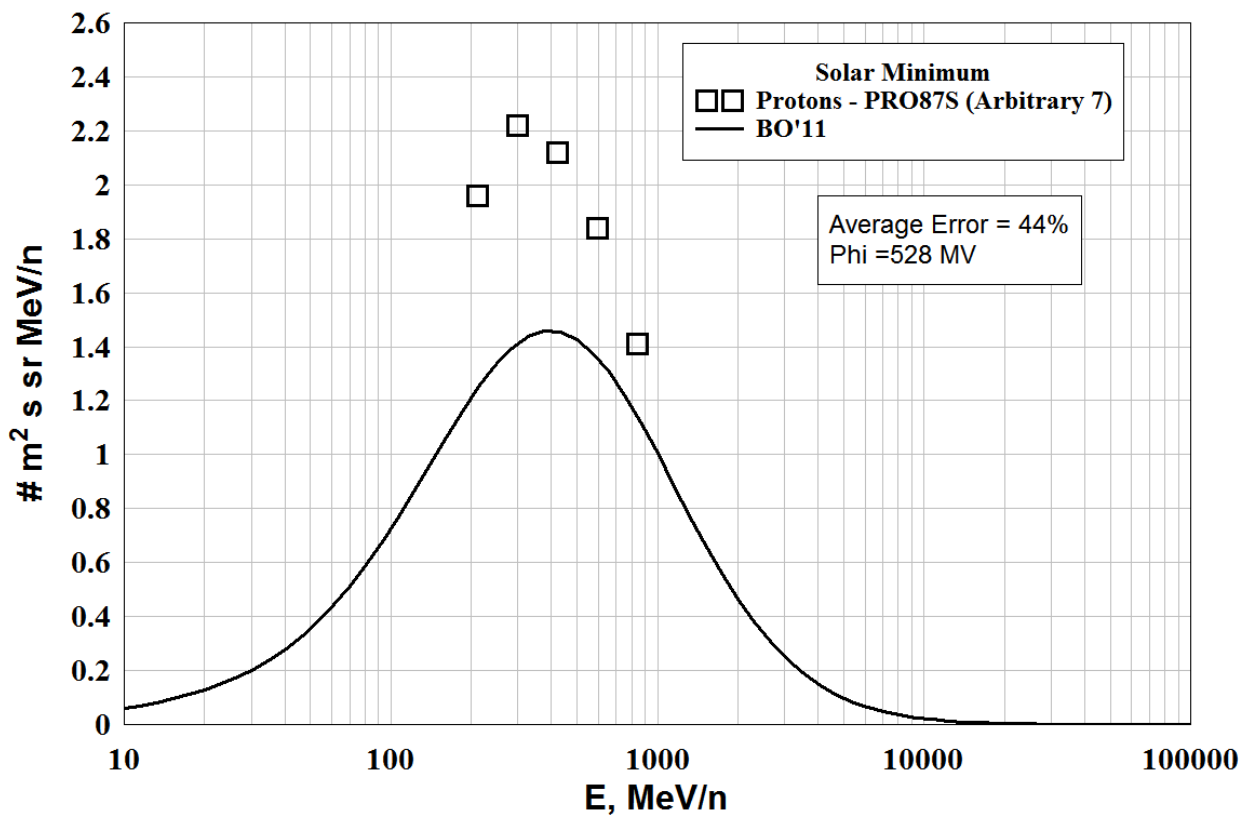
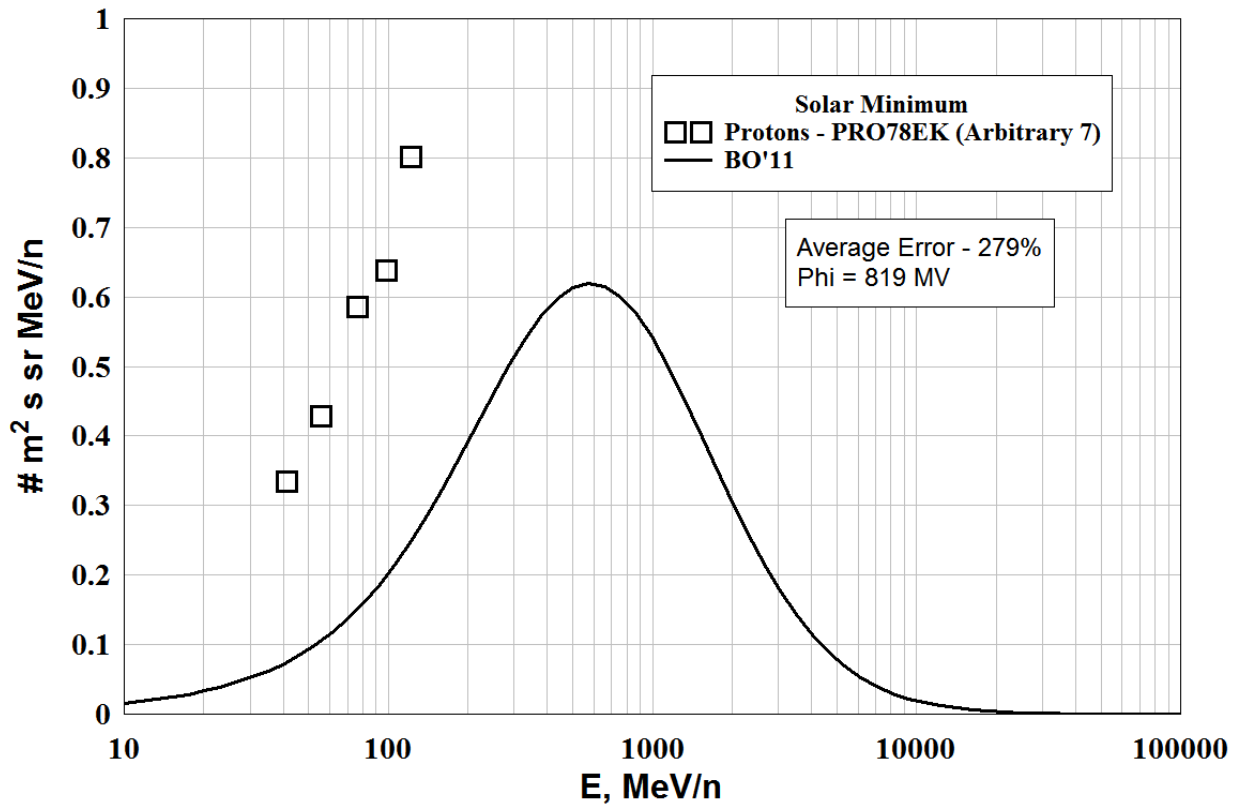


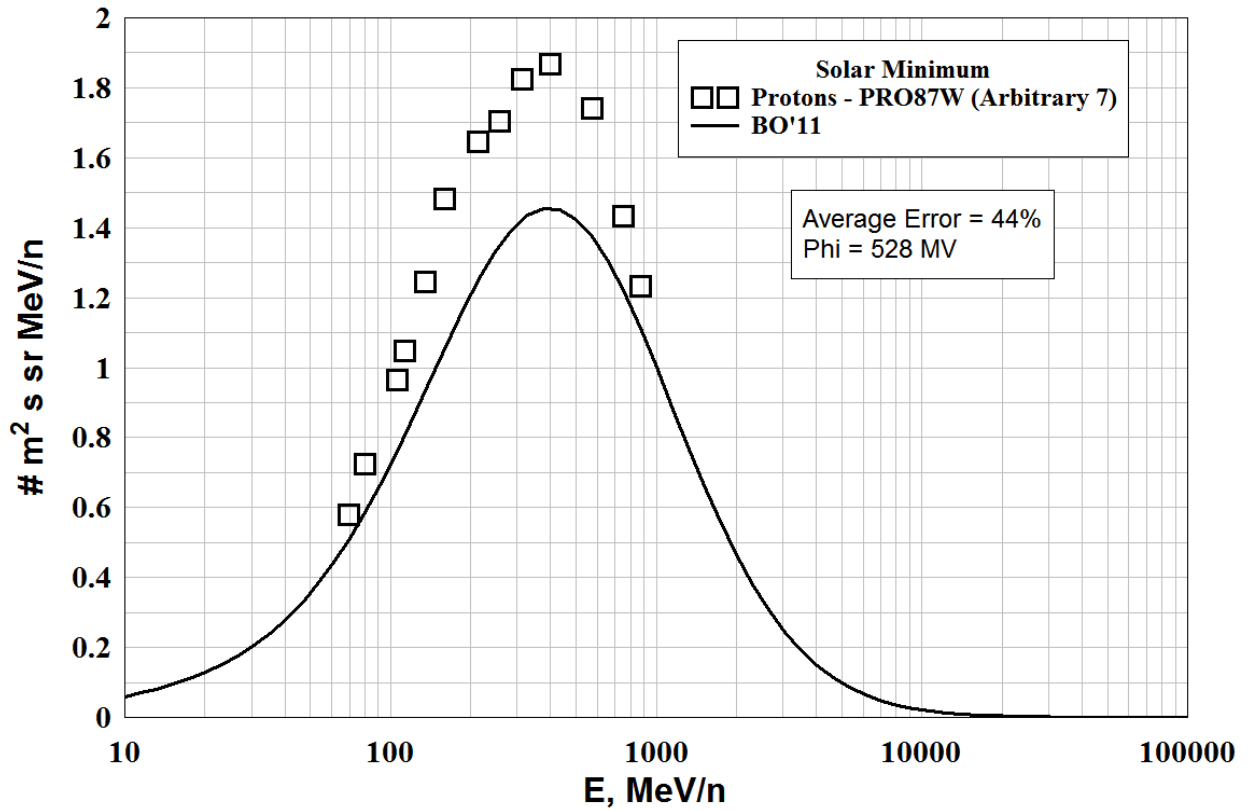








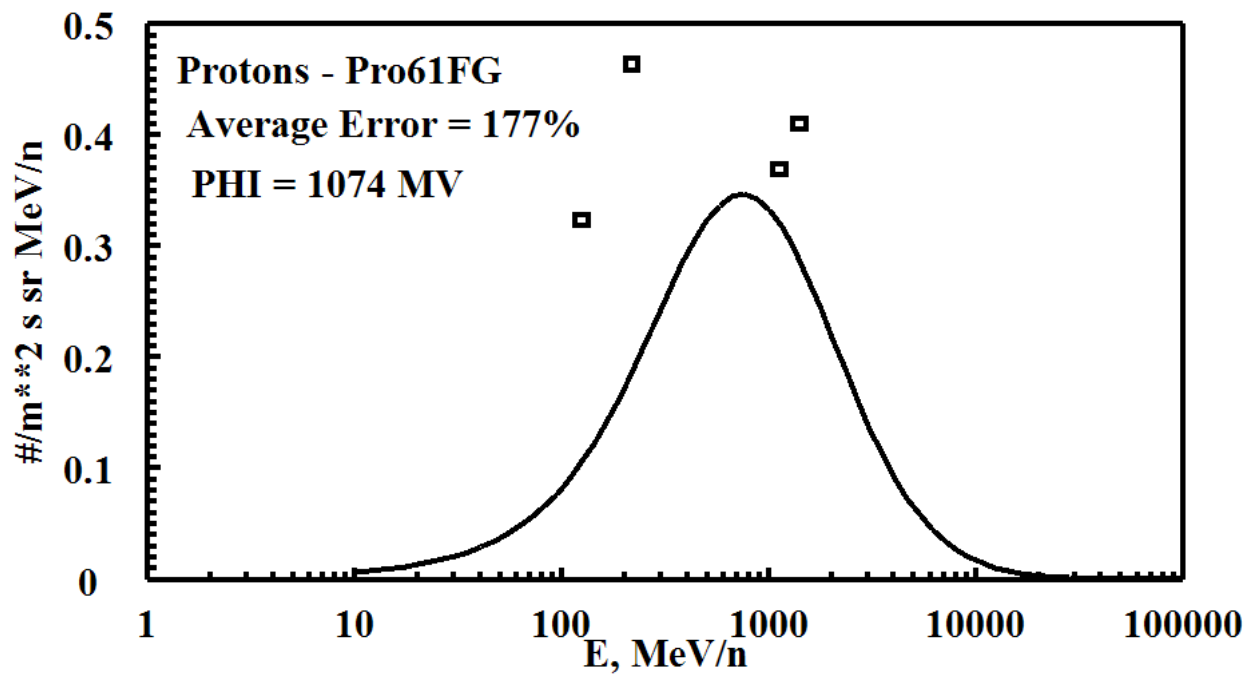
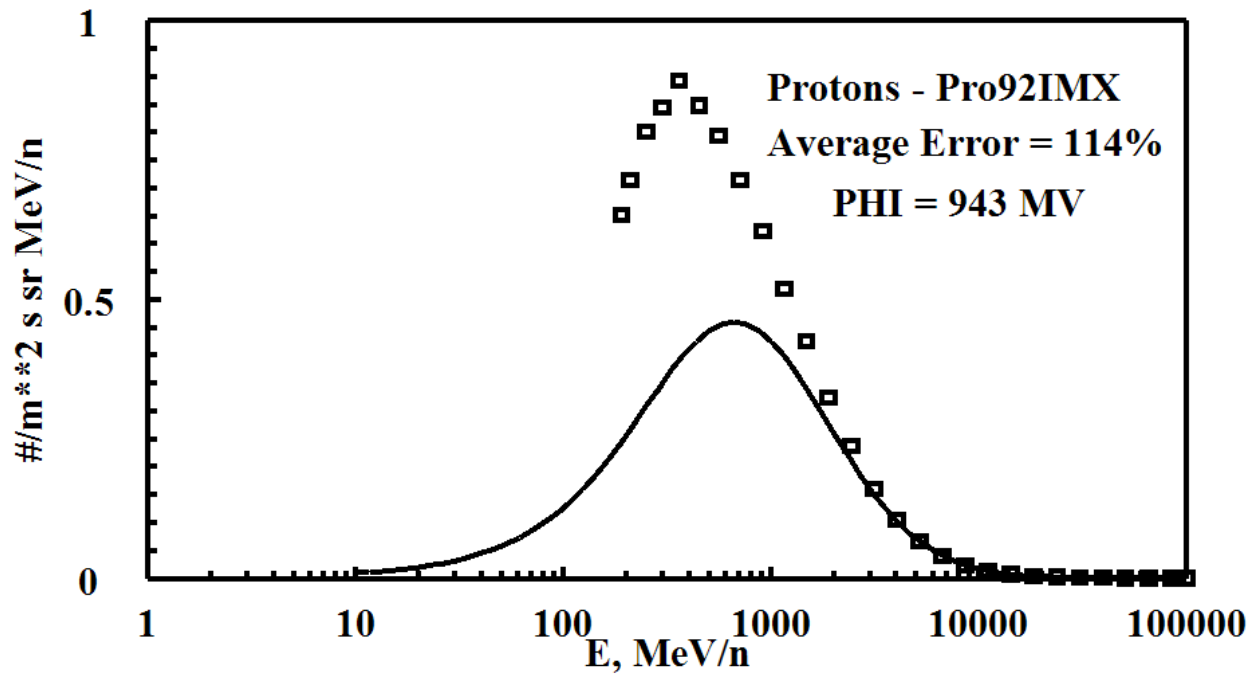


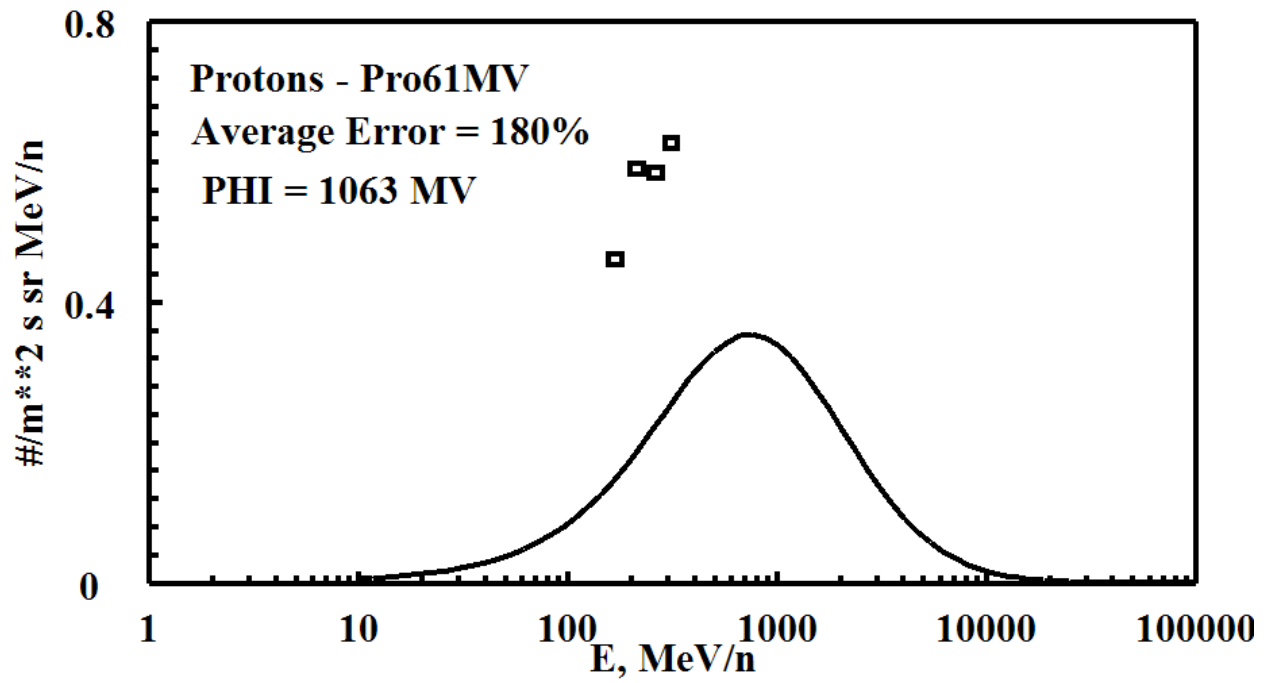
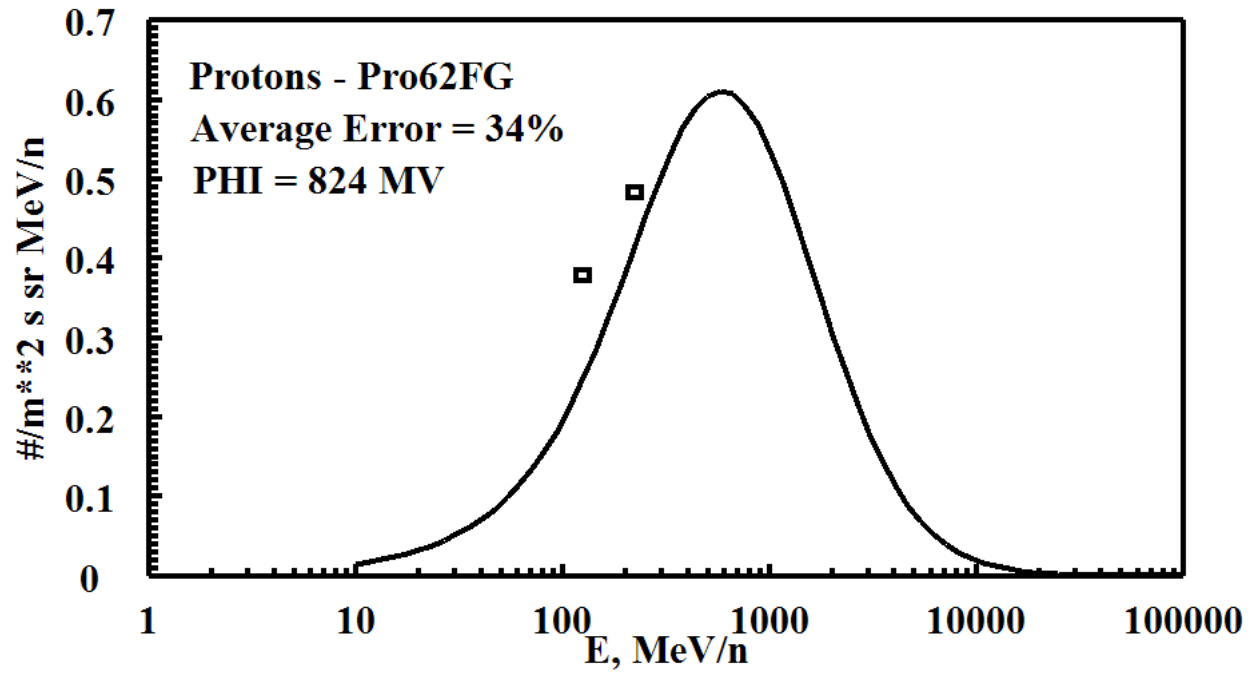


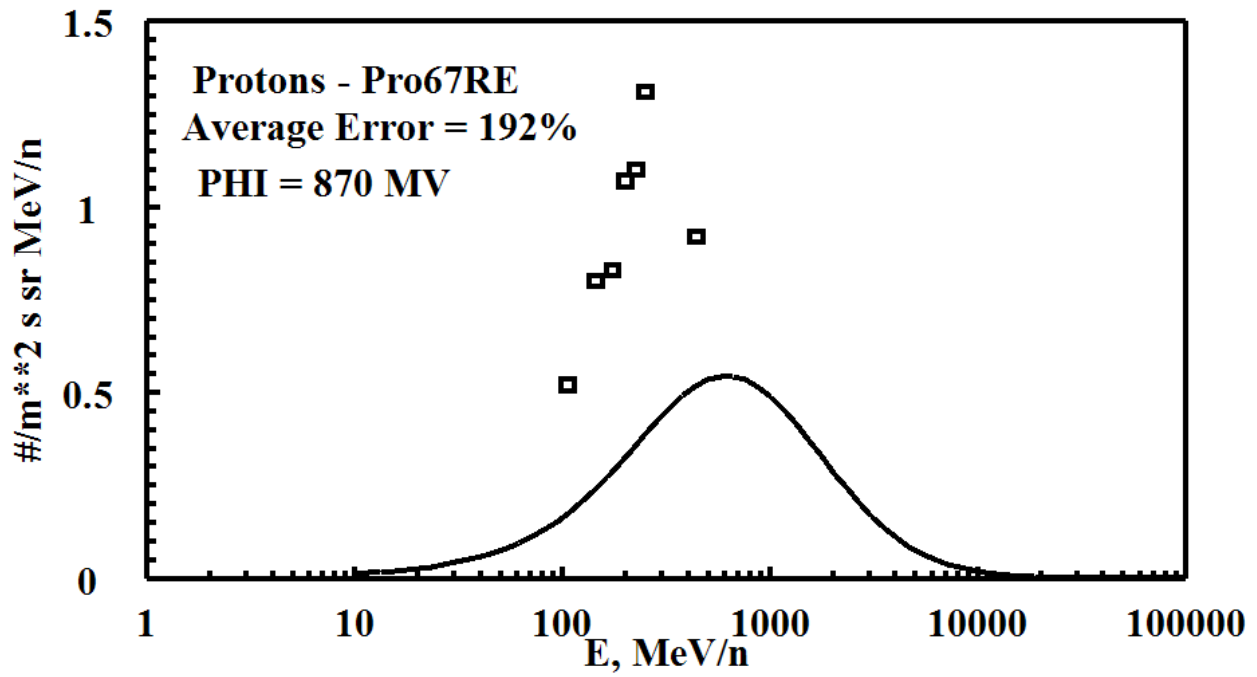
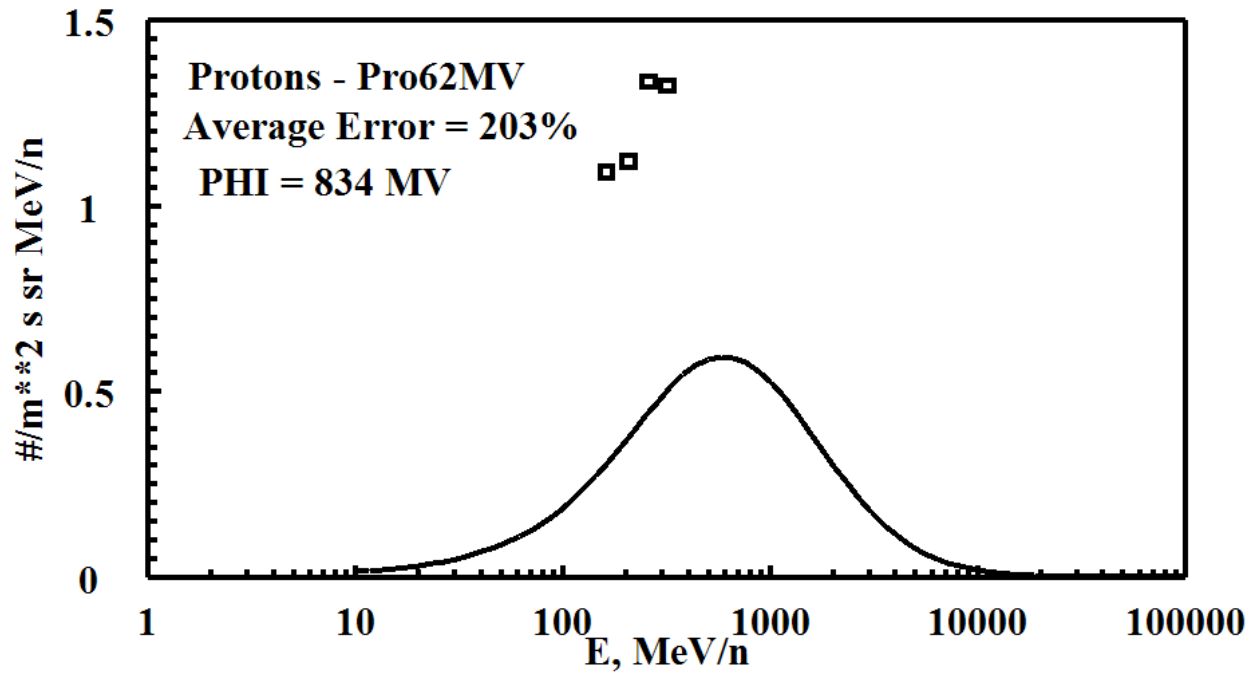
PROTONS - Low Energy, Solar Maximum

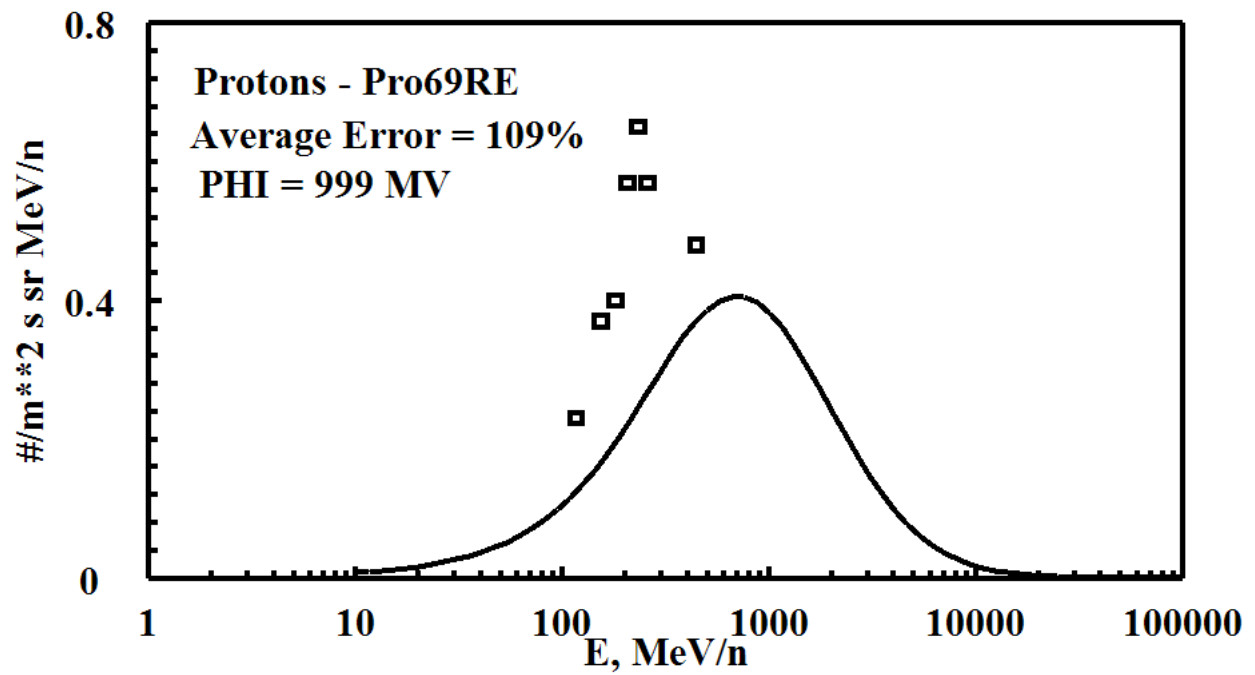
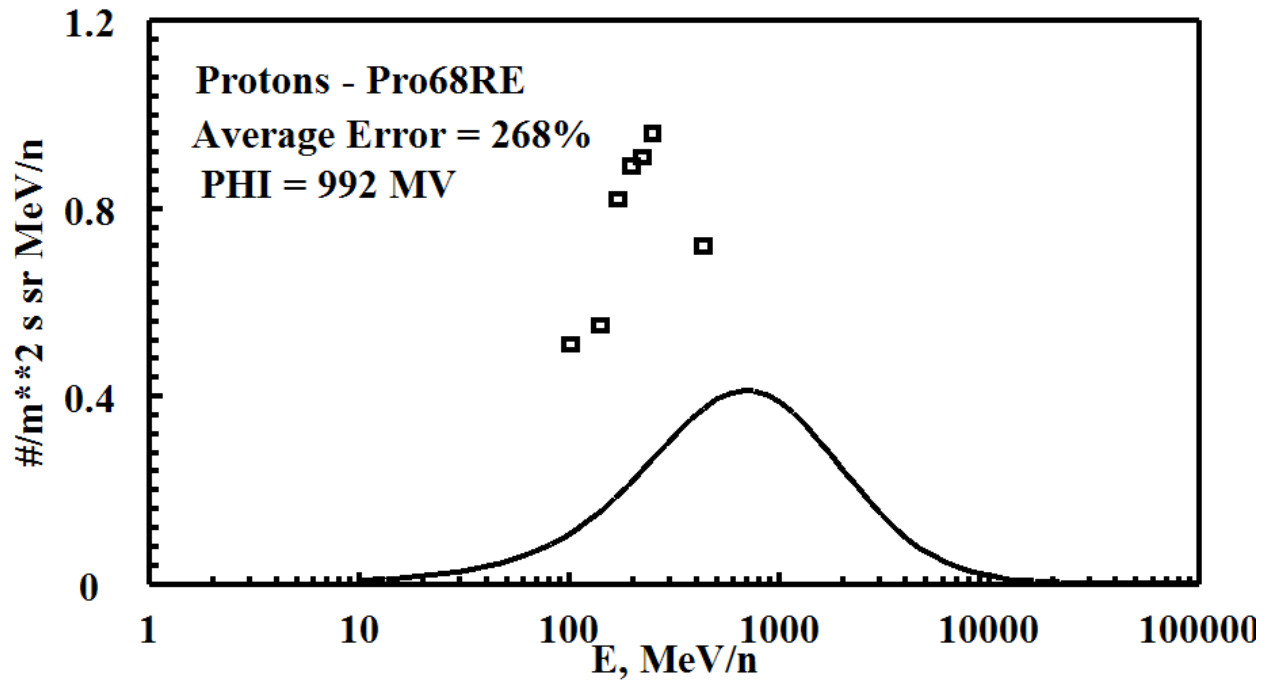
Files Used (Arbitrary 1's)

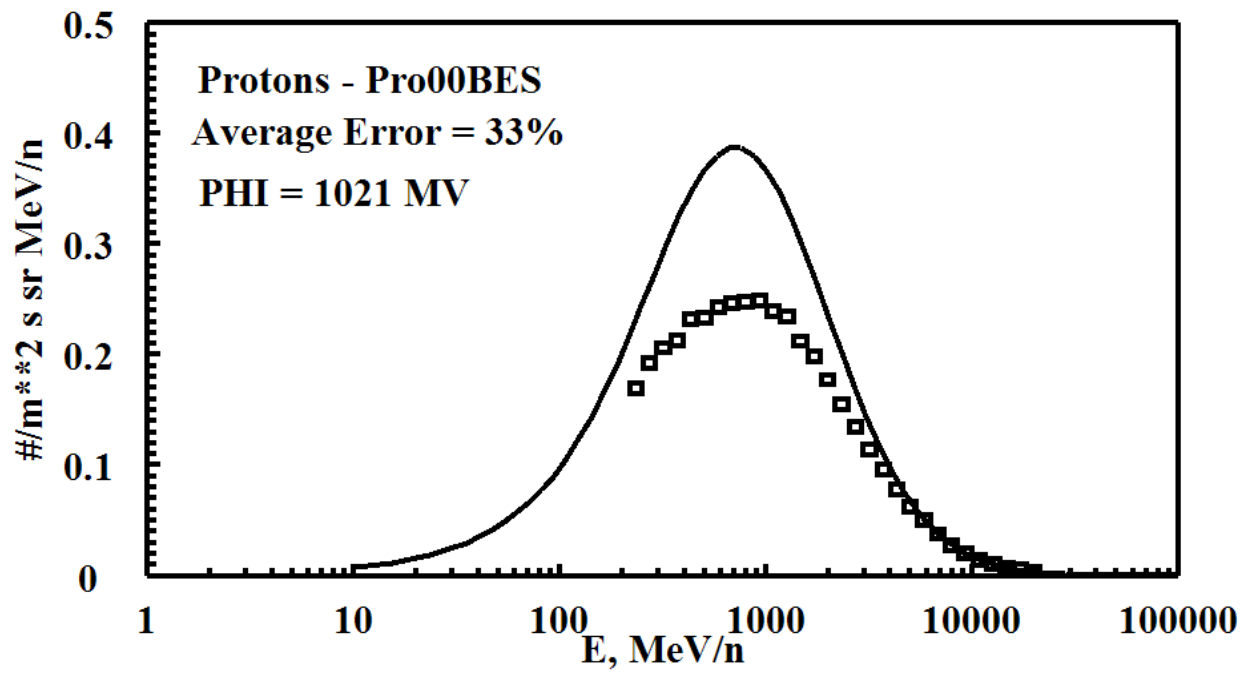
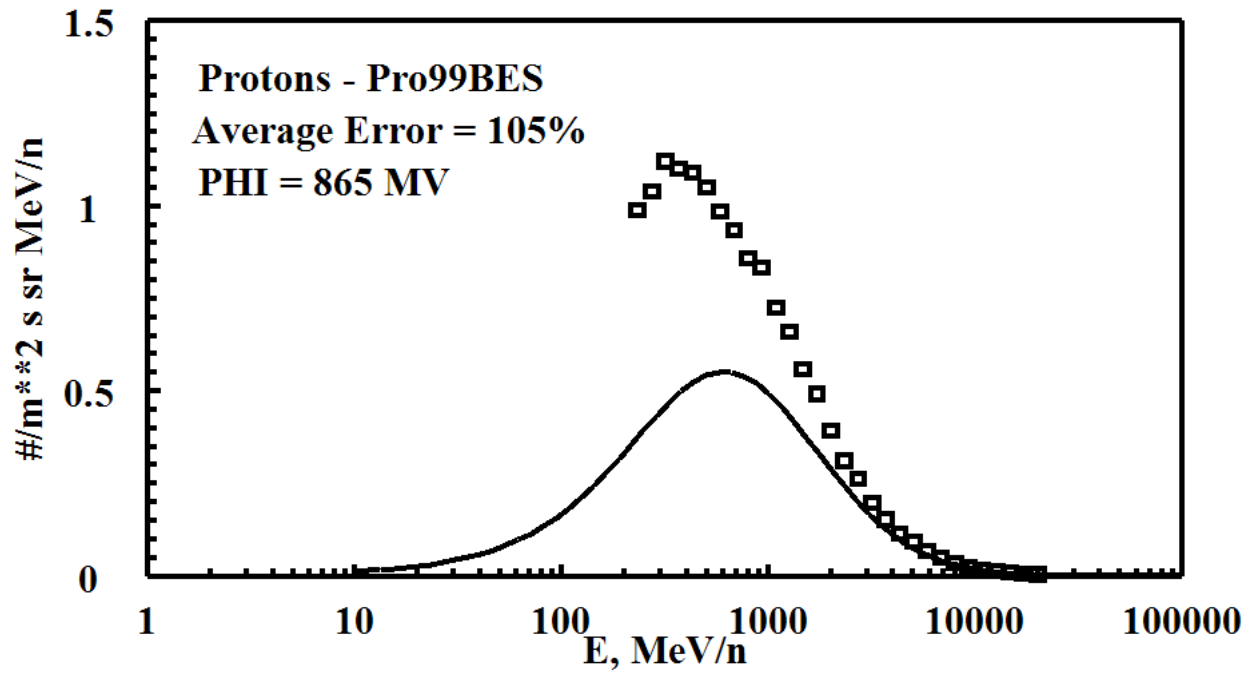
FILE	DATE	PHI (MV)	ERROR=ABS (FLUX-DATA)
Pro92IMX.dat	1992.540	942.8263	113.5180
Pro61FG.dat	1961.515	1073.765	176.6916
Pro62FG.dat	1962.573	823.6523	33.71636
Pro61MV.dat	1961.603	1063.220	180.3427
Pro62MV.dat	1962.542	834.3836	202.9461
Pro67RE.dat	1967.716	869.5131	192.3126
Pro68RE.dat	1968.622	991.5895	267.6558
Pro69RE.dat	1969.538	998.6859	109.4019
Pro99BES.dat	1999.611	865.3713	105.2273
Pro00BES.dat	2000.608	1020.844	32.94044
Pro02BES.dat	2002.600	1029.817	5.189703
BO AVERAGE ERROR =			129.0857

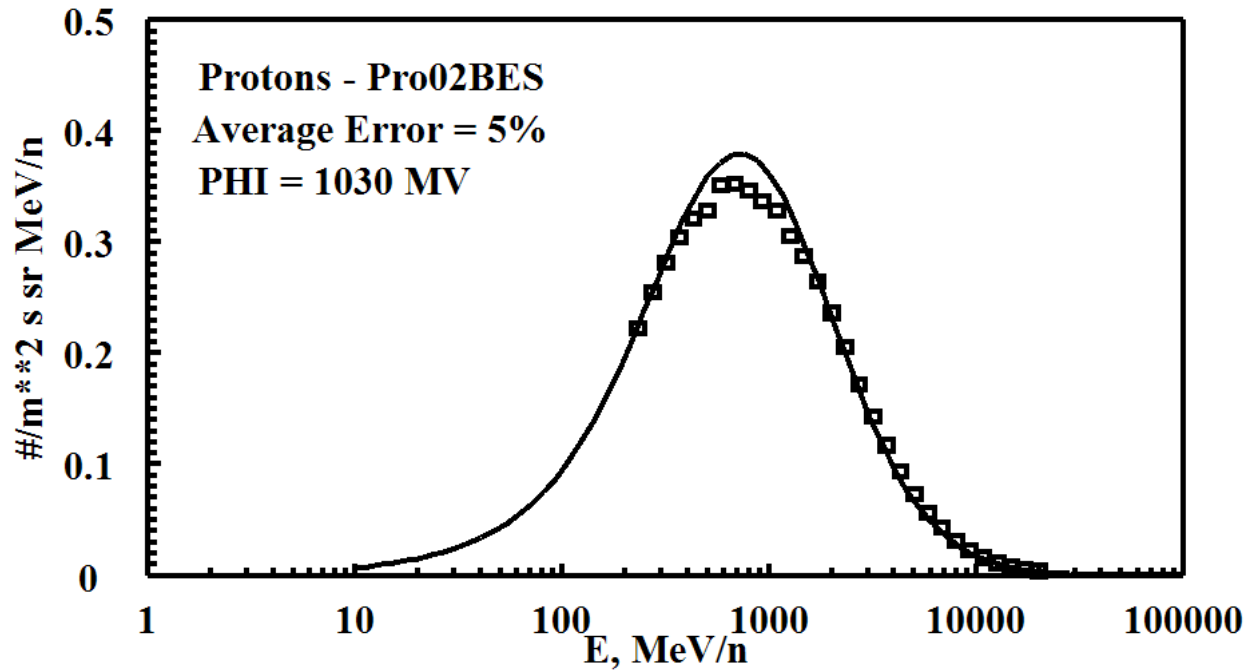








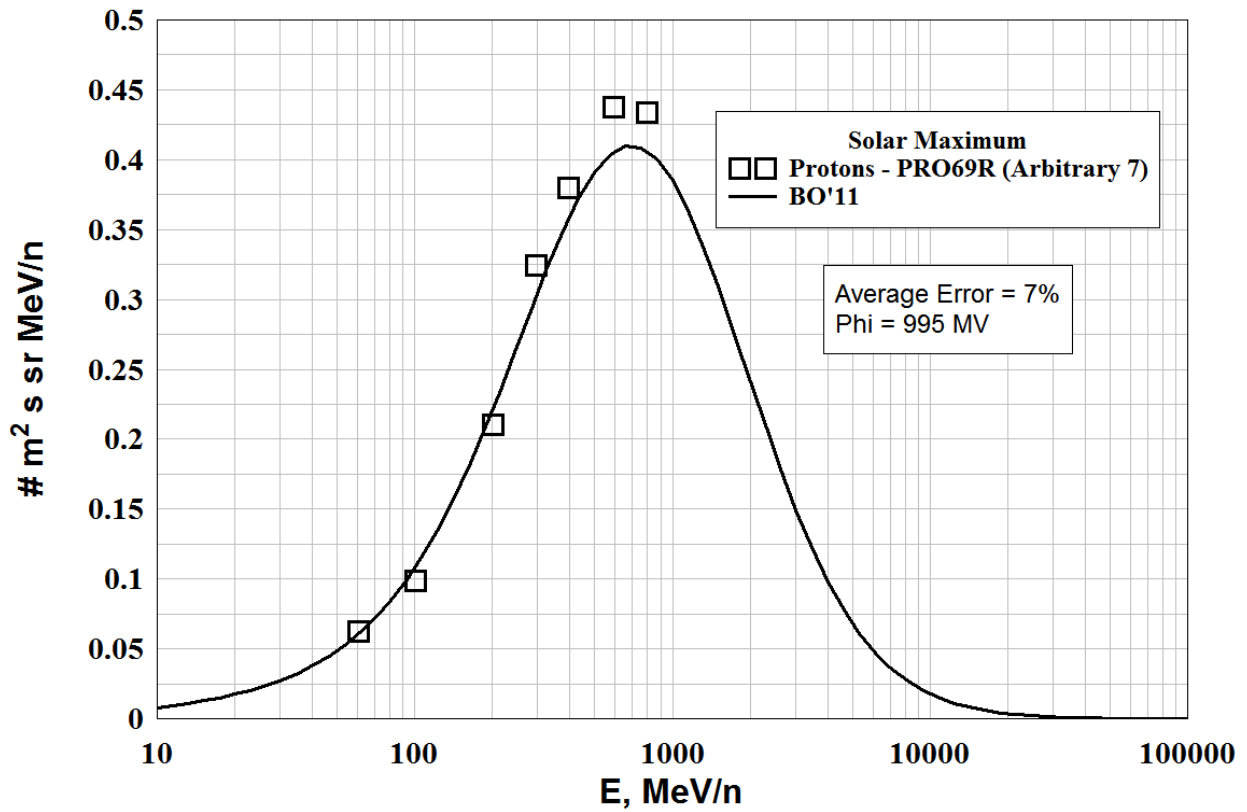
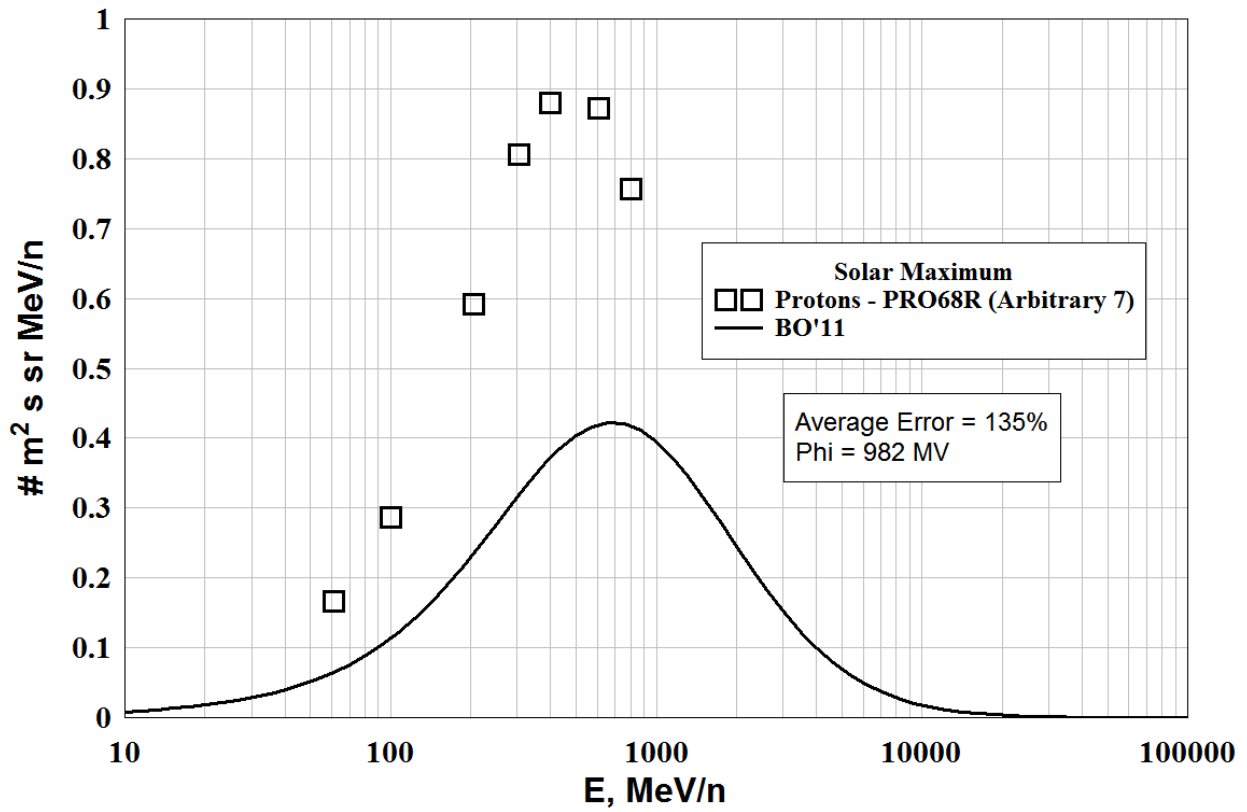


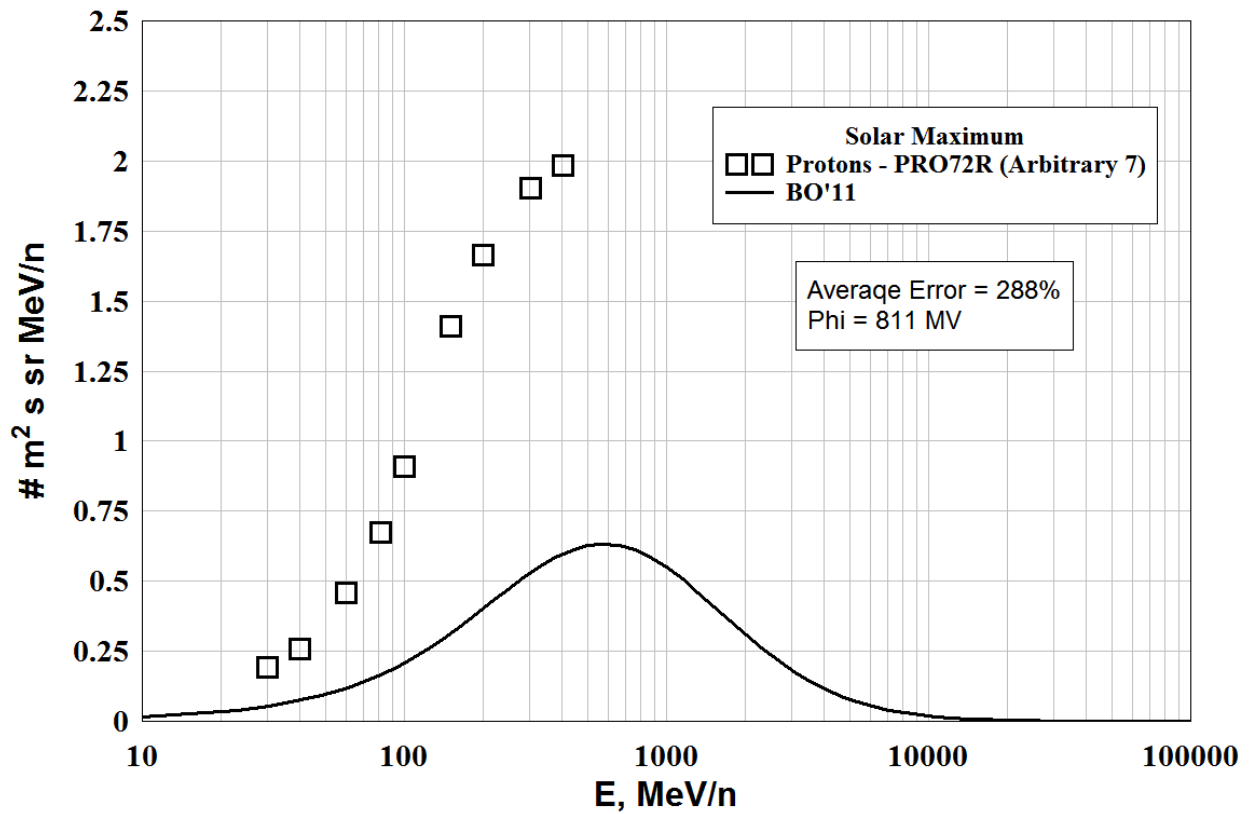
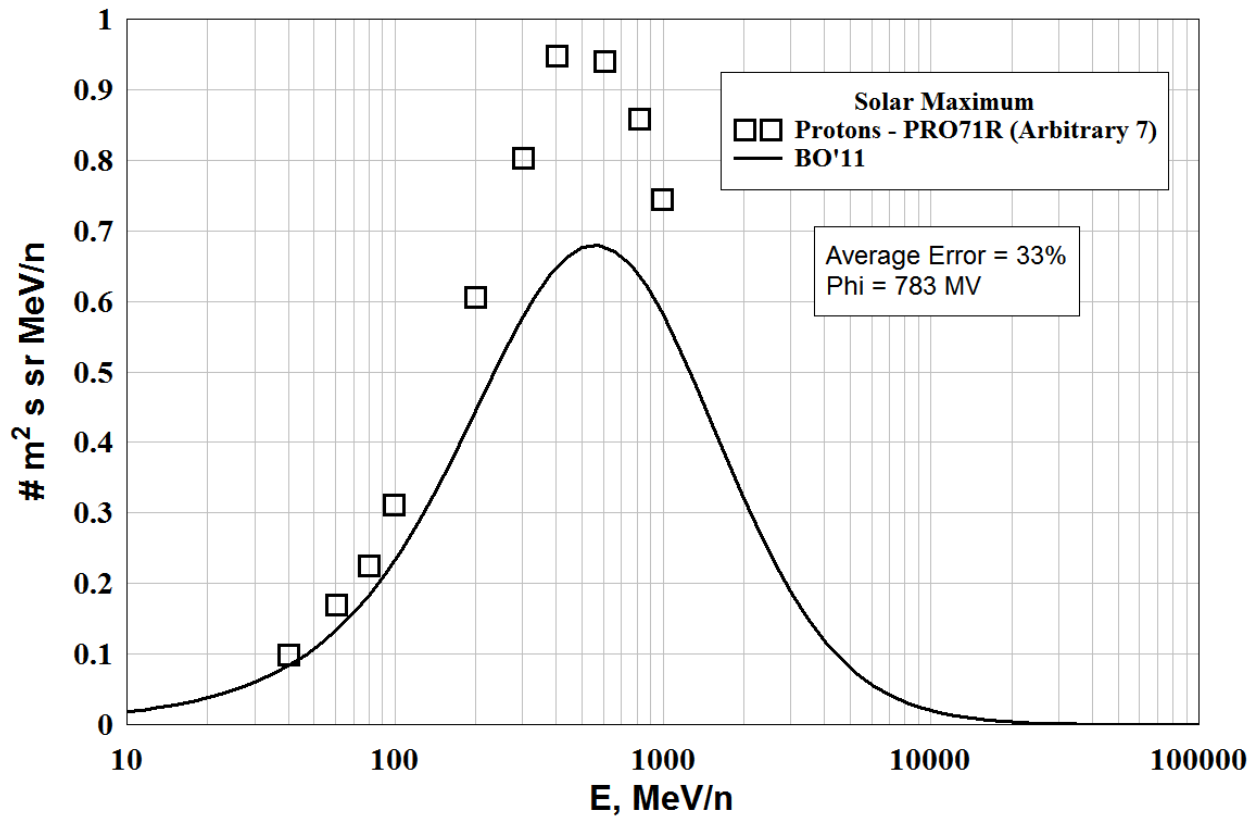


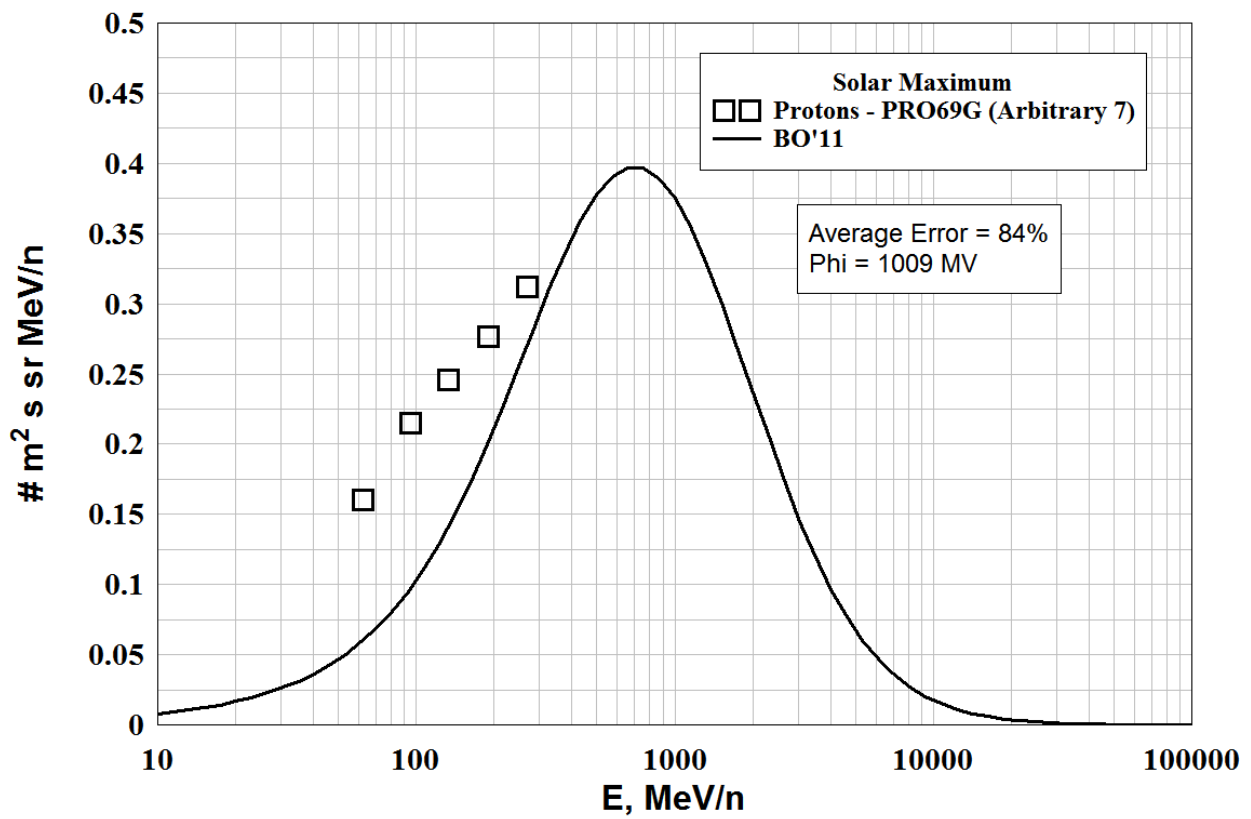
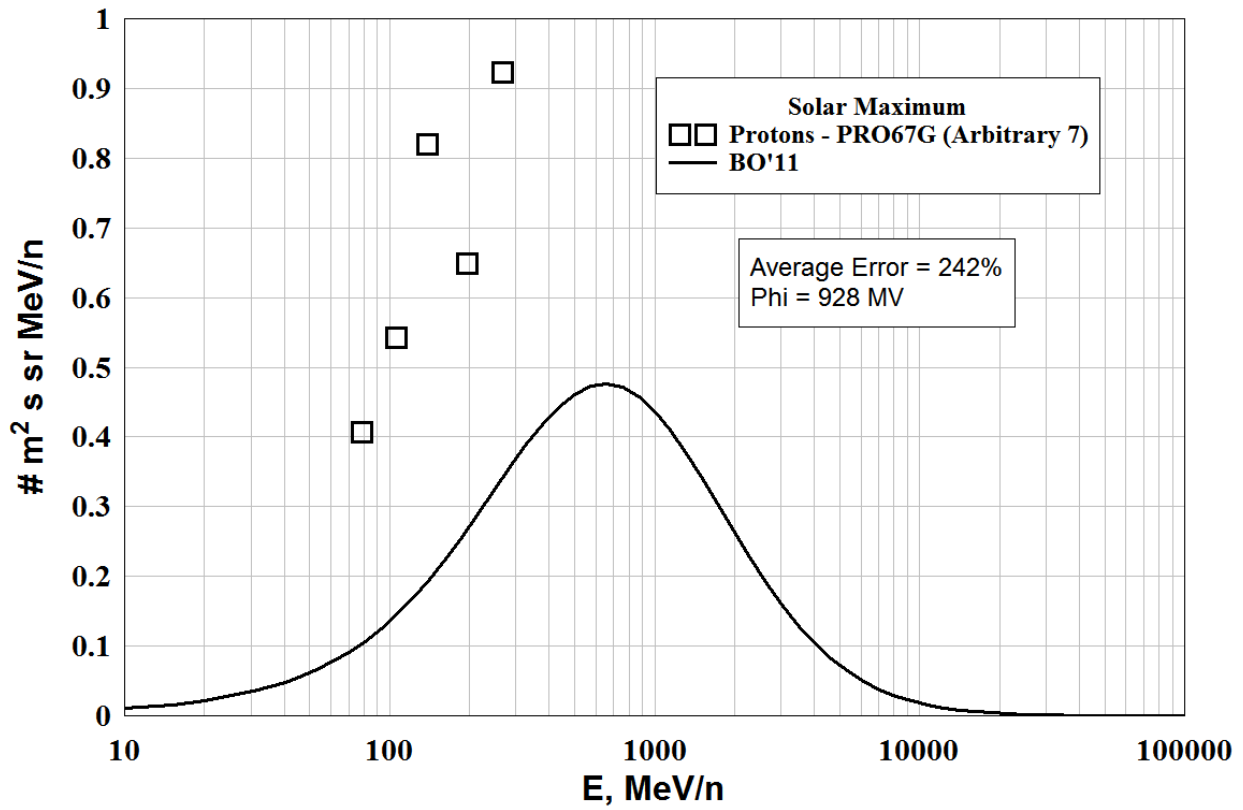
PROTONS - Low Energy, Solar Maximum

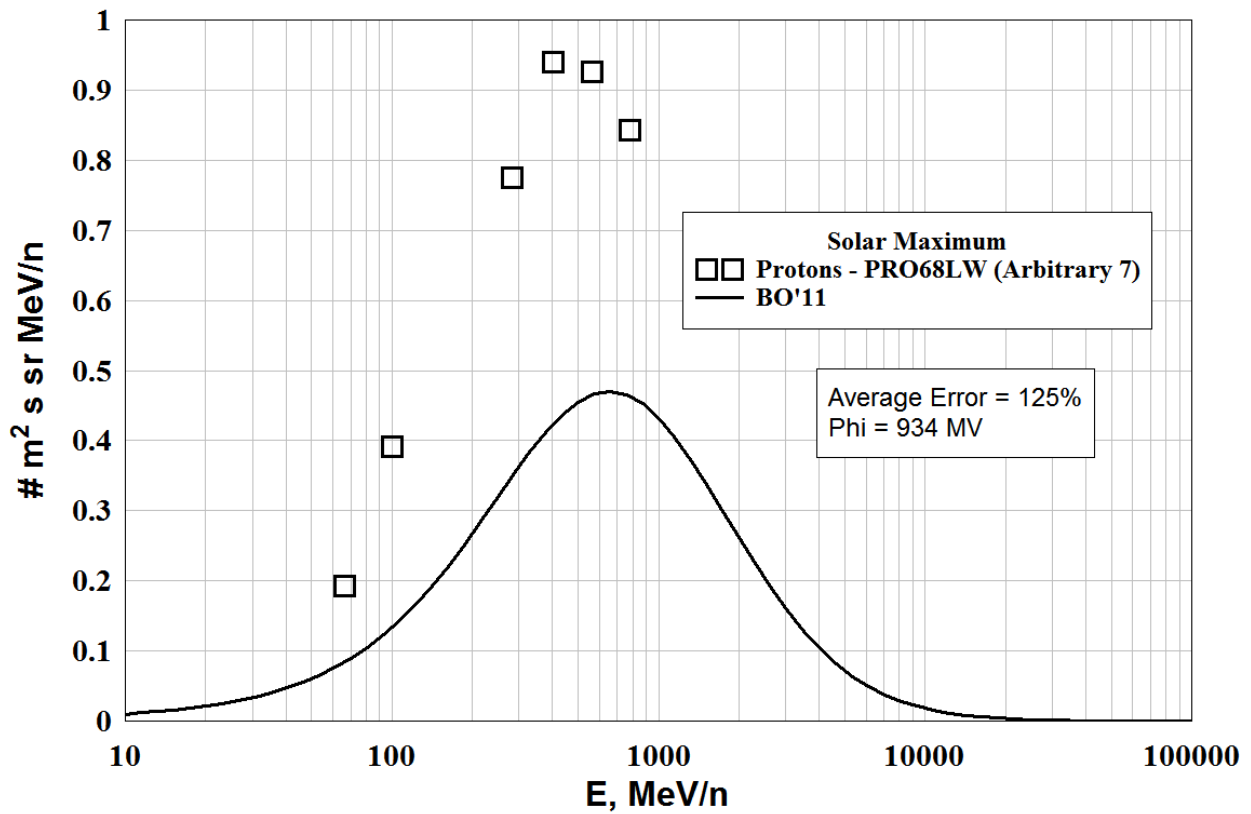
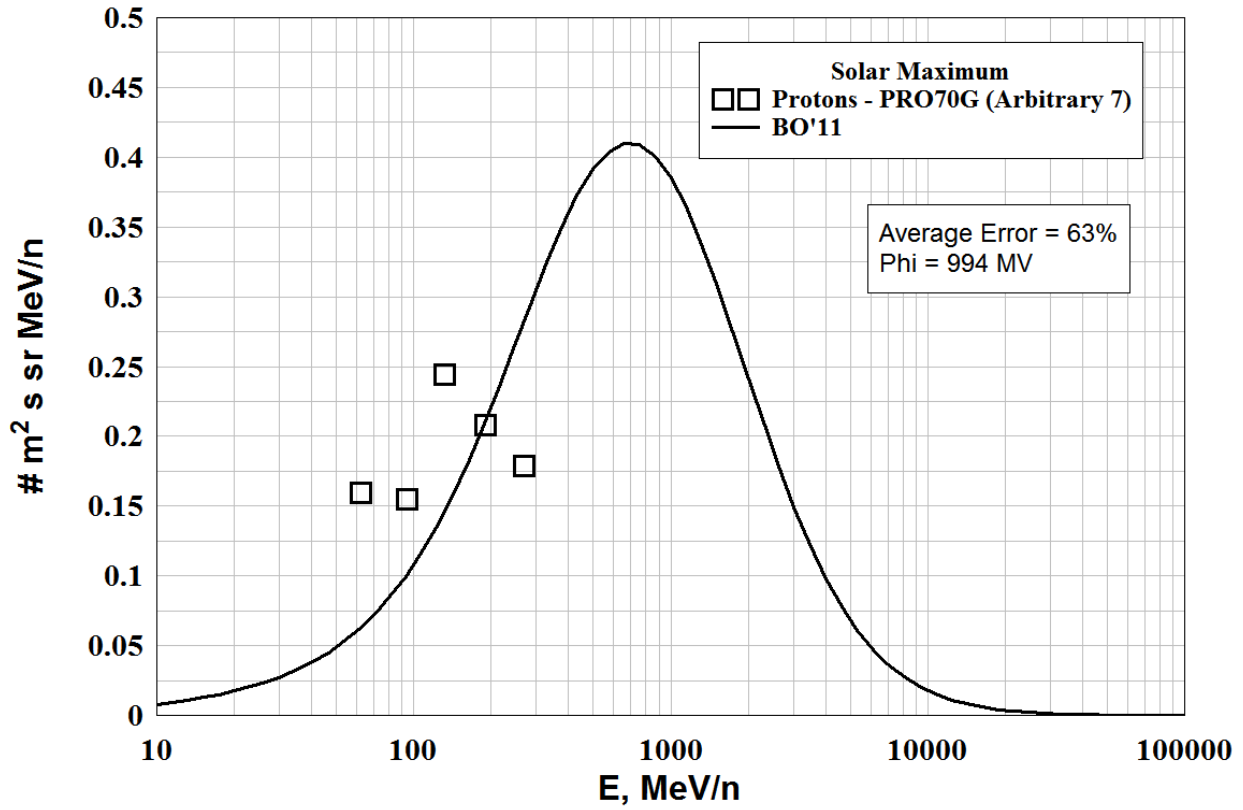
Files Rejected - (Arbitrary 7's)

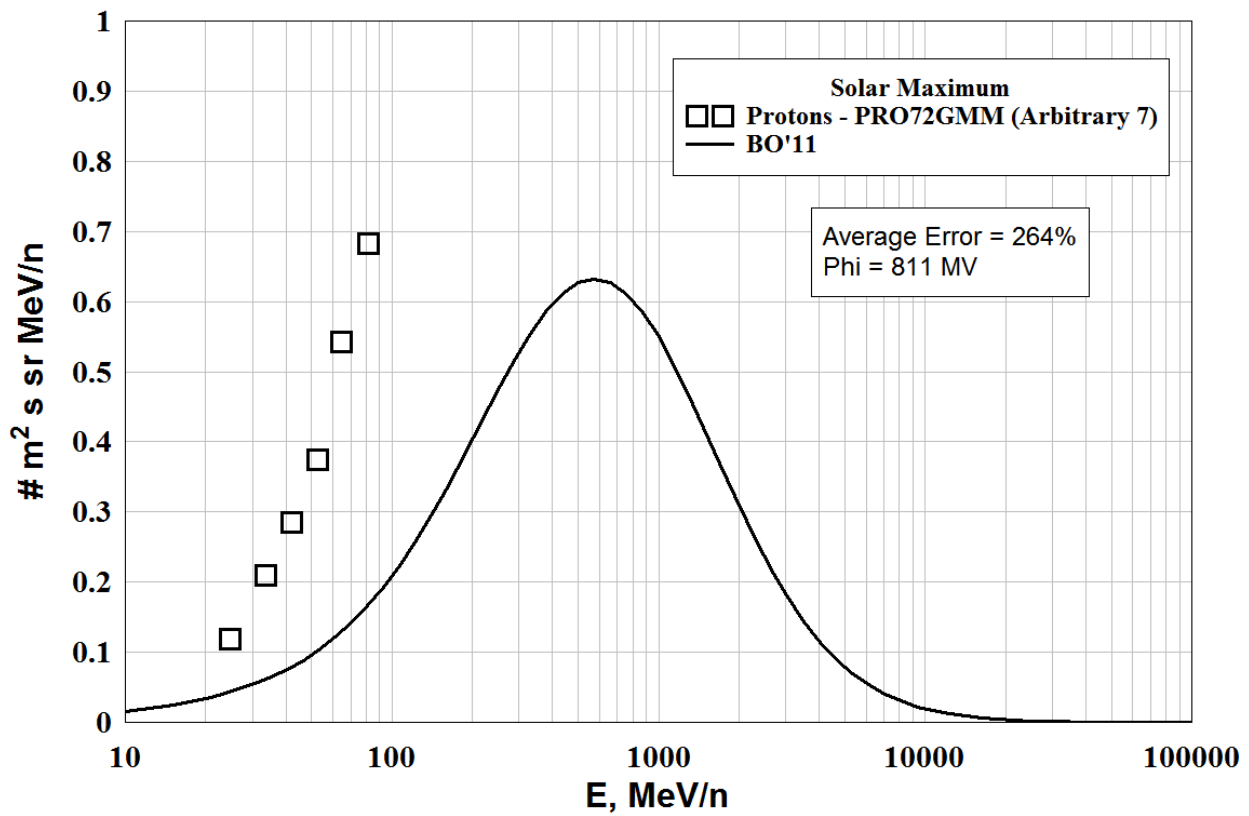
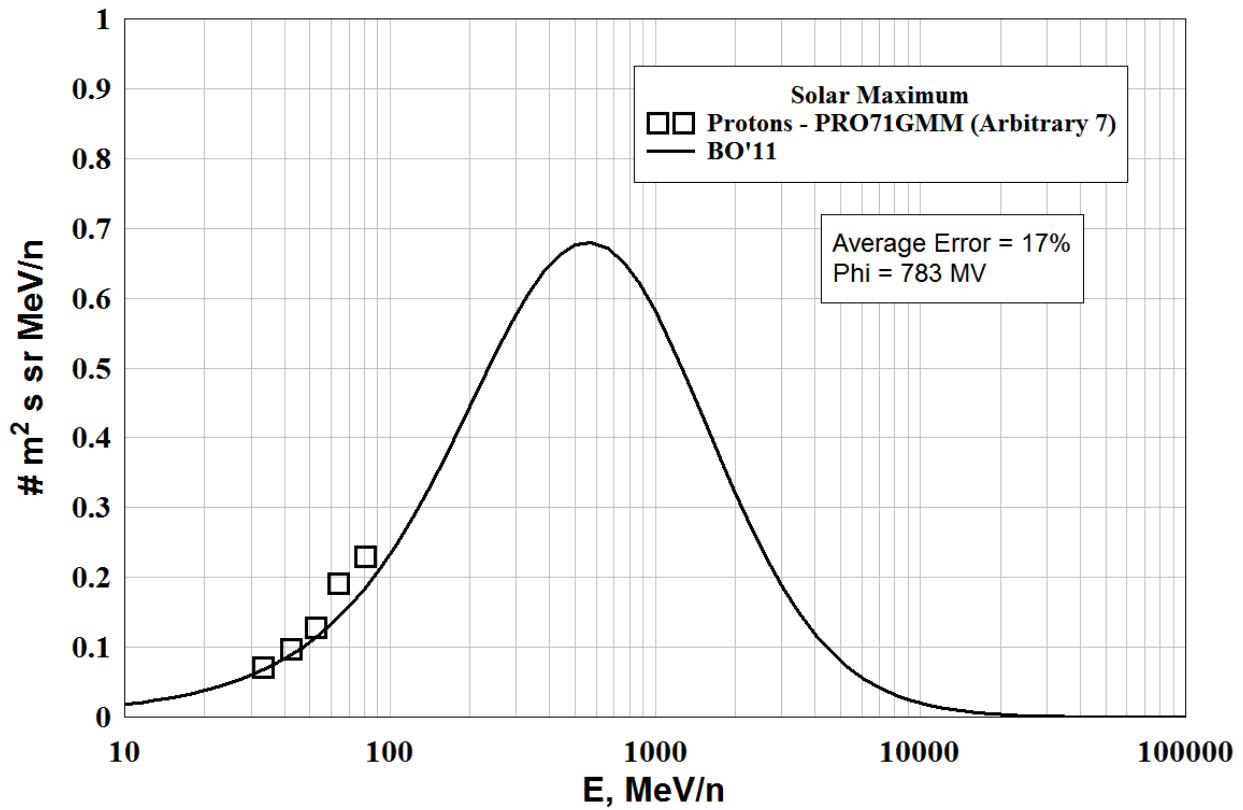
FILE	DATE	PHI (MV)	ERROR=ABS (FLUX-DATA)
Pro68R.dat	1968.581	981.7554	135.4016
Pro69R.dat	1969.041	994.8779	6.619009
Pro71R.dat	1971.515	782.7104	33.03931
Pro72R.dat	1972.332	810.7516	288.1599
Pro67G.dat	1967.988	928.3704	242.4603
Pro69G.dat	1969.471	1008.994	84.08736
Pro70G.dat	1970.474	994.4297	62.62927
Pro68LW.dat	1967.956	933.7995	125.3981
Pro71GMM.dat	1971.427	782.5904	16.93390
Pro72GMM.dat	1972.332	810.7516	263.5408
Pro79Vm.dat	1978.849	887.7434	386.2381
Pro82GMP.dat	1982.499	1183.914	224.4373
Pro84GMP.dat	1984.584	899.1680	133.9511
Pro89W.dat	1989.682	1248.804	37.41331
BO AVERAGE ERROR =			145.7364

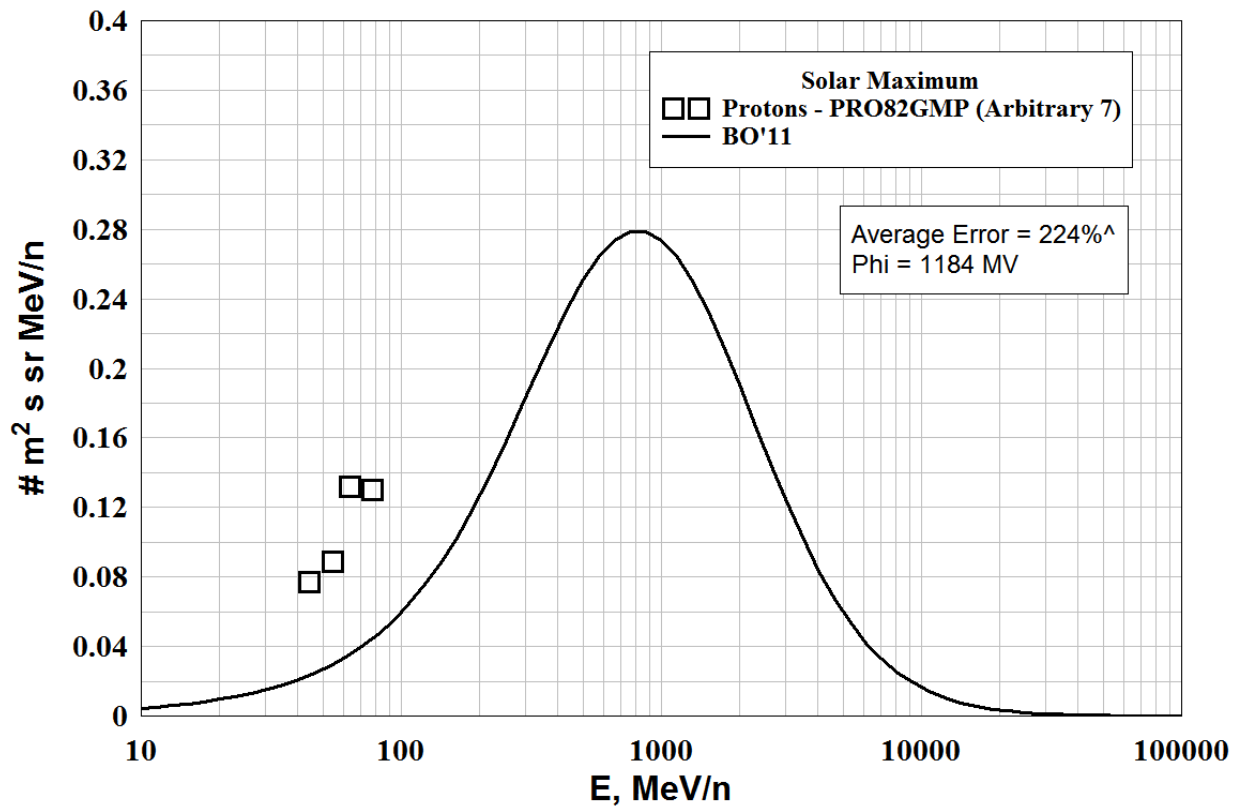
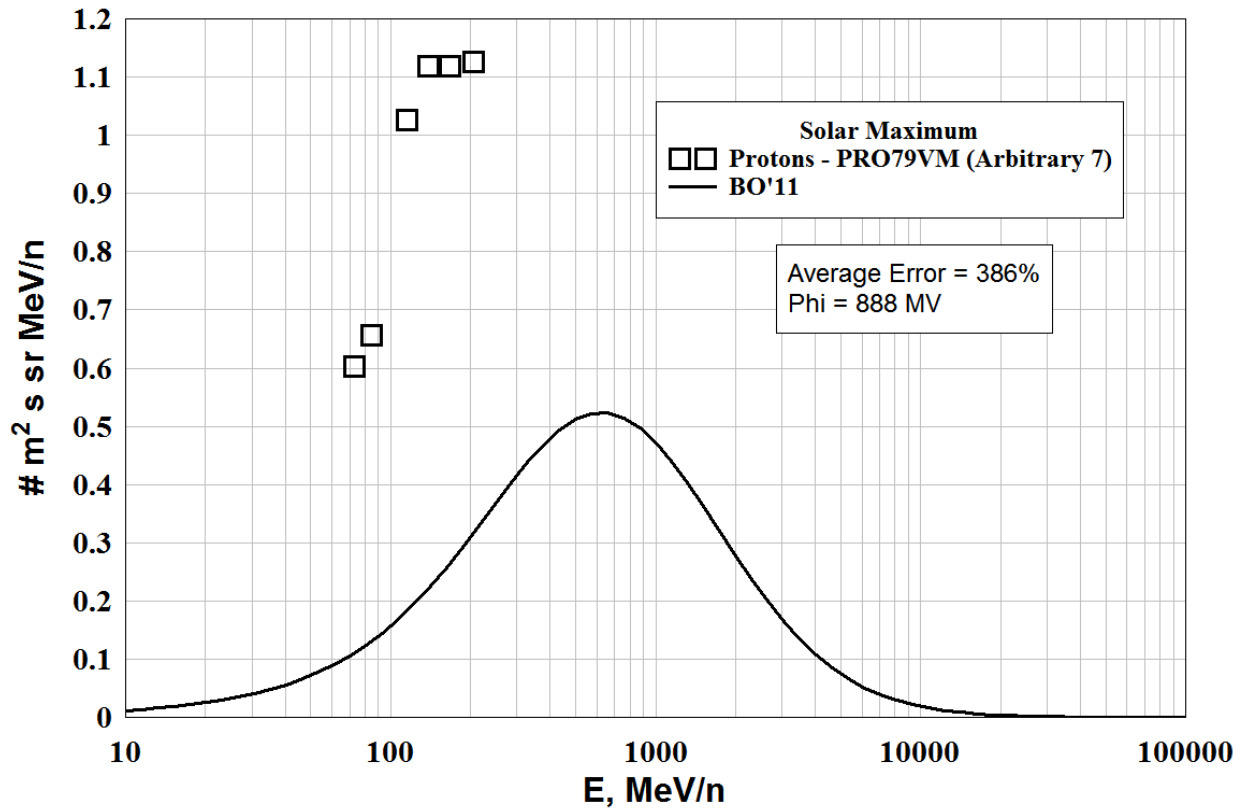


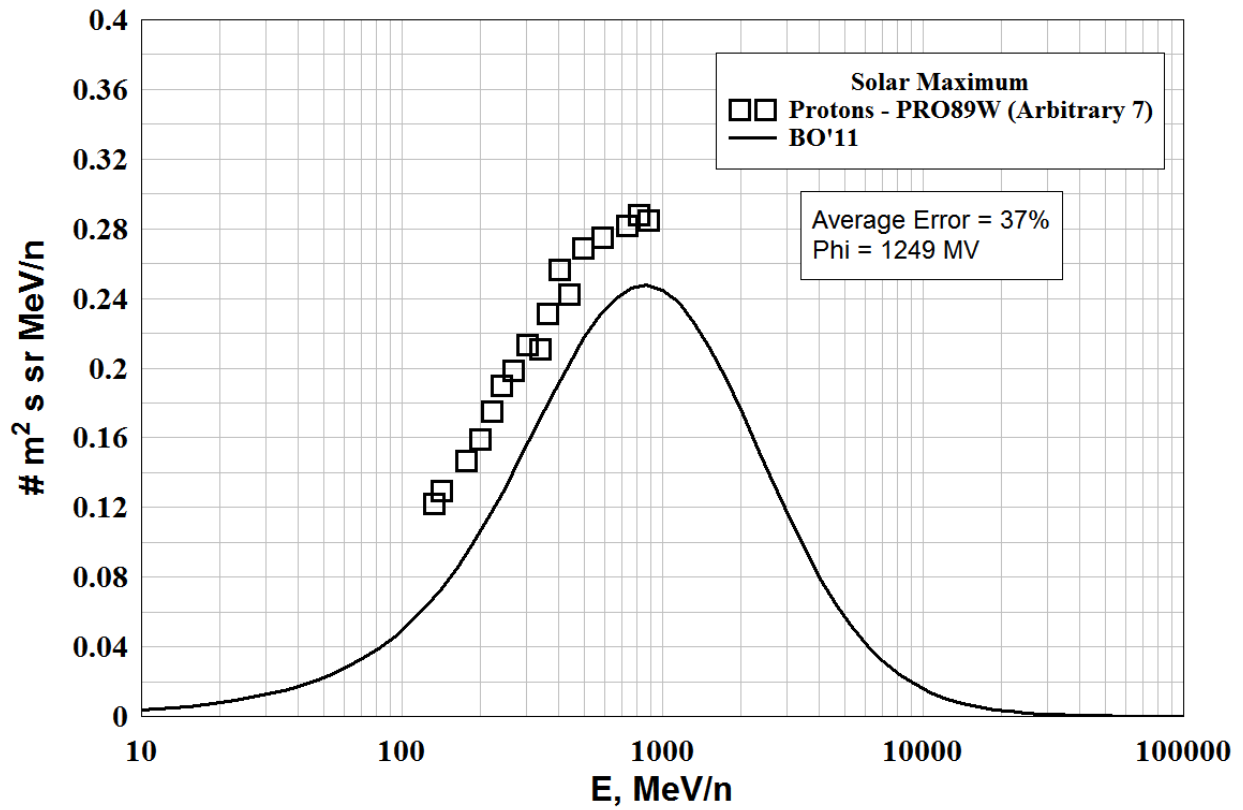
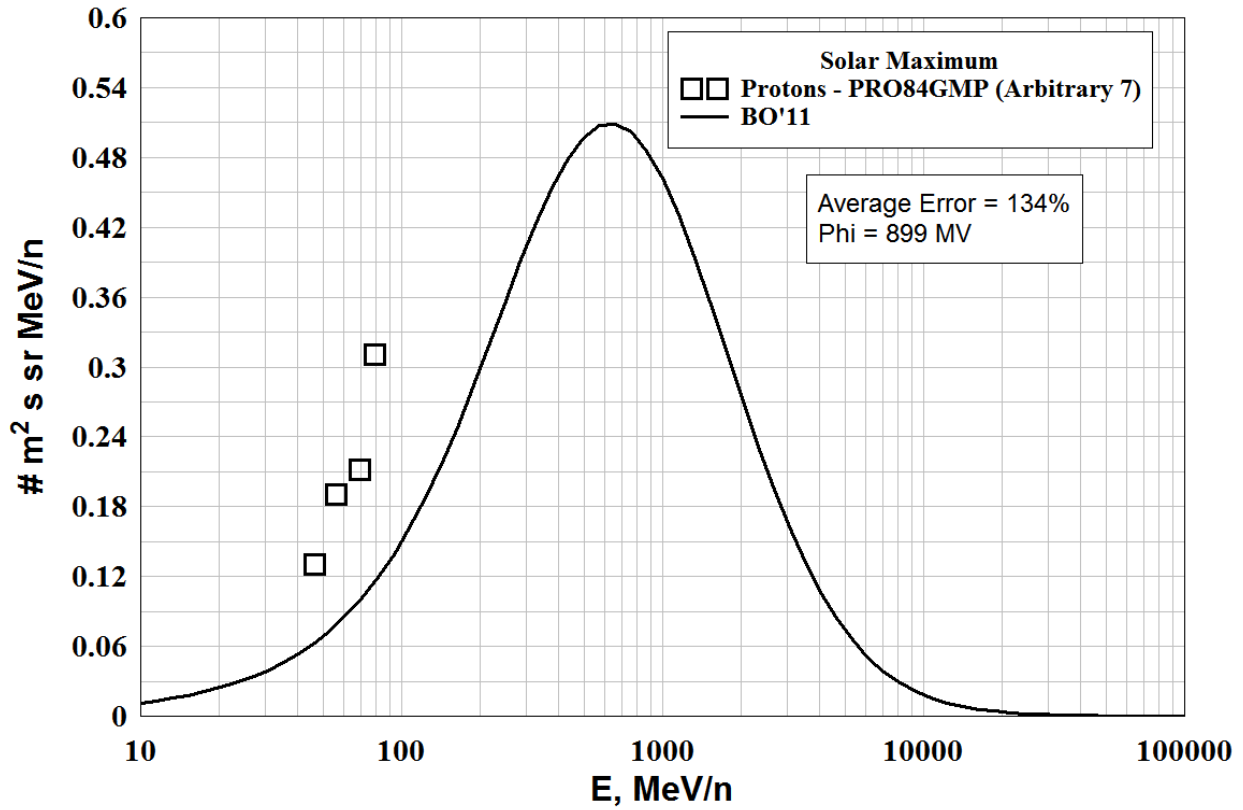










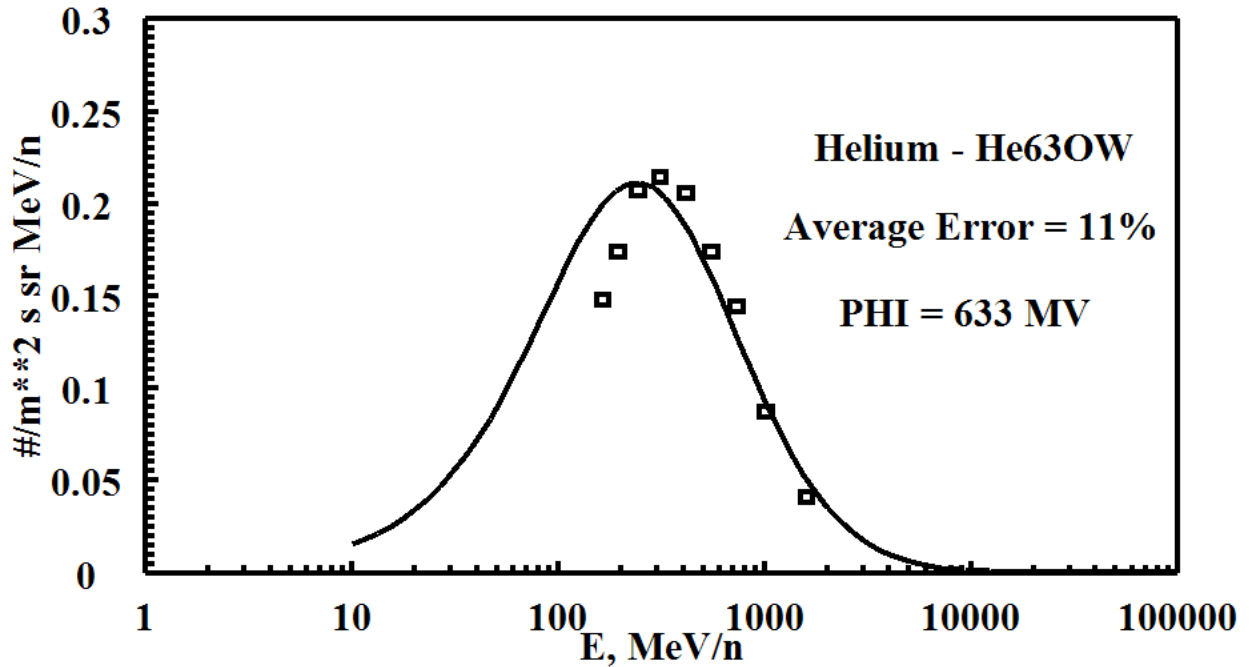


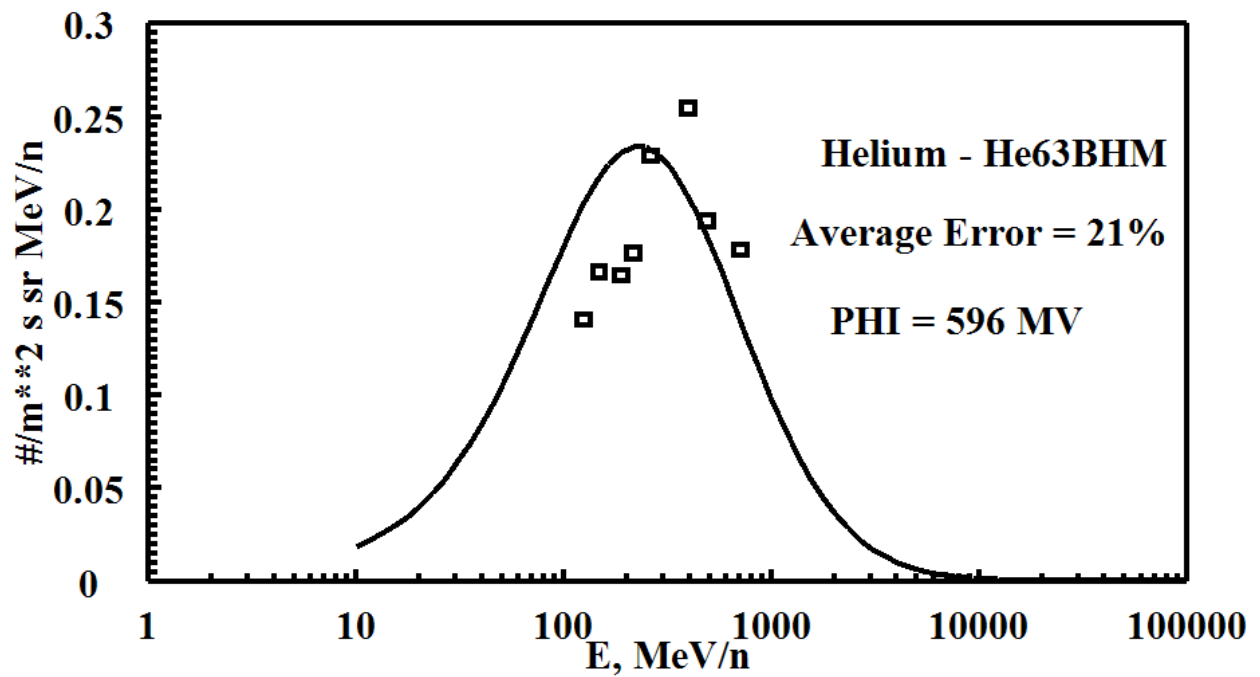
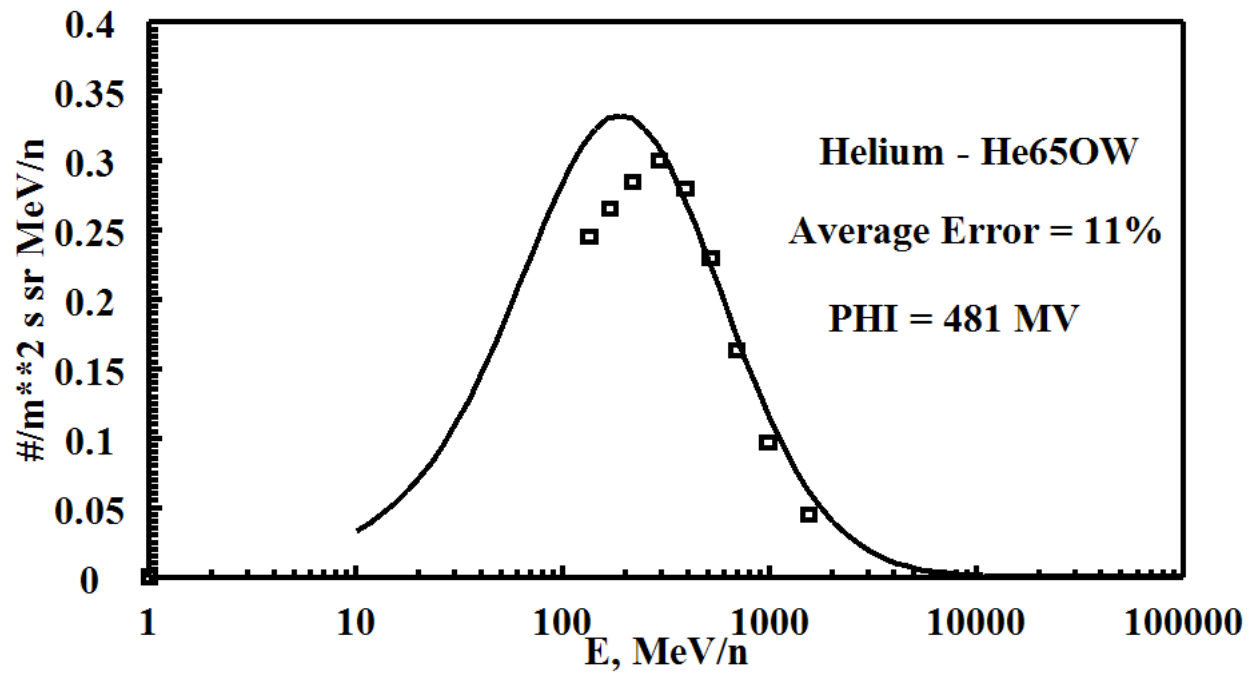
HELIUM - Low Energy, Solar Minimum

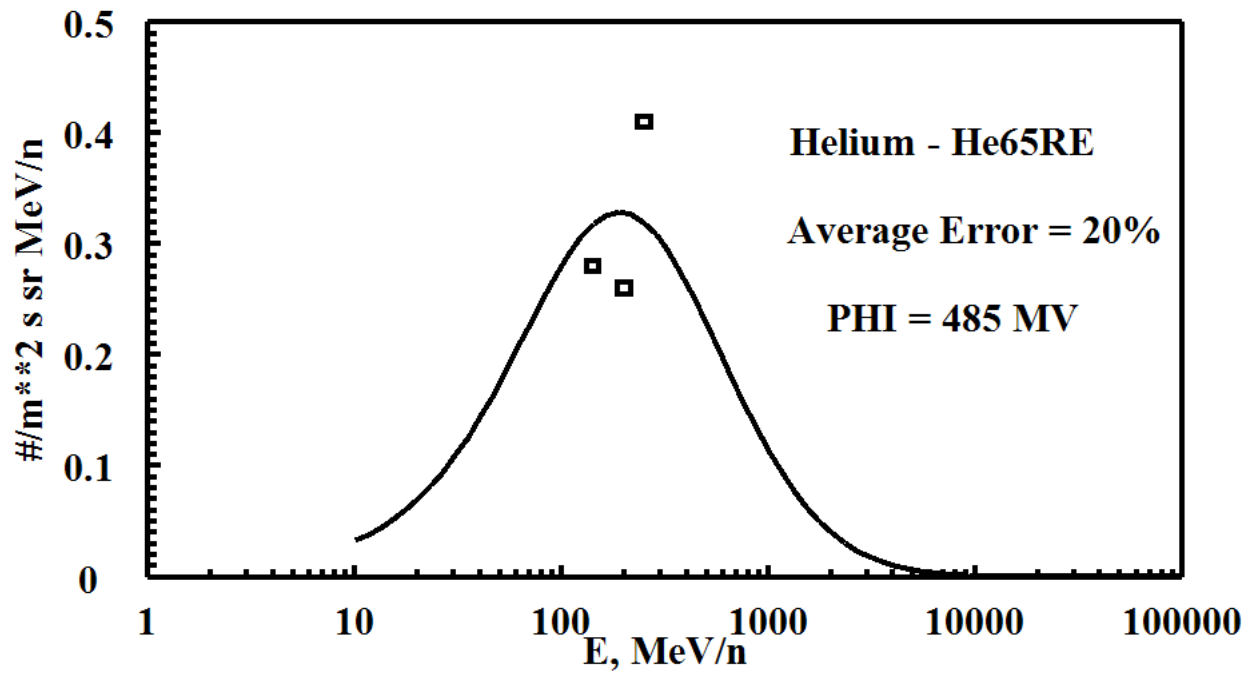
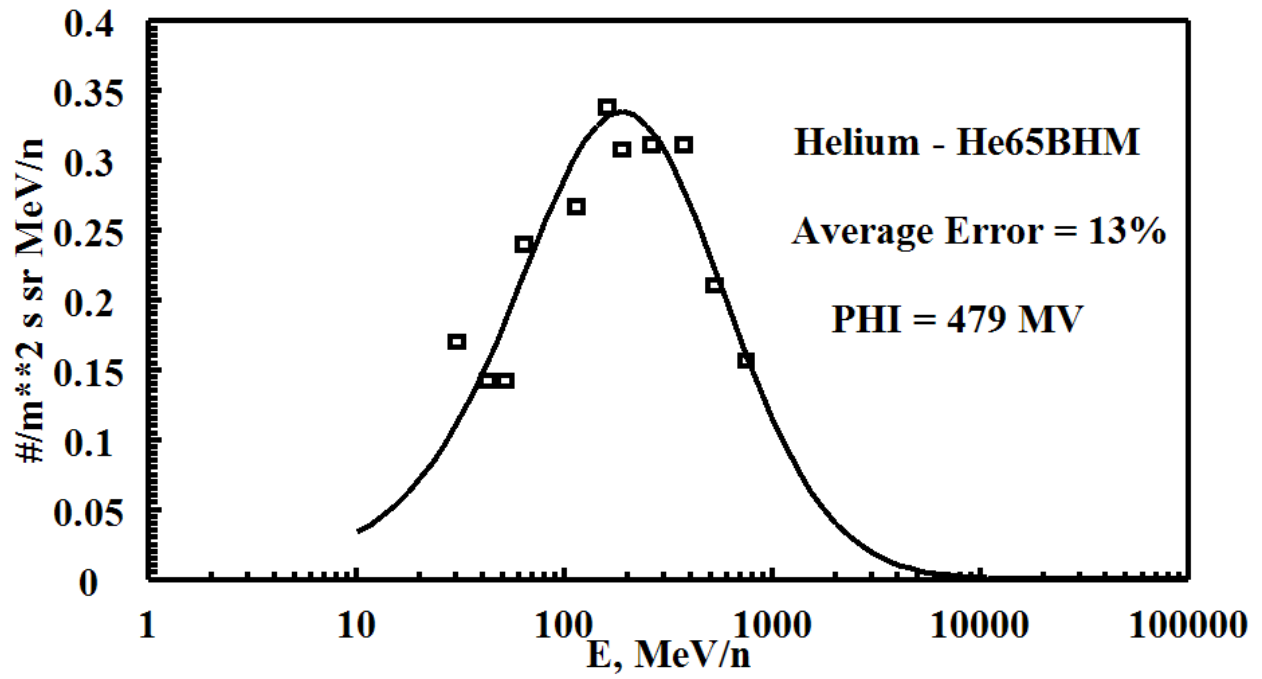
Files Used (Arbitrary 1's)

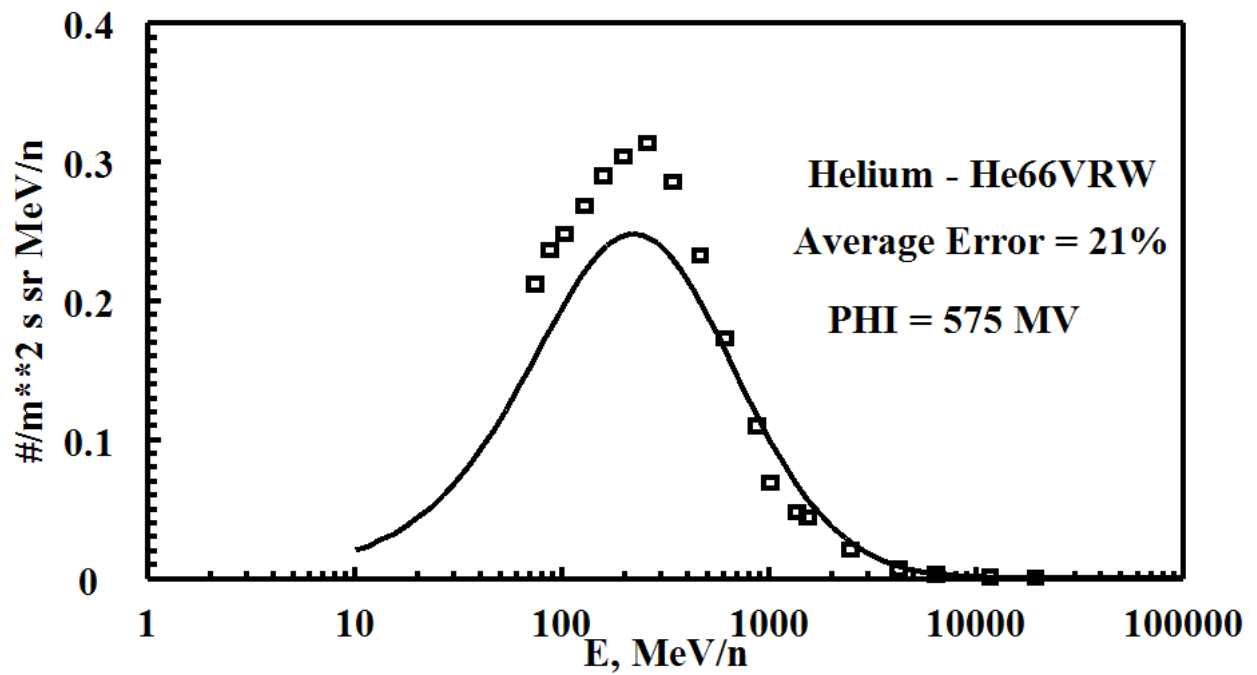
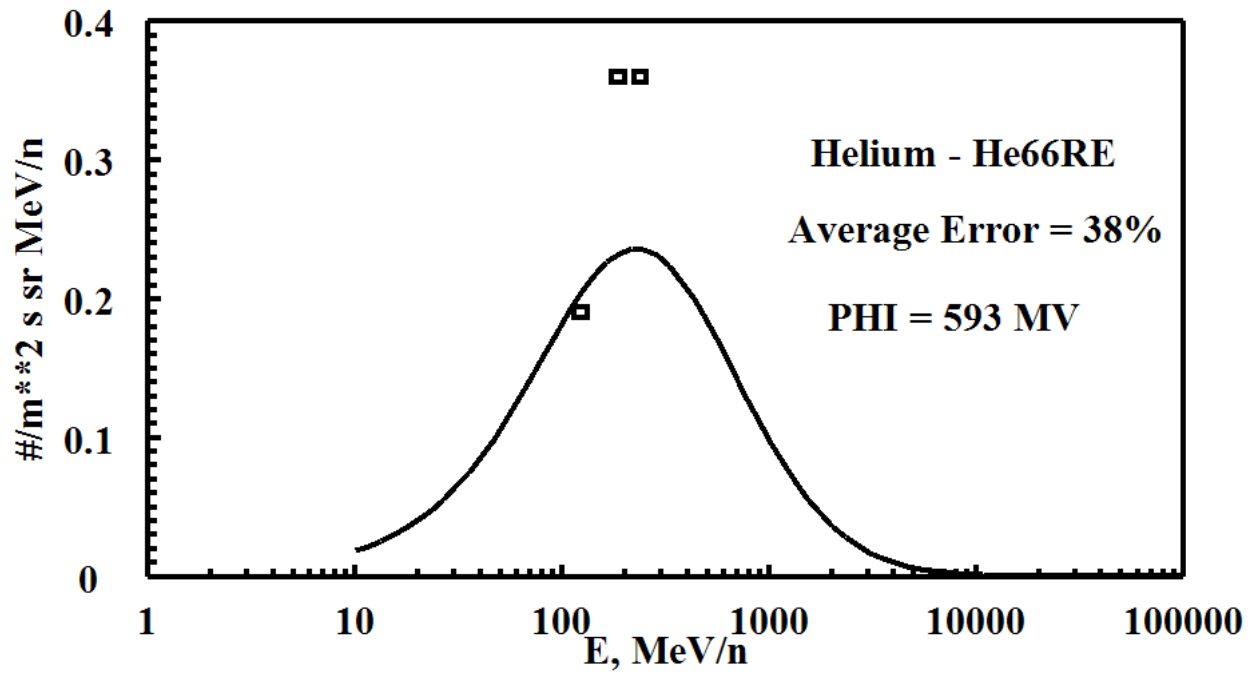
FILE	DATE	PHI (MV)	ERROR=ABS (FLUX-DATA)
He63OW.dat	1963.575	632.7310	11.41053
He65OW.dat	1965.501	481.2304	11.11259
He63BHM.dat	1963.836	596.1647	20.65012
He65BHM.dat	1965.447	479.2167	12.53052
He65RE.dat	1965.627	485.0185	20.43687
He66RE.dat	1966.641	593.0267	38.18496
He66vRW.dat	1966.564	575.2775	21.46687
He66B.dat	1966.499	559.3981	19.02636
He93WSA.dat	1993.567	572.9689	12.92917
He97BES.dat	1997.570	449.6011	11.11594
He98BES.dat	1998.575	547.9679	6.896191
He94Cap.dat	1994.605	495.4308	24.51402

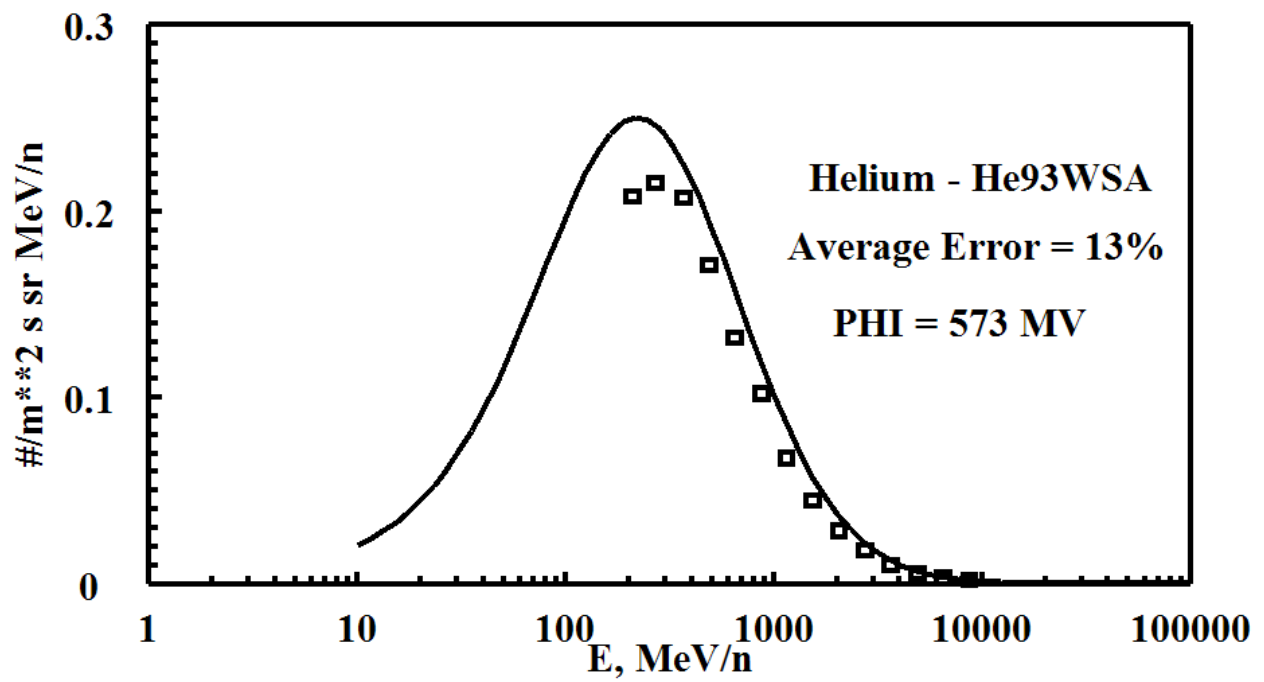
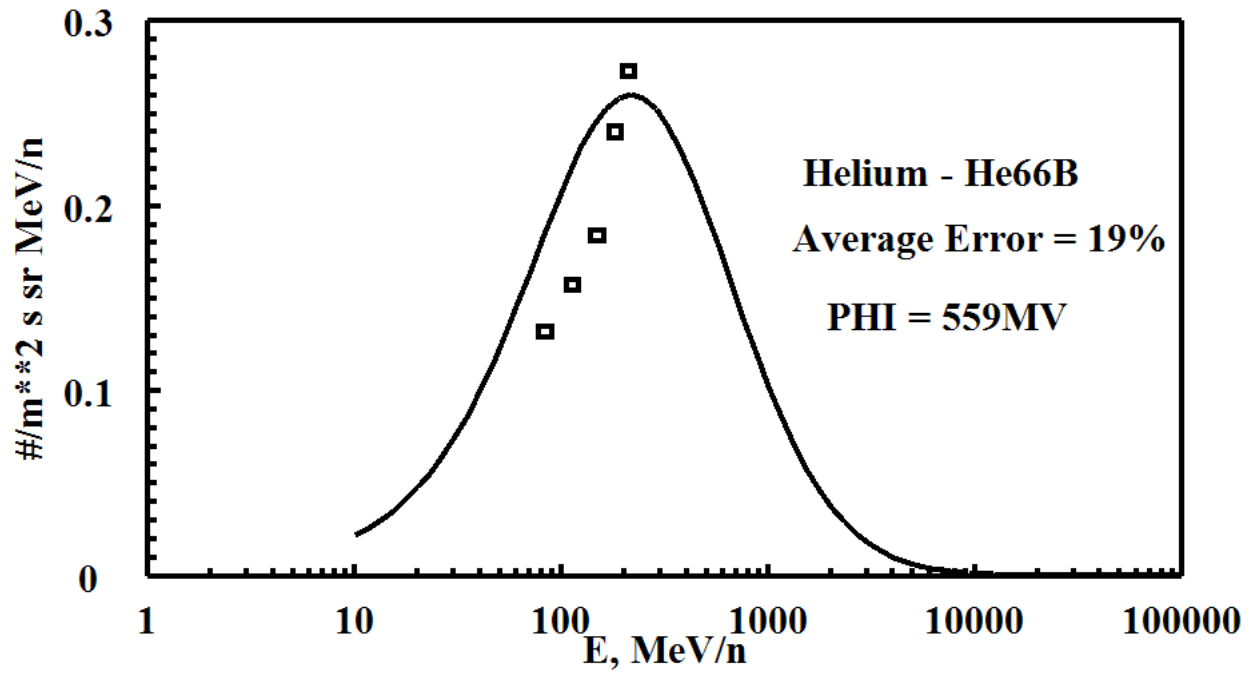
BO AVERAGE ERROR = 17.52284

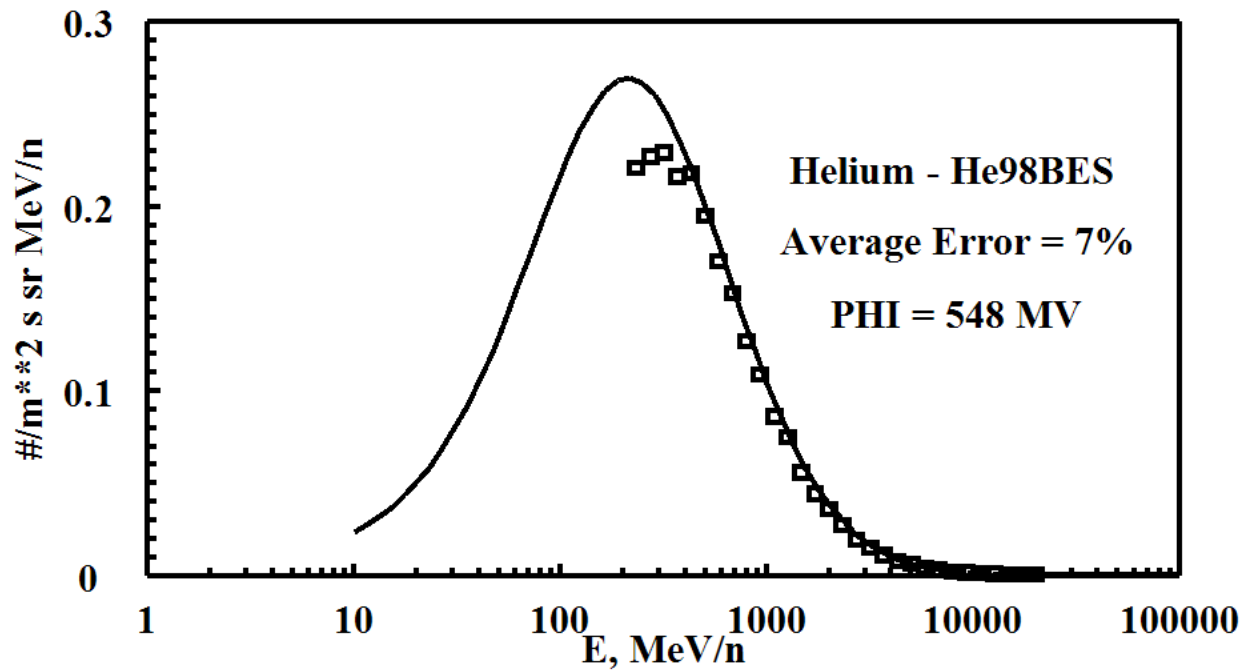
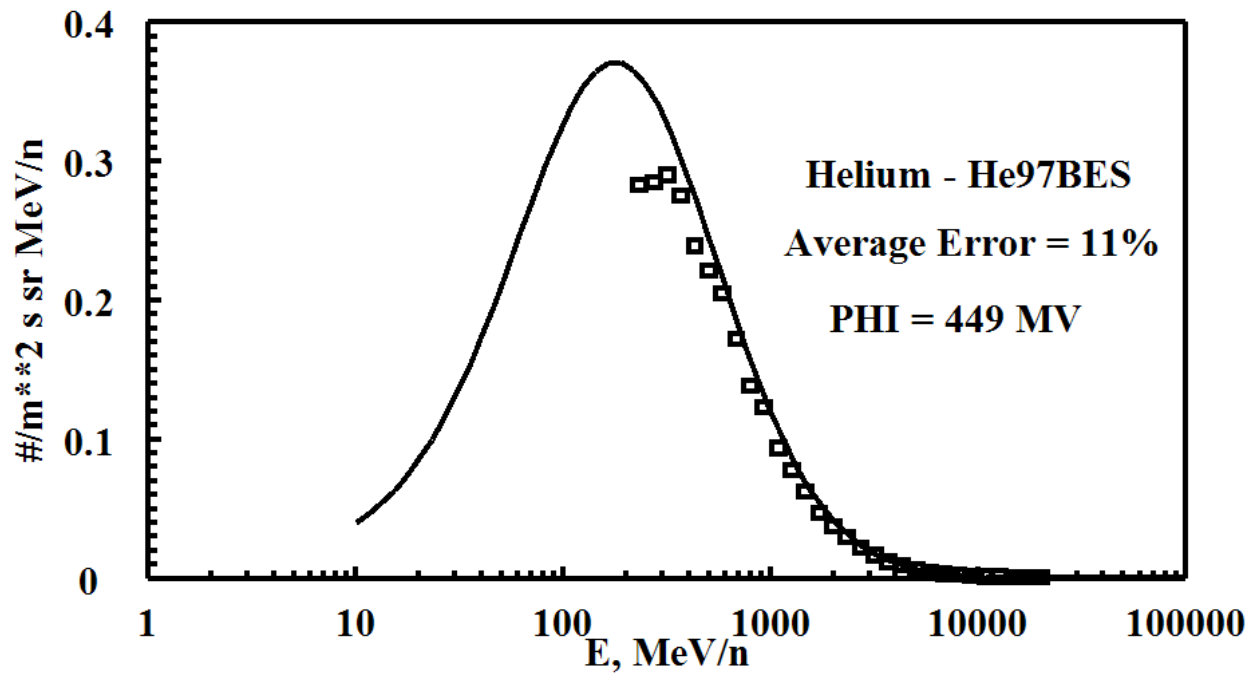


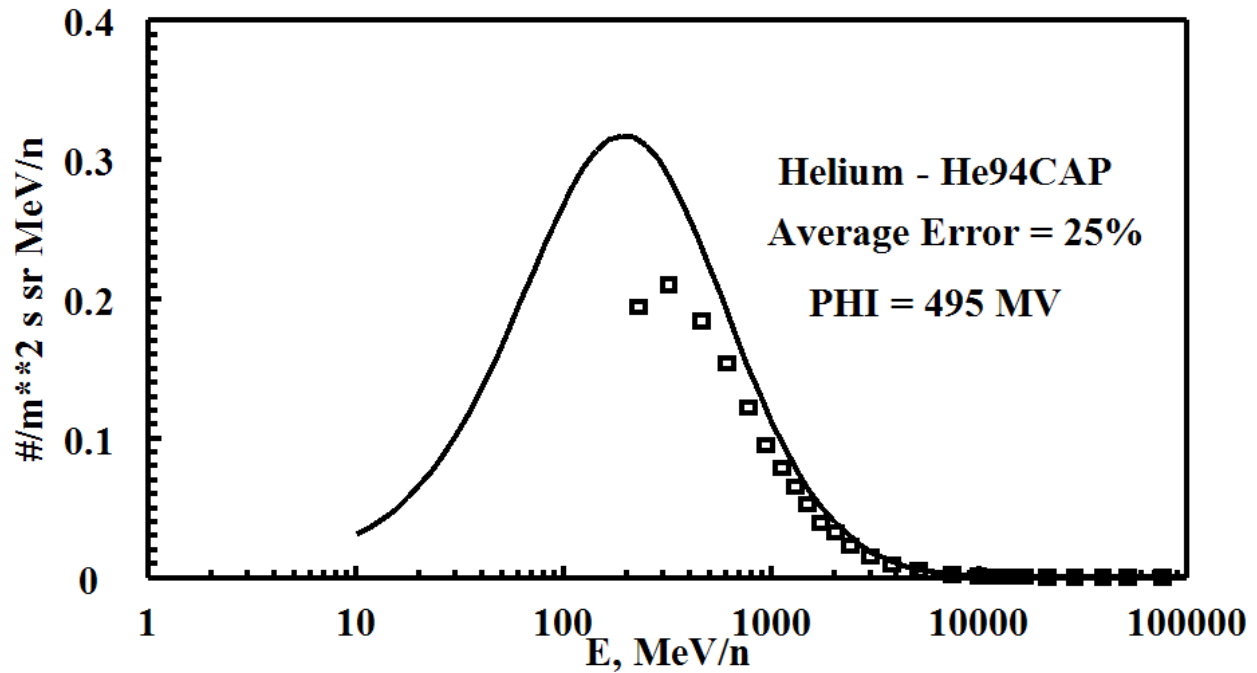








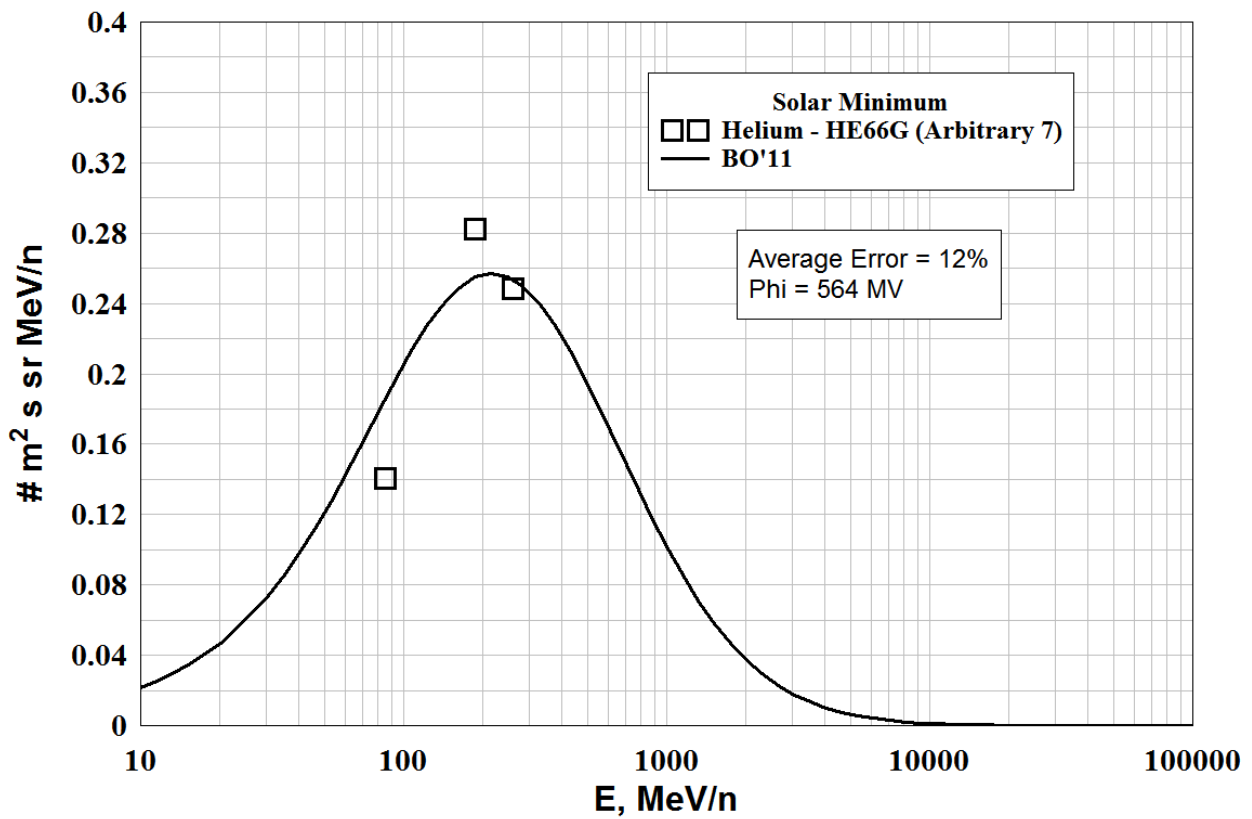
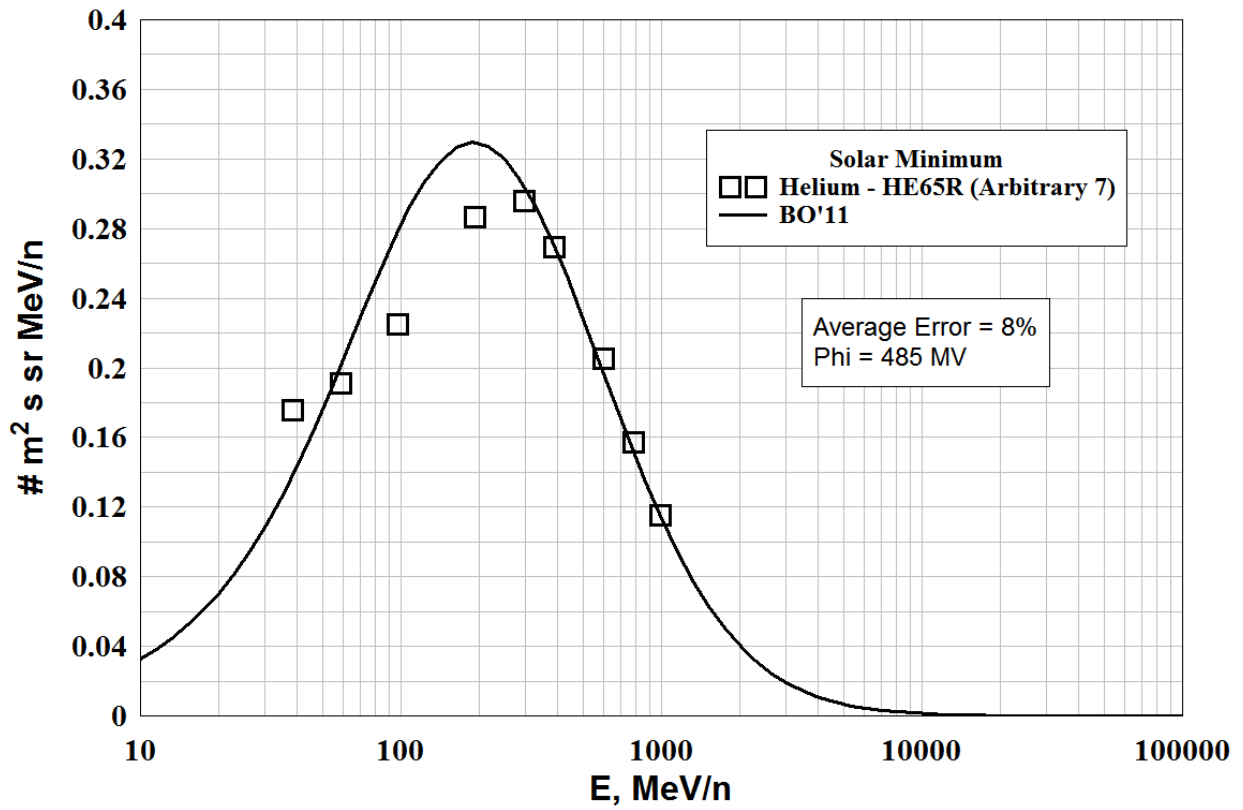


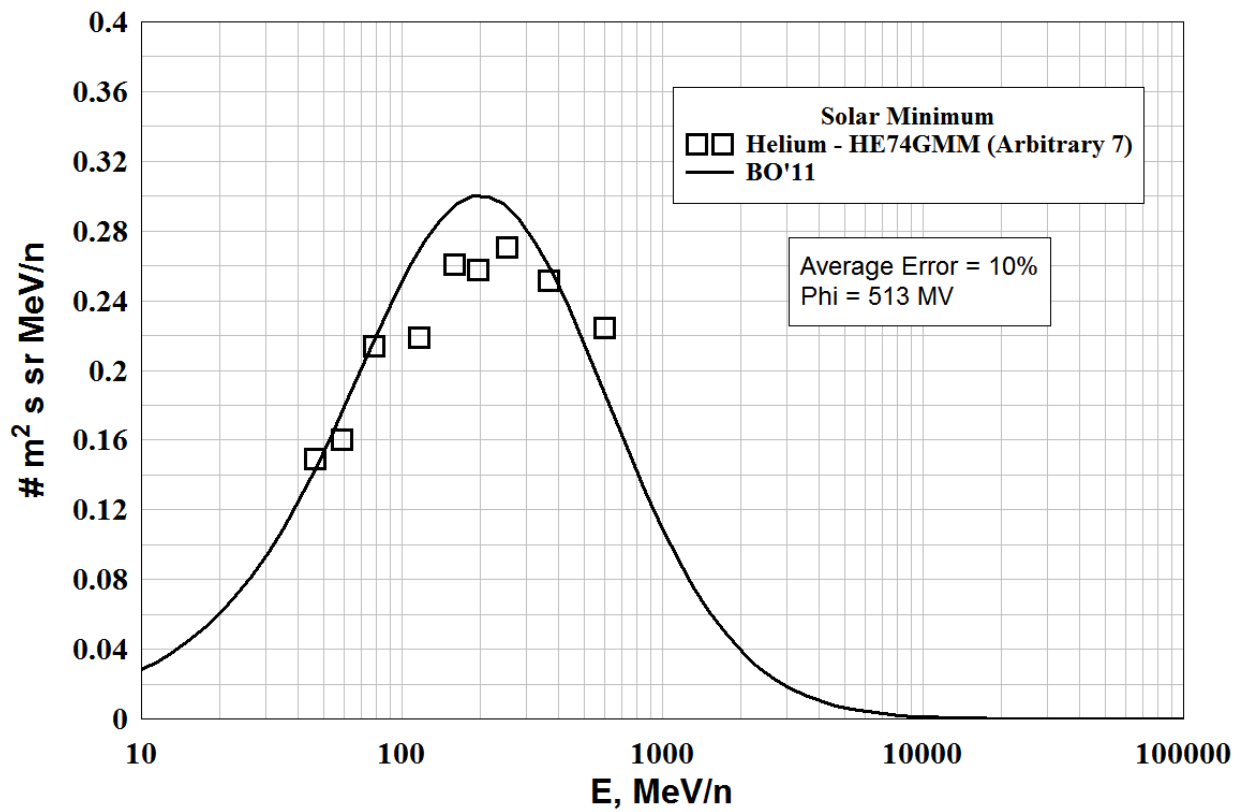
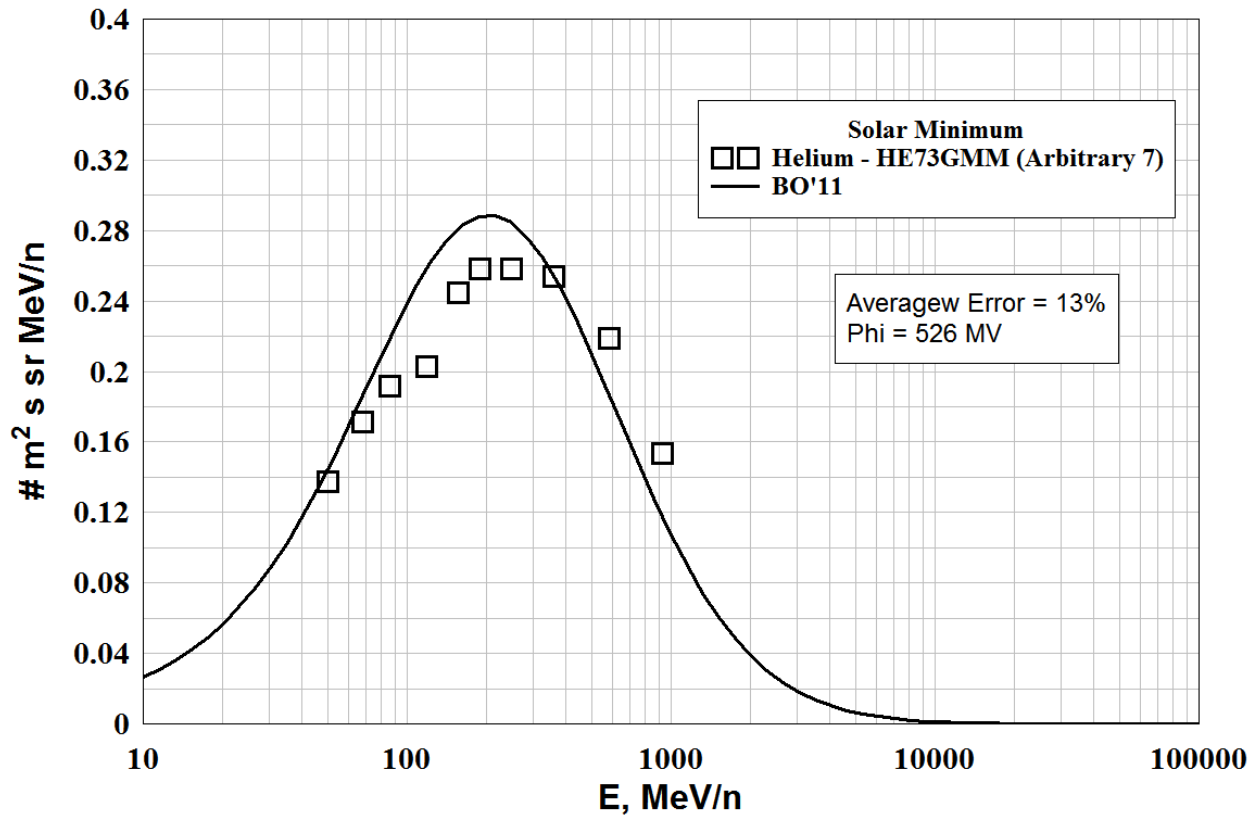


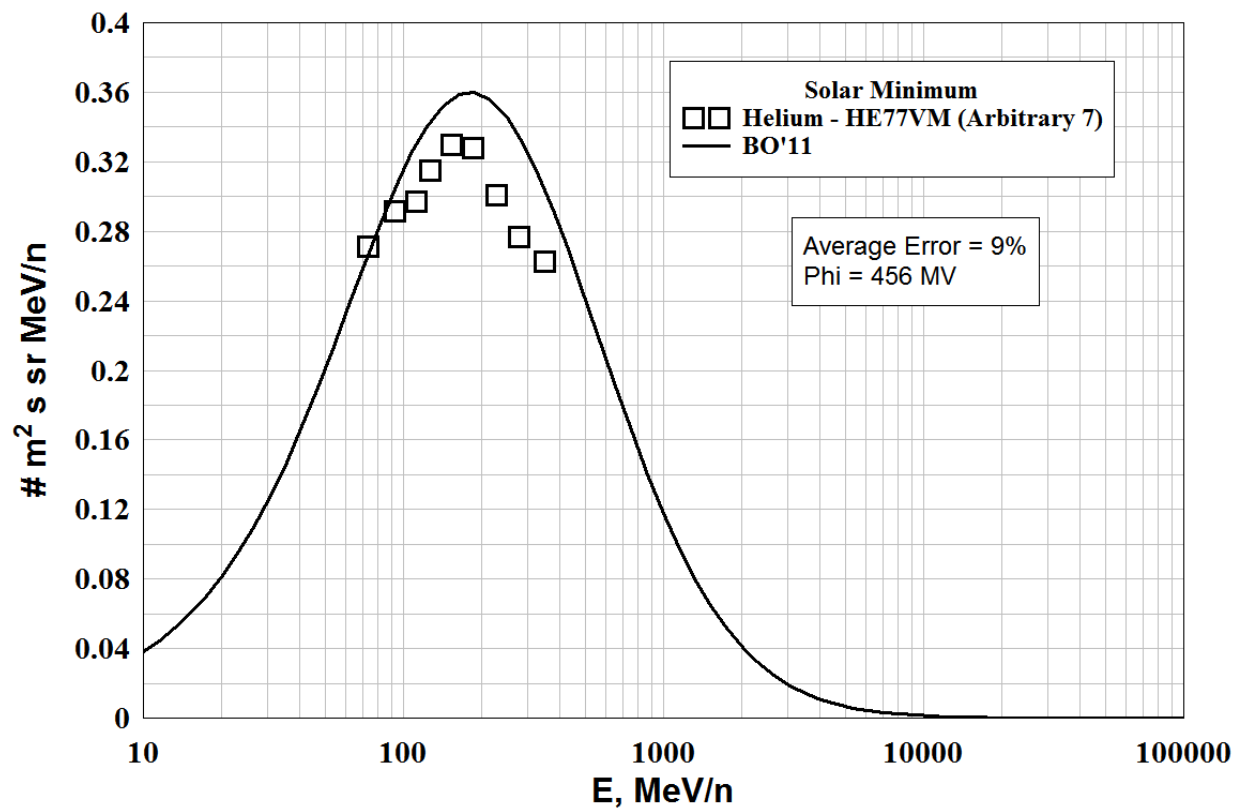
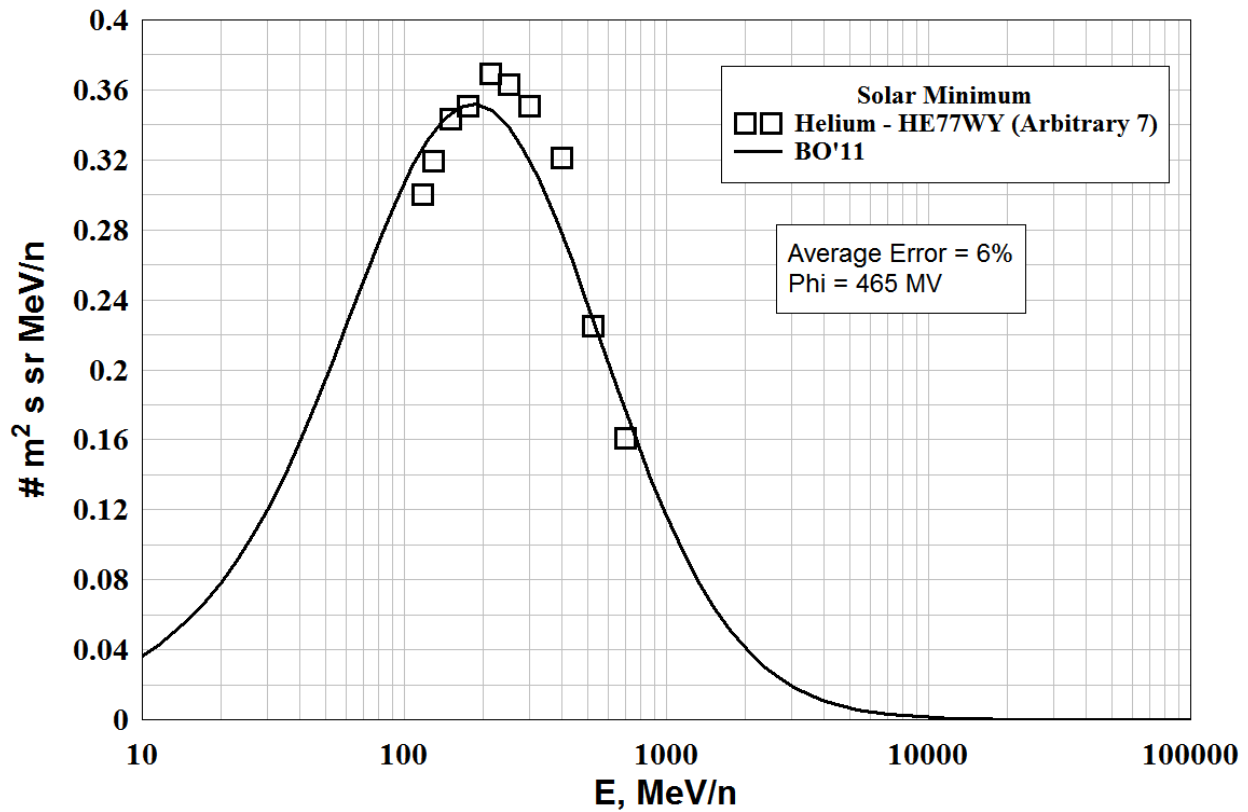
HELIUM - Low Energy, Solar Minimum

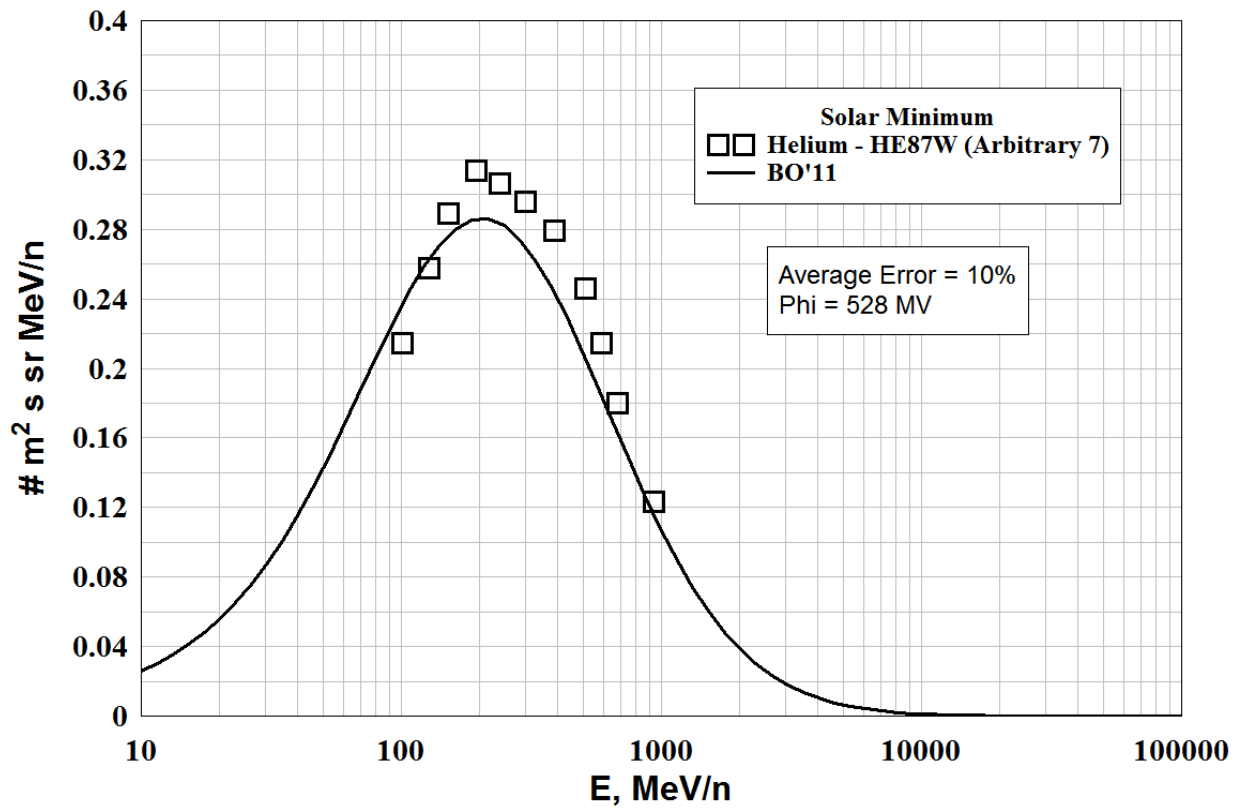
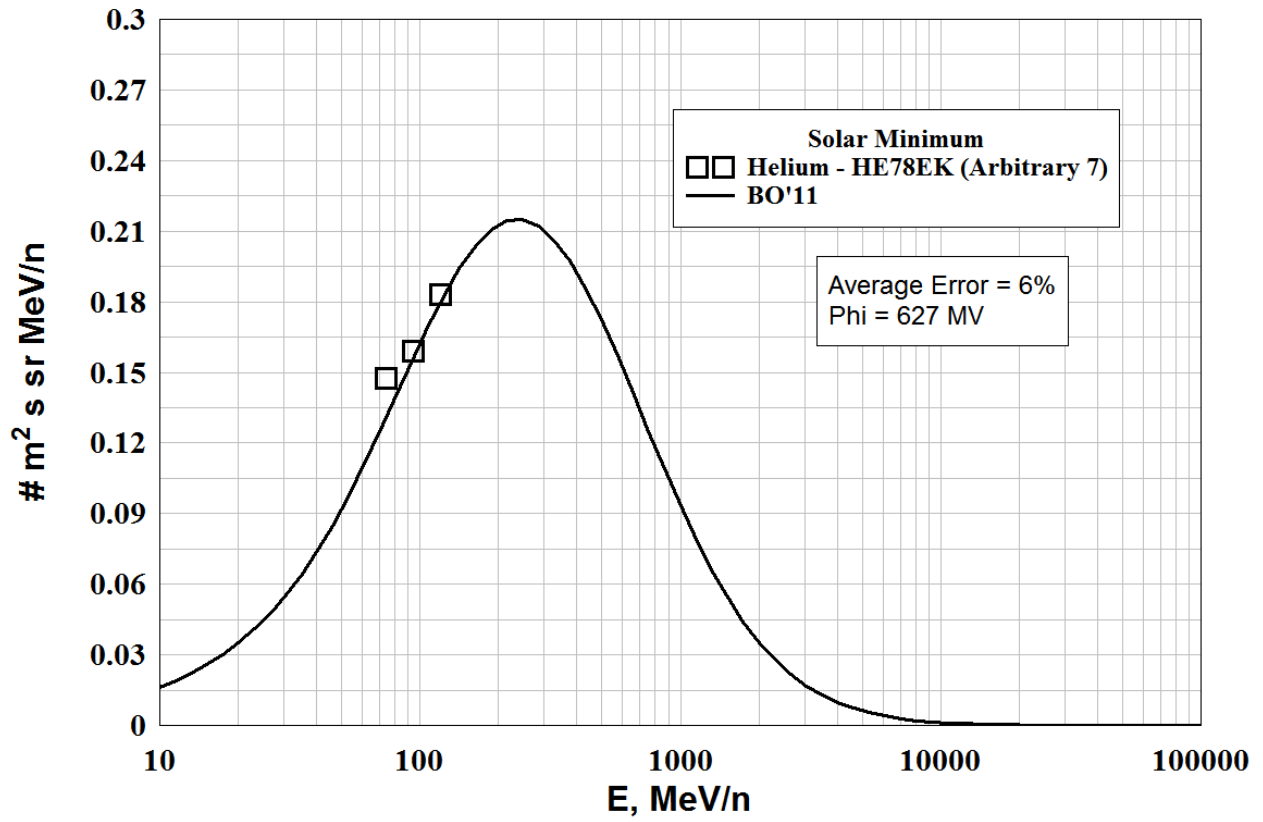
Files Rejected - (Arbitrary 7's)

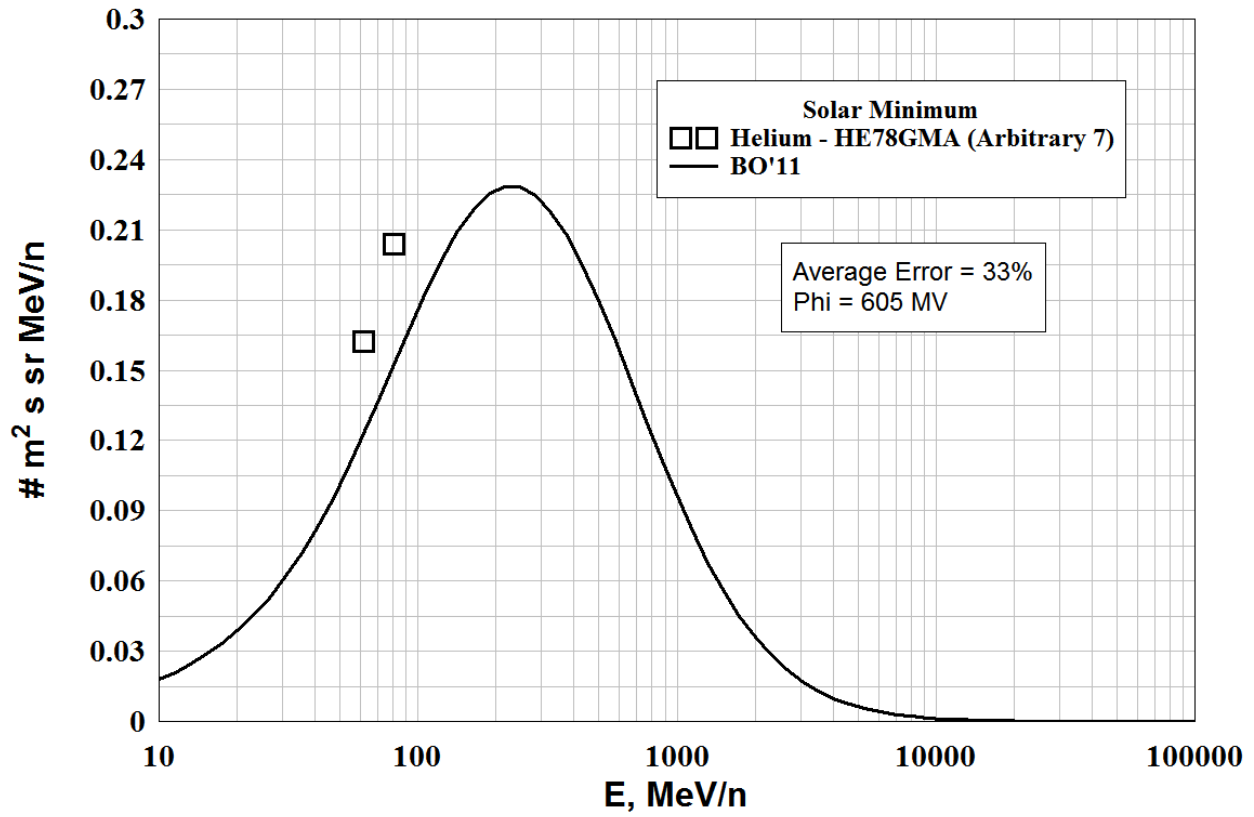
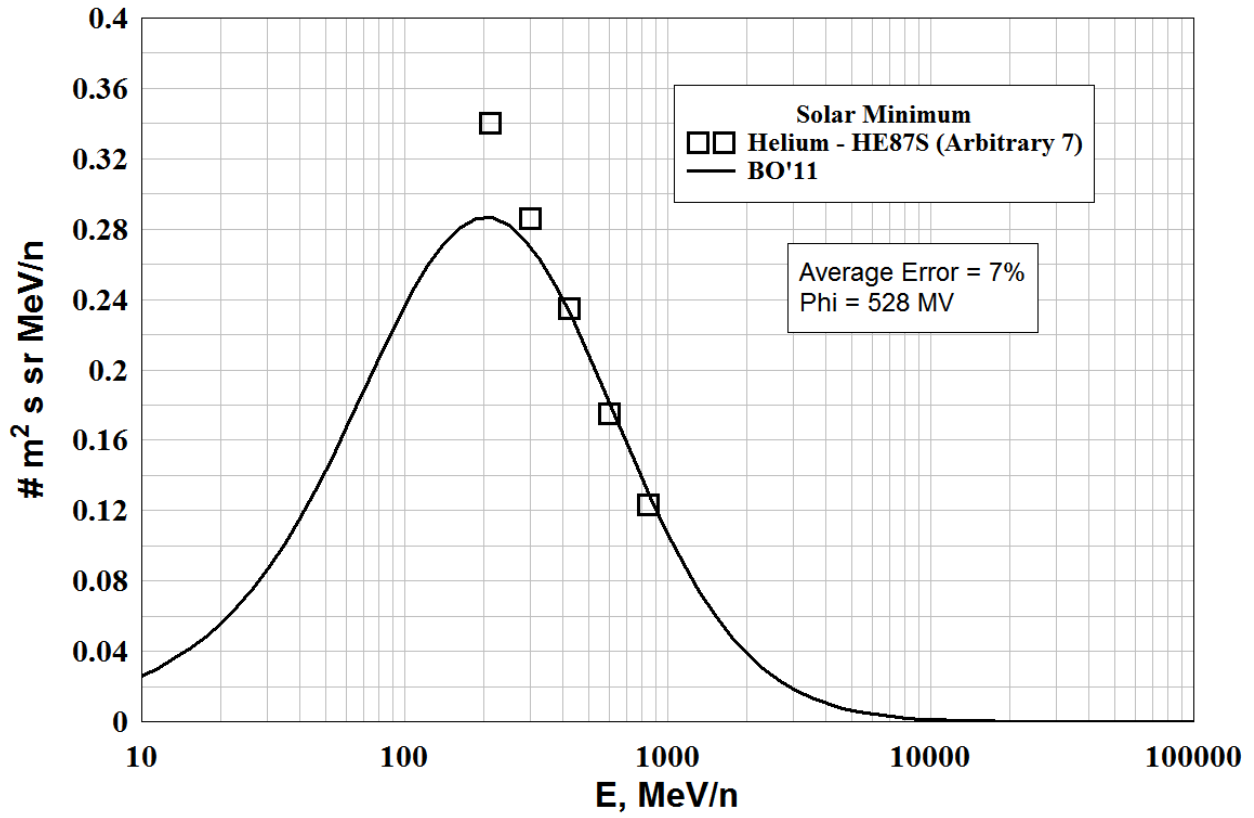
FILE	DATE	PHI (MV)	ERROR=ABS (FLUX-DATA)
He65R.dat	1965.573	484.6338	8.380550
He66G.dat	1966.517	563.7659	12.26126
He73GMM.dat	1973.408	525.5283	12.62536
he74GMM.dat	1974.542	513.0281	9.974391
He77Wy.dat	1977.510	465.1496	6.281869
He77Vm.dat	1977.252	458.5849	9.465549
He78ek.dat	1978.584	626.8853	5.727871
He87W.dat	1987.641	528.4525	10.06009
He87S.dat	1987.638	527.9987	7.012885
He78GMA.dat	1978.430	604.7474	33.48859
He86GMA.dat	1986.384	513.0007	4.387522
He87GMA.dat	1987.600	530.7039	15.75659
BO AVERAGE ERROR =			11.28521

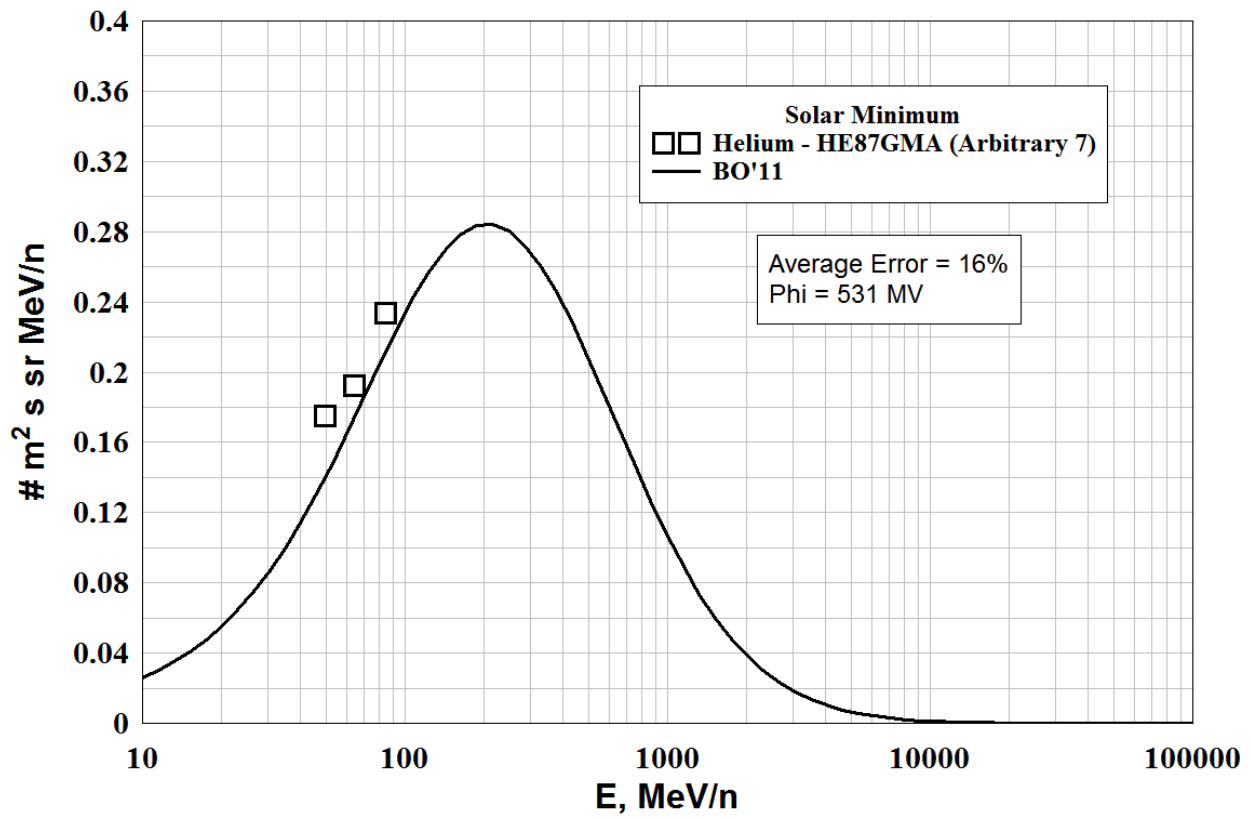
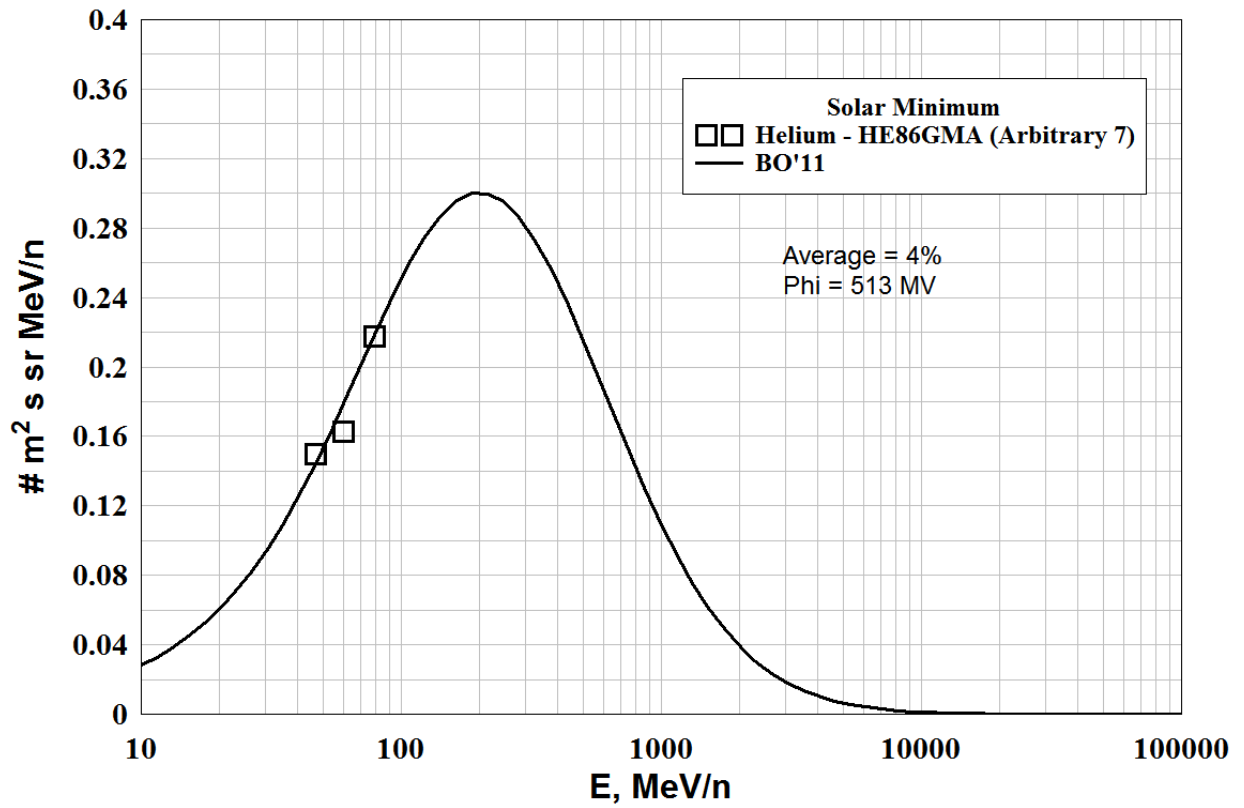






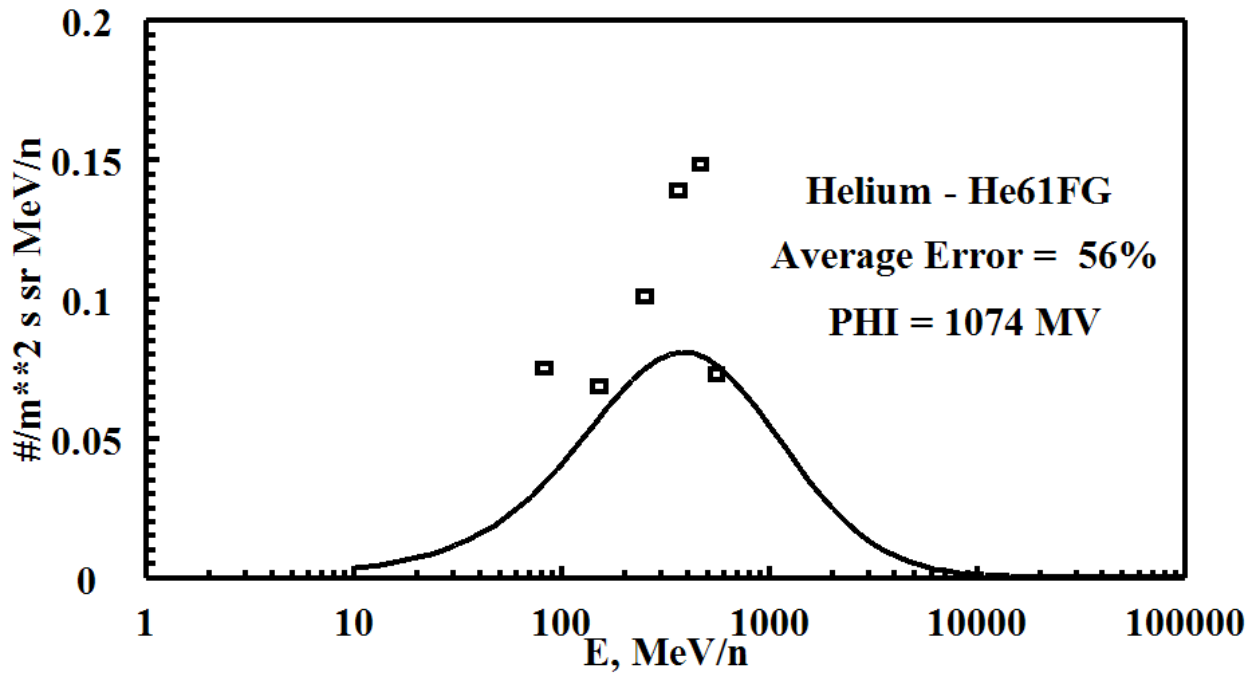


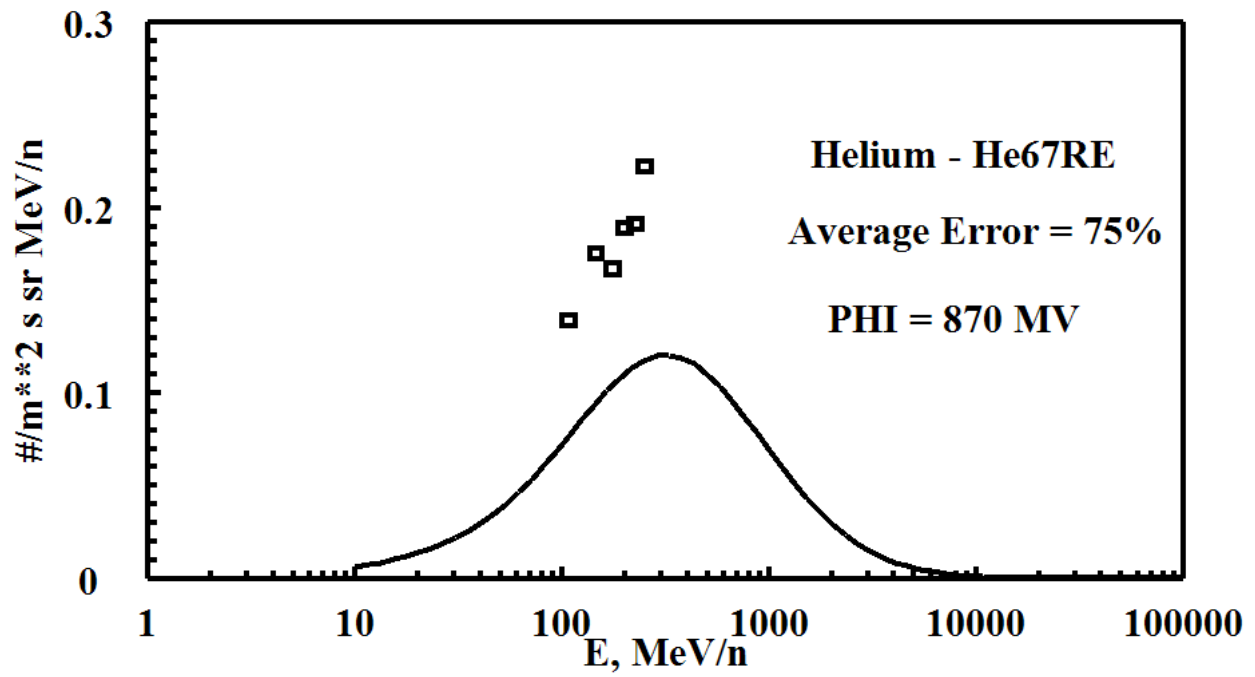
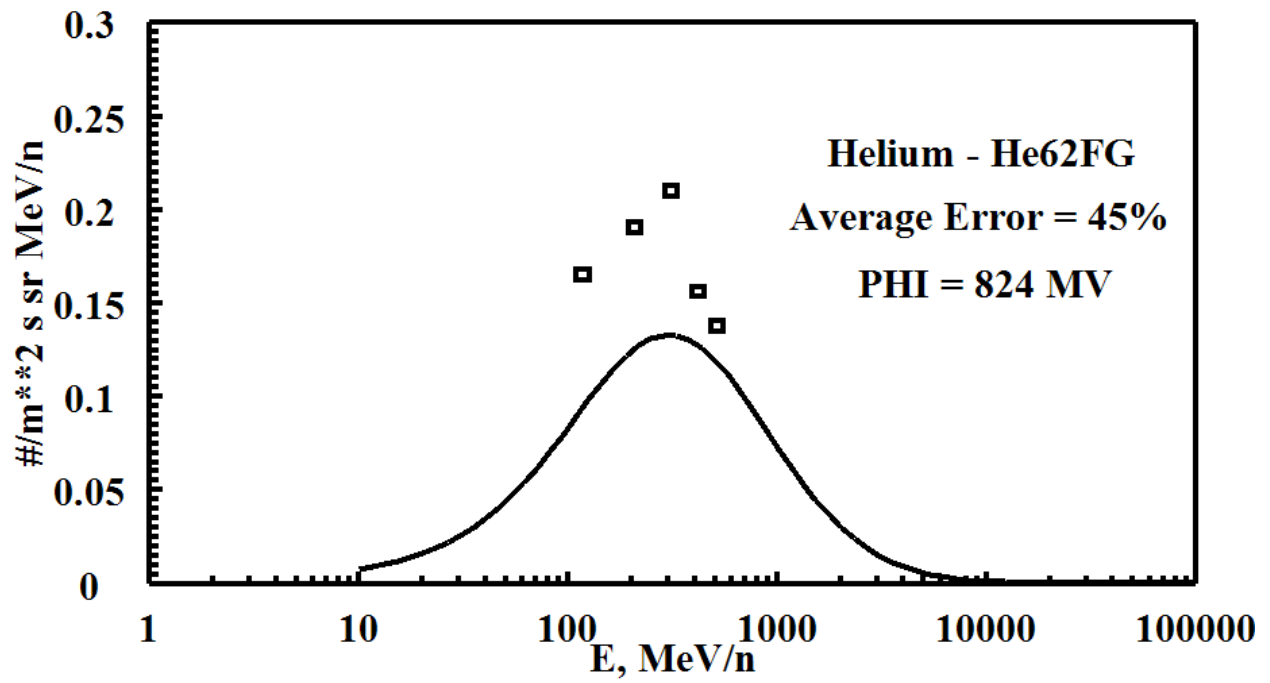


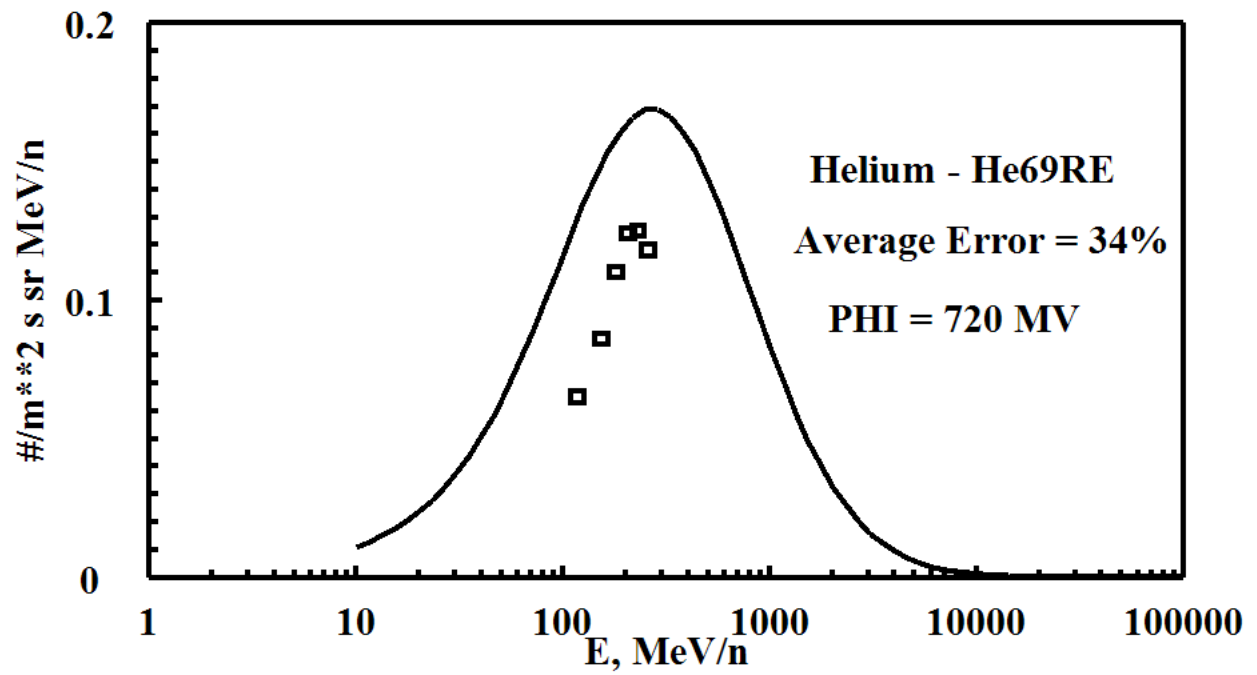
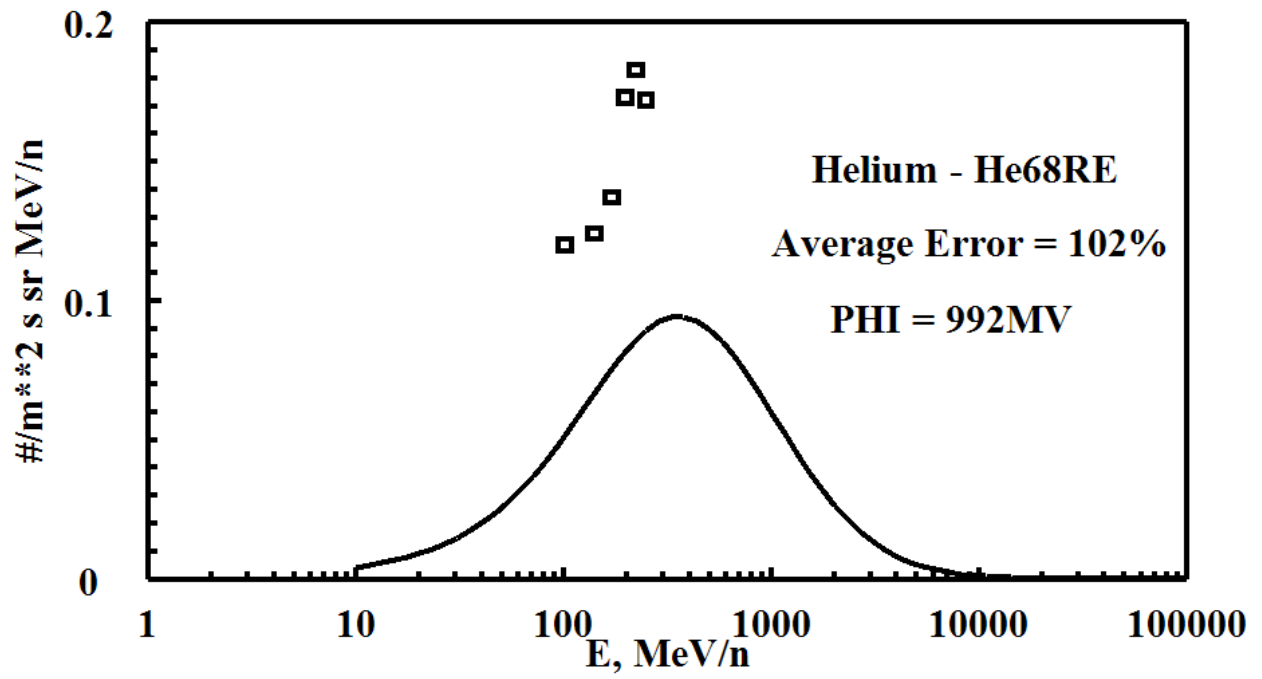


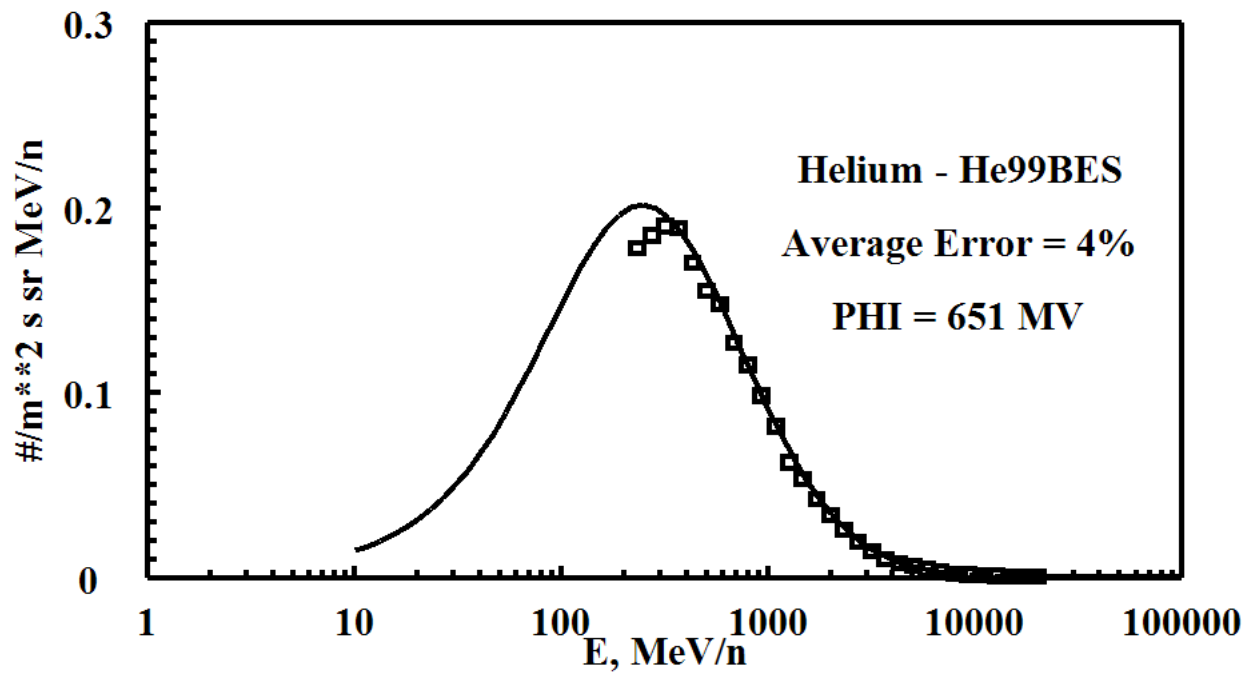
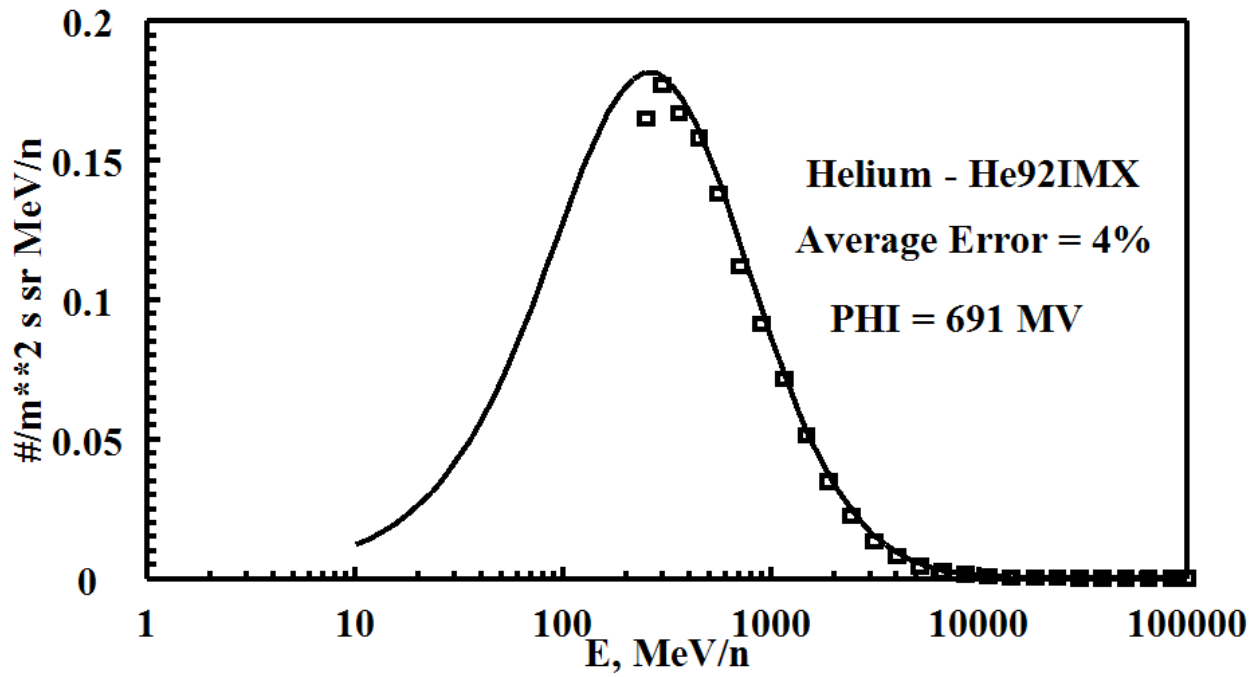
HELIUM - Low Energy, Solar Maximum
Files Used (Arbitrary 1's)

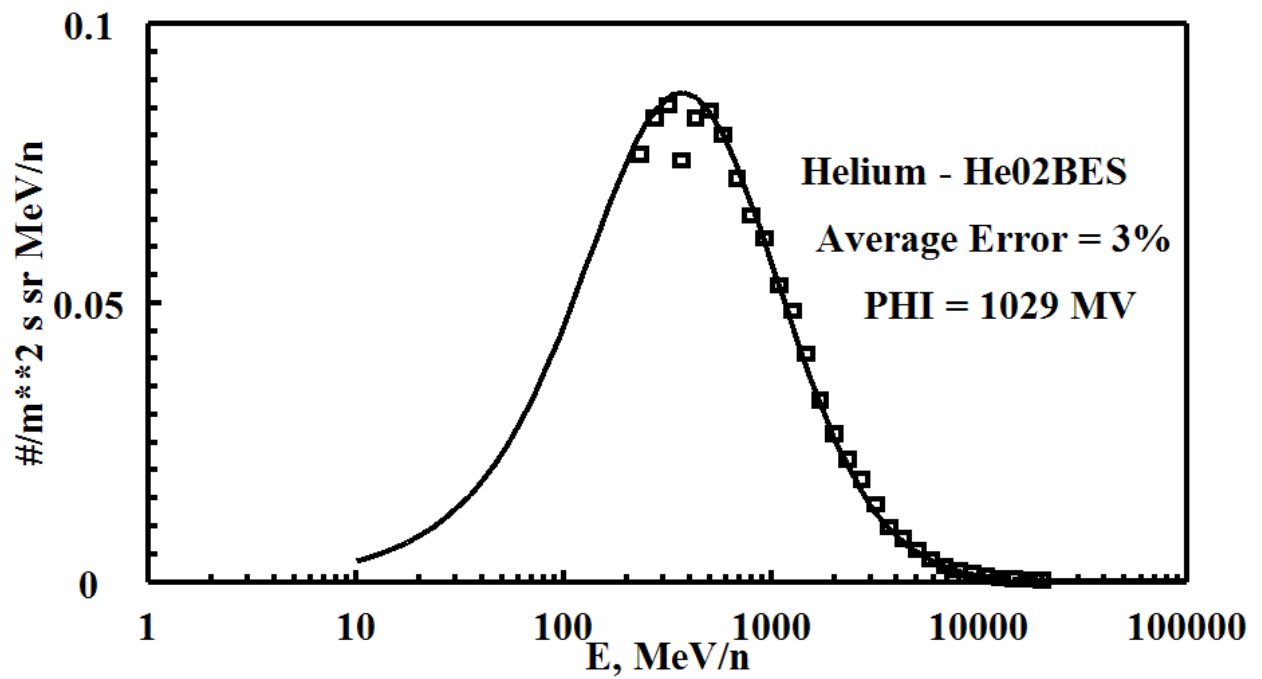
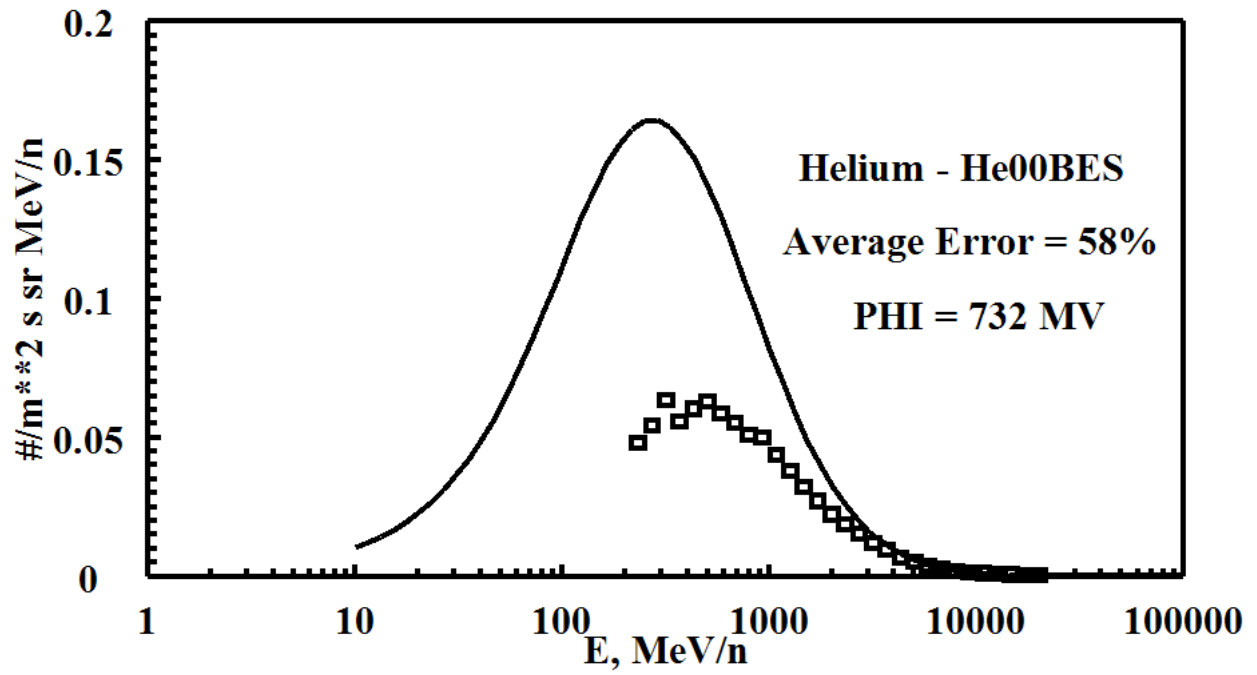
FILE	DATE	PHI (MV)	ERROR=ABS (FLUX-DATA)
He61FG.dat	1961.515	1073.765	56.01486
He62FG.dat	1962.573	823.6523	44.98145
He67RE.dat	1967.716	869.5131	75.17842
He68RE.dat	1968.622	991.5895	102.0424
He69RE.dat	1969.538	720.0593	33.85181
He92IMX.dat	1992.540	691.0951	4.379588
He99BES.dat	1999.611	650.9333	3.593930
He00BES.dat	2000.608	731.5487	57.95938
He02BES.dat	2002.600	1029.817	3.451360
BO AVERAGE ERROR =			42.38369







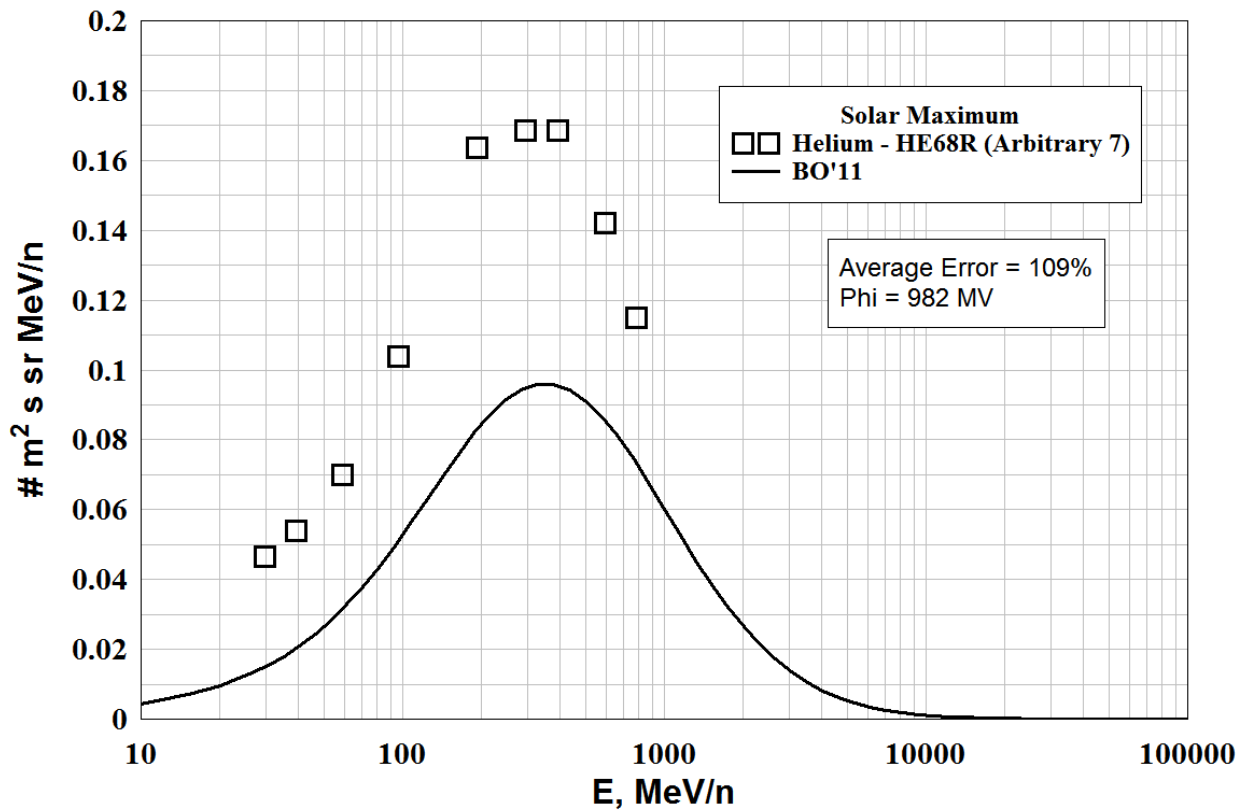


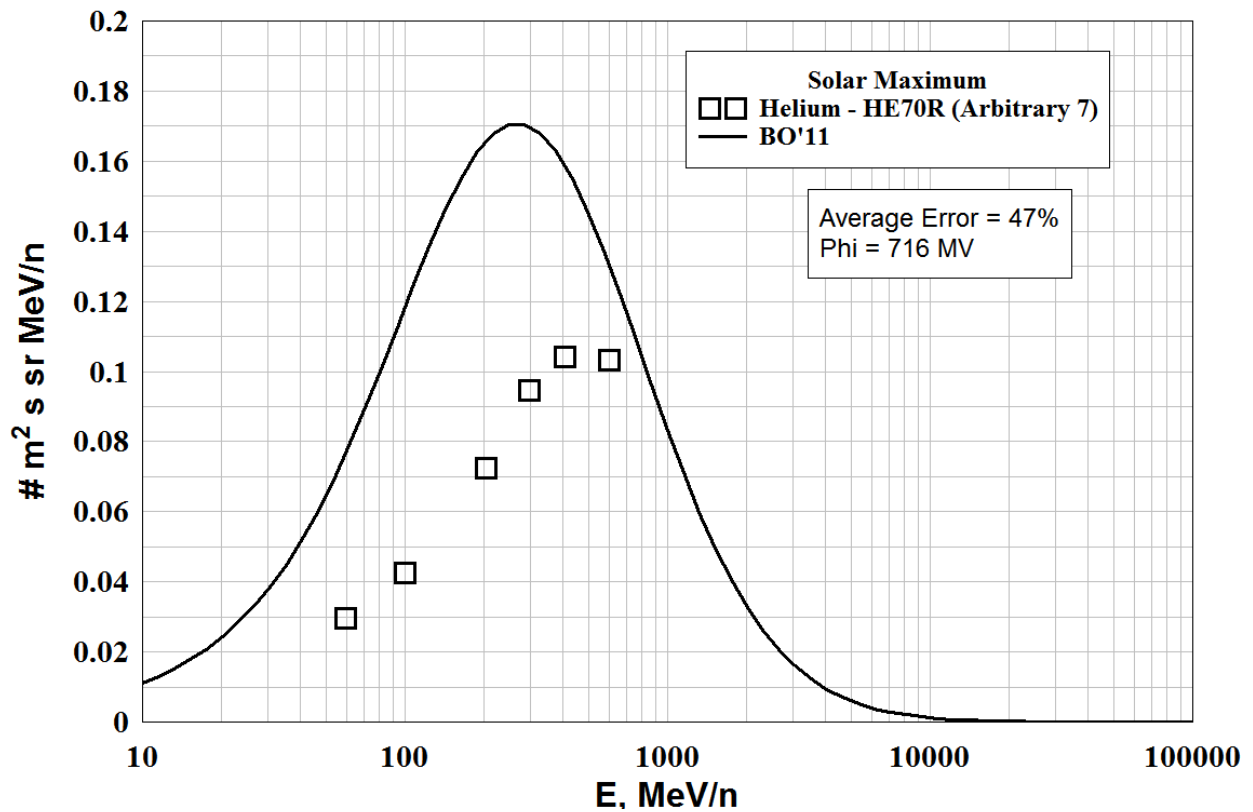
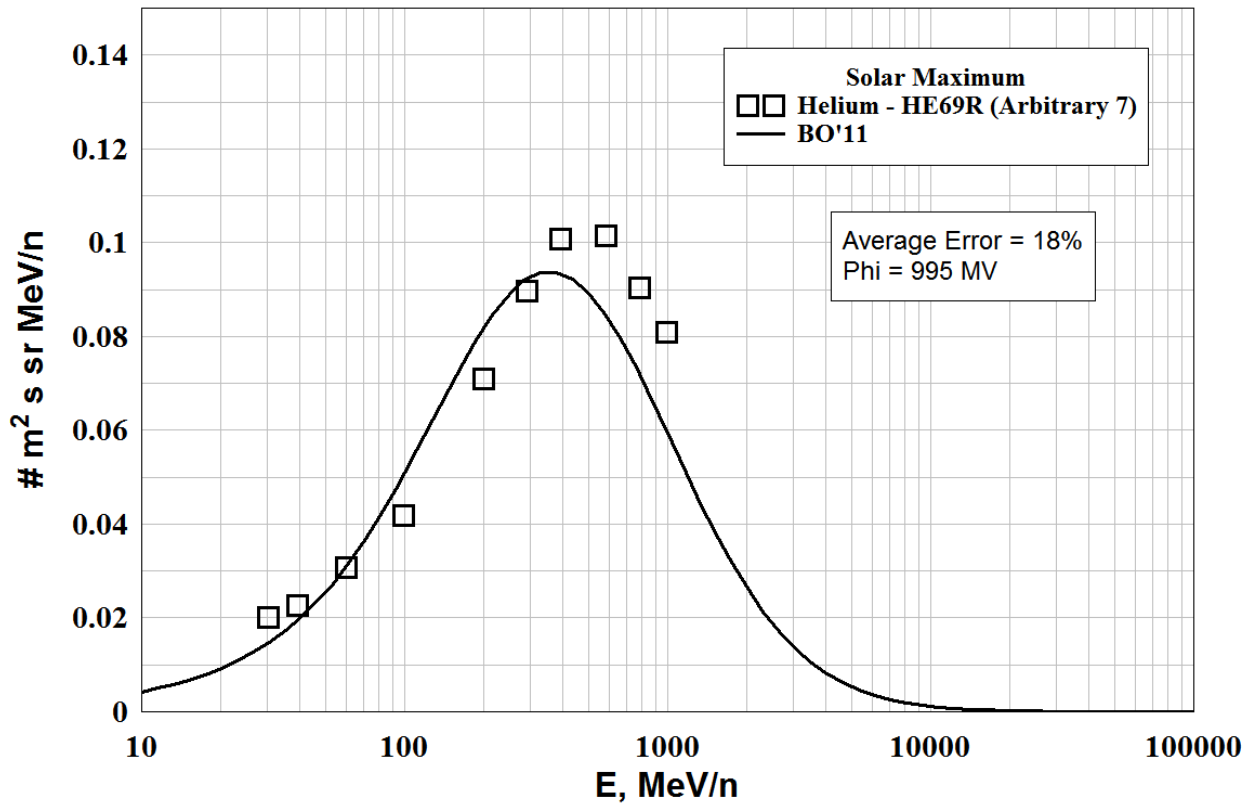


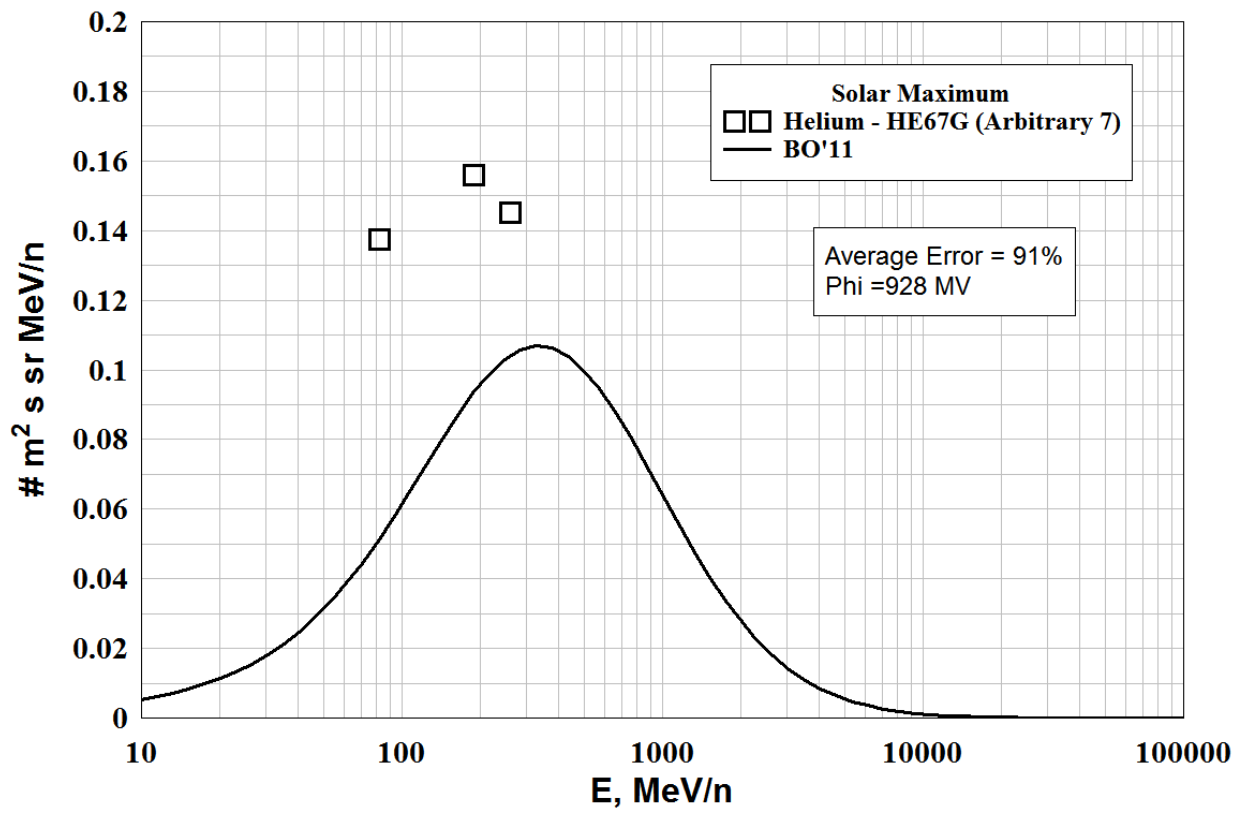
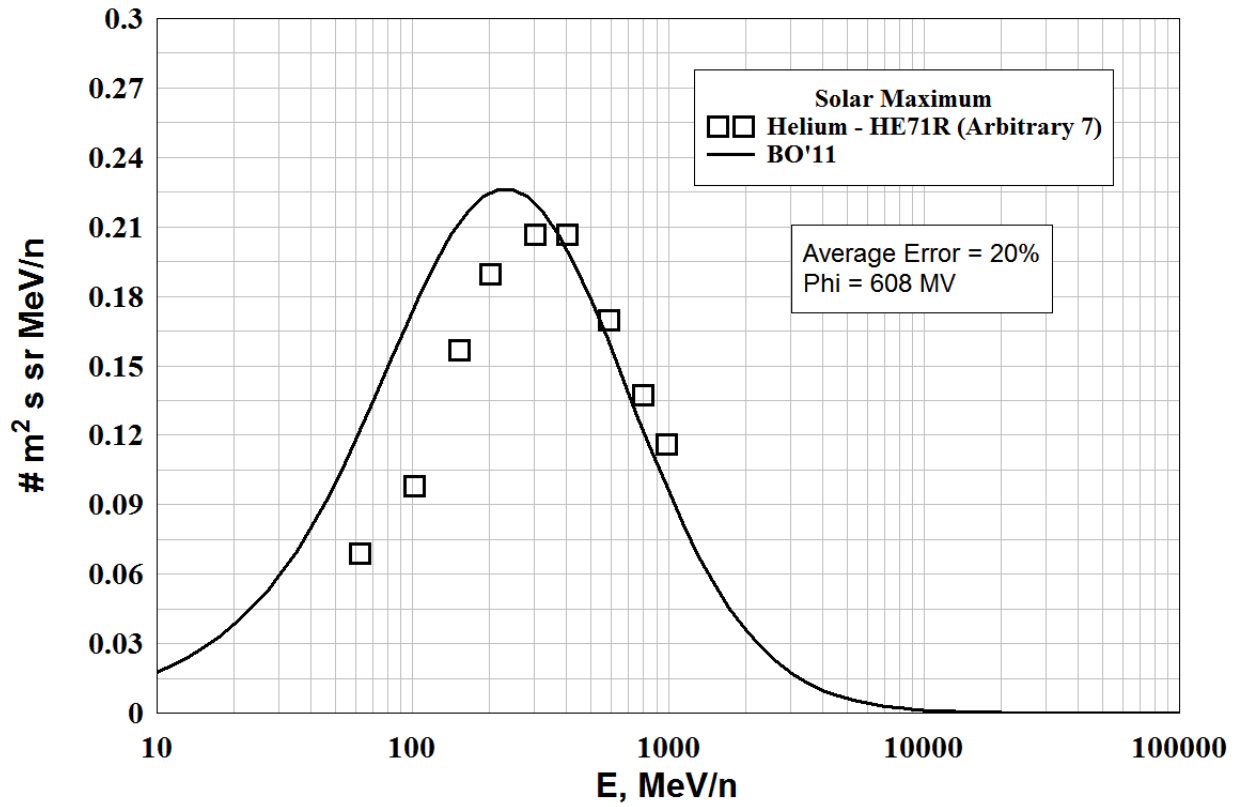
HELIUM - Low Energy, Solar Maximum

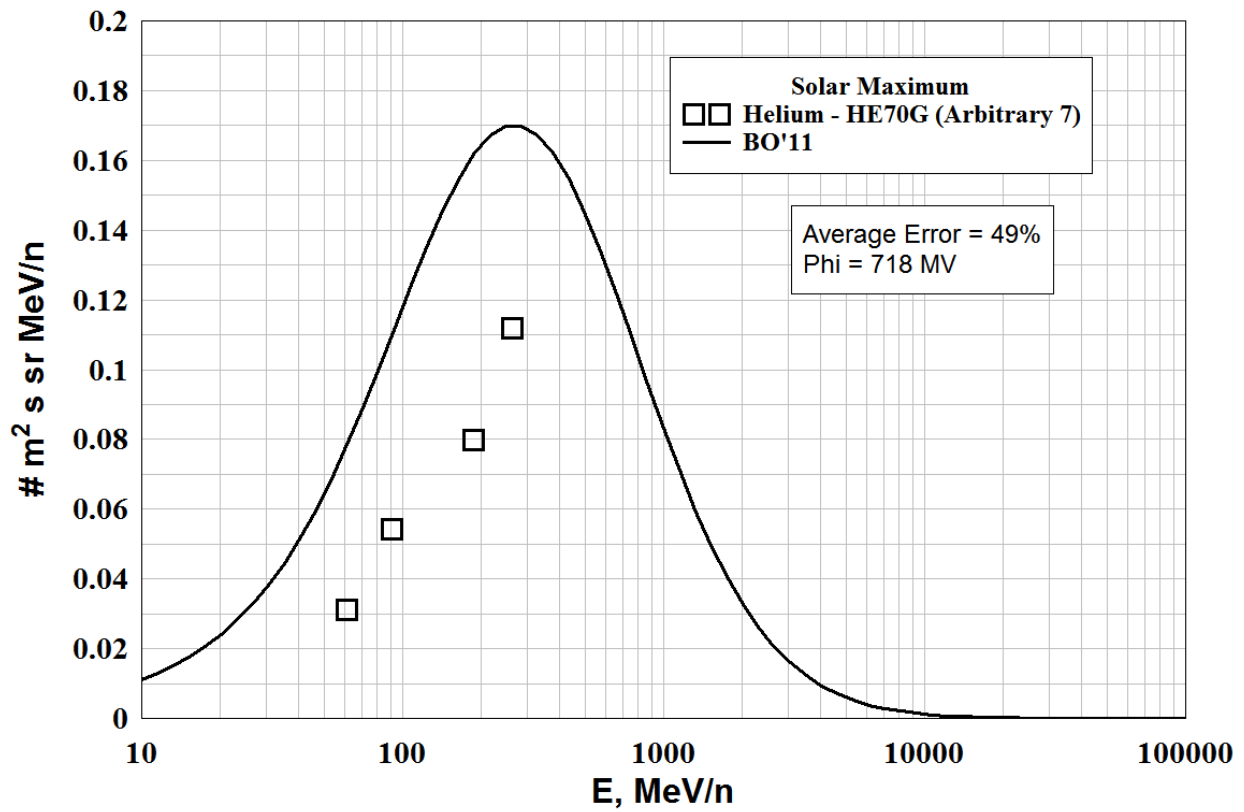
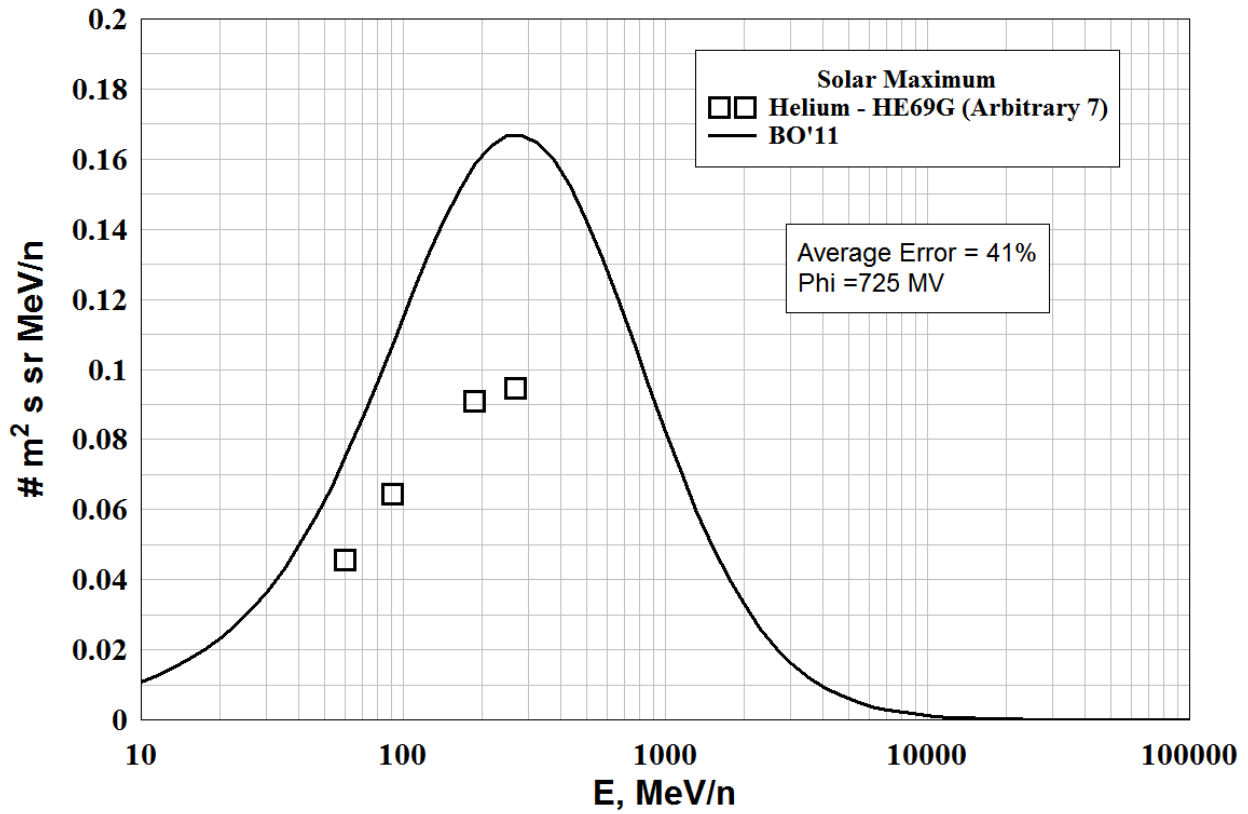
Files Rejected - (Arbitrary 7's)

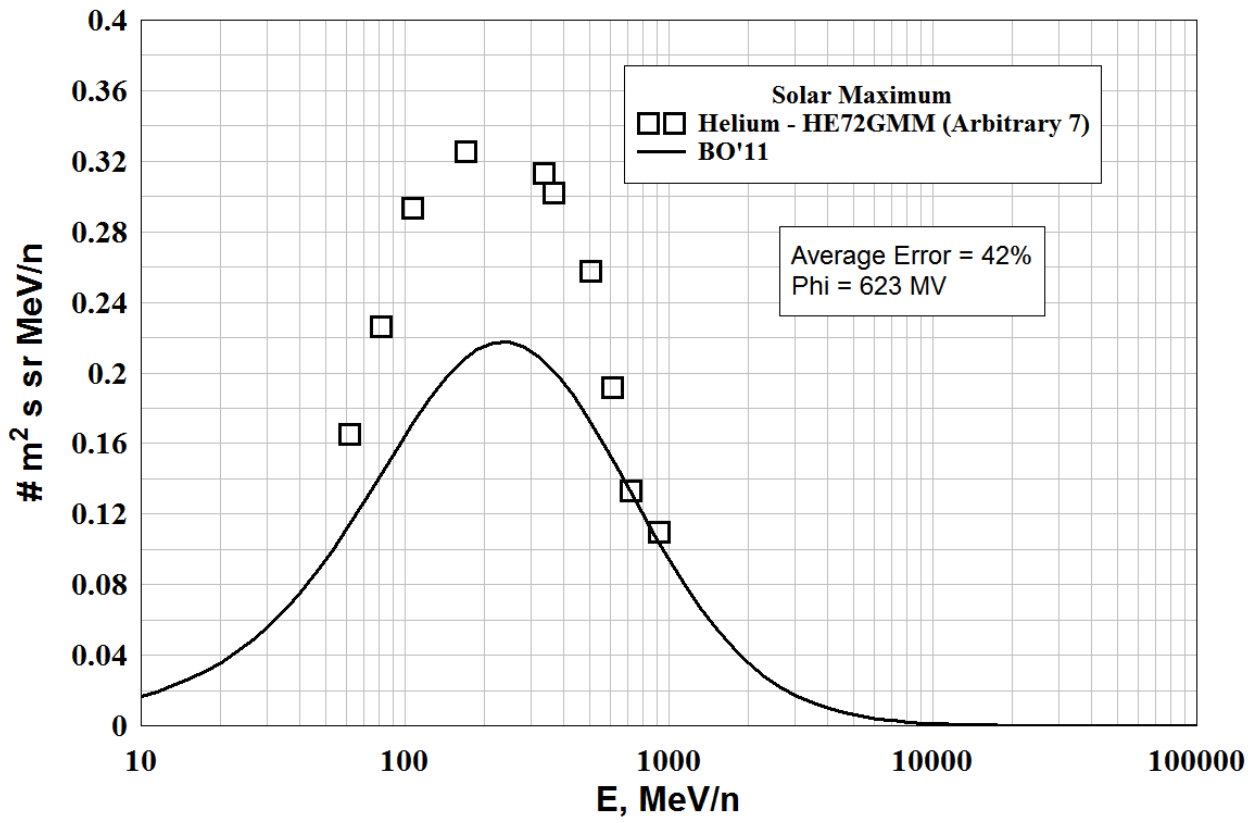
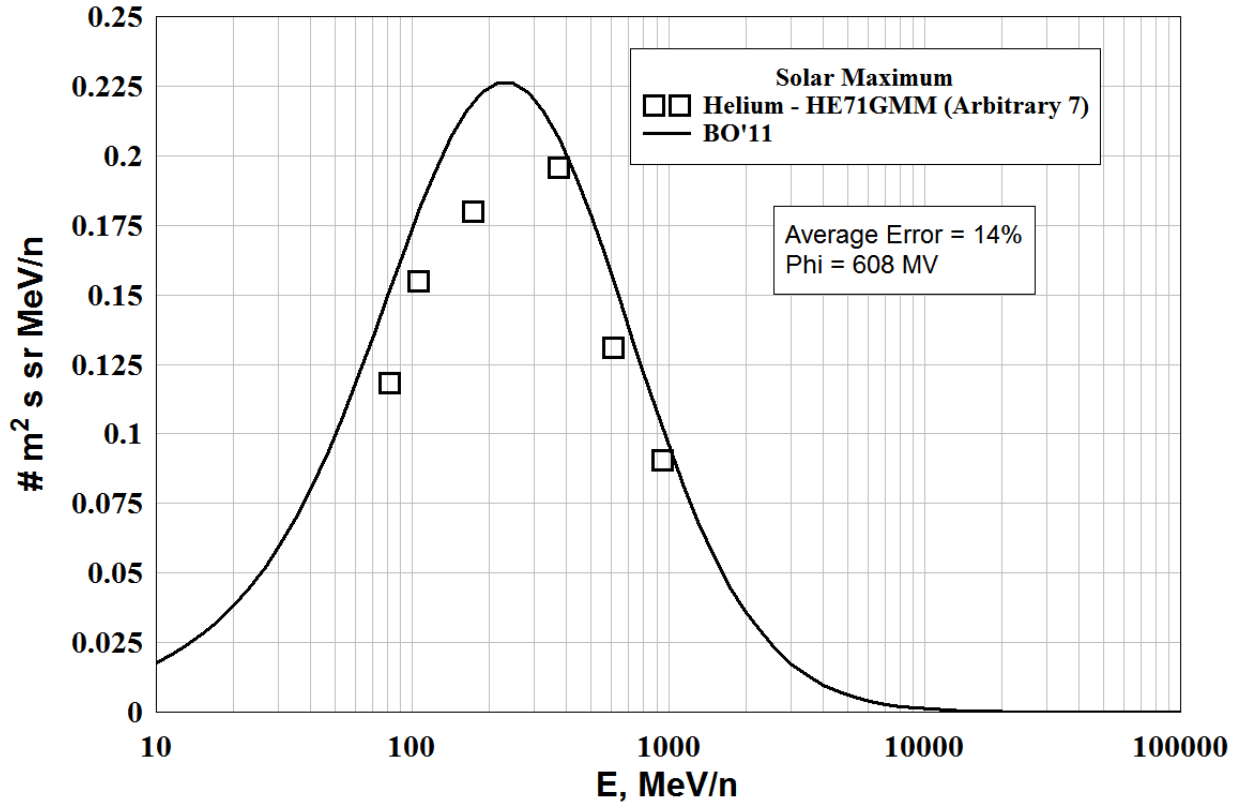
FILE	DATE	PHI (MV)	ERROR=ABS (FLUX-DATA)
He68R.dat	1968.581	981.7554	108.6536
He69R.dat	1969.041	994.8779	17.65793
He70R.dat	1970.526	716.4028	46.76329
He71R.dat	1971.515	608.0721	19.51150
He67G.dat	1967.988	928.3704	91.28412
He69G.dat	1969.471	725.4042	41.10138
He70G.dat	1970.474	717.8524	49.00396
He71GMM.dat	1971.427	608.0098	14.05173
He72GMM.dat	1972.332	622.6121	41.69375
He68LW.dat	1967.956	933.7995	66.35567
He79Vm.dat	1978.849	662.5335	29.26356
He82GMP.dat	1982.499	1183.914	97.14291
He84GMP.dat	1984.584	887.9470	53.54042
He89W.dat	1989.682	1248.804	8.721601
BO AVERAGE ERROR =			48.91040

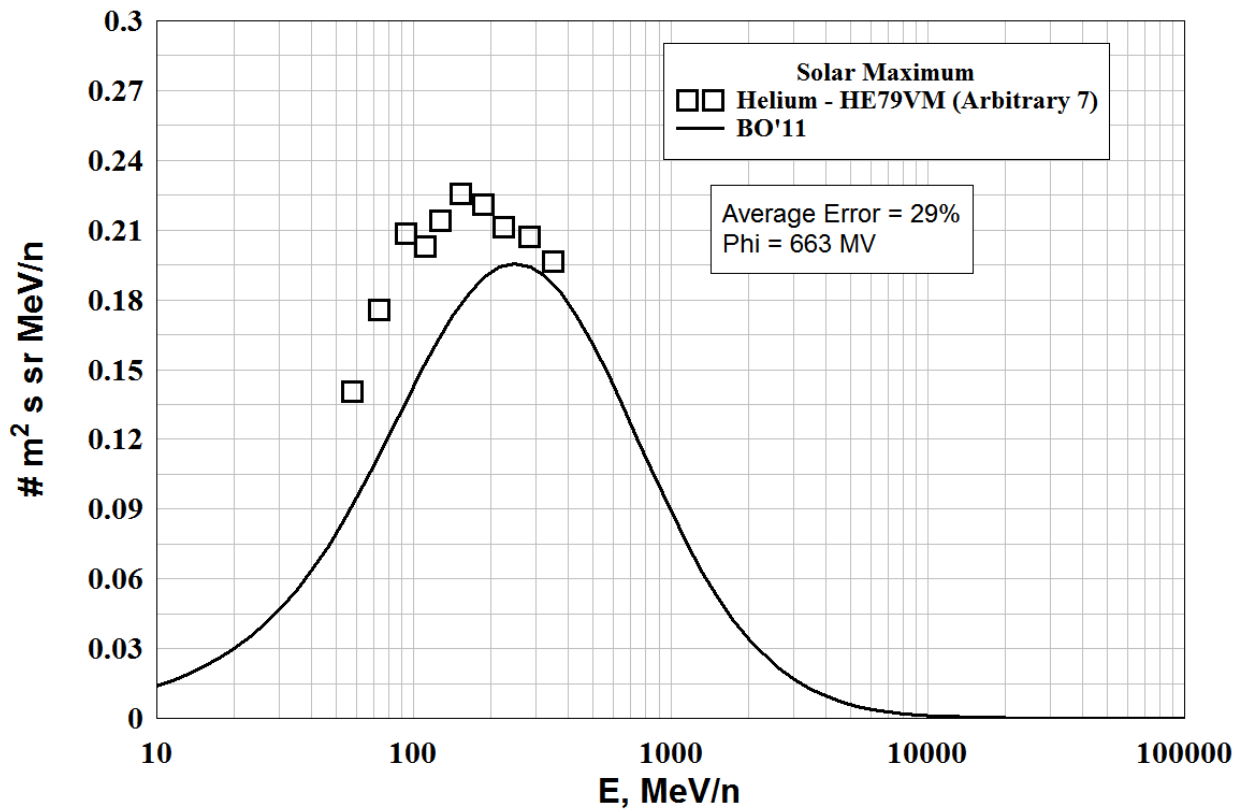
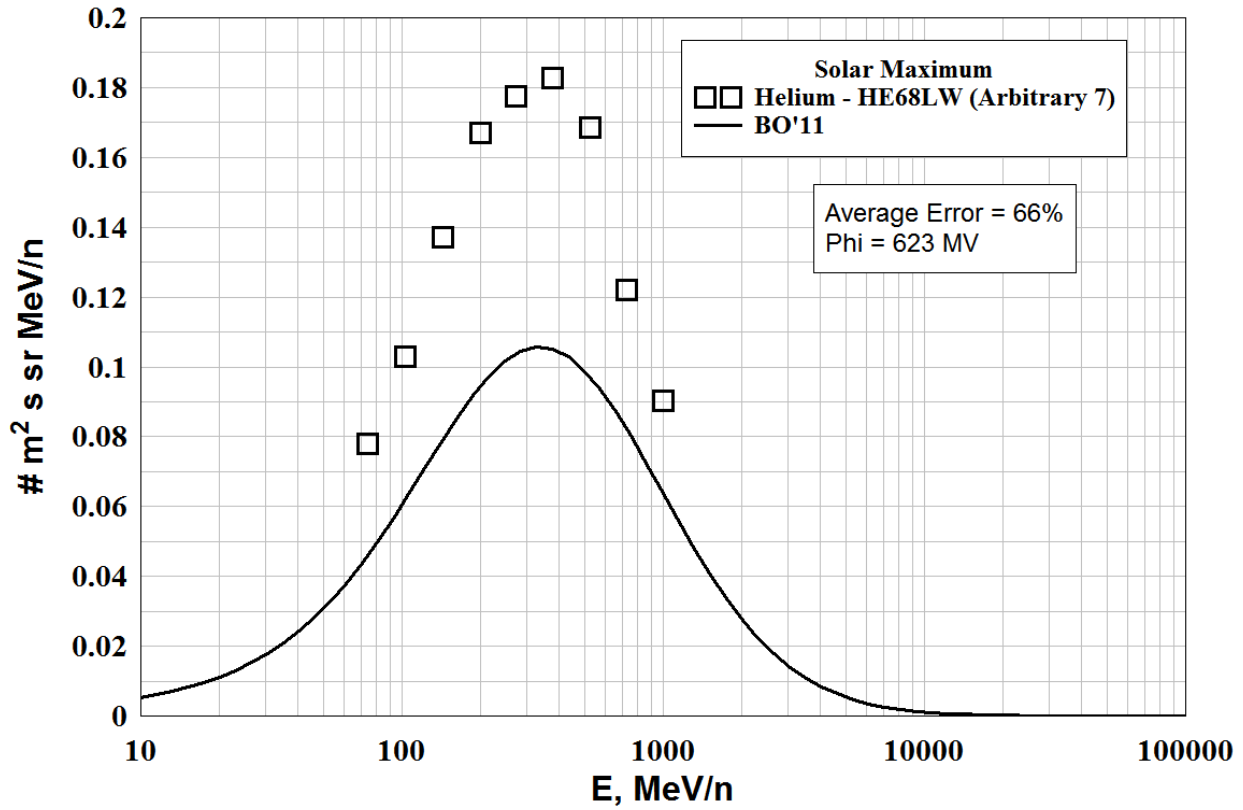


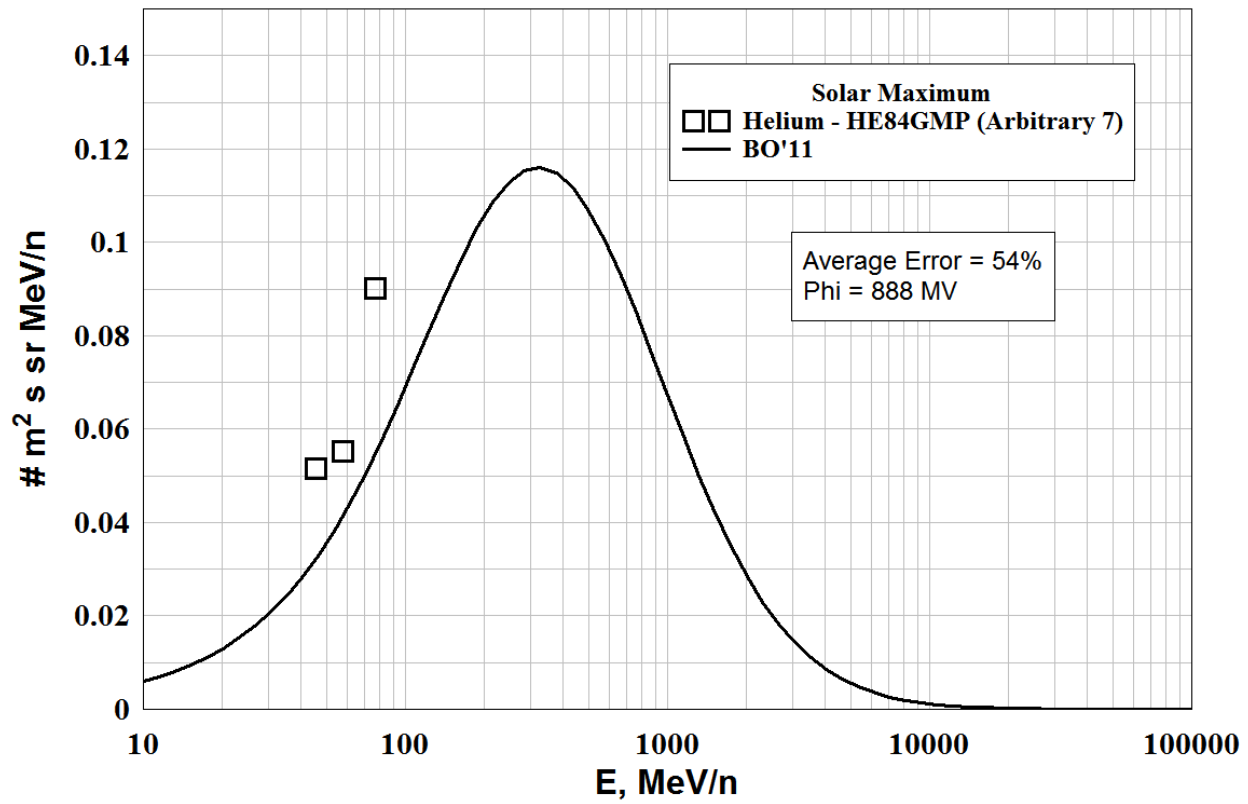
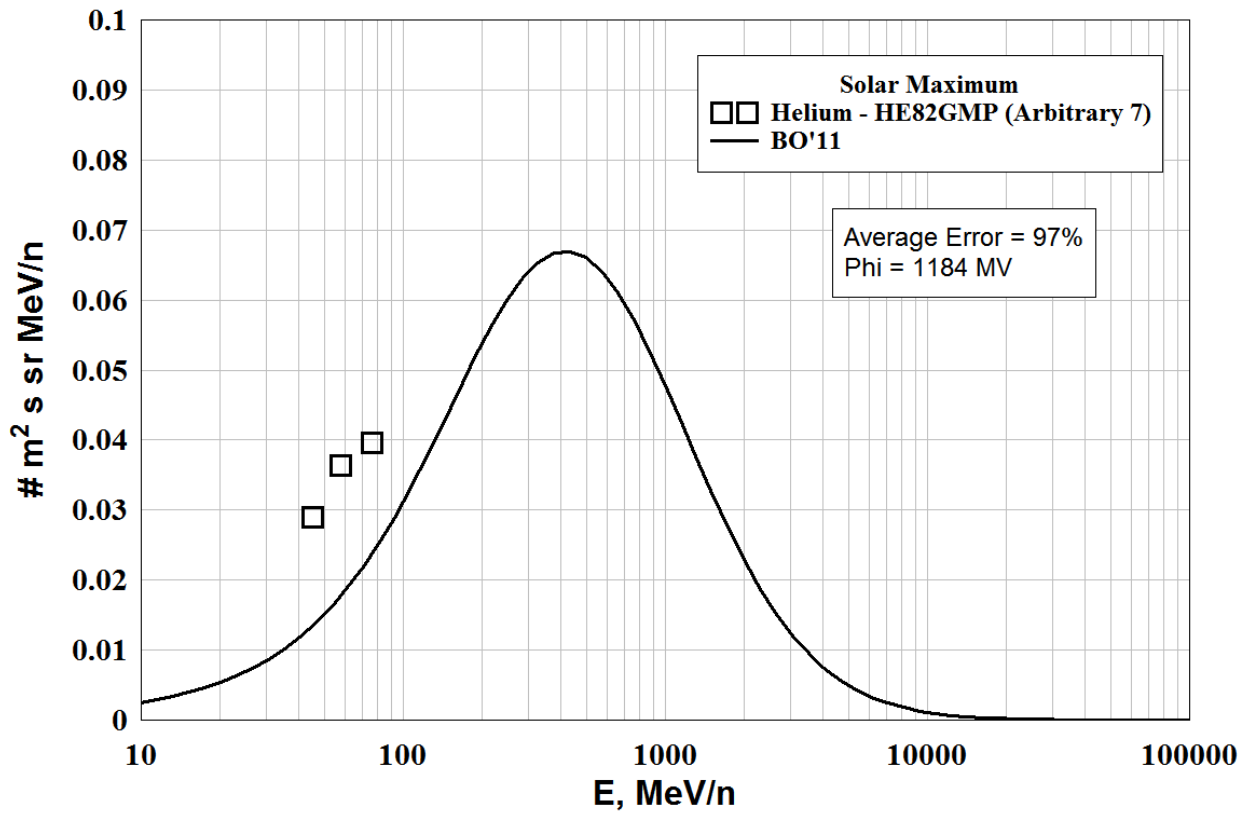


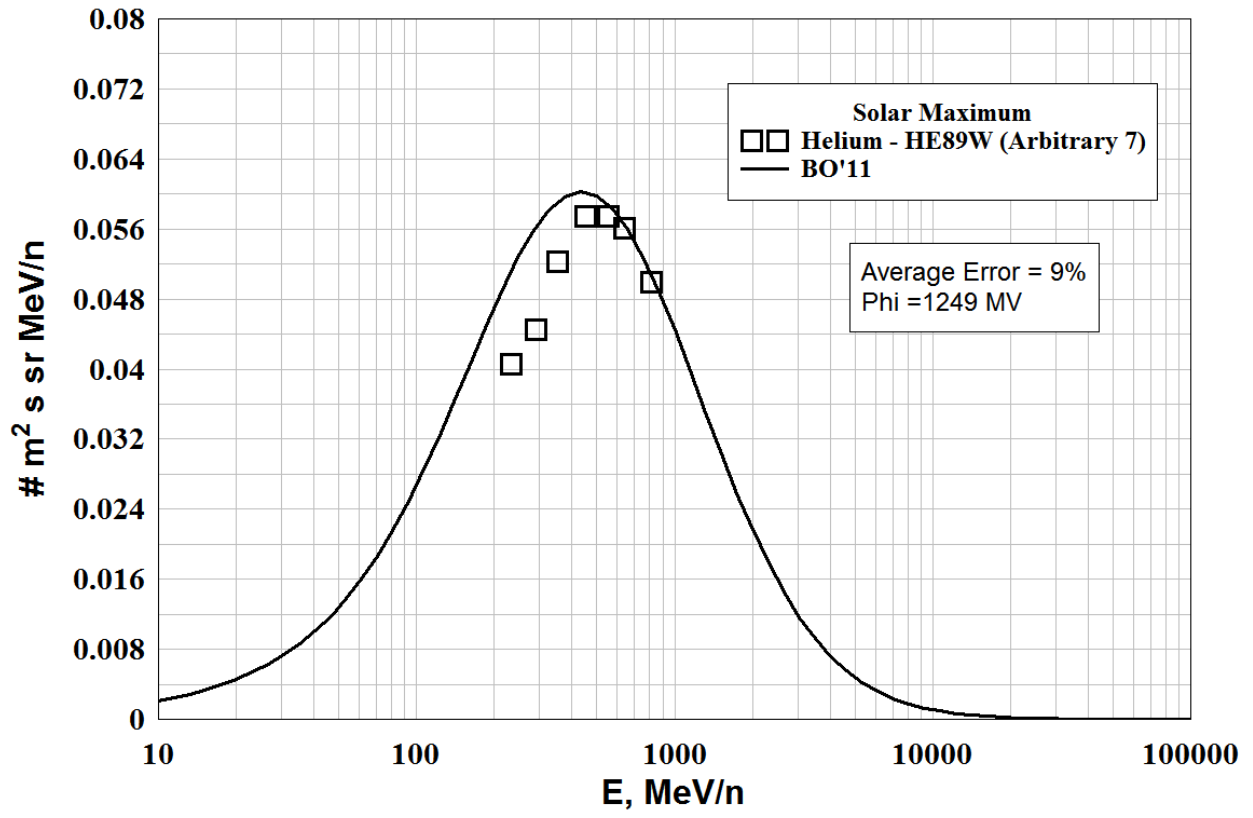




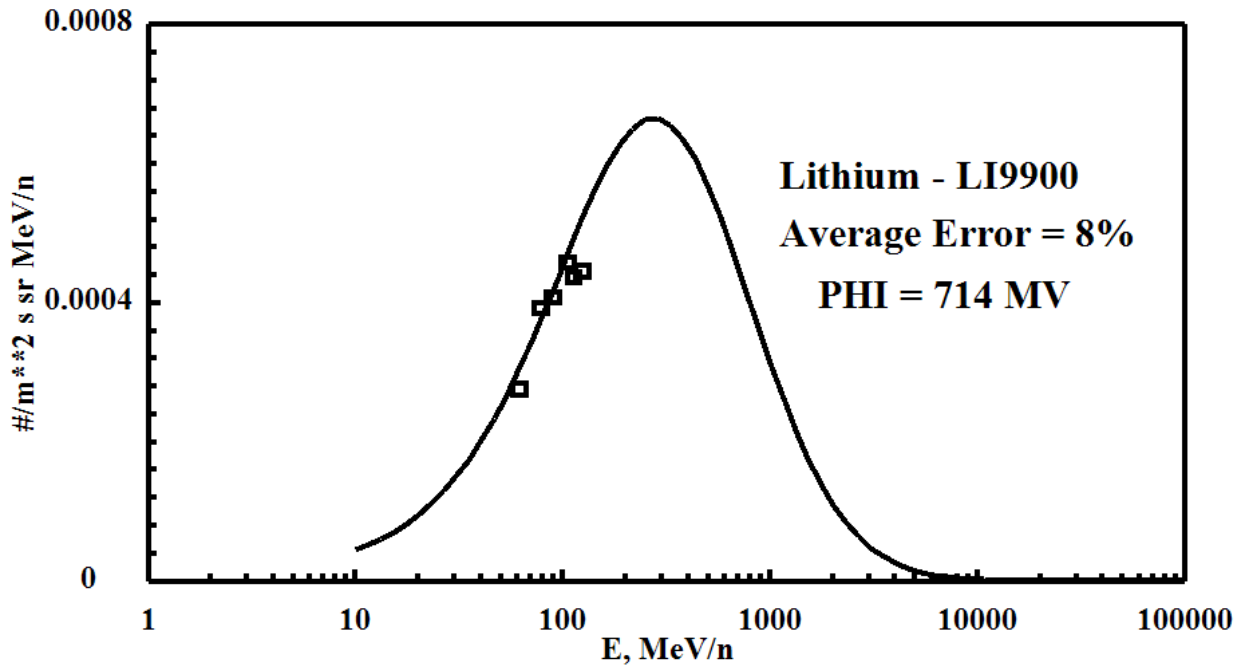
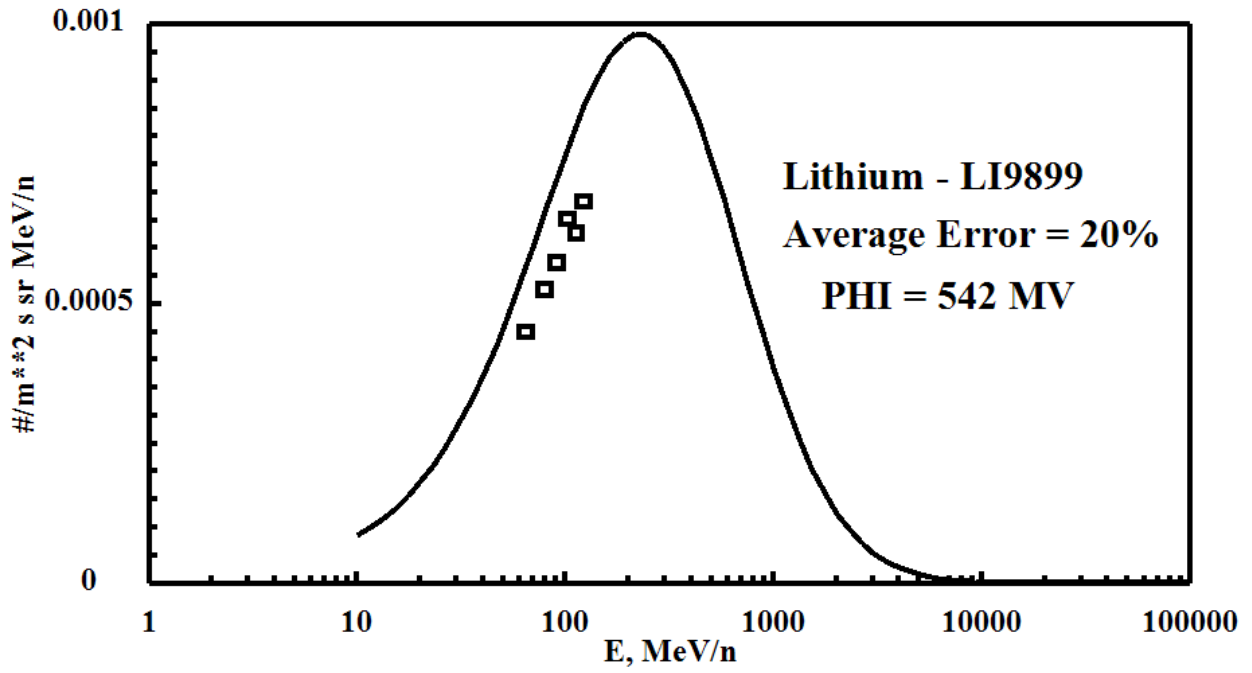


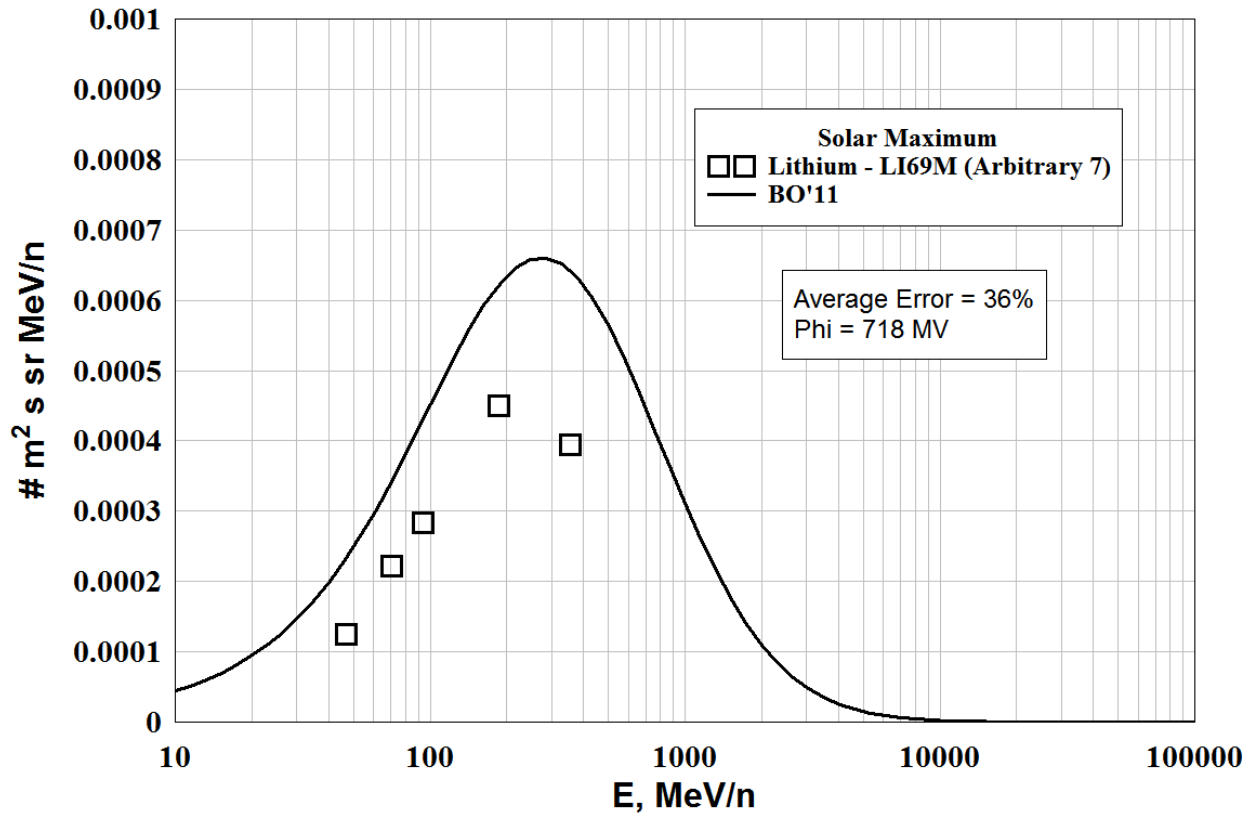




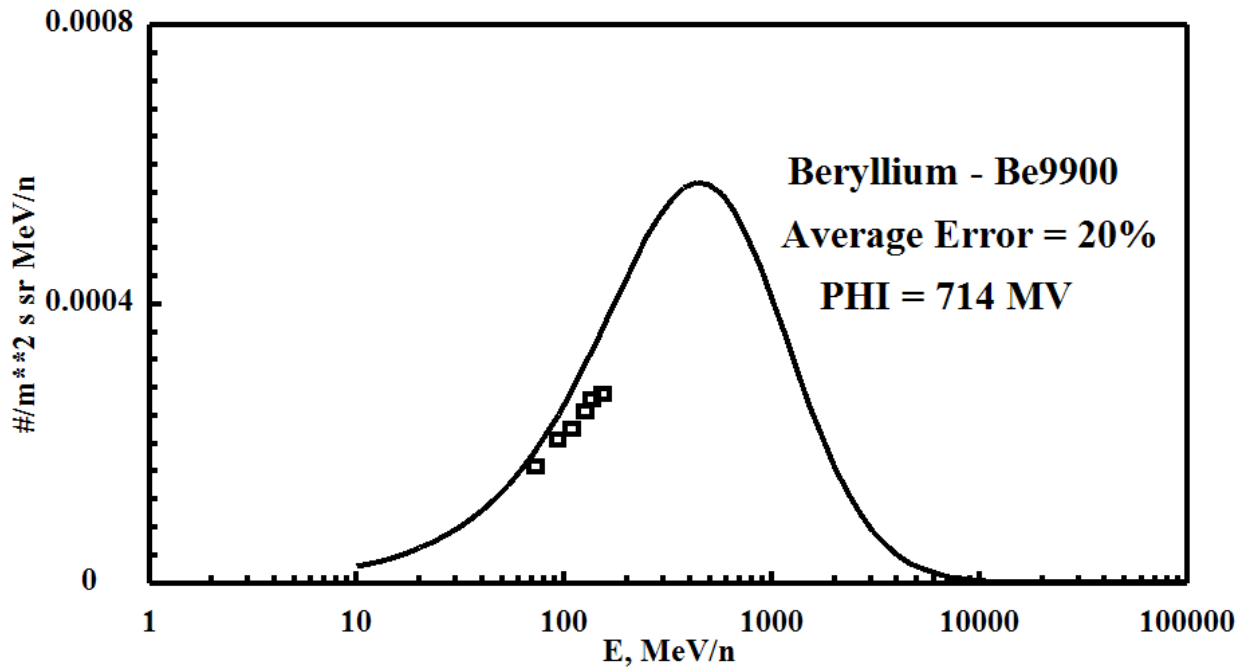
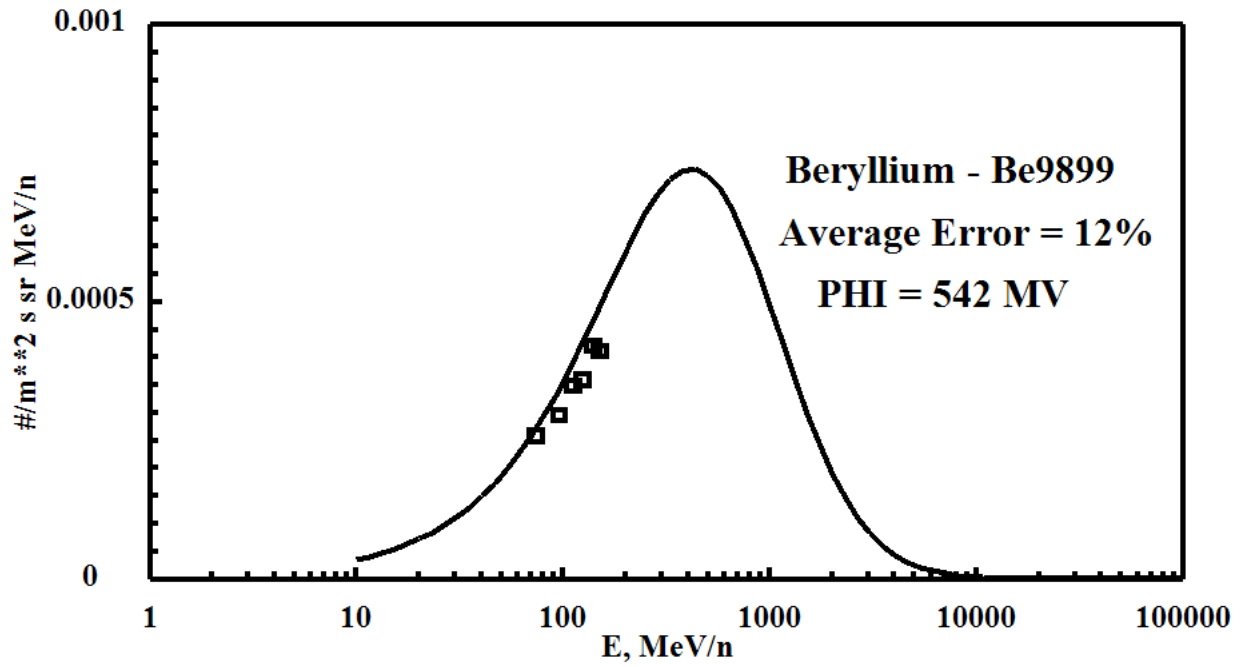


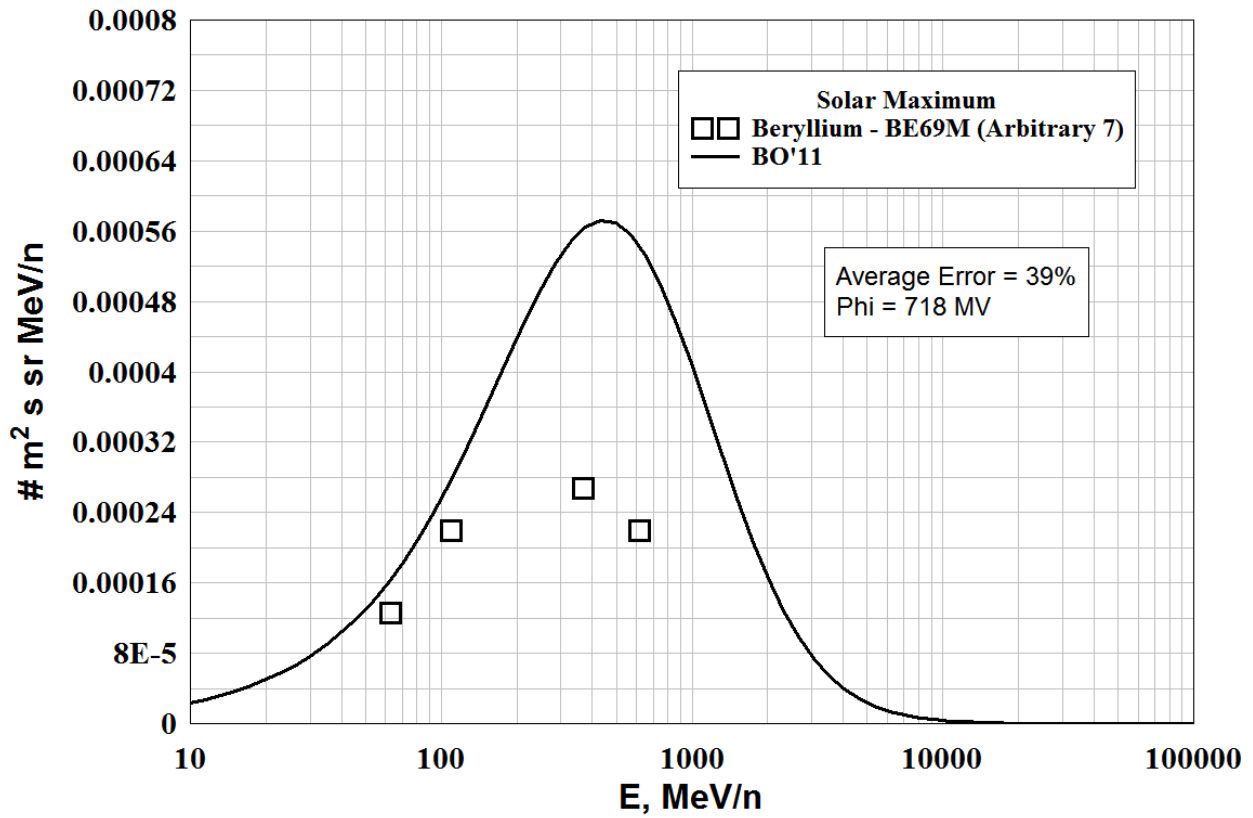
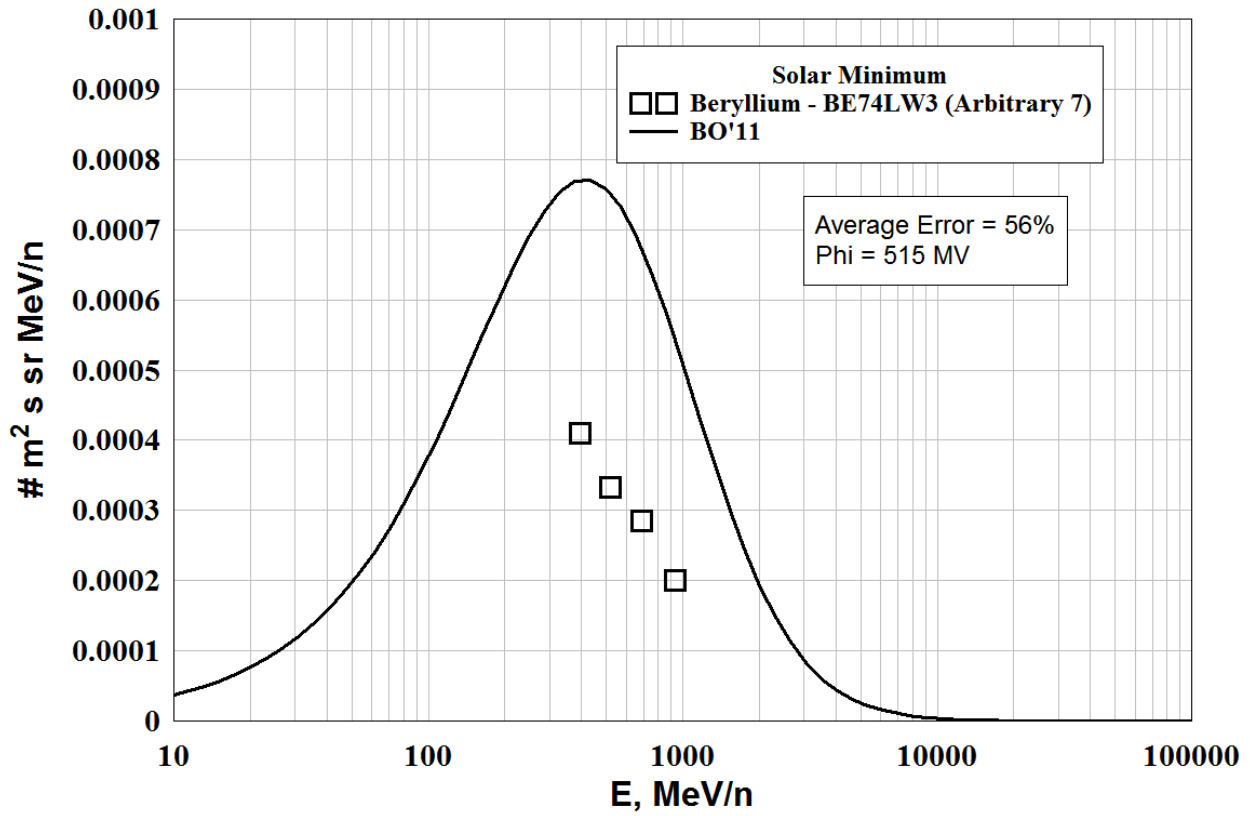
LITHIUM - LOW ENERGY DATA



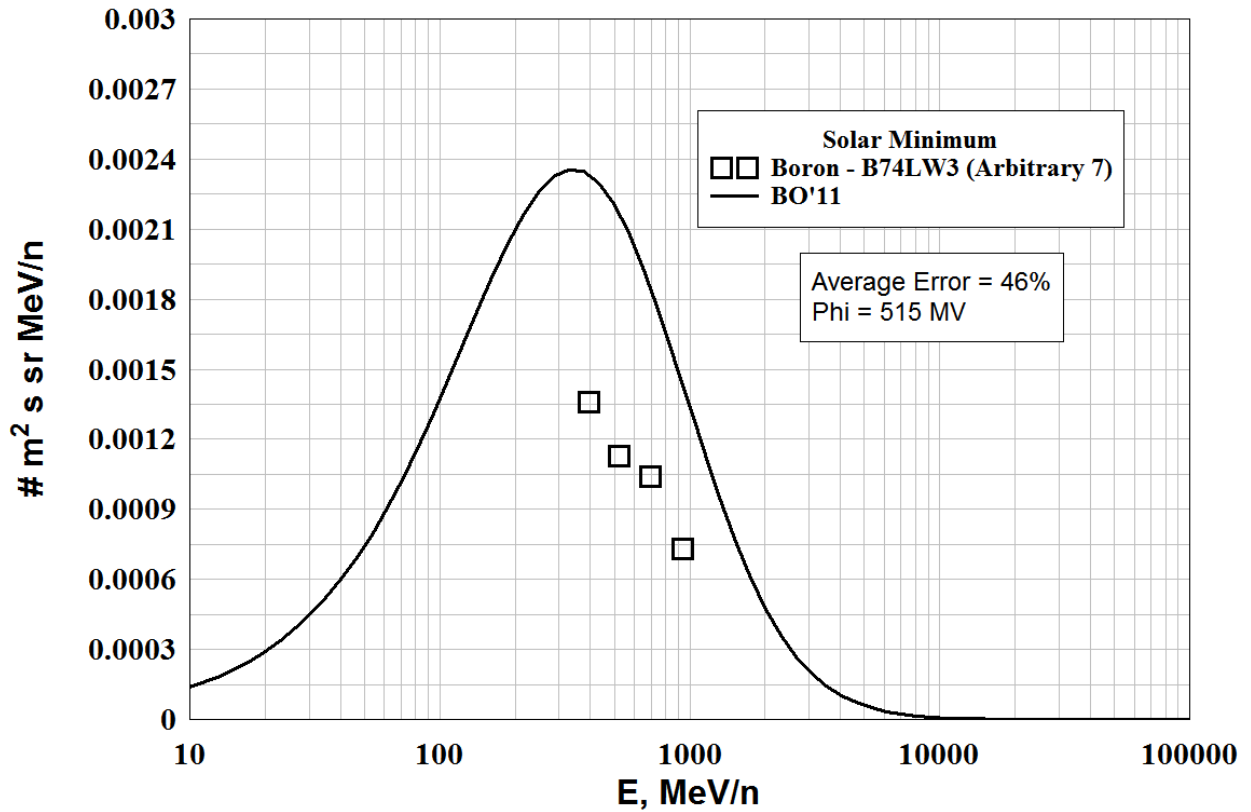
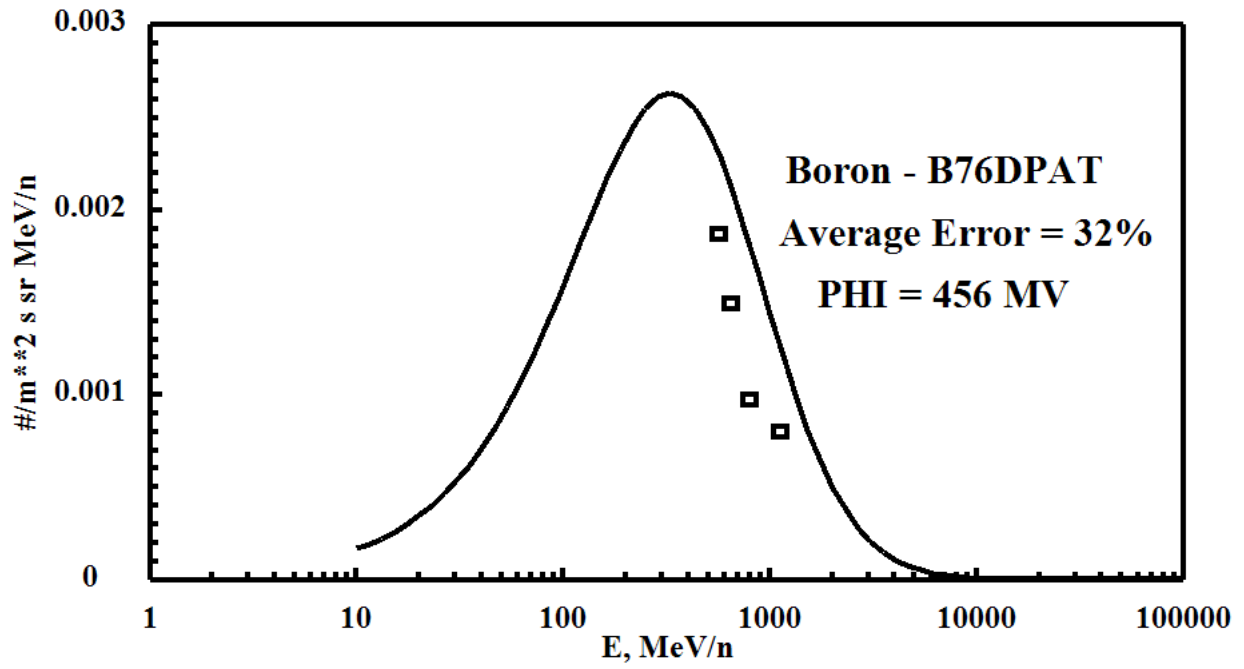


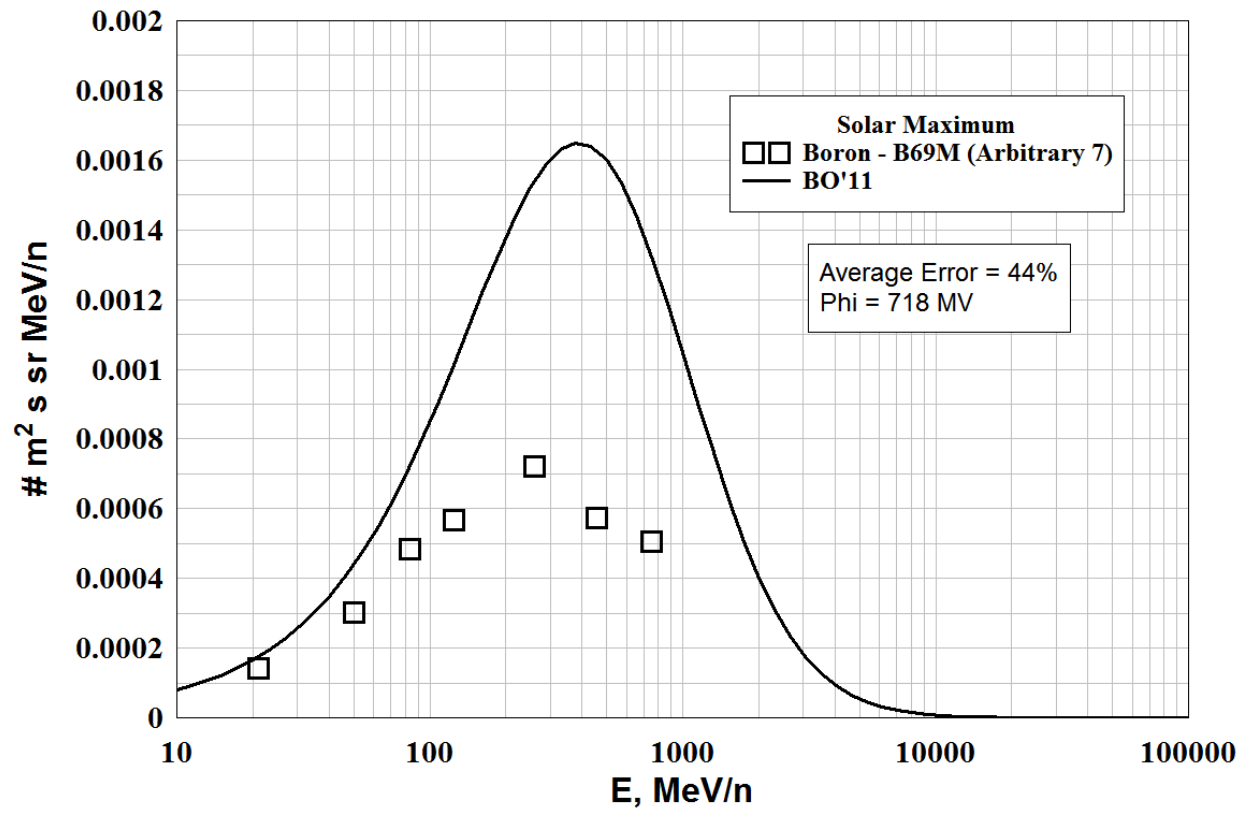
BERYLLIUM - LOW ENERGY DATA





BORON - LOW ENERGY DATA

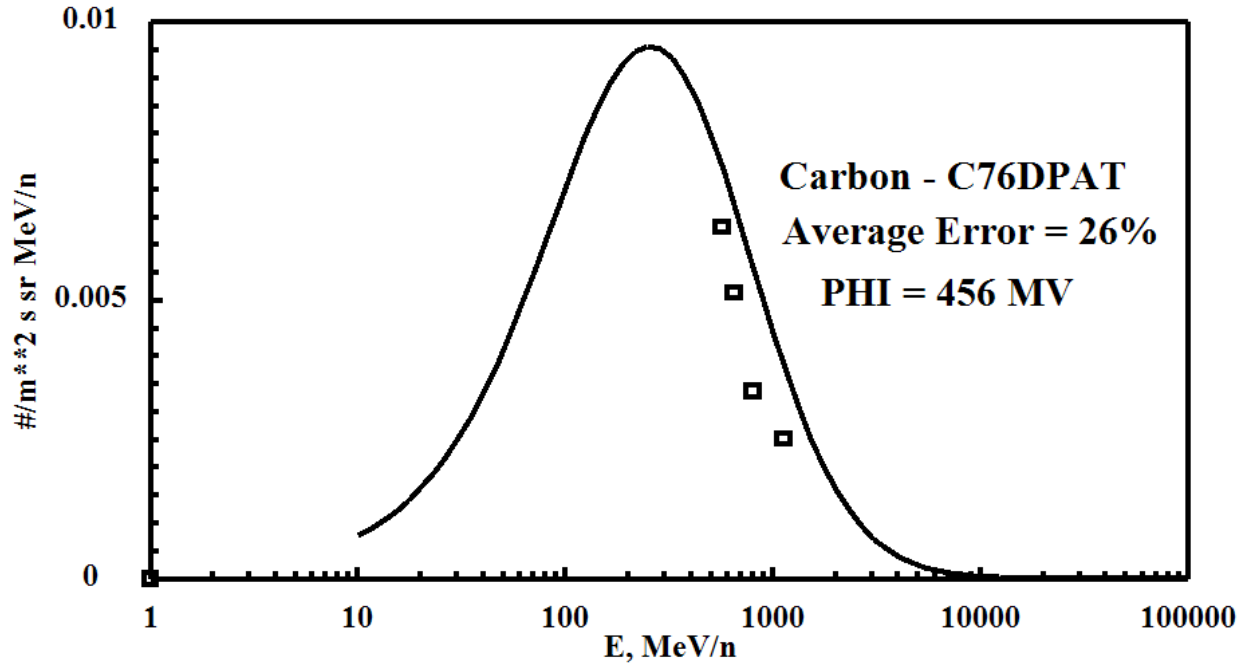




CARBON - Low Energy, Solar Minimum

Files Used (Arbitrary 1's)

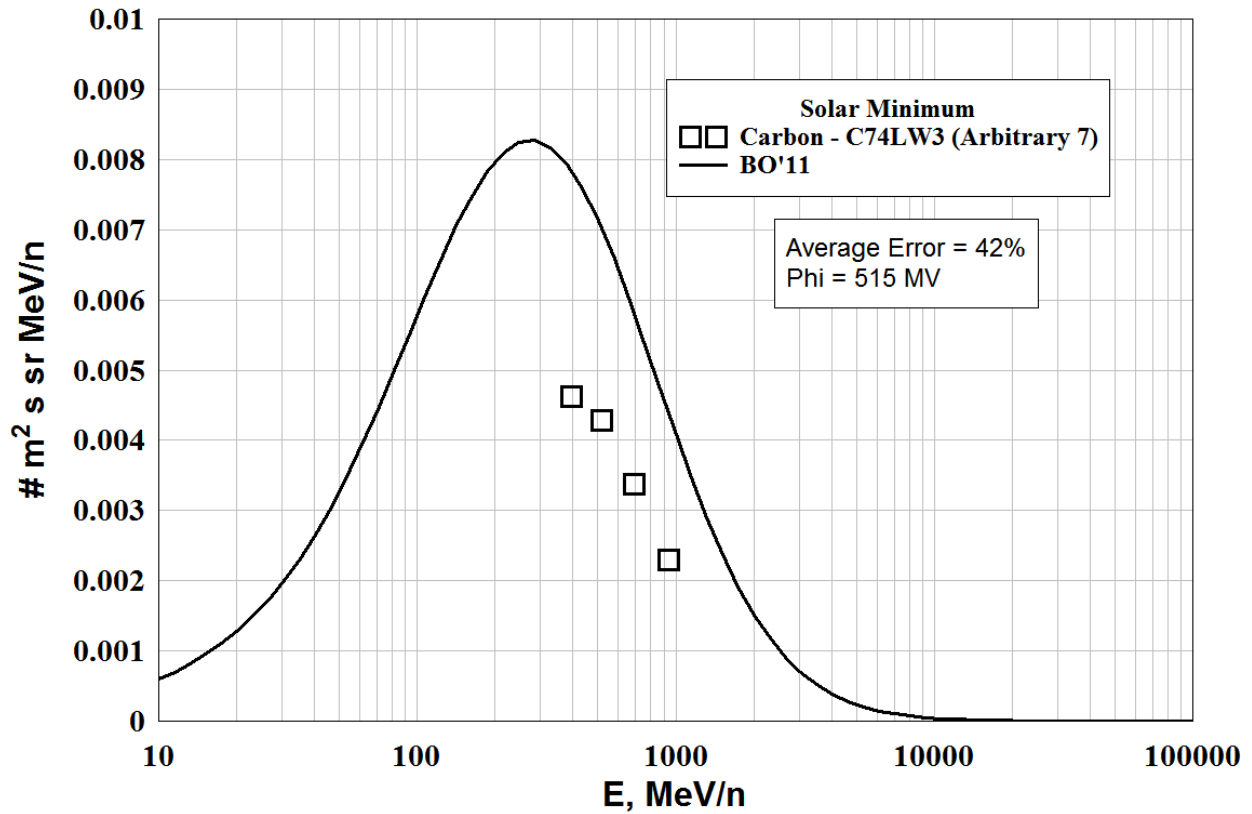
FILE	DATE	PHI (MV)	ERROR=ABS (FLUX-DATA)
C76DPAT.dat	1976.748	455.9699	26.06009
BO AVERAGE ERROR = 26.06009			



CARBON - Low Energy, Solar Minimum

Files Rejected - (Arbitrary 7's)

FILE	DATE	PHI (MV)	ERROR=ABS (FLUX-DATA)
C74LW3.dat	1974.553	515.0297	42.21569
BO AVERAGE ERROR = 42.21569			



CARBON - Low Energy, Solar Maximum

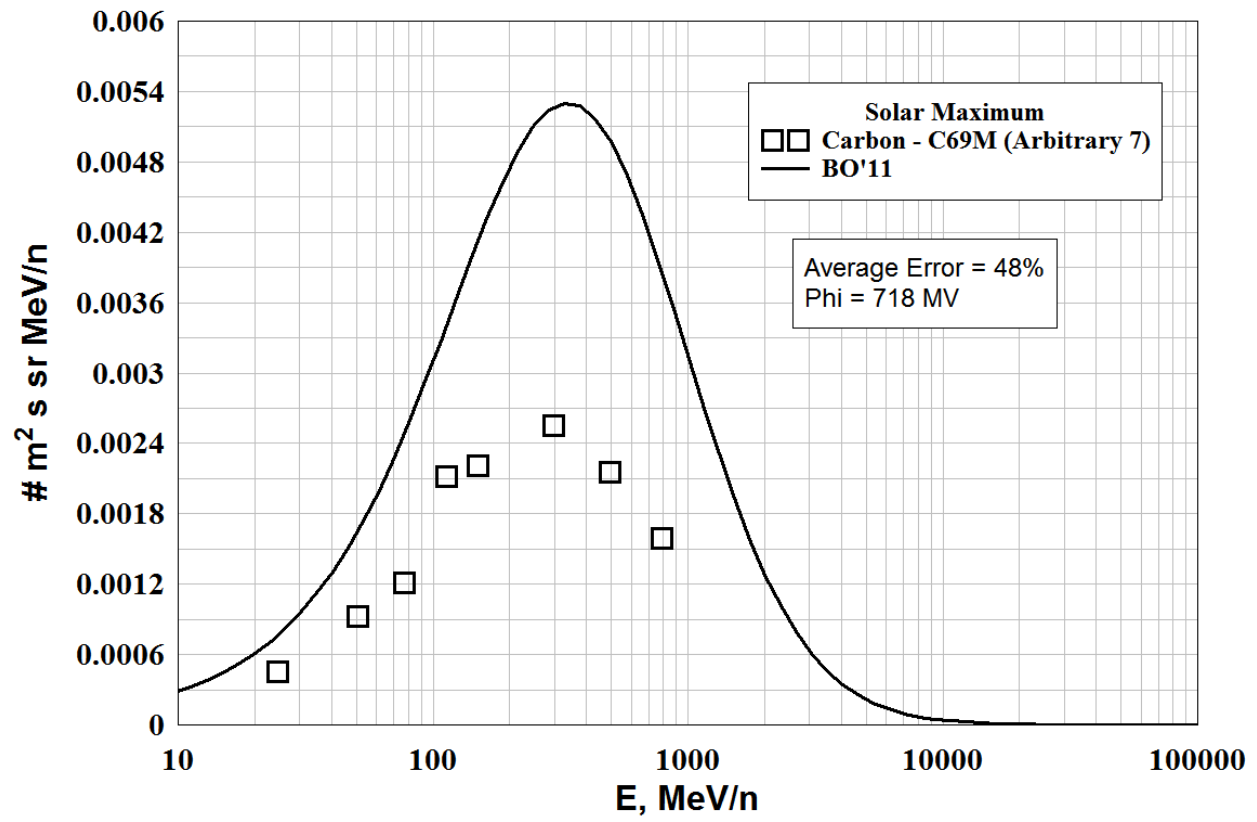
Files Used (Arbitrary 1's)

-----NO FILES-----

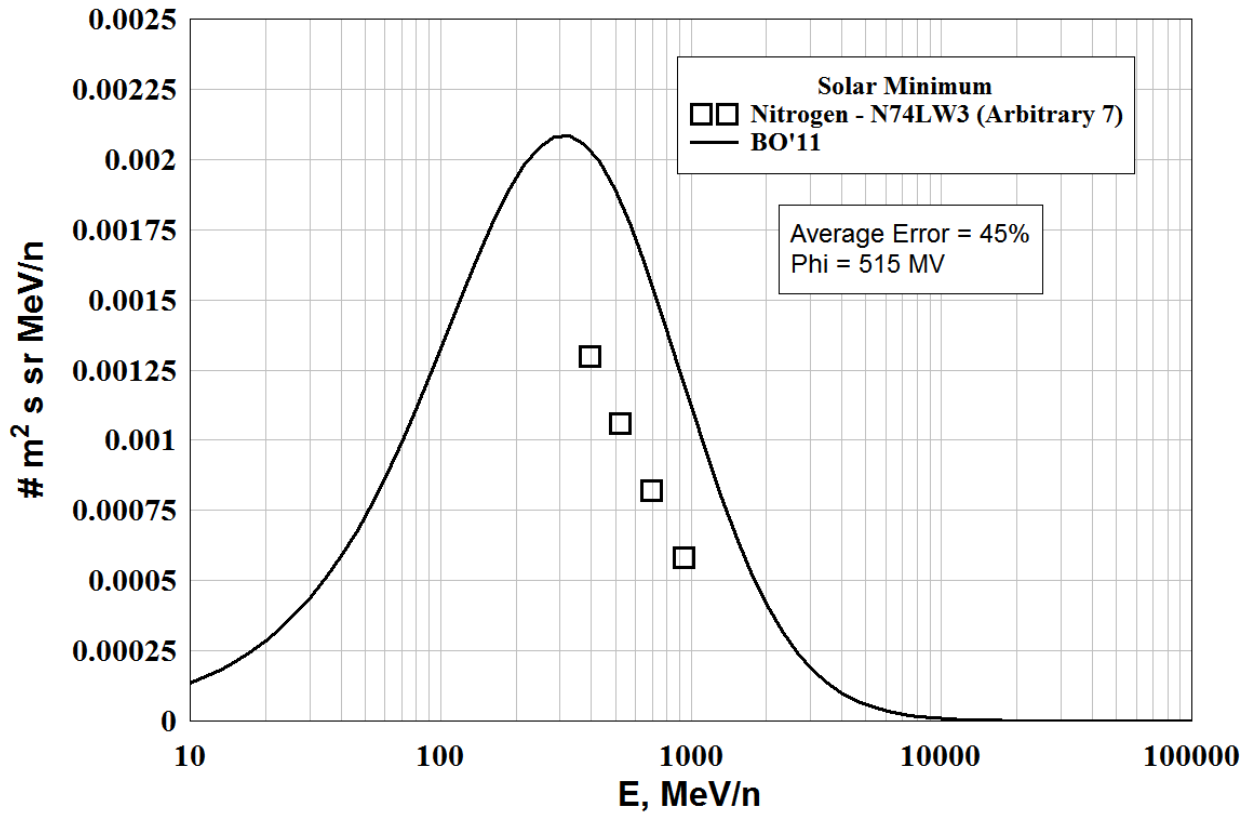
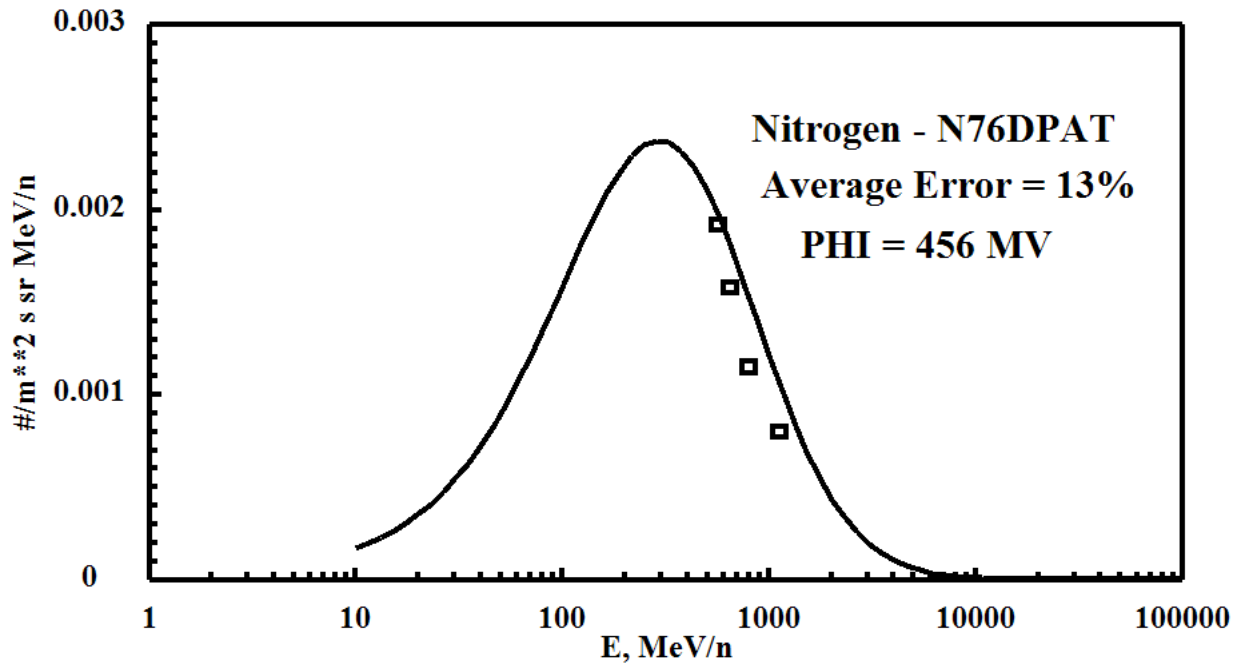
CARBON - Low Energy, Solar Maximum

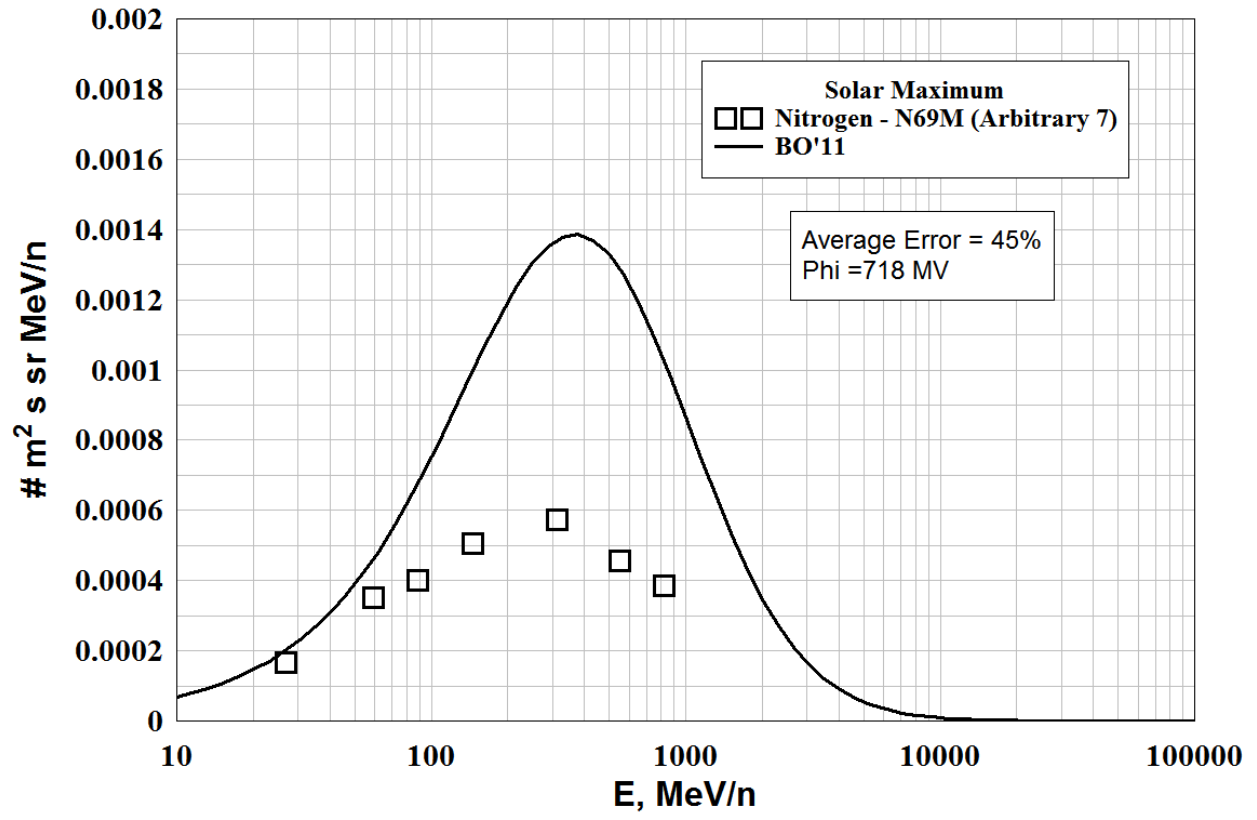
Files Rejected - (Arbitrary 7's)

FILE	DATE	PHI (MV)	ERROR=ABS (FLUX-DATA)
C69M.dat	1969.570	718.0887	48.41494
BO AVERAGE ERROR =			48.41494



NITROGEN - LOW ENERGY DATA

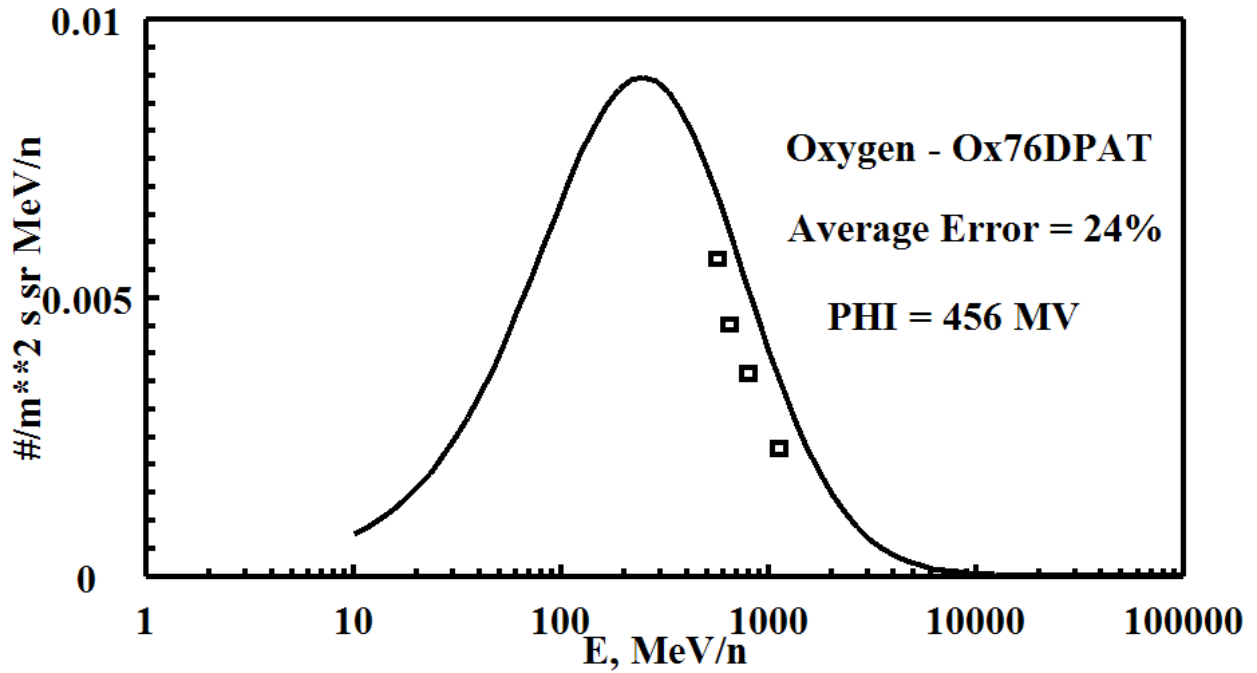




OXYGEN - Low Energy, Solar Minimum

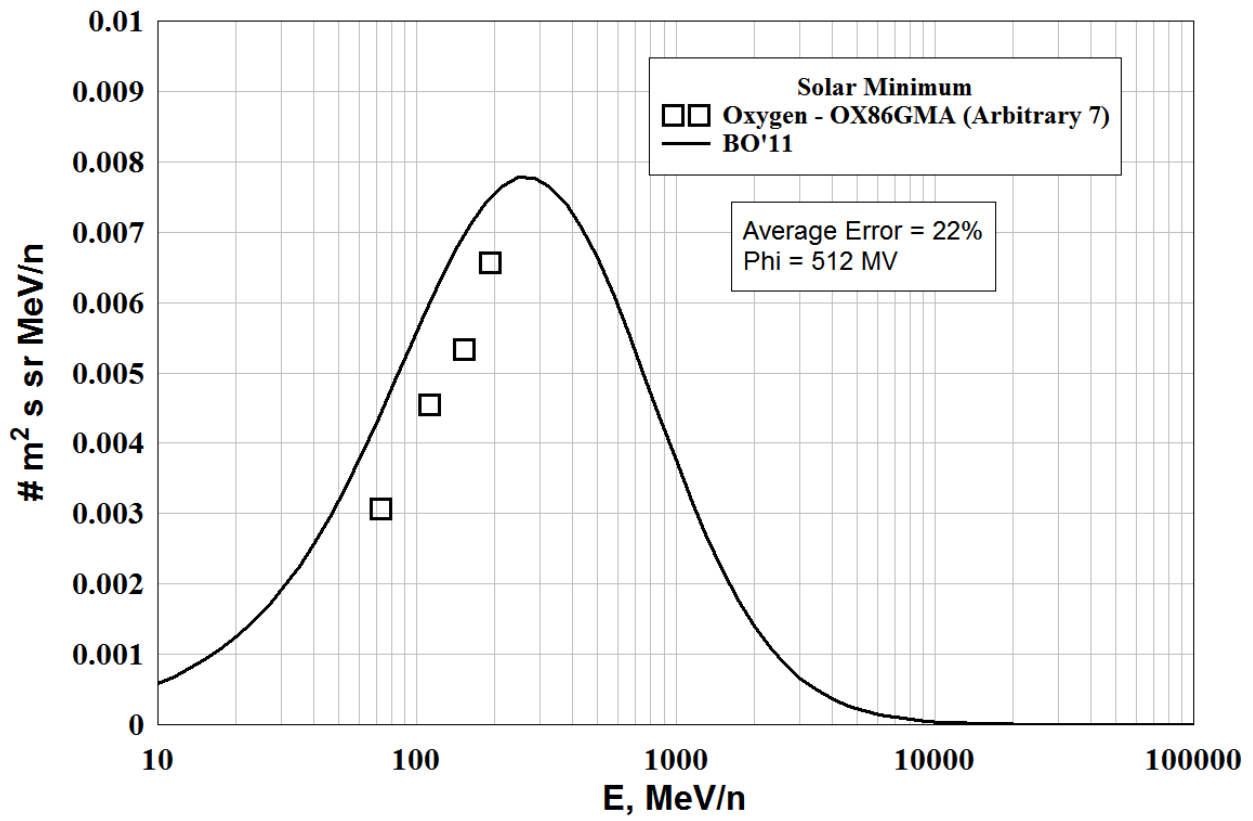
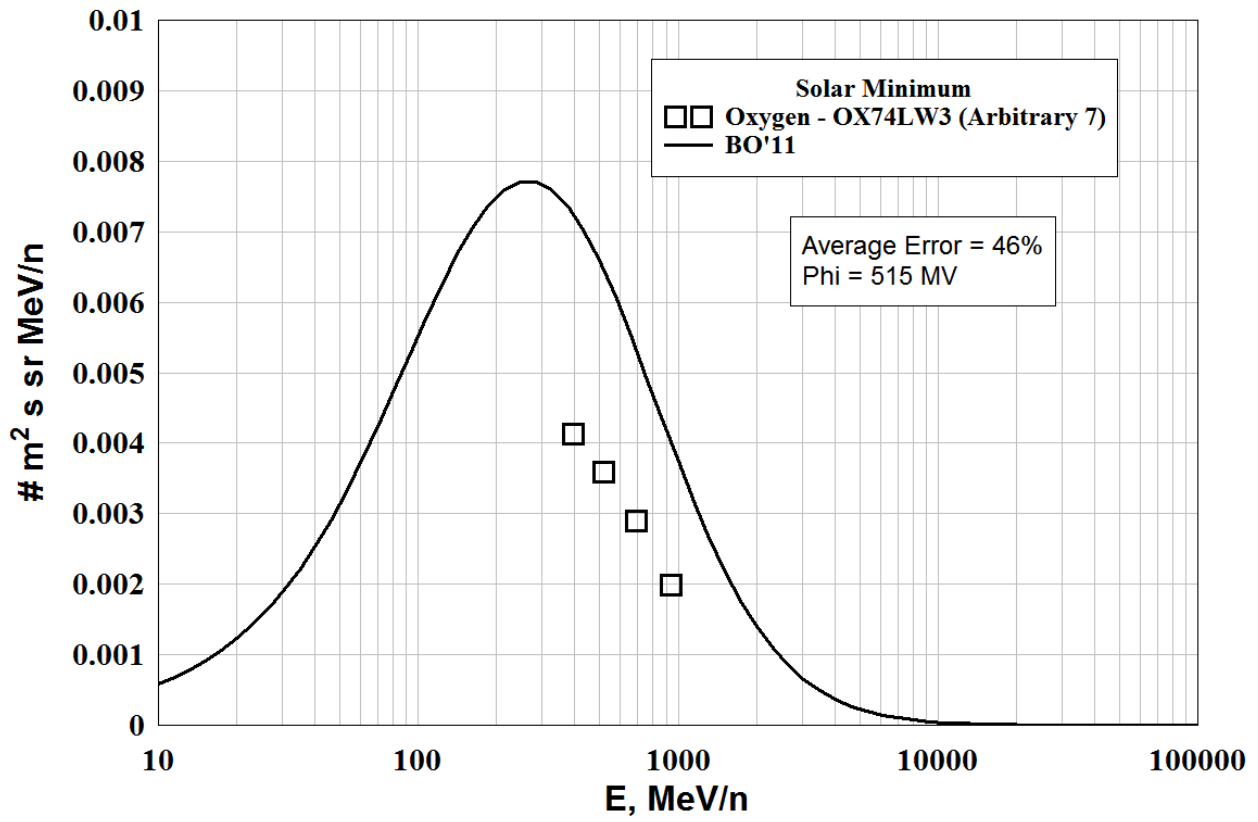
Files Used (Arbitrary 1's)

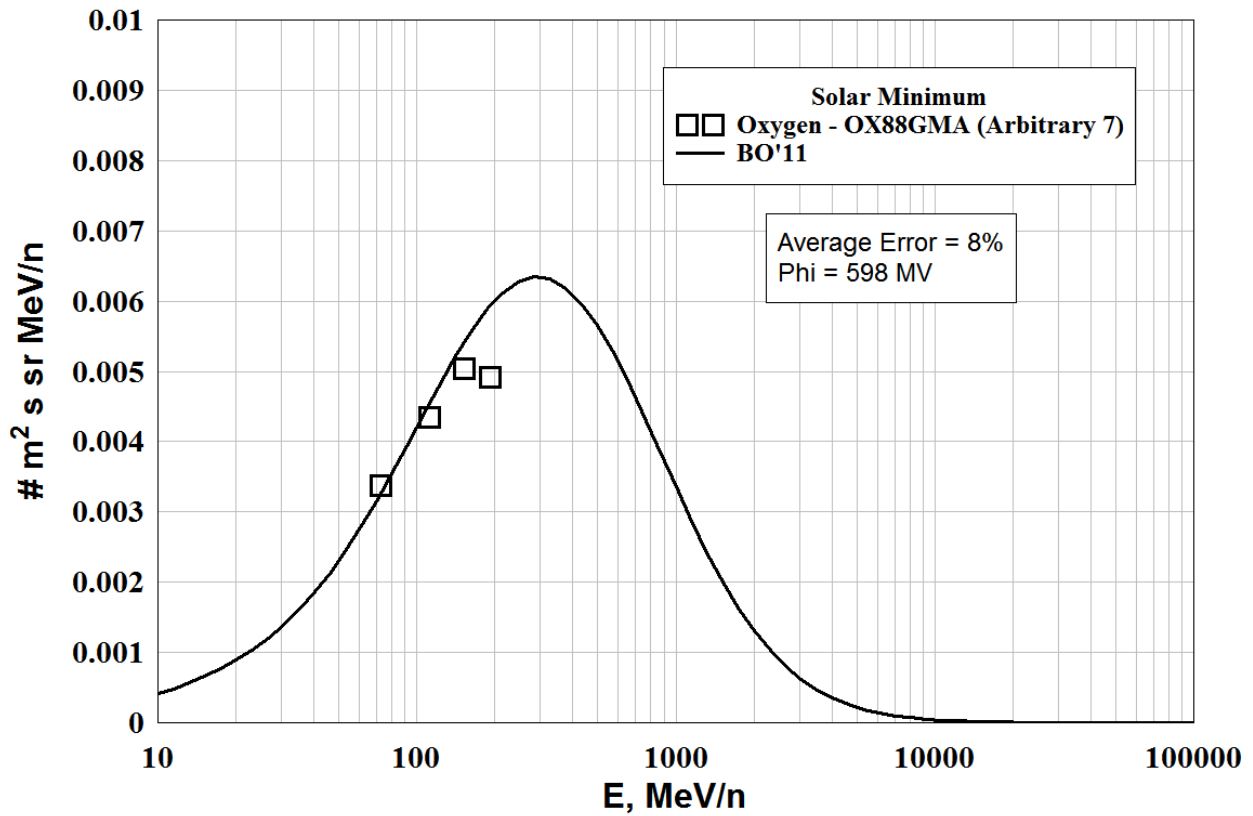
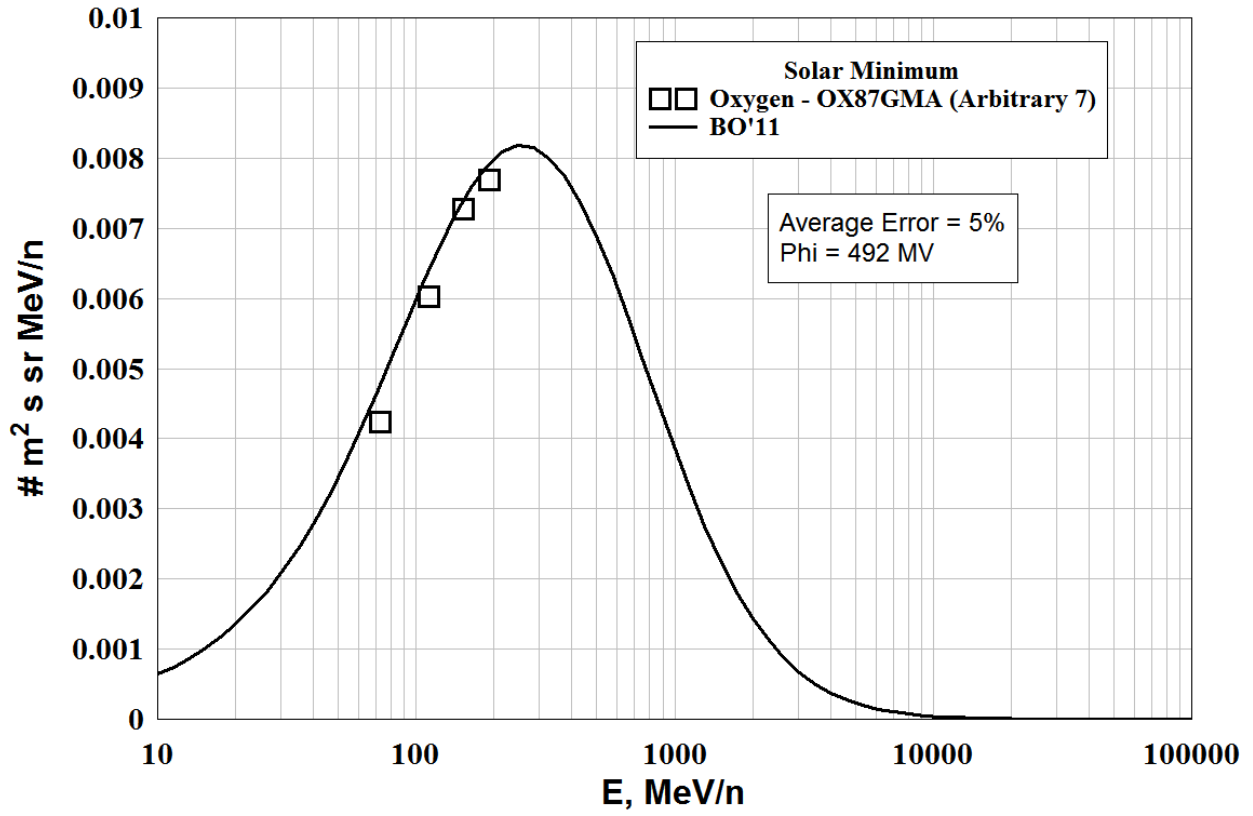
FILE	DATE	PHI (MV)	ERROR=ABS (FLUX-DATA)
Ox76DPAT.dat	1976.748	455.9695	24.19584
BO AVERAGE ERROR = 24.19584			



Files Rejected - (Arbitrary 7's)

FILE	DATE	PHI (MV)	ERROR=ABS (FLUX-DATA)
Ox74LW3.dat	1974.553	515.0297	45.80968
Ox86GMA.dat	1986.288	511.7451	22.46120
Ox87GMA.dat	1987.104	491.9082	5.159821
Ox88GMA.dat	1987.934	597.9689	7.827194
BO AVERAGE ERROR = 20.31448			





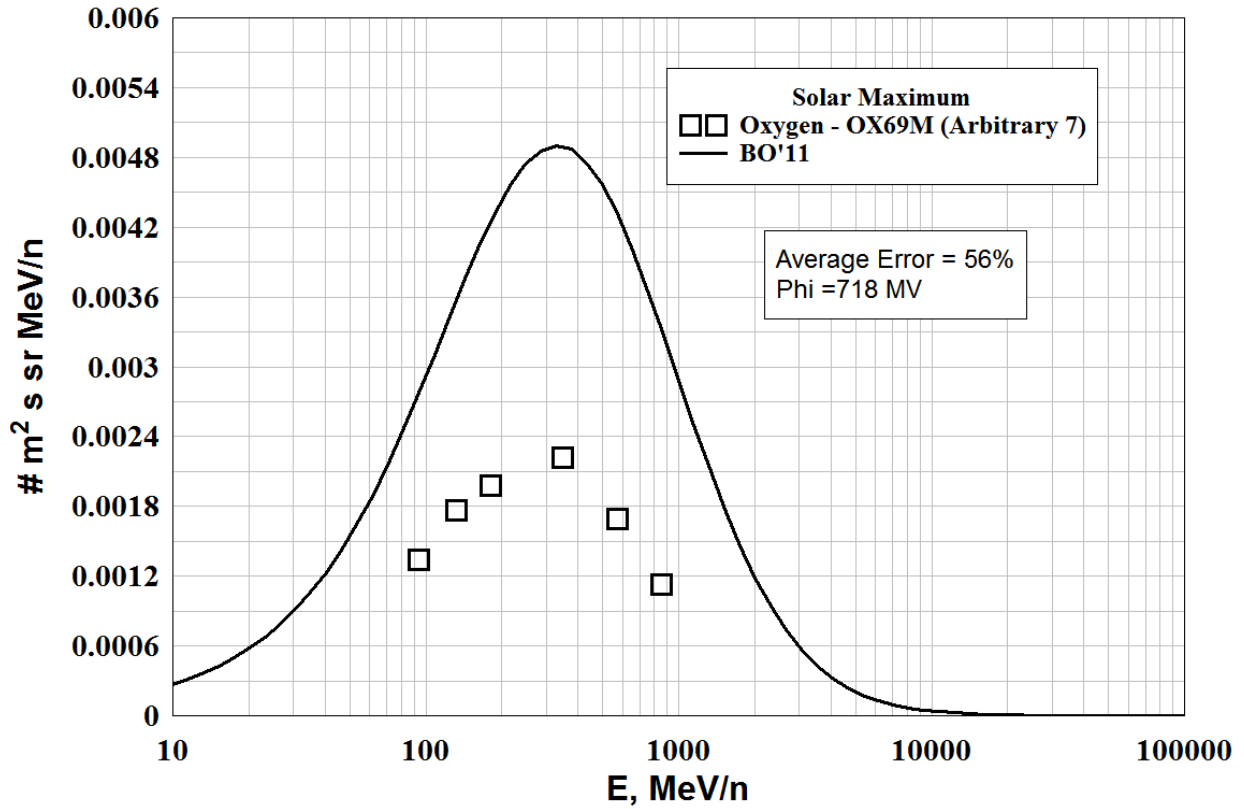
OXYGEN - Low Energy, Solar Maximum

Files Used (Arbitrary 1's)

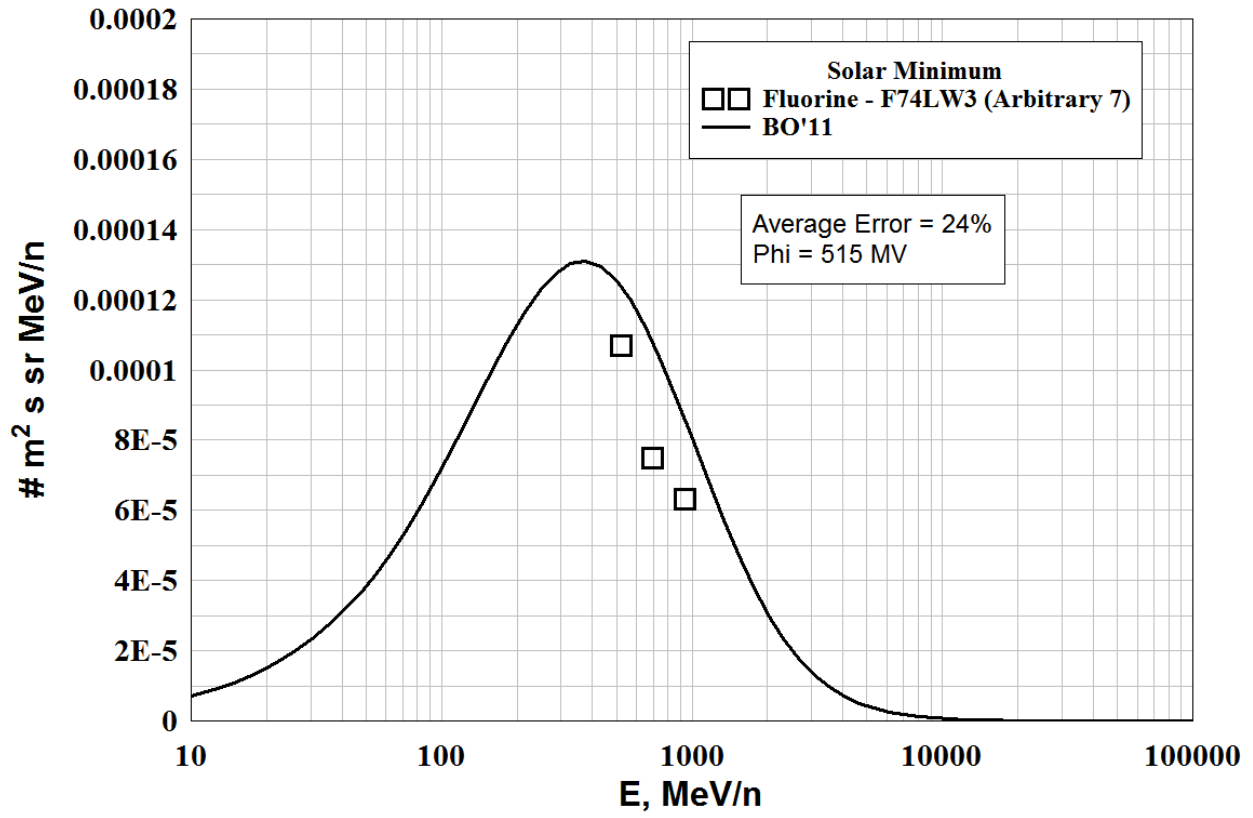
-----NO FILES-----

Files Rejected - (Arbitrary 7's)

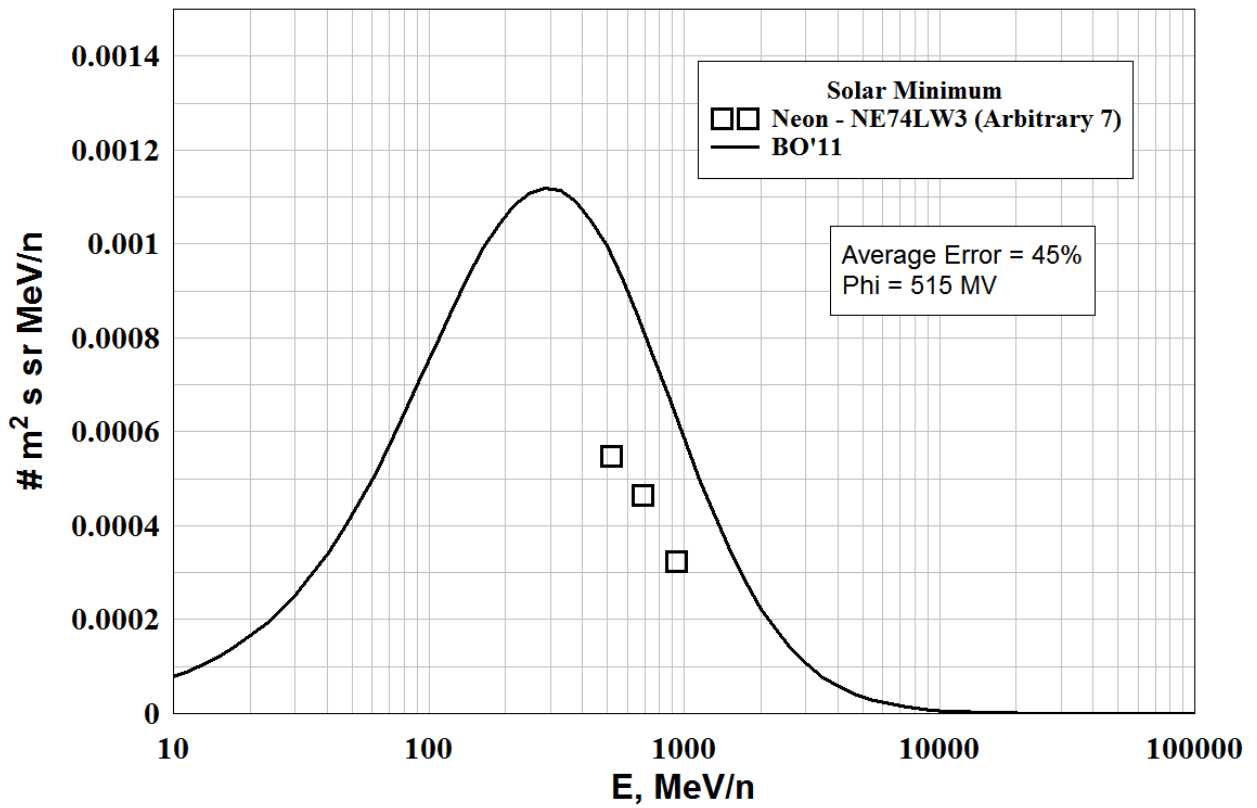
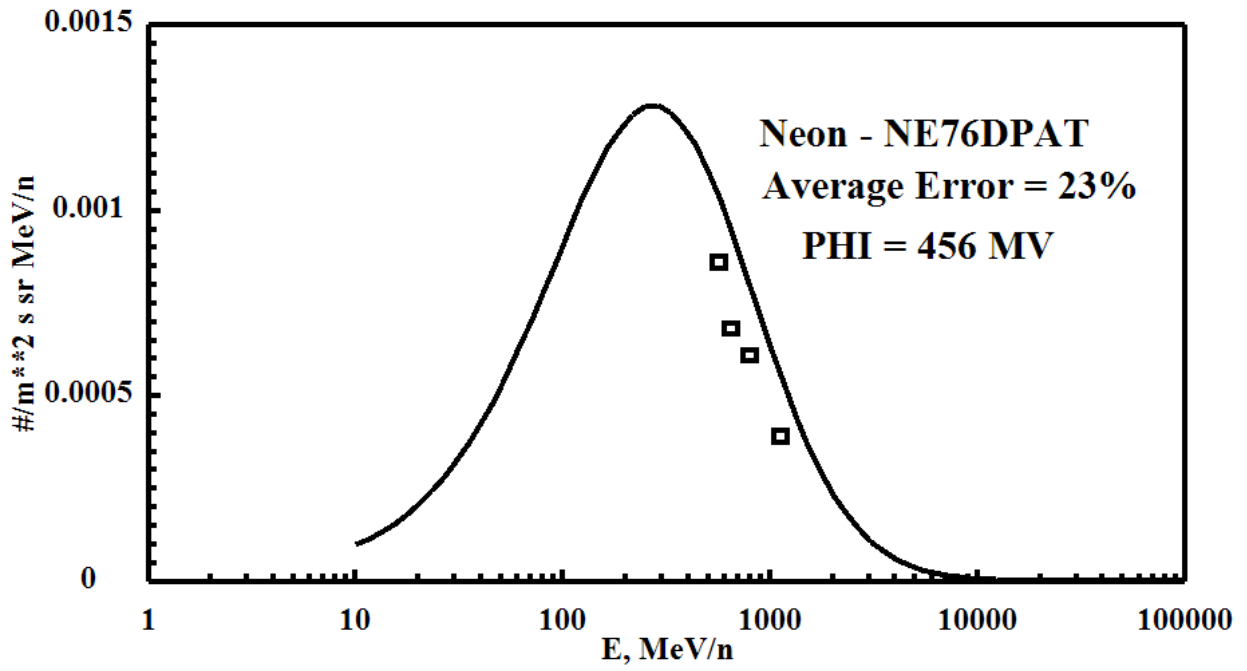
FILE	DATE	PHI (MV)	ERROR=ABS (FLUX-DATA)	
Ox69M.dat	1969.570	718.0887	56.16359	
BO AVERAGE ERROR =		56.16359		



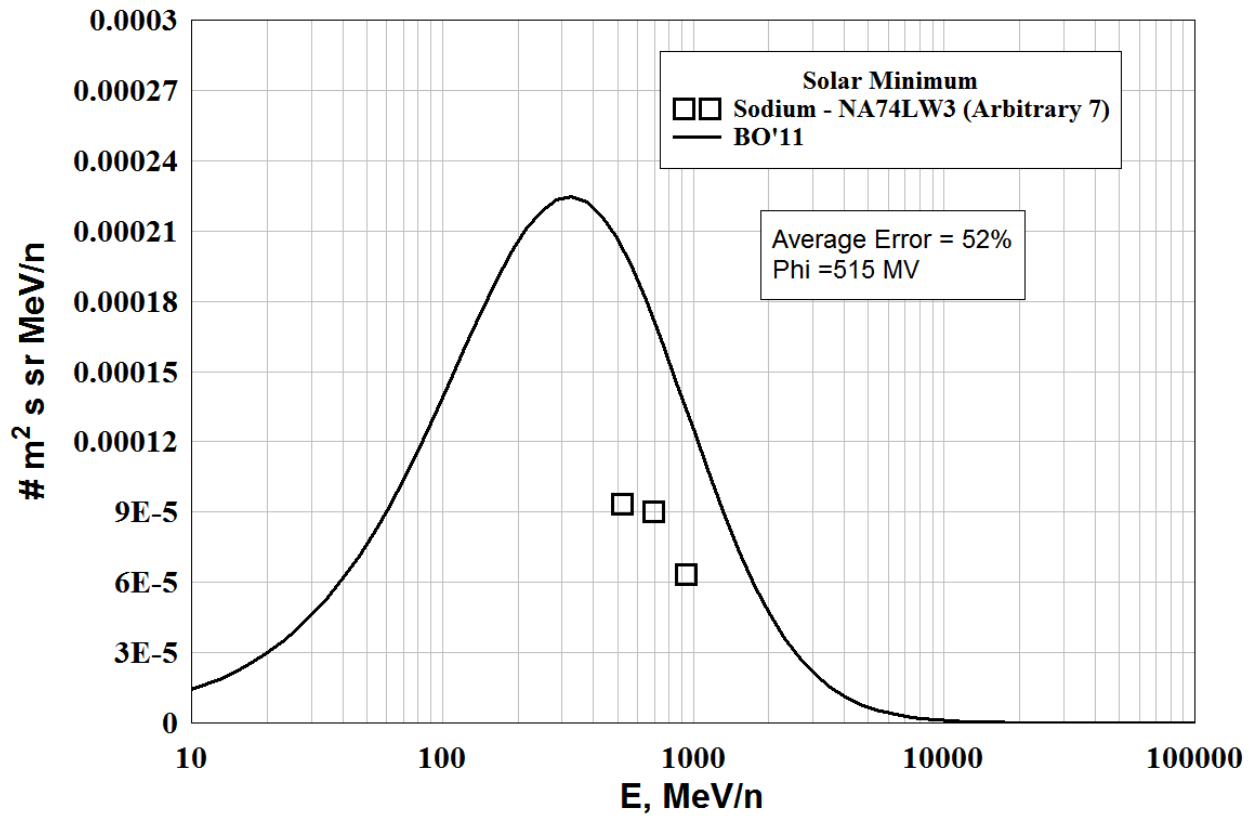
FLOURINE - LOW ENERGY DATA



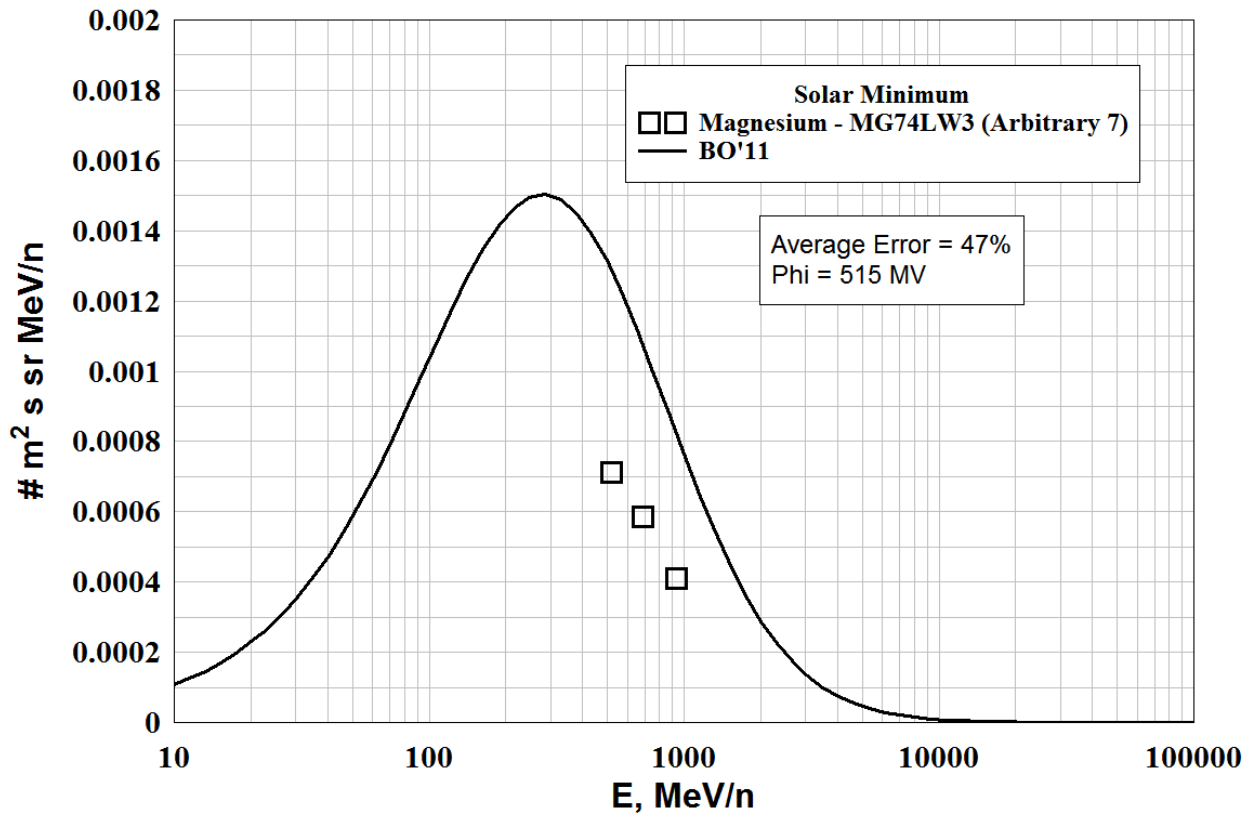
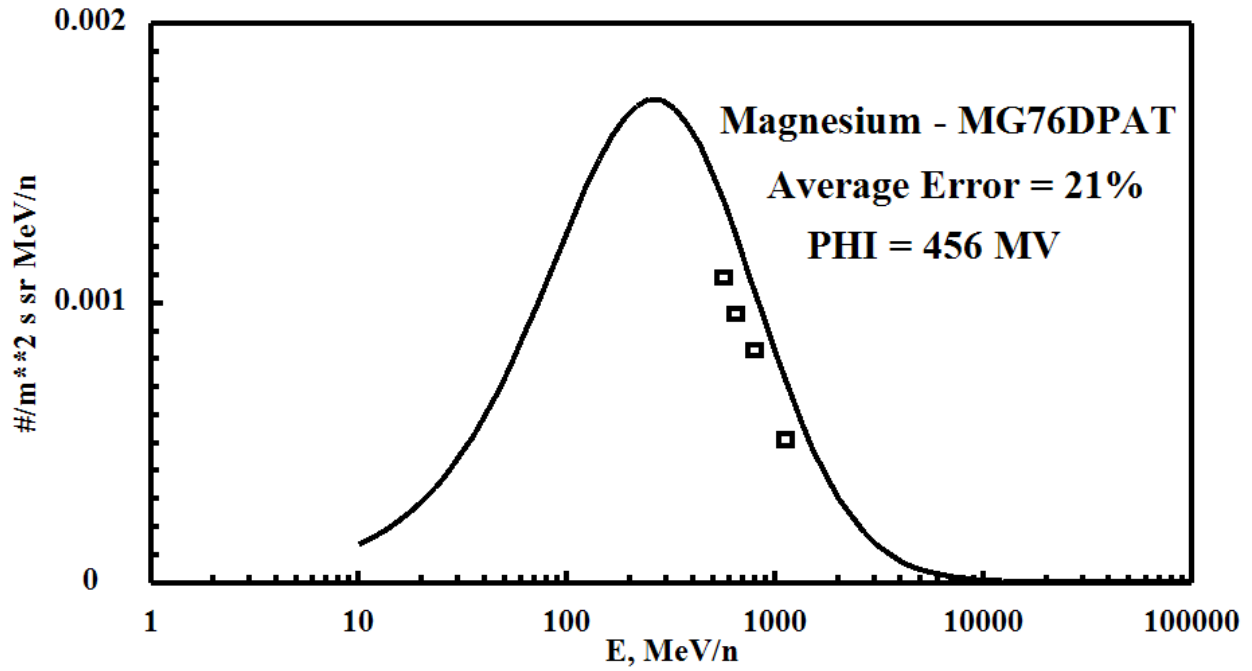
NEON - LOW ENERGY DATA



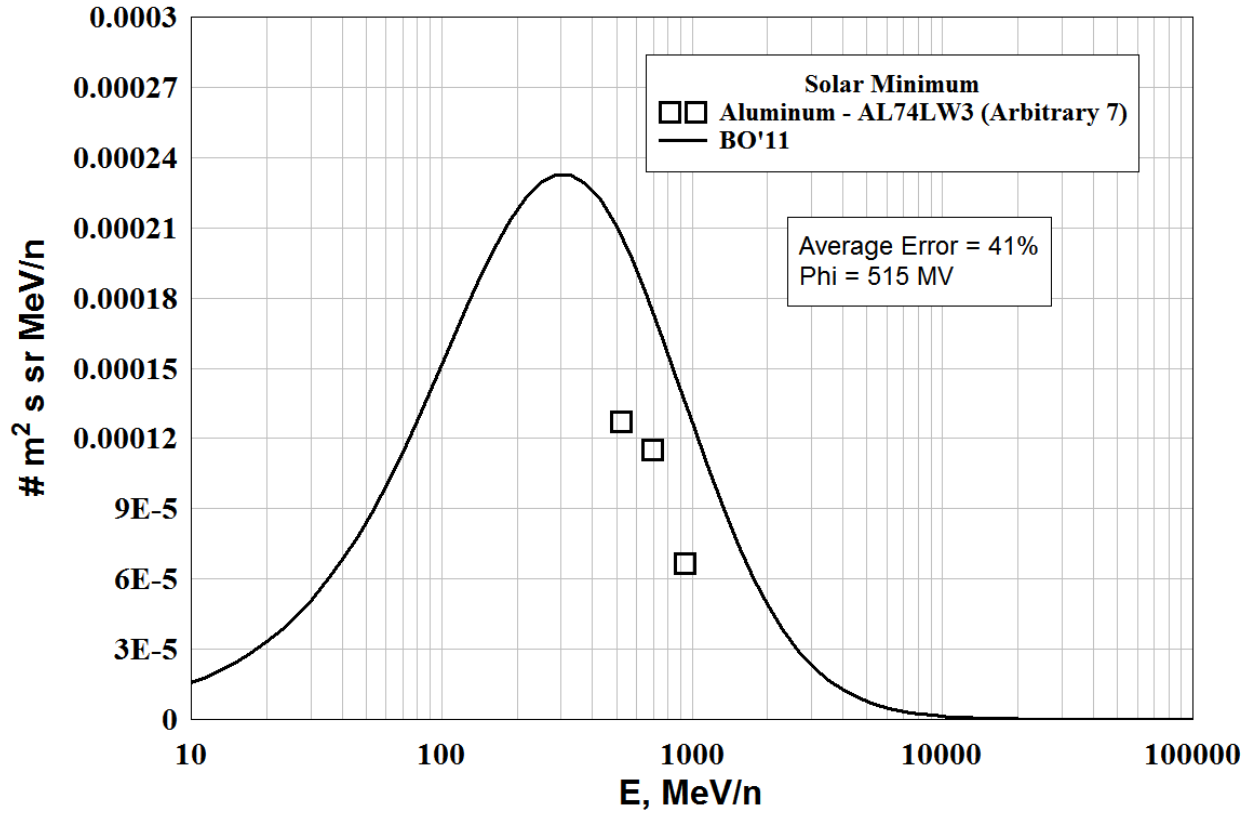
SODIUM - LOW ENERGY DATA



MAGNESIUM - LOW ENERGY DATA



ALUMINUM - LOW ENERGY DATA



SILICON - Low Energy, Solar Minimum

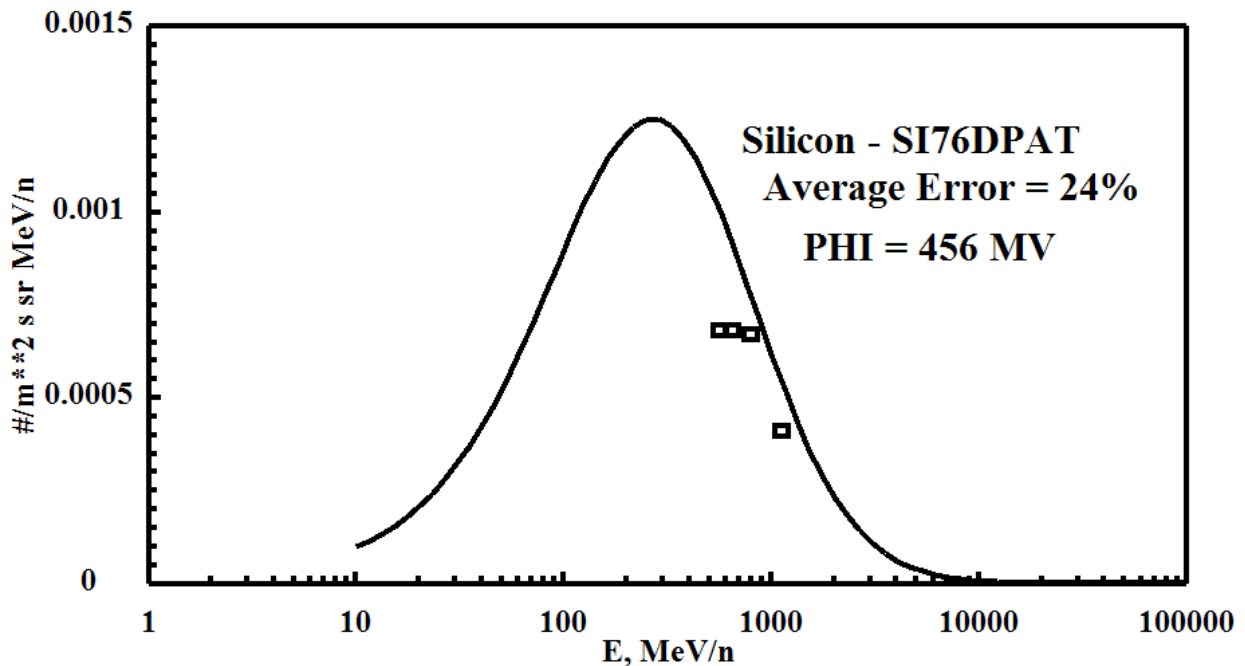
Files Used (Arbitrary 1's)

FILE	DATE	PHI (MV)	ERROR=ABS (FLUX-DATA)
SI76DPAt.dat	1976.748	455.9699	23.79770
BO AVERAGE ERROR = 23.79770			

SILICON - Low Energy, Solar Maximum

Files Used (Arbitrary 1's)

FILE	DATE	PHI (MV)	ERROR=ABS (FLUX-DATA)
SI71B.dat	1971.756	601.9181	29.50120
BO AVERAGE ERROR = 29.50120			

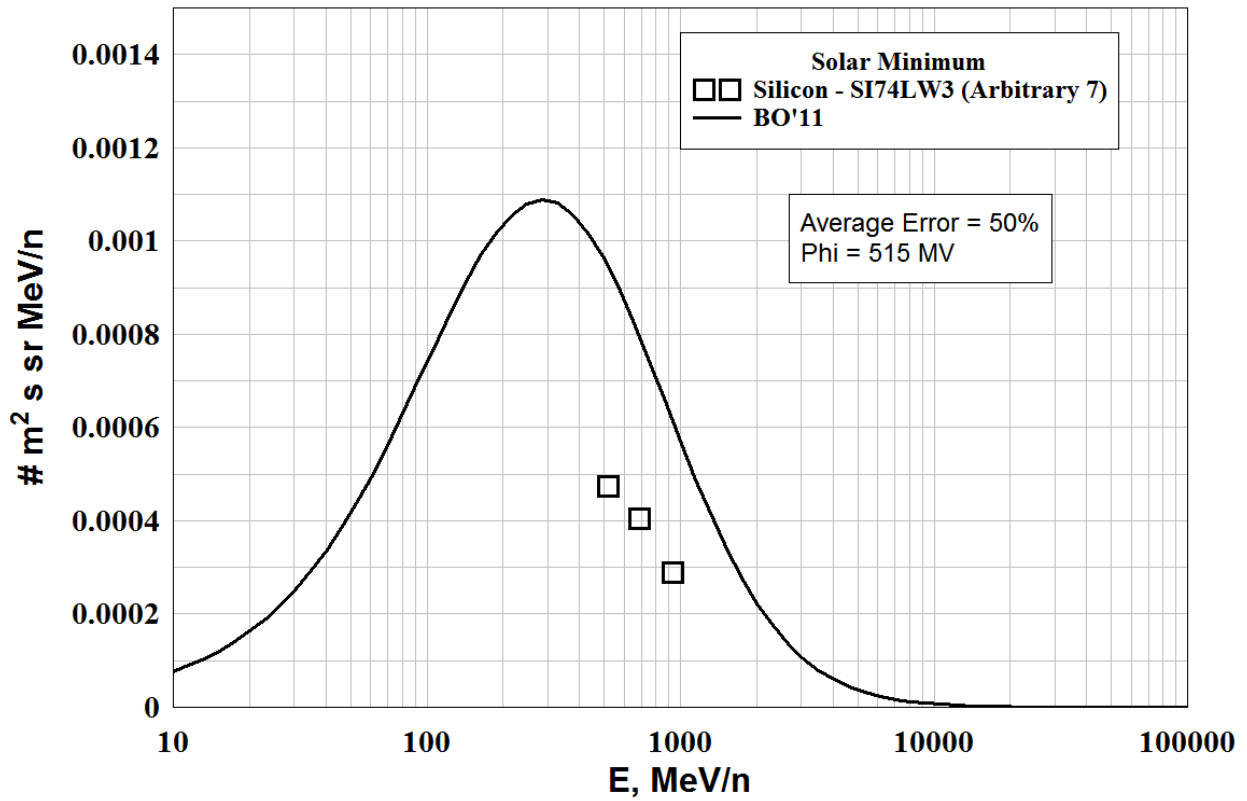
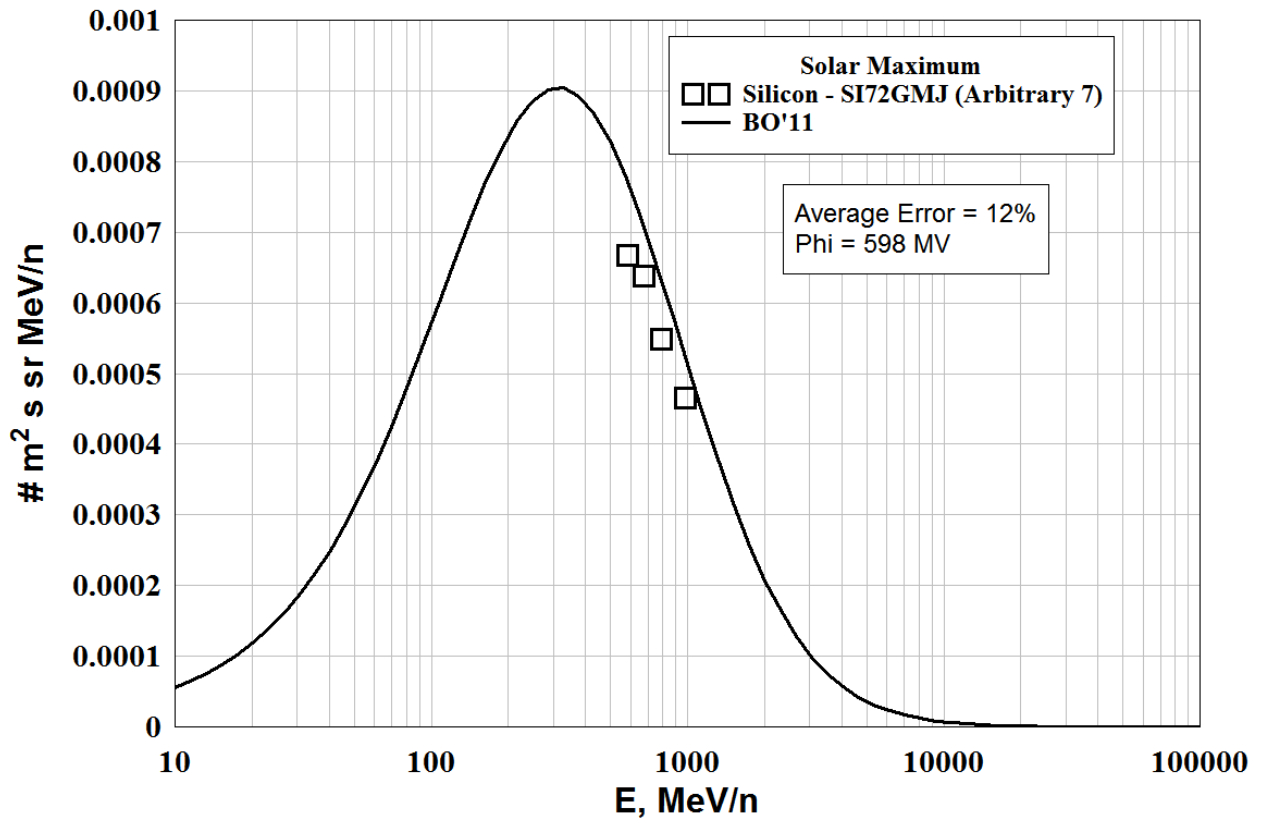


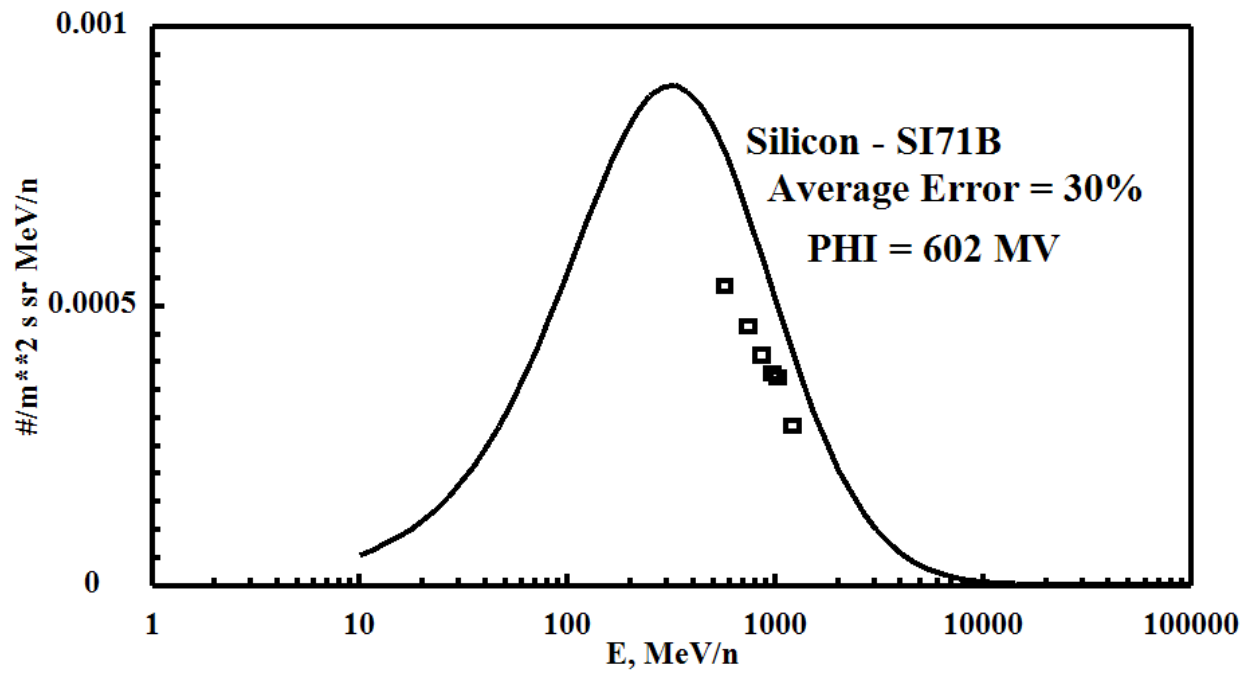
Files Rejected - (Arbitrary 7's)

FILE	DATE	PHI (MV)	ERROR=ABS (FLUX-DATA)
SI72GMJ.dat	1972.668	598.2584	11.98216
BO AVERAGE ERROR = 11.98216			

Files Rejected - (Arbitrary 7's)

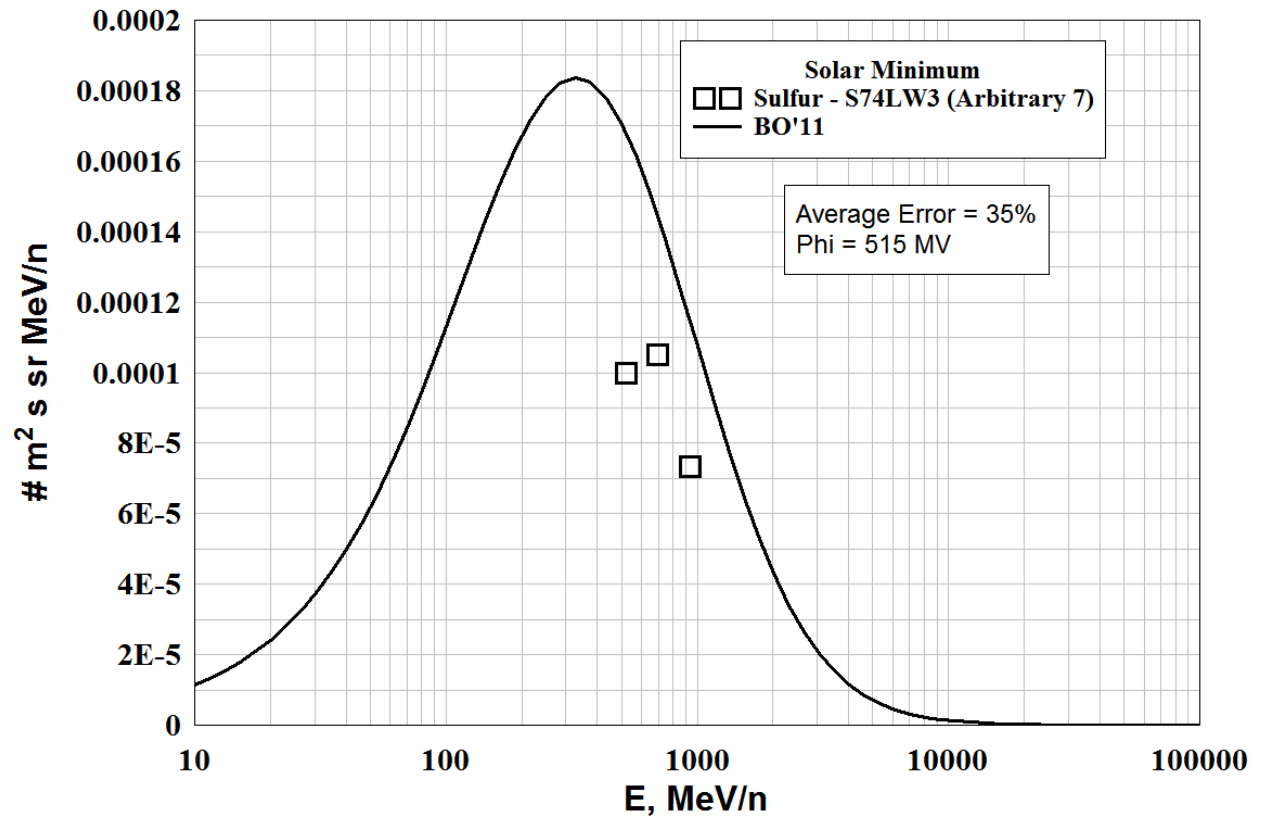
FILE	DATE	PHI (MV)	ERROR=ABS (FLUX-DATA)
SI74LW3.dat	1974.553	515.0297	50.41383
BO AVERAGE ERROR = 50.41383			



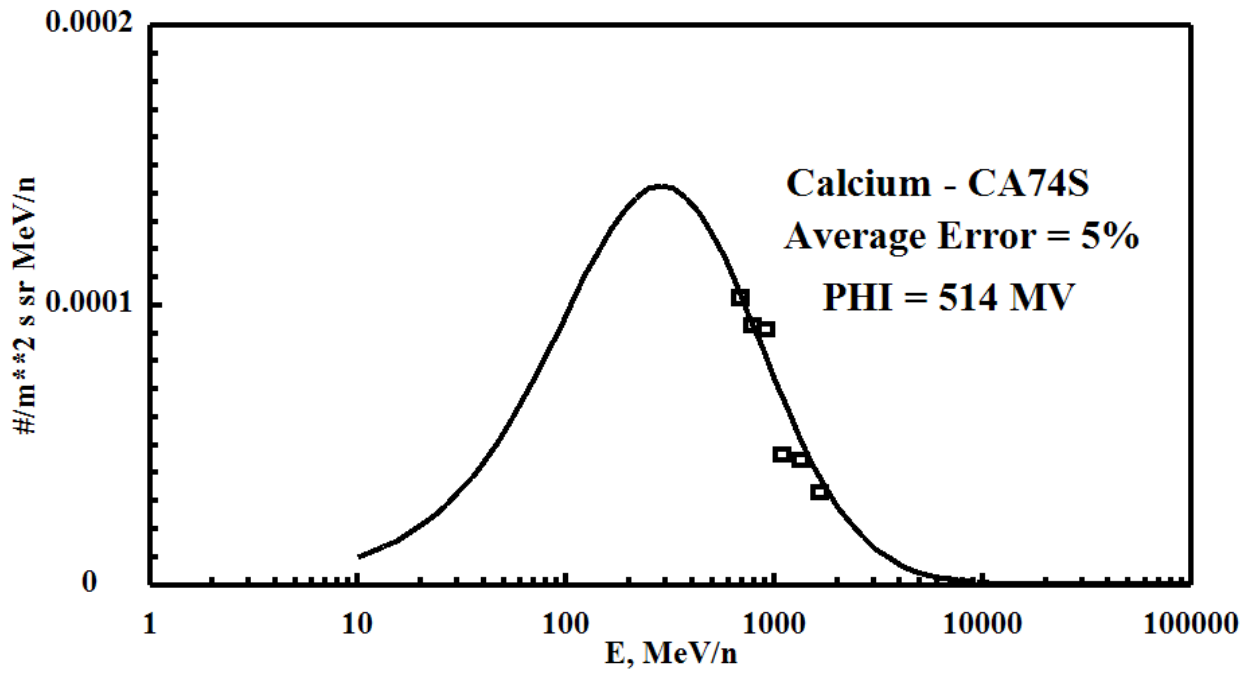
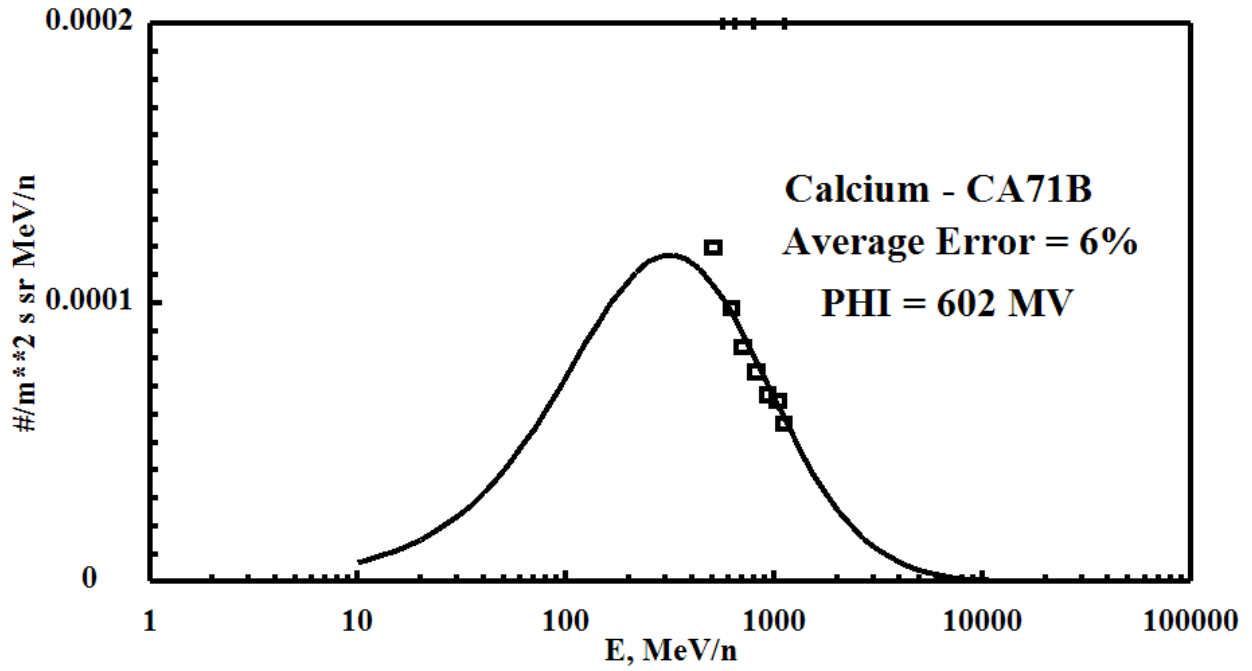


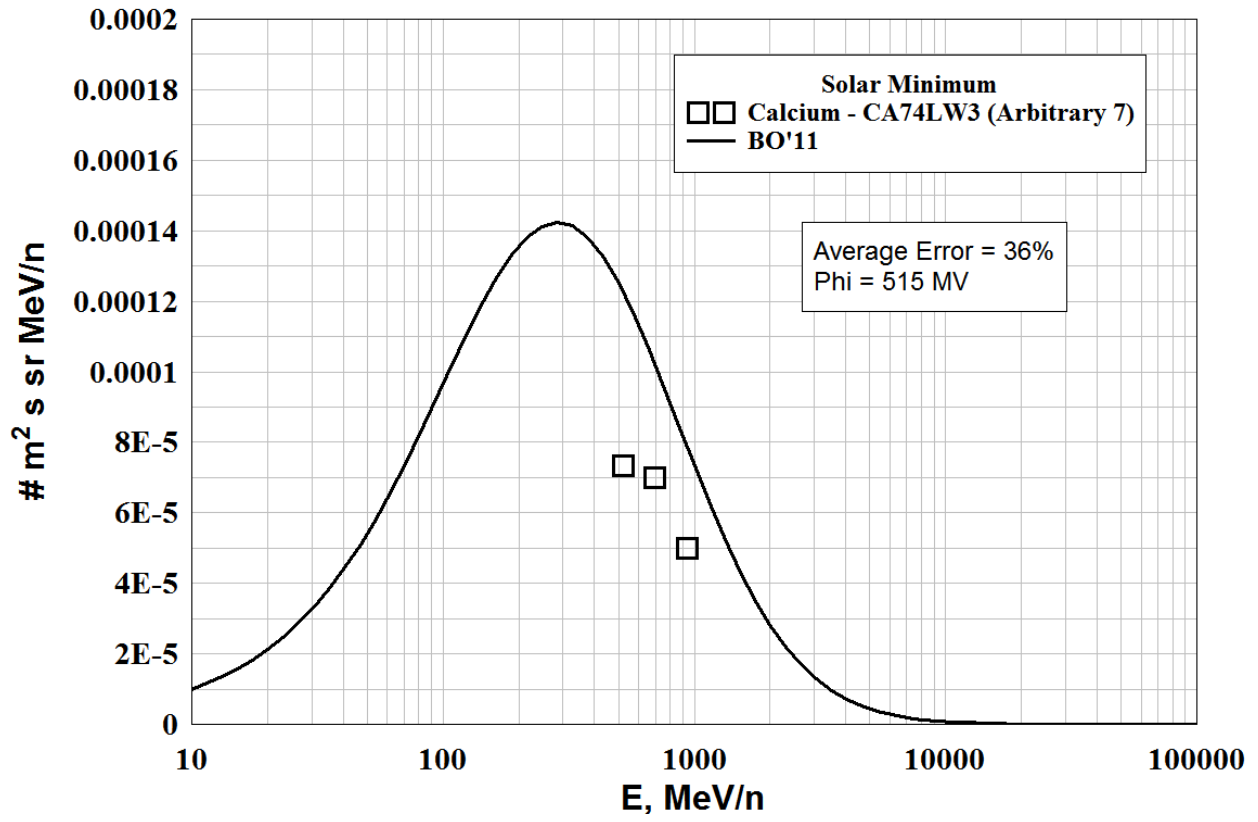
PHOSPHORUS - LOW ENERGY DATA - NONE

SULFUR - LOW ENERGY DATA



CALCIUM` - LOW ENERGY DATA

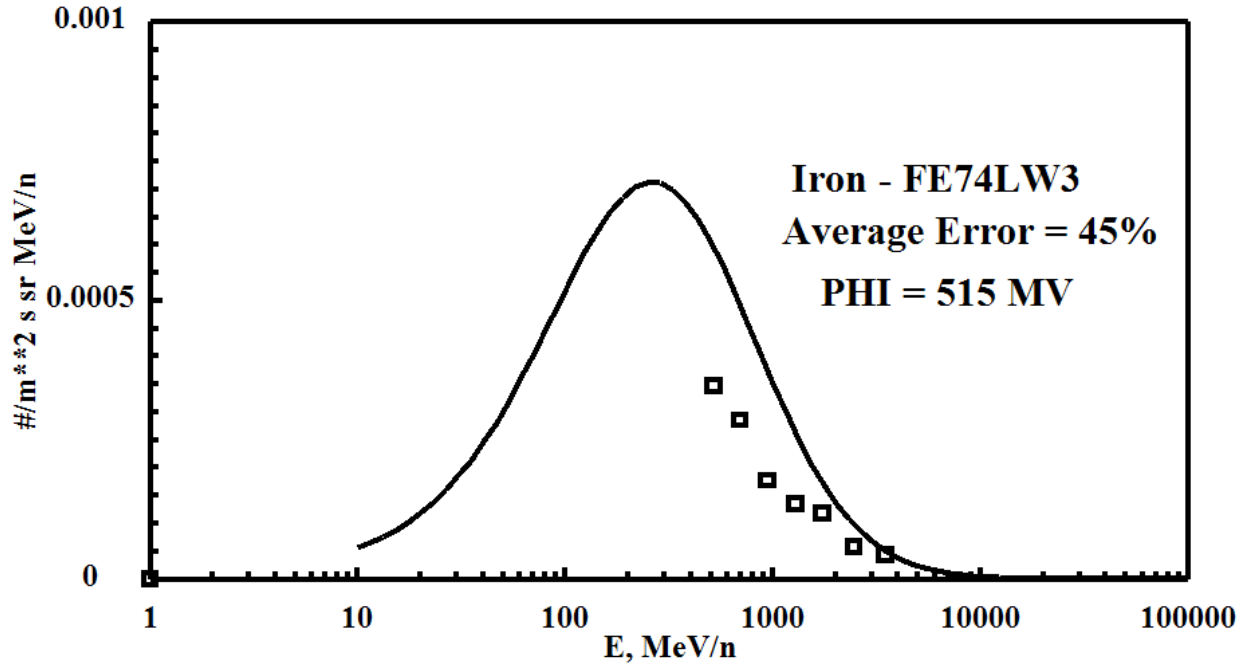


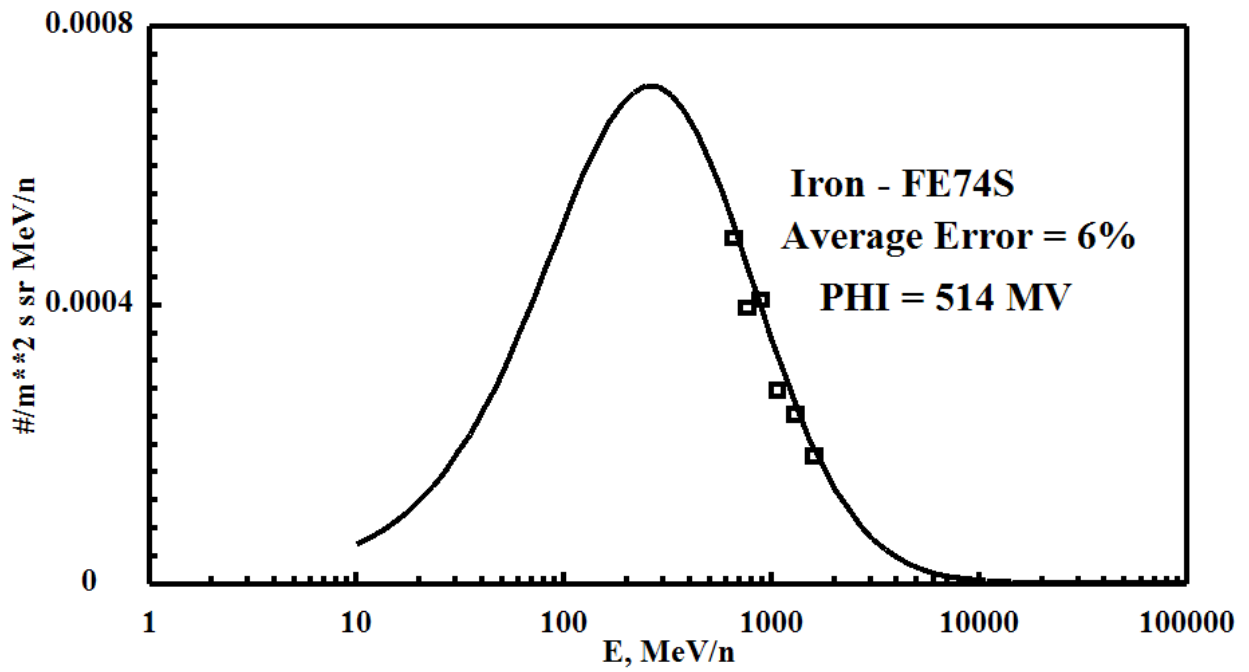
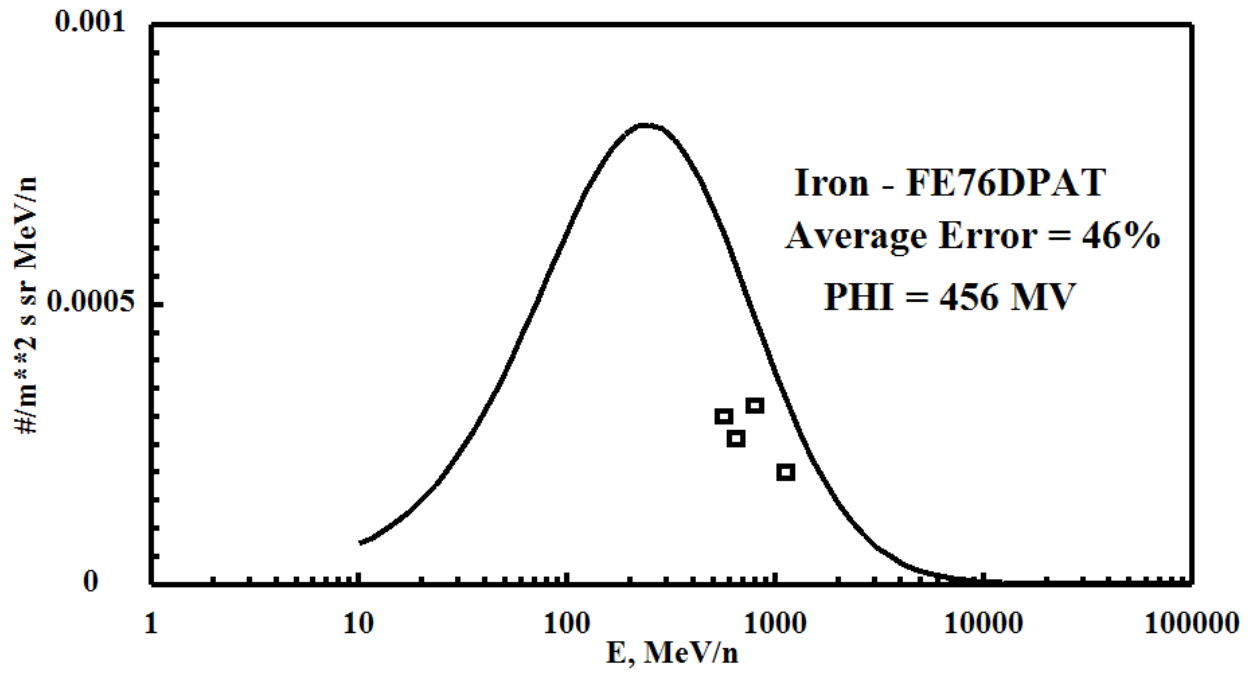


IRON - Low Energy, Solar Minimum

Files Used (Arbitrary 1's)

FILE	DATE	PHI (MV)	ERROR=ABS (FLUX-DATA)
Fe74LW3.dat	1974.553	515.0297	45.46681
Fe76DPAt.dat	1976.748	455.9699	46.30156
Fe74S.dat	1974.603	513.5059	6.138590
BO AVERAGE ERROR =			32.63565

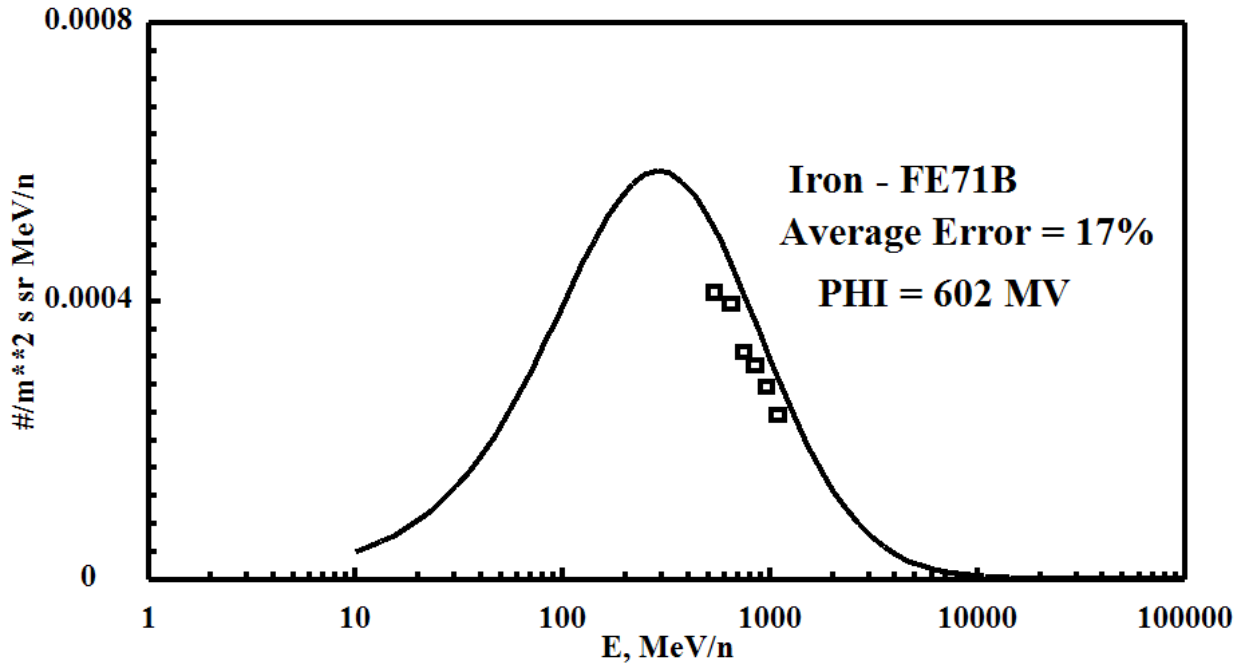




IRON - Low Energy, Solar Maximum

Files Used (Arbitrary 1's)

FILE	DATE	PHI (MV)	ERROR=ABS (FLUX-DATA)
Fe71B.dat	1971.756	601.9181	16.74504
BO AVERAGE ERROR =			16.74504

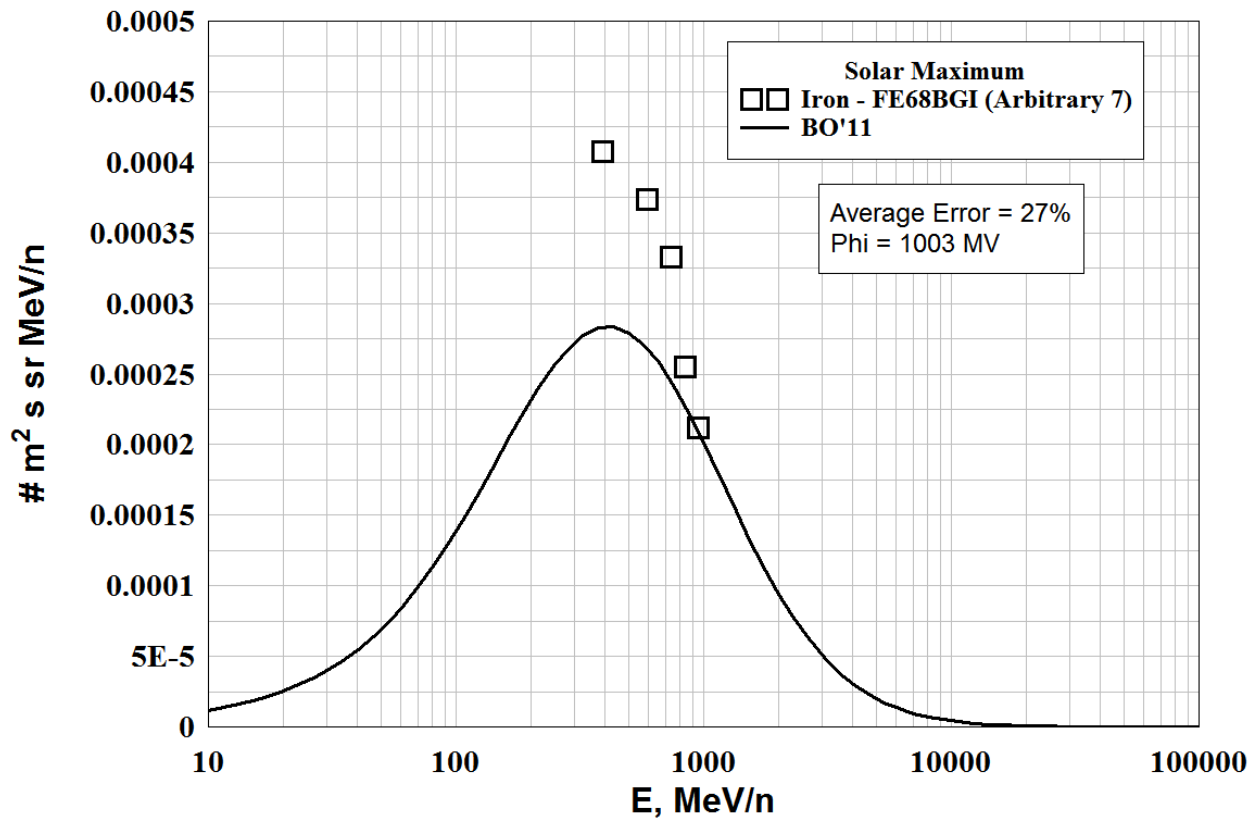
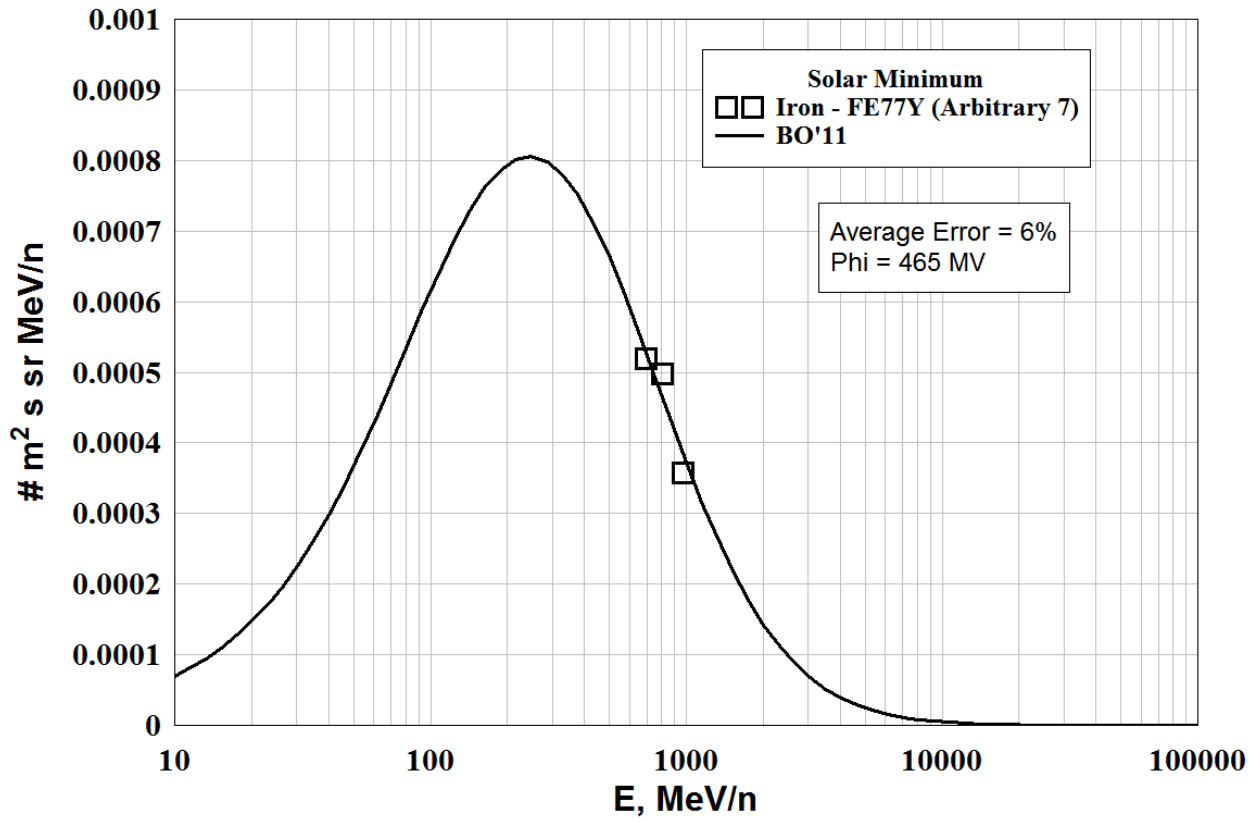


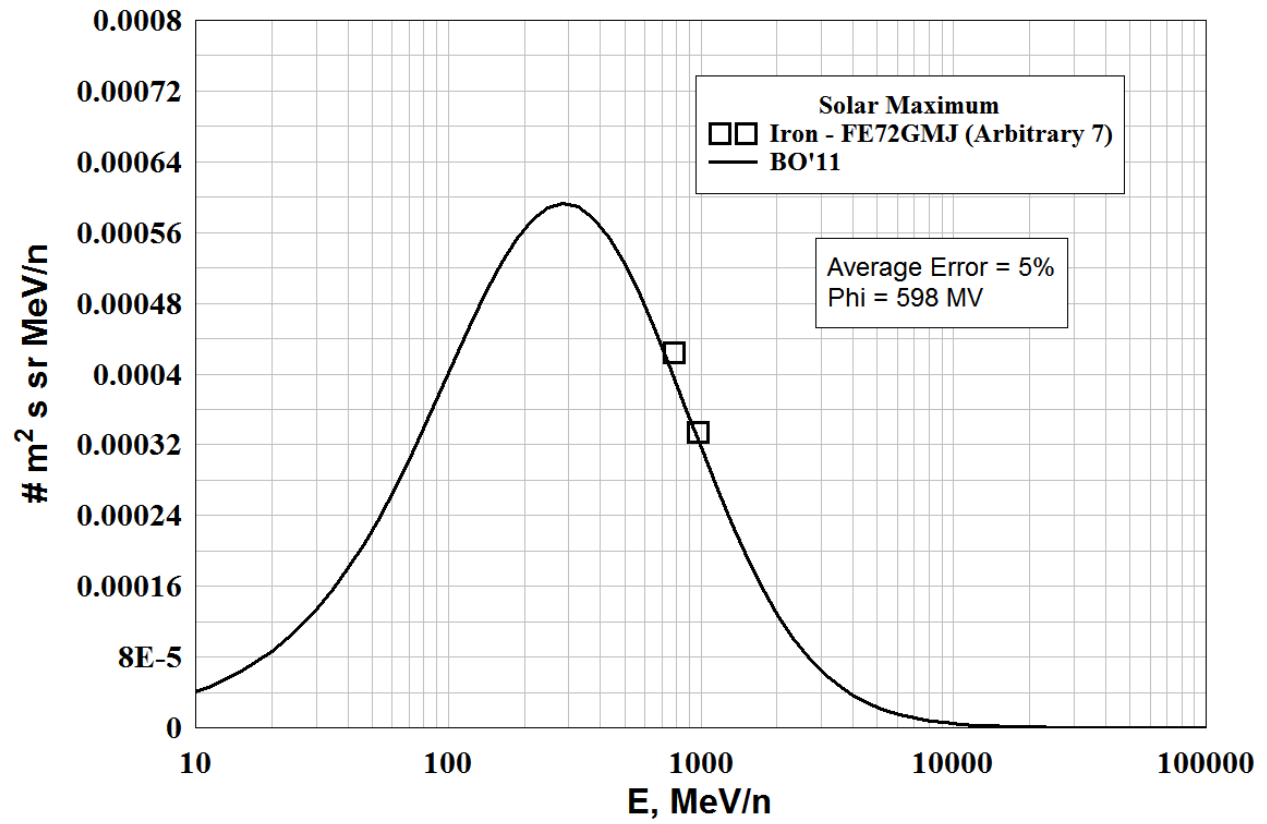
Files Rejected - (Arbitrary 7's)

FILE	DATE	PHI (MV)	ERROR=ABS (FLUX-DATA)
Fe77Y.dat	1977.500	464.6233	5.698211
BO AVERAGE ERROR =			5.698211

Files Rejected - (Arbitrary 7's)

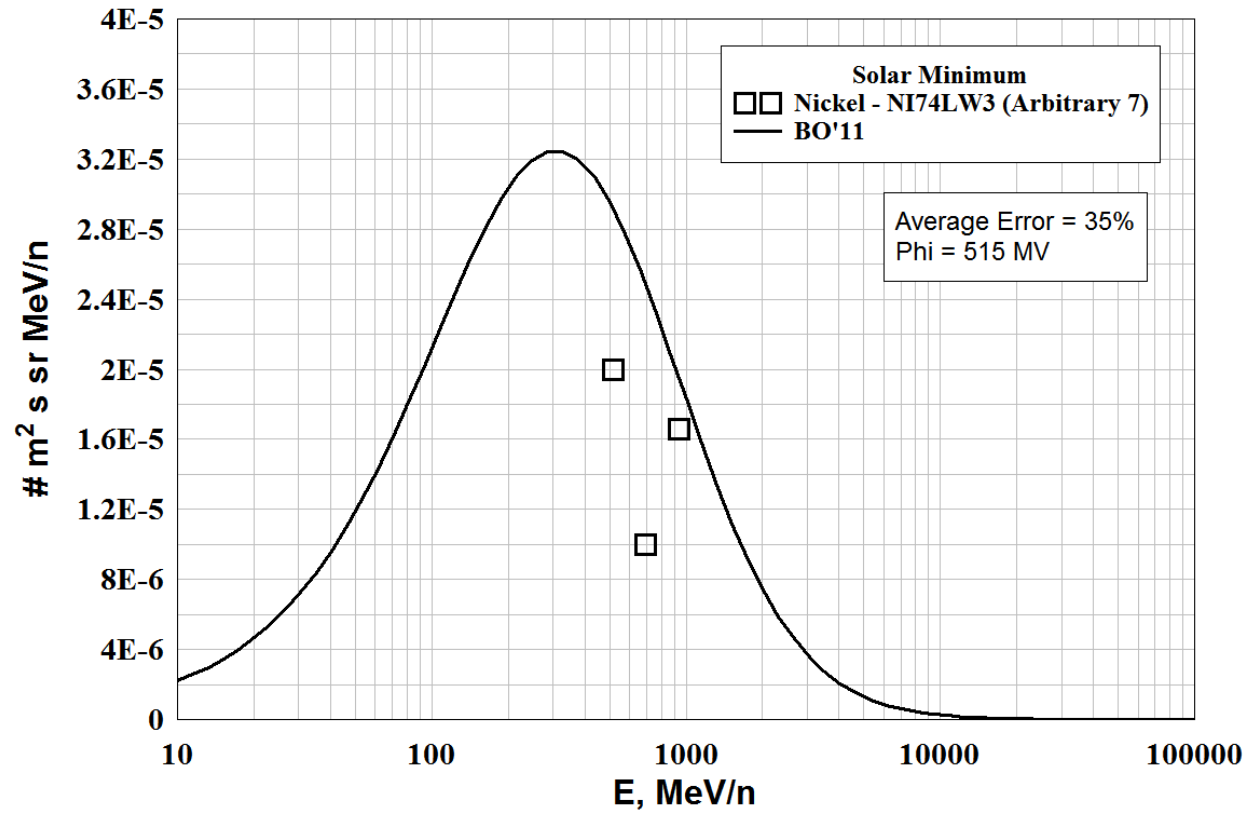
FILE	DATE	PHI (MV)	ERROR=ABS (FLUX-DATA)
Fe68BGI.dat	1968.707	1002.739	26.71205
Fe72GMJ.dat	1972.668	598.2584	5.029116
BO AVERAGE ERROR =			15.87058





COBALT LOW ENERGY DATA - NONE

NICKEL LOW ENERGY DATA



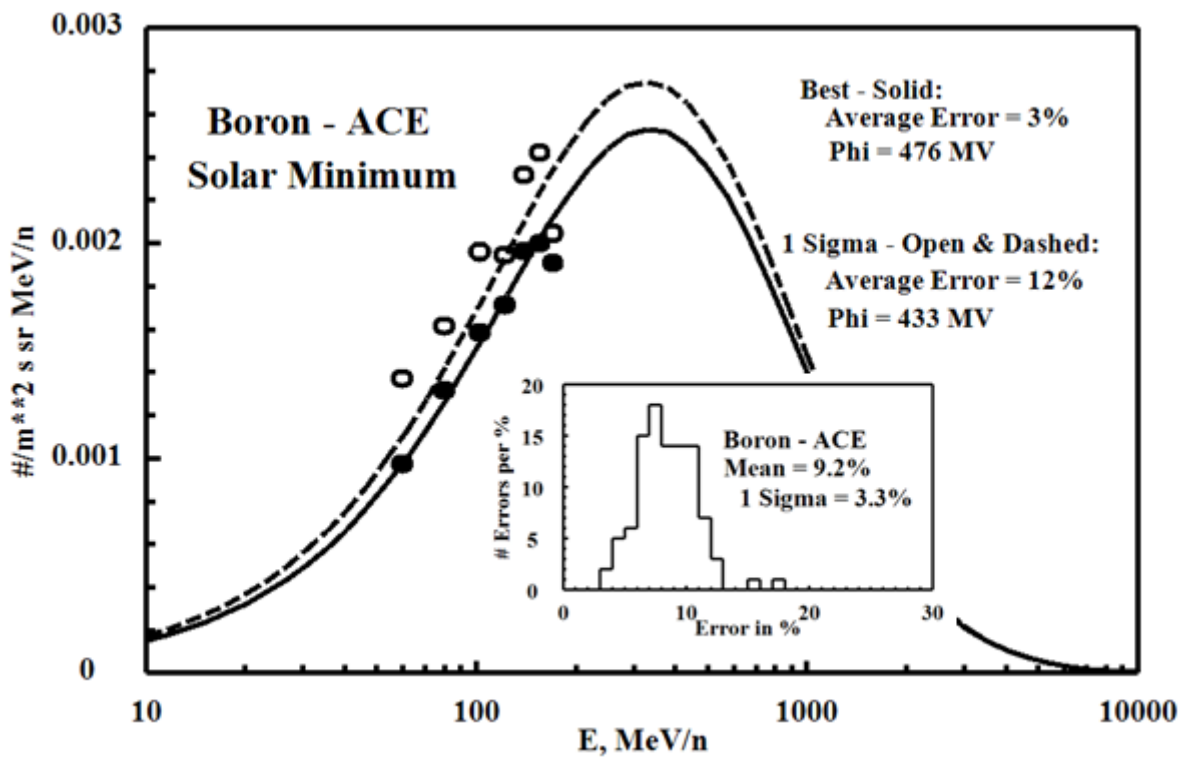
Appendix E: Low Energy ACE Spectra for Solar Minimum and Maximum Periods

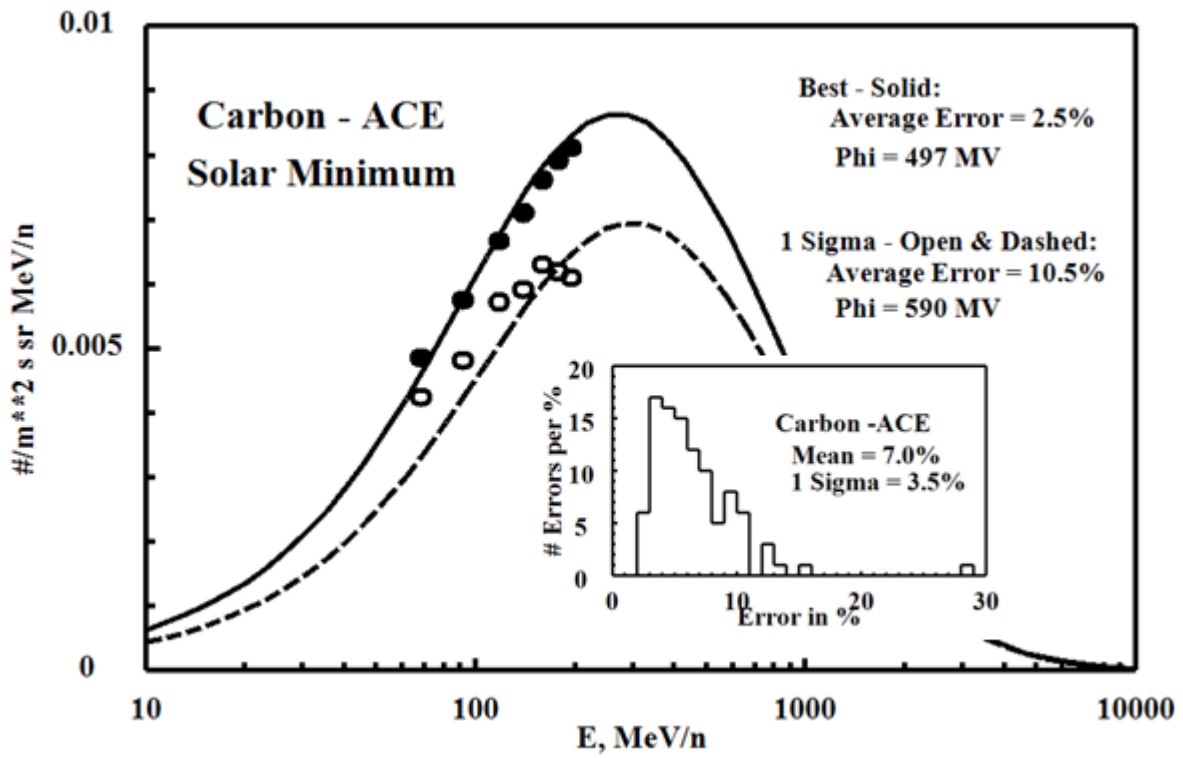
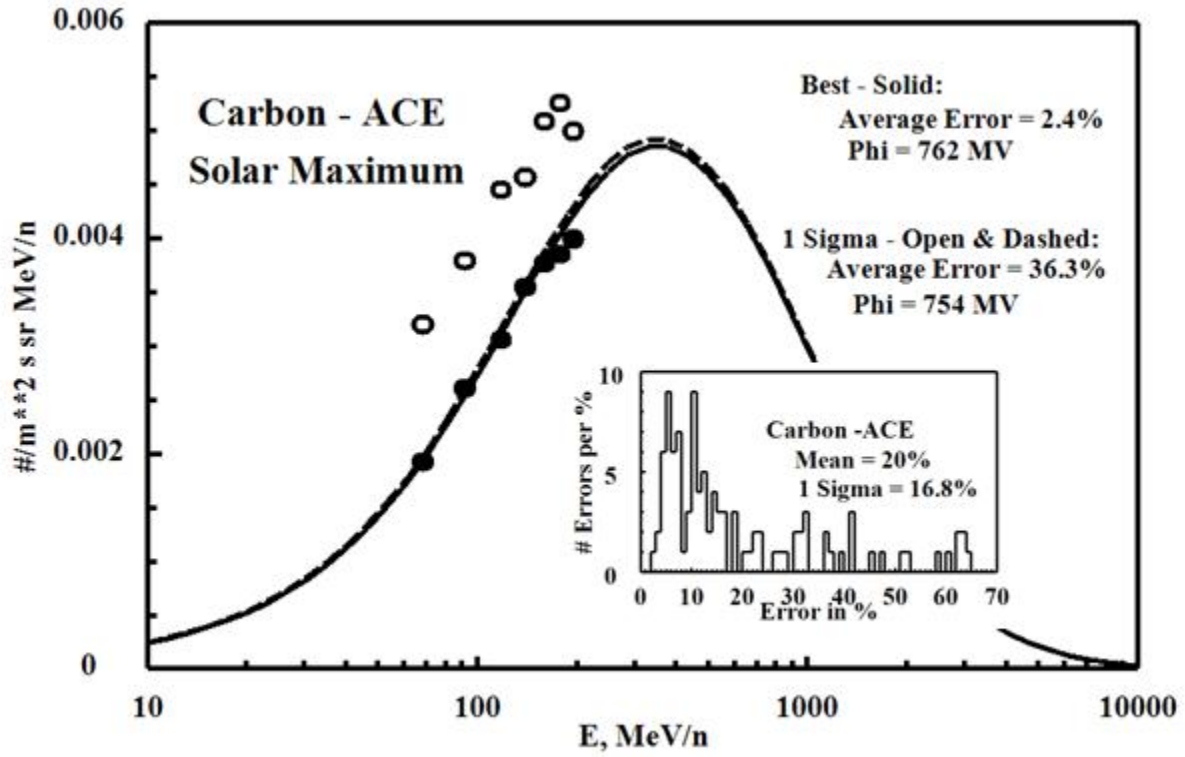
Solid Line = BO'11 Model for
"BEST" ACE Measurements (solid circles)

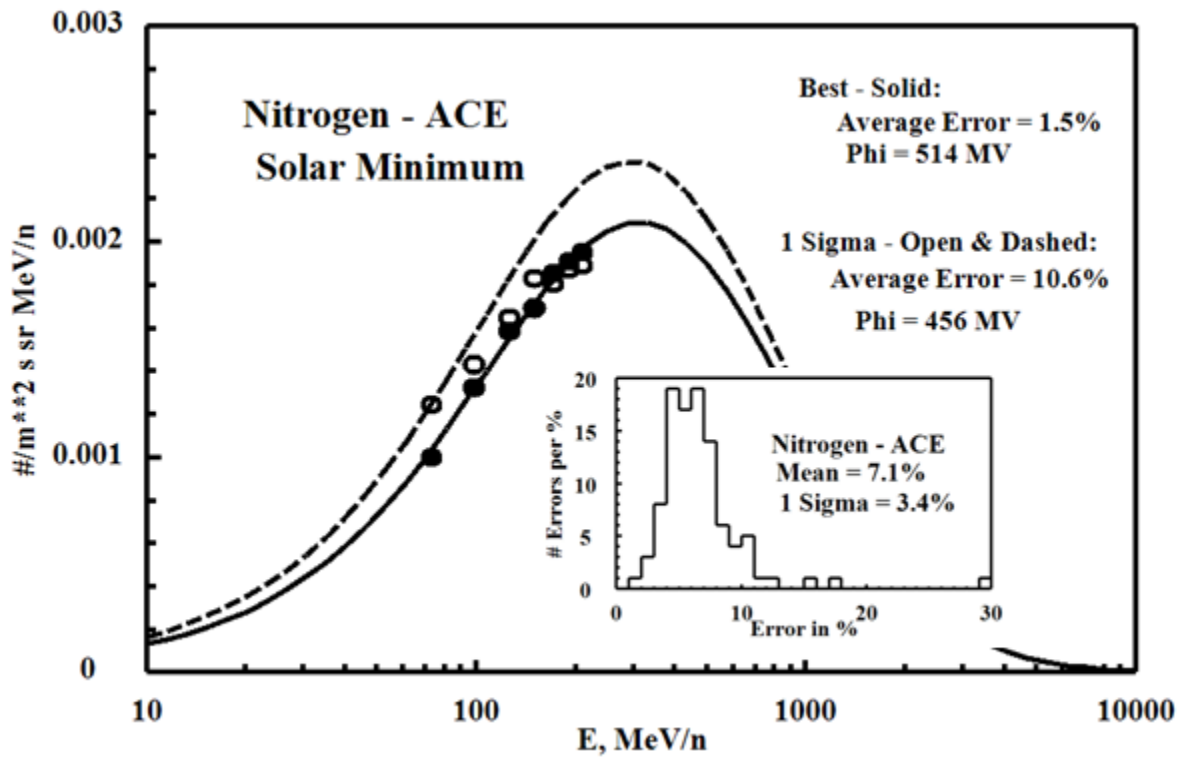
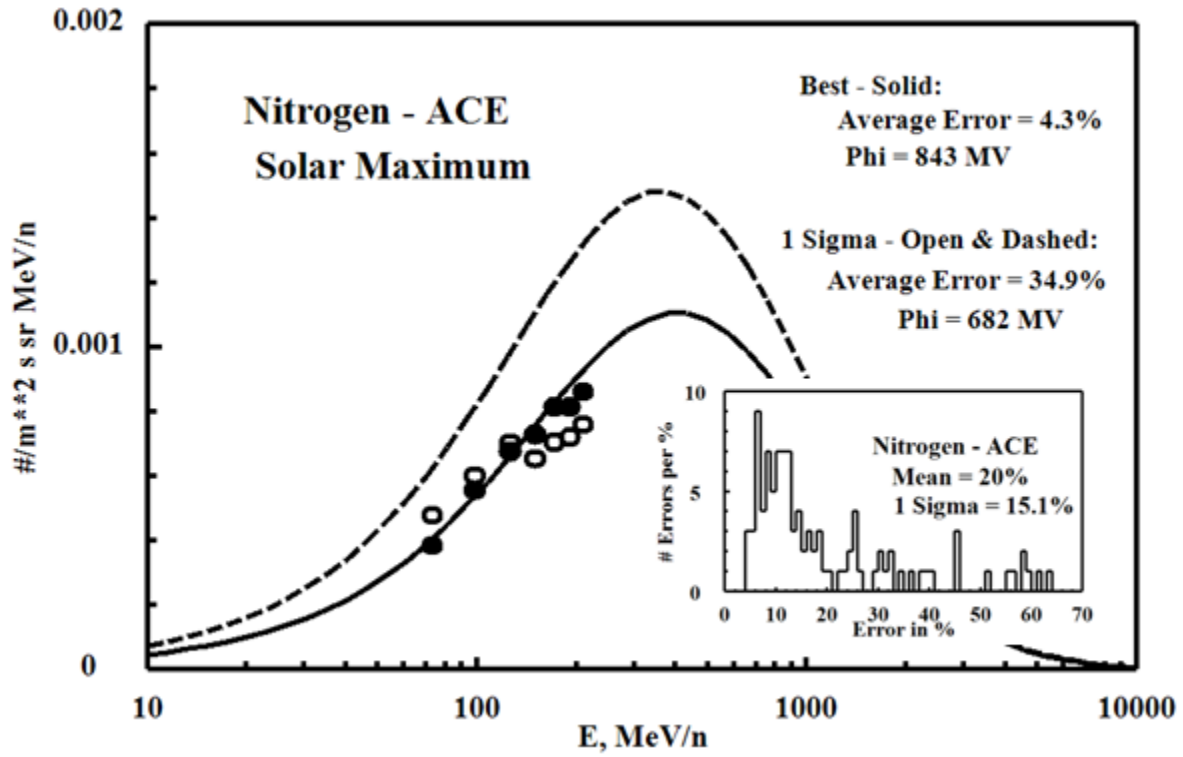
Dashed Line = BO'11 Model for
"1 sigma" ACE Measurements (open circles)

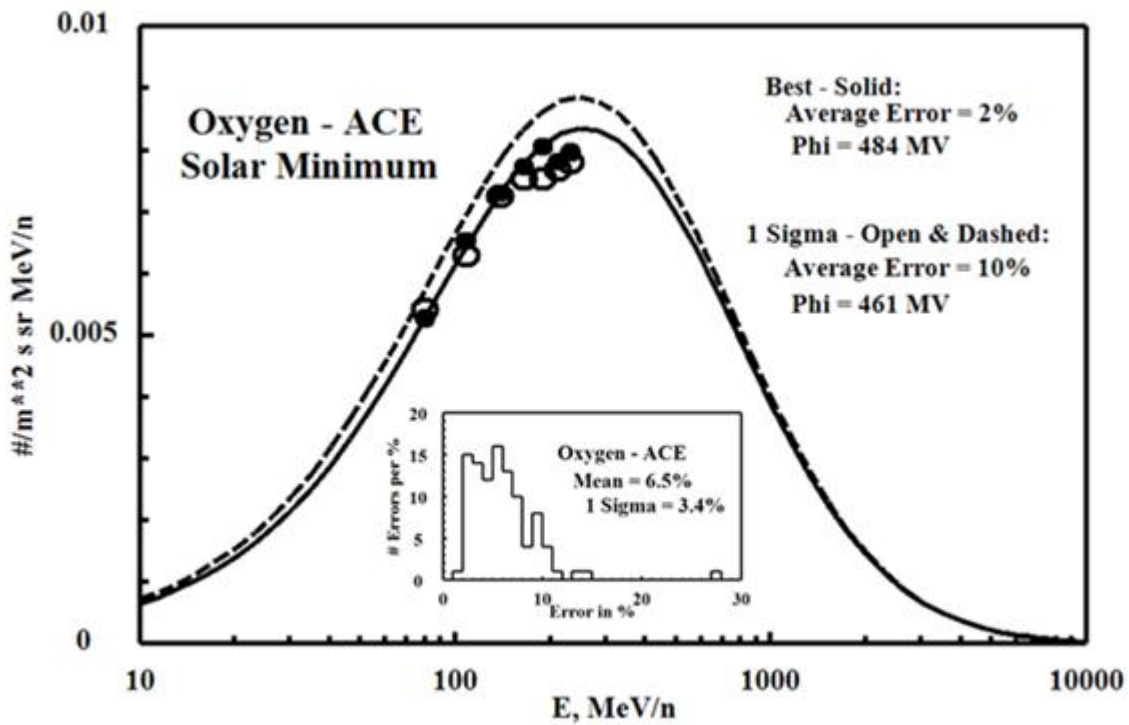
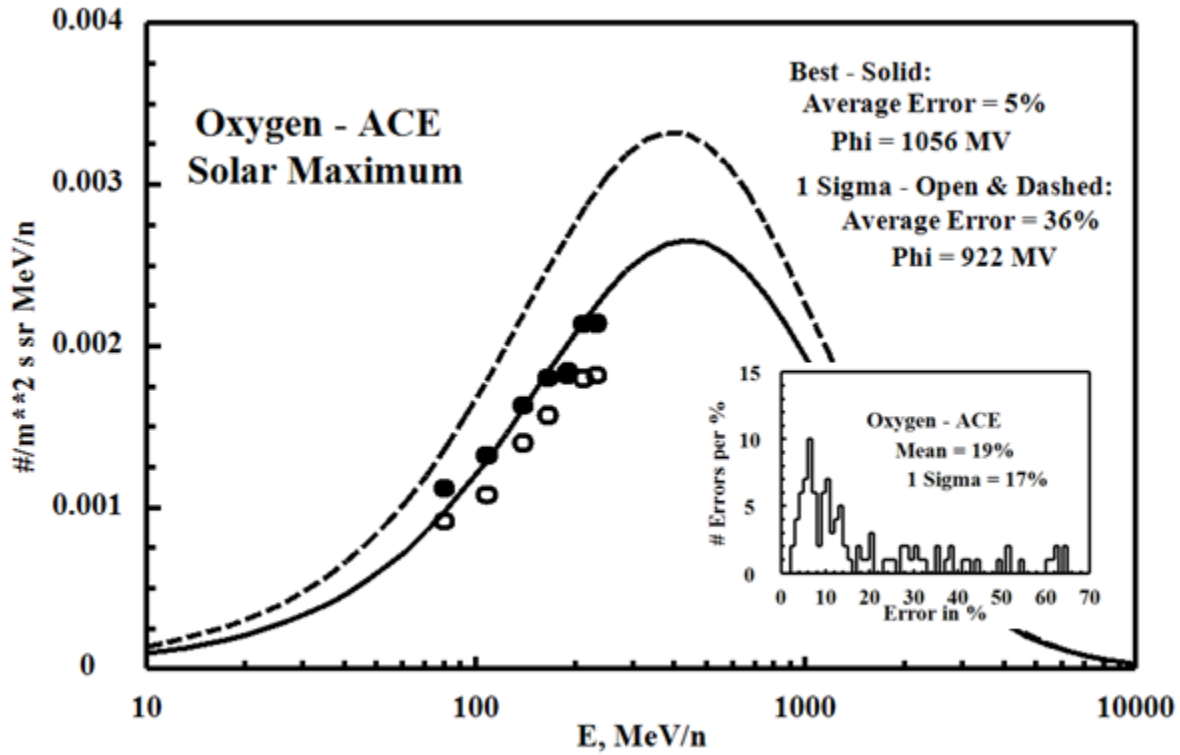
Inset shows distribution of errors based on all ACE measurements made between 1997 and present.

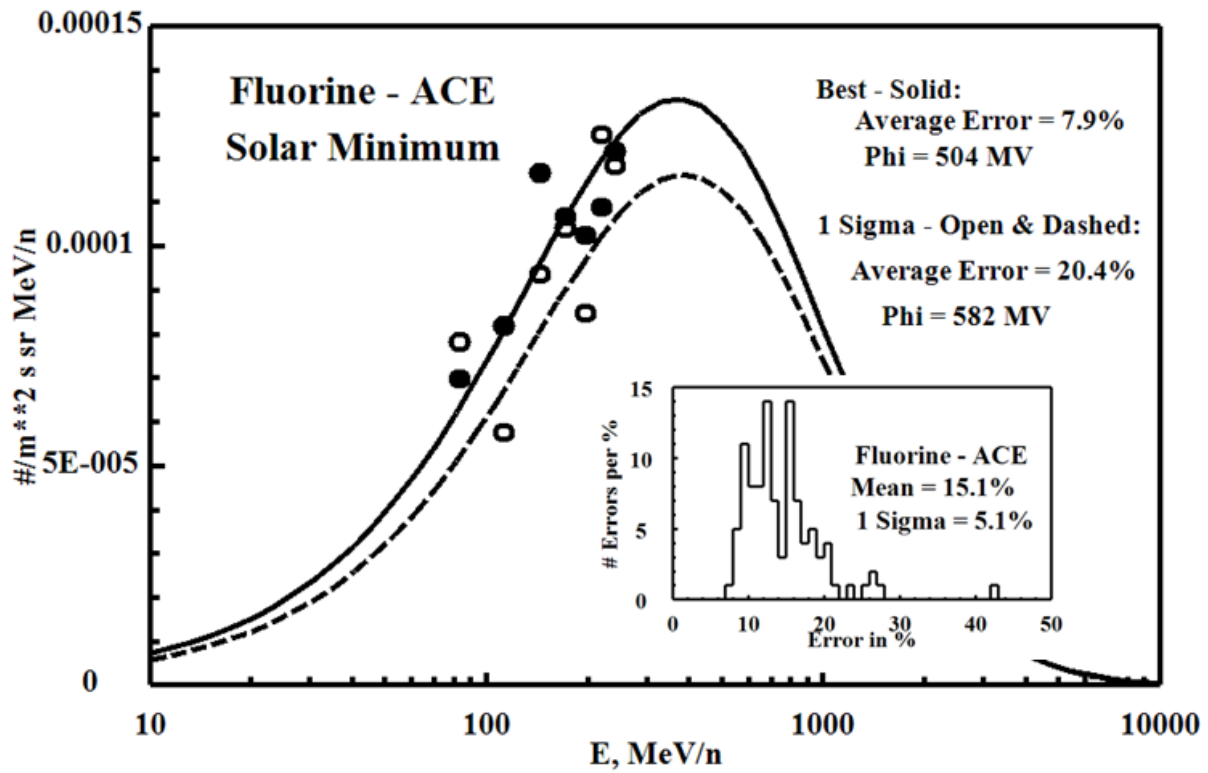
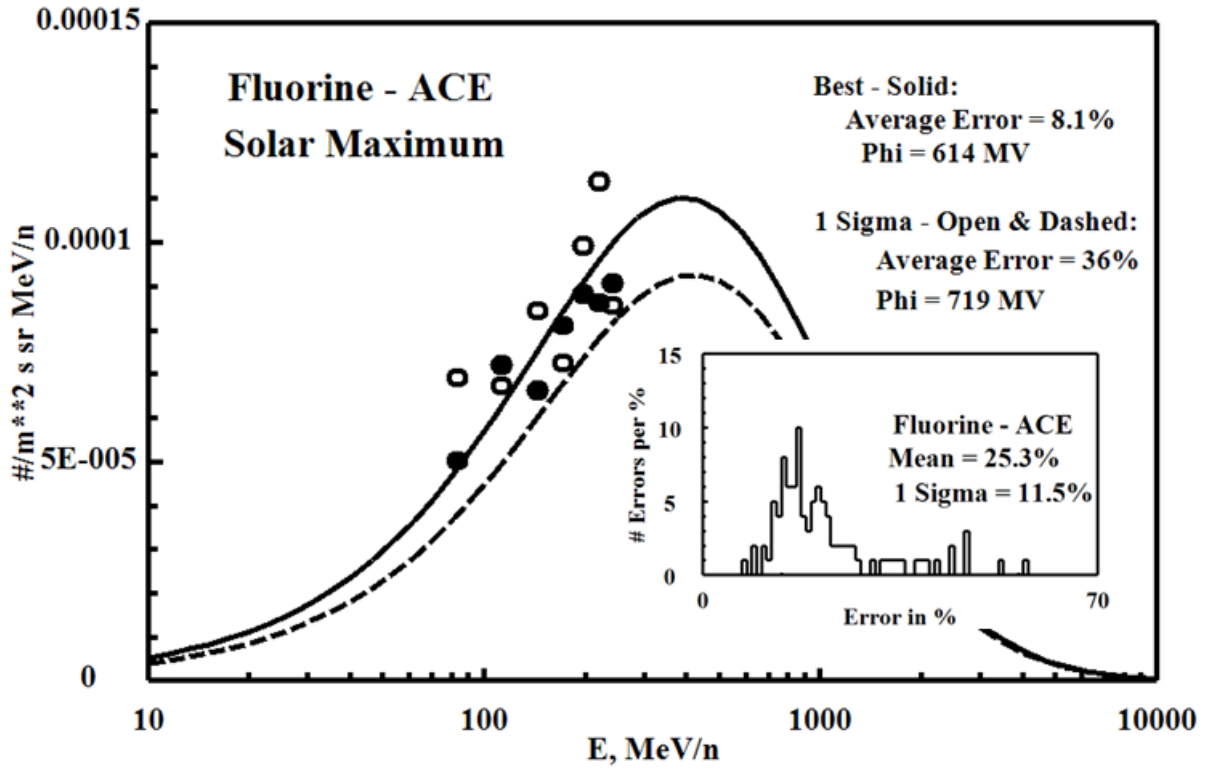
Note that all of fits essentially (84%) lie below the "1 sigma" error fit.

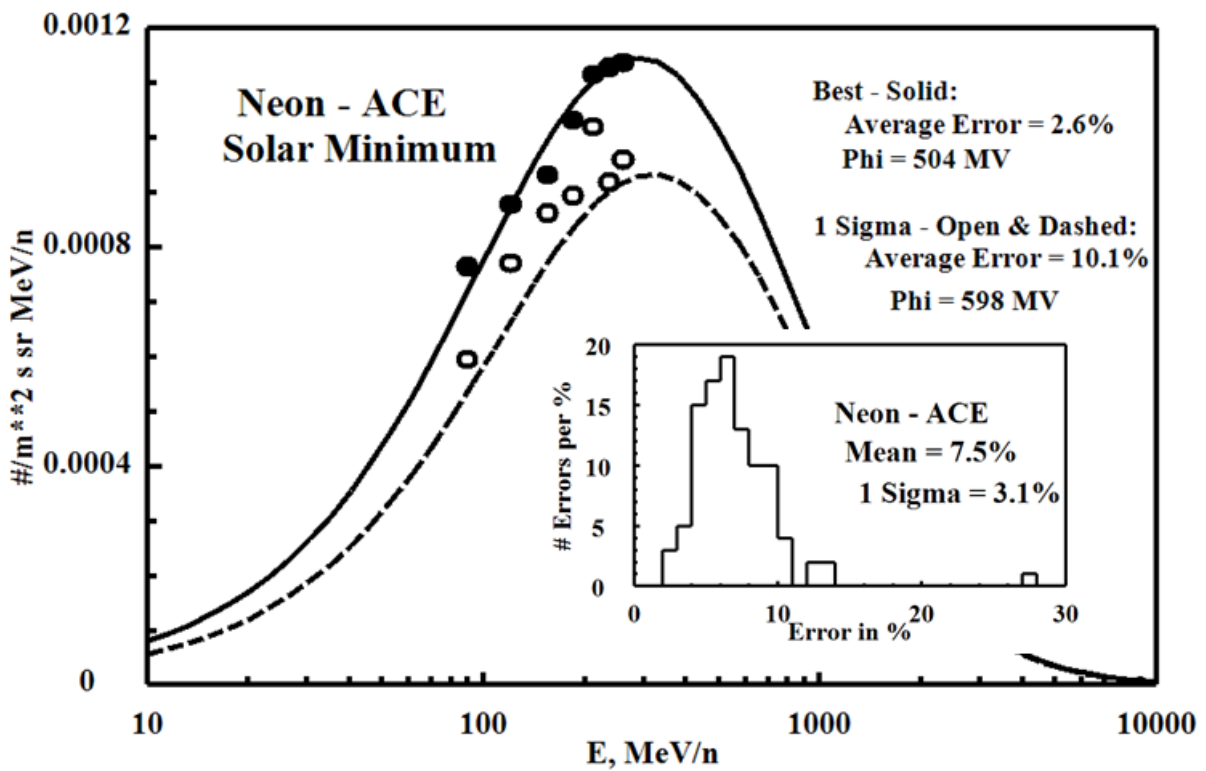
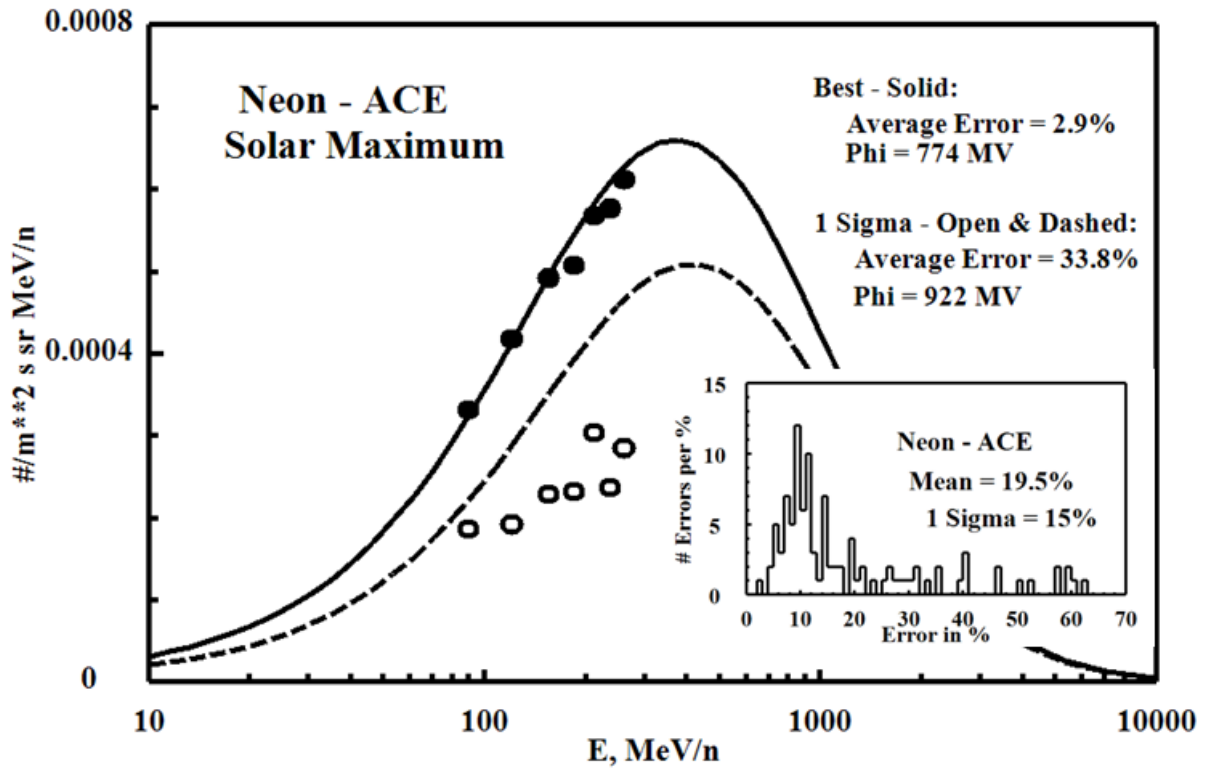


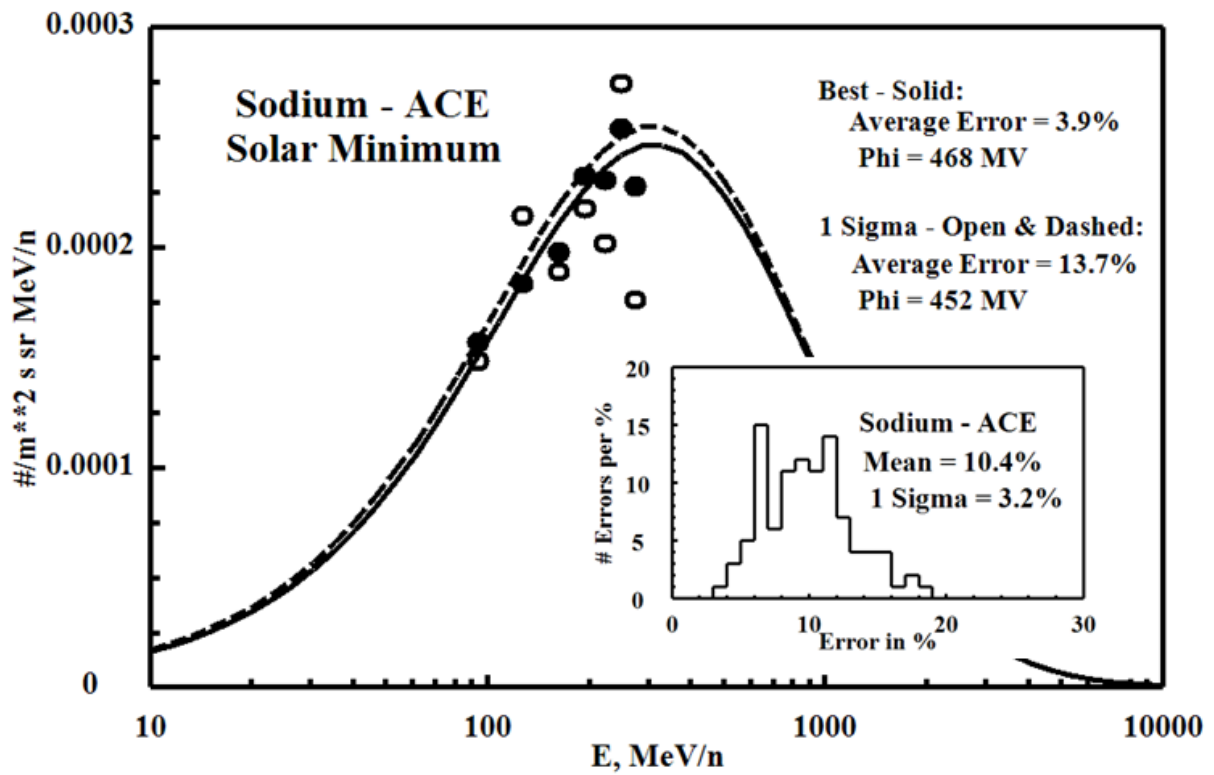
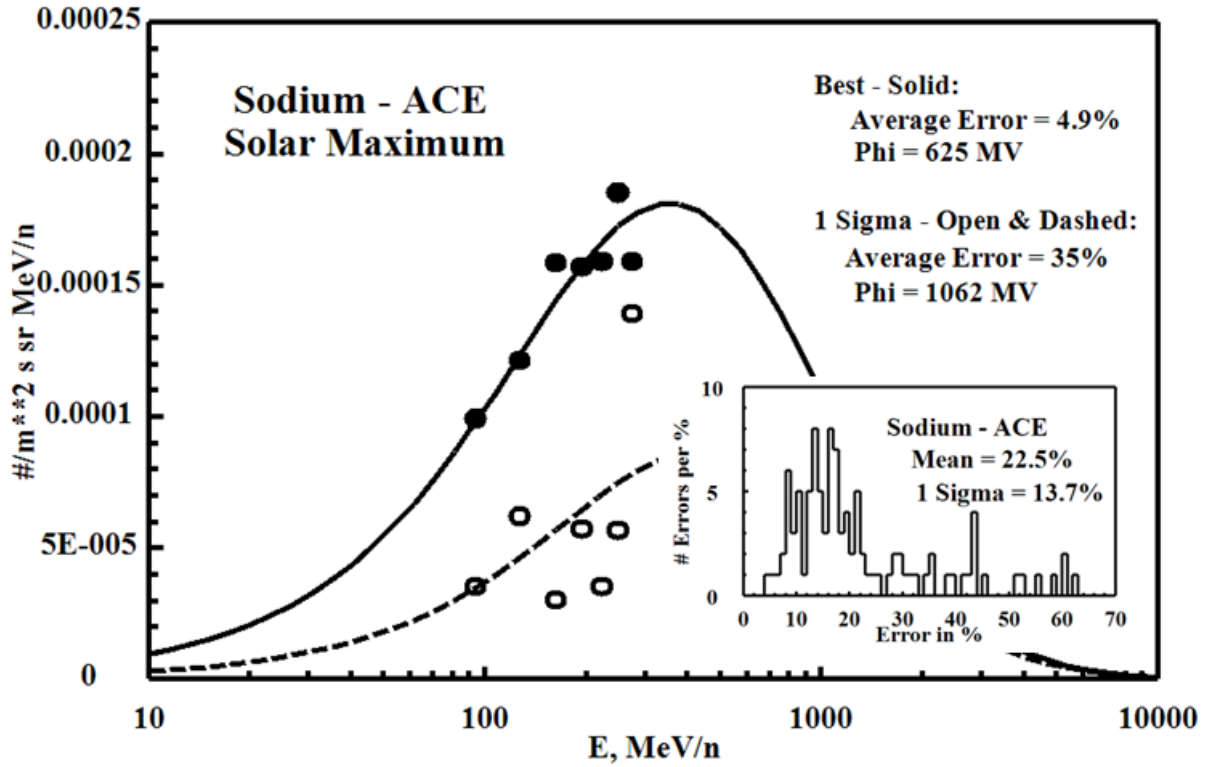


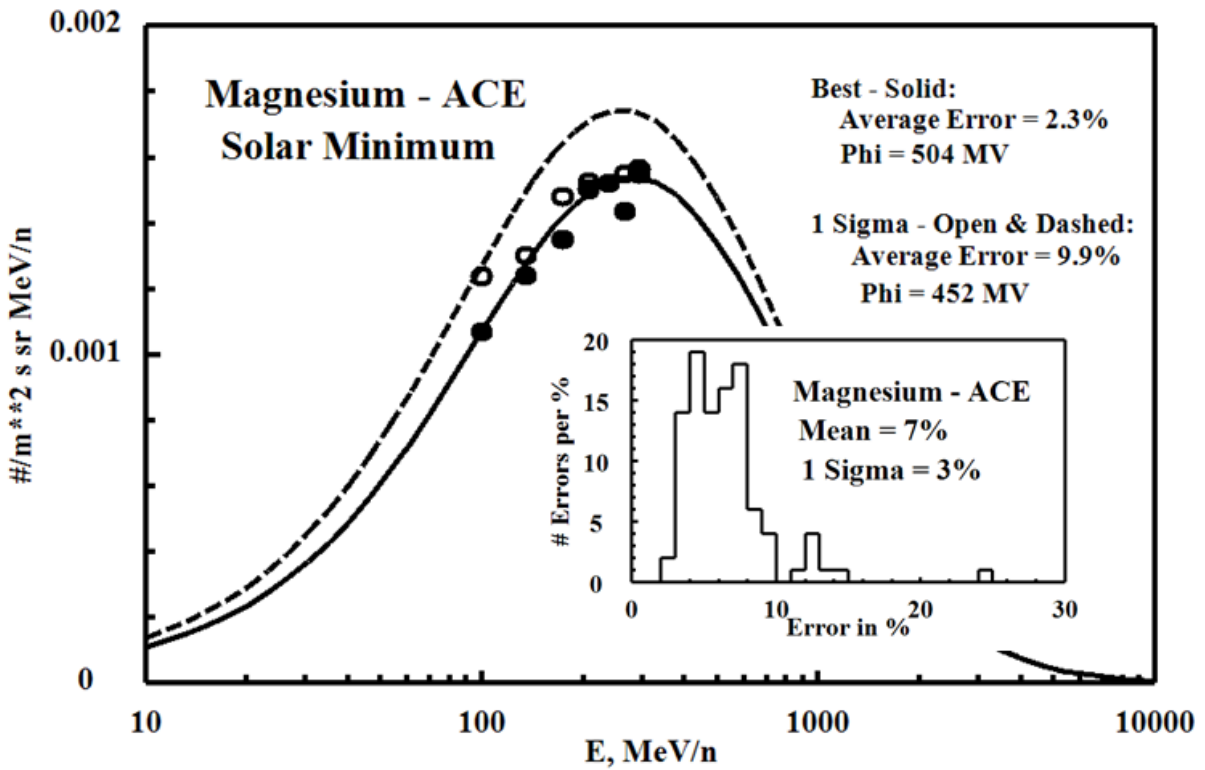
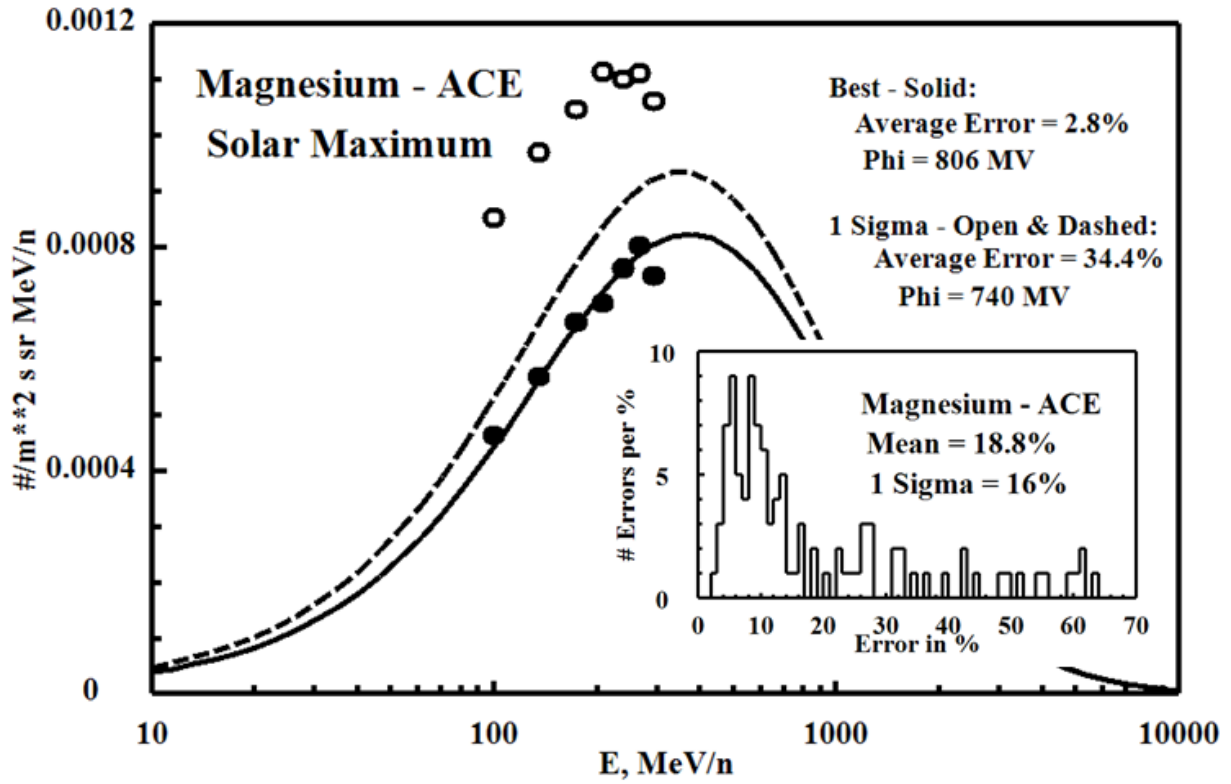


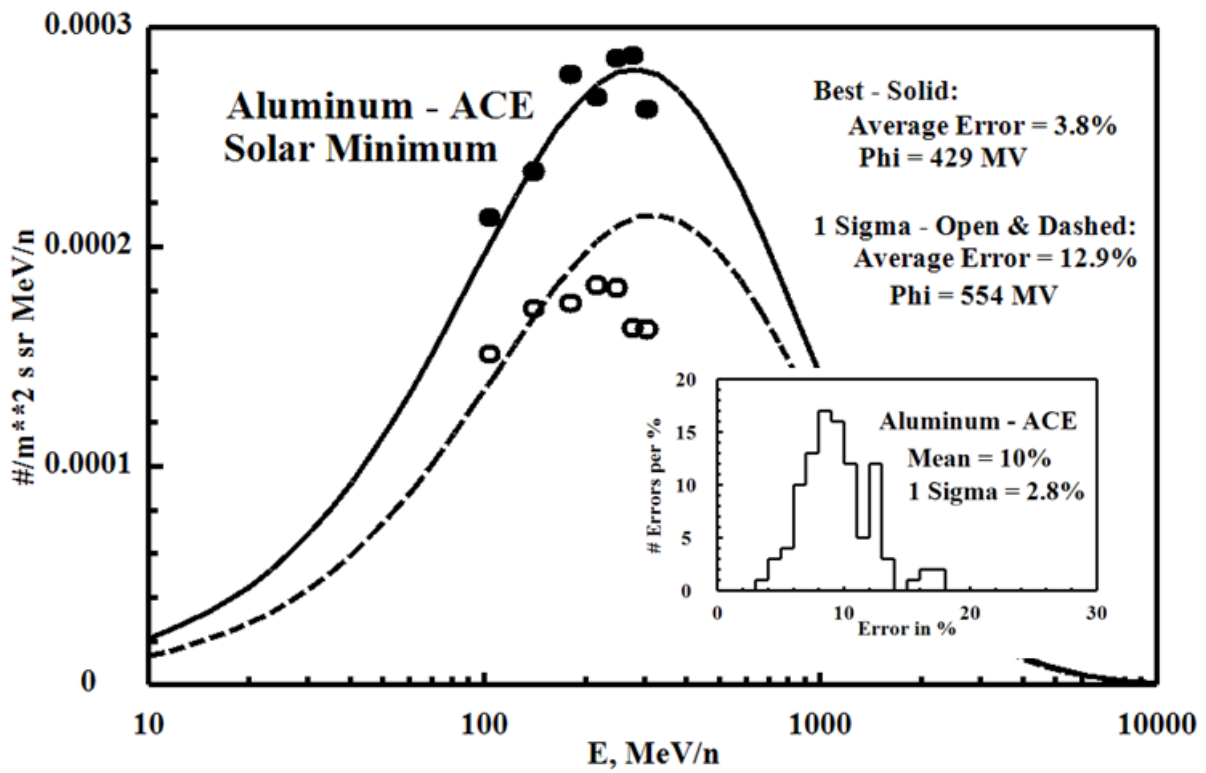
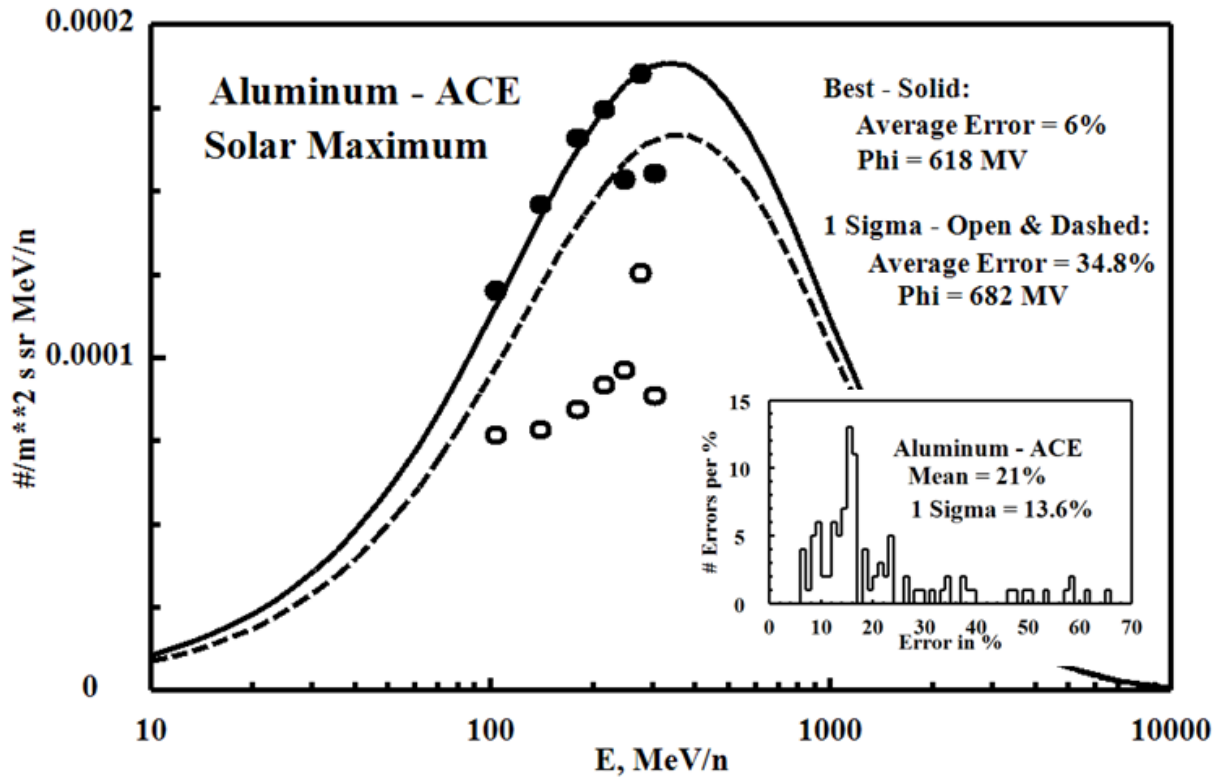


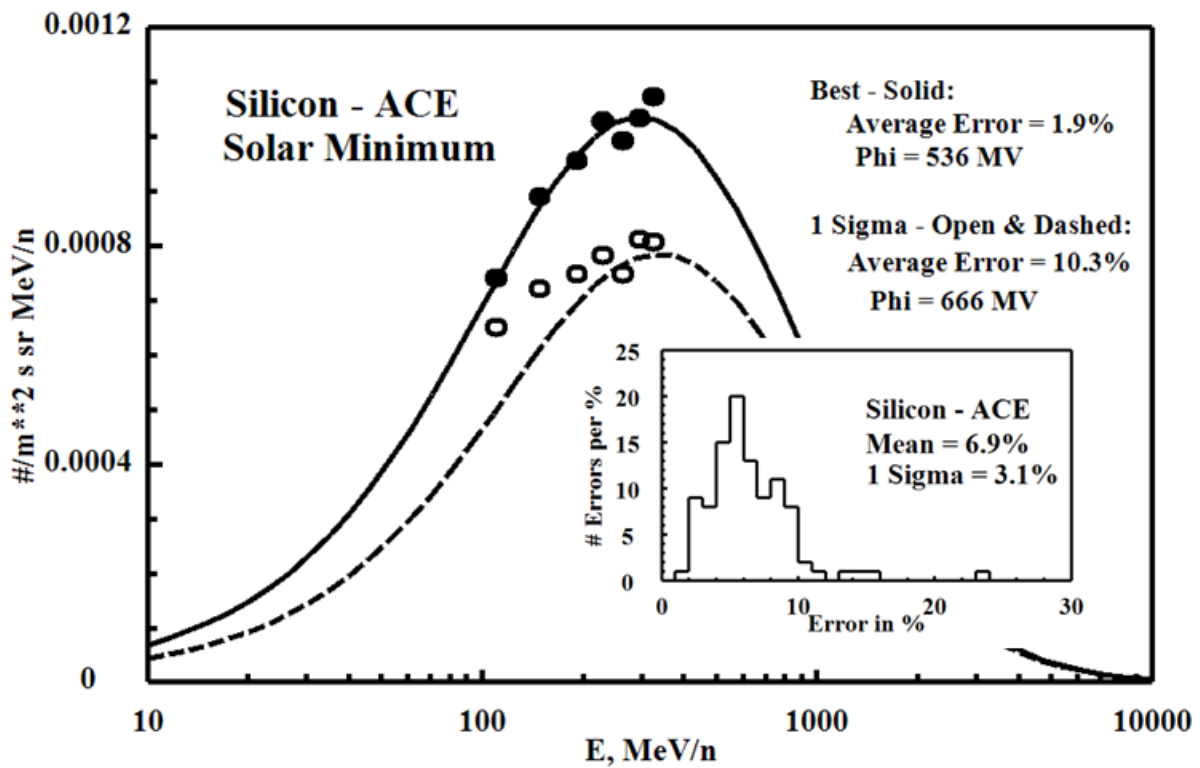
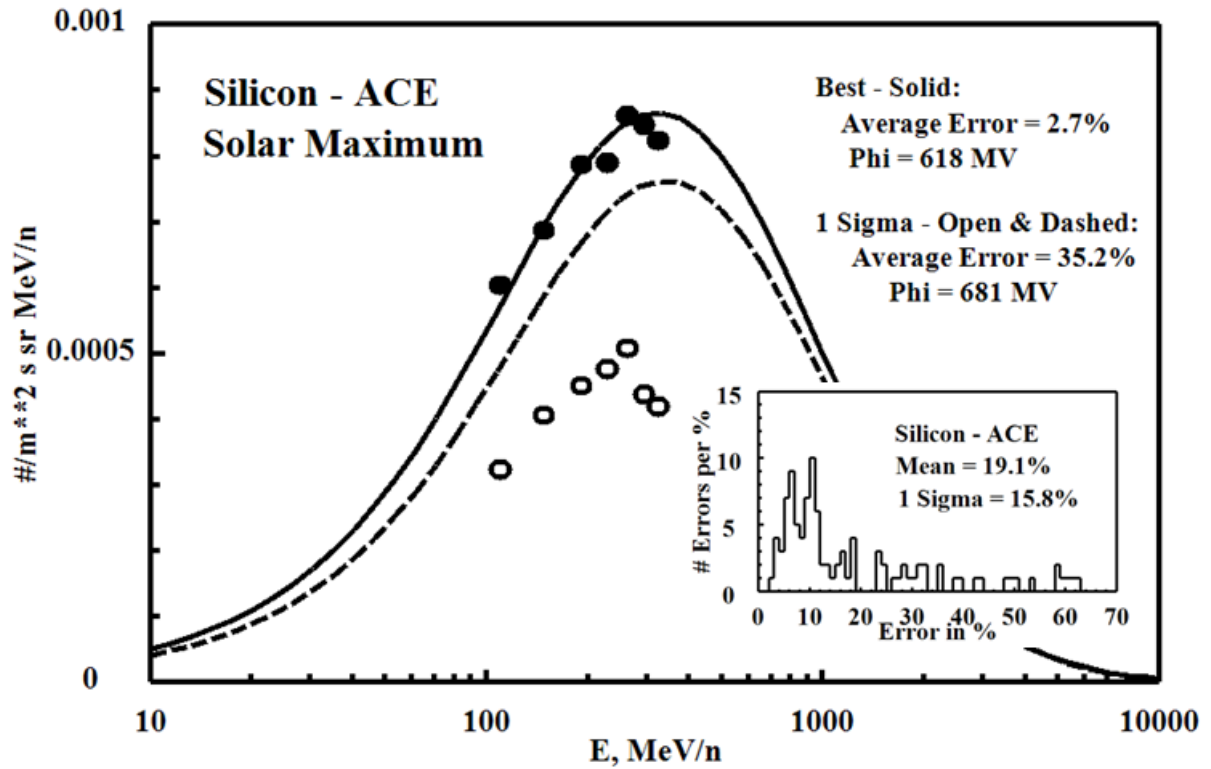


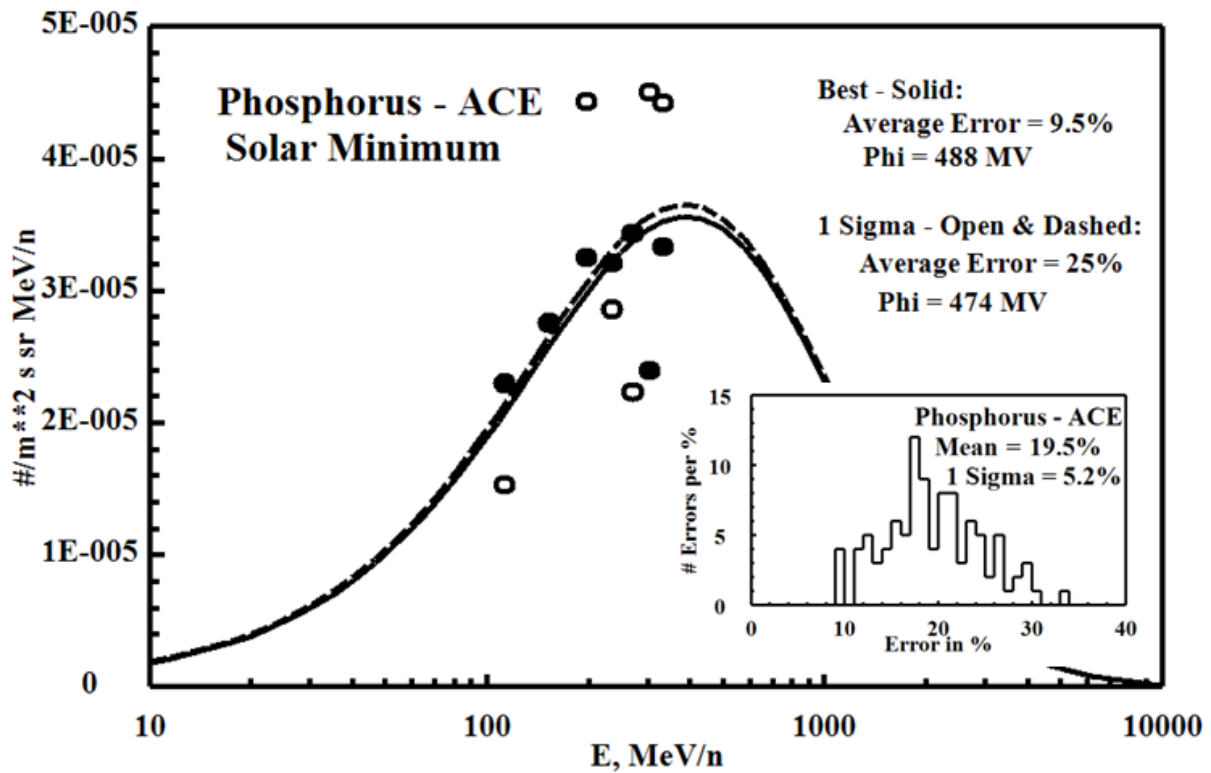
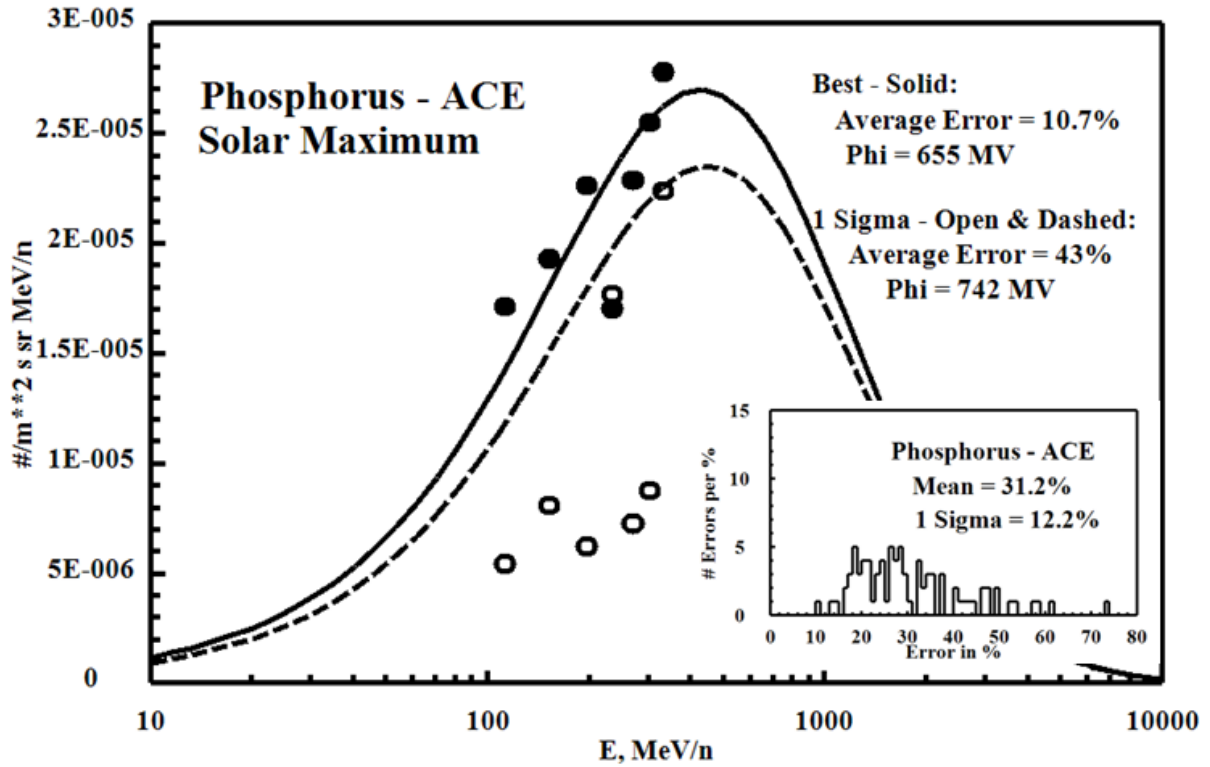


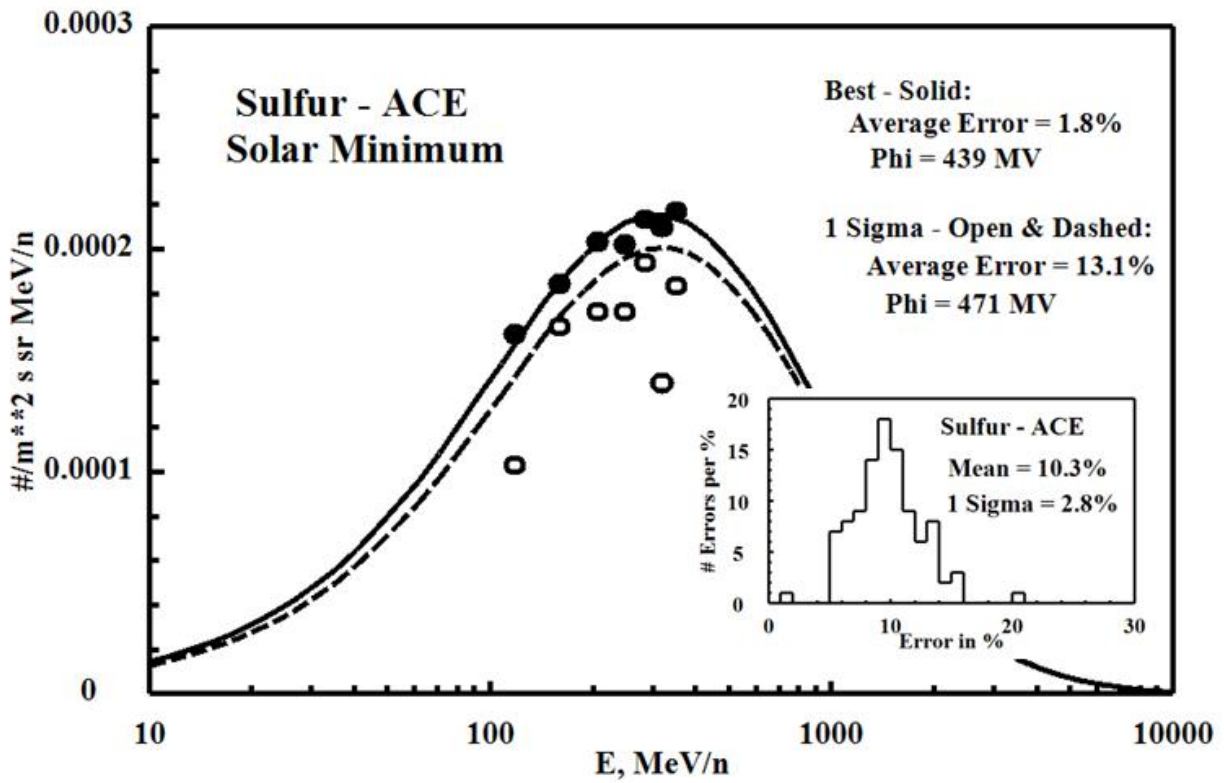
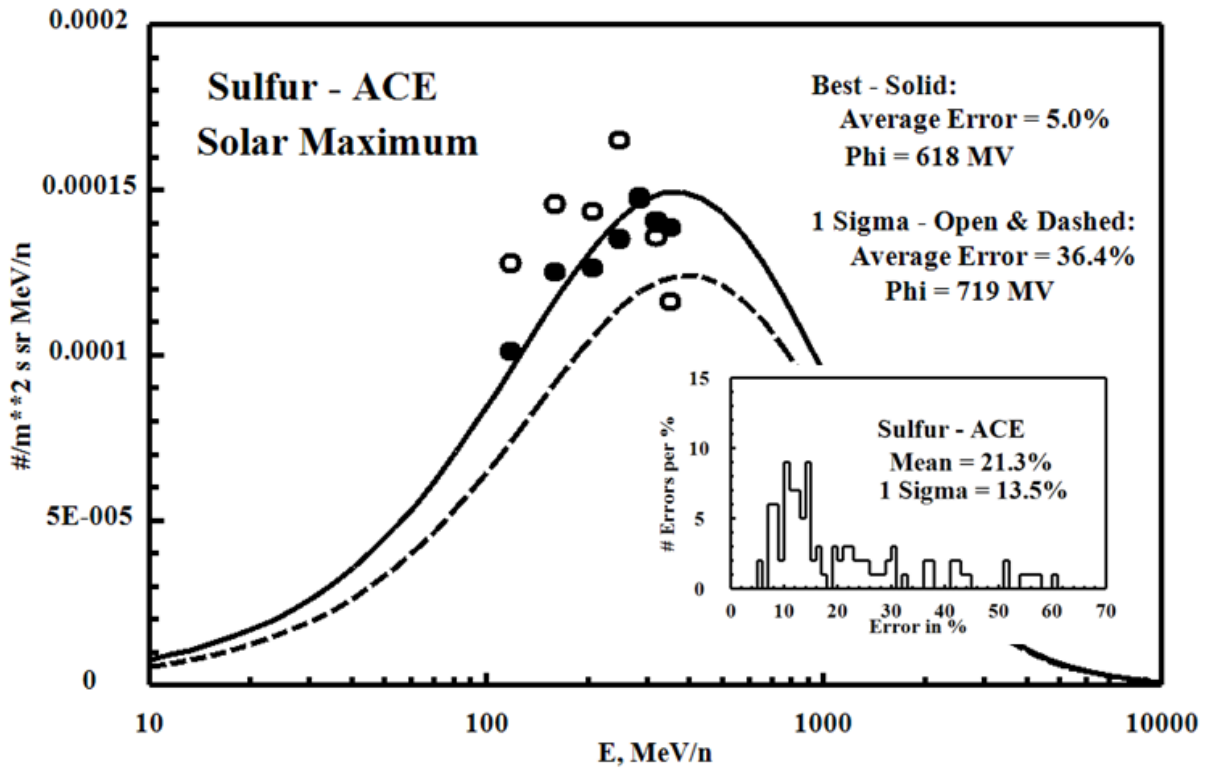


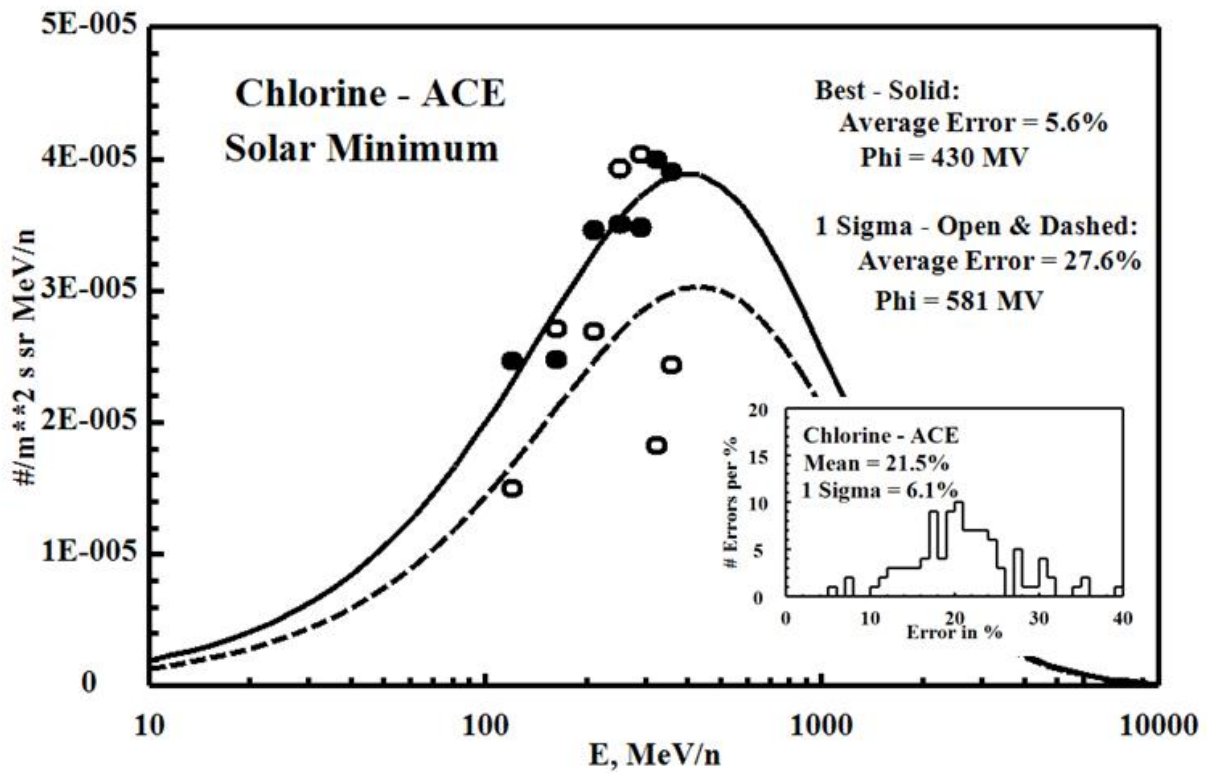
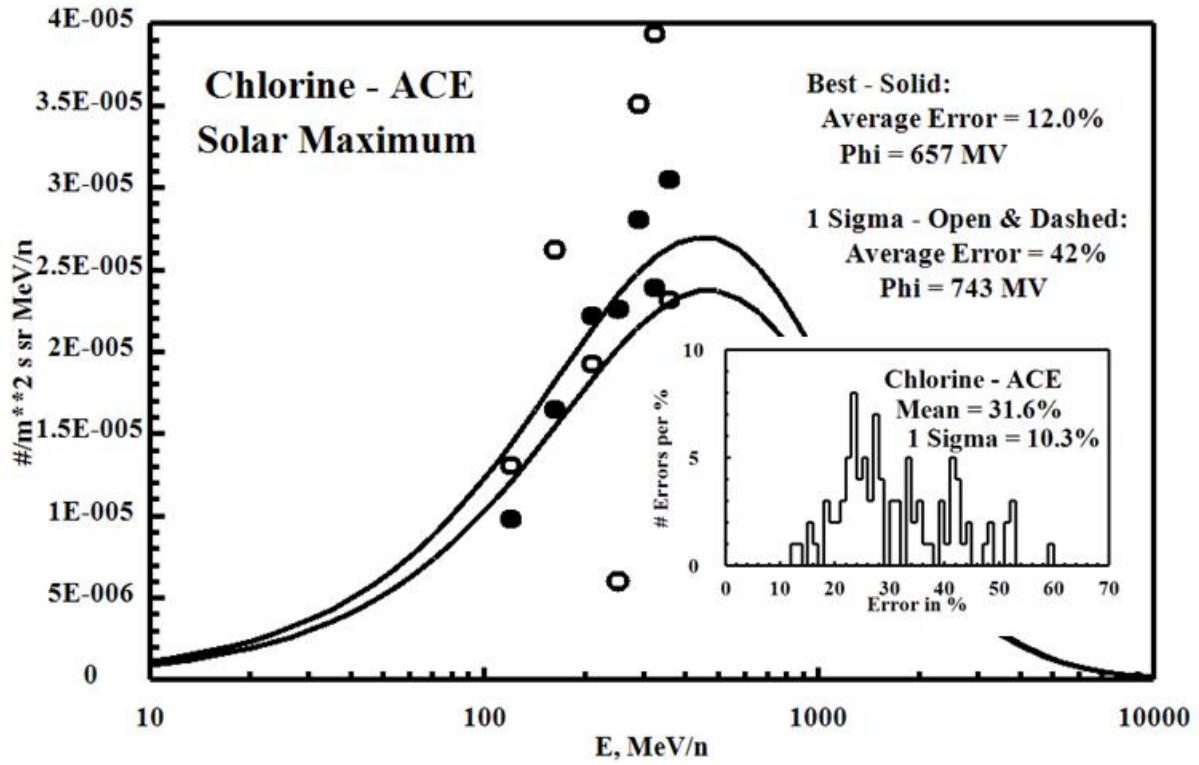


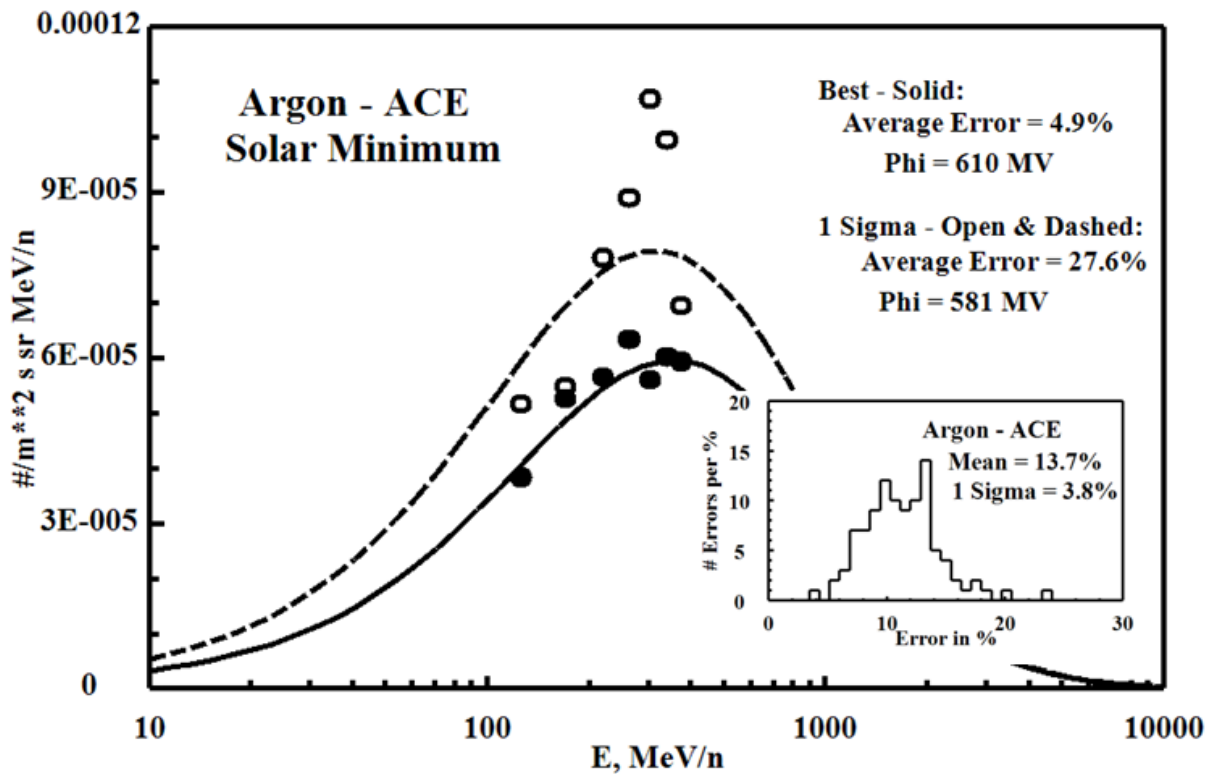
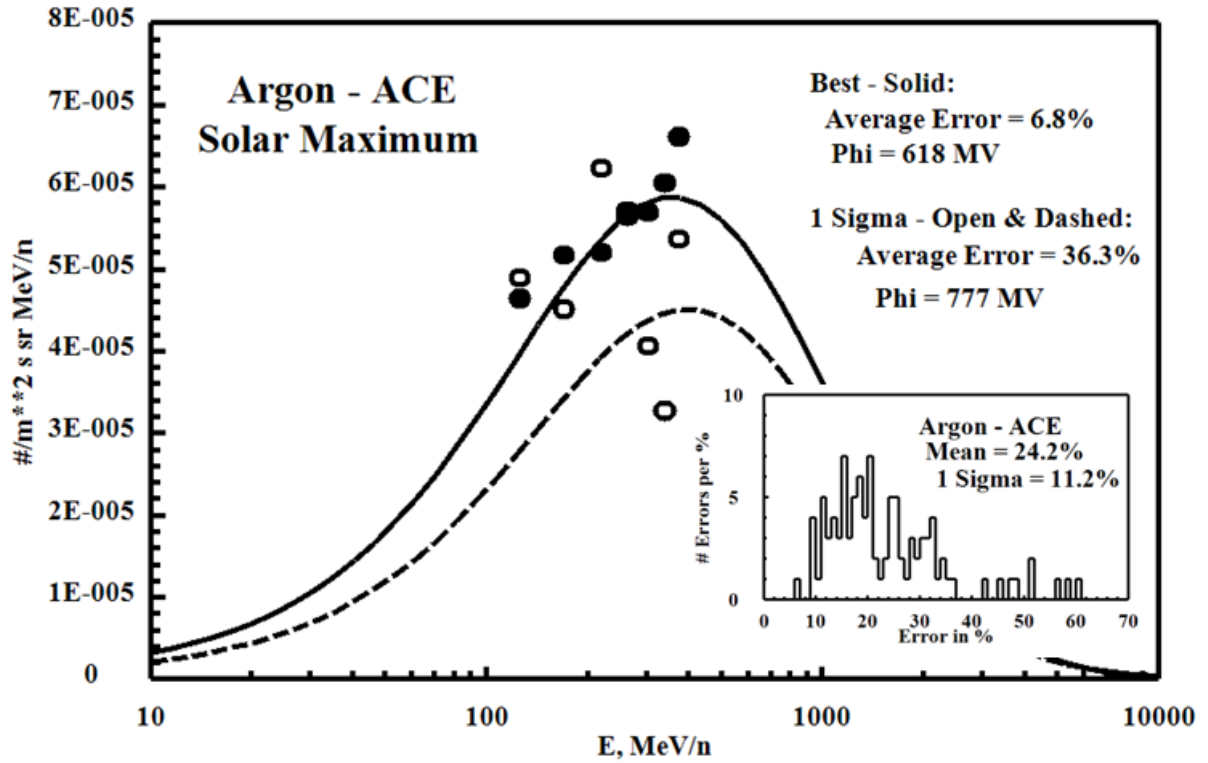


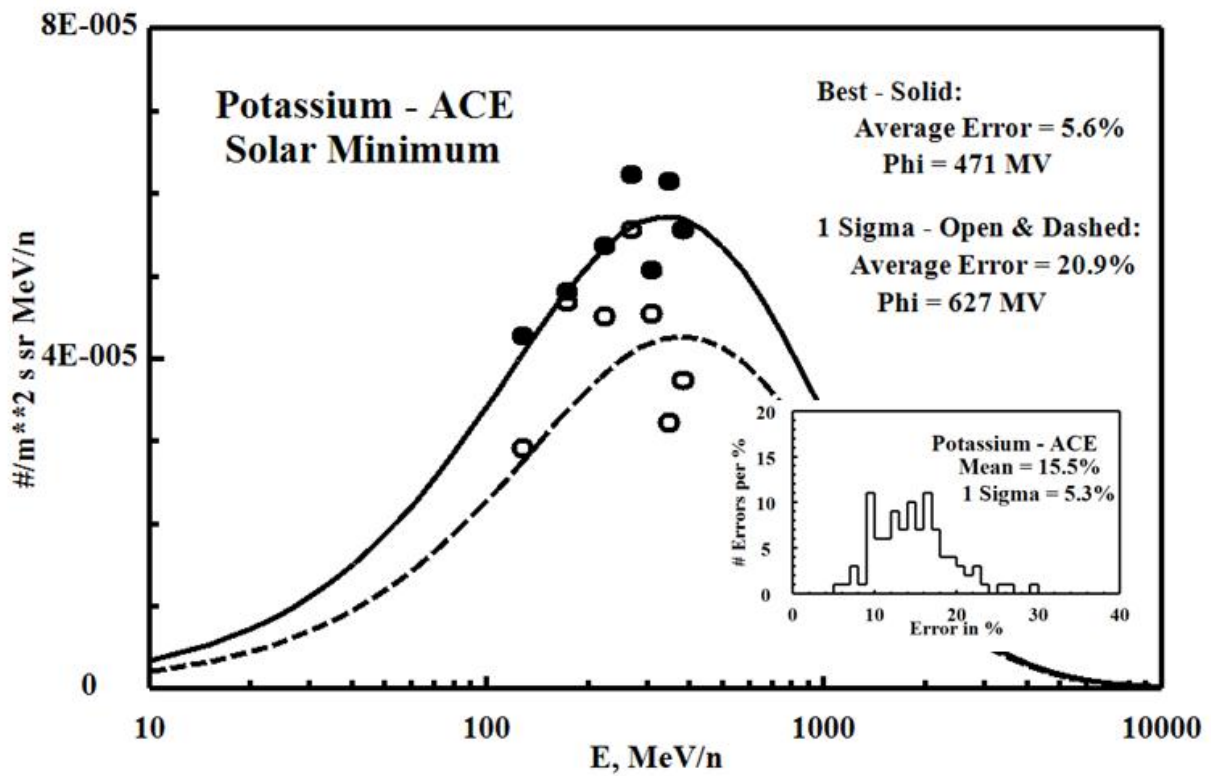
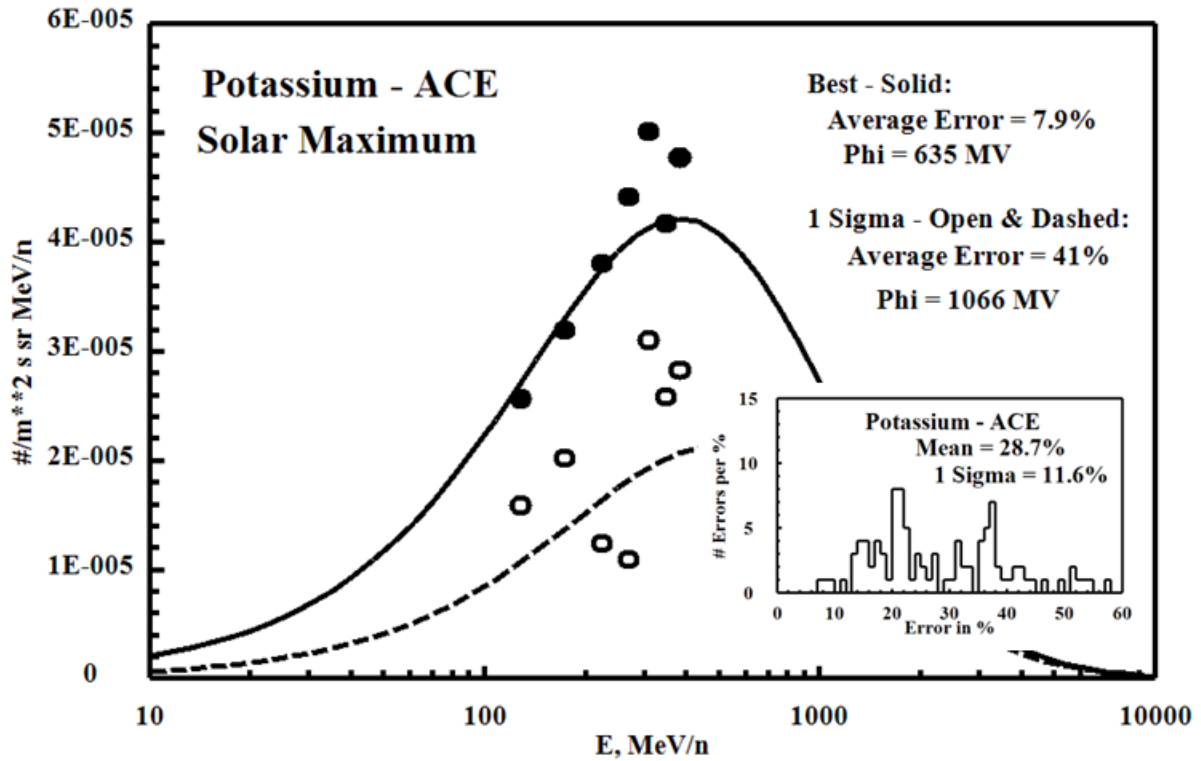


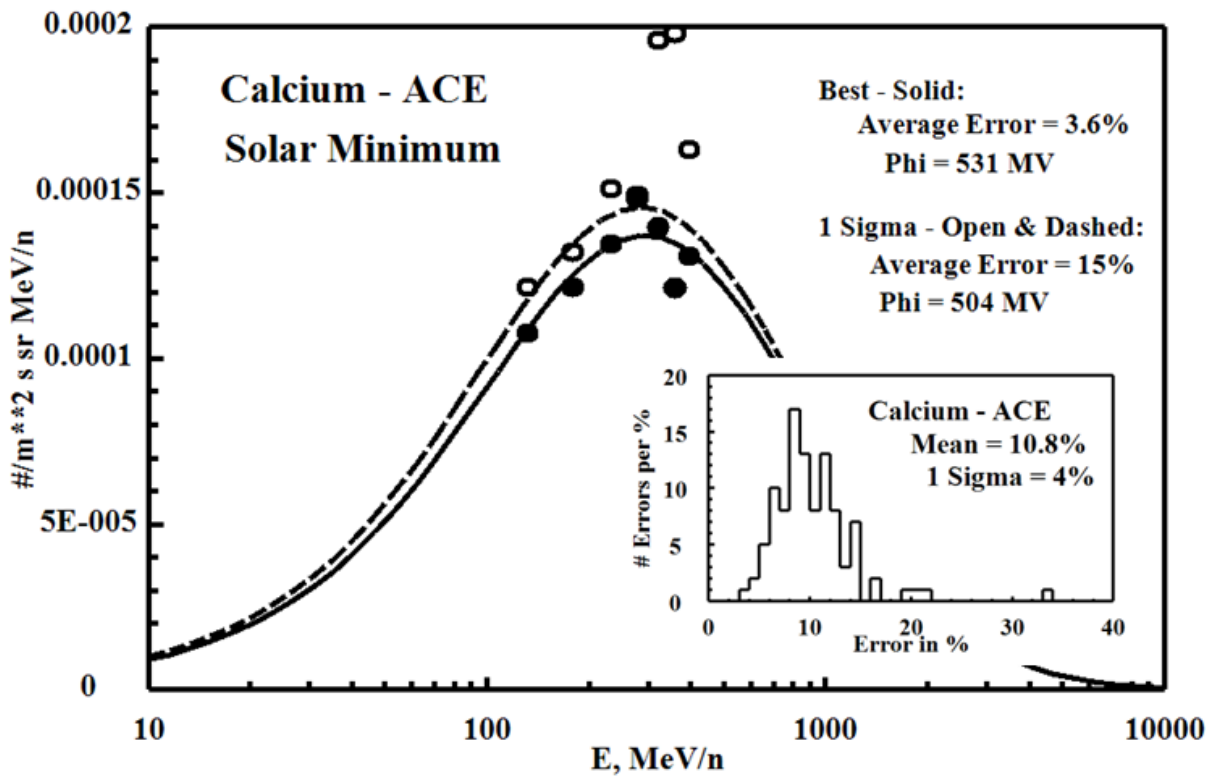
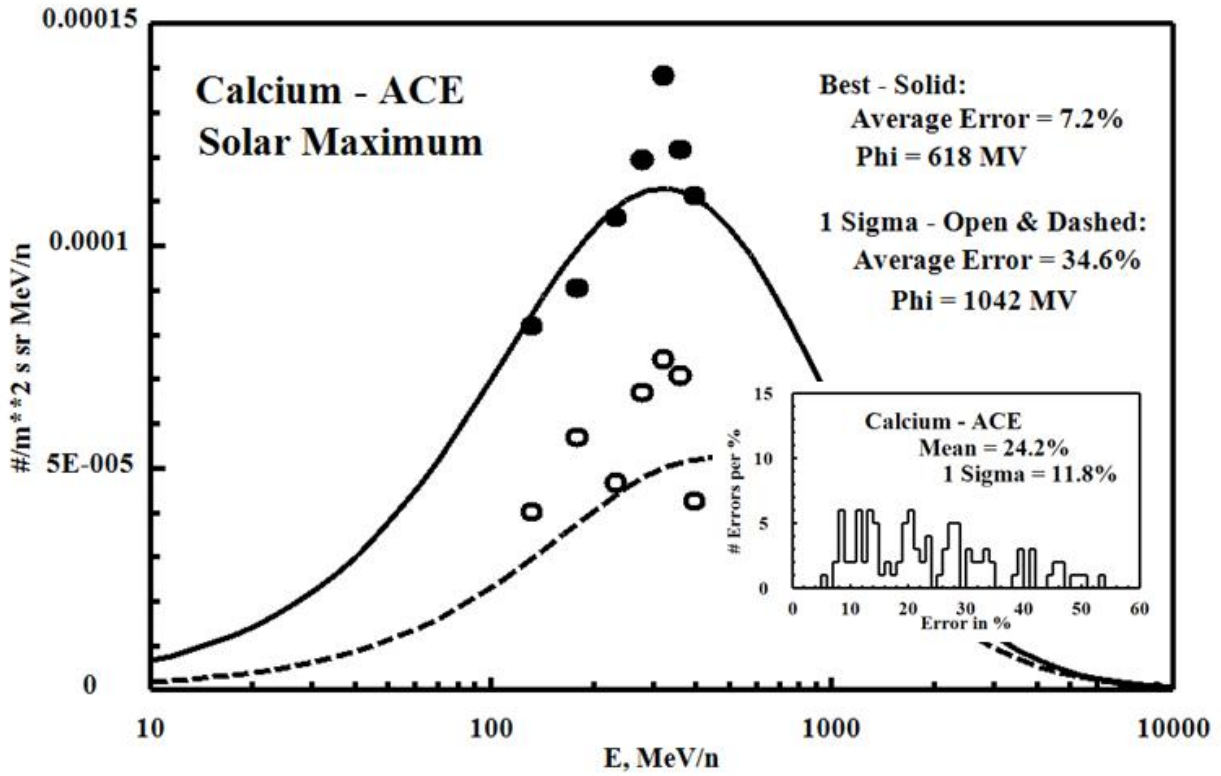


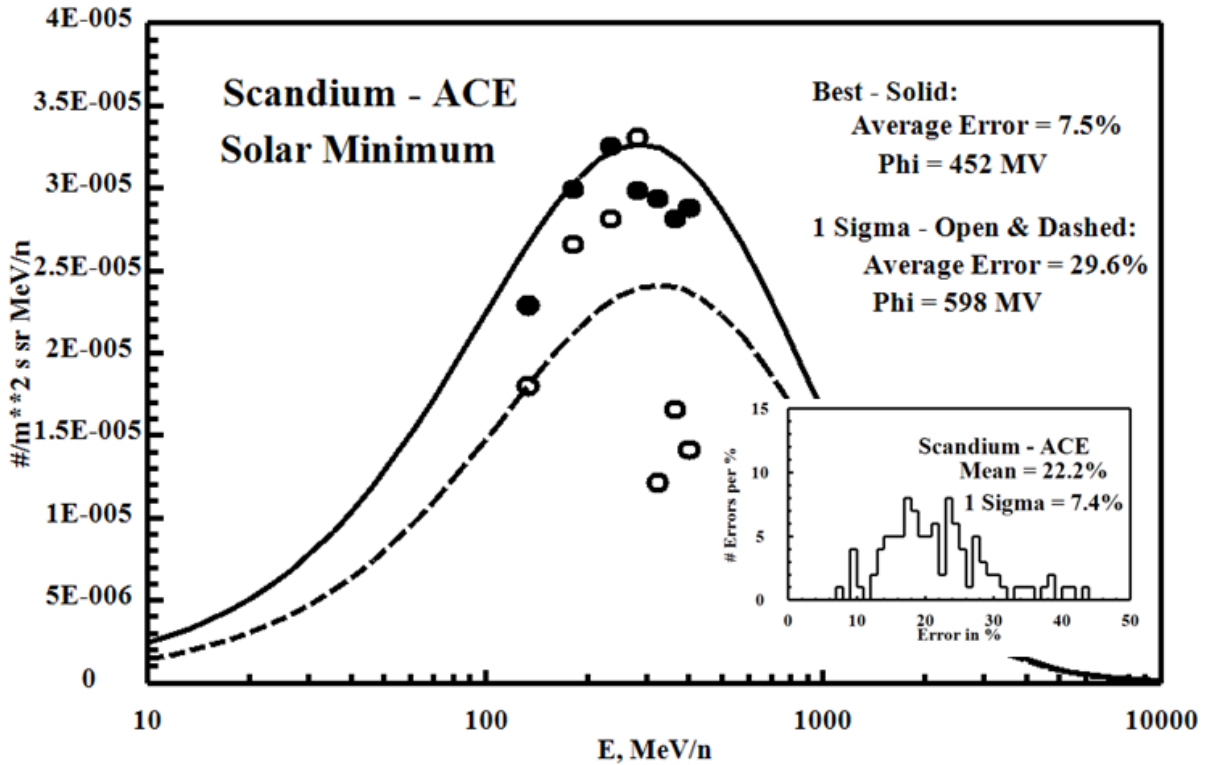
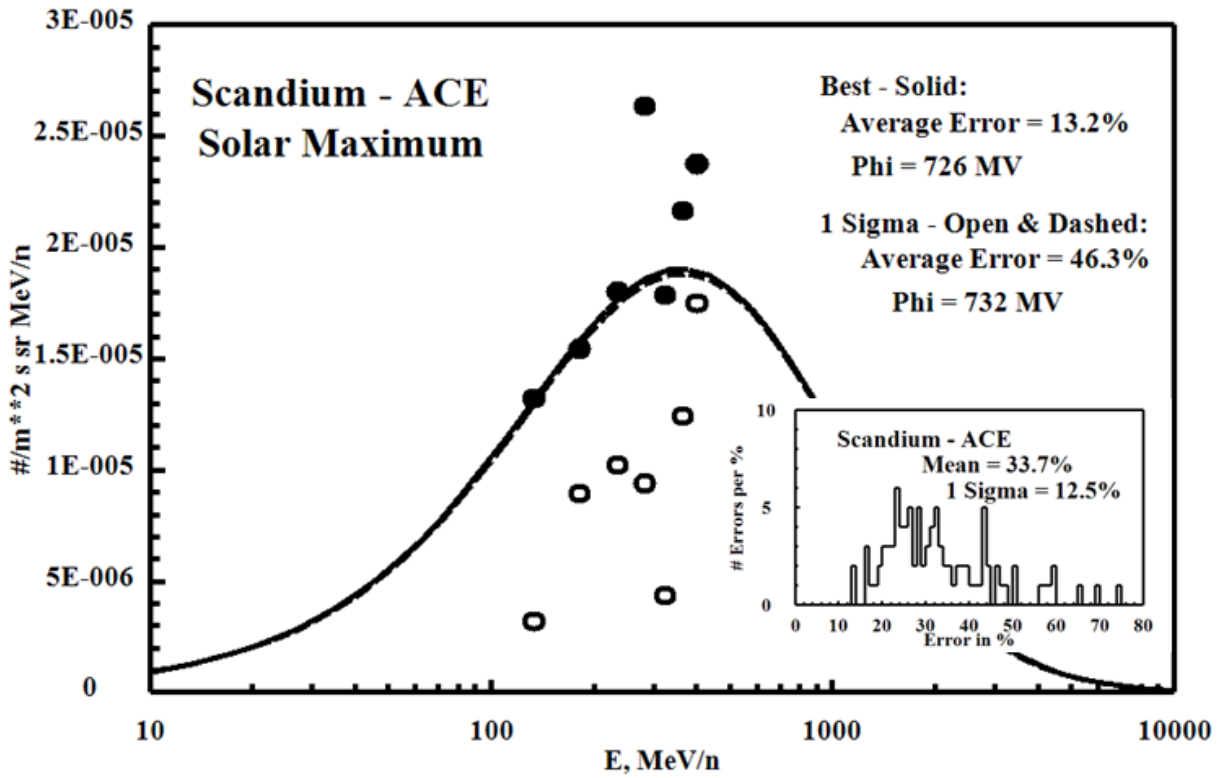


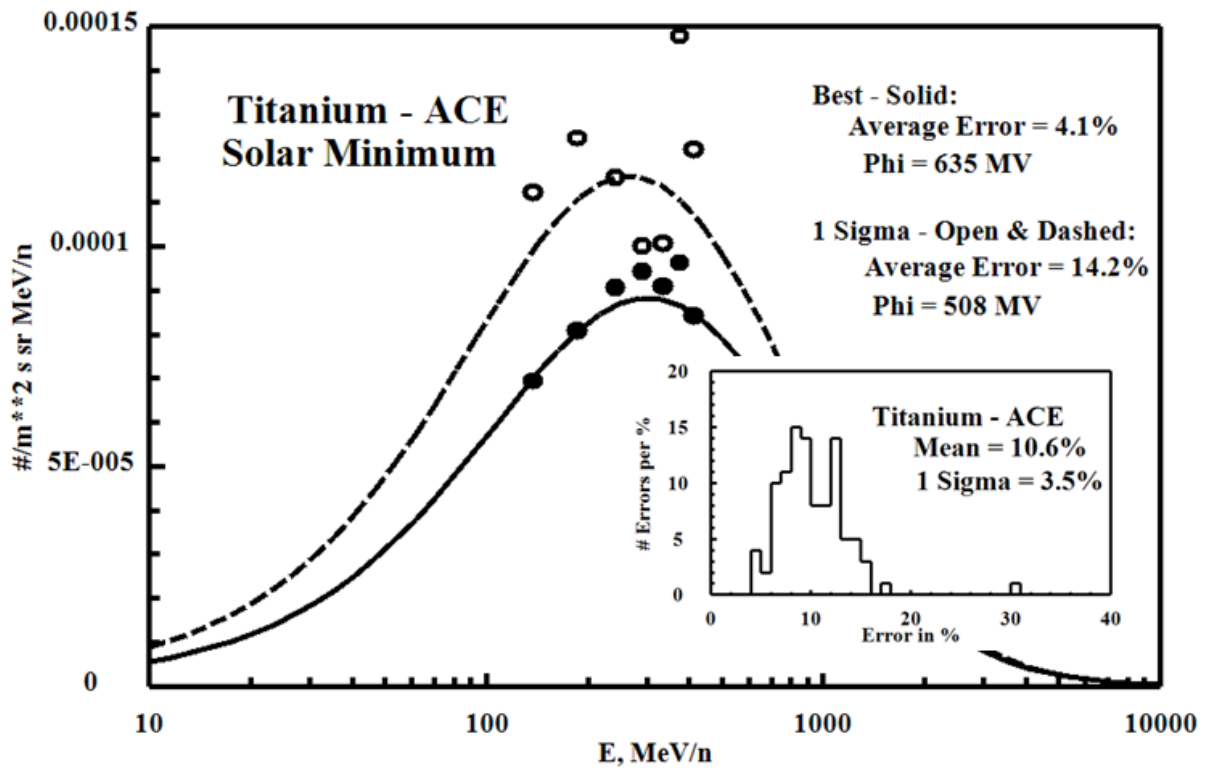
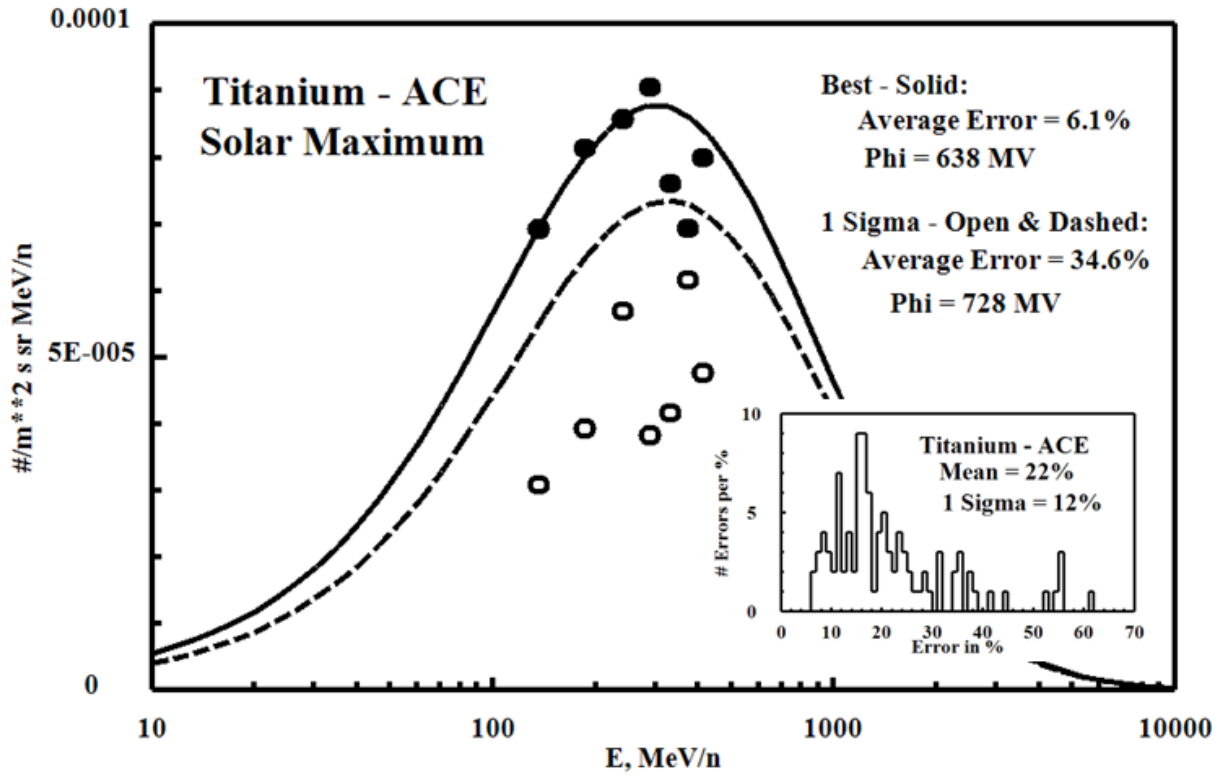


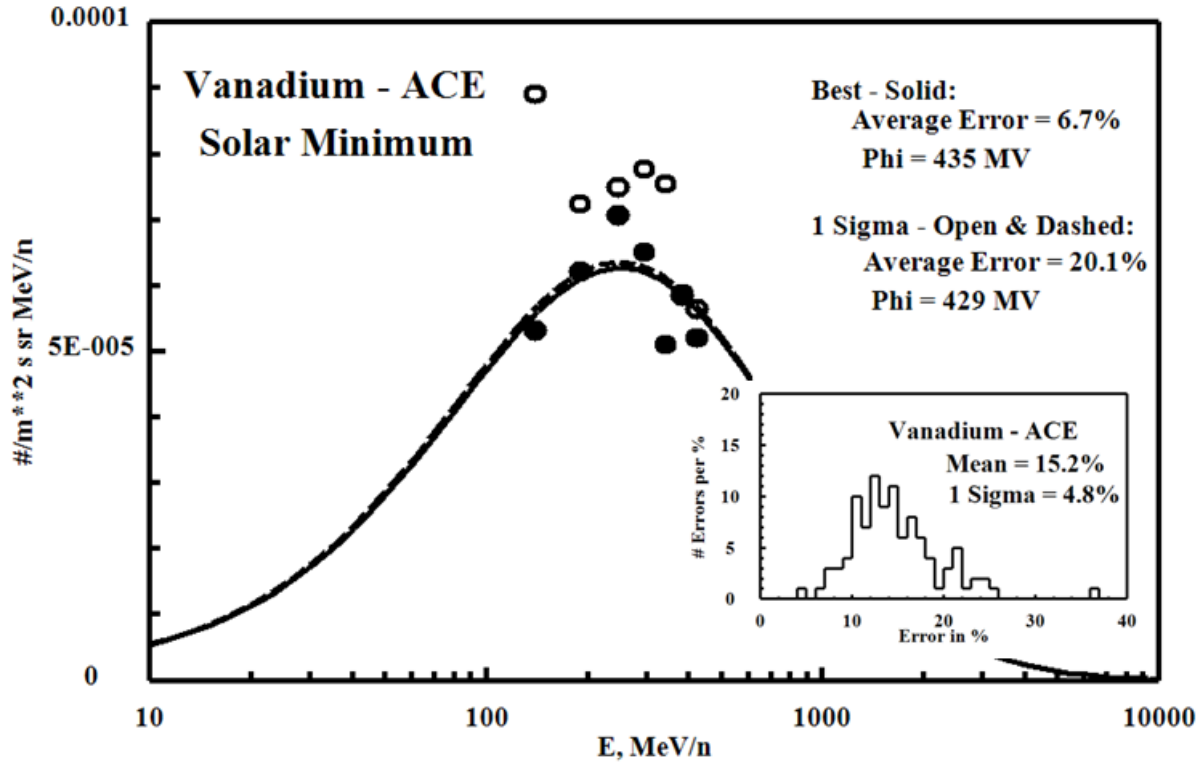
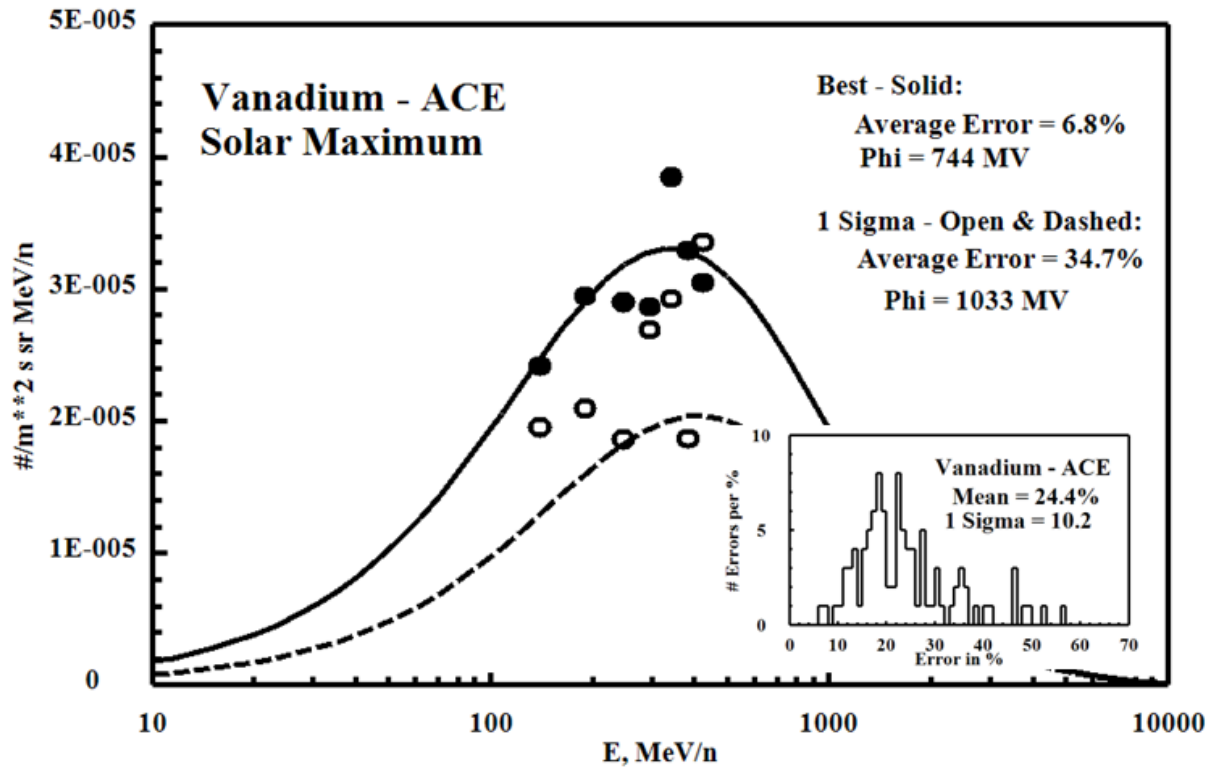


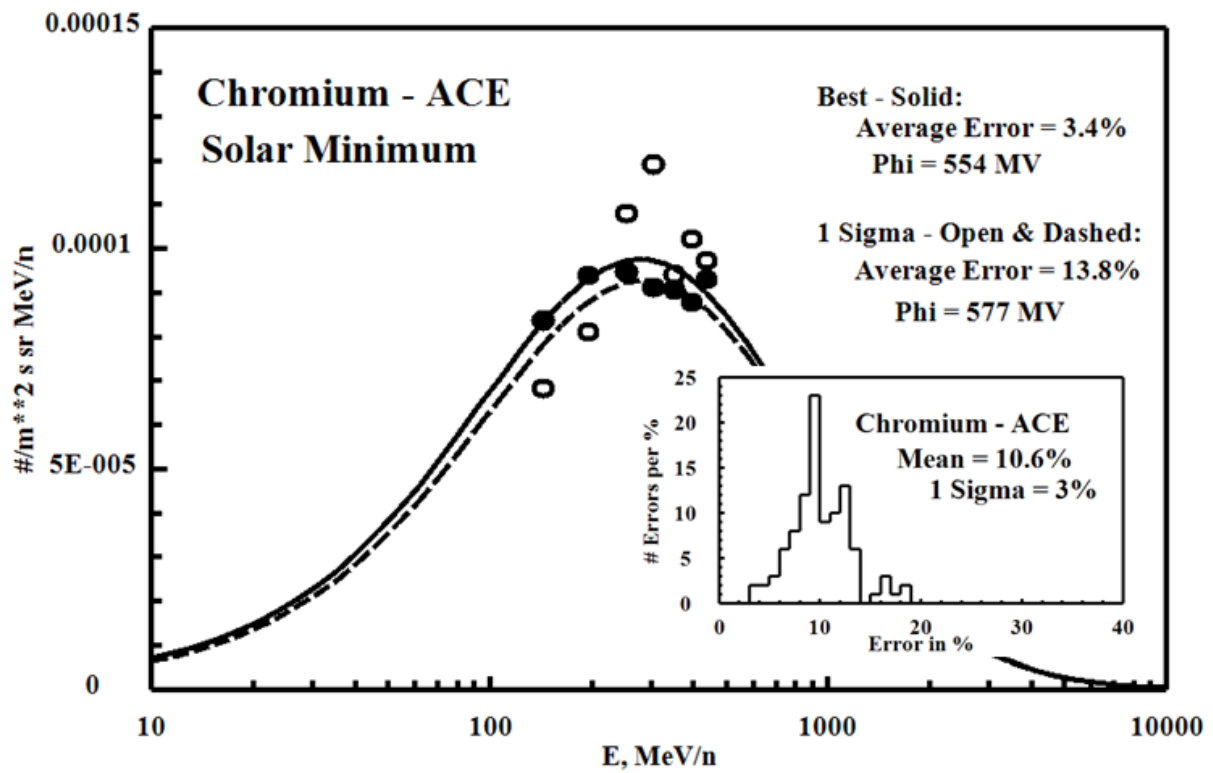
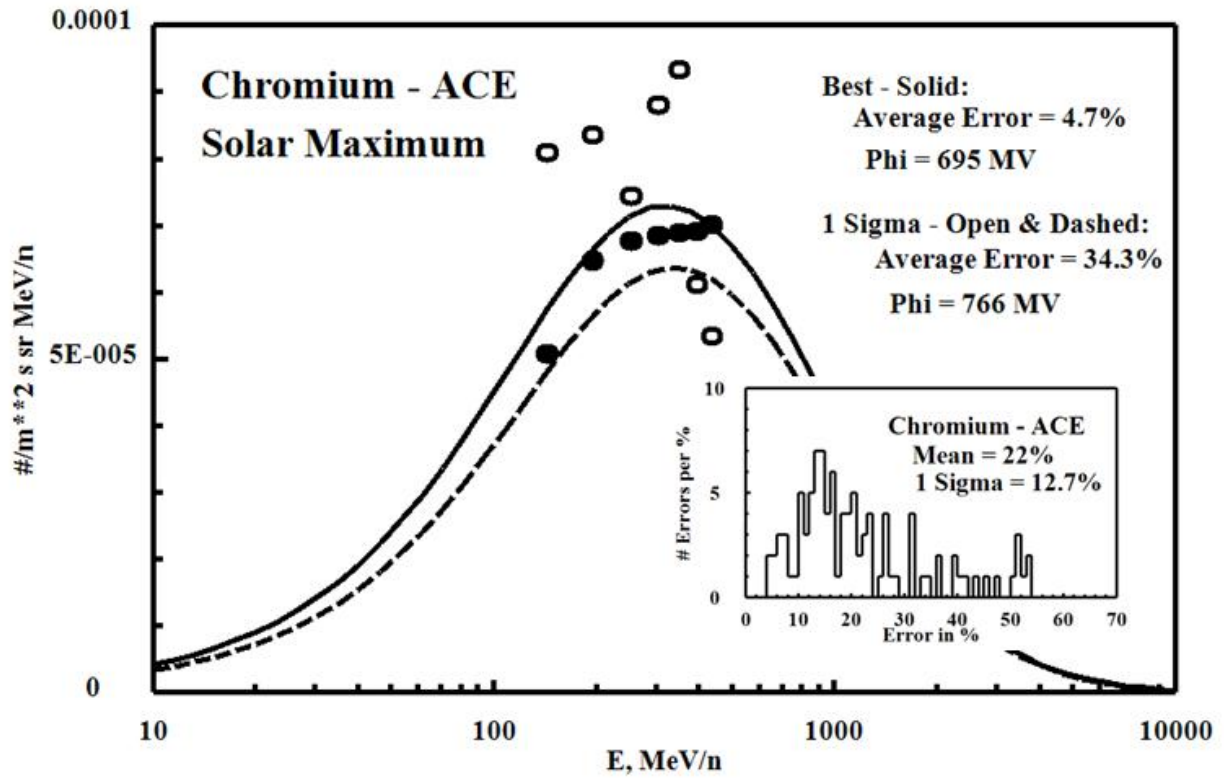


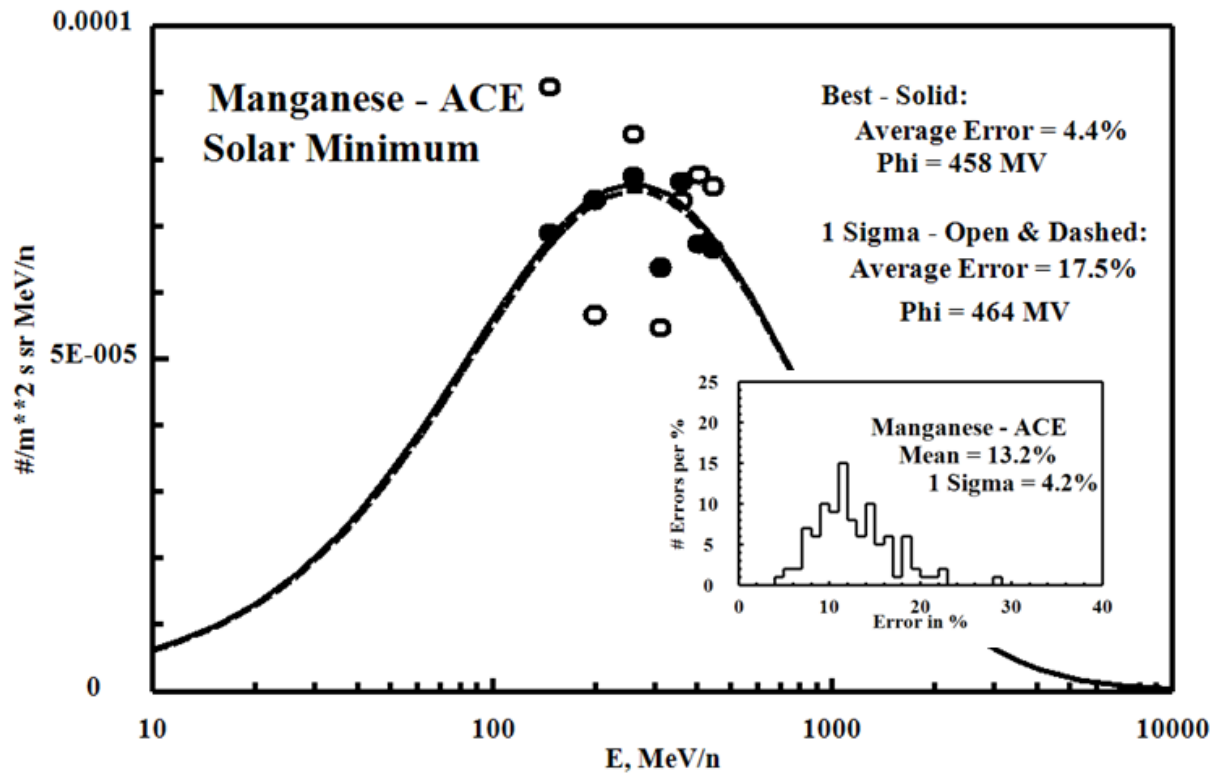
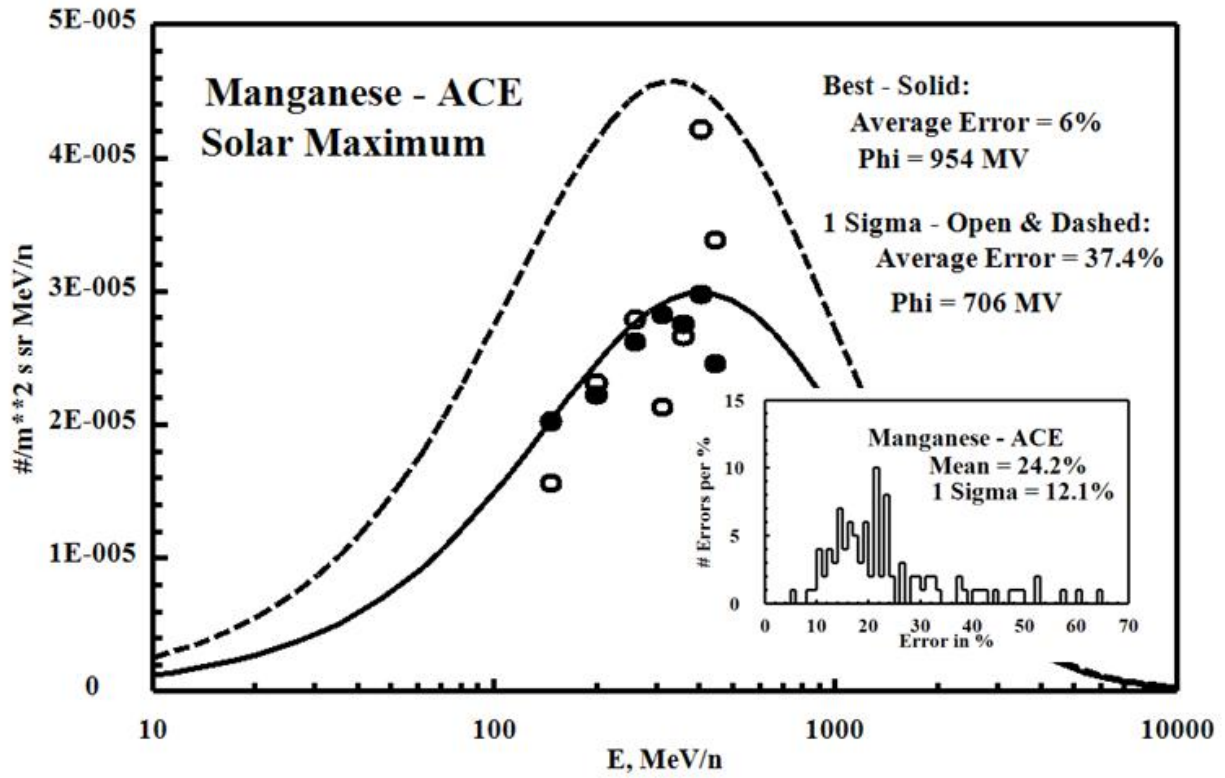


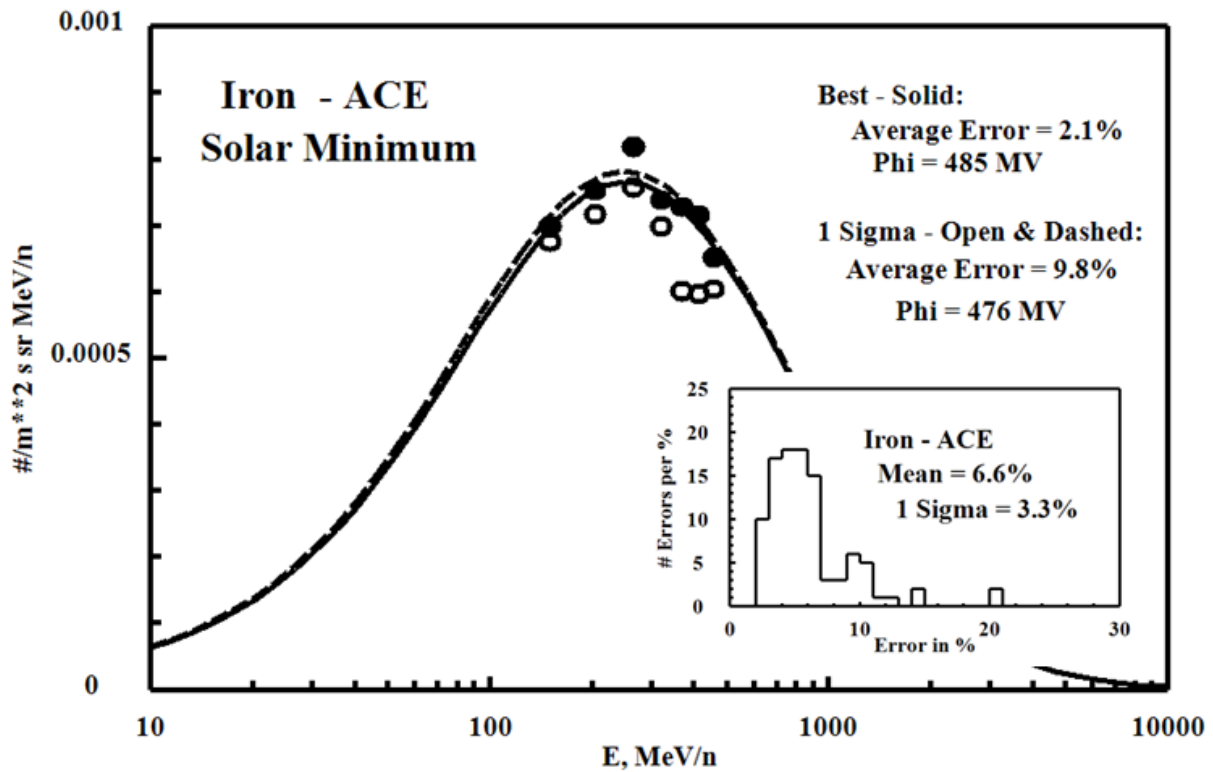
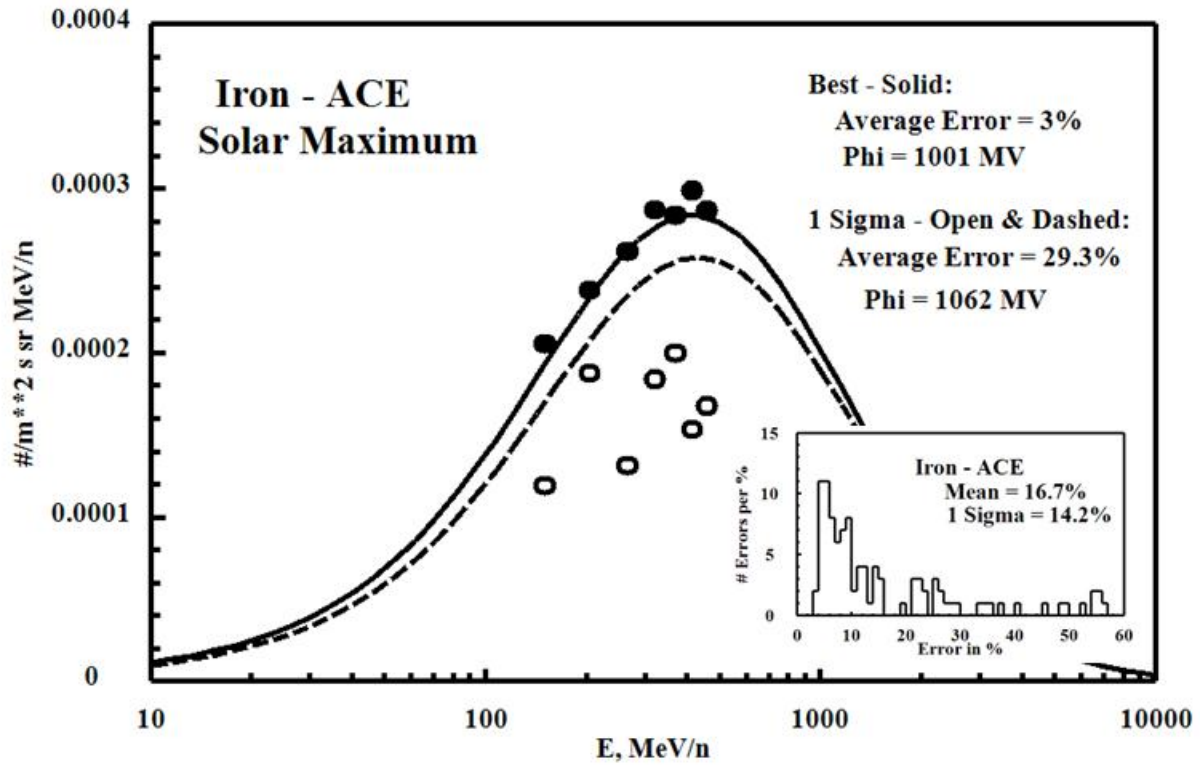


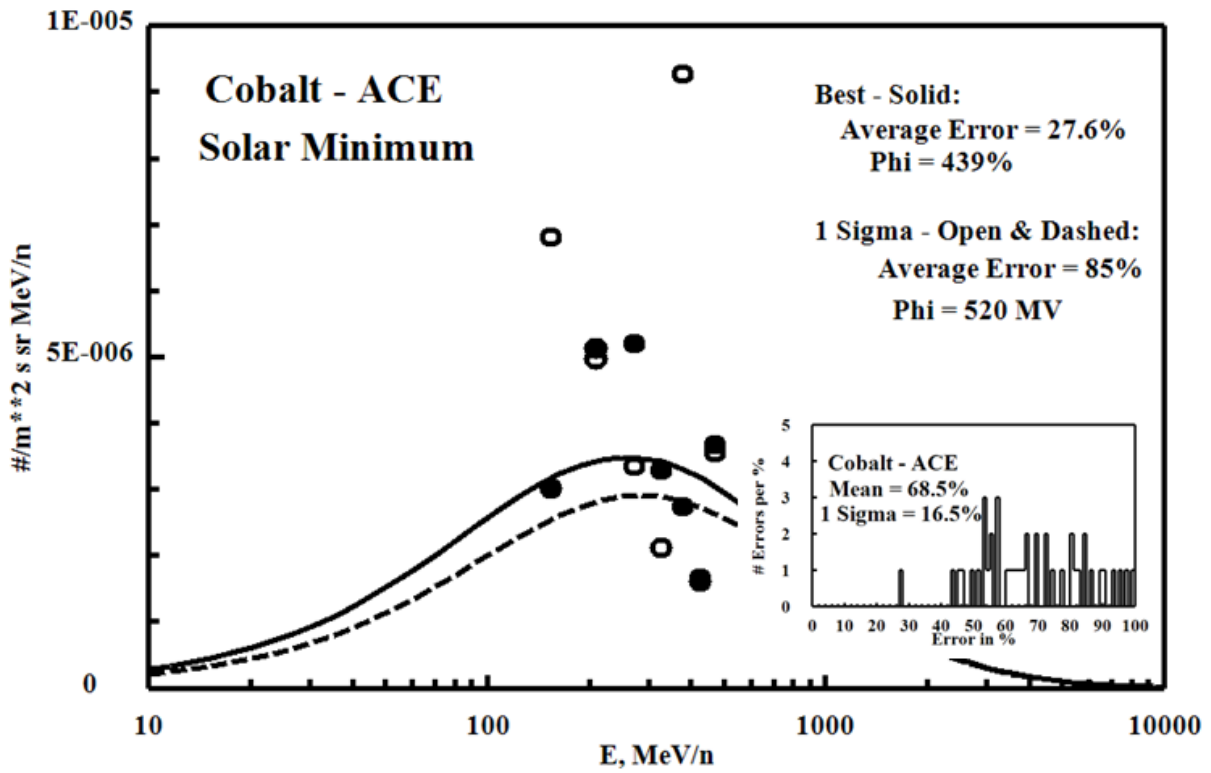
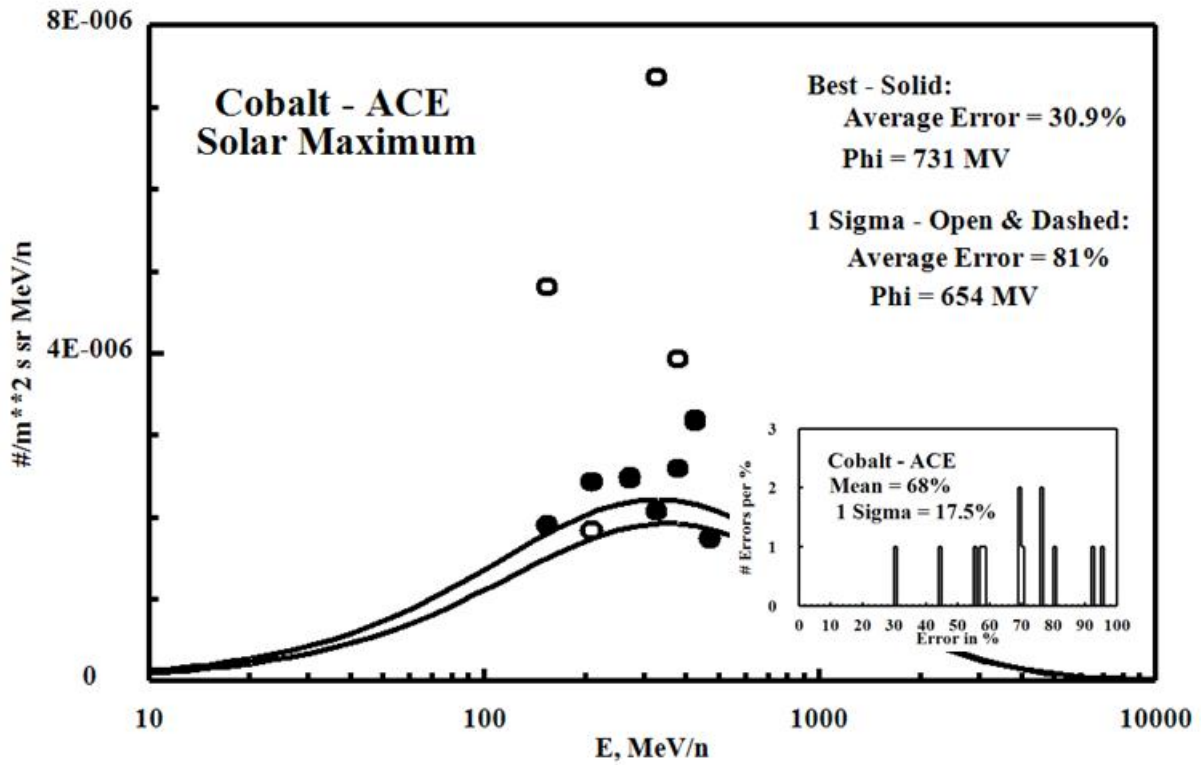


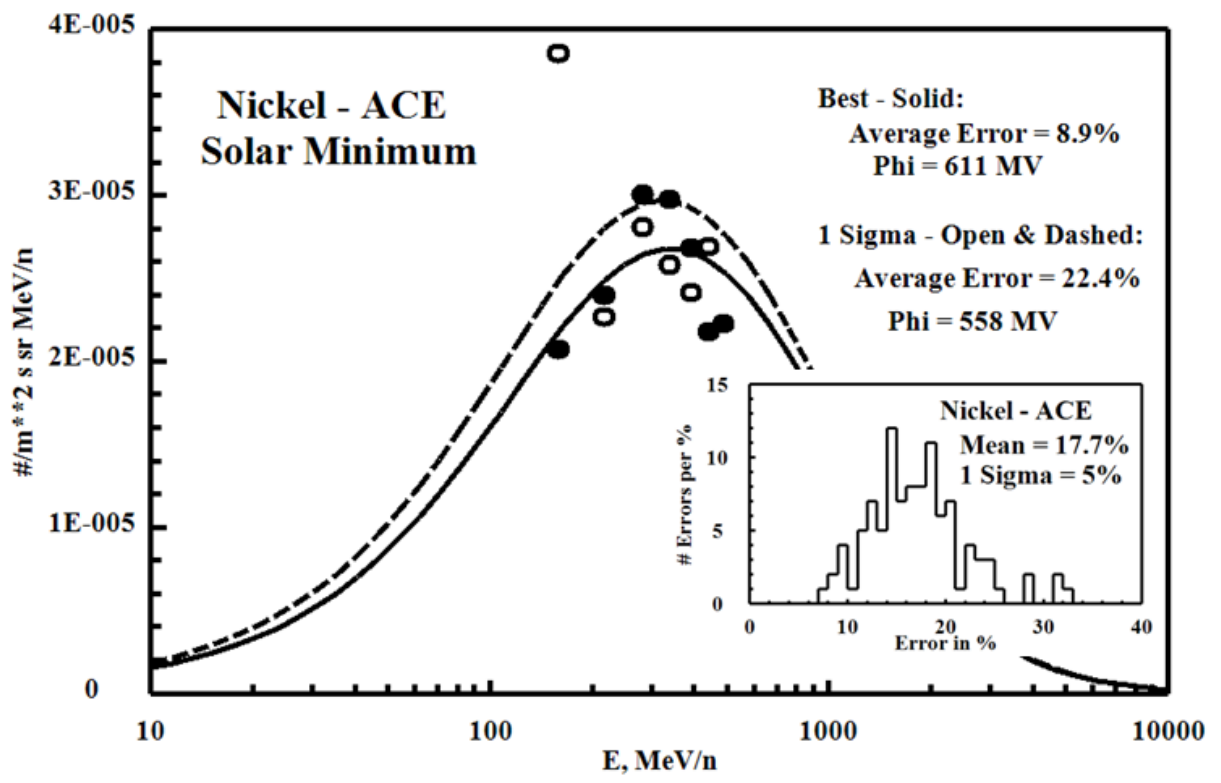
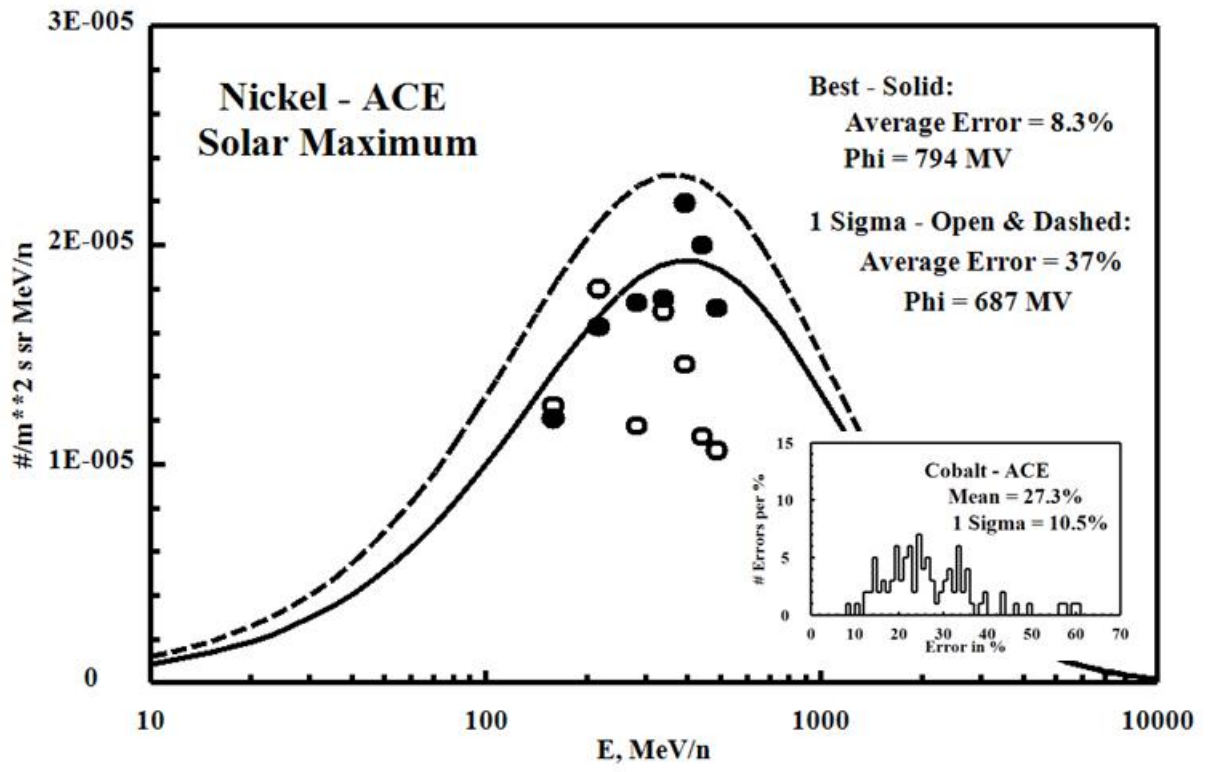












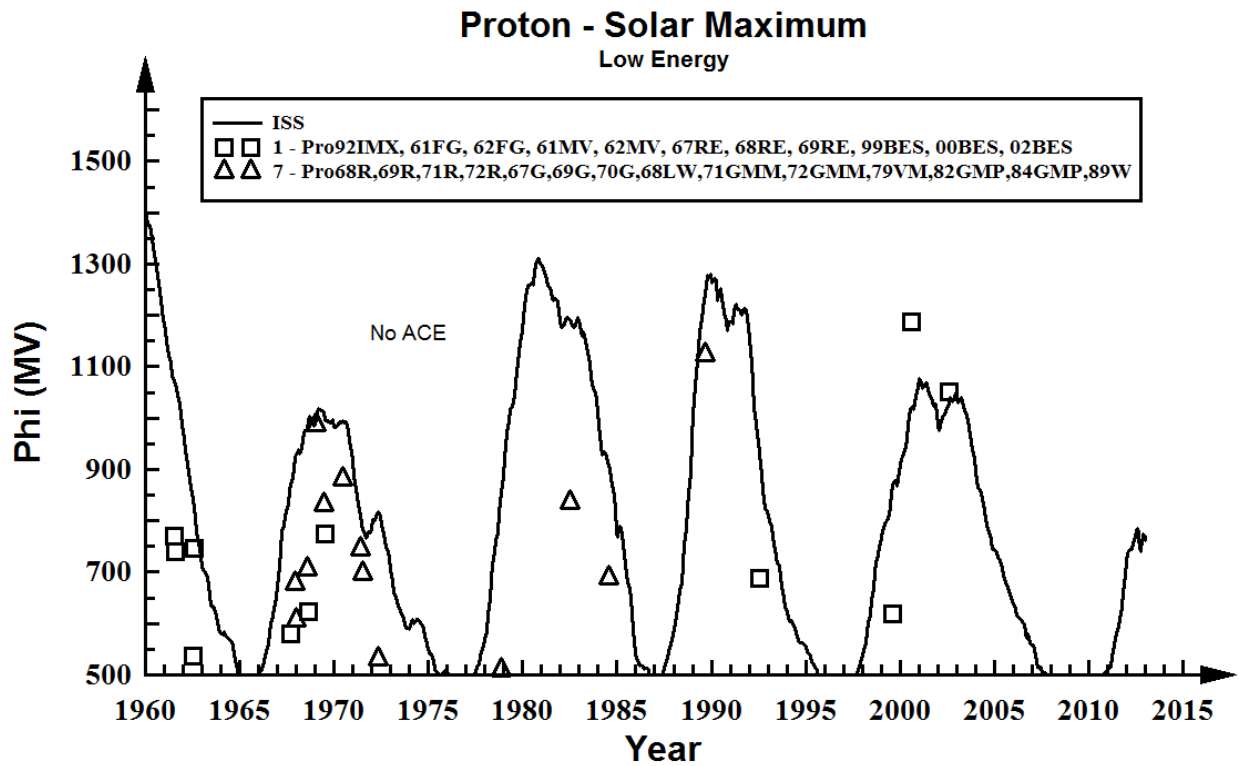
Appendix F: PHI from ISS# ADJUSTED to get Best Model – Data Fit

These plots demonstrate the degree to which the value of PHI (based on sunspot #) determines the spectrum for each of the low energy data measurements for $z=1$ to 28.

Circles, squares, ... are the adjusted values of PHI such that the data measurements fit the most accurately.

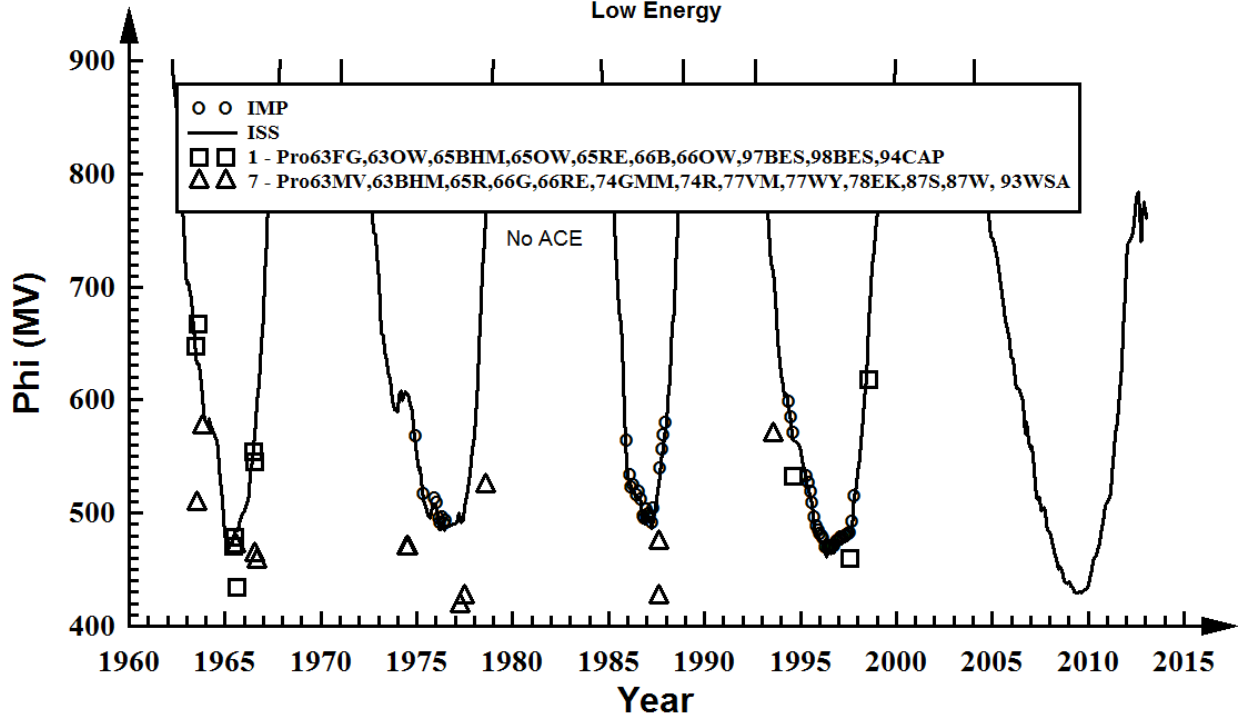
Solid Line = PHI as determined directly from the ISS# (PHIFRISS.DAT)

Adjusted PHI for all low Energy ACE & Arbitrary Data for Solar Minimum and Maximum periods versus time



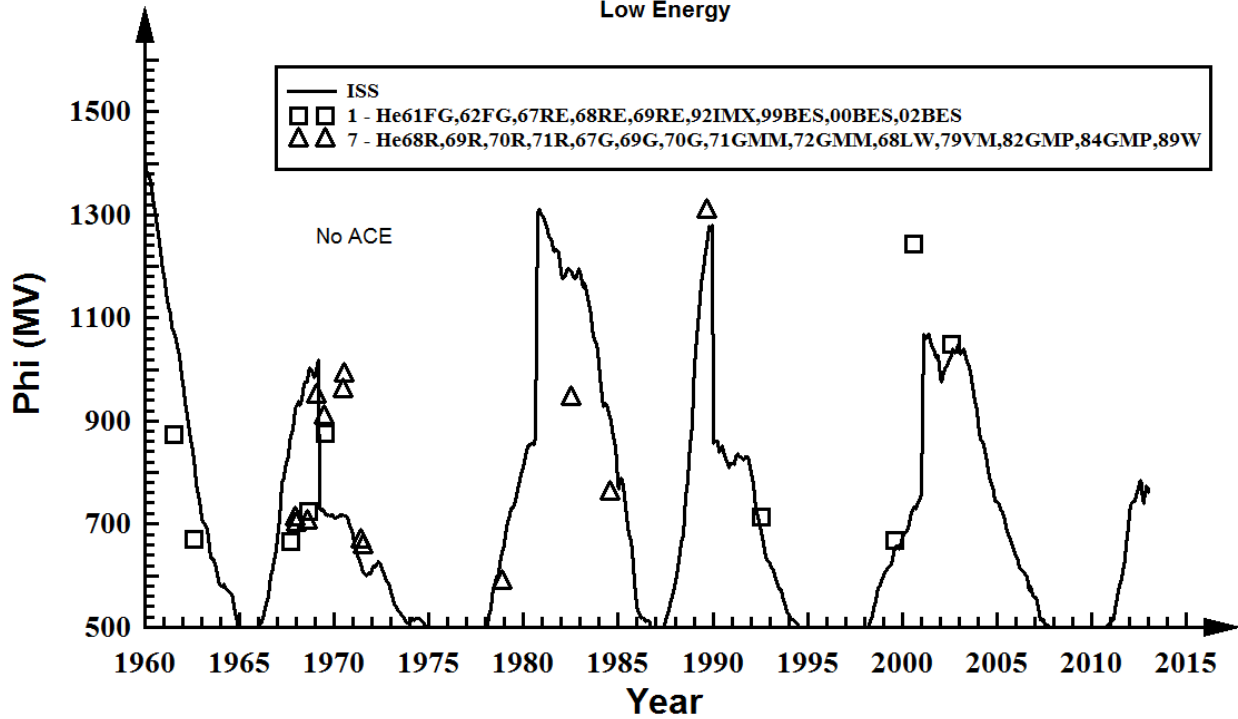
Proton - Solar Minimum

Low Energy



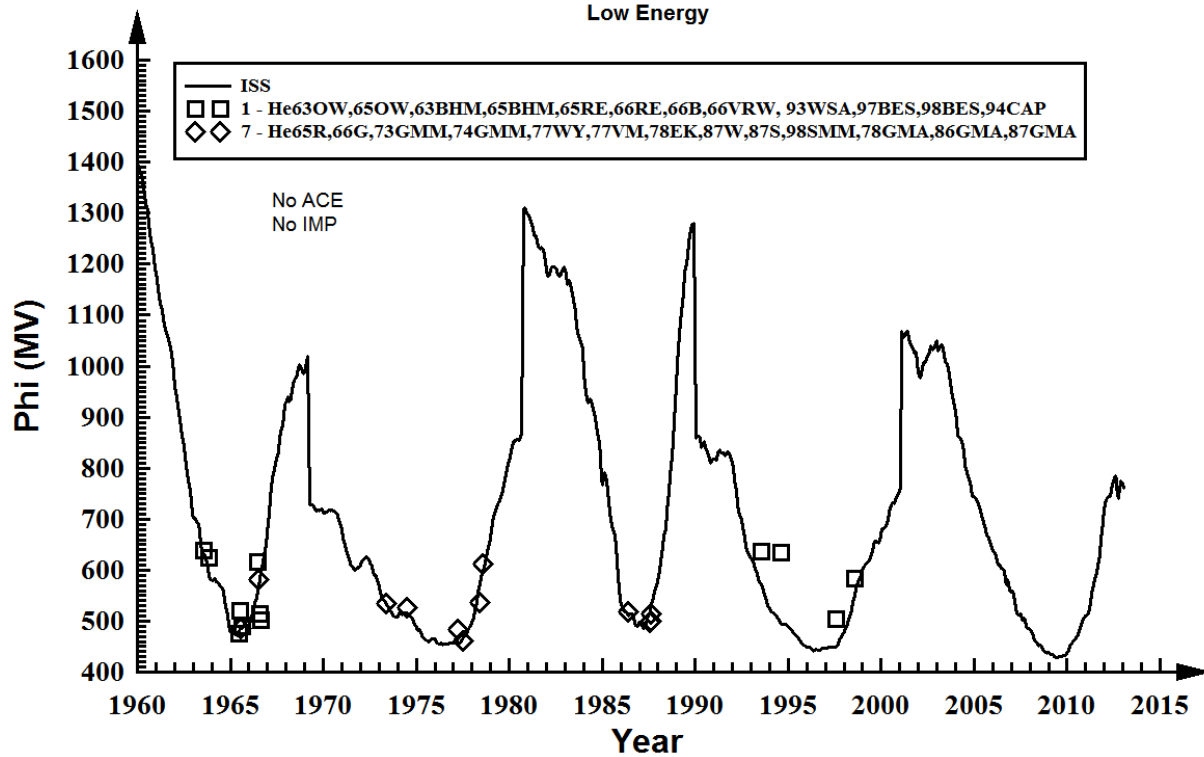
Helium - Solar Maximum

Low Energy



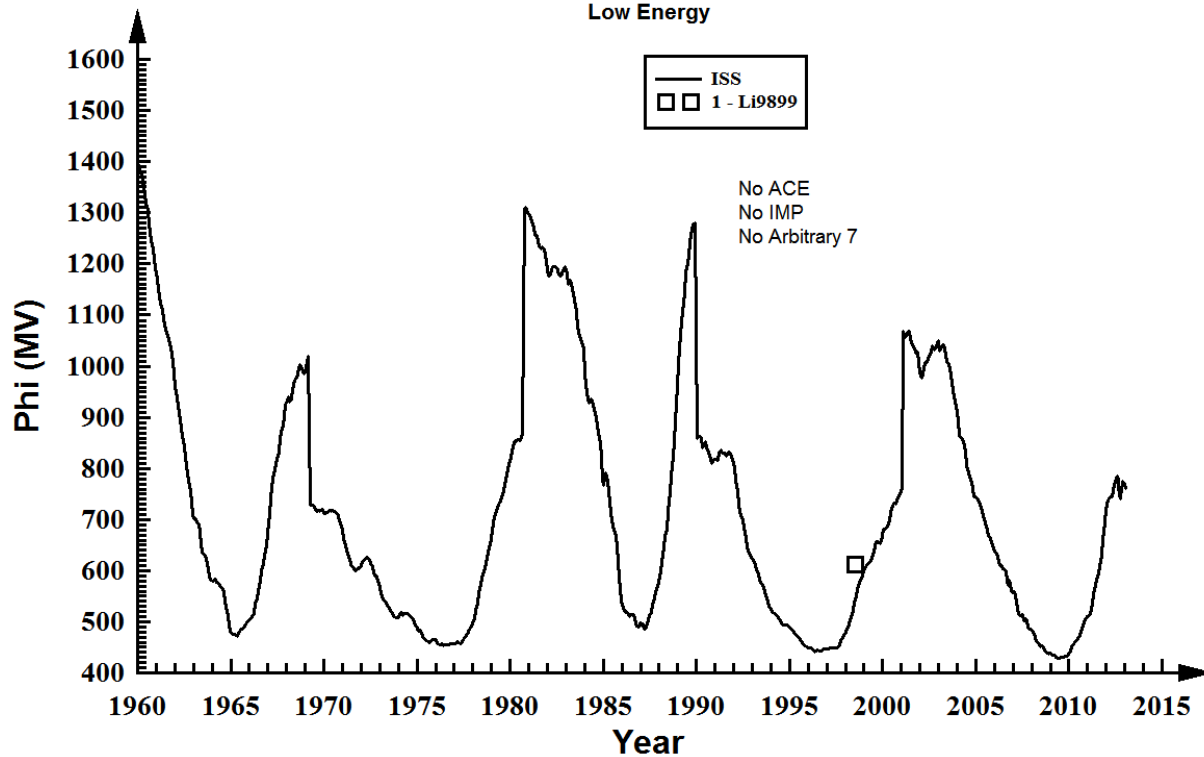
Helium - Solar Minimum

Low Energy



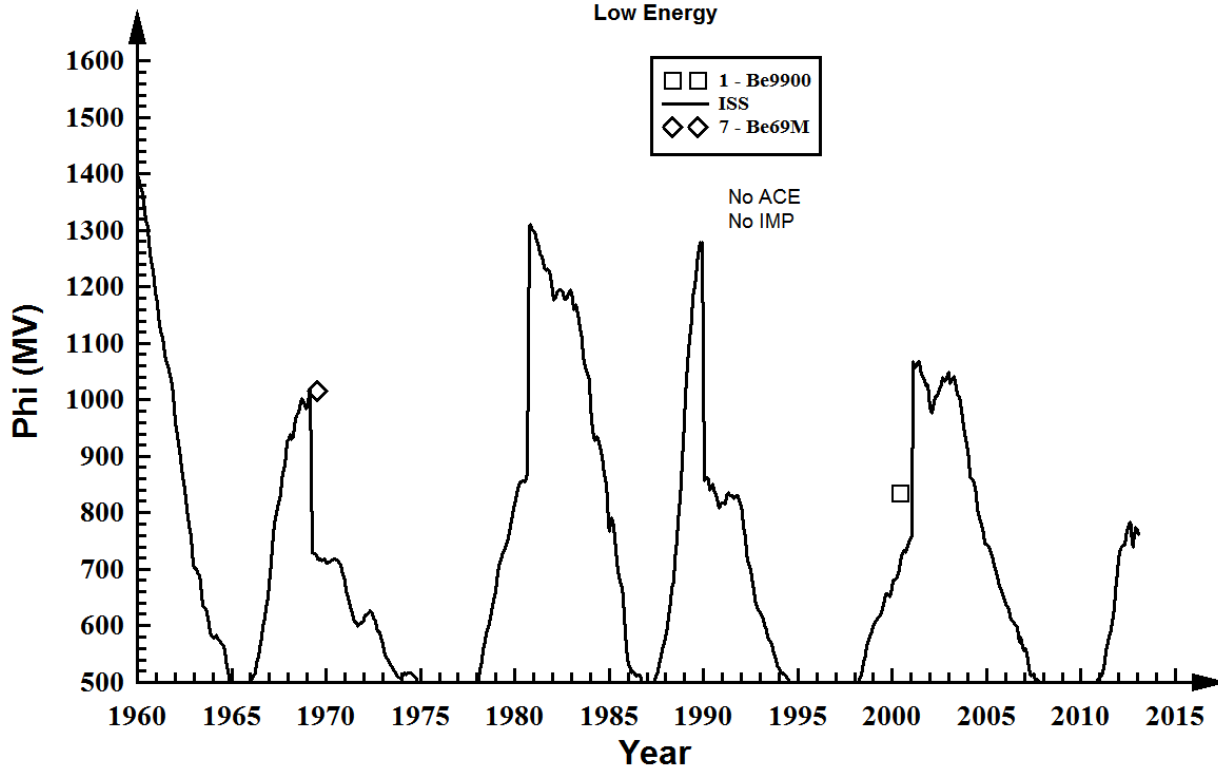
Lithium - Solar Minimum

Low Energy



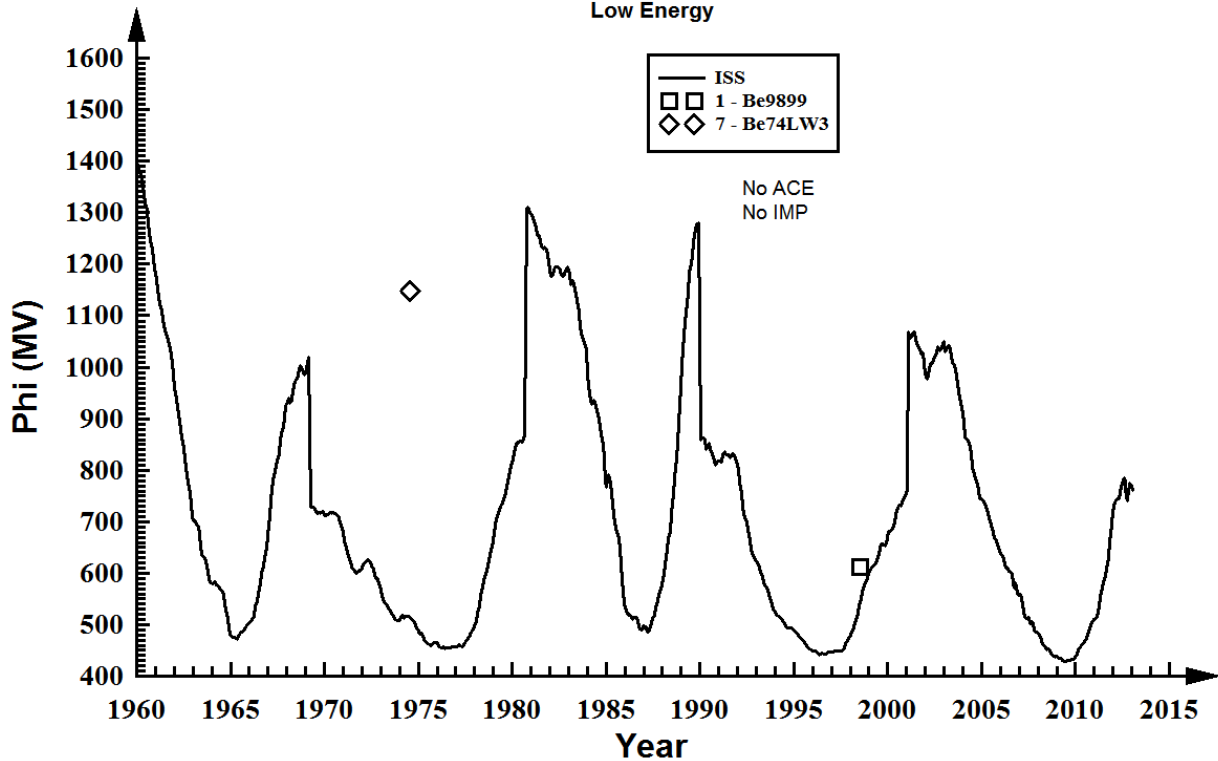
Beryllium - Solar Maximum

Low Energy



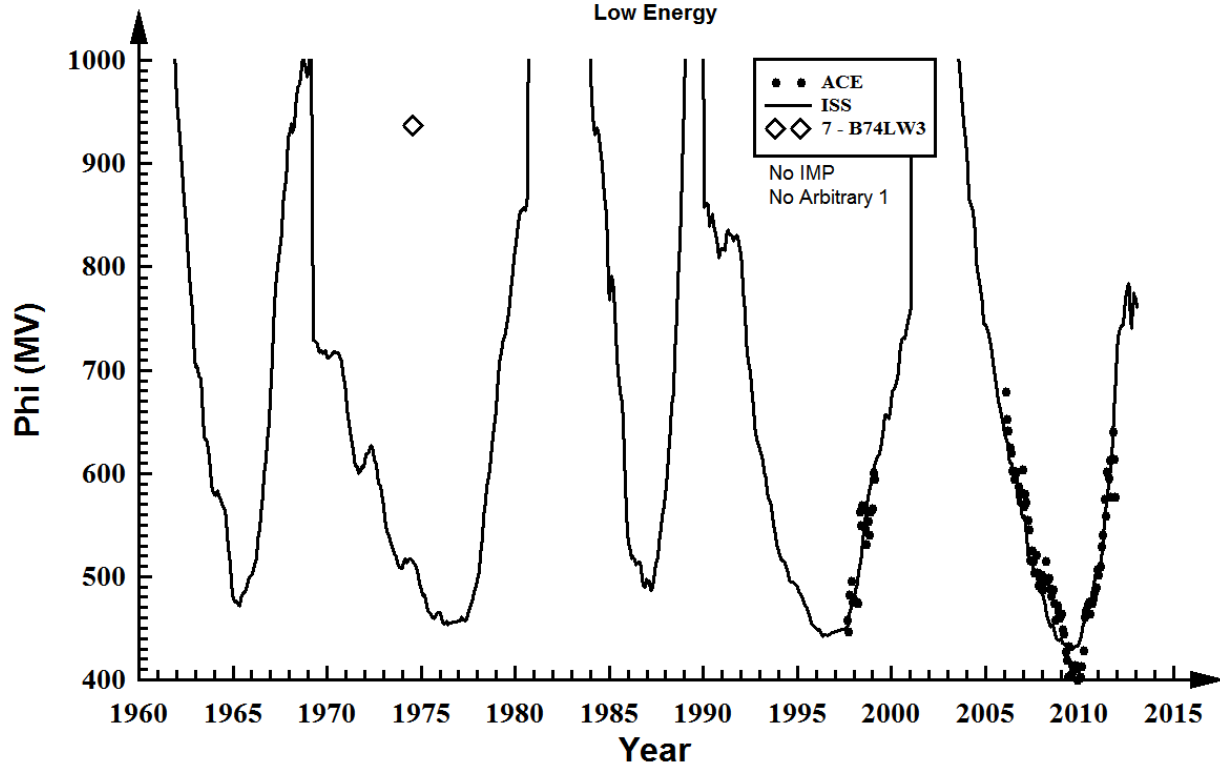
Beryllium - Solar Minimum

Low Energy



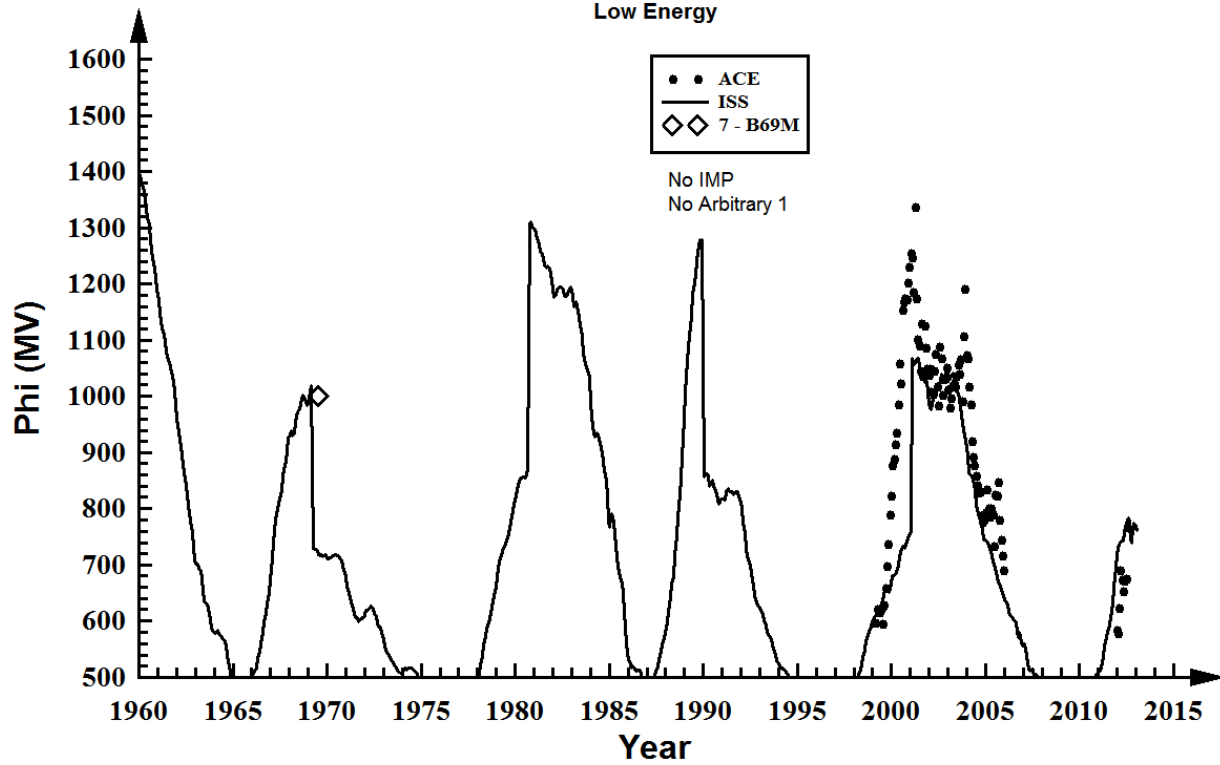
Boron - Solar Minimum

Low Energy



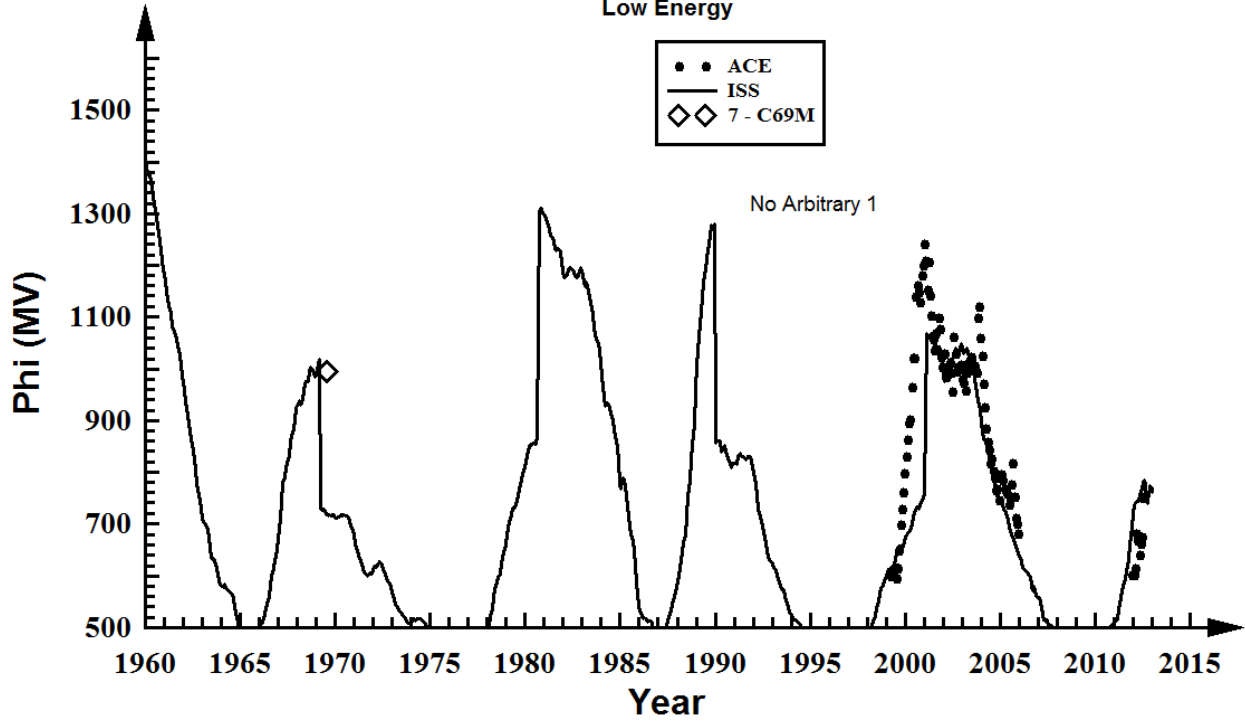
Boron - Solar Maximum

Low Energy



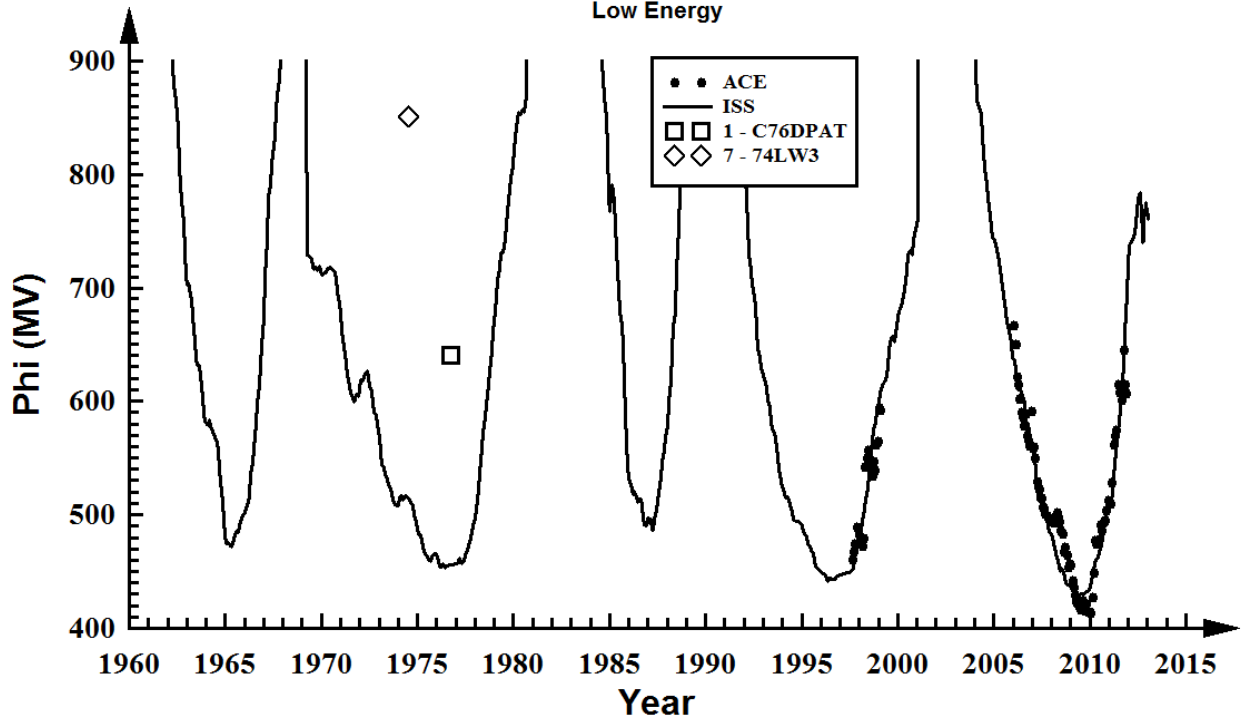
Carbon - Solar Maximum

Low Energy

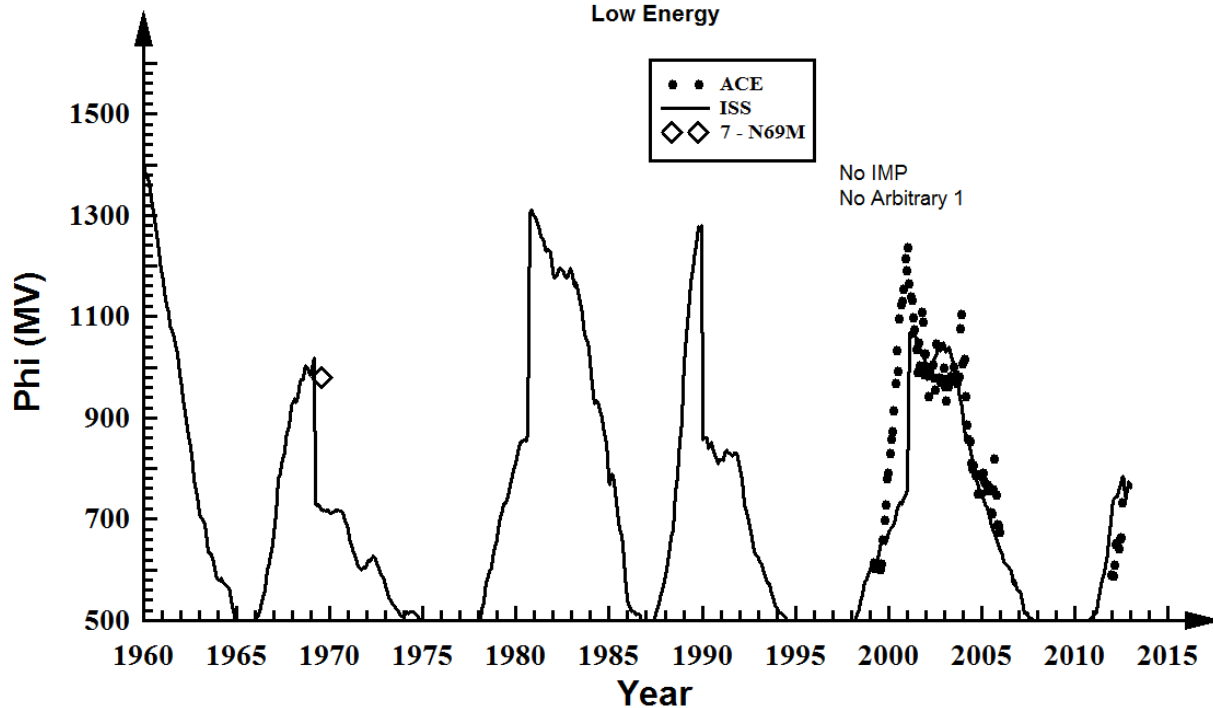


Carbon - Solar Minimum

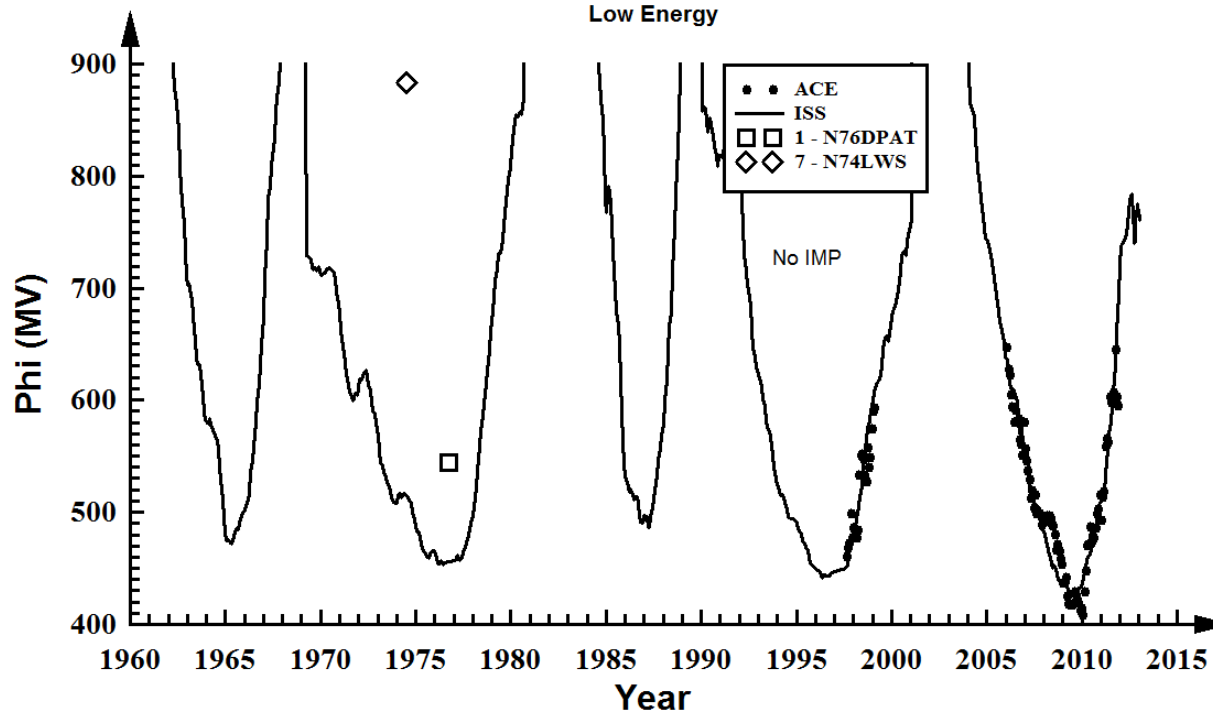
Low Energy



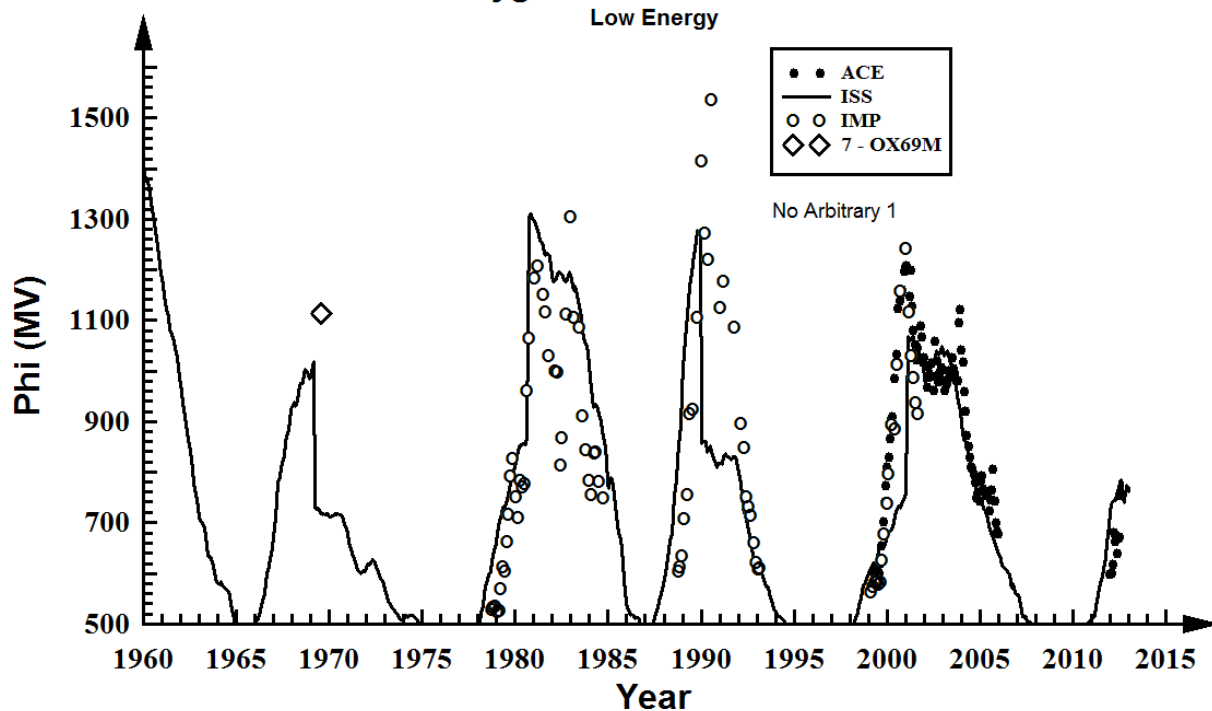
Nitrogen - Solar Maximum Low Energy



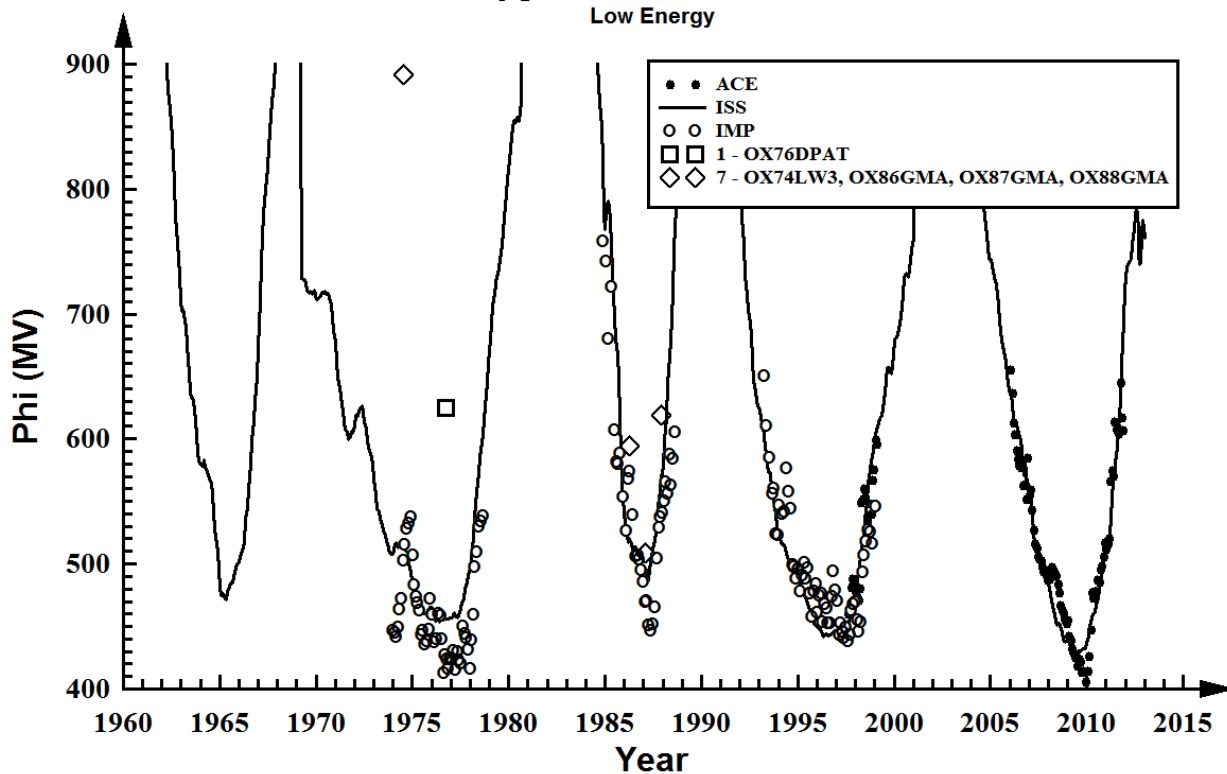
Nitrogen - Solar Minimum Low Energy



Oxygen - Solar Maximum

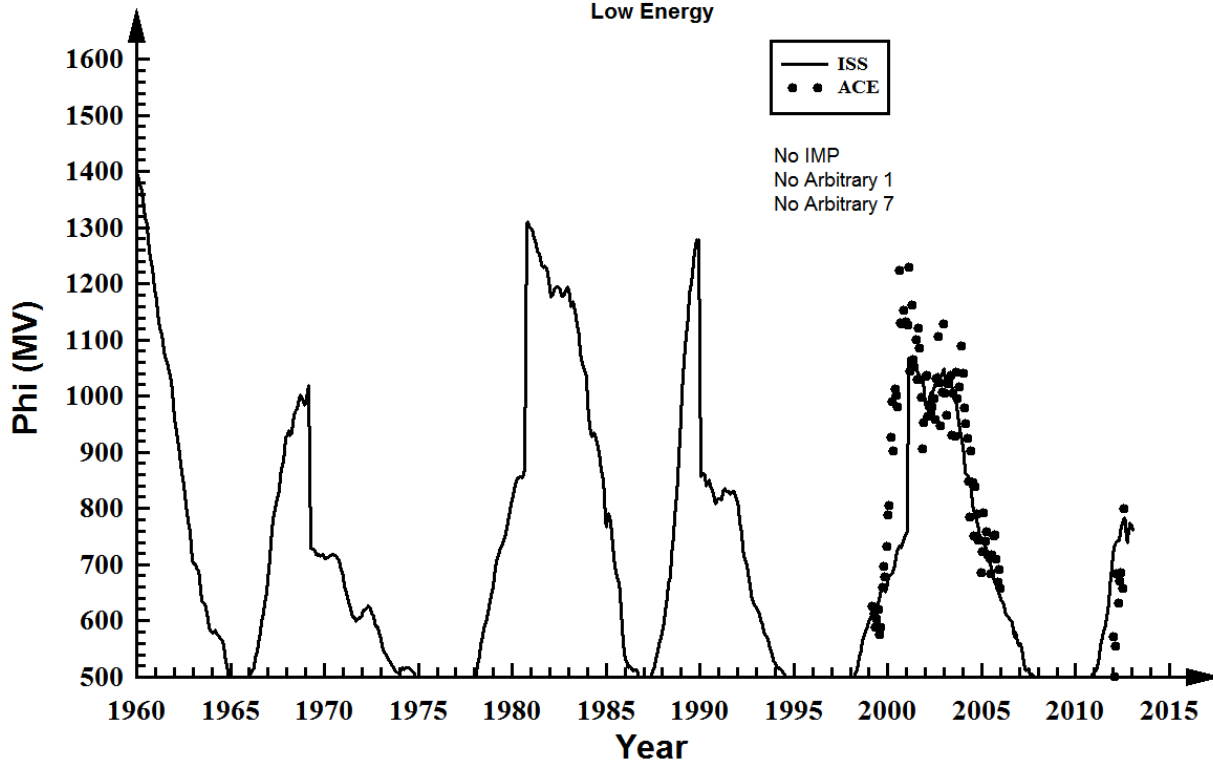


Oxygen - Solar Minimum



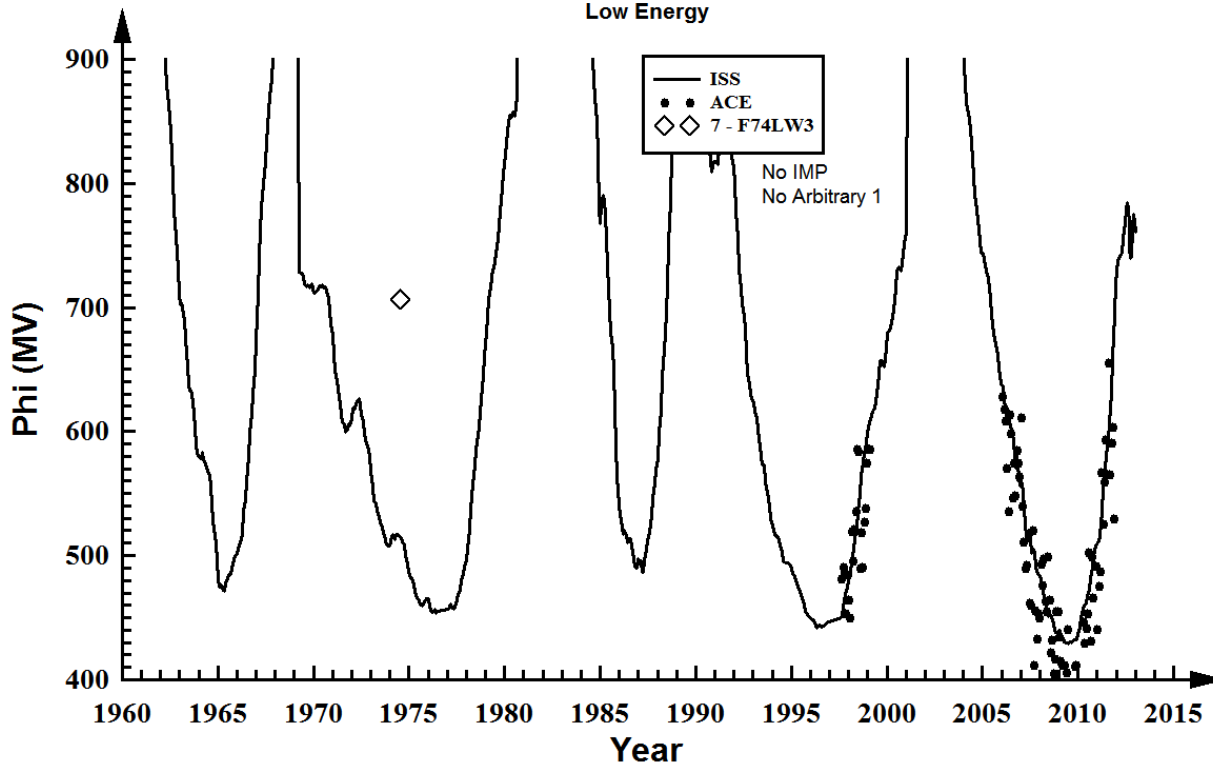
Fluorine - Solar Maximum

Low Energy



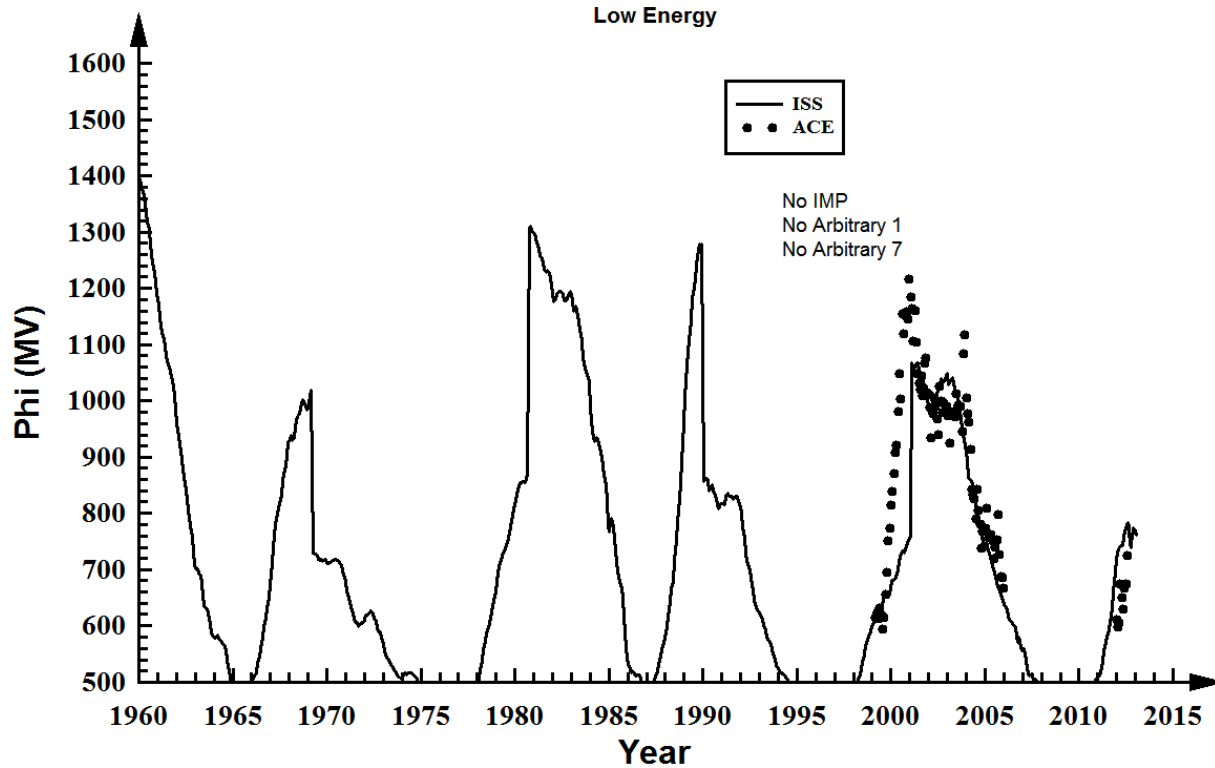
Fluorine - Solar Minimum

Low Energy



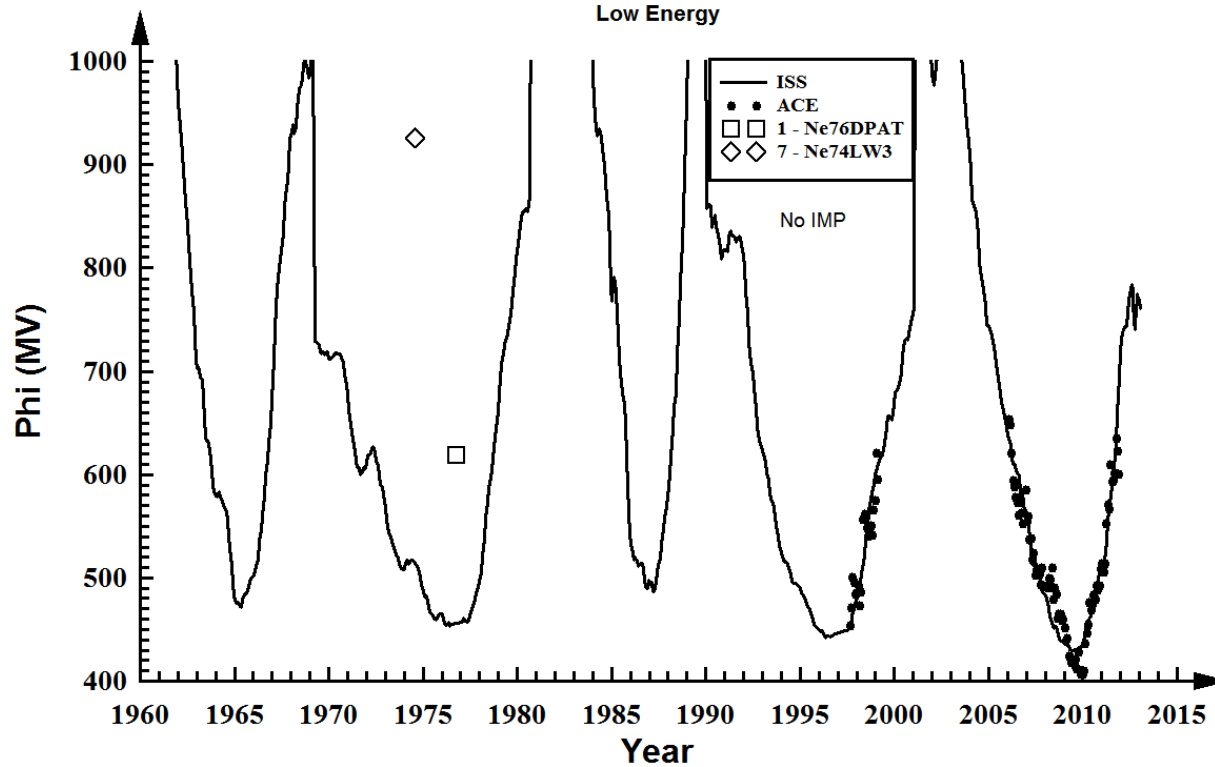
Neon - Solar Maximum

Low Energy



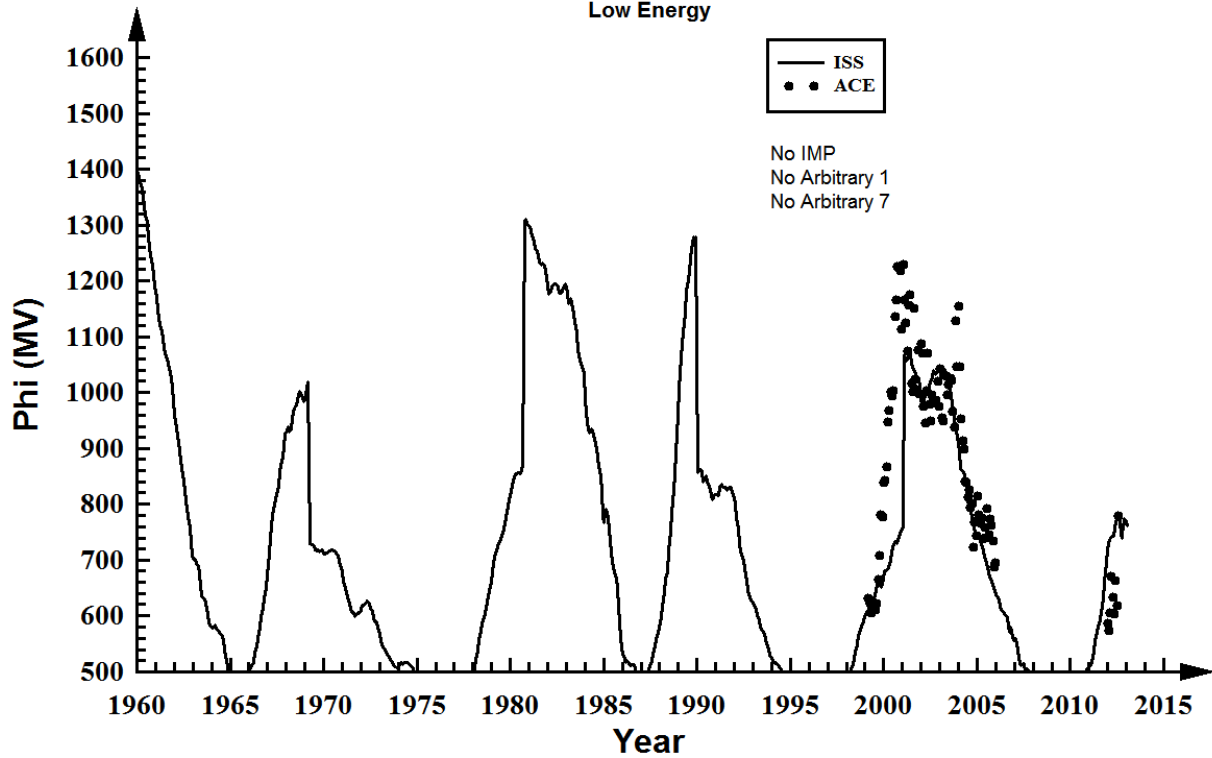
Neon - Solar Minimum

Low Energy



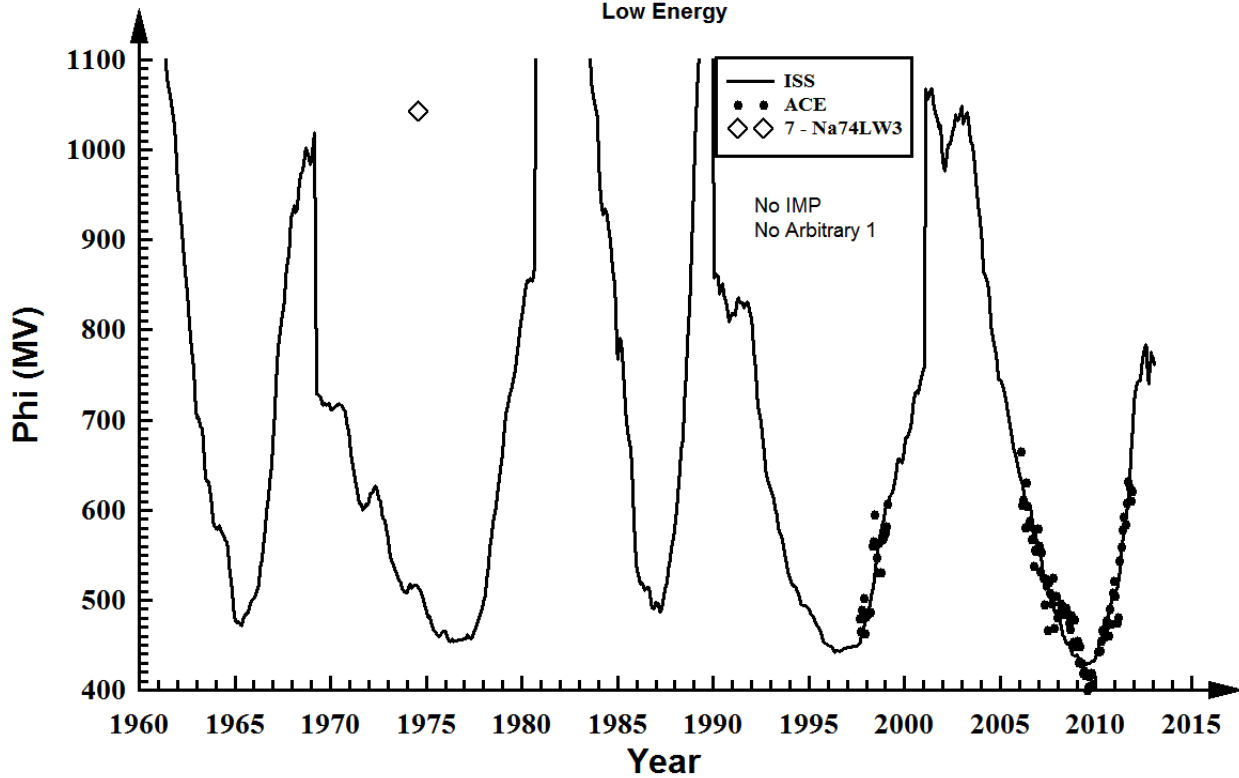
Sodium - Solar Maximum

Low Energy

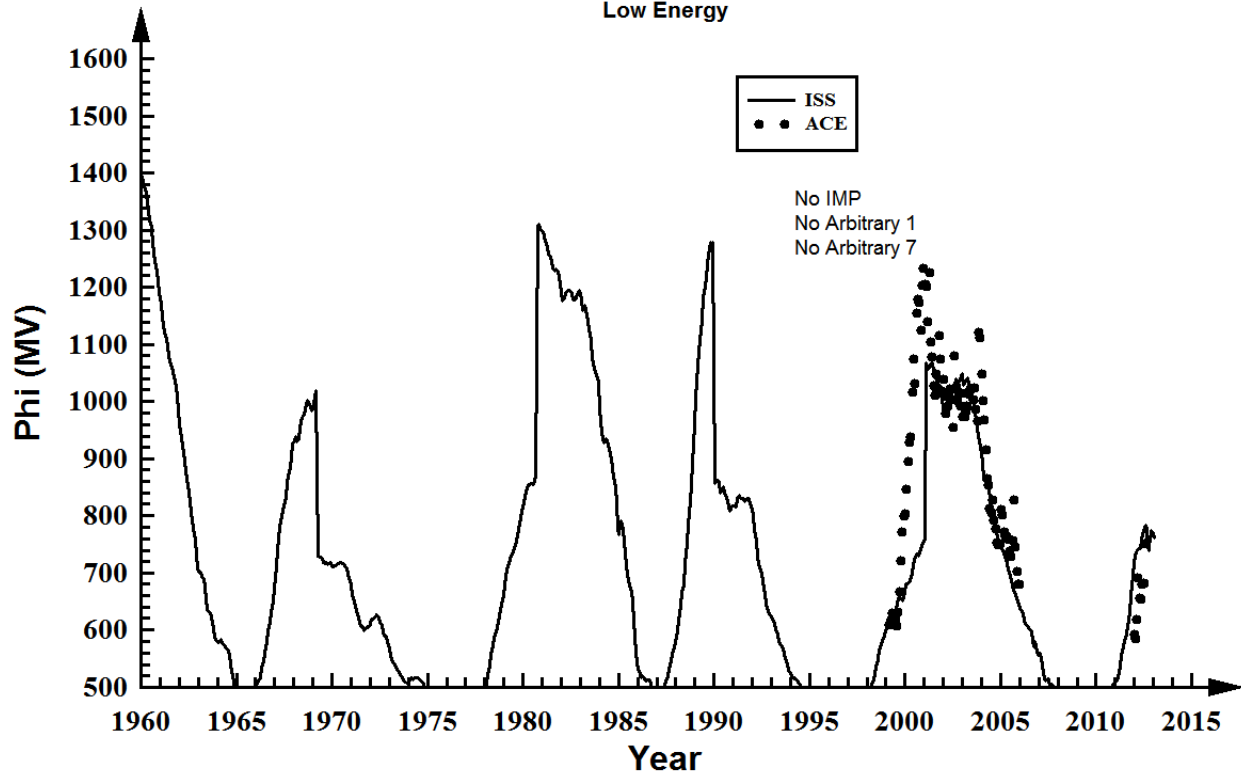


Sodium - Solar Minimum

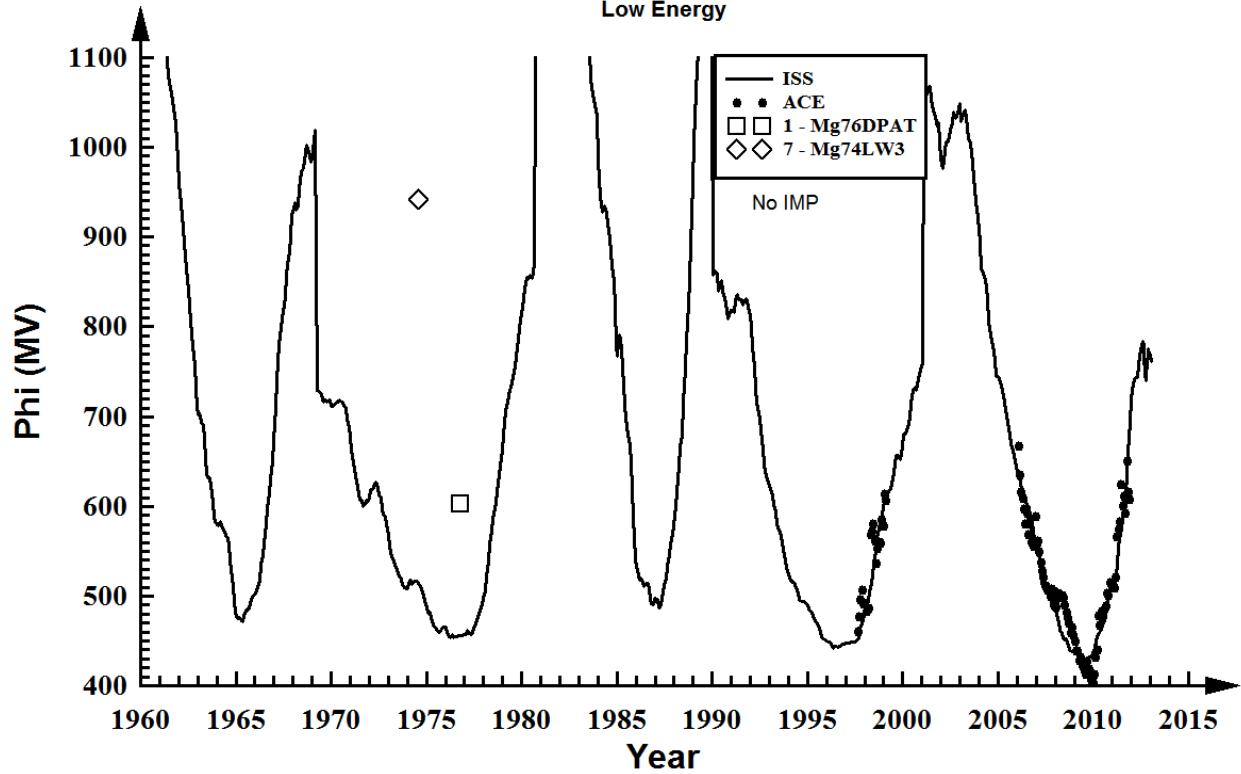
Low Energy



Magnesium - Solar Maximum Low Energy

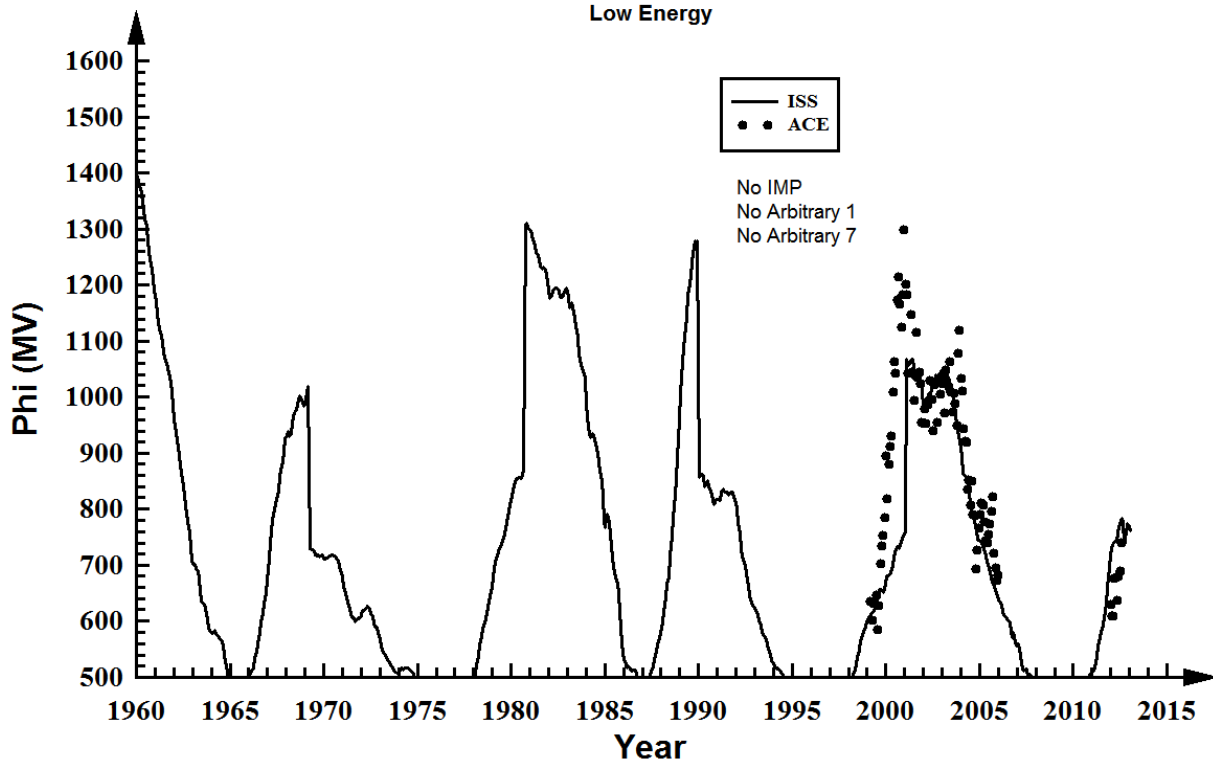


Magnesium - Solar Minimum Low Energy



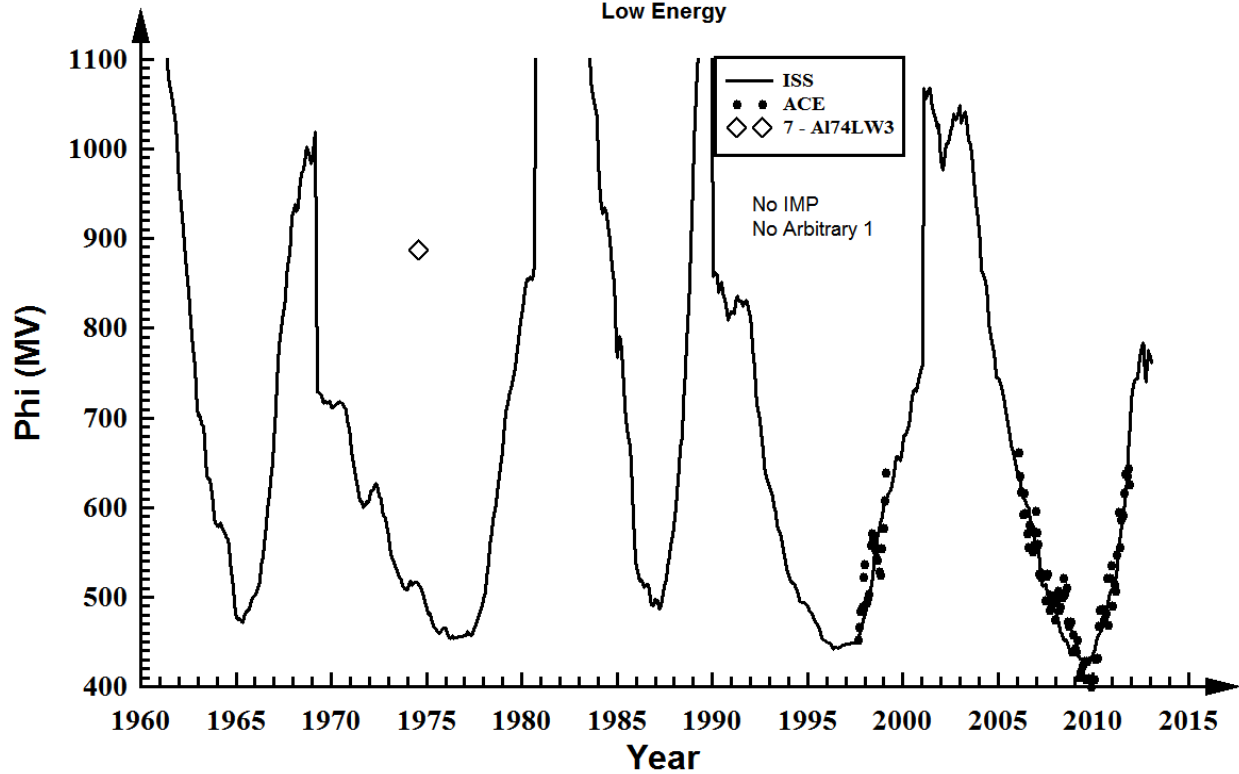
Aluminum - Solar Maximum

Low Energy



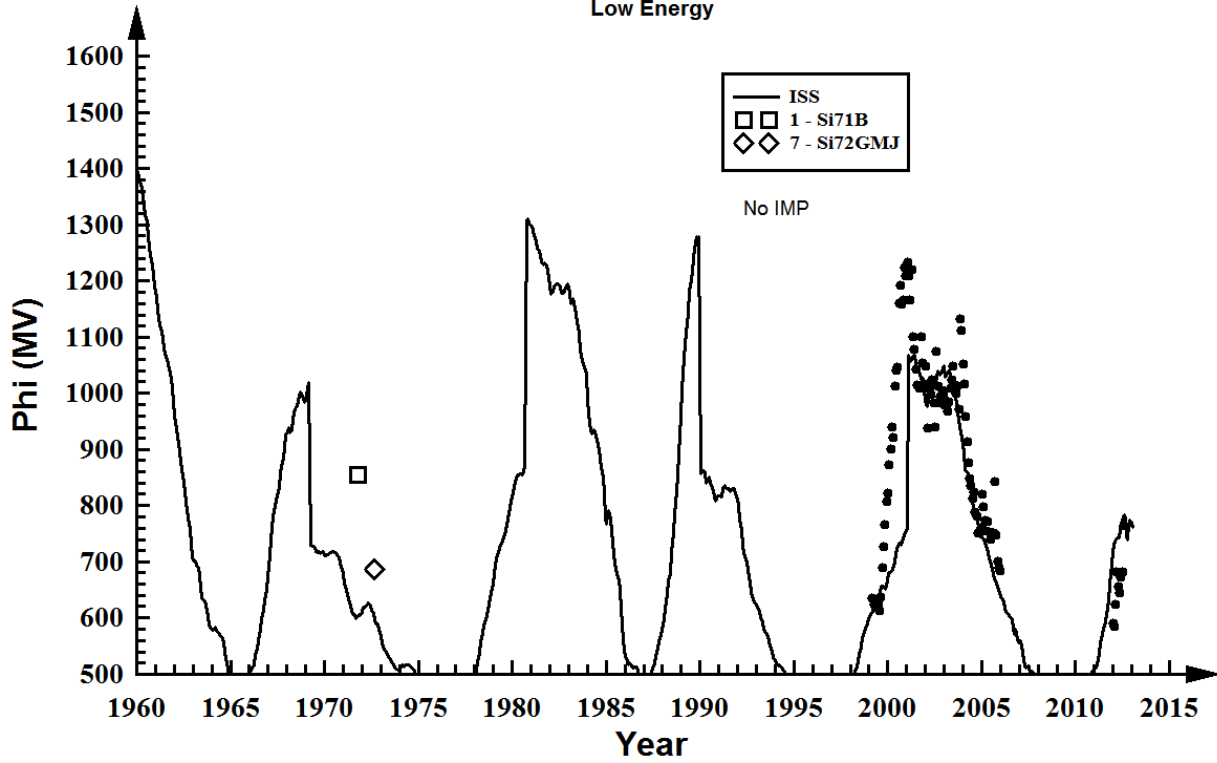
Aluminum - Solar Minimum

Low Energy



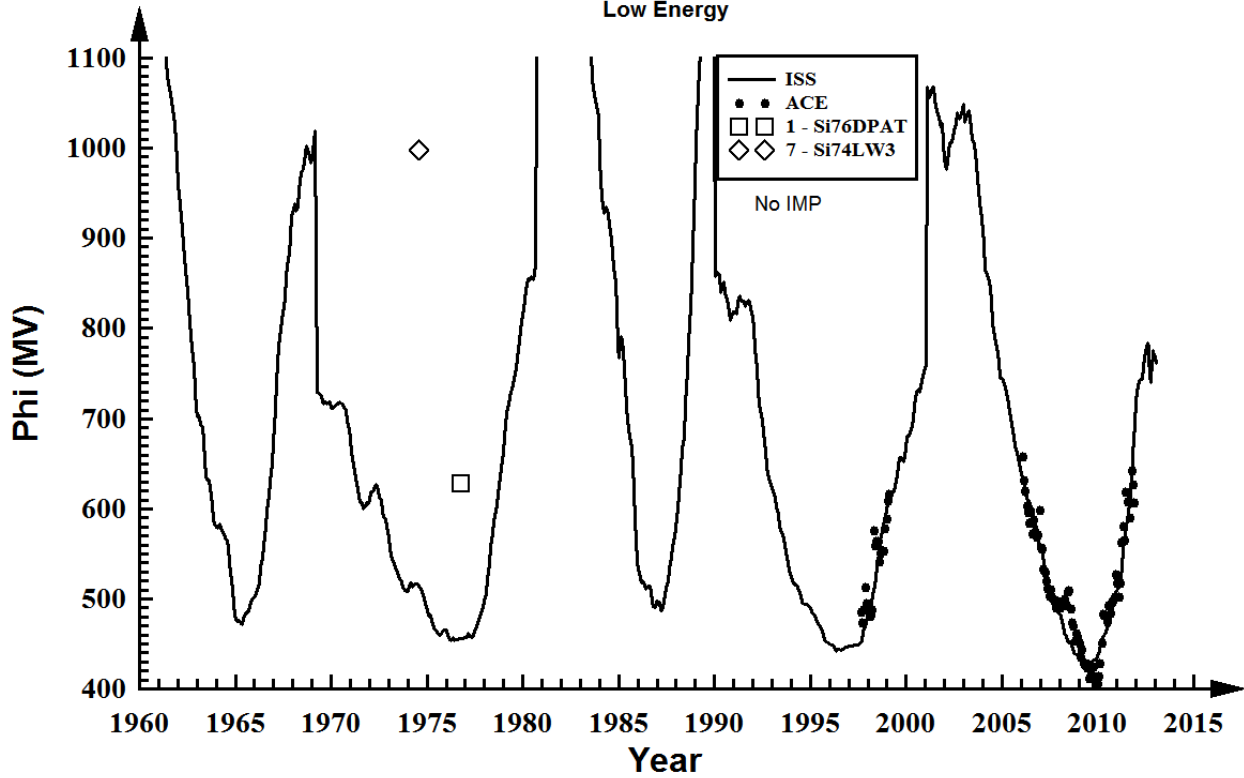
Silicon - Solar Maximum

Low Energy

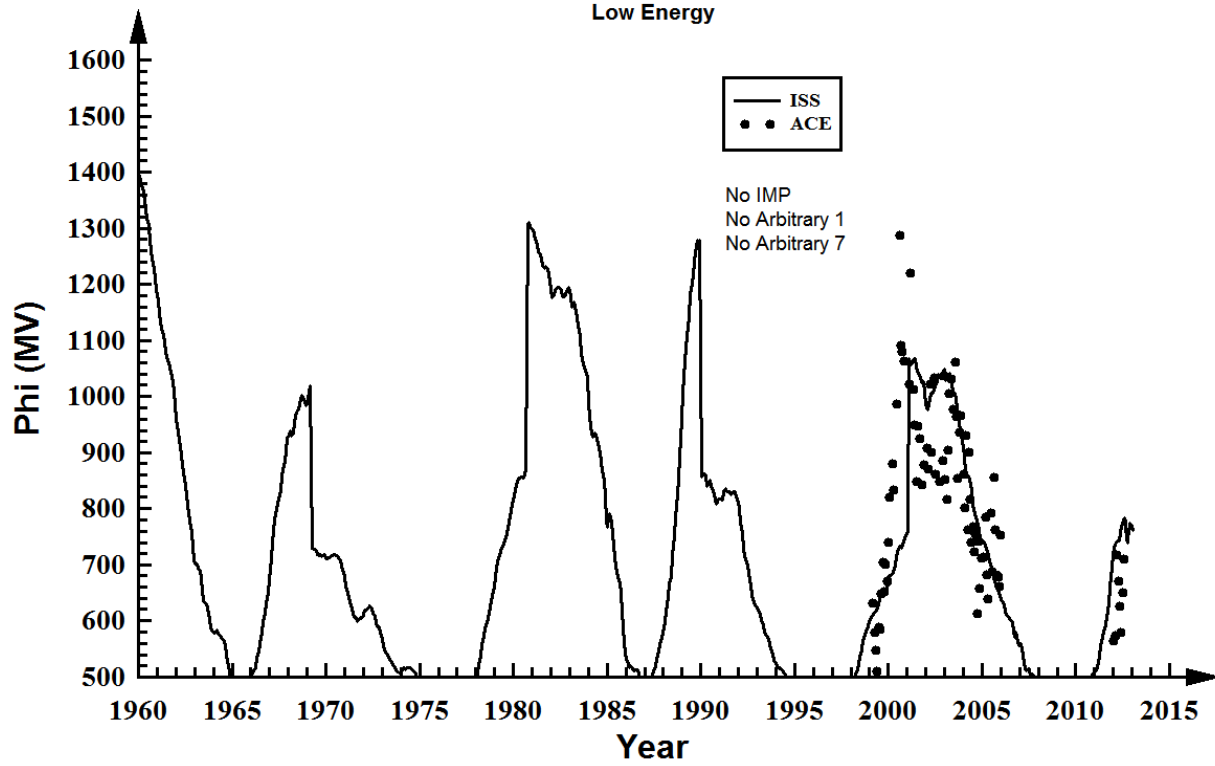


Silicon - Solar Minimum

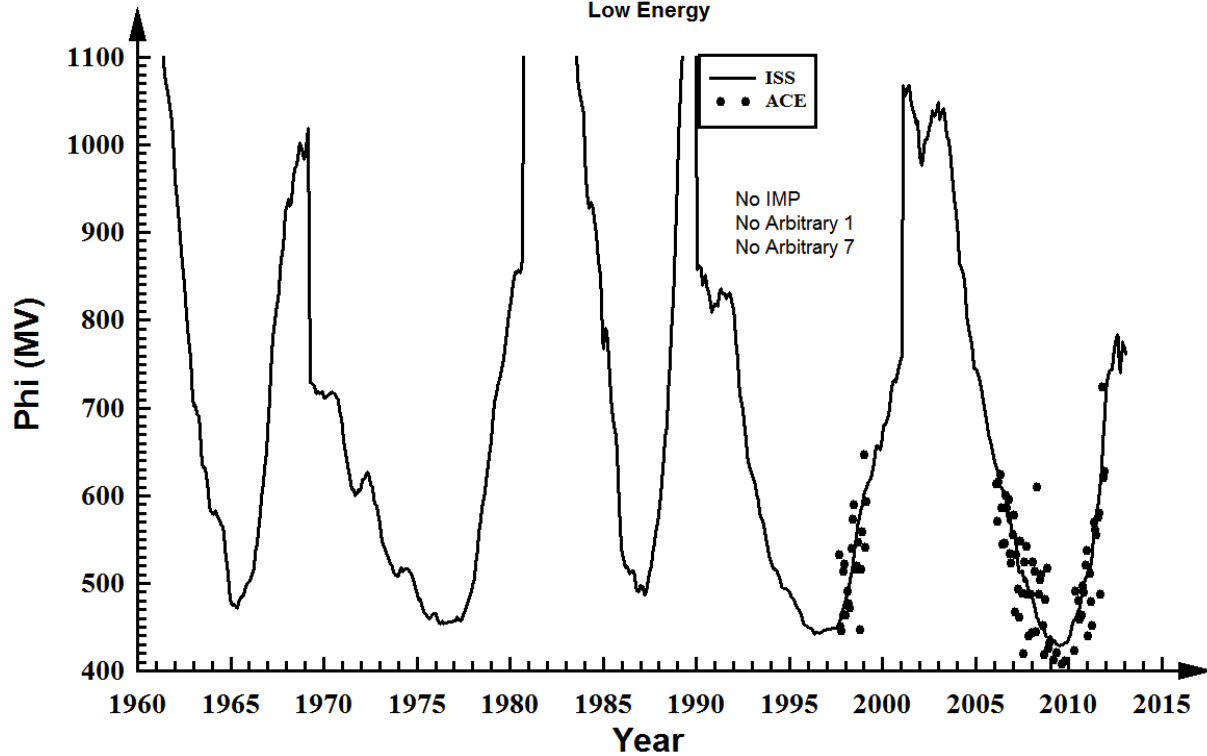
Low Energy



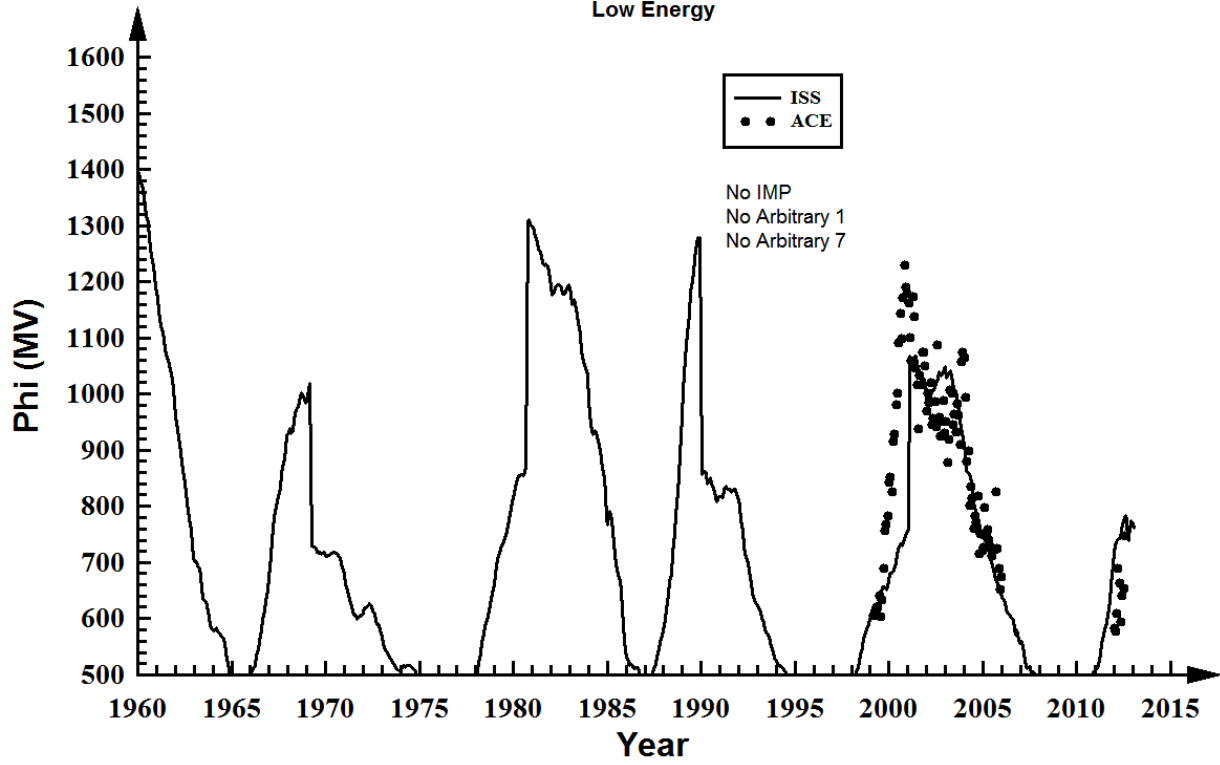
Phosphorus - Solar Maximum Low Energy



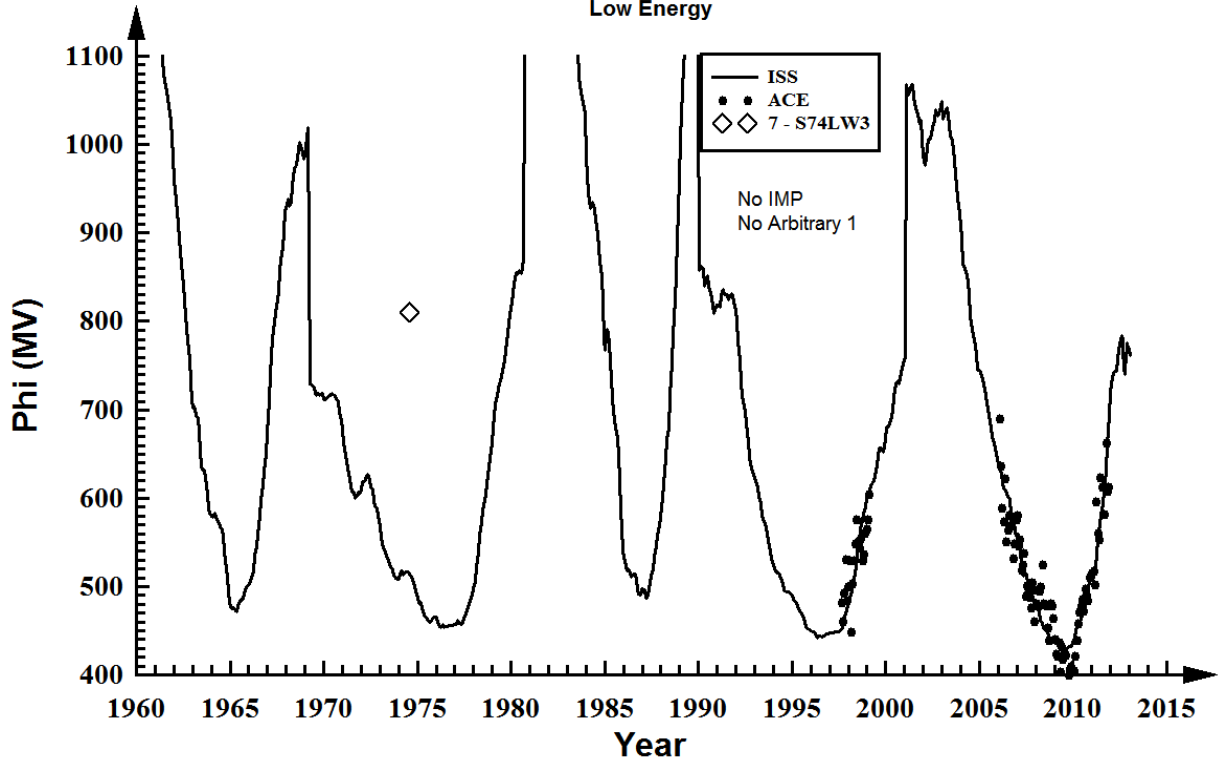
Phosphorus - Solar Minimum Low Energy



Sulfur - Solar Maximum Low Energy

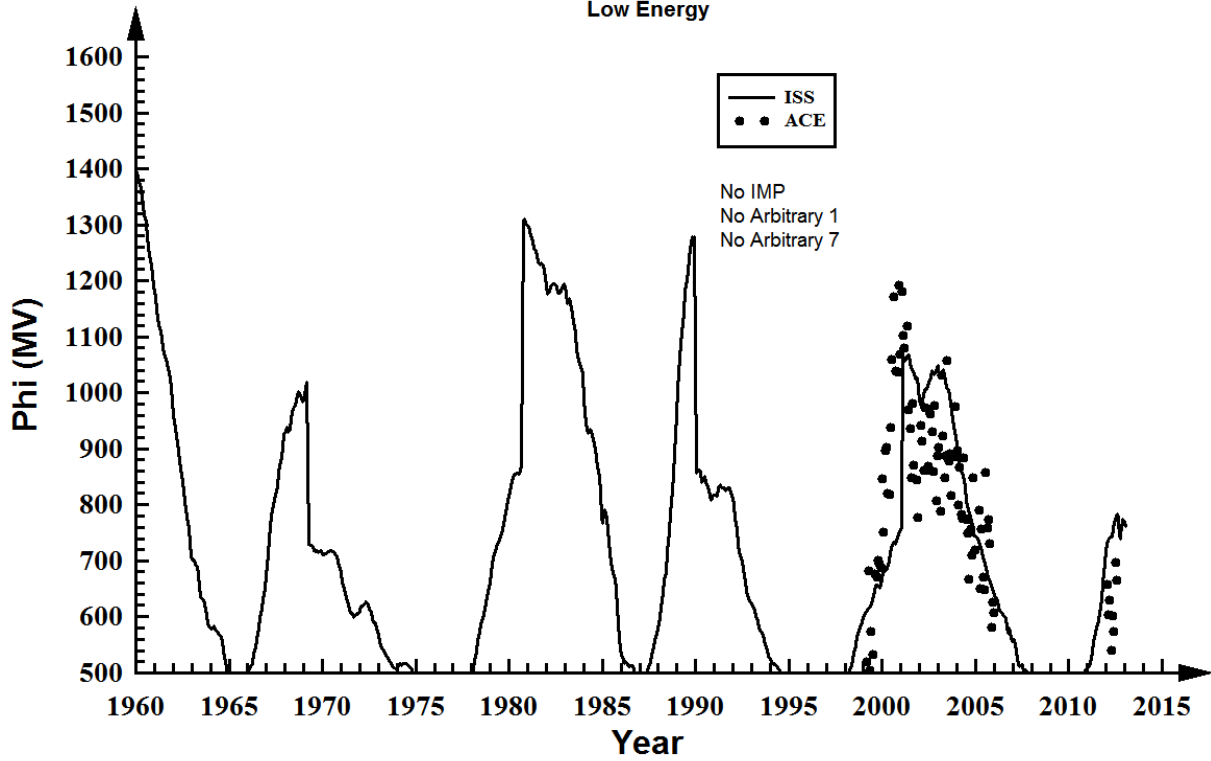


Sulfur - Solar Minimum Low Energy



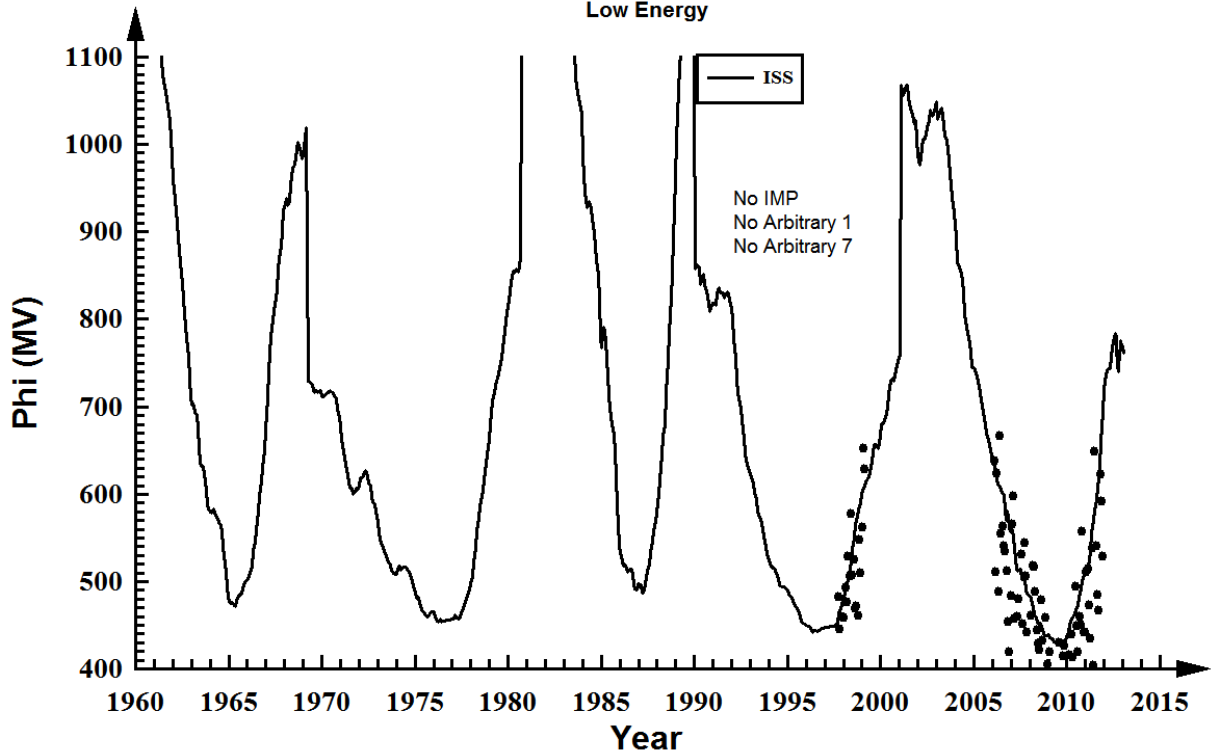
Chlorine - Solar Maximum

Low Energy

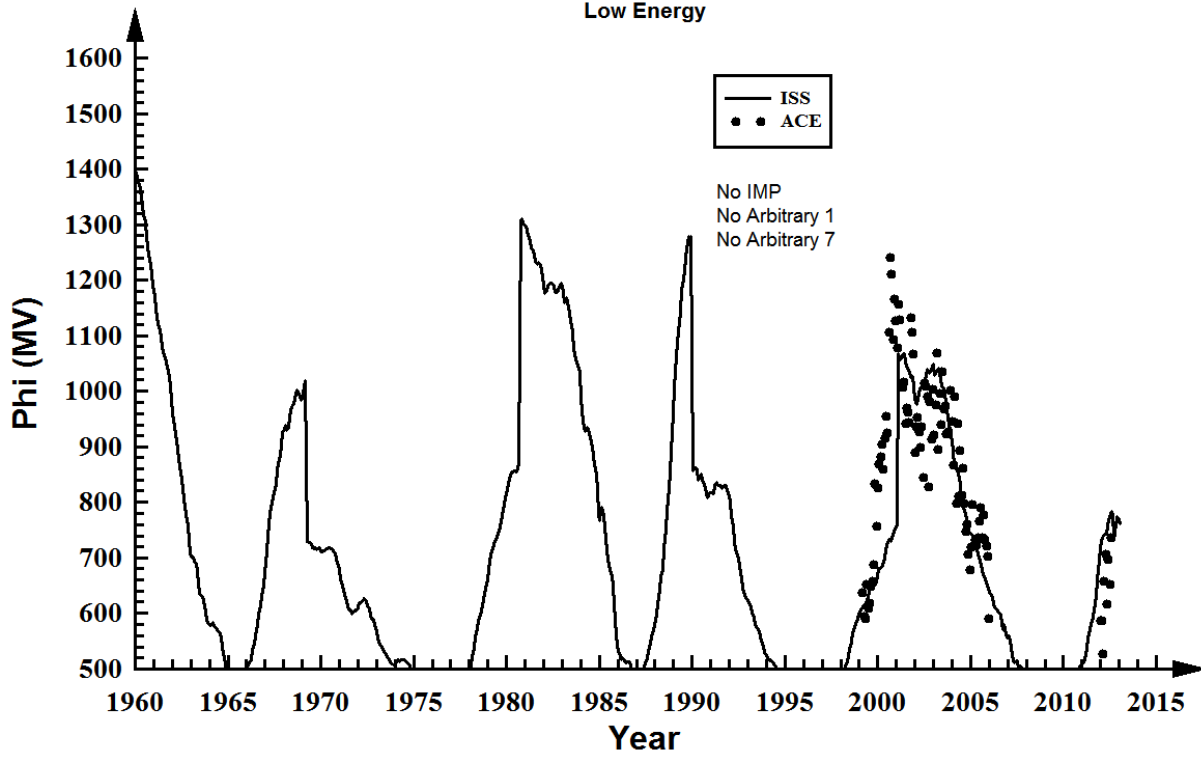


Chlorine - Solar Minimum

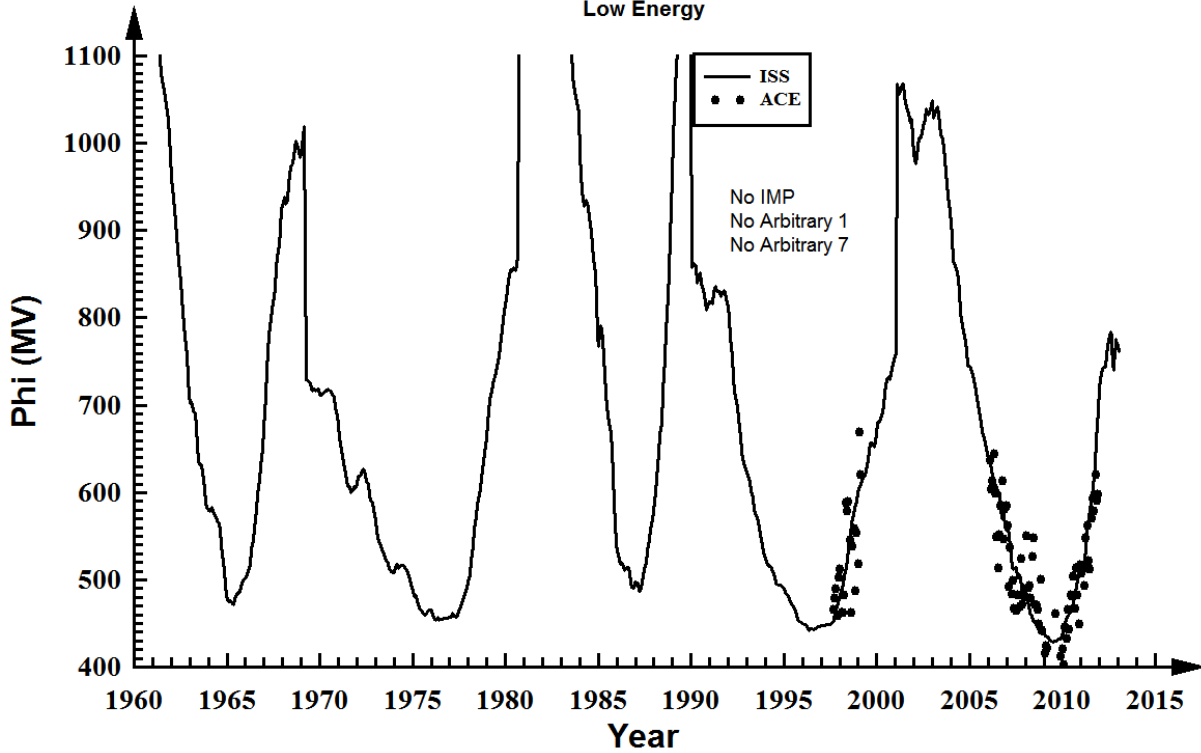
Low Energy



Argon - Solar Maximum Low Energy

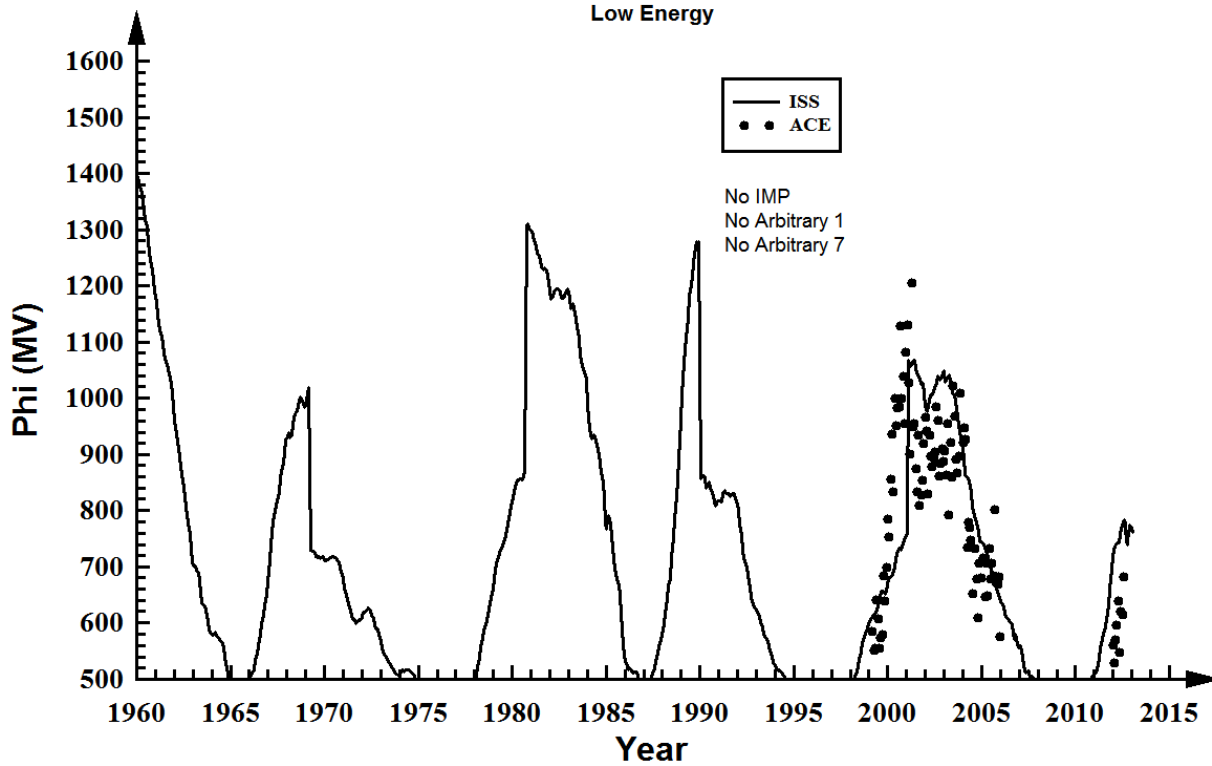


Argon - Solar Minimum Low Energy



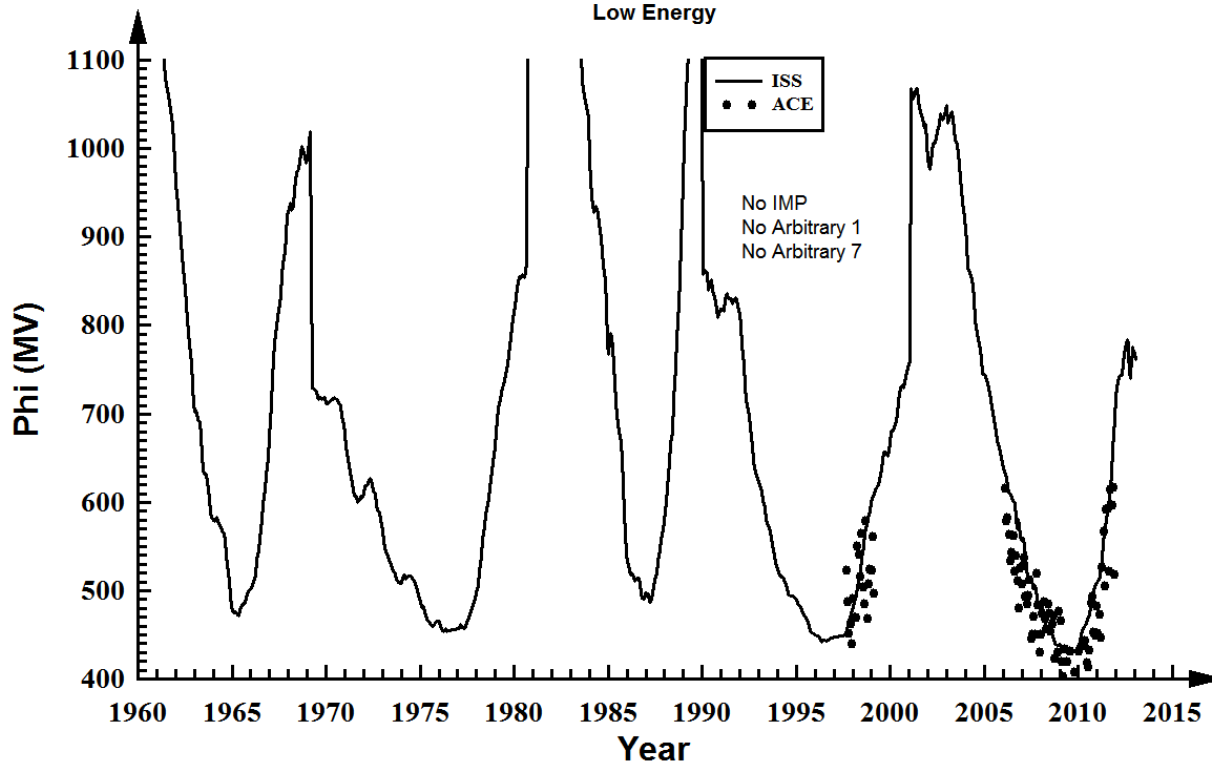
Potassium - Solar Maximum

Low Energy

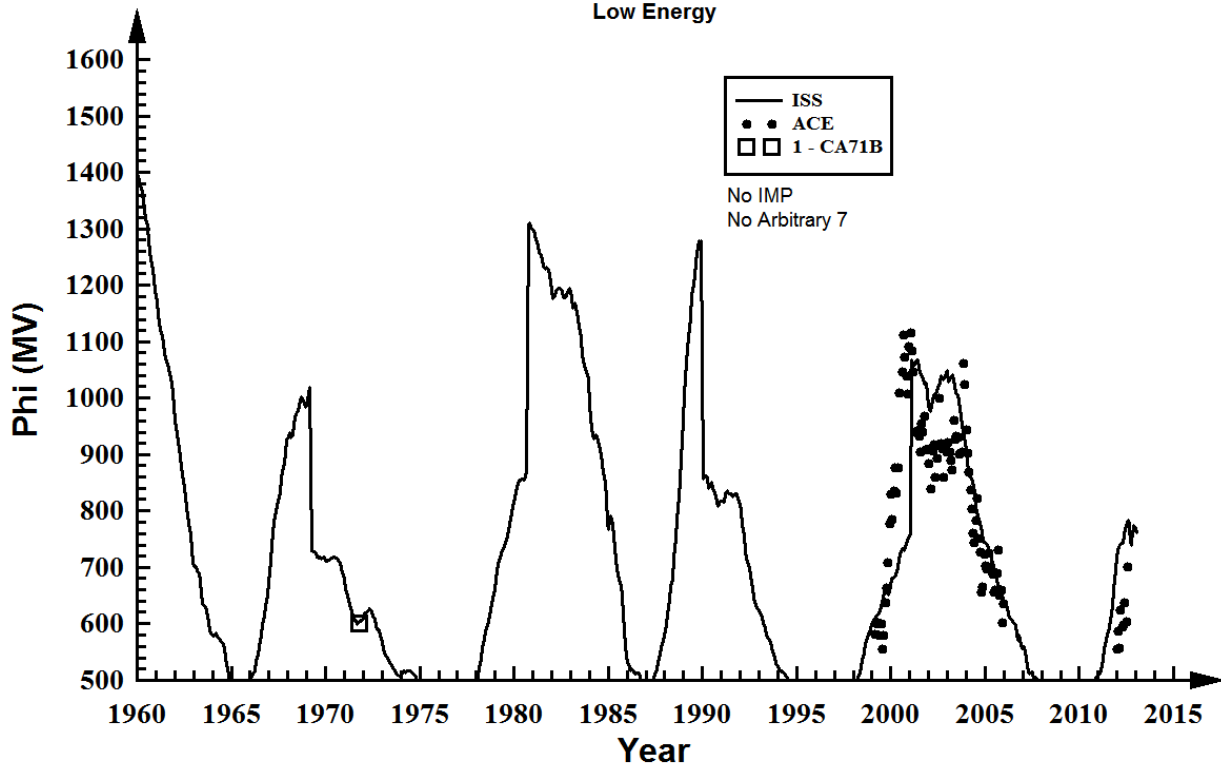


Potassium - Solar Minimum

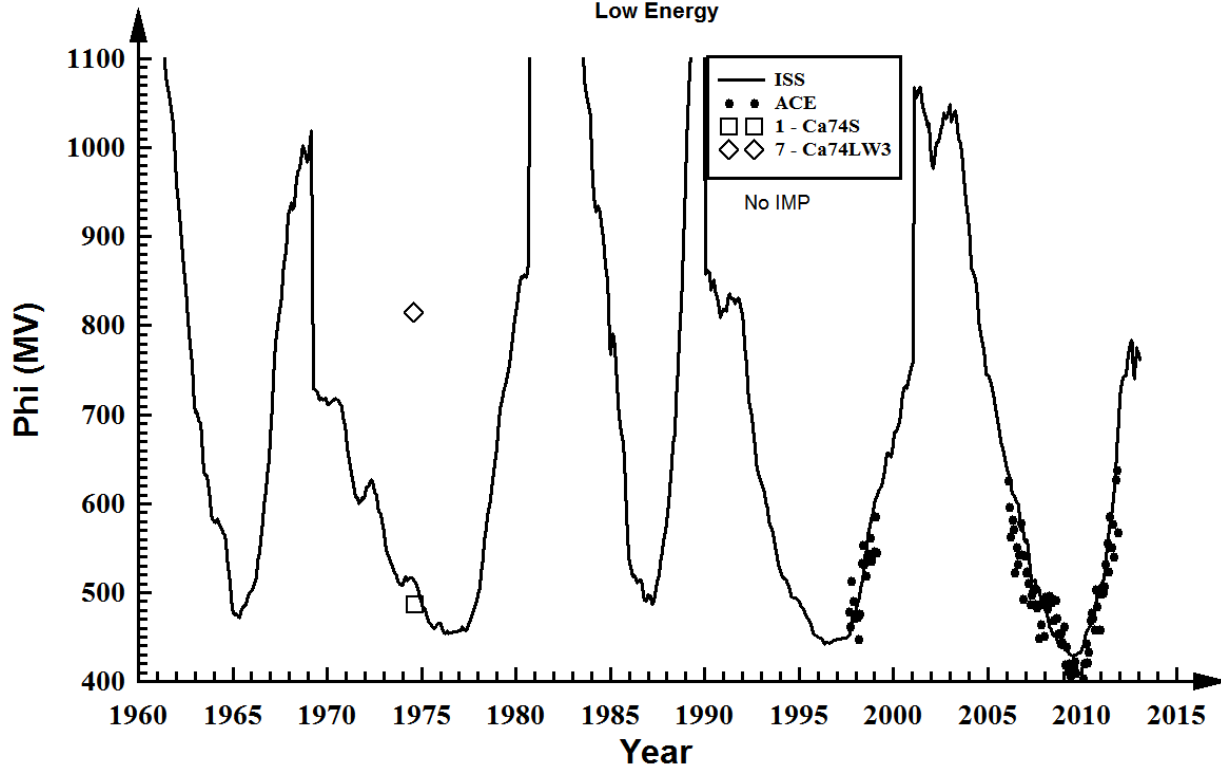
Low Energy



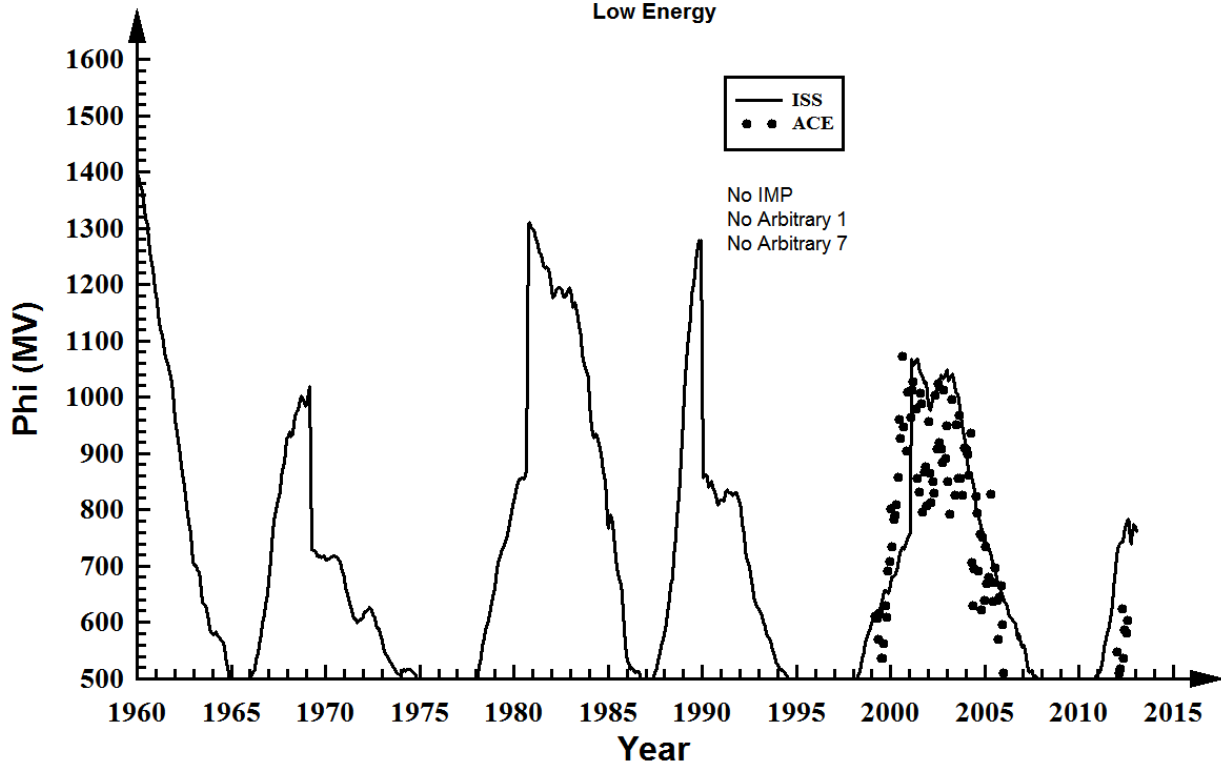
Calcium - Solar Maximum Low Energy



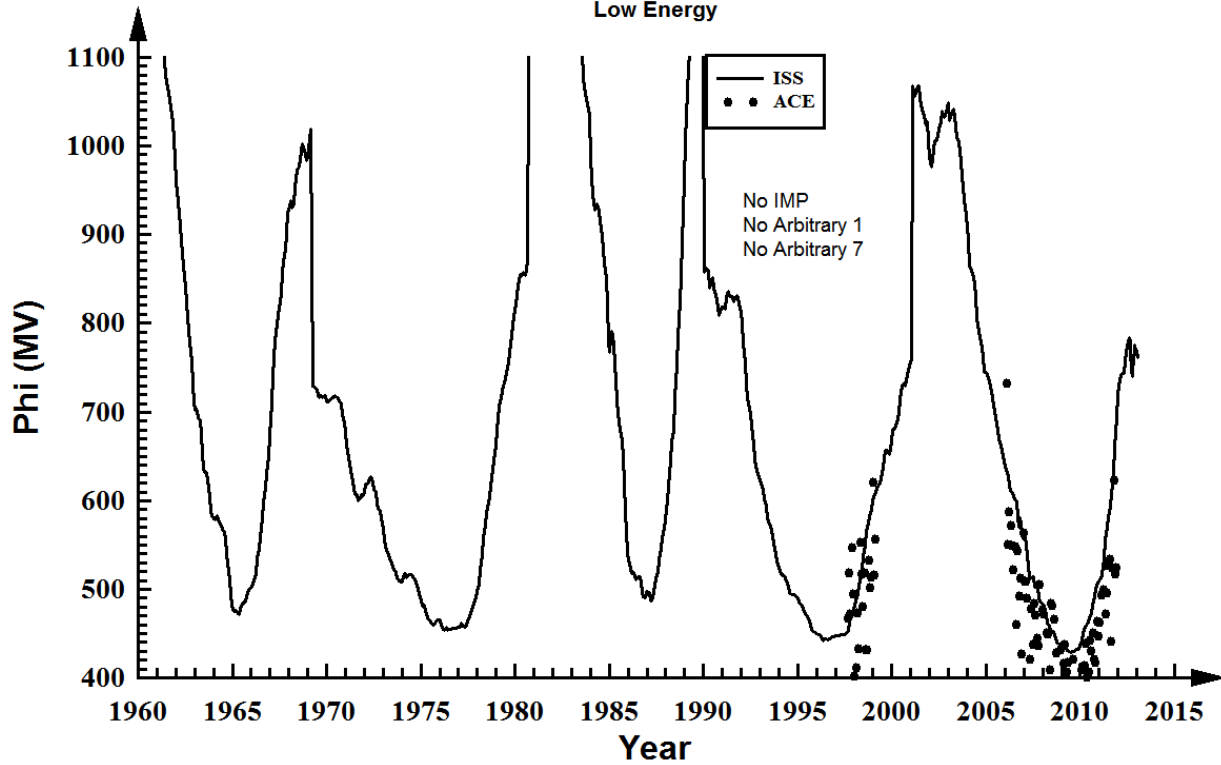
Calcium - Solar Minimum Low Energy



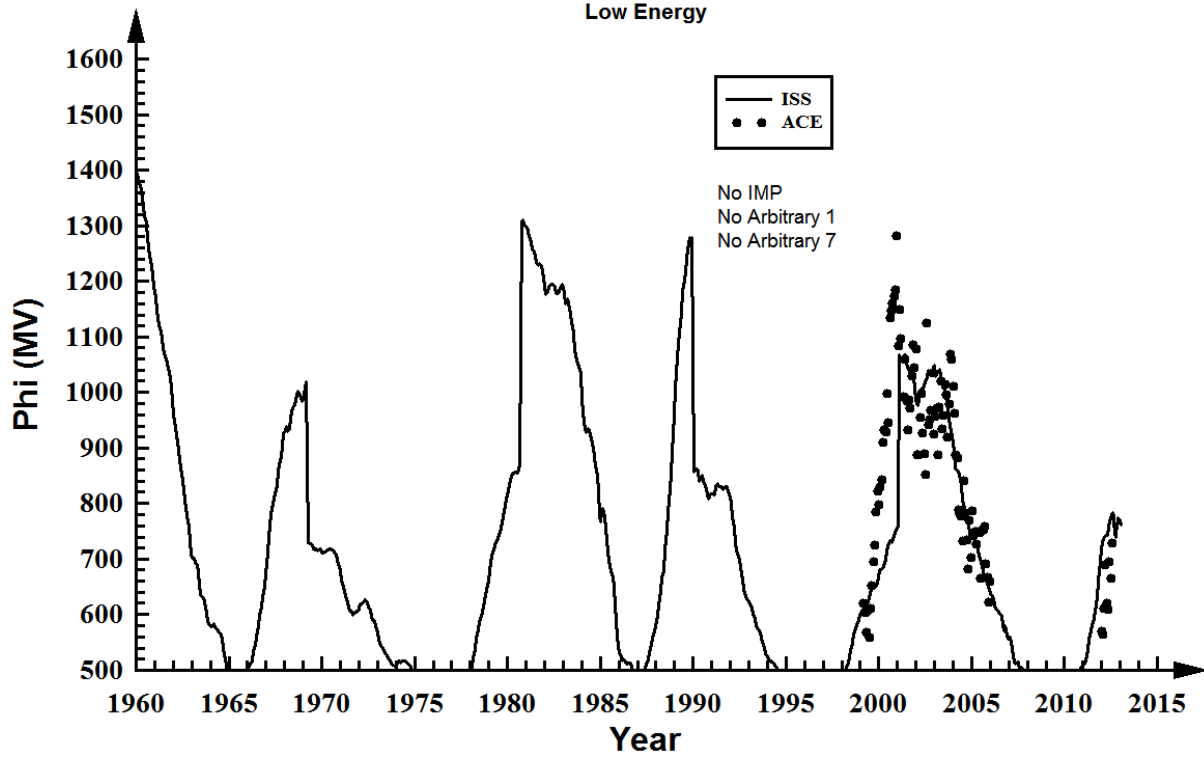
Scandium - Solar Maximum Low Energy



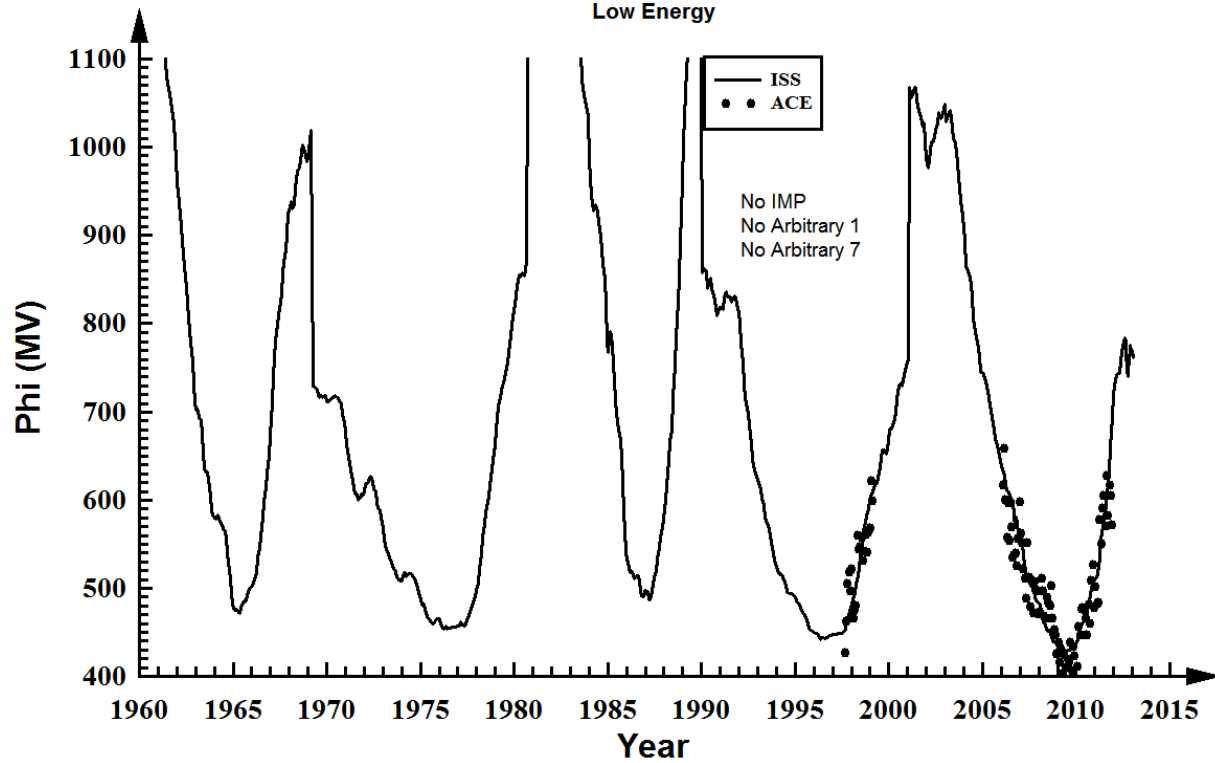
Scandium - Solar Minimum Low Energy



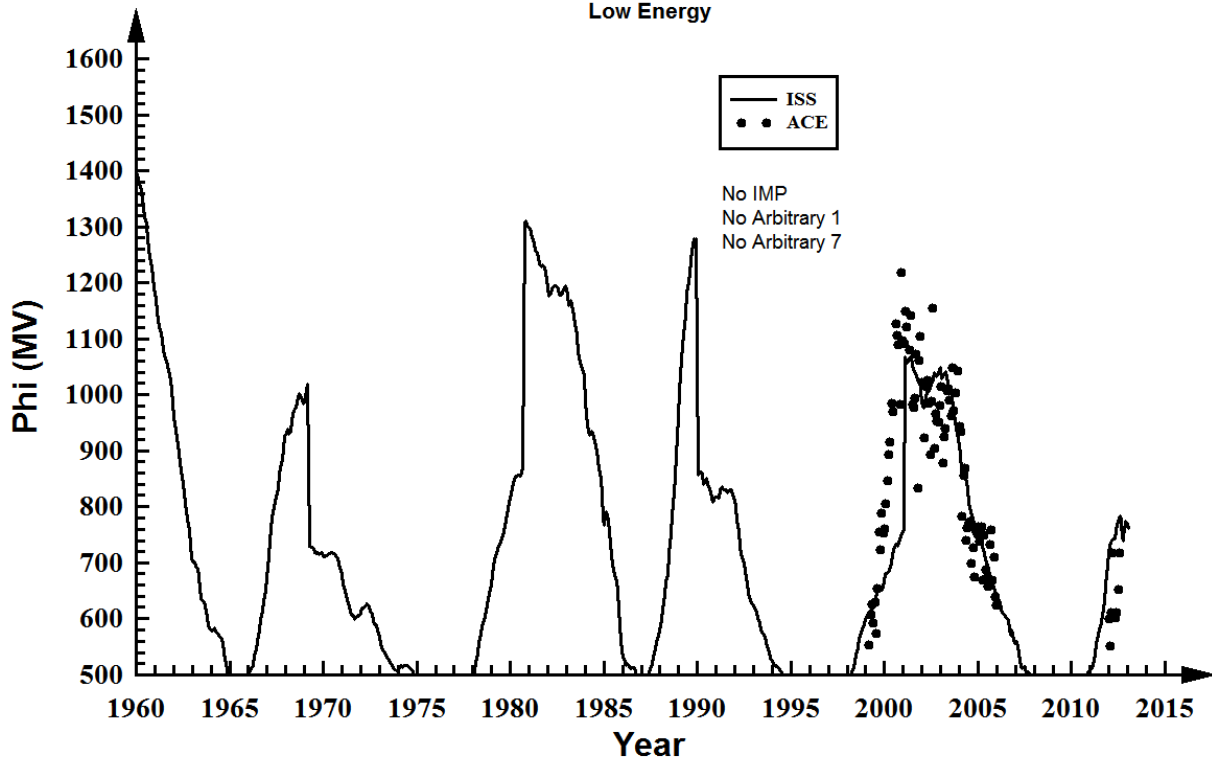
Titanium - Solar Maximum Low Energy



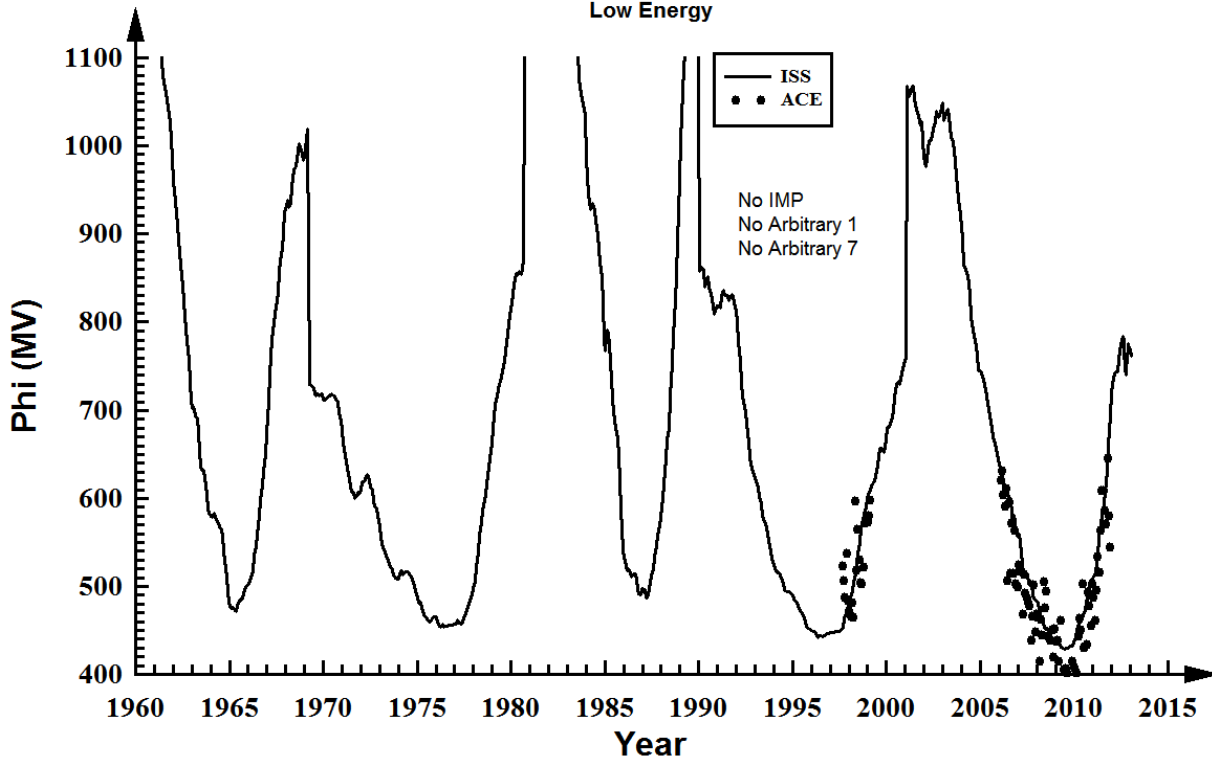
Titanium - Solar Minimum Low Energy



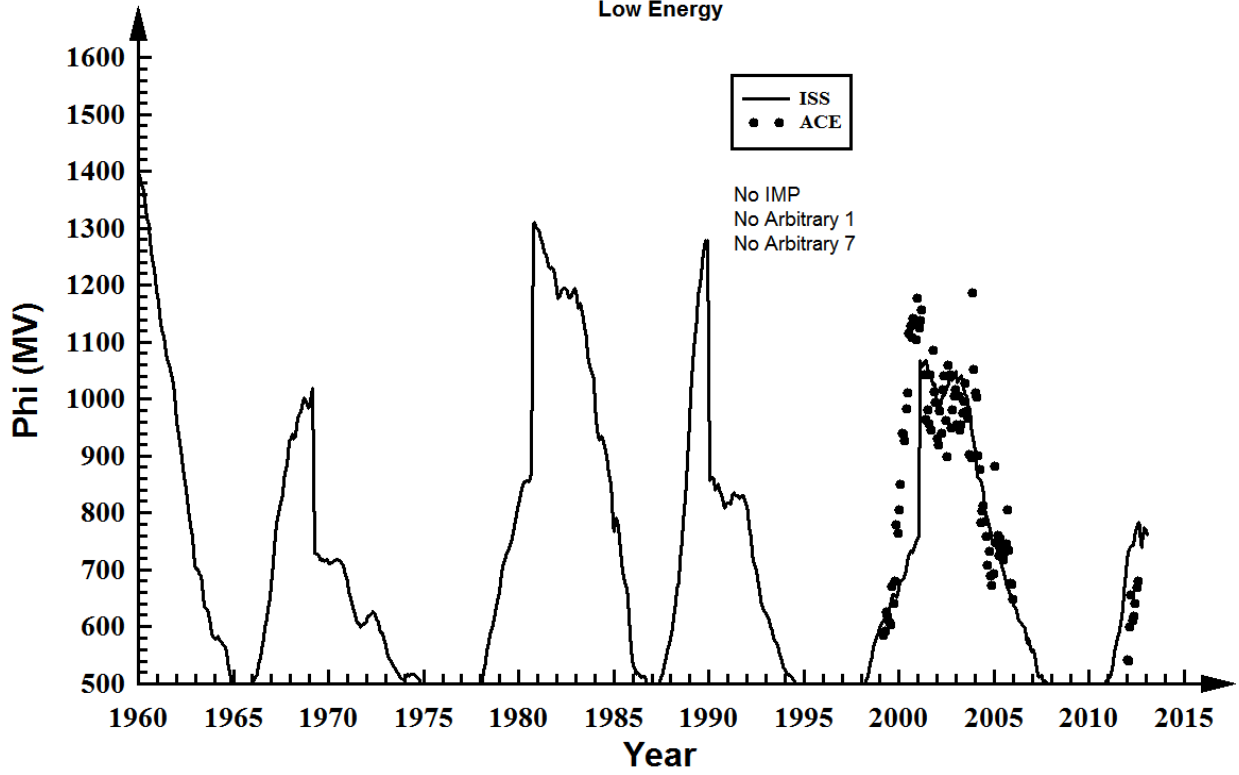
Vanadium - Solar Maximum Low Energy



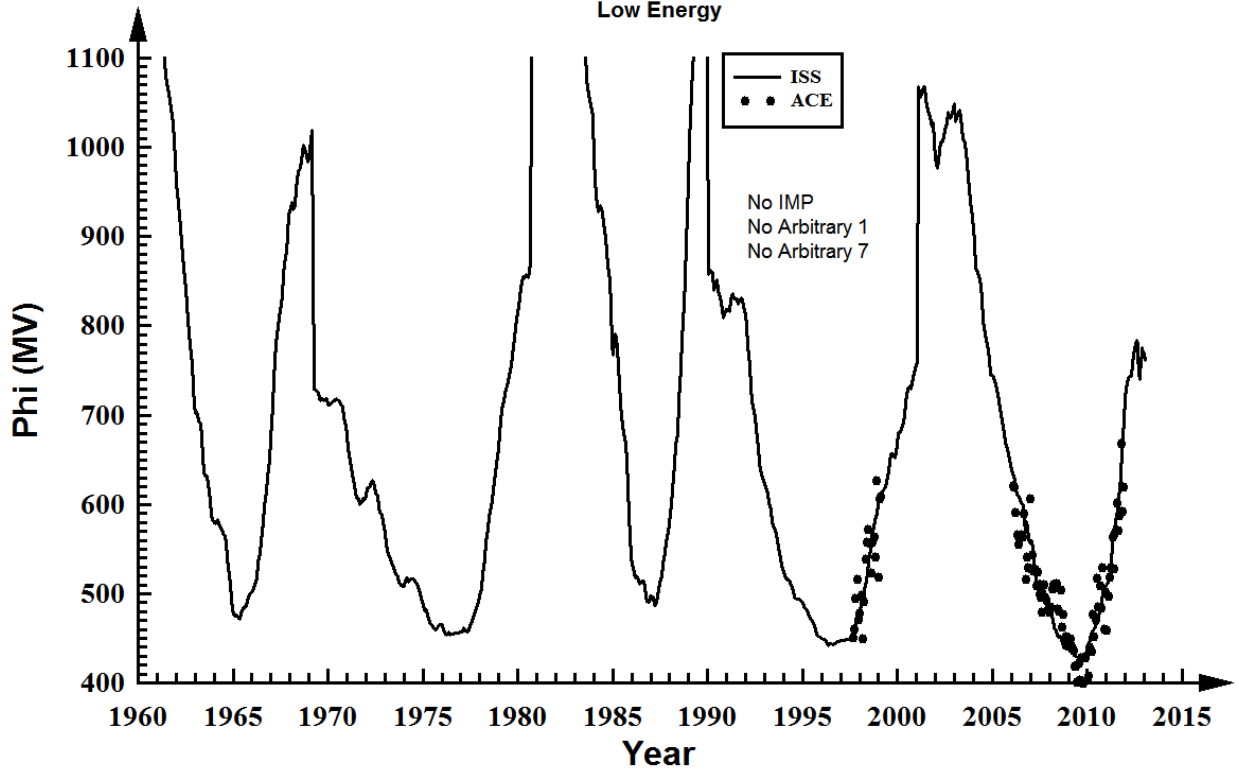
Vanadium - Solar Minimum Low Energy



Chromium - Solar Maximum Low Energy

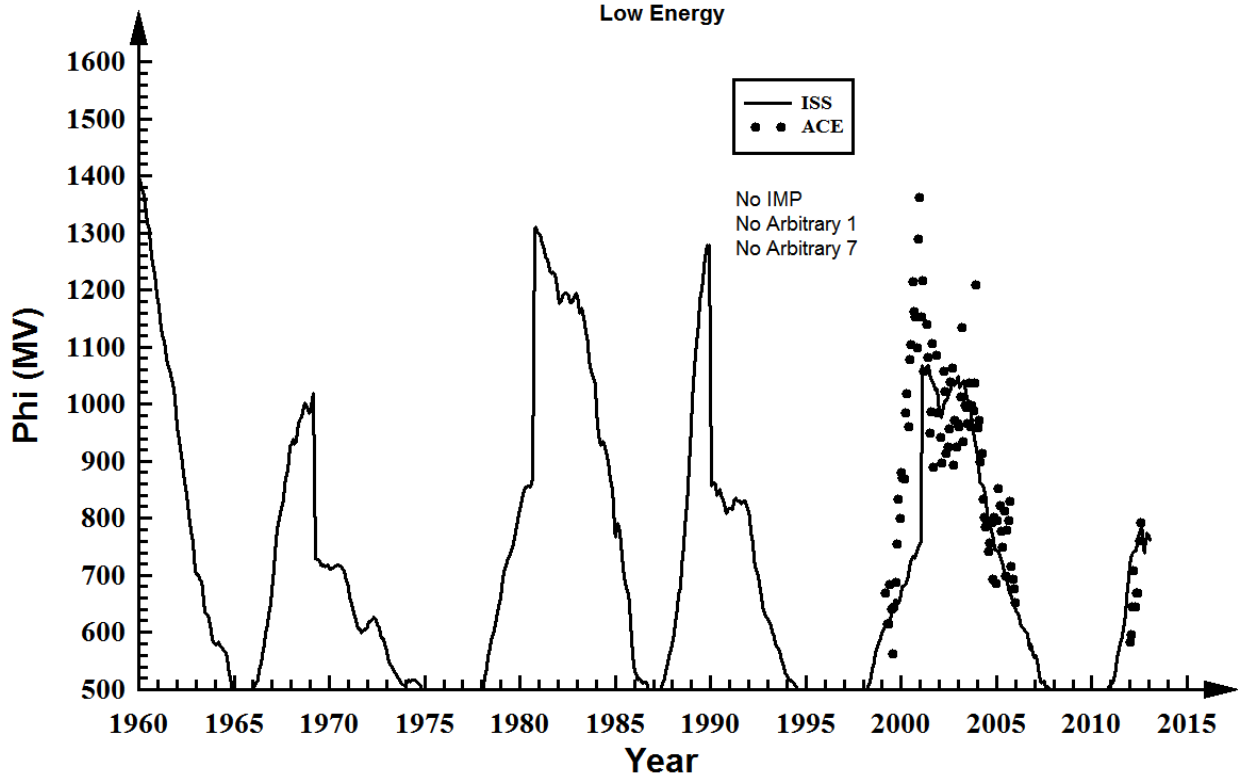


Chromium - Solar Minimum Low Energy



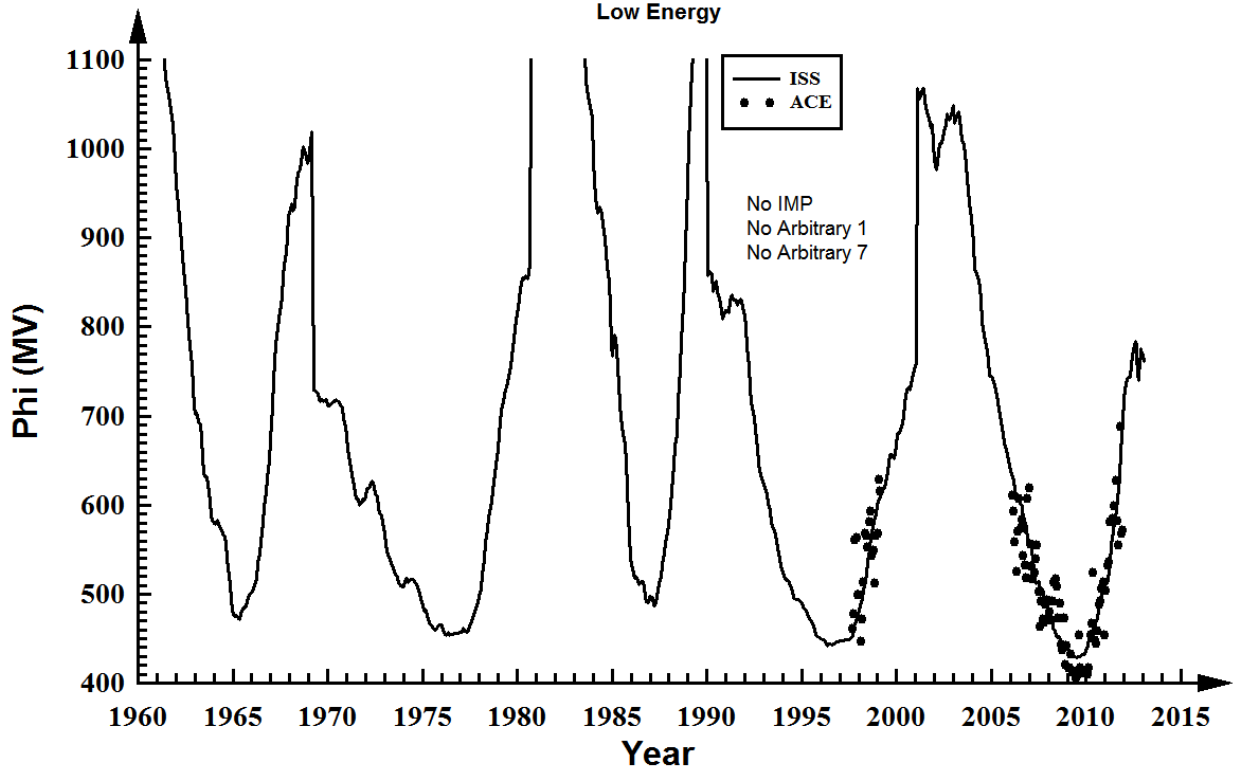
Manganese - Solar Maximum

Low Energy



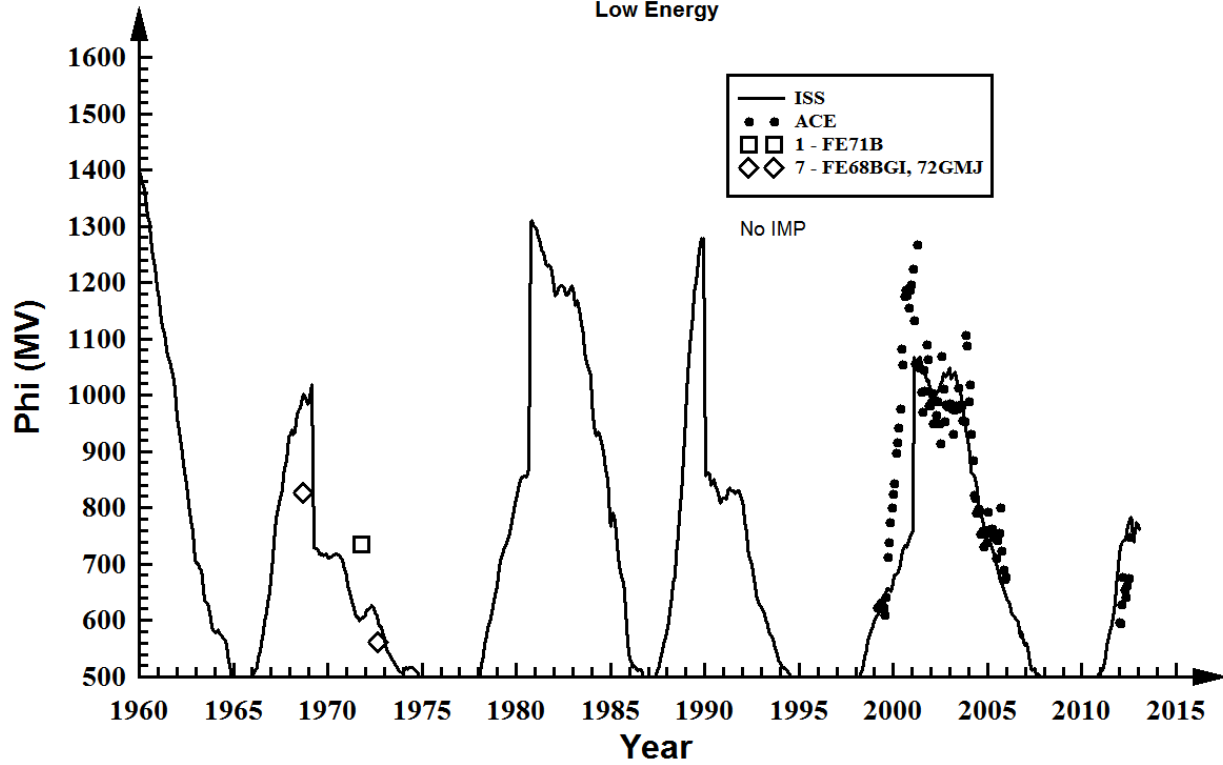
Manganese - Solar Minimum

Low Energy



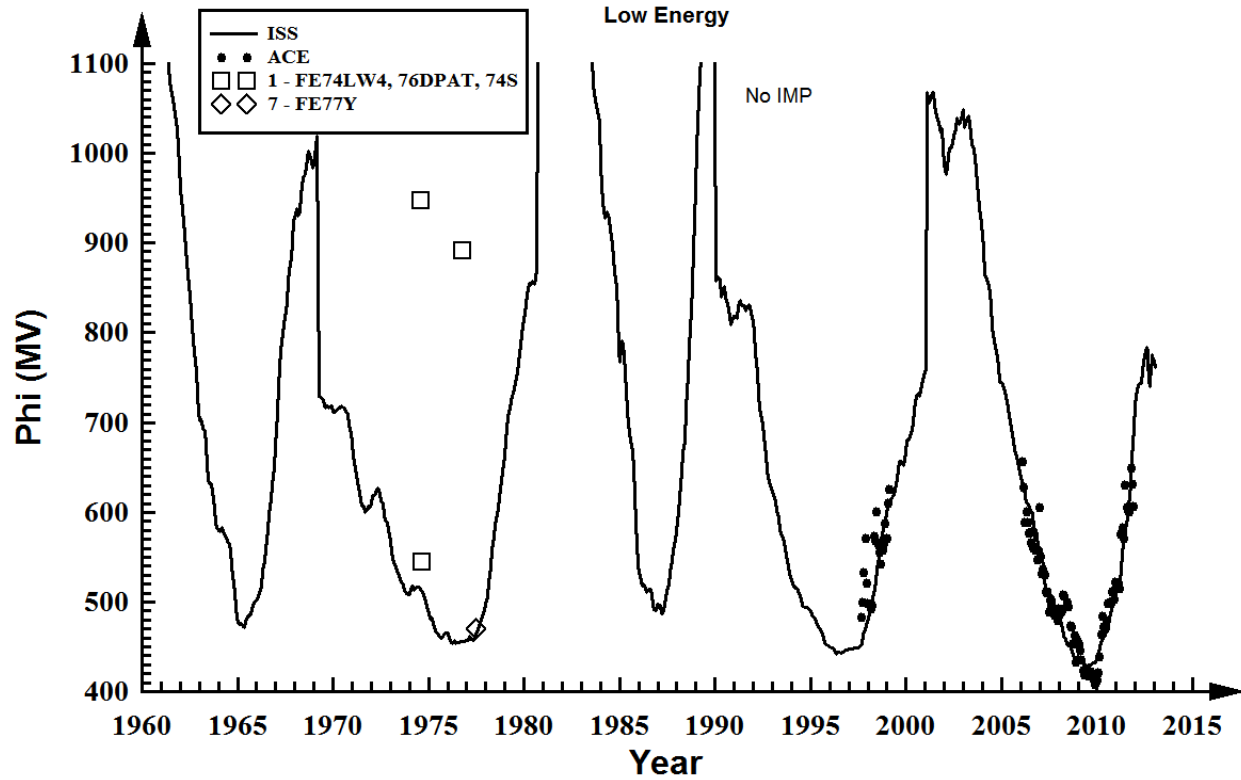
Iron - Solar Maximum

Low Energy

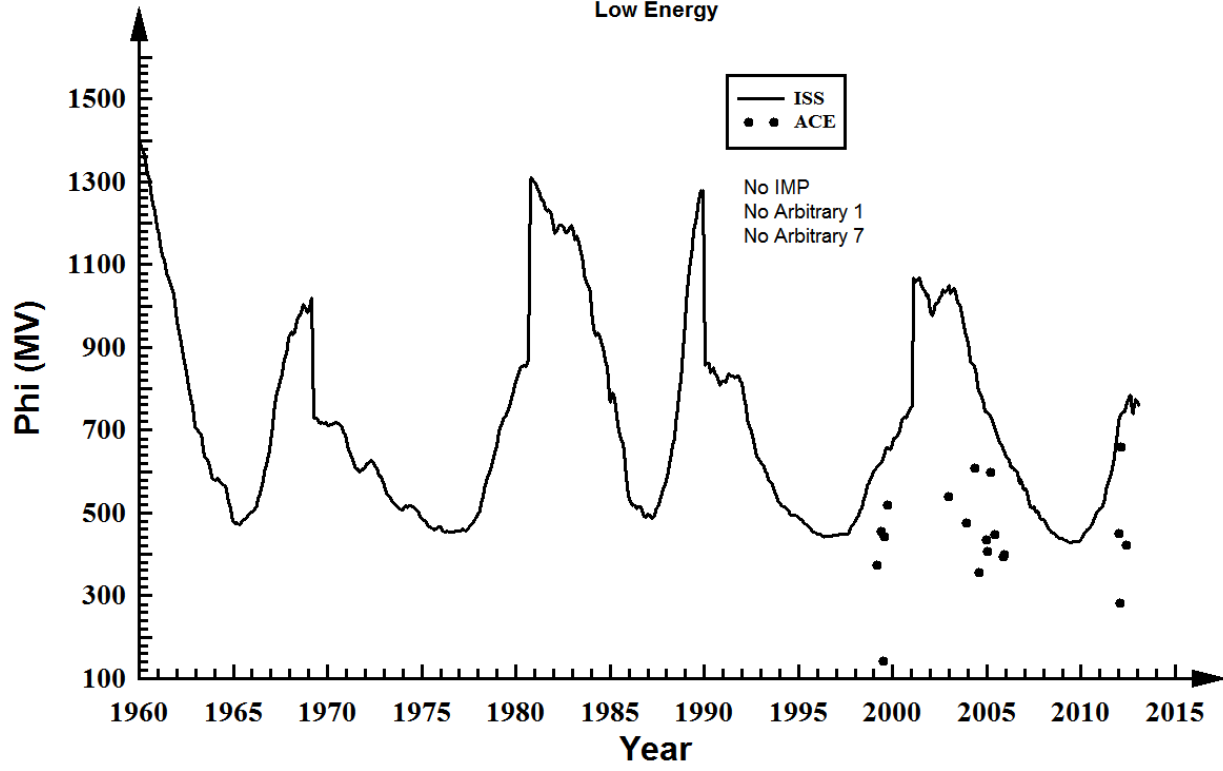


Iron - Solar Minimum

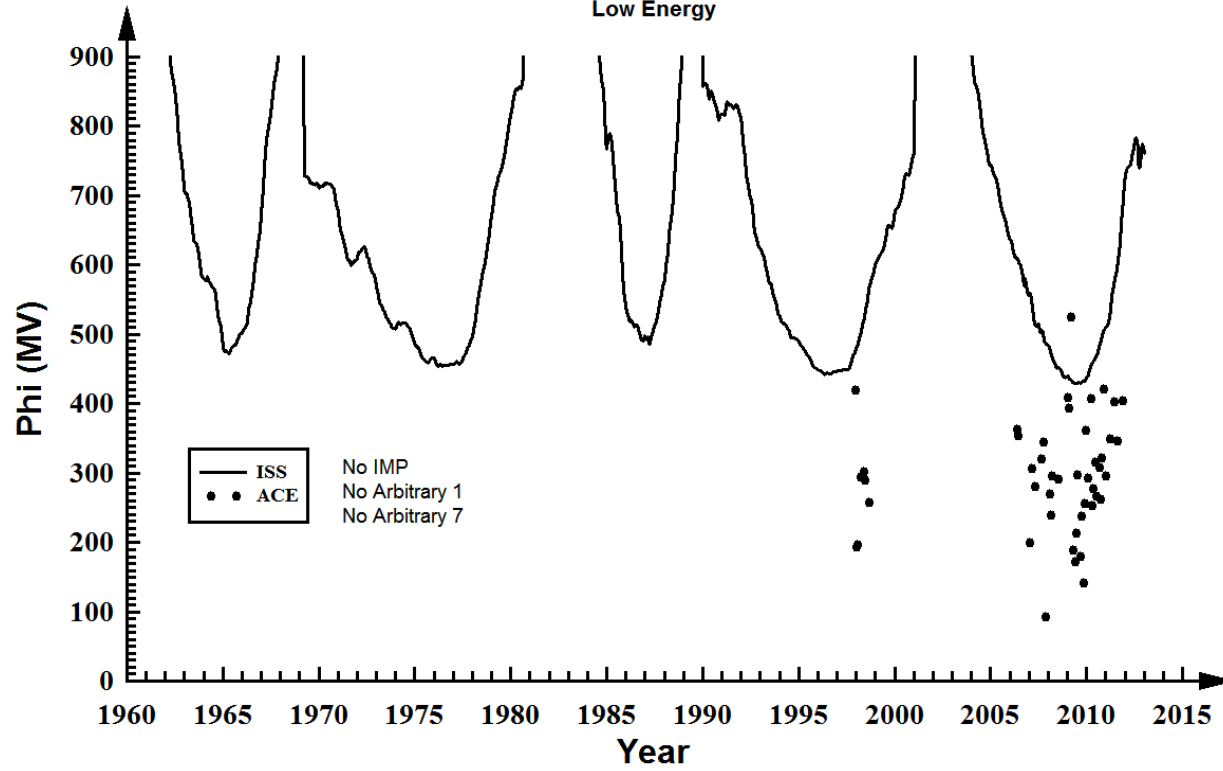
Low Energy



Cobalt - Solar Maximum Low Energy

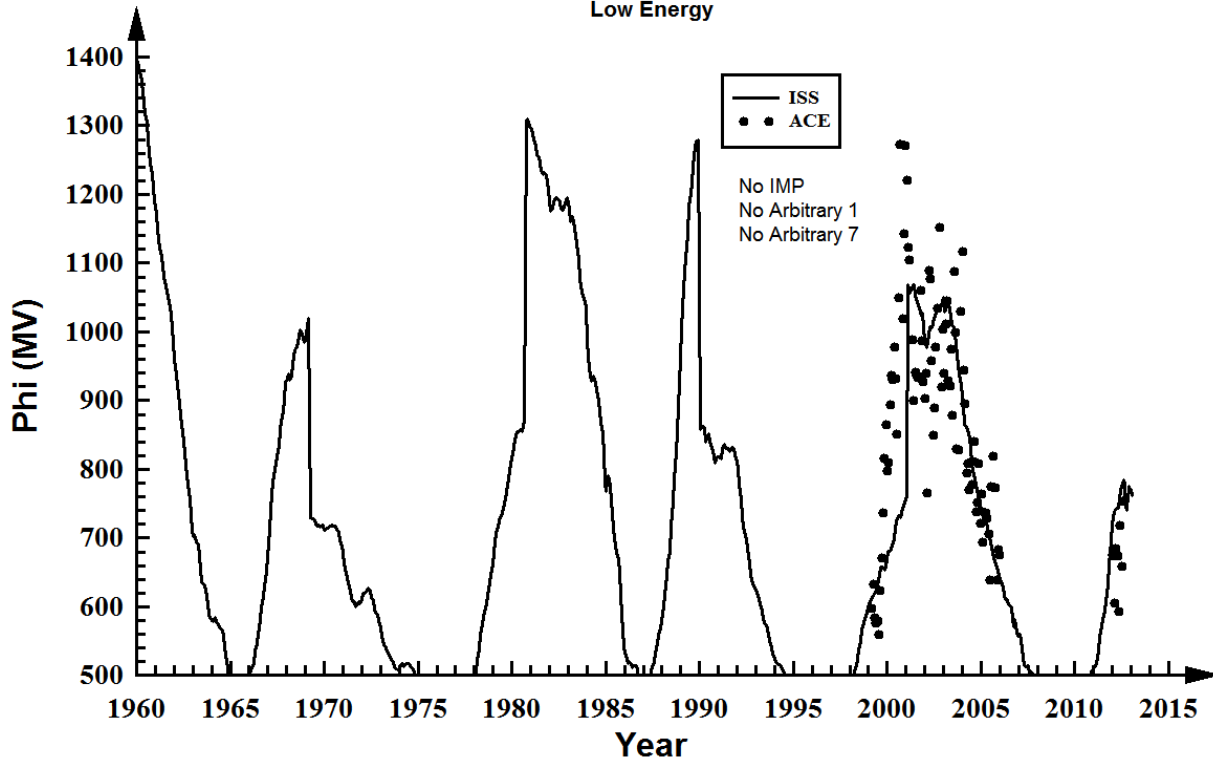


Cobalt - Solar Minimum Low Energy



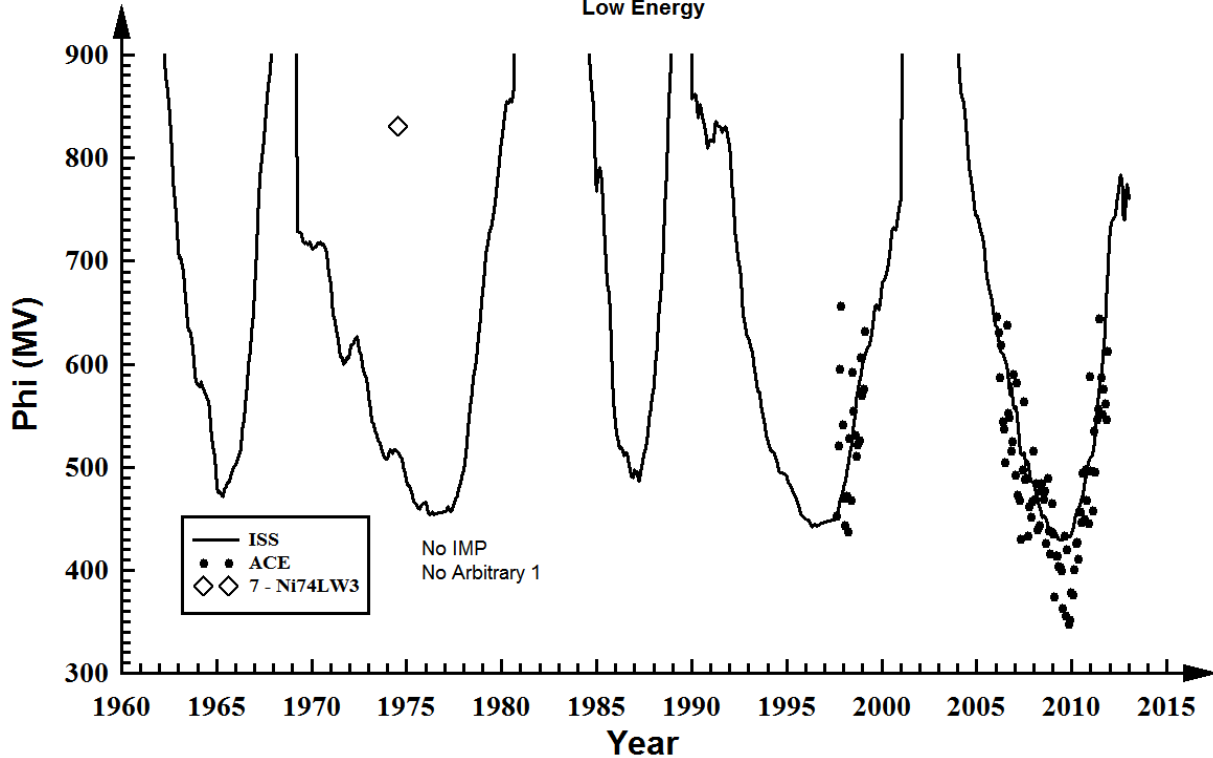
Nickel - Solar Maximum

Low Energy



Nickel - Solar Minimum

Low Energy



REPORT DOCUMENTATION PAGE			Form Approved OMB No. 0704-0188	
Public reporting burden for this collection of information is estimated to average 1 hour per response, including the time for reviewing instructions, searching existing data sources, gathering and maintaining the data needed, and completing and reviewing the collection of information. Send comments regarding this burden estimate or any other aspect of this collection of information, including suggestions for reducing this burden, to Washington Headquarters Services, Directorate for Information Operations and Reports, 1215 Jefferson Davis Highway, Suite 1204, Arlington, VA 22202-4302, and to the Office of Management and Budget, Paperwork Reduction Project (0704-0188), Washington, DC 20503.				
1. AGENCY USE ONLY (Leave Blank)	2. REPORT DATE June 2013	3. REPORT TYPE AND DATES COVERED Technical Publication		
4. TITLE AND SUBTITLE Badhwar-O'Neill 2011 Galactic Cosmic Ray Flux Model Description			5. FUNDING NUMBERS	
6. AUTHOR(S) Engineering Directorate Avionic Systems Division				
7. PERFORMING ORGANIZATION NAME(S) AND ADDRESS(ES) Lyndon B. Johnson Space Center Houston, Texas 77058			8. PERFORMING ORGANIZATION REPORT NUMBERS S-1139	
9. SPONSORING/MONITORING AGENCY NAME(S) AND ADDRESS(ES) National Aeronautics and Space Administration Washington, DC 20546-0001			10. SPONSORING/MONITORING AGENCY REPORT NUMBER TP-2013-217376	
11. SUPPLEMENTARY NOTES				
12a. DISTRIBUTION/AVAILABILITY STATEMENT Unclassified/Unlimited Available from the NASA Center for AeroSpace Information (CASI) 7115 Standard Hanover, MD 21076-1320 Category: 93			12b. DISTRIBUTION CODE	
13. ABSTRACT (Maximum 200 words) The purpose of this work is to provide an accurate Galactic Cosmic Ray (GCR) energy spectrum that can be used by radiation health physicists for astronaut exposures and for Single Event Effect (SEE) rate prediction codes CRÈME-MC and CREME96. GCRs are the major cause of "quiet time" SEEs in spacecraft in the solar system and beyond. Accurate knowledge of the GCR spectrum is needed, especially during solar minimum when the GCR flux is at its maximum. All GCR energy spectra reported in this paper apply in free space – beyond the Earth's magnetosphere. An appropriate magnetic cutoff code should be used to get the GCR flux within the Earth's magnetic field. New results presented here model the "quiet time" GCR flux from 1955 to 2012 and provide the most comprehensive comparison compiled, to date, between model and GCR in-flight measurements made above the magnetic cutoff, from balloons (high latitude) and satellites (high altitude). The Badhwar-O'Neill model parameters are uniquely influenced by measurements from the NASA Advanced Composition Explorer Cosmic Ray Isotope Spectrometer that is measuring the low energy spectrum for all ions from lithium to nickel. This is a significant improvement to the overall accuracy of modeling the true GCR spectrum.				
14. SUBJECT TERMS galactic cosmic rays; galactic radiation; radiation measurement; flux density			15. NUMBER OF PAGES 240	16. PRICE CODE
17. SECURITY CLASSIFICATION OF REPORT Unclassified	18. SECURITY CLASSIFICATION OF THIS PAGE Unclassified	19. SECURITY CLASSIFICATION OF ABSTRACT Unclassified	20. LIMITATION OF ABSTRACT Unlimited	
